



**HAL**  
open science

# Strategy of non-physiological EGFR endocytosis and aptamer-vectorization

Elisabete Cruz da Silva

► **To cite this version:**

Elisabete Cruz da Silva. Strategy of non-physiological EGFR endocytosis and aptamer-vectorization. Molecular biology. Université de Strasbourg, 2020. English. NNT : 2020STRAJ035 . tel-03627278

**HAL Id: tel-03627278**

**<https://theses.hal.science/tel-03627278v1>**

Submitted on 1 Apr 2022

**HAL** is a multi-disciplinary open access archive for the deposit and dissemination of scientific research documents, whether they are published or not. The documents may come from teaching and research institutions in France or abroad, or from public or private research centers.

L'archive ouverte pluridisciplinaire **HAL**, est destinée au dépôt et à la diffusion de documents scientifiques de niveau recherche, publiés ou non, émanant des établissements d'enseignement et de recherche français ou étrangers, des laboratoires publics ou privés.

*ÉCOLE DOCTORALE SCIENCES DE LA VIE ET DE LA SANTE*

Faculté de Pharmacie, CNRS UMR 7021

**THESIS** presented by:

[ **Elisabete CRUZ DA SILVA** ]

Defended on: 15 octobre 2020

to obtain the title of: **Docteur de l'Université de Strasbourg**

Speciality: Molecular and Cellular Biology aspects

**Strategy of non-physiological EGFR endocytosis  
and aptamer-vectorization**

**THESIS directed by:**

[M. LEHMANN Maxime]

Pr, Université de Strasbourg, CNRS UMR 7021

[Mme. CHOULIER Laurence]

Dr, Université de Strasbourg, CNRS UMR 7021

**REPORTERS:**

[M. LALLOUE Fabrice]

Pr, Université de Limoges, EA3842-CAPTuR

[Mme. CERCHIA Laura]

Dr, Institute of Experimental Endocrinology and Oncology "G. Salvatore"

---

**OTHER JURY MEMBERS:**

[Mme. FAUROBERT Eva]

Dr, Université de Grenoble Alpes, Institute of Advanced Biosciences

[Mme. TOMASETTO Catherine-Laure]

Dr, Université de Strasbourg, IGBMC

*C'est le temps que tu as perdu pour ta rose qui fait ta rose si importante.*

*Petit Prince- Antoine de Saint-Exupéry*

# Acknowledgements

I would like to respectfully acknowledge Pr. Fabrice Lalloué, Dr. Laura Cerchia, Dr. Eva Faurobert and Dr. Fabien Alpy for accepting being part of my thesis' jury, reading and evaluating my work.

I would like to sincerely thank my supervisors Prof. Maxime Lehmann and Dr. Laurence Choulier, my parents in science, for all the time spent teaching me and sharing with me their knowledge, for giving me support in all moments and help me growth professionally and personally.

Respectful thanks to Dr. Monique Dontenwill by accepting me into her team and all the support given along my thesis.

Warm thanks to all members from Dontenwill and Rondé teams. The shared knowledge and work give always more fruits than lonely trees.

Thank you to Saidu Sani, Marina Pierrevelcin, Marina Ingremeau, Raphaël Cathagne, Sylvie Egloff, Marie-Cécile Mercier, Magalie Lambert, Imtiaz Ali and to all master students with who I had the pleasure to work with. Moments spent with you are unforgettable ones.

Grateful thanks to our collaborators Prof. Stephane Dedieu, Dr. Christophe Schneider and Dr. Jessica for all the hard work and the useful advices given. Also thank you to Phillipe Carl and Romain Vauchelles for their help in image analysis.

A warm remembering of Isabelle Lelong-Rebel, my grandmother of science and cups of coffee.

Even though work is a major part of my life, it would be impossible to succeed without my friends and family.

Special thank you to all my friends, mainly to Vanessa Henriques, Kalina Radoynovska, Olga Agrici, Daniel Morgado and Daniela Moura. Not forgetting Kenny Schumacher, Christophe Bruckert, Nicolas Rayroux, Rémy Halliez, Michaële Hémono, Carine Laurent, Florence Hermal and Nadja Groysbeck.

Even far away, my family is my strongest motivation and to them I dedicate all my achievements.

For all the love, support and affection I would like to thank my family. My uncle and my aunt for being my second parents. Inês, Pedro and Telma my dearest non-blood sisters and brother. Claudia and her family to bring warm love to our life. Thank you to Lambert's family to all support.

My father and my grandfather kept guiding me and giving me strength during all these moments.

My favorite and dearest person in the world, my little queen, my mother/grandmother made me the strong woman that fights to achieve always the highest and hardest objectives.

To Bastienzito all my love and all my gratitude for the incontestable support, patience and love.

My PhD is one of the best moments of my life! Thank you to all!

# Table of contents

Acknowledgements .....	ii
Table of contents .....	iv
List of tables .....	vii
List of figures .....	viii
Liste of annexes.....	ix
List of Abbreviations.....	x
Synopsis .....	xvi
Introduction .....	1
1. Glioblastoma .....	1
1.1 Definition .....	1
1.2. Glioblastoma classifications.....	1
1.3 Main GBM hallmarks.....	4
1.3.1 Glioblastoma Invasive behavior.....	4
1.3.2 GBM heterogeneity as a cause of tumor aggressiveness and therapy resistance.....	6
1.4 Glioblastoma Treatment.....	9
1.5 Predictive and prognostic factors of GBM.....	10
1.6 New therapeutic approaches in GBM .....	11
1.6.1 Targeted therapies .....	12
1.6.2 Metabolism targeting.....	12
1.6.3 Immunotherapy .....	14
2. Epidermal growth factor receptor .....	17
2.1 Generality on EGFR.....	17
2.2 EGFR signaling .....	19
2.2.1 Ras/Raf/MEK/MAPK signaling pathway .....	19
2.2.2 PI3K signaling pathway .....	19
2.2.3 STAT signaling pathway.....	20
2.2.4 PLC- $\gamma$ signaling pathway .....	20
2.3 Endocytic pathway of EGFR.....	21
2.4 EGFR trafficking.....	22
2.4.1 Ligand-induced EGFR trafficking .....	22
2.4.2 Stress-induced EGFR trafficking dysregulation .....	24
2.5 EGFR a therapeutic target in GBM.....	25

2.5.1 Oncogenic activity of EGFR in GBM.....	25
2.5.2 EGFR trafficking dysregulation in GBM.....	26
2.5.3 Anti-EGFR therapies and clinical trials .....	28
3. Integrins.....	36
3.1 The integrin family.....	36
3.2 Integrin Structure.....	37
3.3 Integrin signaling pathways .....	38
3.4 Integrins and cancer .....	41
3.4.1 Integrin trafficking fuel cancer cell migration and invasion.....	43
3.4.2 Role of integrins in resistance to anti-tumor therapies.....	46
3.4.3 Integrins and GBM.....	47
4. Aptamers as alternative to antibodies.....	52
4.1 Conformation .....	52
4.2 Advantages of aptamers .....	52
4.3 Disadvantages of aptamers.....	54
4.4 SELEX .....	56
4.4.1 Protein-SELEX.....	56
4.4.2 Cell-SELEX .....	57
4.4.3 Protein-SELEX versus cell-SELEX.....	58
4.4.4 Other SELEX methodologies.....	58
4.5 Applications of Aptamers.....	59
4.5.1 Aptamers as Therapeutics .....	60
4.5.2 Aptamers as diagnostic tools.....	67
5. Objectives.....	70
Material and Methods.....	72
Results .....	83
Introduction Articles 1 and 2.....	84
Article 1 .....	86
Article 2.....	106
General conclusions of Articles 1 and 2.....	129
Introduction to Article 3 and to recent results.....	131
Article 3.....	134
Recent results on aptamers targeting different cell-surface receptors, biomarkers of GBM .	150

General conclusions .....	162
Conclusion.....	163
References .....	178
Résumé .....	205
Annexes.....	I
Résumé .....	XLVI
Résumé en anglais.....	XLVI



## List of tables

<b>Table 1: EGFR trafficking dysregulation in GBM</b> .....	30
<b>Table 2: ADC in clinics</b> .....	33
<b>Table 3: Integrin overexpression in cancer</b> .....	42
<b>Table 4: Aptamer versus monoclonal antibody</b> .....	55
<b>Table 5: Aptamers in clinical trials</b> .....	64
<b>Table 6: Dilutions of antibodies used</b> .....	73
<b>Table 7: Concentration of inhibitors used</b> .....	73
<b>Table 8: Cell lines used</b> .....	74
<b>Table 9: Sequences of aptamers used</b> .....	76
<b>Table 10: Target affinity of EGFR-TKIs.</b> .....	166

## List of figures

<b>Figure 1: Algorithm used on WHO CNS tumor classification in 2016</b> .....	4
<b>Figure 2: Metabolism of TMZ in aqueous solution</b> .....	13
<b>Figure 3: HER family. A family of 4 receptors tyrosine-kinase</b> .....	18
<b>Figure 4: ATP binding site of tyrosine kinase domain</b> .....	18
<b>Figure 5: EGFR signaling.</b> .....	21
<b>Figure 6: EGFR membrane trafficking.</b> .....	24
<b>Figure 7: EGFR-targeting therapies.</b> .....	34
<b>Figure 8: Structures of EGFR-TKI</b> .....	35
<b>Figure 9: Integrin family</b> .....	38
<b>Figure 10: Integrin structure.</b> .....	39
<b>Figure 11: Integrin conformations</b> .....	39
<b>Figure 12: Integrin trafficking in cell migration</b> .....	45
<b>Figure 13: Integrin/EGFR crosstalk as response to therapy</b> .....	46
<b>Figure 14 : Strategies targeting integrins in clinical trials.</b> .....	51
<b>Figure 15: SELEX</b> .....	59
<b>Figure 16: Aptamer-internalization mechanisms</b> .....	68
<b>Figure 17: Perspectives of the present work</b> .....	164
<b>Figure 18: GME effect on inactive integrin trafficking</b> .....	169
<b>Figure 19: GME effect on active integrin trafficking</b> .....	170
<b>Figure 20: Gefitinib effect on cetuximab (CTX) internalization</b> .....	171
<b>Figure 21: Gefitinib increases ABT-414 efficiency</b> .....	172
<b>Figure 22: Illustration of clinical applications of aptamers targeting GBM cell-surface biomarkers</b> .....	173
<b>Figure 23: Illustration of the putative intracellular trafficking, by RME ('receptor mediated endocytosis'), of aptamers targeting cellular receptors and conjugated to siRNAs</b> .....	175

## Liste of annexes

<b><u>Annex 1</u></b> Draft of Review : A systematic review of glioblastoma molecular targeted therapies in Phases II, III, IV clinical trials.....	II
<b><u>Annex 2</u></b> Review : Role of Integrins in Resistance to Therapies Targeting Growth Factor Receptors in Cancer .....	IV
<b><u>Annex 3</u></b> Publication in collaboration with Dr. Guy Zuber team.....	XXXII

## List of Abbreviations

**A**CK1 - Activated Cdc42-associated kinase 1

ADC - Antibody-drug conjugate

ADCC- Antibody dependent cell cytotoxicity

ADMIDAS - Adjacent Metal Ion-Dependent adhesion site

$\alpha$ -KG -  $\alpha$ -ketoglutarate

ALDH1 - Aldehyde Dehydrogenase 1

AMPA -  $\alpha$ -amino-3-hydroxy-5-methyl-4-isoxazolepropionic acid *receptor*

AP-2 - Adaptor protein 2

AptDC – Aptamer-drug conjugate

AsiC – Aptamer-siRNA chimera

ATP - Adenosine triphosphate

ATRX - Alpha-thalassemia/mental retardation, X-linked

**B**BB - Blood-brain barrier

**C**AR-T - Chimeric antigen receptor T cells

CAF - Cancer-associated fibroblasts

Cbl - Casitas B-lineage Lymphoma

CCL2 - C-C Chemokine Ligand 2

CD- Cluster of differentiation

CDK - Cyclin-dependent kinases

CDKN2A - Cyclin dependent kinase inhibitor 2A

CEA - Carcinoembryonic antigen

CpG - Cytosine-phosphate-guanine

CME- Clathrin-mediated endocytosis

CMTM - Chemokine-like factor-like MARVEL transmembrane domain

CNS - Central nervous system

CTC - Circulating tumor cells

CTLA4 - Cytotoxic T-lymphocyte-associated protein 4

CXCL2 - C-X-C - Chemokine Ligand 12

CXCR-4 - C-X-C chemokine receptor type 4

## **D**<sub>a</sub> – Dalton

DAG - Diacylglycerol

DNA - Deoxyribonucleic acid

DNM2- Dynamin-2

## **E**<sub>CM</sub> - Extracellular matrix

EEA1 - Early endosome antigen 1

EGF - Epidermal growth factor

EGFR - Epidermal growth factor receptor

EMEM- Eagle's minimum essential medium

EPS15- Epidermal growth factor receptor substrate 15

ER - Estrogen receptor

ERC- Endocytic recycling compartment

ESCRT - Endosomal sorting complex required for transport

## **F**<sub>A</sub> - Focal adhesion

FAK - Focal adhesion kinase

FBS – Fetal Bovine Serum

FDA - Food and drug administration

FIP- Family Interacting Proteins

FISH - Fluorescence in-situ hybridization

FRET - Fluorescence resonance energy transfer

## **G**<sub>BM</sub> - Glioblastoma

G-CIMP - Glioma-CpG island methylator phenotype

GDP – Guanosine diphosphate

GFAP - Glial fibrillary acidic protein

GLS – Glutaminase

GME – Gefitinib-mediated endocytosis

GOLPH3 - Golgi phosphoprotein 3

GPCR - G-protein-coupled receptors

Grb2- Growth factor receptor-bound protein 2

GSC - Glioma stem-like cells

GSK-3 $\beta$ - Glycogen synthase kinase 3 beta

GTP – Guanosine triphosphate

**H**GF - Hepatocyte growth factor

HIV - Human immunodeficiency virus

HLA - Human leukocyte antigen

HNSCC - Head and Neck Squamous Cell Carcinoma

HRP - Horseradish peroxidase

**I**DH - Isocitrate dehydrogenase

IGFR - Insulin-like growth factor receptor

IHC- Immunohistochemistry

IL - Interleukin

ILK - Integrin linked kinase

ILV - Intraluminal vesicle

**L**IF – Leukemia inhibitory factor

LOX - Lysyl oxidase

LRP-1 - Low density lipoprotein receptor-related protein 1

**M**APK - Mitogen-activated protein kinase

MDM2 - Mouse double minute 2 homolog

MGMT - O-6-methylguanine-DNA methyltransferase

MIDAS- Metal Ion-dependent adhesion site

miR – micro RNA

MMAE – Monomethyl auristatin-E

MMAF - Monomethyl auristatin-F

MMP - Metalloprotease

MRI - Magnetic resonance imaging

MSLC - Mesenchymal stem-like cells

MTAP - Methylthioadenosine phosphorylase

MUC1 - Mucin 1

MVB - Multivesicular body

**N**ADP - Nicotinamide adenine dinucleotide phosphate

NAMPT - Nicotinamide phosphoribosyltransferase

NCE - Non-clathrin endocytosis

NF1 - Neurofibromatosis 1

NF- $\kappa$ B – Nuclear factor -  $\kappa$ B

NHE9 - Na<sup>+</sup>/H<sup>+</sup> exchanger isoform 9

NOS – Not otherwise specified

NSCLC - Non- Small Cell Lung Cancer

NTRK - Neurotrophic Receptor Tyrosine Kinase

NVAMD - Neo-vascular age-related macular degeneration of the retina

**P**ARP - Poly(ADP-ribose) polymerases

PCR - Polymerase chain reaction

PD-1 - Programmed cell death protein 1

PDGFR - Platelet-derived growth factor receptor

PD-L1 - Programmed cell death protein ligand 1

PDX - Patient derived xenograft

PEG - Poly ethylene glycol

PET - Positron emission tomography

PIP - Phosphatidylinositol

PKC- Protein Kinase C

PLC - Phospholipase C

PLGA - Poly (D,L-lactic-co-glycolic acid)

PRMT5 - Protein arginine methyltransferase 5

PSA - Prostate specific antigen

PSMA - Prostate-specific membrane antigen

PTEN - Phosphatase and tensin homolog

PTP1B - Protein-tyrosine phosphatase 1B

**R**ab- Ras-associated binding

RAF – Rapidly Accelerated Fibrosarcoma

RAS – Reticular Activating System

Rb - Retinoblastoma

RCP - Rab-coupling protein

RGD - Arginine-glycine-aspartic acid

RNA - Ribonucleic acid

RNF11 - RING finger protein 11

ROS - Reactive oxygen species

RPA – Robotic automatization process

RT - Radiotherapy

RT-PCR - Reverse transcription polymerase chain reaction

RTK - Receptor tyrosine kinase

**S**ELEX - Selective evolution of ligands by exponential enrichment'

Shc- Src homology 2 domain-containing

SPECT - Single-photon emission computed tomography

SNARE- Soluble N-ethylmaleimide sensitive factor receptor

SNP - Single nucleotide polymorphisms

SNX17 - Sorting nexin 17

STAM - Signal transducing adaptor molecule

STAT - *Signal* transducers and activators of transcription

STX8 - Syntaxin-8

SyMBS - Synergistic metal ion binding site

**T**AM - Tumor-associated macrophages

TAZ- Transcriptional coactivator with PDZ-binding motif

TCGA – The cancer genome atlas

TERT - telomerase reverse transcriptase

TFPI - Tissue Factor Pathway Inhibitor

TGF - Transforming growth factor

TGN - Trans-Golgi network

TIC - Tumor initiating cells

TIMP – Tissue inhibitors of MMP

TK - Tyrosine kinase



TKI - Tyrosine kinase inhibitor

TLR4 - Toll-like receptor 4

TMZ - Temozolomide

**U**PA - Urokinase-type plasminogen activator

USA- United States of America

UV - Ultraviolet

UIM- ubiquitin-interacting motifs

**V**EGF - Vascular endothelial growth factor

VEGFR - Vascular endothelial growth factor receptor

**W**HO - World health organization

WT - Wild-type

**X**NA - Xeno nucleic acid

**Y**AP- Yes-Associated Protein

**Z**EB - Zinc finger E-box binding protein

**2'**-OH - 2'-hydroxyl

**2**-HG - 2-hydroxyglutarate

# Synopsis

This thesis manuscript entitled “Strategy of non-physiological EGFR endocytosis and aptamer-vectorization”, will be presented as follow:

## **Introduction:**

An overview on glioblastoma (GBM) characteristics and therapeutic challenge is presented, followed by the description of two GBM therapeutic targets (EGFR (Epidermal Growth Factor Receptor) and  $\alpha 5\beta 1$  integrin (expression, oncogenic signalling pathway, intracellular trafficking and targeted therapies). Finally, aptamers, small nucleic acids molecules, also called chemical antibodies, are described as antibodies alternative for vectorization and detection tools.

## **M&M:**

The description of methodologies I performed during my PhD in the four different projects presented in results are described.

## **Results:**

My PhD research results, presented in three scientific articles and one section of recents results, followed two main objectives:

(1) the description of the effect of tyrosine kinase inhibitors of EGFR used in clinic on the endocytosis of the two therapeutic targets described herein in glioma cell models. We first described that in different GBM cell lines, EGFR-tyrosine kinase inhibitors trigger exuberant endocytosis of EGFR and  $\alpha 5\beta 1$  integrin, which may modulate glioma cell invasiveness under therapeutic treatment (Blandin, Cruz da Silva et al., 2020). In order to better understand the molecular mechanism, we identify several proteins involved in this non-physiological endocytosis (Cruz da Silva et al, under writing).

(2) the validation of aptamers targeting integrin or EGFR, as an alternative to antibodies, for diagnosis and intracellular delivery of cytotoxic agents. We first described and characterized aptamer H02, a new aptamer targeting  $\alpha 5$  integrin. Its affinity and specificity toward GBM cells and tumoral tissues expressing  $\alpha 5$  integrin were determined (Fechter, Cruz Da Silva et al.,

2019). EGFR-targeting aptamers are studied in the 4<sup>th</sup> section. Integrin  $\alpha 5$  and EGFR targeting aptamers were used in aptafluorescence in GBM cells and tissues (Cruz da Silva, under writing).

## **Discussion**

Finally, a critical discussion about the main experimental results of my thesis is presented. Some preliminary results and future perspectives are also presented.

## **Annexes**

Annex 1 presents a draft of a revue about glioblastoma molecular targeted therapies in Phases II, III, IV clinical trials (Cruz da Silva et al., under writing).

Annex 2 presents a revue about the role of integrins in therapy resistance to tyrosine kinase receptor-targeted therapies in cancer (Cruz da Silva et al., 2019)

Annex 3 presents a scientific article characterizing gold particles conjugated to cetuximab for future GBM treatment using targeted radiotherapy. This work is the result of a collaboration with Dr. Guy Zuber team (Groysbeck et al., 2019).

# Introduction

# 1. Glioblastoma

## 1.1 Definition

Central nervous system (CNS) tumors represent approximately 3% of the cancer cases worldwide (Miranda-Filho et al., 2017). In 2016, were reported 330 000 incident cases of CNS cancer and 227 000 deaths in the world (Patel et al., 2019). Glioblastoma (GBM) is the most common and most aggressive malignant tumor in CNS representing 60% of all brain tumors in adults (Hanif et al., 2017). Despite numerous efforts, the median survival is around 15 months (Hanif et al., 2017; Thakkar et al., 2014). GBM can develop anywhere in the brain, but preferentially in the supratentorial region, having edema surrounding the tumor (Thakkar et al., 2014). GBM is more prominent in men than women, with a median age of incidence of 64 years old (Tamimi and Juweid, 2017).

The risk factors associated with GBM development include therapeutic or high-dose radiation, decreased susceptibility to allergy, immune factors and genetic alterations (Bondy et al., 2008). Overactive immune response resulting in allergic and/or autoimmune conditions is associated with reduced risk glioma (Safaeian et al., 2013). Genome-wide association studies associated germline variants with an increased risk for development of GBM. 27 single nucleotide polymorphisms (SNP) were associated with glioma genetic risk (DeAngelis, 2001; Kinnersley et al., 2018; Thakkar et al., 2014). Moreover, increased telomere length was described as a risk factor for glioma. This association is based on analysis of blood cells, however, no data is available in brain cells (JAMA Onc, 2017).

GBM symptoms are variable depending on tumor localization and volume. GBM can appear progressively with neurologic deficit, cognitive problems, intracranial hypertension syndrome, and epileptic seizures. The usual symptoms involve headache, seizures, nausea, vomiting and hemiparesis. Cranial magnetic resonance imaging is the reference exam in brain tumor doubts, that allows differential diagnosis between brain tumor, stroke and encephalopathy (DeAngelis, 2001; Thakkar et al., 2014).

## 1.2. Glioblastoma classifications

The World Health Organization (WHO) classification of CNS tumors dated from 2007 described 3 major groups: astrocytoma (grade I to IV), oligodendroglioma (grade II to III) and

oligoastrocytoma (grade II to III). Brain tumors were classified according to their anatomopathological features: histological and grade elements. Histological analysis describes the most frequent cell types (astrocytes, oligodendrocytes or mix) and possible morphological similarities with normal glia. While in grading, malignancy criteria such as like cell density, nuclear atypia, number of mitoses, micro vascularization and necrosis are evaluated (Louis et al., 2007). In 2016, a new classification has emerged based on an integrated diagnostic with phenotypic and genotypic characteristics (Figure 1) (Louis et al., 2016).

GBMs are now classified as grade IV diffuse astrocytic and oligodendroglial tumors. These tumors are further segregated based on Isocitrate dehydrogenase (IDH) status. 90% of GBM expressed wildtype IDH and the remaining 10% share a genetic driver mutation on *IDH1* and rarely on *IDH2* genes (Cohen et al., 2013). The 3 isocitrate dehydrogenases are encoded by 5 different genes. IDH1 is found in the cytoplasm and peroxisomes where it participates in lipid and glucose metabolism. While IDH2 and IDH3 are found in mitochondria. IDH1 protects cells against oxidative stress from oxygen reactive species by catalyzing the decarboxylation of isocitrate from  $\alpha$ -ketoglutarate ( $\alpha$ -KG) in the citric acid cycle to produce NADPH from NADP<sup>+</sup> (Madala et al., 2018; Smolková and Ježek, 2012). The evaluation of IDH status is established by immunohistochemistry to detect the mutant protein and by *IDH* gene sequencing. In 91% of the cases, the mutation consists in the replacement of an arginine by a histidine in position 132. Mutated *IDH1* R132H results in a decrease of  $\alpha$ -KG and NADPH production. As a consequence, glutathione (GSH) levels are reduced, and deoxyribonucleic acid (DNA) methylation and hypoxia are increased (Dang et al., 2009). IDH status is used as prognostic factor in GBM. GBM patients with mutated *IDH* have a longer survival than *IDH* WT patients and present small tumor size and less necrotic lesions (Madala et al., 2018).

When IDH evaluation cannot be performed, the tumor is classified as GBM NOS (not otherwise specified) (Louis et al., 2016).

### Primary and secondary GBM

Contrary to secondary GBMs, primary GBMs are diagnosed without clinical or histologic evidence of a previous lesions.

Primary GBMs represent 90% of all GBM and usually affect older patients (over 55 years old). They are characterized by frequent necrotic and ischemic areas. Genetically, primary GBMs

are characterized by a wildtype *IDH* status, *erbB1* amplification (40% of cases), phosphatase and tensin homolog (PTEN) mutations (45% of cases), p16 deletions and hTERT promotor mutations. The chromosomal events associated to this GBM subgroup are:

- amplification of the 7p12 region, that encodes *erbB1*.
- amplification of the 12q14 region, that encodes *CDK4* and *MDM2* genes. Thus, p53 and Rb1 pathways are disrupted.
- homozygous deletion of 9p, that encodes *p16*, *p15* and *p14 ARF* genes.
- loss of heterozygosity of 10q, that encodes the *PTEN* gene, leading to a constitutive activation of PI3K (Phosphoinositide 3-kinase)/AKT pathway.

Secondary GBM affect young patients and are characterized by less necrotic areas and genetic alterations found in low grade tumors such as *TP53*, Platelet-derived growth Factor Receptor-alpha (*PDGFR-α*), Retinoblastoma1 (*Rb1*), *ATRX*, and *IDH1*. They are associated with a significantly better prognosis (Behin et al., 2003; DeAngelis, 2001).

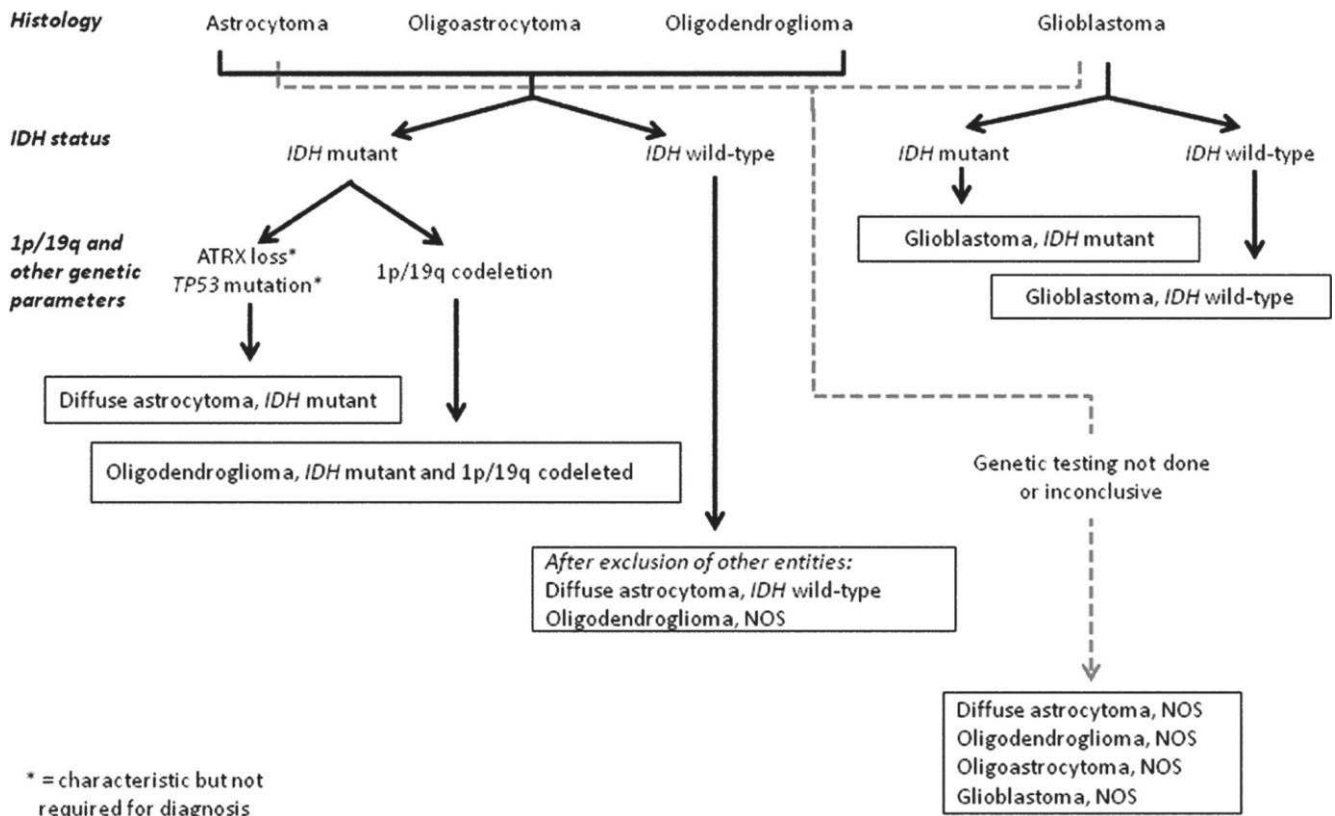


**Figure 1: Algorithm used on WHO CNS tumor classification in 2016.** CNS tumors are first divided by their histological features. Glioblastomas are now divided into *IDH*-wild type (about 90 % of GBM cases), and *IDH*-mutant. *IDH*-mutant correspond to younger patients and present a better prognosis of survival. Another denomination is used when *IDH* evaluation cannot be performed (GBM NOS). The other tumors are also divided accordingly with *IDH* mutation, 1p/19q codeletion, *TP53* mutation and *ATRX* loss. NOS nomination is given when genetic testing is not available or inconclusive. Adapted from (Louis et al., 2016).

## 1.3 Main GBM hallmarks

### 1.3.1 Glioblastoma Invasive behavior

Highly invasive growth is a GBM hallmark. GBM cell invasion can promote therapy resistance (Lefranc et al., 2018; Vehlow and Cordes, 2013).

GBM cells can develop a tumor in the opposite hemisphere from the primary site or even produce a multifocal GBM tumor. However, GBM rarely metastasizes outside of the brain. (Thakkar et al., 2014). Syngeneic GBM cells were orthotopically implanted into rat to study cell invasion profiles. GBM cells moved along blood vessel wall, neural fibers of corpus callosum and astrocytes of glia limitans. When GBM cells migrate along blood vessels, they present a spindled shape with a single pseudopodium extended toward the movement direction through polarization of actin polymerization. Brain parenchyma migration is achieved by multiple pseudopodia pointed in different directions (Hirata et al., 2012).

Most of the time, migrating GBM cells adopt a mesenchymal phenotype, dependent on the adhesion to the extra cellular matrix (ECM) and their remodulation. Modification on cell shape, position and tissue architecture are needed for effective invasion together with PI3K signaling and small GTPase activation. GBM cells interact with ECM mainly through integrins and their adhesomes, and acid hyaluronan receptor CD44 (Alves et al., 2011; Cha et al., 2016). ECM proteins are overexpressed in GBM parenchyma (Lal et al., 1999). Hyaluronan, collagen, fibronectin and laminin present in brain parenchyma are some of the main ligands of integrins and CD44 (Giese and Westphal, 1996; Rape et al., 2014). ECM is remodeled by serine proteases, cysteine proteases and metalloproteases (MMP). The most studied serine protease is the complex urokinase-type plasminogen activator (uPA) / uPA receptor that activates plasmin and degrades fibronectin and laminin (Deryugina and Quigley, 2012). While a common cysteine protease is Cathepsin B, that is involved in laminin and collagen degradation and thus GBM invasion (Mohanam et al., 2001). Moreover, the most important MMPs involved in GBM cell invasion are MMP-2 and -9 (Hagemann et al., 2012). The inhibition of these MMPs leads to less migration and invasion in glioma cell lines and glioma cells xenografts (Badiga et al.,



2011; Kesanakurti et al., 2012). Tissue inhibitors of MMP (TIMP) modulate the proteases activity by forming complexes and reducing cell invasion (Valente et al., 1998).

Glutamate enhances cancer cell invasion through activation of AMPA receptors. AMPA receptor expression correlates with  $\beta$ 1 integrin expression, focal adhesion kinase (FAK) activation and cell invasion (Piao et al., 2009). Moreover, exosomes release from GBM cells upon radiation enhances tumor migration via FAK signaling (Arscott et al., 2013).

Crosstalk between GBM cells and cells from their microenvironment enhances cancer cells migration and invasion. For instance, the perivascular niche regulates glioma stem-like cells (GSCs) and promotes GBM invasion. Using co-culture of patient-derived GBM spheroids with brain endothelial cells in microfabricated collagen gels, McCoy et al have recently shown that endothelial cells increase GBM invasiveness and growth through enrichment of GSC via secretion of interleukin-8 (IL-8) (McCoy et al., 2019). Moreover, crosstalk between GBM cells and mesenchymal stem-like cells (MSLCs) boosted GBM invasion into parenchymal brain tissue. This mechanism is dependent of p38-MAPK (Mitogen-activated protein kinase)/ZEB1 signaling (Lim et al., 2020). Interaction between GBM cells and astrocytes can promote tumor cell invasion (Zhang et al., 2020a). Astrocytes remodel ECM by enhancing MMP expression and activation of uPAR signal (Le et al., 2003). Astrocytes secrete cytokine IL-6 that induces cytomembrane MMP14 in glioma cells. Thus, MMP2 is activated and promotes glioma cell migration and invasion (Chen et al., 2016b).

Communication within tumor site and surroundings through extracellular vesicles is also possible. For example, miR-21-positive extracellular vesicles released by GBM cells enhance macrophages proliferation. On the other hand, macrophages also transfer miR-21 positive extracellular vesicles to GBM cells, increasing signal transducer and activator of transcription 3 (STAT3) activity and thus stimulating cell invasion, proliferation and therapy resistance (Buruiană et al., 2020).

Brain tumor cells form thick and long cellular protrusions, called tumor microtubes, to interconnect multicellular networks. Tumor microtubes were identified in GBM xenograft via longitudinal intravital two-photon microscopy (Osswald et al., 2015). Tumor microtubes facilitate cell proliferation, cell invasion into healthy brain tissue, and transfer of molecules and organelles between tumor and stromal cells (Osswald et al., 2015). Moreover, these networks protected cells from radiotherapy and chemotherapy cytotoxicity (Weil et al., 2017). In other

tumors, mitochondrial transfer through tumor microtubules rescued apoptotic cells and facilitate cell invasion (Lu et al., 2017; Wang and Gerdes, 2015).

### 1.3.2 GBM heterogeneity as a cause of tumor aggressiveness and therapy resistance

Interestingly, the name multiforme was proposed thanks to the presence of different histological regions of pseudo-palisading necrosis, hemorrhage and angiogenesis. At the genetic level, GBM has various deletions, amplifications and point mutations that activate different signal pathways (Holland, 2000). GBM presents a high inter-patient and inter-tumoral variability, that makes GBM a very aggressive and resistant tumor (Parker et al., 2015).

#### 1.3.2.1 Inter-tumoral heterogeneity

Using microarray analysis on a cohort of two hundred human GBM biopsies, the group of Verhaak demonstrates for the first time a great inter-tumoral heterogeneity between patients. Verhaak classification divided GBM on 4 groups: classical, mesenchymal, proneural and neural (Verhaak et al., 2010).

Classical GBM are characterized by high levels of *erbB1* transcription and they are more responsive to therapy with a better prognosis compared to other groups. The mesenchymal GBM presents high expression of ECM remodeling genes (*CHI3L1*, *MET* and *CD44*). The proneural subtype is characterized by alterations of *PDGFRA*, point mutations in *IDH1* and *TP53* mutations, and is correlated with a worst survival prognosis. This group was further divided according to the G-CIMP methylation status (Verhaak et al., 2010). The majority of GBM non-methylated G-CIMP exhibits chromosome 7 amplification and chromosome 10 loss. However, methylated G-CIMP proneural seems to result from a low-grade glioma evolution (Ozawa et al., 2014). Finally, the neural subtype is characterized by the expression of neuronal markers such as *NEFL*, *GABRA1*, *SYT1* and *SLC12A5* (Verhaak et al., 2010).

The main limitation of Verhaak's study is that it was based on a single GBM biopsy. It does not consider different areas of tumor or even infiltrated cells on surrounding parenchyma. Moreover, proportion between tumor cells and normal microenvironment cells are unknown by using single biopsies.

Later on, the same group published a study based on a transcriptome analysis of *IDH*-WT GBM tissues and cells which showed the existence of only 3 groups partly shaped by tumor immune environment. The neural subgroup was eliminated and considered as a microenvironment normal tissue. The mesenchymal group presented the worst survival. Comparison of matched primary and recurrent tumors revealed tumor plasticity with subtype change (Wang et al., 2017a).

The existence of different areas inside the same tumor and the capacity of a subtype of cells to evolve highlights the intra-tumoral heterogeneity, not yet explored in Verhaak's papers.

### 1.3.2.2 Intra-tumoral heterogeneity

Intra-tumoral heterogeneity plays a major role in tumor development and therapy resistance.

Using fluorescence in-situ hybridization (FISH) analysis, Snuderl et al. described a mosaic amplification of RTKs (Epidermal Growth Factor Receptor (EGFR), c-MET, PDGFRA) in GBM adjacent cells. All subpopulation participated in tumor growth and all shared early genetic changes from a common precursor (Snuderl et al., 2011).

Sottoriva et al studied the copy-number and gene expression of 38 biopsies from 9 patients and demonstrated the presence of different GBM subgroups inside the same tumor (Sottoriva et al., 2013). Another study using single-cell transcriptomic analysis corroborated the previous study. Interestingly, GBM with cells derived from more than one subgroup have a worst prognostic (Patel et al., 2014).

Using single-cell RNA (ribonucleic acid)-sequencing of 28 tumors, genetic and expression analysis of TCGA tumors and single-cell lineage, a recent study showed the complex and dynamic intra-heterogeneity of GBM tumors (Neftel et al., 2019). Four subtypes of GBM cells were identified, each one characterized by specific genetic alterations (*CDK4*, *EGFR*, *PDGFRA*, *NF1*). GBM subtypes are highly influenced by the tumor microenvironment, and present a huge plasticity since a single cell can generate all four subtypes with multiple possible transitions (Neftel et al., 2019).

Tumor plasticity have important impact on clinical outcome. This plasticity can be seen in the appearance of a recurrent tumor with a different molecular signature than the previous resected tumor. This transition of molecular characteristics is associated with GBM radiation resistance

(Bhat et al., 2013). A primary tumor characterized by proneural molecular markers gives rise to a recurrent tumor with mesenchymal characteristics. This transition is regulated by tumor-associated macrophages (TAM) through NF- $\kappa$ B activation (Bhat et al., 2013). Short-term relapse GBMs presented a high amount of M2 macrophages upon radiotherapy. Moreover, NF1 deficiency was associated with increased TAM infiltration (Wang et al., 2017a).

The presence of tumor initiating cells (TIC) or GSC creates tumors with cells genetically different, giving a certain tumor plasticity. These cells have some stem cell properties such as: renewing capability, unspecialized characteristics and capability to become differentiated cells (Bonavia et al., 2011). These cells are identified by their capacity of self-renewal and to initiate a tumor (Rahman et al., 2011). Neural stem and progenitor cells are cell types present in the brain, expressing both CD133+. In Singhs *et al* study, CD133+ cells with stem cell properties *in vitro* were isolated from human brain tumors. CD133+ GBM cells represent between 3-30% of the tumor. These cells were able to produce tumors in NOD-SCID (non-obese diabetic, severe combined immunodeficient) mice. These tumors resemble the original human tumor with the same expression of markers (nestin, MIB-1, GFAP, MAP2). Moreover, CD133+ initiating cells were shown to give rise to differentiated cells. Sub-populations of TIC have high levels of SOX2, OCT4, and NANOG, all known to maintain self-renewal and cellular proliferation (Singh et al., 2004). Moreover, these cells are known to be highly resistant to therapy. They survive to standard therapy and can give rise to a recurrence. Therefore, strategies targeting GSC cells can overcome GBM therapy resistance. One of these strategies is the use of ALDH1 inhibitors. *ALDH1A1* encodes the aldehyde dehydrogenase 1 family member A1 protein and is enriched in GSC promoting TMZ GBM resistance. *ALDH1A1* expression is promoted by long noncoding RNAs TP73-AS1 (Mazor et al., 2019). Combination of ALDH inhibitors with the Stupp protocol is in clinical trials and may have efficacy in some GBM patients (Huang et al., 2019a).

The spatial and temporal intra-tumoral heterogeneity are major causes for tumor recurrence.

Spatially, 90% of times, recurrence occurs in peritumoral areas, that usually contains tumoral cells in one third of the area (Lemée et al., 2015). Genetically, cells from primary site mainly expressed anti-apoptotic genes while cells from peritumoral site expressed survival genes. Moreover, peritumoral cells are more proliferative, invasive and resistant to therapy (Lemée et al., 2015). Additionally, genome sequencing of primary tumor and its recurrence demonstrated that distant recurrence presents divergence mutational landscape from primary tumor (Kim et

al., 2015). Demonstrating once more that migrating cells are submitted to a totally different evolution than cells on primary site. Another interesting area is the physiological site of neurogenesis, the subependymal zone. In GBM, this area contains approximately 65% of tumoral cells and is associated to recurrence (Piccirillo et al., 2015).

Usually, the recurrent tumor presents a different genetic signature compared to the primary tumor, suggesting a temporal heterogeneity and adaptation to stress (treatment). Interestingly, the mesenchymal subgroup, being aggressive and resistant to therapy, seems to be genetically stable temporally, with similarities between primary and recurrent tumors. However, the GBM proneural and classical subgroups change genetically to survive therapy and to acquire a more mesenchymal profile (Wang et al., 2017a).

Furthermore, inter-cooperation between tumoral cells and surrounding microenvironment facilitates therapy resistance and tumor recurrence. The microenvironment is composed by different cells (macrophages, endothelial cells, pericytes, astrocytes) and different extracellular matrix components, that can modify the phenotype of tumor cells (Bonavia et al., 2011). For example, tumor-associated astrocytes are activated upon direct contact with GBM cells. They facilitate tumor progression, proliferation, migration, evasion of immune system and chemoradiotherapy resistance of tumor cells (Zhang et al., 2020a). Moreover, different tumor cells can cooperate with each other. For instance, mutant EGFRvIII expressing cells enhance EGFR WT cells proliferation by secretion of IL-6 and LIF (Bonavia et al., 2012; Inda et al., 2010). Furthermore, oxygen gradient and vascularization induce a certain cell adaptation to environment and thus promote tumor heterogeneity. Each tumoral cell that migrates to different areas, adapts to the new microenvironment through additional mutations. Interestingly, the expression of RTK are spatially distinct (Little et al., 2012; Szerlip et al., 2012). For example, PDGFR positive cells are usually found on highly vascularized areas, while EGFR positive cells are detected in more hypoxic sites (Little et al., 2012).

## 1.4 Glioblastoma Treatment

Whenever possible surgical resection is the first therapeutic step for the treatment of GBM. It reduces and decompress the tumor area. Complete tumor resection is associated with increased survival. To facilitate tumor removal, a fluorescence molecule derived from 5-aminolevulinic acid is used during surgical resection to enhance the contrast between normal and tumoral tissues (Ferraro et al., 2016). However, due to the highly invasive nature of the GBM and the

late diagnosis, resections are only partial. Chemo- and radio-therapies are required. Until 2005, surgical resection was followed by radiotherapy (RT) and chemotherapy with carmustine, a nitrosourea drug with alkylating function, as adjuvant treatment (DeAngelis, 2001). In 2005, an improved protocol was established (Stupp et al., 2005). The efficiency of this protocol was verified in the clinical trial (NCT 22981/26981) where concomitant administration of an alkylating chemotherapeutic, temozolomide (TMZ), with RT upon surgical resection, together with adjuvant TMZ resulted in a better treatment. Improved survival was observed for TMZ/RT compared to RT alone (for recursive partitioning analysis (RPA)-III 21 months versus 15 months, while for RPA-IV 16 versus 13 months, respectively) for GBM patients with minimal levels of toxicity (Mirimanoff et al., 2006). The radiotherapy used in Stupp protocol is a fractionated focal type, with irradiation of 2 Gy/ fraction, once a day for five days/week, for a period of six weeks (total of radiation given is 60Gy).

The choice of chemotherapeutic drugs needs to be rational and follows several criteria. The drug should have (i) a low molecular weight to be able to cross the blood-brain barrier (BBB), (ii) a high lipidic solubility, (iii) a low ionization, and (iv) a minimal protein binding capability (Newton, 2006). TMZ is an oral alkylating agent with small size (194 Da) possessing all these characteristics. TMZ is a pro-drug that is spontaneously converted to an active metabolite, imidazole-4-carboxamide that can methylate DNA (Figure 2), in N-7 or O-6 positions of guanine residues (Agarwala and Kirkwood, 2000; Zhu et al., 2014). The rationale of giving TMZ concomitantly with RT is based on:

- A daily administration of low doses has a greater intensity of activity without additional toxicity (Newlands et al., 1992; Wick et al., 2009),
- After RT, O-6-methylguanine-DNA methyltransferase (MGMT) enzyme is activated and repairs DNA damage. A continued administration of alkylating agents like TMZ reduces MGMT expression (van Niftrik et al., 2007),
- A synergy effect is observed by the concomitant use of TMZ and RT (Parisi et al., 2015).

## 1.5 Predictive and prognostic factors of GBM

In GBM, young patient's age, tumor cerebral location and maximal tumor resection are good prognostic factors. Other molecular biomarkers may be considered as valuable genetic prognostic factors.

*IDH*-mutant gliomas present hypermethylation at a large number of loci, known as cytosine-phosphate-guanine (CpG) island. This GBM CpG island methylator phenotype is called G-CIMP. G-CIMP occurs in 10% of GBM, mainly in secondary GBM (Seymour et al., 2015; Thakkar et al., 2014). G-CIMP positive tumors present a better prognosis (Noushmehr et al., 2010). *IDH* mutation and 1p/19q deletion associated with high expression of *CHI3L1*, a gene coding a secreted glycoprotein involved in ECM remodulation and inflammation, and low expression of *NTRK2*, a gene coding a neurotrophic RTK-2 that induces neuronal differentiation and survival, defines an unfavorable prognosis of glioma patients (Deluche et al., 2019). *ATRX* mutations cause alternative lengthening of telomeres and are associated with *IDH1/2* and *TP53* mutations in secondary GBM. *TERT* mutations, more frequently found in primary GBM than in secondary GBM, are correlated with *erbB1* amplification and a shorter patient survival. EGFR overexpression is associated with worse prognosis in younger patients with *TP53*-wildtype tumors (Simmons et al., 2001). *MGMT* is implicated in DNA repair and resistance to alkylating therapy. *MGMT* gene promotor is rich in CpG, which methylation reduces *MGMT* expression. The *MGMT* promotor is hypermethylated in approximately 50% of GBM and is associated with *IDH1/2* mutations. *MGMT* promotor hypermethylation is a predictive factor for alkylating therapy and is associated with a better survival (Yu et al., 2020).

Moreover, several others molecular alterations that are studied in preclinical and clinical studies can be used as predictive factors or therapeutic targets to better treat GBM patients. Molecular studies (Ceccarelli et al., 2016; Verhaak et al., 2010) are not yet used in GBM treatment algorithm. In the last years, the several clinical trials on GBM patients clearly showed the need to better stratify patients and provide a more personalized treatment related to the genetic signature and evolution of GBMs.

Even with treatment, the median survival is around 15 months (Hanif et al., 2017; Thakkar et al., 2014). GBM is still incurable and most tumors give rise to a recurrence.

## 1.6 New therapeutic approaches in GBM

The standard care of GBM (Stupp protocol) has not changed since 15 years. Currently, several studies are being made to develop new treatments. However, most of them are disappointing.

### 1.6.1 Targeted therapies

GBM molecular characterization identified molecular biomarkers involved in tumor progression that can be targeted in order to impair tumor aggressiveness. Therapies inhibiting specifically these biomarkers are called targeted-therapies.

In annex 1 (manuscript under writing), we are currently describing all targeted-therapies tested in 259 GBM clinical trials. Within these clinical trials, proteins involved in tumor growth and migration, cell cycle and cell death's escape, angiogenesis, and unlimited replication were targeted. These studies, being extensively described in this draft (Annex 1), are not repeated in this paragraph.

### 1.6.2 Metabolism targeting

GBMs redirect metabolism to the macromolecule synthesis and antioxidant regeneration mediating tumor progression and therapy resistance (Zhou and Wahl, 2019).



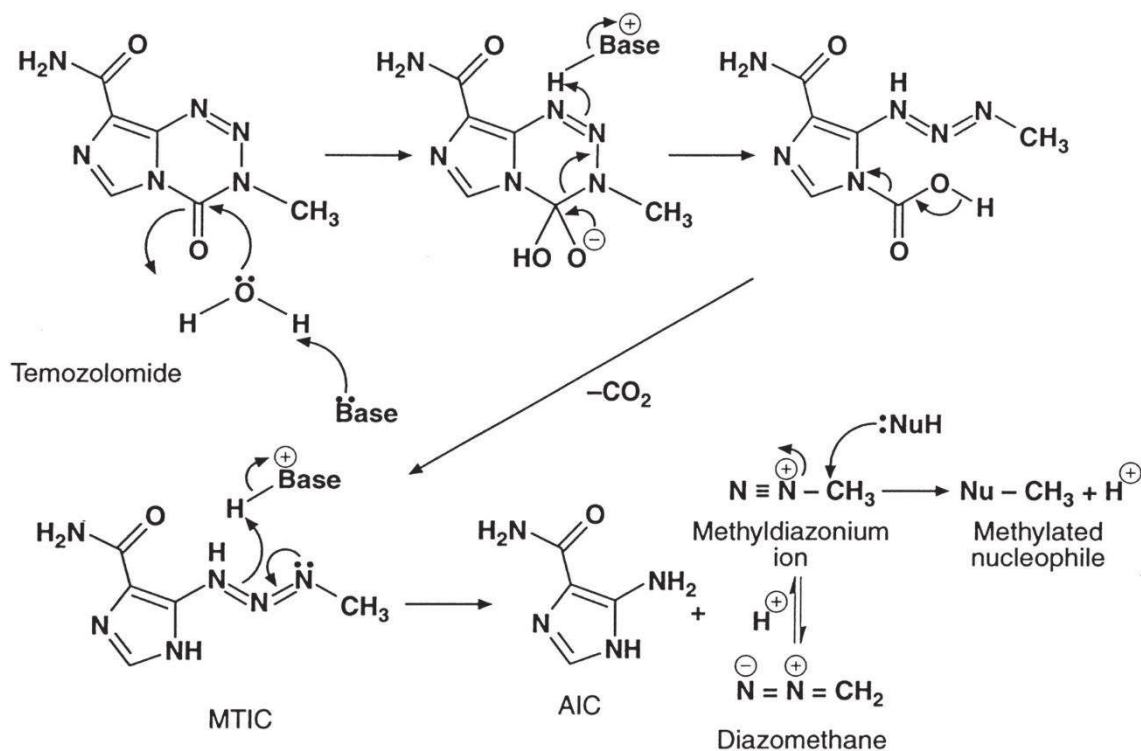


**Figure 2: Metabolism of TMZ in aqueous solution.** When it enters in contact with basic pH solutions like blood or tissues, TMZ undergoes hydrolysis and gives rise to the active metabolite MTIC. MTIC originates the reactive methyldiazonium ion, and 5-aminoimidazole-4-carboxamide (AIC) that will be excreted by the urine. Adapted from (Agarwala and Kirkwood, 2000; Newlands et al., 1997).

Isoform-selective IDH inhibitors suppress 2-HG production. Preclinical studies using an inhibitor of mutant *IDH1* showed the impairment of glioma cell growth (Rohle et al., 2013). Six inhibitors of the mutated *IDH1/2* enzymes are being tested in glioma phase I and II clinical trials (Kaminska et al., 2019). An IDH1-R132H targeting peptide vaccine was evaluated in a phase I (NOA-16) on GBM patients to evaluate safety, tolerance and immune response (Platten et al., 2018). One-carbon (1C) metabolism is based on a series of connected metabolic pathways, including methionine and folate cycles. This metabolic process is essential to provide methyl groups for the synthesis of DNA, polyamines, amino acids, creatine, and phospholipids (Clare et al., 2019). Interestingly, methionine-restricted diet increases cell response to radio and chemotherapy in mice, by depleting circulating antioxidant agents and nucleotide levels (Gao et al., 2019). Methionine can be inhibited in cancer treatment by blocking protein arginine methyltransferase 5 (PRMT5). In cancer cells, depletion of 5-methylthioadenosine phosphorylase (MTAP), an enzyme involved in the methionine pathway, promotes PRMT5 dependency. Moreover, PRMT5 inhibition selectively killed MTAP-null cancer cells (Kryukov et al., 2016). Interestingly, MTAP is deleted in half of GBM tumors (Cerami 2012). An ongoing clinical trial (NCT02783300) addresses the potential interest of PRMT5 inhibitor in several solid tumors including GBM (Zhou and Wahl, 2019).

NAD<sup>+</sup> is a critical metabolic co-factor that affects base excision repair and single strand break repair pathways through Poly(ADP-ribose) polymerases (PARPs) (Almeida and Sobol, 2007). NAD<sup>+</sup> is highly present in GBM since its metabolic enzyme nicotinamide phosphoribosyltransferase (NAMPT) is often upregulated in GSC (Gujar et al., 2016). This pathway can be blocked using NAMPT inhibitors. Clinical trials of NAMPT inhibitors as monotherapy have been discontinued due to toxicity and minimal activity (Sampath et al., 2015). Another way to block this pathway is to use PARP inhibitors. PARP can be inhibited by two mechanisms: (i) antagonist competition with NAD<sup>+</sup> at PARP catalytic site and (ii) PARP entrapment to DNA. Concomitant PARP inhibition with RT/TMZ reduced tumor size in human glioma xenografts (Blakeley et al., 2015). GBM preclinical studies of PARP inhibition increased cell radio-sensitivity (Barazzuol et al., 2013; Russo et al., 2009).

Glutamine breakdown contributes to GBM growth and survival (Zhou and Wahl, 2019). Glutaminase (GLS), which converts glutamine to an ammonium ion and glutamate, is a therapeutic target in many cancers. A glutaminase inhibitor CB-839 sensitized IDH mutant cells to radiation *in vitro* and *in vivo* (McBrayer et al., 2018). A phase Ib clinical trial in IDH-mutated GBM patients is using CB-839 in combination with the Stupp protocol (NCT03528642). Also combination with a PARP inhibitor, talazoparib, is being tested in GBM patients (NCT03875313) (Annex 1). Recently, EGFR was described as a promotor of glutamine metabolism, through ELK1 phosphorylation to activate *GDHI* transcription and thus glutaminolysis (Yang et al., 2020). This correlation can be exploited by using concomitant glutaminase inhibitor and EGFR-targeted therapies. This combination improved anti-EGFR therapy efficiency in preclinical models of colorectal cancer (Cohen et al., 2020). Also this combination provoked metabolic crisis and cell death in mouse lung cancer xenografts (Momcilovic et al., 2017).

### 1.6.3 Immunotherapy

One hallmark of GBM is its highly immunosuppressive profile. This opens the opportunity to use immunotherapy, already successful in the treatment of other solid tumors, to improve GBM suppression.

Nobel prize for medicine 2018 awarded the discovery of checkpoint inhibitors and their use for cancer therapy. Inhibitors of immune checkpoints such as PD-1, PD-L1, and CTLA-4 increase immune activation (McGranahan et al., 2019). In GBM clinical trials, immune checkpoints

inhibitors are being used in monotherapy or combined with other immune stimulating therapies. However, serious concerns exist due to severe complications, even fatal, upon over activation of immune system in the brain (Leitinger et al., 2018).

The vast existence of tumor-associated antigens opened ways to use them as tumor identification card. Vaccines can induce a specific immune response against tumor antigens by teaching patient own immune system to better fight cancer cells. Nowadays, the use of tumor antigen vaccines is restricted to some conditions. Before administration, tumoral antigen expression has to be confirmed. Patients are stratified based on their human leukocyte antigen (HLA) type as well (McGranahan et al., 2019). Several tumor antigens (HER-2, IL13Ra2, MAGE-1, and survivin) are restricted to specific HLA types (class I restricted cytotoxic T cell or class II restricted helper T cell). For targeting these antigens, vaccines need to present the antigen on restricted HLA alleles to generate an immune response (Zhang et al., 2007a). In GBM, single-tumor-antigen vaccines targeting EGFRvIII mutation (rindopepimut) (Annex 1) improved median survival of mice with hetero- and orthotopic GBM xenografts (Heimberger et al., 2003). A phase III clinical trial combining rindopepimut with TMZ did not improve patient survival compared to control (Weller et al., 2017). A phase II with an anti-VEGF (vascular endothelial growth factor) antibody, bevacizumab, showed beneficial results that need to be confirmed in a larger patient set (Reardon et al., 2020). Another target of interest is survivin, a member of the inhibitor of apoptosis family. Survivin overexpression is associated with worst prognostic in GBM, ovarian, breast cancer (Chakravarti et al., 2002; Tong et al., 2019). A single-tumor-antigen vaccine against surviving (SurVaxM) has been developed and is currently tested in association with check-point inhibitor or TMZ (NCT04013672 and NCT02455557, respectively). Furthermore, a multi-targeting vaccine, SL701, targets IL-13Ra2, ephrin A2, and survivin (McGranahan et al., 2019; Peereboom et al., 2018). Moreover, vaccines can be customized according to resected tumor analysis. Two promising custom vaccines (HSPPC-96 (Prophage) and DC-Vax-L) are tested as single agent or in combination with checkpoint inhibitors (McGranahan et al., 2019).

Another immunotherapy is based on the use of chimeric antigen receptor- T (CAR-T) cells which are autologous or allogeneic T cells modified to recognize a tumor antigen. CAR-T recognize tumor cells through their extracellular domain, while their intracellular domain activates T cell. Clinical trials using CAR-T cells in hematological cancers have shown promising results (Miliotou and Papadopoulou, 2018). However, solid tumors fail to respond

to infusions of CAR-T cells. Several studies are being made to overcome CAR-T efficiency obstacles and to better stratify patients through companion tests (Ma et al., 2019). The GBM tumor antigens used as targets in CAR-T cells are IL-13Ra2, EGFRvIII, and HER2. Several clinical trials are studying the range of different administration ways. Encouraging results concern safety and penetrance of CAR-T cells were achieved, although effect on tumor growth and recurrence are less convincing (McGranahan et al., 2019).

*Intra-heterogeneity is usually associated with therapy failure. Thus, it would be important to perform tumor molecular analysis in distinct biopsies from different parts of the tumor. However, not only genetic profile can affect tumor biology and therapy response. In this thesis we will evaluate how membrane cell surface receptor trafficking can affect GBM cell evasion and response to targeted-therapies.*

## 2. Epidermal growth factor receptor

Forty years ago, Cohen identified a 170 kDa protein able to bind EGF which possess a kinase activity, called EGFR (Cohen et al., 1980). EGFR overexpression contribution to cancer progression was first described few years later (Thompson and Gill, 1985). Since then, large amount of data established that EGFR signaling network promotes cancer cell survival, growth and invasion and is therefore critical for tumor progression (Jones and Rappoport, 2014; Normanno et al., 2006).

### 2.1 Generality on EGFR

EGFR belongs to the *HER* gene family, which contains four genes encoding transmembrane receptors: EGFR (*HER1*), ERBB2 (*HER2*), ERBB3 (*HER3*) and ERBB4 (*HER4*) (Figure 3) (Olayioye et al., 2000). EGFR is a 170 kDa glycoprotein, with 1186 amino acids and is composed by three main domains: an extracellular ligand-binding domain (ectodomain), a hydrophobic transmembrane domain and a cytoplasmic tail bearing a tyrosine kinase domain (Roskoski, 2014; Wieduwilt and Moasser, 2008).

The ectodomain contains four subdomains: two leucine-rich subdomains and two cysteine-rich subdomains. The leucine domains directly bind to the various ligands (domains I and III), while the cysteine domains (domains II and IV) are involved in interaction and homo- and hetero-dimerization with other receptors. The leucine domain is different among all family members, giving them ligand specificity (Berasain and Avila, 2014; Wieduwilt and Moasser, 2008).

The cytoplasmic domain contains a highly conserved bi-lobed tyrosine kinase (TK). HER3 lacks TK activity, and it must form heterodimers to activate signaling pathways. Between the two lobes exists an ATP binding site (Figure 4). The activation of the receptor by ligand binding creates an extended conformation followed by receptor dimerization. Interaction between the N-lobe of one domain with the C-lobe of another domain transphosphorylates the receptor on tyrosine residues and creates many phosphorylated docking sites (Harari, 2004; Roskoski, 2014; Wieduwilt and Moasser, 2008) .

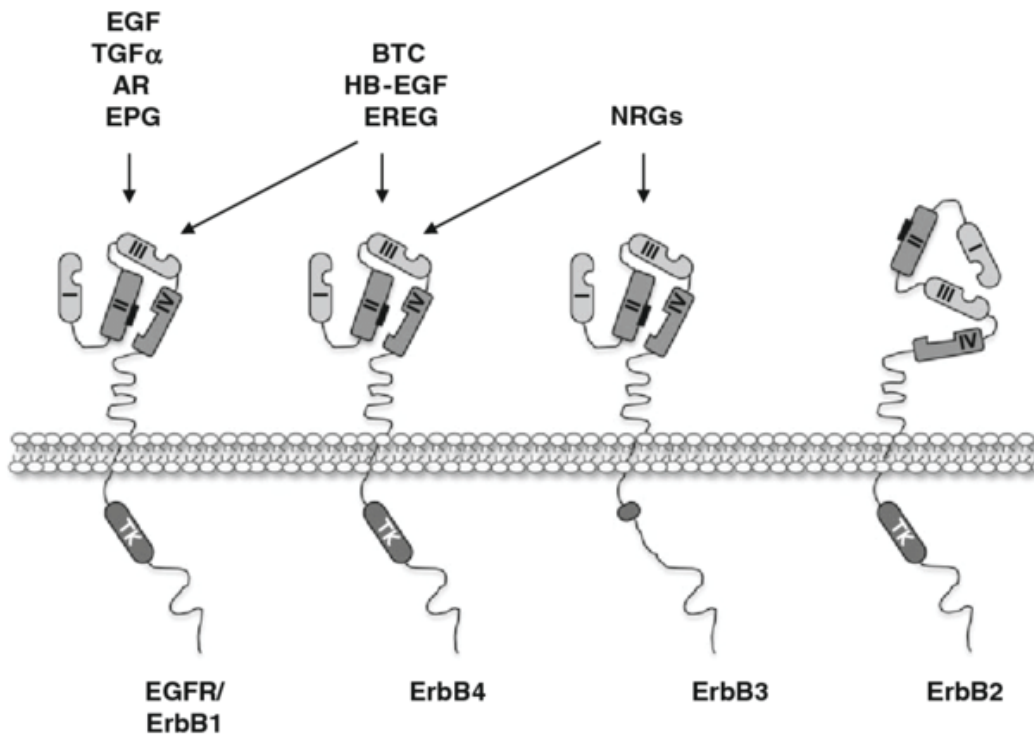


**Figure 3: HER family.** A family of 4 receptors tyrosine-kinase. HER1, HER2 and HER4 present an intracellular tyrosine kinase domain, while HER3 lacks this domain. Extracellular domains I and III play a part in ligand binding, while domains II and IV participate in homo- and hetero-dimerization upon ligand-binding. Adapted from (Berasain and Avila, 2014).

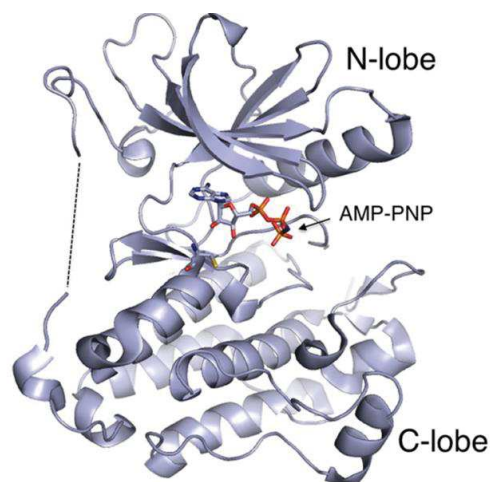


**Figure 4: ATP binding site of tyrosine kinase domain.** ATP binding site was evaluated using AMP-PNP, a non-hydrolysable analogue of ATP, and was found to be located between N- and C- lobes of TK domain. Adapted from (Heppner et al., 2016)

The EGFR known ligands are EGF, TGFA/TGF- $\alpha$ , amphiregulin, epigen/EPGN, BTC/betacellulin, epiregulin/EREG and HBEGF/heparin-binding EGF (Harari, 2004; Wieduwilt and Moasser, 2008). They are synthesized as membrane-anchored precursors. EGF needs to be proteolytically released to be active, whereas HBEGF promotes receptor activation while anchored to the membrane (Dong et al., 2005). Upon ligand binding, EGFR is stabilized

in open conformation and a homo- (with EGFR) or hetero- (with other receptors of ErbB family) dimerization is occurring. Moreover, EGFR can also be activated by ligand-independent mechanisms induced by unphysiological stimuli (such as oxidative stress, UV, and irradiation), by others RTK (such as c-MET, IGFR), by G-protein coupled receptors (GPCRs) and adhesion receptors like integrins (Sheng and Liu, 2011; Siwak et al., 2010).

## 2.2 EGFR signaling

Once activated, the phosphorylated tyrosine residues in the intracellular tail act as docking sites for signaling molecules and endocytic adaptors. EGFR mostly activates Ras/Raf/MEK/MAPK, PI3K, PLC- $\gamma$  and STAT signaling cascades (Figure 5).

### 2.2.1 Ras/Raf/MEK/MAPK signaling pathway

The RAS/RAF/MAPK signaling pathway stimulates cell proliferation, migration, differentiation and vascular angiogenesis (Wieduwilt and Moasser, 2008). This pathway starts with the binding of the adaptor protein Grb2 to residues pTyr1068 and pTyr1173 (Batzer et al., 1994). Grb2 interacts with SOS, a GTP exchange factor that stimulates GTP-binding to the monomeric GTPase RAS and its subsequent activation. RAS-GTP binds to and activates the serine kinase RAF, a cascade of serine phosphorylation is then initiated, from RAF to ERK via the kinase MEK. ERK is translocated to the nucleus, activating other kinases and/or transcription factors. Alternatively, ERK pathway can be activated by the recruitment of the protein Shc to EGFR via their SH2 domains (Pelicci et al., 1992). Once phosphorylated by activated EGFR, Shc binds to Grb2 and activates the RAS/RAF/MEK/ERK pathway (Rozakis-Adcock et al., 1992).

### 2.2.2 PI3K signaling pathway

On the other hand, PI3K/Akt pathway enhances tumor cell survival and apoptosis. Human expresses 3 classes of PI3K. Within class I PI3K, mammals have 4 catalytic isoforms (p110  $\alpha$ ,  $\beta$ ,  $\gamma$ , and  $\delta$ ) and 7 regulatory subunits (p85 $\alpha$ , p85 $\beta$ , p55 $\alpha$ , p50 $\alpha$ , p55 $\gamma$ , p84, p101). p110 $\alpha$  catalytic isoform forms a dimer with a p85 regulatory subunit through binding of domain ABC to a coiled-coil region inter-SH2 domain (iSH2). p85 interacts to EGFR, either directly through SH2 domain binding to pTyr residues, or indirectly via-Gab1 interaction (Carpenter et al., 1990; Harari, 2004; Wieduwilt and Moasser, 2008). Upon activation, PI3K phosphorylates the

3'-hydroxyl group of the inositol ring of a phospholipid from the plasma membrane (phosphatidylinositol-4,5-bisphosphate (PIP<sub>2</sub>)), converting it to phosphatidylinositol (3,4,5)-trisphosphate (PIP<sub>3</sub>) (Whitman et al., 1988). PIP<sub>3</sub> recruits AKT to the plasma membrane by its PH domain. PDK1, also mobilized to the plasma membrane by PIP<sub>3</sub>, partially activates AKT by phosphorylation of Thr308 residue in the kinase domain. AKT needs Ser473 phosphorylation in the C-terminal domain to achieve full activation, by mTORC2 complex, PDK2 or integrin-linked kinase (ILK) (Knight et al., 2006; Vanhaesebroeck et al., 2012). Upon full activation, AKT dissociates from PIP<sub>3</sub> and phosphorylates several cytosolic and nuclear proteins. This signaling pathway is negatively regulated by the tumor suppressor protein PTEN, a phosphatase that dephosphorylates PIP<sub>3</sub> to form PIP<sub>2</sub>, shutting down the signal.

### 2.2.3 STAT signaling pathway

Upon binding to activated EGFR, STAT3 dimerizes and is translocated into the nucleus. STAT3 acts as a transcription factor to regulate cell proliferation, differentiation, survival and apoptosis (Jorissen et al., 2003).

### 2.2.4 PLC- $\gamma$ signaling pathway

Moreover, EGFR can also directly interact with phospholipase C-  $\gamma$  (PLC- $\gamma$ ) through pTyr992 residue. PLC- $\gamma$  activation catalyzes PIP<sub>2</sub> hydrolysis into IP<sub>3</sub> and DAG. Herein, DAG can activate PKC, a family of serine kinases involved in cell proliferation, survival, migration and adhesion. PLC- $\gamma$ /EGFR interaction leads to actin reorganization and asymmetric motile phenotype (Normanno et al., 2006).

EGFR activation is attenuated by tyrosine dephosphorylation of active receptor, through phosphatases such as density-enhanced phosphatase-1 and protein-tyrosine phosphatase 1B (PTP1B). Their catalytic activities remove the docking sites that stimulates cell signaling (Sebastian et al., 2006).



Upon EGFR activation, the receptor is internalized. EGFR endocytosis and intracellular trafficking closely regulates receptor activity and tumor progression.

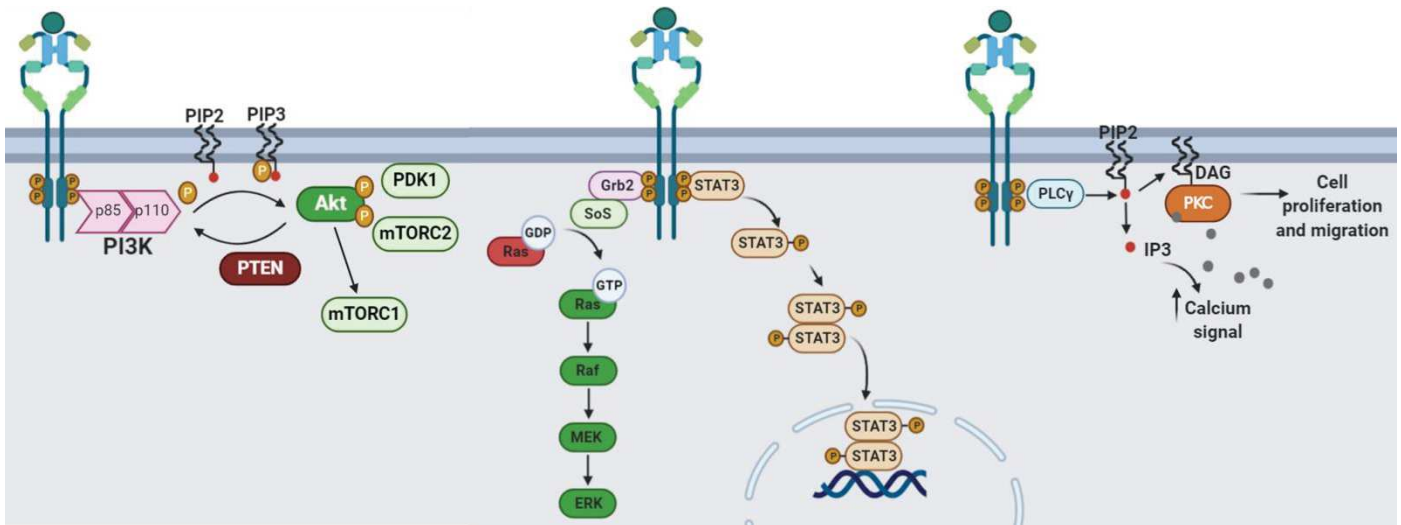


**Figure 5: EGFR signaling.** EGFR through four main signaling pathways (PI3K/AKT, MAPK, STAT3 and PLC- $\gamma$ ) promotes tumor cell proliferation, survival and invasion.

## 2.3 Endocytic pathway of EGFR

EGFR membrane localization and signaling function is tightly regulated by receptor endocytosis and intracellular trafficking. Unstimulated EGFR is internalized at a very slow rate and its rarely degraded, returning back to the plasma membrane, whereas ligand binding and kinase activation increase the endocytic constant rate (Caldieri et al., 2018). Ligand-induced endocytosis can occur through different pathways classified as clathrin-mediated endocytosis (CME) and non-clathrin dependent endocytosis (NCE), depending on receptor homo- or heterodimers formation, ligand type and concentration. For instance, EGF and TGF $\alpha$  induce CME, while HB-EGF or high EGF concentration promotes NCE. Furthermore, NCE leads to 90% of EGFR degradation while CME has a more important impact on spatial and temporal signaling control with signal amplification on clathrin-coated pits and a rate of 70% of recycled EGFR (Henriksen et al., 2013; Sigismund et al., 2008).

EGFR ubiquitination is a critical signal for the endocytosis since it determines endocytic route and receptor fate (degradation or recycling) (Caldieri et al., 2018). The E3 ligase, Cbl, directly binds to EGFR pTyr1045 residue or to Grb2 (Sorkin and Goh, 2008). After binding, Cbl ubiquitinates lysine residues in the EGFR kinase domain. Lys63 polyUb chains and multi-monoUb are the most common ubiquitin residues. Cbl remains associated to EGFR throughout the endocytic route (Caldieri et al., 2018). EGFR Protein tyrosine kinase Substrate 15 (Eps15),

a scaffolding protein, interacts with ubiquitinated motif of EGFR, allowing the binding to a major endocytic adaptor, AP-2.

AP-2 mediates the link of the receptor to the clathrin-coated pit (Parachoniak and Park, 2009; Sigismund et al., 2005; Tomas et al., 2014). Generation of an endocytic vesicle requires plasma membrane invagination and fission. AP-2 increases clathrin coat stiffness, facilitating cargo sequestration and coated vesicle formation (Lherbette et al., 2019). Dynamin, a family of GTPase proteins is involved in the fission of the vesicle and consequently in EGFR endocytosis (Sousa et al., 2012). Three isoforms of dynamin (dynamin-1, dynamin-2 and dynamin-3) have been identified in humans. Dynamin-2 (DNM2) is ubiquitously expressed while dynamin-1 is expressed only in neurons and dynamin-3 in brain, testis and lung cells. After GTP binding, dynamin assembles as helical polymers in the neck of clathrin pit. GTP hydrolysis mediates dynamin conformation change generating forces that results in fission by constriction or stretching (Ferguson and De Camilli, 2012; Sundborger and Hinshaw, 2014).

## 2.4 EGFR trafficking

### 2.4.1 Ligand-induced EGFR trafficking

After endocytosis, independently of the entry route, EGFR reaches early endosomes and is addressed either to recycling endosomes to return back to the plasma membrane or to late endosomes for degradation through an endosomes progressive maturation (Caldieri et al., 2018; Tomas et al., 2014). The two Eps15 existing isoforms have different roles in EGFR membrane trafficking. Eps15s, which lacks the ubiquitin-interacting motifs (UIMs), promotes EGFR transfer to the endocytic recycling compartment (ERC) via Ras-associated binding 11 (Rab11) (Chi et al., 2011), while eps15b interacts with Hrs (hepatocyte growth factor-regulated tyrosine kinase substrate), a vesicular transport protein with a double zinc finger domain, and sorts EGFR to multi-vesicular bodies (MVBs) (Figure 6) (van Bergen en Henegouwen, 2009; Komada and Soriano, 1999; Roxrud et al., 2008).

The small GTPase Rab proteins family, which are regulated by a dynamic cycling between their GTP-bound (active) form to their GDP-bound (inactive) form (Jovic et al., 2010), are critical regulators of endocytosis and membrane trafficking. Rab5 and its effectors, like early-endosome antigen 1 (EEA1), are involved in the (i) regulation of cargo entry from the plasma membrane to the early endosomes, (ii) generation of early endosome components such as

phosphatidylinositol-3-phosphate (PtdIns(3)P) lipid, (iii) early endosome homotypic fusion, (iv) early endosome motility on actin and microtubules, and (v) regulation of endosomal signaling pathways. Ligand-activated EGFR is sorted to Rab5-positive early endosomes, and continuously activated Rab5 induces EGFR accumulation in enlarged endosomes (Dinneen and Ceresa, 2004).

Rab11 together with Rab4 and Rab25 is involved in EGFR recycling. Rab11 promotes EGFR/ $\beta$ 1 integrin recycling and enhanced epithelial migration (Caswell et al., 2008; Palmieri et al., 2005). Rab4 promotes enlarged early endosomes that prolong EGFR activation in breast cancer cells (Tubbesing et al., 2020). Rab4 dominant negative reduces EGFR recycling and degradation, demonstrating an important role of Rab4 in early endosome sorting (McCaffrey et al., 2001). Rab25 favors EGFR recycling and its overexpression is associated with *in vitro* and *in vivo* cancer cell resistance to radiotherapy, and lung adenocarcinoma and nasopharyngeal carcinoma's patients worst prognosis (Zhang et al., 2020b). Moreover, Rab25 overexpression is associated with EGFR-tyrosine kinase inhibitor (TKI) resistance in non-small cell lung cancer (NSCLC) patients (Wang et al., 2019b). Rab7 is required to the transfer of receptors from late endosomes to lysosomes (Vanlandingham and Ceresa, 2009) and its activity correlates with EGFR degradation (Ceresa and Bahr, 2006). Rab35 is activated by EGF, leading to EGFR degradation and attenuation of EGFR signaling (Zheng et al., 2017).

Increase in H<sup>+</sup> concentration in endosomal compartment differently influence ligand/receptor interaction and dictates EGFR membrane trafficking. In acidic endosomal environment, TGF $\alpha$  dissociates from EGFR leading to its inactivation, Cbl detachment and consequent receptor deubiquitylation. This cascade of events promotes a fast EGFR recycling. On the other hand, EGF/EGFR interaction is more stable at low pH and ligand-bound receptor is mostly degraded in lysosomes (Longva et al., 2002).

Ubiquitinated EGFRs are sorted along the degradative pathway by the ESCRT (endosomal sorting complexes required for transport) complexes. ESCRT machinery is composed by 4 cytosolic protein complexes (ESCRT-0, ESCRT-I, ESCRT-II, and ESCRT-III) that are involved in membrane remodeling and, for example, in MVB biogenesis (Frankel and Audhya, 2018; Williams and Urbé, 2007). ESCRT-0 complex recognizes ubiquitinated EGFR in early endosomes and induces receptor sorting into MVB. In the MVB, a complex is formed between Hrs and STAM1/2 (signal transducing adaptor molecule 1 and 2), followed by a sequential recruitment of ESCRT-I, -II and -III to the MVB membrane. After cargo transfer between the

different ESCRT complexes, ESCRT-III drives inner MVB membrane invagination forming intraluminal vesicles (ILVs) into which ubiquitinated EGFR is found (Caldieri et al., 2018). ILVs are then released from MVBs into the lumen of the lysosome.

Spatio-temporal regulation of EGFR signalling is under the control of its endocytic trafficking. Dynamin inhibition revealed that EGFR predominantly activates MAPK or AKT signaling pathways at the plasma membrane. Receptor internalization and consequently degradation is associated with signaling shutdown. However, other reports demonstrated that receptor can also signal through its trafficking journey inside endosomal compartments. Endosomal EGFR signaling suppressed cell apoptosis induced by serum starvation (Wang et al., 2002).

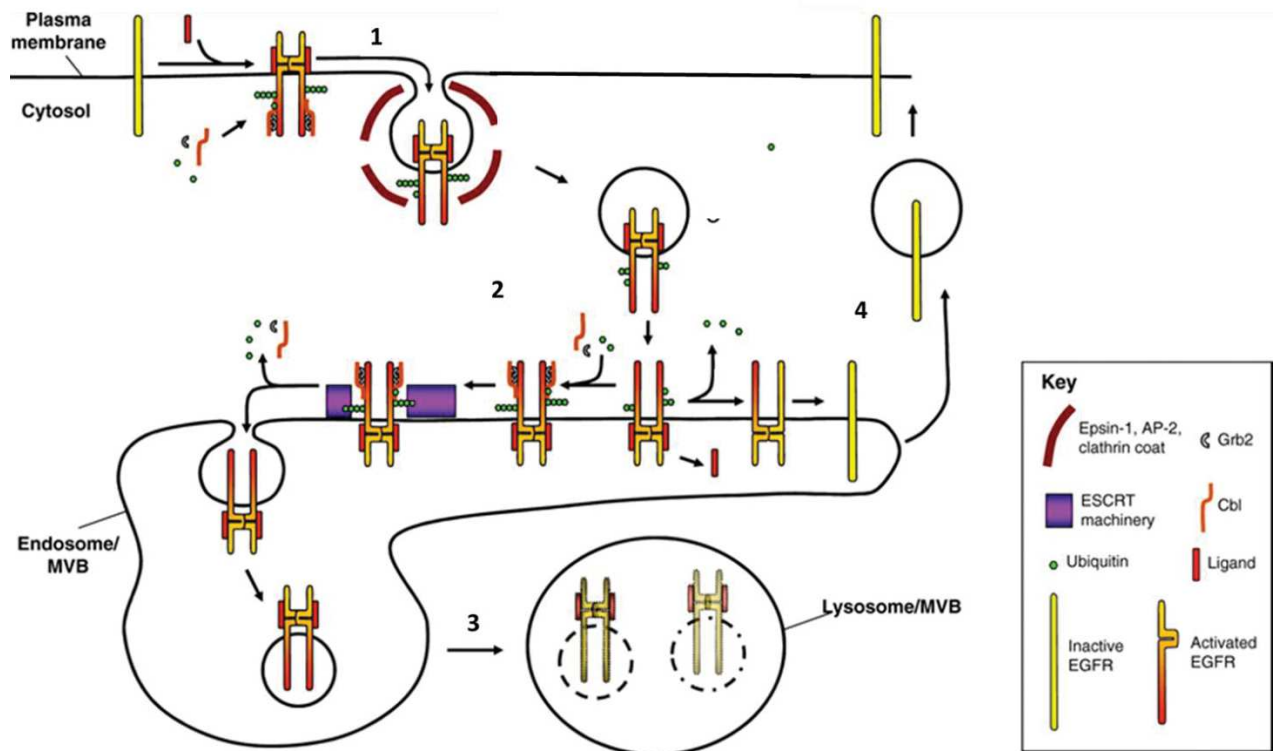


**Figure 6: EGFR membrane trafficking.** 1- Upon ligand binding, EGFR is activated, ubiquitinated by Cbl and recruited into clathrin-coated pits. 2- EGFR interacts with ESCRT machinery on early endosomes, and it is sorted to MVBs and finally to lysosomes for degradation (3). 4- When EGFR ligand dissociates, EGFR is deactivated, deubiquitinated and recycled to the plasma membrane. Adapted from (Madhus and Stang, 2009).

### 2.4.2 Stress-induced EGFR trafficking dysregulation

Studies made in HeLa cells and in head and neck cancer cells demonstrated that stress stimulus such as radiation (UVB and UVC) or chemotherapy can affect EGFR traffic and play a role in cancer progression independently of DNA damage (Tomas et al., 2017). The possible

generation of reactive oxygen species alters kinase/phosphatases equilibrium, promoting EGFR activation independently of ligand binding (Tomas et al., 2017). UV-stimulated internalization is tyrosine kinase-independent (Oksvold et al., 2002). It requires phosphorylation of EGFR serine and threonine residues (Oksvold et al., 2004) and continuous stress-activated p38-MAPK (MAPK14) activation (Zwang and Yarden, 2006). Cisplatin has also been shown to induce p38 MAPK-dependent EGFR internalization and therapy resistance in breast cancer cells (Winograd-Katz and Levitzki, 2006). Stress conditions can induce also EGFR degradation, that contrary to stress-induced endocytosis does not require p38, but it is catalyzed by caspase-3 activity (Peng et al., 2016). p38-MAPK can activate Rab5 by phosphorylating its effectors EEA1 and GDI, promoting thus EGFR internalization and endosomal fusion (Cavalli, 2001). UV and cisplatin-induced EGFR endocytosis seems to use a different route compared to EGF-induced EGFR endocytosis. Stress-induced internalized EGFR is accumulated and trapped in a lyso-bisphosphatidic acid-rich MVB, different from the MVB containing EGF-induced endocytic EGFR, after early-endosome sorting by WASH complex (nucleation-promoting factor that activates actin cytoskeleton regulator Arp2/3 (Duleh and Welch, 2010). This stress-induced EGFR intracellular retention is ubiquitin-independent but requires ESCRT complex and ALG-2-interacting Protein X (ALIX) (Tomas et al., 2015). These intraluminal vesicles do not fuse with lysosomes but are able to back-fuse with the MVB-limiting membrane and move towards the cell surface after p38 inhibition. Stress-induced EGFR is activated after internalization and endosomal retention (Tomas et al., 2015). EGFR signaling from these perinuclear compartments delayed apoptosis induced by UVC or cisplatin, but afterwards cell death happens maybe due to prolonged p38 signal (Tomas et al., 2017).

## 2.5 EGFR a therapeutic target in GBM

### 2.5.1 Oncogenic activity of EGFR in GBM

In GBM, *erbB1* is amplified in 40-60% of the cases after gene rearrangement and/or focal amplification is often associated with mutations (Frederick et al., 2000). The most common EGFR mutation (occurred in more than 50% of the cases) is the loss of exons 2-7 corresponding to a 801 base pair deletion and giving rise to EGFRvIII (Huang et al., 2009). The amino acids 6 to 273 are replaced by a glycine residue, resulting in a 145 kDa glycoprotein with constitutive, ligand-independent activation. The constitutive activation is potentiated by the reduced

interaction with E3-ligase Cbl, leading to a decreased degradation of the receptor (Normanno et al., 2006). Other mutations occurring are a N-terminal truncation (EGFRvI), deletion of exons 14 – 15 (EGFRvII), deletion of exons 25 – 27 (EGFRvIV), C-terminal truncation (EGFRvV) and C-terminal duplications and truncations.

GBM is a highly heterogeneous tumor, presenting variable EGFR expression in certain group of cells (Neftel et al., 2019; Snuderl et al., 2011; Verhaak et al., 2010). Histological studies showed a heterogeneous distribution of EGFR in GBM tissues. EGFR expression was found diffuse within the tumor mass (Hatanpaa et al., 2010), or more focalized in tumor edges (Okada et al., 2003), being associated with GBM invasion.

Several studies clearly established that activation of downstream signaling pathways by EGFR overexpression promoted GBM cell proliferation, migration and invasion, tumor growth and angiogenesis (An et al., 2018). PI3K signal is amplified by EGFR overexpression in GBM, but also by PTEN lost in 45% of GBM. Additionally, mutations in the regulatory domain of PI3K were found in GBM leading to an aberrant PI3K activation and signal (Wang et al., 2004a). Moreover, PI3K signaling pathway targeting through inhibition of mTOR provides GBM regression (Fan et al., 2017; Zhang et al., 2015b). However, clinical application of rapamycin (mTOR inhibitor) and its analogs had few relevant responses in GBM (Xu et al., 2017a). PKC/PI3K/AKT inhibitor, enzastaurin, induced glioma cell apoptosis and suppress proliferation in U87 MG cell line, and reduced tumor growth and angiogenesis in mouse xenografts (Graff et al., 2005). Enzastaurin was evaluated in a GBM phase III clinical trial as monotherapy (Wick et al., 2010). Even though enzastaurin was well tolerated and had less toxic effects compared to lomustine, it failed to demonstrate clinical benefit (Wick et al., 2010). MAPK in GBM is involved in glioma cell invasion, in neo-angiogenic processes and in neural stemness (Sangpairoj et al., 2016). Inhibition of this pathway decreases tumor growth in glioma xenografts (Campbell et al., 2014). In GBM, EGFR can phosphorylate the co-expressed EGFRvIII, promoting its nuclear translocation where it can interact with STAT3, increasing preclinical tumor aggressiveness (Fan et al., 2013).

### 2.5.2 EGFR trafficking dysregulation in GBM

Over the years, different studies have showed that EGFR membrane trafficking is often altered in tumors including GBM and contributes to disease progression (Table 1). Recent reports

indicate that endocytic pathway may be used as pertinent predictive molecular biomarkers and therapeutic tools *in vivo* and in clinics (Chew et al., 2020; Joseph et al., 2019; Ye et al., 2019).

Golgi phosphoprotein 3 (GOLPH3) was initially identified as a Golgi protein through its binding to phosphatidylinositol-4-phosphate (Bell et al., 2001; Dippold et al., 2009). It was showed to regulate membrane receptor trafficking, including EGFR, in *drosophila* (Korolchuk et al., 2007). GOLPH3 is overexpressed in GBM and other solid tumors, and is considered as “Golgi oncoprotein” (Sechi et al., 2015). Through interaction and inactivation of Rab5, overexpressed GOLPH3 dampens EGFR endocytosis, promoting tumoral progression both *in vitro* and *in vivo*. Downregulating GOLPH3 promotes EGFR internalization and degradation, and decreases downstream PI3K-AKT-mTOR signaling (Zhou et al., 2017). Moreover, GOLPH3 increases GBM sensitivity to EGFR-TKI gefitinib treatment (Wang et al., 2019c). On the other hand, compared to monotherapies, co-delivery of siRNA targeting GOLPH3 and gefitinib in brain tumors reduces cancer progression and improves mice survival (Ye et al., 2019).

NHE9 is a  $Na^+/H^+$  channel, first identified in autism where it induces hyperacidification of sorting endosomes and cellular trafficking defects (Kondapalli et al., 2013). NHE9 is highly expressed in brain tissues (Kondapalli et al., 2014). In GBM, NHE9 overexpression promotes GBM invasion by stimulating EGFR recycling and signaling through restriction of luminal acidification of endosomes and therefore bypass EGFR turnover. The higher EGFR density at the plasma membrane promoted by NHE9 makes GBM more resistant to EGFR-TKI (Kondapalli et al., 2015). NHE9 expression is downregulated by microRNA 135a (miR-135a) in U87 cells (Gomez Zubieta et al., 2017).

Mig-6 was originally identified as a mitogen-inducible gene and its depletion induced tumor formation (Zhang et al., 2007b). Mig-6 regulates EGFR trafficking and signaling by promoting EGFR endocytosis and degradation, reducing EGFR activity and consequently GBM cell proliferation (Walsh and Lazzara, 2013; Ying et al., 2010). Mig-6 binds to the SNARE protein STX8 promoting EGFR trafficking into late endosomes and further receptor degradation (Ying et al., 2010). In GBM, miR-148a expression is associated with a more aggressive cell phenotype and a patient poor prognosis. MiR148-a by targeting Mig-6 reduces EGFR transition to late endosomes and lysosomes and consequently EGFR degradation (Kim et al., 2014).

Galectins are a family of  $\beta$ -galactosidase-binding proteins usually involved in cell-cell and cell-matrix interactions. Galectin-3 plays an important role in cancer cell adhesion, growth, differentiation, apoptosis, and tumor angiogenesis (He et al., 2019). Galectin-3 impairs EGFR endocytosis and inhibits keratinocytes migration (Liu et al., 2012). Galectin-3 is overexpressed in breast, gastric, colorectal, liver and brain cancers. Its expression is associated with patient poor prognosis (He et al., 2019) and radio- and chemotherapy resistance in GBM cell lines (Wang et al., 2019a). Galectin-3 inhibition sensitizes esophageal squamous cell to gefitinib treatment, by decreasing EGFR endocytosis in resistant cells (Cui et al., 2015). Another interesting protein is sortilin, a member of the vacuolar protein sorting 10 protein family of sorting receptors (Marcusson et al., 1994). Sortilin low expression is associated with higher grade of lung cancer and a worst patient prognosis. Sortilin downregulation leads to sustained EGFR signaling and EGFR-promoted cell proliferation by decreasing EGFR internalization. Sortilin binds to EGFR at the plasma membrane even if sortilin usually is found in trans-golgi network (TGN). EGFR/sortilin interaction and consequent internalization was independent of ligand-binding and receptor activation. Sortilin expression in gefitinib resistance cells promotes a more responsive phenotype to the treatment (Al-Akhrass et al., 2017). Moreover, sortilin expression is elevated in high-grade glioma and is associated with patient poor prognosis. Increased levels are present in the mesenchymal subtype of GBM (Xiong et al., 2013). Sortilin induces GBM invasion through Glycogen synthase kinase 3  $\beta$  (GSK-3 $\beta$ )/ $\beta$ -catenin/Twist. Sortilin inhibition suppressed EMT-like mesenchymal transition, glioma cell migration and invasion (Yang et al., 2019). Moreover, membrane trafficking of EGFR WT and EGFRvIII are not the same. EGFRvIII is poorly internalized and is recycled back to the plasma membrane rather than being degraded. EGFRvIII prolonged presence in the plasma membrane sustains a signaling pathway different from the EGFR WT. This impaired degradation is due to a deficient receptor ubiquitination by Cbl as its binding site to EGFR pTyr1045 is hypo-phosphorylated (Grandal et al., 2007; Han et al., 2006; Schmidt et al., 2003).

### 2.5.3 Anti-EGFR therapies and clinical trials

Several EGFR-targeted therapies have been developed including antagonist antibodies, TKIs, anti-EGFR antibody-drug conjugated (ADC) (Figure 7), antisense gene or immunotherapies (CAR-T and vaccines based therapies) (Xu et al., 2017b). In the present thesis, only TKI and antibody based targeted therapies will be described in detail. GBM clinical trials using EGFR-inhibitors are reviewed in Annex 1.



## Tyrosine kinase inhibitors

TKIs are small synthetic molecules derived in most of the case from a quinazoline core (Figure 8). TKIs bind to intracellular tyrosine kinase domain of the receptor through a hydrogen bond. TKIs are homologous to adenosine triphosphate (ATP), competing for the ATP-binding domain of the kinases. TKIs prevent tyrosine kinase activation, EGFR autophosphorylation and downstream signaling pathway (Sun et al., 2015).

Gefitinib is a first-generation EGFR-TKI that reversibly inhibits the TK activity of isolated EGFR with an  $IC_{50}$  in the nanomolar range around 0.023  $\mu$ M (Wakeling et al., 2002). *In vivo*, gefitinib needs to be used in higher concentrations (*in vivo*/cell lines around 0.8-4  $\mu$ M) in order to block EGFR phosphorylation due to the existence of intracellular ATP (Anderson et al., 2001; Arteaga and Johnson, 2001). However, at higher concentrations gefitinib can also inhibit others RTK such as erbB2 (Arteaga and Johnson, 2001). Gefitinib is metabolized by cytochrome P450, a family of highly polymorphic genes that contribute to the inter-individual variability response to gefitinib treatment (Cersosimo, 2004; Lin and Lu, 2001). Gefitinib selectively inhibits EGFR-positive glioma cell invasion (Parker et al., 2013). In clinic, gefitinib was approved by FDA in 2015 for the treatment of metastatic NSCLC harboring EGFR-activating mutations such as EGFR exon 19 deletions or exon 21 (L858R) substitution mutations (Kazandjian et al., 2016).

Erlotinib, another first-generation TKI, was approved by FDA as a monotherapy for previously treated, locally advanced or metastatic NSCLC in 2004. In 2005, erlotinib was approved in combination with gemcitabine for a first-line treatment of locally advanced pancreatic cancer (Rocha-Lima and Raez, 2009). *In vitro*, erlotinib downregulates pro-invasive genes in GBM cells, leading to a reduced glioma cell invasion (Lal et al., 2002) and reduces cell viability of six human derived GSC (Griffero et al., 2009).

**Table 1: EGFR trafficking dysregulation in GBM**

Protein	Protein Function	Expression status in GBM	Impact on EGFR trafficking	Impact on GBM biology	References
GOLPH3	Peripheral membrane protein of Golgi	Overexpression	↓ EGFR endocytosis	↑ PI3K-AKT-mTOR signaling ↑ Tumor progression	Zhou et al., 2017
NHE9	NA <sup>+</sup> /H <sup>+</sup> channel	Overexpression	↑ EGFR recycling and signaling	↓ endosomal luminal acidification ↑ GBM invasion ↑ ERK, Cyclin D and AKT ↑ GBM TKI resistance	Kondapalli et al., 2015
Mig-6	Cytoplasmic protein	Loss	↓ EGFR endocytosis and degradation	↓ EGFR trafficking into late endosomes (normally Mig-6 binds to SNARE protein STX8) ↑ cell proliferation ↑ miR-148a downregulates Mig-6	Walsh and Lazzara, 2013 Ying et al., 2010 Kim et al., 2014
Sortilin	Membrane in the vacuolar protein sorting 10 protein	Expressed	EGFR endocytosis	↑ GBM cell proliferation ↑ GBM p-EGFR ↑ GBM invasion	Al-Akhrass et al., 2017 Yang et al., 2019

The second-generation of TKI, afatinib, dacomitinib and lapatinib, are characterized by their irreversible binding to EGFR-TK ATP pocket (Chang et al., 2016). In 2018, FDA indicated afatinib for the first-line treatment of metastatic NSCLC with no EGFR resistant mutations (T790M) but with EGFR-activating mutations (exon 19 deletion, L858R,L861Q, G719X or S768I) (Ricciuti et al., 2018). Afatinib was also approved for lung squamous cell carcinoma in 2016 (Ricciuti et al., 2018; Soria et al., 2015). Dacomitinib is a multi-HER family targeting TKI approved by FDA in 2018 for the treatment of NSCLC with EGFR activating mutations (Lavacchi et al., 2019). *In vitro*, dacomitinib inhibits GBM cell viability, self-renewal, and proliferation. *In vivo*, continuous administration is needed to reduce tumor growth rate (Zahonero et al., 2015). Lapatinib, an EGFR/ErbB2 inhibitor, was approved by FDA in 2010 in combination with capecitabine for first-line treatment of metastatic breast cancer. Moreover, lapatinib can also be combined with letrozole, an aromatase inhibitor, for the treatment of

postmenopausal women with HER2-positive breast cancer (Liao et al., 2010). Lapatinib inhibited cell proliferation of GSC cells (Clark et al., 2012).

In NSCLC, even tumors responding to gefitinib or erlotinib treatment develop resistance upon one year, mainly associated with the occurrence of T790M mutation on the kinase domain (50-60% of cases) (Majem and Remon, 2013). Third generation TKI (osimertinib and rociletinib) were developed to overcome T790M mutation (Wang et al., 2016). Since 2018, osimertinib is indicated for first-line treatment of NSCLC (Ito and Hataji, 2018). Preclinical promising results showed osimertinib efficiency on EGFRvIII positive GBM cells (Chagoya et al., 2020), making this TKI a promising therapeutic agent even though no clinical studies has started yet.

1<sup>st</sup> and 2<sup>nd</sup> generation of EGFR-TKI as monotherapy, or in co-treatment with Stupp protocol, bevacizumab or multi-kinase inhibitor sorafenib as adjuvant therapy did not provide patient beneficial in GBM clinical trials (Annex 1). Undergoing preclinical studies aim to develop new approaches to sensitize GBM cells to EGFR TKIs either by targeting reductant signaling pathways (Day et al., 2020; Goodwin et al., 2018), affecting modulators of EGFR trafficking (Ye et al., 2019) or by inducing autophagy (Liu et al., 2020).

### Antagonist antibodies

One of the best known anti-EGFR therapeutic antibody is cetuximab, a chimeric murine IgG1 antibody with high specificity for EGFR. Cetuximab is an EGFR antagonist, preventing ligand binding and receptor activation. However, therapeutic anti-tumor efficiency relies also on its antibody dependent cell cytotoxicity (ADCC) activity (Kimura et al., 2007). It was approved by FDA on February 2004 for colorectal cancer treatment with KRAS wild type. KRAS mutation status is a predictive factor for anti-EGFR therapy response (Lièvre et al., 2006). Use of cetuximab was expanded to head and neck squamous cell carcinoma (HNSCC) in 2006. Panitumumab is a fully humanized antibody against EGFR, approved by FDA on September 2006 for treatment of colorectal cancer with KRAS wild type. Both antibodies are given by intravenous injection (Zhu, 2007).

Nimotuzumab is a humanized anti-EGFR antibody which requires a bivalent binding, thus this antibody preferentially targets cells with high level of EGFR expression and have less cytotoxic effects in healthy tissues. Nimotuzumab shows anti-tumor activity associated with absence of

severe secondary toxicity (Garrido et al., 2011). Nimotuzumab is currently approved in USA and Europe as an orphan drug for glioma and pancreatic cancer (Ramakrishnan et al., 2009).

Preclinical studies using cetuximab with RT and chemotherapeutic drugs showed a beneficial additive effect on GBM cells and tumors (Eller et al., 2005). Two Phase II studies with cetuximab did not show any therapeutic benefit as monotherapy (Combs et al., 2008) or in combination with bevacizumab and irinotecan (Hasselbalch et al., 2010). Strategies to overcome cetuximab resistance are being studied through dual targeting of other erbB members (Iida et al., 2014) or other signaling pathways (Lu et al., 2019). New antibody constructions are exploring tumor heterogeneity (Jo et al., 2012) or EGFR overexpression (Iida et al., 2013) to override therapy resistance. Nimotuzumab presented a prolonged survival when co-treated with RT (Solomón et al., 2013). However, a phase III showed no benefit on patient survival (Westphal et al., 2015). More encouraging results in a recent phase II with Stupp protocol demonstrated increased survival in GBM patients with high EGFR expression levels (Du et al., 2019).

#### Antibody-drug conjugates

The inefficiency of conventional anti-EGFR therapies (TKIs and antibodies) created the need for the development of new therapeutic strategies. Antibody–drug conjugates (ADCs) combine monoclonal antibodies linked to active cytotoxic agents. ADCs have exhibited strong clinical benefits in cancer therapy by delivering selectively drugs to antigen-positive tumor cells. Actually, eight ADCs are approved by FDA (Table 2), two of them target ErbB2.

Among the 40 ADCs in cancer clinical trials, three are targeting EGFR (Polakis, 2016). Two of them (IMGN289 and AMG595) are conjugated to maytansinoid DM1 (derivative of maytansine). DM1 is a potent microtubule polymerization inhibitor that was indicated as the ideal payload for an ADC since it displays almost 100 times higher cytotoxicity than other chemotherapeutic agents (Oroudjev et al., 2010; Yang et al., 2016).

**Table 2: ADC in clinics**

<b>ADC</b>	<b>Target</b>	<b>Condition</b>
Brentuximab vedotin (Adcetris)	CD30	Hodgkin lymphoma and primary cutaneous anaplastic large cell lymphoma
Trastuzumab emtansine (Kadcyla)	HER2	HER2-positive breast cancer
Gemtuzumab ozogamicin (Mylotarg)	CD33	Acute myelogenous leukemia
Inotuzumab ozogamicin (Besponsa)	CD22	B-cell precursor acute lymphoblastic leukemia
Polatuzumab vedotin- pii (Polivy)	CD79b	Diffuse large B-cell lymphoma
Enfortumab vedotin (Padcev)	Nectin-4	Urothelial cancer
Trastuzumab deruxtecan (Enhertu)	HER2	HER2-positive breast cancer
Sacituzumab govitecan (Trodelvy)	Trop-2	Triple-negative breast cancer

Furthermore, AMG 595 and depatuxizumab mafodotin (ABT-414) are being tested in clinics for GBM treatment. AMG 595 can recognize specifically EGFRvIII positive cells, while ABT-414 recognizes both EGFR WT and EGFRvIII in highly expressing cells (Hamblett et al., 2015; Phillips et al., 2016). ABT-414 is a humanized anti-EGFR antibody linked to monomethyl auristatin F (MMAF) by a non-cleavable maleimidocaproyl linkers. Its potential was demonstrated in preclinical *in vitro* and *in vivo* studies (Phillips et al., 2016) and in phase I/II clinical trials (Narita et al., 2019). A phase II suggested a role for ABT-414 in combination with TMZ (Van Den Bent et al., 2020). Unfortunately, ABT-414 did not demonstrate a survival benefit in the Phase III INTELLANCE-1 study (NCT02573324).

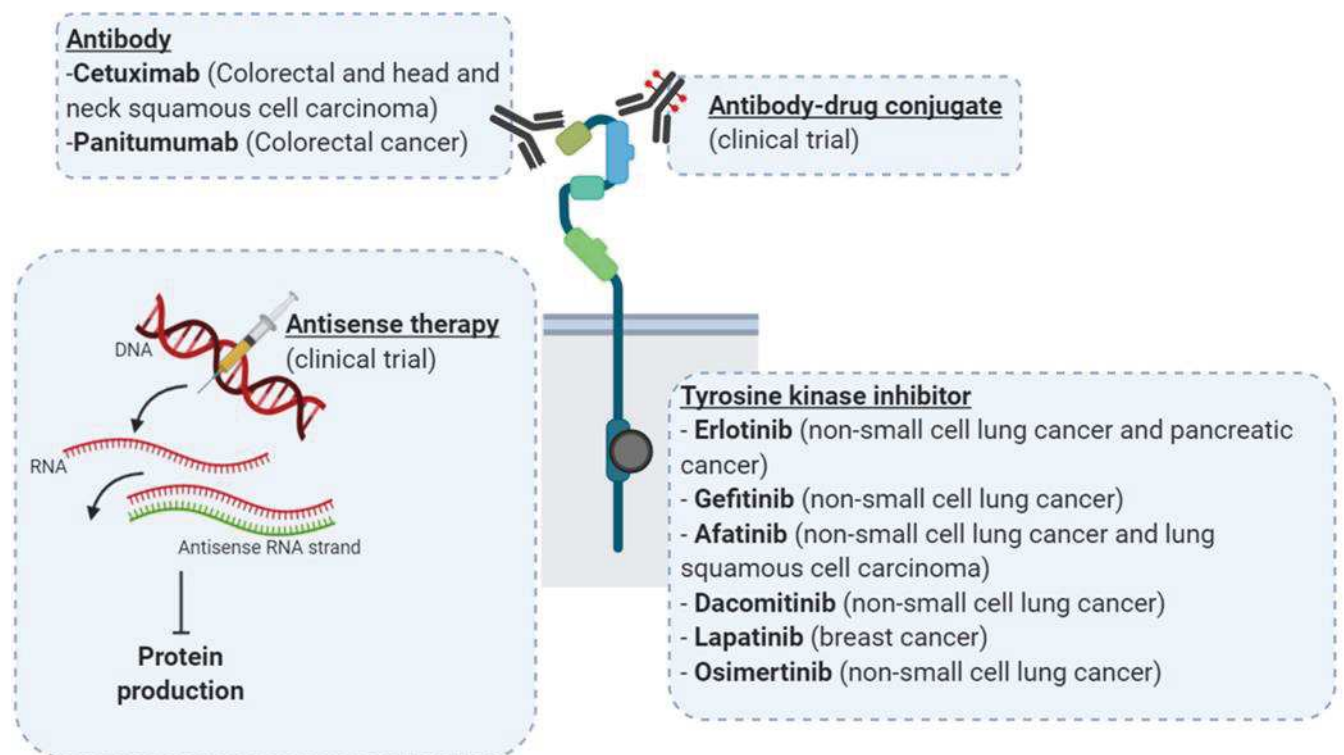
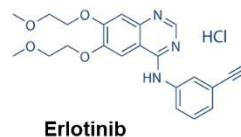
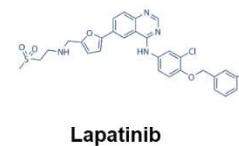
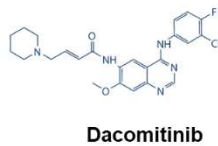
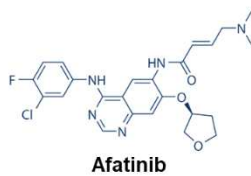


**Figure 7: EGFR-targeting therapies.** EGFR can be inhibited by impairing ligand-binding (antibody) or activation of tyrosine-kinase domain (tyrosine kinase inhibitor). Moreover, EGFR can be used as a target for therapeutic vectorization using antibody-drug conjugate. Antisense therapy that inhibits EGFR mRNA is tested in clinical trials.

First generation



Second generation



Third generation

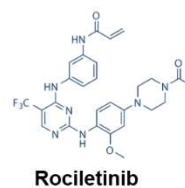


Figure 8: Structures of EGFR-TKI. Adapted from Selleckchem database.

## 3. Integrins

In normal tissues, integrins, a family of cell surface adhesion receptors, are expressed in all cell types in a tissue-dependent way (Lowell and Mayadas, 2012). Integrins and their ligands are involved in early stages of embryonic development such as fertilization, implantation and blastula formation (Tarone et al., 2000). Integrins play important roles during physiological tissue development, remodeling and homeostasis by controlling cell growth, survival, and motility and due to their role in keeping the cell stemness and determining cell fate. For example, integrin  $\alpha 5$  controls pancreatic duct lineage differentiation via actin-YAP1-Notch mechanotransduction (Mamidi et al., 2018). Often overexpressed in solid tumors, integrins contribute to cancer cell survival, proliferation, invasion, and stemness maintenance and play a major role in disease progression and resistance to therapies (Blandin et al., 2015; Cruz da Silva et al., 2019; Harburger and Calderwood, 2009).

### 3.1 The integrin family

Integrins are a family of transmembrane heterodimeric glycoproteins composed by non-covalent association of  $\alpha$  and  $\beta$  subunits. In Human, this family is composed by 24 integrins, originated by combination between 18  $\alpha$  subunits and 8  $\beta$  subunits. Each integrin can bind to one or more ligands including ECM proteins or cell surface receptors (Figure 9) (Takada et al., 2007).

Based on the evolutionary history of  $\alpha$  subunits and their ligand specificity, integrins' family is divided in four sub-families. One group is composed by integrins that recognize an arginine-glycine-aspartic acid (RGD) motif on their ligands, for example ECM proteins such as fibronectin, vitronectin or fibrinogen. Other groups are composed by the laminin- or collagen-binding integrins and finally by the leukocyte integrins. Collagen-binding and leukocyte integrins come from the same large group of integrins that differ structurally from the others integrins due to their  $\alpha$  subunit (Barczyk et al., 2010; Takada et al., 2007) (Figure 9).



## 3.2 Integrin Structure

Structurally, integrins possess 3 domains (Figure 10). The globular extracellular domain contains between 700 and 1000 amino acids and allows ligand binding. After exists a linear transmembrane domain with 20 to 30 amino acids and a cytoplasmic domain, containing 70 amino acids, with the notable exception of the  $\beta_4$  subunit that possess a cytoplasmic domain with 1000 amino acids. The cytoplasmic domains of  $\beta$  subunits are composed of one or two specific and conserved motifs NPxY and NPxxY. Through these motifs,  $\beta$  subunits interact with several intracellular proteins that contain a PTB domain (Takada et al., 2007). 3D structures of human  $\alpha_V\beta_3$  and  $\alpha_{IIb}\beta_3$  integrins were determined and used to model other integrins structures (Xiao et al., 2004; Xiong et al., 2001, 2002).

As mentioned above,  $\alpha$  subunits diverged during evolution and can be split into two structural subgroups. The extracellular domain of the  $\alpha_5$ ,  $\alpha_6$ ,  $\alpha_7$ ,  $\alpha_8$ ,  $\alpha_9$ ,  $\alpha_V$ ,  $\alpha_{IIb}$  subunits is composed by a  $\beta$ -propeller with 7 repeated sequences of 60 amino acids, and a linear region with thigh, genu and calfs 1/2 domains. Moreover, these subunits are processed by the furin convertases, the two polypeptides remaining linked by a disulfide bridge (Lissitzky et al., 2000). The subunits  $\alpha_1$ ,  $\alpha_2$ ,  $\alpha_{10}$ ,  $\alpha_{11}$ ,  $\alpha_M$ ,  $\alpha_L$ ,  $\alpha_D$ ,  $\alpha_X$ ,  $\alpha_E$  possess an  $\alpha$ -I domain between two repeated sequences of  $\beta$ -propeller domain (Figure 9) (Barczyk et al., 2010; Takada et al., 2007). The extracellular domain of the  $\beta$ -subunit is composed of 7 domains: one domain- $\beta$ -I-like (domain  $\beta_a$ ), one hybridization domain, one domain PSI (plexin, semaphoring and integrin) and four EGF-like domains (Figure 10) (Takada et al., 2007). Integrin-ligand interaction was described by comparing the crystal structures of RGD-bound and unbound integrins (Xiong et al., 2001, 2002). The ligand binding site is found on the interface between  $\alpha$ -subunit (precisely domain  $\beta$ -propeller) and  $\beta$ -subunit (precisely domain  $\beta$ -I) (Xiong et al., 2001, 2002). ECM proteins binding is bridged by divalent cations (calcium, magnesium, manganese) and the MIDAS motif (Metal Ion-dependent adhesion site). The MIDAS motif is present on  $\alpha$ -I or  $\beta$ -I domains. In  $\beta$ -I domains, the MIDAS motif is flanked by the ADMIDAS (Adjacent Metal Ion-Dependent adhesion site) and the SyMBS (synergistic metal ion binding site) motifs (Zhang and Chen, 2012).

### 3.3 Integrin signaling pathways

Studies on the platelet integrin  $\alpha\text{IIb}\beta\text{3}$  or on the leucocyte integrins, revealed that integrins are mainly expressed as resting state at the cell surface and required to be activated to fulfill their adhesive function (Durrant et al., 2017; Huang et al., 2019b). Structural and functional analysis showed that, remarkably, integrins can adopt three conformations: bent and closed conformations of low affinity, an extended and closed conformation and extended and open fully active conformations (Figure 11) (Takada et al., 2007). However, a recent electronic microscopy study showed that integrins can adopt a larger array of conformation states *in vitro*, suggesting a more complex and diversified regulation of integrin conformations *in vivo* (Miyazaki et al., 2018). Cryo-electronic microscopy data analysis of  $\alpha\text{v}\beta\text{3}$  and  $\alpha\text{v}\beta\text{8}$  integrins showed that  $\alpha\text{v}\beta\text{3}$  integrin can adopt a bent low affinity conformation, while  $\alpha\text{v}\beta\text{8}$  integrin is only found in extended conformation and shifts from a low affinity to a high affinity conformation (Cormier et al., 2018). Because they share the same  $\alpha\text{v}$ , this suggest that  $\beta$  subunit plays a major role in the integrin conformational dynamics.

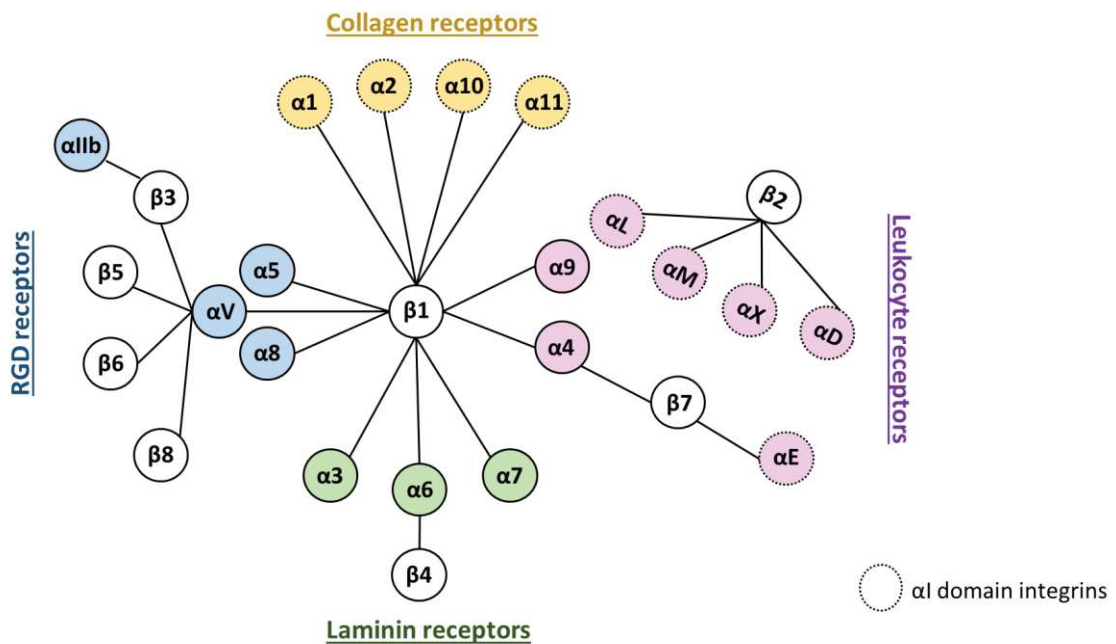


**Figure 9: Integrin family.** Integrin ligand specificity depends on  $\alpha$  subunit. Depending on ligand, integrin family is divided in four subgroups: RGD, Collagen, Laminin and Leukocyte. In Collagen and Leukocyte integrins exist heterodimers that are structurally different from the others since they have an extra domain in the  $\alpha$  subunit ( $\alpha\text{I}$  domain).

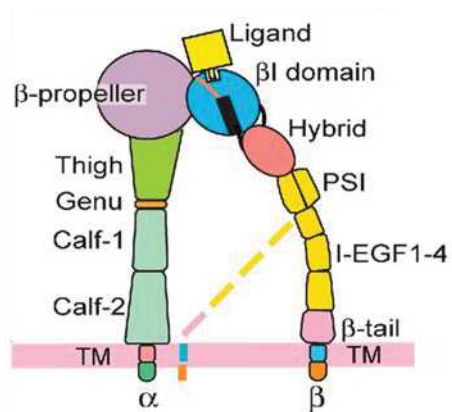


**Figure 10: Integrin structure.** Schematic of  $\alpha$  and  $\beta$  integrin domain organization. The pink loop and black bar represent the 6-7 loop and 7-helix of the I domain, respectively.

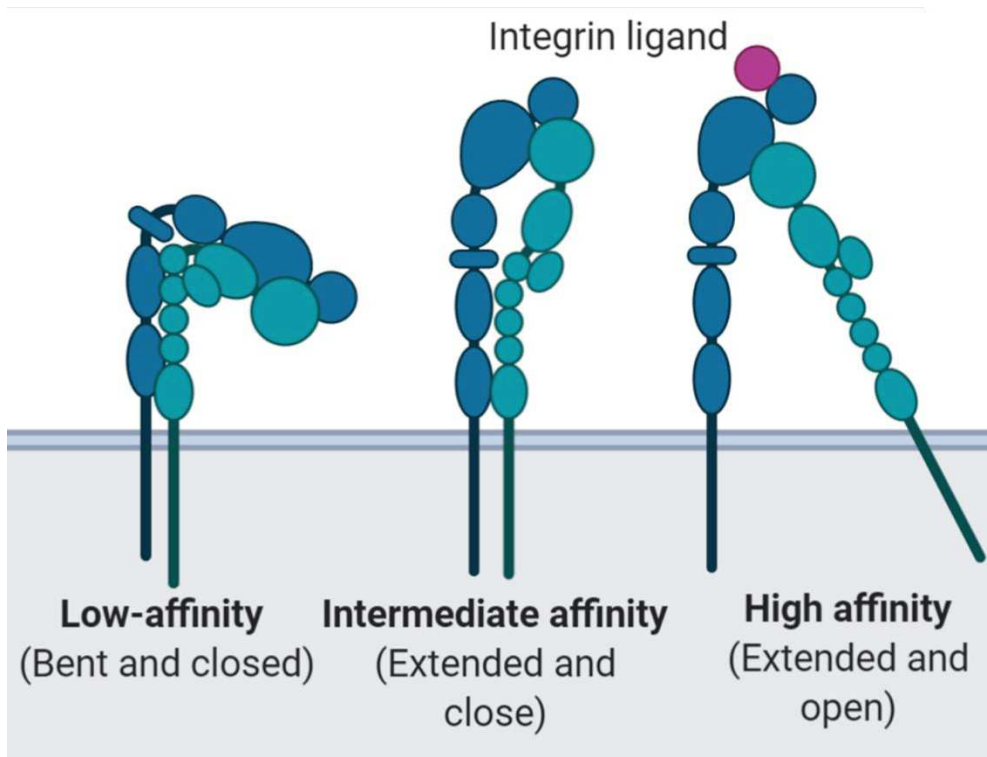


**Figure 11: Integrin conformations.** Integrin changes conformation as response to intracellular stimulus like talin binding. The different conformations have different affinities for ligands. A close and bent conformation has low binding affinity. A full-activated extended and open integrin has maximal affinity to ligand binding. The conformational change starts in extracellular  $\beta$ -subunit that achieves a complete extension. Then occurs a separation of the cytoplasmic leg domains.

The conformational changes occurs in the extracellular  $\beta$ -subunit followed by the separation of the intracellular domains of both subunits (Askari et al., 2009; Barczyk et al., 2010).

Binding of cytoplasmic proteins, like talins or kindlins, to the cytoplasmic tail of  $\beta$ -integrins is a crucial step in integrin activation. This binding breaks saline bridge between the two integrin subunits and reorganizes the extracellular domains to increase ligand affinity in an opened and extended conformation (Campbell and Humphries, 2011). Interestingly, talin regulates integrin affinity and kindlin its avidity (Sun et al., 2019). Moreover, filamins and other proteins compete with talin for the binding to  $\beta$ -integrin tails, whereby filamin inhibits integrin activity (Kiema et al., 2006). Upon activation and adhesion to ECM, integrins form clusters, and connect with numerous intracellular proteins to form a complex network called “adhesome”. Adhesome is a highly dynamic multi-protein structure involved in cell survival, polarity and migration (Winograd-Katz et al., 2014). The first description of adhesome emerged from an *in silico* study that identified 180 components interacting between each other (Zaidel-Bar and Geiger, 2010; Zaidel-Bar et al., 2007). Proteomics analysis identified hundreds of proteins including protein kinases, cytoskeleton adaptors, phosphoproteins and others (Robertson et al., 2017). Despite important and dynamic variations in composition of the integrin adhesome that depends the nature of the integrins, or of their ligand, the cell type or ECM rigidity, a consensus adhesome has emerged (Horton et al., 2015). For example, integrins need to recruit cytoplasmic kinases, such focal adhesion kinase (FAK), ILK and Src, in order to transduce biochemical signals. Upon ligand binding, FAK is recruited to the intracellular domain of  $\beta$  integrin via FERM (4.1/ezrin/radixin/moesin) domain, where FAK is autophosphorylated (Tyr397), creating a docking site for Src (Dunty et al., 2004). The complex FAK/Src activates several downstream signaling cascades like NF- $\kappa$ B, MAPK and PI3K. The recruitment of cytosolic signaling molecules can also transactivate RTK (VEGFR, FGFR, EGFR...) activity (Barczyk et al., 2010; Cruz da Silva et al., 2019; Harburger and Calderwood, 2009; Schlaepfer et al., 1997). Interestingly, studies in cancer cells revealed that integrin signaling is even more complex. For instance, inactive integrin interacts with the RTK c-MET to promote FAK signal from an autophagy-related endomembrane. This inside-in signaling promoted anchorage-independent survival, tumor growth and cancer cell dissemination to form metastasis (Barrow-McGee et al., 2016).

Moreover, integrins can promote a bidirectional mechanotransduction signal. Particularly integrin adhesome senses microenvironmental changes in rigidity and elasticity, affecting

cytoskeleton organization, cellular morphology and gene transcription. Outside-in mechanotransduction activates YAP and TAZ, two Hippo pathway transcriptional activators. In rigid substrates, integrin clusters favor actomyosin-dependent intracellular tension and activate YAP/TAZ, leading to cell elongation and polarization. While soft substratum promotes cells roundness due to reduced focal adhesion maturation, actomyosin contractility and YAP/TAZ activation (Prager-Khoutorsky et al., 2011; Totaro et al., 2018). Integrin-mediated mechanotransduction also modulates gene expression via nesprin and activation of serum response factor-mediated transcription involved in cancer metastasis (Baarlink et al., 2013; Esnault et al., 2014). Besides, ECM rigidity can also alter integrin expression and therefore focal adhesion dynamics (Yeh et al., 2017). Additionally, integrin transduces cell tension to the surrounding ECM, in an inside-out signal. For example, cancer-associated fibroblasts (CAFs) can apply mechanical forces to external ECM through actomyosin contractility to increase environment rigidity or promote ECM fibers formation (fibrillogenesis) (Goetz et al., 2011).

### 3.4 Integrins and cancer

As known from the cancer hallmarks, tumor microenvironment is as important as the mutation burden of the tumors, and stimulates cancer cell survival, proliferation, migration and immune escape (Hanahan and Weinberg, 2011). ECM has been associated with tumor aggressiveness, metastases and tumor recurrence (Paolillo and Schinelli, 2019; Poltavets et al., 2018; Stevens et al., 2017). Integrins signaling pathway activates cancer cell survival, growth, invasion and therapy resistance (Blandin et al., 2015; Cruz da Silva et al., 2019; Harburger and Calderwood, 2009).

Although integrins do not have any mutation associated with cancer, integrins are often overexpressed in solid tumors, being associated with cancer progression and patient worst prognosis. Integrin expression varies in cancer in function of the heterodimer nature, the cell type or state of disease. Table 3 summarizes variation of expression of integrins in cancer.

Integrin crosstalk with growth factor receptors is involved in tumor progression and therapy resistance (Cruz da Silva et al., 2019; Ivaska, 2011). Integrin/RTK crosstalk was described in a review found in annex 2, and therefore will not be repeated extensively in this paragraph (Cruz da Silva et al., 2019).

**Table 3: Integrin overexpression in cancer.** Adapted from (Blandin et al., 2015; Desgrosellier and Cheresch, 2010; Schaffner et al., 2013)

Tumor	Integrin
Melanoma	$\alpha 5\beta 1$ and $\alpha v\beta 3$
Prostate cancer	$\alpha v\beta 3$
Pancreas cancer	$\alpha 5\beta 1$ and $\alpha v\beta 3$
Ovarian cancer	$\alpha 5\beta 1$ , $\alpha v\beta 3$ and $\alpha 4\beta 1$
GBM	$\alpha 5\beta 1$ , $\alpha v\beta 3$ , $\alpha v\beta 5$ , $\alpha 7\beta 1$ , $\alpha v\beta 8$
Colon cancer	$\alpha 5\beta 1$ and $\alpha v\beta 6$
NSCLC	$\alpha 5\beta 1$
Breast cancer	$\alpha v\beta 3$ and $\alpha 6\beta 4$
Cervical cancer	$\alpha v\beta 3$ and $\alpha v\beta 6$

Integrin can affect RTK signaling. For example, integrin  $\alpha 5\beta 1$  participates in EGFR-PI3K and MAPK signaling (Morozevich et al., 2012). Integrin/RTK complexes can stimulate cell invasion (Morello et al., 2011; Williams and Coppolino, 2014). Inhibition of EGFR using an aptamer, a nucleic acid structure also called chemical antibody, blocked EGFR/ $\alpha v\beta 3$  integrin interaction and prevented vasculogenic mimicry events in triple negative breast cancer (Camorani et al., 2017). Vasculogenic mimicry is a blood supply, independent of angiogenesis and endothelial cells (Fernández-Cortés et al., 2019).

In addition to being expressed in cancer cells, integrins are also overexpressed by non-tumoral cells such as CAFs and endothelial cells. CAFs change ECM composition and increase ECM rigidity by mechanotransduction (Goetz et al., 2011) and also through the controlled release of lysyl oxidase (LOX) enzymes, an ECM protein crosslinking enzyme (Cox et al., 2013). LOX expression in CAF cells can be enhanced by  $\alpha v$  integrin and TGF $\beta$  signal transduction (Khan and Marshall, 2016). Moreover, upon  $\alpha 2\beta 1$  integrin binding to collagen, LOX expression is increased (Gao et al., 2016). This CAF-mediated excessive production of fibrillary ECM proteins and ECM remodeling creates tumor microenvironment fibrosis, called desmoplasia (Jang and Beningo, 2019). Moreover, CAF enhances cancer cell invasion through  $\alpha 3$  and  $\alpha 5$  integrin that promotes matrix remodeling and creation of tracks in the matrix that guide cancer cell migration (Grasset et al., 2018).

During tumor angiogenesis, endothelial cells upregulate  $\alpha v\beta 3$  and  $\alpha v\beta 5$  integrin expression to enhance endothelial cell proliferation, migration and survival (Avraamides et al., 2008;

Friedlander et al., 1995; Stupack and Cheresch, 2003). Also integrin  $\alpha 5\beta 1$  is expressed in cancer-associated endothelial cells, and contributes to angiogenesis and tumor growth through a VEGF-mediated process (Kim et al., 2000).

Exosomes are extracellular vesicles secreted by cells that allow communication between tumor primary cells and distant tissues. Tumor exosome integrins determine organotropic metastasis,  $\alpha 6\beta 1$  and  $\alpha 6\beta 4$  integrins bind to lung fibroblasts and epithelial cells, while  $\alpha v\beta 5$  integrin binds to liver Kupffer cells. On metastatic niche, integrins in the exosomes trigger the expression of ECM proteins (laminin and Src in lung fibroblasts, and fibronectin in liver fibroblasts) and pro-inflammatory S100 proteins that help cancer cell survival (Hoshino et al., 2015).

### 3.4.1 Integrin trafficking fuel cancer cell migration and invasion

Integrins constantly travel inside the cells whatever their bent or open conformation state (Arjonen et al., 2012). This constant flow allows better sensing of the microenvironment and adaption to its physical and biochemical changes (Moreno-Layseca et al., 2019). Regulation of integrin endocytosis is under the control of the  $\beta$ -subunit, via a conserved NPxY/NxxY motif in the cytoplasmic domain that interacts with clathrin-mediated endocytosis adaptors and others accessory proteins such as EPS8, Dab2 and Numb (Calderwood et al., 2003). Nevertheless, some integrin  $\alpha$ -subunits contain a Yxx $\phi$  motif that can interact with AP-2 and promote clathrin-mediated endocytosis (De Franceschi et al., 2016).

#### Integrin recycling controls invasive cell migration

During cell migration, precise control of cell adhesion and of focal adhesion turnover coordinates cell protrusions, tail retractions and cytoskeletal forces. Integrin recycling plays an important role in this regulation (Figure 12).

Rab35, the first oncogenic Rab protein identified (Wheeler et al., 2015), interplays with EGFR function and trafficking to promote cancer cell migration (Ye et al., 2018; Zheng et al., 2017). When Rab35 is inactivated,  $\alpha 5\beta 1$ -integrin is internalized and recycled by the small GTPase Arf6 (Allaire et al., 2013). Arf6-dependent  $\alpha 5\beta 1$  recycling can be inhibited by Src-mediated phosphorylation of an ECM transmembrane heparan sulfate proteoglycan syndecan-4, promoting  $\alpha v\beta 3$  recycling. This leads to a stabilization of focal adhesion and promotion of cell migration (Morgan et al., 2013).  $\alpha 5\beta 1$  integrin also interacts with Rab25 to recycled to specific invasive protrusions in 3D-ECM (Caswell et al., 2007), facilitating focal adhesion disassembly

and rear cell detachment in metastatic ovarian carcinoma cells (Dozynkiewicz et al., 2012). APPL1 is a double-edge sword, on one side it inhibits  $\alpha 5\beta 1$  integrin endocytosis, and on the other side it promotes integrin recycling to adhesion sites, keeping high levels of integrin at cell surface and thus promoting cell migration (Diggins et al., 2018). Also, APPL1 is required for rapid recycling of  $\beta 1$  integrins and EGFR, and thus increases focal adhesion turnover and cell migration (Lakoduk et al., 2019). Rabgap1 facilitates active  $\beta 1$  integrin recycling by attenuating Rab11 activity and promoting breast cancer migration (Samarelli et al., 2020). On the other hand, Rab11-mediated recycling of integrin  $\beta 1$  can be stimulated by LRP-1 in thyroid cancer cells (Theret et al., 2017). Moreover, this recycling favors brain metastasis through efficient engagement of breast cancer cells with brain ECM (Howe et al., 2020). In glioma cells, the Na<sup>+</sup>/H<sup>+</sup> exchanger 5 is overexpressed and promotes  $\beta 1$  recycling and glioma cell invasion (Kurata et al., 2019).

$\beta 3$  integrin recycling is also important for cell migration. Internalization and traffic to recycling endosomes of  $\beta 3$  integrin upon binding to Rab34, enhances breast cancer cell migration and invasion (Sun et al., 2018). Evidences showed that  $\beta 3$  integrin recycling is mediated by a Rab5-effector Rabaptin-5 and Rab4, promoting 3D invasion on vitronectin-rich environments (Christoforides et al., 2012).

### Integrin endosomal signal

Endocytosed ligand-unbound integrins can be kept in an active state inside the endosomes by talin while interacting with FAK. Furthermore, they move from Rab5-early endosomes to Rab11-recycling endosomes to be recycled to the cell front for adhesion assembly and directional cell migration (Nader et al., 2016). Active  $\beta 1$  integrin leads to sustained c-MET endomembranar signalling required to anchorage-independent cell growth and *in vivo* invasion in zebrafish (Barrow-McGee et al., 2016). In endosomal compartment, Rab21 stabilizes  $\beta 1$ -integrin /FAK interaction to stimulate a signalling pathway that suppress anoikis and promotes survival of metastatic cancer cells (Alanko et al., 2015).



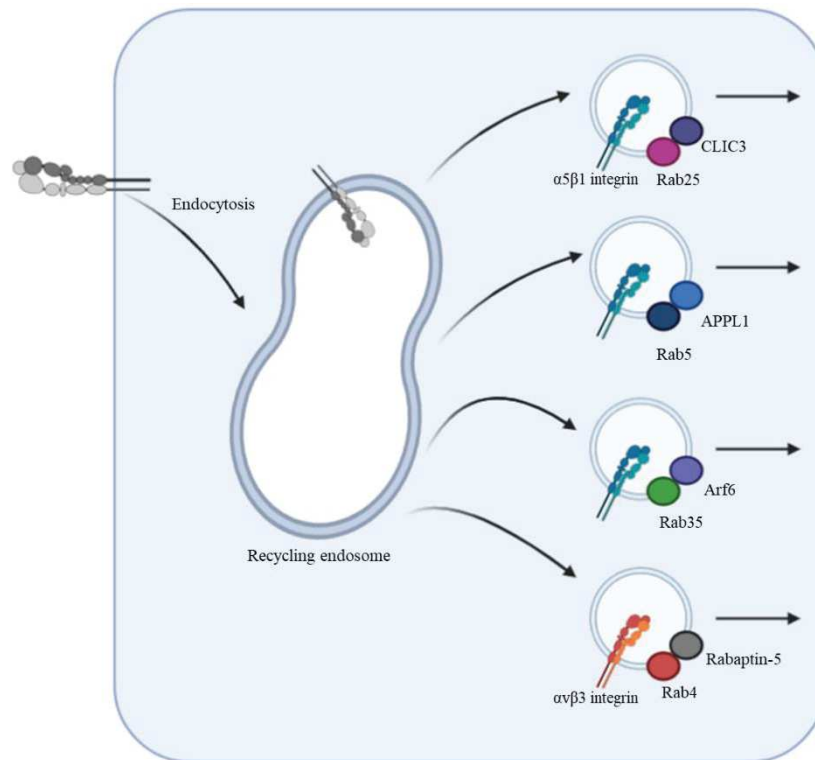


**Figure 12: Integrin trafficking in cell migration.**  $\alpha 5\beta 1$  integrins can be recycled via Rab25/CLIC3 pathway to drive cell migration in 3D environments. APPL1 decreases internalization and increases recycling of  $\alpha 5\beta 1$  integrin in migrating cells. Inhibition of Rab35 promotes Arf6-dependent  $\alpha 5\beta 1$  recycling.  $\alpha v\beta 3$  integrins can be recycled by a Rab4-Rabaptin-5 pathway to drive vitronectin-rich-3D migration.

### Integrin/RTK journey together in trafficking

Furthermore, integrin crosstalk with other membrane receptors can also control their endosomal trafficking. It has been demonstrated that blocking  $\alpha v\beta 3$  integrin with cilengitide promoted  $\alpha 5\beta 1$  integrin recycling to ruffling protrusions at the cell front of migrating cells. Recycling of  $\alpha 5\beta 1$  integrin requires integrin association with Rab-coupling protein (RCP). Moreover, integrin promotes interaction of EGFR with RCP, and therefore  $\alpha 5\beta 1$  integrin coordinates a jointed recycling of both receptors and a promotion of Akt signaling and a migratory profile in 3D-matrices (Figure 13) (Caswell et al., 2008). Also, c-MET/integrin co-recycling mediated by RCP drives cancer cell invasion (Muller et al., 2013, 2009). Morphological changes induced by c-MET and integrin activity can modulate cell migration and invasion. c-MET activation leads to a collective mesenchymal cell invasion in a 3D Matrigel. HGF-induced cell invasion, mediated by HIP-1, needs transient RhoA activation and  $\beta 1$ -integrin turnover. Sustained c-MET activity stimulates integrin-independent cell rounding mediated by the constitutive activation of RhoA (Mai et al., 2014).

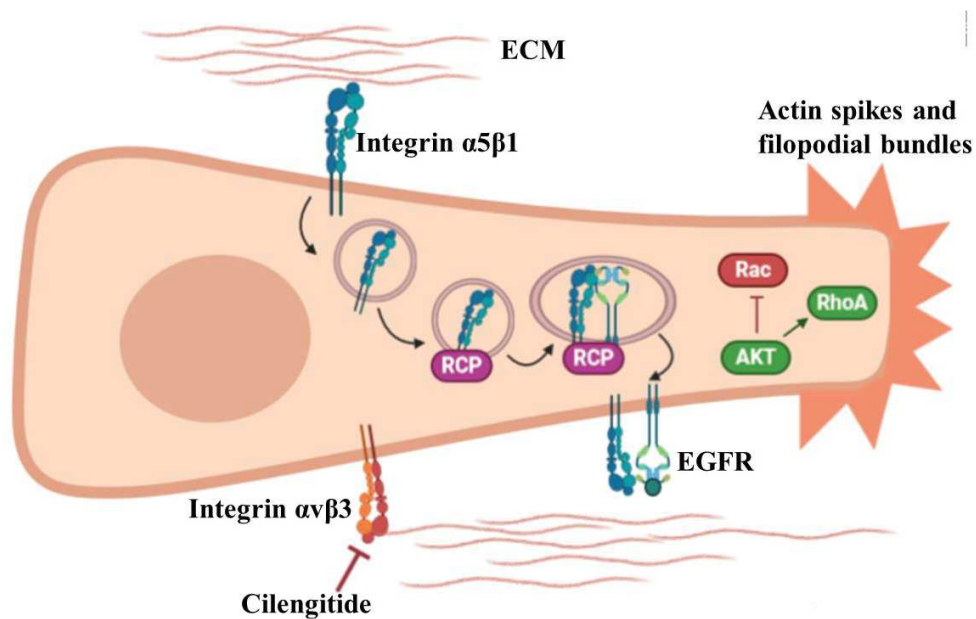


**Figure 13: Integrin/EGFR crosstalk as response to therapy.** Blocking of  $\alpha v \beta 3$  integrin with cilengitide enhances  $\alpha 5 \beta 1$  integrin and EGFR recycling to ruffling protrusions at the cell front of migrating cells. This interaction is mediated by Rab-coupling protein (RCP) and promotes Akt signaling and cell migration in 3D-matrices through formation of actin spikes and filopodial bundles. Adapted from (Caswell et al., 2008a).

### 3.4.2 Role of integrins in resistance to anti-tumor therapies

Numerous studies described the role of integrin in chemo- and radiotherapy. This resistance can be mediated by integrin expression and signaling, and also integrin crosstalk with RTK.

For example,  $\beta 1$  integrin promotes paclitaxel resistance in breast cancer by inhibiting drug-induced apoptosis (Aoudjit and Vuori, 2001). Integrin interacts with CXCR4 chemokine receptor enhancing small cell lung cancer cells adhesion to matrix and stromal cells. Thus, stromal cells protected cancer cells from chemotherapy-induced apoptosis (Hartmann et al., 2005). In GBM,  $\alpha 5 \beta 1$  integrin prevents p53 activation leading to TMZ resistance (Janouskova et al., 2012; Renner et al., 2016a). EGFR/ $\beta 1$  integrin complex is involved in radiotherapy response, since its formation is considered as a prognostic factor in glioma (Petrás et al., 2013) and inhibition of complex sensitizes cancer cells to radiotherapy (Eke et al., 2013, 2015). However, simultaneous inhibition of  $\beta 1$  integrin and EGFR in HNSCC spheroids (Zscheppang et al., 2016) and colon carcinoma (Poschau et al., 2015) did not improve radiotherapy efficacy. For instance, integrin  $\beta 8$  promotes GSC differentiation and radio-resistance (Malric et al., 2019). Combined radiotherapy and integrin  $\alpha v$  blockage in nasopharyngeal carcinoma xenografts reduced tumor size (Ou et al., 2012).

Moreover, numerous reports describe that functional synergy between integrins and RTK triggers resistance to targeted therapies (Cruz da Silva et al., 2019; Ivaska, 2011). These results being described in detail in the revue added in annex 2 of the thesis (Cruz da Silva et al., 2019), are briefly summarized herein.  $\beta 1$  integrin plays a role in endothelial cell migration and survival, in angiogenesis, and in anti-angiogenic therapy resistance (Jahangiri et al., 2014). Micro-array analysis in bevacizumab-resistant GBM showed  $\alpha 5$  integrin and fibronectin overexpression (DeLay et al., 2012). Interestingly,  $\beta 1$  integrin and c-MET crosstalk represents an anti-angiogenic therapy resistance mechanism (Jahangiri et al., 2017; Mitra et al., 2011). Ligand-activated VEGFR-2 binds to both  $\alpha 5\beta 1$  integrin and c-MET, blocking  $\beta 1$  integrin/c-MET complex formation. When cells are treated with bevacizumab, VEGF binding to VEGFR-2 decreases, and thus  $\beta 1$  integrin/c-MET complex is promoted. This complex activates the AKT signaling pathway and thus resistance to anti-angiogenic therapies (Jahangiri et al., 2017). EGFR-TKI resistance in NSCLC cells has been correlated with  $\beta 1$  integrin expression (Deng et al., 2016; Ju et al., 2010; Kanda et al., 2013). Moreover,  $\beta 1$  integrin inhibition sensitizes NSCLC to TKIs *in vitro* and *in vivo* (Deng et al., 2016; Kanda et al., 2013; Morello et al., 2011). In pancreatic ductal adenocarcinoma cells,  $\beta 1$  integrin overexpression promotes the FAK/Src/Akt pathway, activating EGFR independently of ligand binding. This EGFR signaling enhances cell growth and cetuximab resistance (Kim et al., 2017).

### 3.4.3 Integrins and GBM

Several integrins ( $\alpha v\beta 3$ ,  $\alpha v\beta 5$ ,  $\alpha 6\beta 4$ ,  $\alpha 5\beta 1$ ,  $\alpha v\beta 6$ ,  $\alpha 6\beta 1$ ,  $\alpha v\beta 8$ ,  $\alpha 2$ ,  $\alpha 3$ ,  $\alpha 4$ ,  $\alpha 7$ ,  $\alpha 10$ ) are overexpressed in GBM either in cancer cells or endothelial cells and contribute to cancer progression and resistance to therapies (Blandin et al., 2015; Gingras et al., 1995; Haas et al., 2017; Malric et al., 2017; Munksgaard Thorén et al., 2019), making integrins interesting therapeutic targets (Figure 14).

#### Integrins $\alpha v\beta 3$ and $\alpha v\beta 5$

$\alpha v\beta 3$  and  $\alpha v\beta 5$  integrins bind to RGD-containing ECM proteins such as vitronectin and fibronectin. They are overexpressed in cancer cells and in cancer-associated endothelial cells compared to normal tissue (Bello et al., 2001; Gladson, 1996; Schittenhelm et al., 2013). These integrins are mainly involved in tumoral angiogenesis, their inhibition induces endothelial cells apoptosis and reduces tumoral neo-vessel formation (Brooks et al., 1994; Mahabeleshwar et al., 2008). Moreover, a GBM subtype dependent of  $\alpha v\beta 3$  integrin activates YAP/TAZ/Glut3 (high-

affinity glucose transporter) pathway that enhances cancer cell stemness (Cosset et al., 2017). Integrins  $\alpha\beta3$  and  $\alpha\beta5$  signaling promotes chemo- and radiotherapy resistance in glioma cells (Haeger et al., 2020; Mikkelsen et al., 2009; Monferran et al., 2008). Their overexpression in tumor is associated with patient poor prognostics (Bello et al., 2001; Schittenhelm et al., 2013; Schnell et al., 2008), and thus appraising their targeted therapy.

Cilengitide is a cyclic RGD pentapeptide inhibitor of  $\alpha\beta3$  and  $\alpha\beta5$  integrins (Mas-Moruno et al., 2010). In preclinical studies, it was efficient as anti-angiogenic and as anti-tumoral agent *in vitro* and *in vivo* (Brooks et al., 1994; Mikkelsen et al., 2009; Yamada et al., 2006). The first clinical trials were in pancreatic carcinoma (Friess et al., 2006) and melanoma (Kim et al., 2012), where it showed no beneficial effect. But, in a GBM phase I/II, cilengitide as concomitant and adjuvant treatment to standard treatment, showed promising results (Stupp et al., 2010) (Annex 1). Afterwards, in newly diagnosed GBM patients with methylated MGMT expression, a phase III clinical trial (CENTRIC) was performed in which cilengitide was used in combination with radio- and chemotherapy (Stupp et al., 2014). Next, a companion phase II trial (CORE) tested cilengitide with standard treatment in MGMT unmethylated patients (Nabors et al., 2015). Unfortunately, both studies did not show any clinical benefit. Cilengitide also failed to provide a beneficial outcome in phase II in HNSCC and NSCLC, when administrated with cetuximab and cisplatin or platinum-chemotherapy, respectively (Vansteenkiste et al., 2015; Vermorken et al., 2014). Cilengitide failure in clinical trials can be explained by its rapid plasma clearance or inadequate perfusion of the brain tumor environment or even the possibility of tumorigenic effect of low doses of cilengitide. Continuous infusion of cilengitide improves drug accumulation on site, since cilengitide has a short half-life of 3-5 hours. The pharmacokinetics of cilengitide is not yet studied in combination with GBM standard treatment (O'Donnell et al., 2012). Failure of cilengitide can also be explained by some preclinical studies. For instance, low concentrations of cilengitide have been shown to promote VEGF-mediated angiogenesis by increasing VEGFR2 recycling to the cell surface, thus promoting angiogenesis and tumor growth (Reynolds et al., 2009). In another study, cilengitide promotes the association of RCP with  $\alpha5\beta1$  integrin and EGFR, and thus drives their recycling back to the plasma membrane to cell front protrusions. At the plasma membrane, EGFR can signal and activate AKT pathway to promote tumor migration in 3D matrices (Caswell et al., 2008). Moreover, genetic approaches showed that  $\beta3$  and  $\beta5$  integrin-deficient mice are characterized by enhanced tumor angiogenesis (Reynolds et al., 2002).

It is hoped that stratification of patients could improve therapies based on  $\alpha v\beta 3$  inhibition. A retrospective study analysed  $\alpha v\beta 3/ \alpha v\beta 5$  expression of patients that participated in CORE and CENTRIC clinical trials.  $\alpha v\beta 3$  integrin expression may predict integrin inhibition benefit in patients without MGMT promoter methylation (Weller et al., 2016). Another study identified a subset of GBM more sensitive to cilengitide treatment in mice, characterized by a high level of expression of  $\alpha v\beta 3$  integrin and glucose transporter (Glut3) (Cosset et al., 2017).

### Integrin $\alpha 5\beta 1$

The fibronectin receptor,  $\alpha 5\beta 1$  integrin, presents higher expression levels in GBM tissues compared to adjacent normal tissue (Gingras et al., 1995; Janouskova et al., 2012). This overexpression is associated with worse patient prognosis (Janouskova et al., 2012; Lathia et al., 2014). Preclinical data demonstrated the role of  $\alpha 5\beta 1$  integrin in glioma cell growth and survival (Färber et al., 2008; Kesanakurti et al., 2013), cell motility (Blandin et al., 2016; Mallawaarachy et al., 2015; Patil et al., 2015) and therapy resistance (Janouskova et al., 2012; Martinkova et al., 2010; Renner et al., 2016a). Integrin  $\alpha 5\beta 1$  inhibition reduced *in vitro* cell proliferation and *in vivo* tumor size (Färber et al., 2008). Integrin  $\alpha 5\beta 1$  activated  $\beta$ -catenin pathway to stimulate GBM cell migration (Ray et al., 2014; Renner et al., 2016b). siRNA depletion of  $\alpha 5$  integrin reduced invadopodia formation in U87 cells (Mallawaarachy et al., 2015). Inhibition of  $\alpha 5\beta 1$  integrin promoted p53 activation and sensitized GBM cells to TMZ (Janouskova et al., 2012; Renner et al., 2016a). Also, integrin  $\alpha 5\beta 1$  inhibited TMZ-induced apoptosis and stimulated p53-dependent cell senescence, inducing chemotherapy resistance (Martinkova et al., 2010). Inhibition of  $\beta 1$  integrin/EGFR complexes sensitized cancer cells to RT (Eke et al., 2013, 2015). Moreover,  $\alpha 5\beta 1$  integrin is involved in tumor angiogenesis (Dudvarski Stanković et al., 2018; Li et al., 2012; Lugano et al., 2018).  $\alpha 5\beta 1$  integrin promotes brain endothelial cells proliferation in response to cerebral hypoxia, demonstrating the interest of targeting integrin as an anti-angiogenic therapy (Li et al., 2012). Integrin  $\alpha 5\beta 1$  expression on endothelial cells stimulated GBM vascularization in *in vivo* models.  $\beta 1$  integrin-mediated fibronectin fibrillogenesis in endothelial cells promotes GBM tumor vascularization *in vivo* (Li et al., 2012).

Several integrin  $\alpha 5\beta 1$  inhibitors have been tested in other solid tumor or angiogenic situations, however in GBM where integrin is a therapeutic target of interest, just phase I and II clinical studies were realized. Further studies are needed to better evaluate the efficiency of these targeted-therapies.

Volociximab is a chimeric antibody inhibiting  $\alpha 5\beta 1$  integrin, used as anti-angiogenic for solid tumors and wet age-related macular degenerative disease (Raab-Westphal et al., 2017). In ovarian cancer, a phase II with volociximab as monotherapy in platinum-resistant patients showed to be inefficient but tolerated (Bell-McGuinn et al., 2011). The tolerance and pharmacokinetics were further evaluated in a phase I in NSCLC. Volociximab was combined with carboplatin and paclitaxel and revealed a well-tolerance and a preliminary efficiency (Besse et al., 2013). Despite the important role of  $\alpha 5\beta 1$  integrin in neo-angiogenesis, volociximab remains inefficient. Other antibodies targeting  $\beta 1$  integrin were used in clinical trials. Antibody OS2966 received orphan drug designation by FDA for the treatment of GBM in 2014 and for ovarian cancer in 2015, after presenting active action in preclinical studies. In 2019, OS2966 was used as investigational new drug in a phase I GBM clinical trial (OncoSynergy, 2019). The monoclonal antibody P5 was in phase III clinical trial for lung adenocarcinoma (Kim et al., 2016). RGD-like inhibitors FR248 and K34c are selective to  $\alpha 5\beta 1$  integrin at the nanomolar range. Their affinity was determined by inhibition tests on cell adhesion on purified integrins (Heckmann et al., 2008; Rechenmacher et al., 2013). These inhibitors reduced glioma cell migration (Ray et al., 2014) and sensitized cells to TMZ in p53-WT GBM cells (Martinkova et al., 2010). Different integrin targeted strategies have developed the use of RGD integrins as vectors for drug or immunotherapy delivery. An internalized-RGD, specific to integrin and neuropilin 1, allowed the uptake of irinotecan-loaded-nanoparticles on pancreatic adenocarcinoma to reduce metastasis (Liu et al., 2017). Another molecule JSM-6427 induces cell death of endothelial cells and, thus, inhibits ocular neo-angiogenesis (Maier et al., 2007). A phase I clinical trial was completed in macular degeneration treatment and did not show any signs of toxicity (NCT00536016). The non-RGD peptide ATN-161 mimics the synergy domain of fibronectin. A phase I clinical trial in resistant solid tumors showed a disease-stabilization upon ATN-161 treatment (Cianfrocca et al., 2006). It was also used with carboplatin in a phase I/II in GBM (NCT00352313). A RGD peptide was fused to a Fc-domain of an immunoglobulin to induce ADCC, and administered with an anti-PD-1 antibody. Overall the treatment was well-tolerated and showed antitumor efficacy in murine models of cancer (Kwan et al., 2017).

#### Other potential integrins as therapeutic target in GBM

An RGD-binding  $\beta 8$  integrin is overexpressed in GBM cells, promoting their invasion through Rho activation by sequestering a Rho GTPase (Reyes et al., 2013). Moreover,  $\alpha v\beta 8$  integrin is

expressed in GSC and stimulates TGF $\beta$ 1 signaling to maintain stem perivascular niche (Guerrero et al., 2017; Malric et al., 2019). Combination of radiotherapy and  $\beta$ 8 integrin blockade significantly induced GSC apoptosis (Malric et al., 2019).

Collagen is overexpressed in GBM parenchyma and is associated with tumor angiogenesis and progression (Mammoto et al., 2013; Pointer et al., 2017). A collagen-receptor, integrin  $\alpha$ 10 $\beta$ 1, was found overexpressed in GBM tissues and cells. Integrin  $\alpha$ 10 expression enhanced GBM cell proliferation and migration (Munksgaard Thorén et al., 2019).

Laminins are present in blood vessel basement membranes and are overexpressed in GBM (Ljubimova et al., 2006). Laminin interaction with integrin  $\alpha$ 7 $\beta$ 1 promotes GBM progression. Integrin  $\alpha$ 7-laminin interaction promotes GSC growth and invasion. Integrin  $\alpha$ 7 blockage reduced xenografts tumors size and invasion (Haas et al., 2017). Also laminin interaction with integrin  $\alpha$ 6 activates STAT3 signaling leading to methylation of important genes for GSC, increasing their aggressivity and therapy resistance (Herrmann et al., 2020).

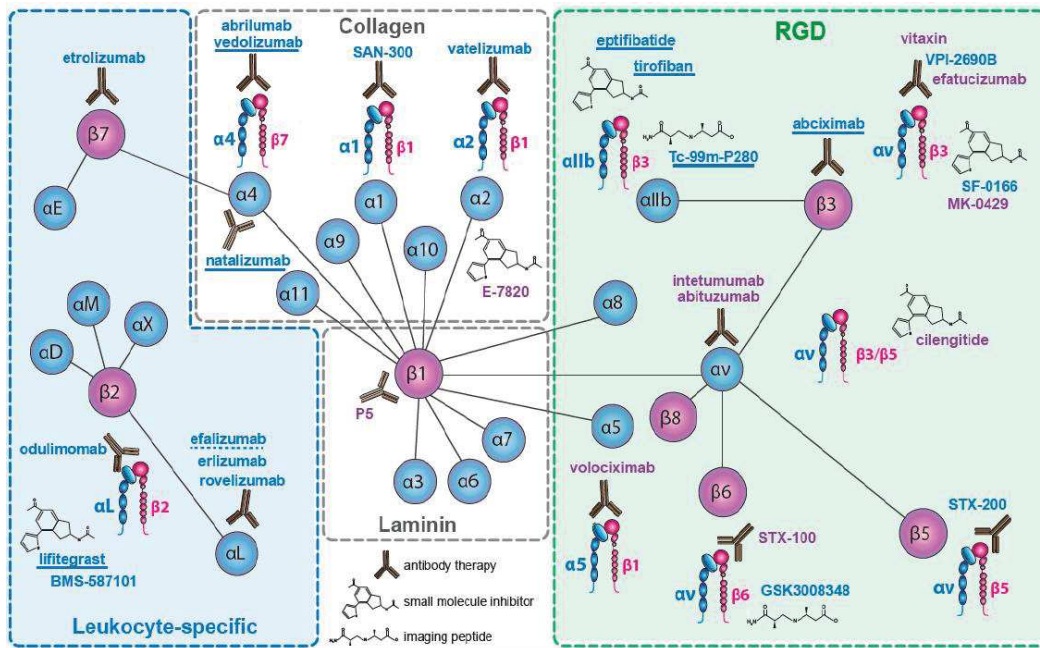


**Figure 14 : Strategies targeting integrins in clinical trials.** Out of the 24 integrins, nineteen have been considered as pertinent therapeutic targets as anti-inflammatory or anti-aggregating molecules and cancer treatment. Four integrin antagonists have proven their effectiveness and are used in human clinics for the treatment of chronic inflammation or coronary syndrome. Unfortunately, until now no clinical trial showed any benefit in targeting integrins for cancer treatment (drugs in violet). Underlined drugs are commercialized and broken underlined were withdrawn. Adapted from (Raab-Westphal et al., 2017)

## 4. Aptamers as alternative to antibodies

Aptamers are oligonucleotides of single stranded DNA (ssDNA) or RNA. Aptamers recognize various targets (proteins, small molecules, nucleic acids, sugars, lipids, virus, cells, biopolymers,...) with high affinity and selectivity. The name aptamer derives from the latin *aptus* which means to fit (Nimjee et al., 2017). Moreover, the ability of the aptamer to bind selectively to its target is based on the aptamer three dimensional structure which allows it to bind to the target via non-covalent interactions (Zhu and Chen, 2018).

### 4.1 Conformation

The aptamer three-dimensional conformation is dependent on the sequence of the nucleotides, therefore aptamers can acquire a vast amount of different conformations. RNA aptamers can fold into more varied three-dimensional conformations compared to ssDNA aptamers. This advantage is due to their 2'-hydroxyl (2'-OH) group on ribose and the non-Watson-Crick base pairing (Zhu et al., 2015b). The G-quadruplex conformation is a guanine enriched structure of RNA or ssDNA in which the guanines associate between themselves via non-covalent interactions. This structure allows the folding in a stable conformation with the maximum interactions possible between nucleotides.

### 4.2 Advantages of aptamers

Aptamers are analogous to antibodies in their vast target recognition and possible applications and therefore aptamers are also called chemical antibodies. Aptamers possess numerous advantages over antibodies (Table 4), like smaller size, temperature stability, self-refolding, lack of immunogenicity and toxicity, chemical synthesis with high batch fidelity (Zhou and Rossi, 2017; Zhu and Chen, 2018). Even with all differences, aptamers and antibodies are more complementary than enemies.

Aptamers seem to have a larger panel of potential targets than antibodies. Antibodies need animal immune reactions for their production and only substances that provoke an immune response can be used as antibody targets. Research are being made to replace whole antibodies for antibody, in order to substitute animals or cells use. Aptamers can be screened for a wide array of molecular targets, including toxins or poorly immunogenic targets (Zhou and Rossi, 2017).



Aptamers are more stable than antibodies and have an unlimited shelf-life. Hard conditions of pH, temperature and salt concentration, for example, cause antibody irreversible denaturation. This might limit antibody storage time and conditions. Contrary to antibodies, aptamers are thermally stable and therefore their denaturation is reversible. After heating, aptamers are able to refold when cooled down to room temperature, making aptamers adapted for long term storage. Moreover, as aptamers are selected *in vitro*, some of these non-physiological conditions can be implemented during selection. This advantage can be used to identify aptamers against targets only available in these harsh conditions (Zhou and Rossi, 2017).

Aptamers normally are composed of 15 to 50 nucleotides and they have a molecular weight ranging from 5 to 15 kDa. Aptamers size is between antibodies (150 kDa) and small peptides (1-5 kDa). This small size of aptamers versus antibodies, improved the permeability of aptamers in tissues (Lakhin et al., 2013).

Advances in chemical modifications and bioconjugation allow easier aptamer's modification. Increasing biostability of aptamers, conjugation to fluorogenic or radioisotope reporters or with therapeutic agents and keeping reproducibility are possible. Even some steps can be automated. While antibodies are subjected to a limited panel of chemical modifications (Zhou and Rossi, 2017).

When considering molecules for therapeutic uses not only pharmacodynamics or pharmacokinetics are to be kept in mind, but also the immunogenicity of the molecule. Except if desired, therapeutic agents should not elicit any immune response. Most antibodies induce immune response due to their constant domain. This effect has been reduced with humanized antibodies but not fully eliminated (Ryman and Meibohm, 2017). Aptamers present low immunogenicity and/or toxicity reactions associated to their nature. This statement seems to be based on the sole clinical phases I and II of the aptamer Mucagen. But conjugation with poly ethylene glycol (PEG), for example, can induce a certain immunogenicity. Relatively to this problem, REG aptamer's phase III was stopped due to allergies induced by PEG (Ganson et al., 2016; Lincoff et al., 2016). For pharmaceutical companies, the time and price of molecule production have strong impacts. Aptamers appear to be more advantageous than antibodies. Since antibody production requires the use of animals or cells, their production is very expensive. The costs of aptamer production is believed to be considerable reduced compared to antibodies. The *in vivo* element in antibody production turns large-scale and homogeneity between batches more difficult. On another hand, aptamers are chemically synthesized, so

independent of any biological system, reducing the risk of bacterial or viral contamination, reducing the variation from batch to batch and having a huge bioethical advantage (Lakhin et al., 2013). Furthermore, actual technologies of automated DNA/RNA synthesis allow an easy, cost-effective and a large-scale production of any chemical modified aptamer (Jayasena, 1999; Nimjee et al., 2017; Zhou and Rossi, 2017; Zhu and Chen, 2018).

### 4.3 Disadvantages of aptamers

However, aptamers have disadvantages as well. They suffer from the action of nucleases and renal clearance, decreasing their circulating half-life. Mainly RNA aptamers are highly susceptible to nucleases activity. They can be eliminated from the circulation within seconds (Zhou and Rossi, 2017). To circumvent this disadvantage, aptamers can be chemical modified to render them resistant to nucleases and thus increase their stability. These chemical modifications include 3' end capping strategies, phosphodiester backbone, sugar ring modifications and/or mirror image (Ni et al., 2017). The capping strategies are accomplished by inverting the nucleotide at the 3'-terminus, creating an oligonucleotide sequence with two 5'-termini and no 3' since 3'-exonuclease activity is considerably higher than the 5' one (Keefe et al., 2010). The nucleophilic attack occurs in the 2'-OH group. So, sugar ring modifications like the replacement of 2'-OH for 2'-fluoro or amino reduce aptamer susceptibility to nucleases (Ruckman et al., 1998). Mirror image technique is based on spiegelmers (Vater and Klussmann, 2015). RNA-spiegelmers are RNA-aptamers composed by L-ribose units linked by phosphodiester bonds. L-ribose units are enantiomers (non-superimposable mirror images) of WT-nucleic acid sugars D-ribose units. L-ribose is more resistant to nucleases and therefore more stable *in vivo*. The SELEX process is performed on WT-RNA with enantiomer of the target. After aptamer identification, the sequences which bind to the target are synthesized with L-riboses. This technique only covers small proteins domains or peptides as targets since enantiomeric targets need to be synthetically prepared (Keefe et al., 2010; Ni et al., 2017).

However, due to their "small" size, aptamers are easily submitted to renal clearance. Molecular mass cut-off for the renal glomerulus is 30-50 kDa. Strategies such as the addition of bulky groups, like PEG, poly (D,L-lactic-co-glycolic acid) (PLGA) or cholesterol groups, on 5' of aptamers, increase aptamer size and render them resistant to renal filtration (Healy et al., 2004; Keefe et al., 2010).

The chemical diversity of a four nucleotides based DNA/RNA library may be limited compared to a 20 amino acids based library (Zhou and Rossi, 2017). But we should have in mind that the specificity of aptamers is not due to their sequence but to their tertiary structure (Tan and Fang, 2015). One aptamer can adopt different conformations and therefore detect different targets (Ruscito and DeRosa, 2016). Moreover, new synthetic nucleotides called Xeno nucleic acid (XNA) are created. For example, the addition of modified nucleotide triphosphate increases protein binding through direct hydrophobic contacts between aptamer and a proteic target (Hasegawa et al., 2016). Besides increasing aptamers diversity, XNA also increased their resistance to nucleases (Rangel et al., 2018).

**Table 4: Aptamer versus monoclonal antibody**

	<b>Aptamer</b>	<b>Monoclonal antibody</b>
Size	>5 000 Da	150 000 Da
Target potential	Any small molecule, biopolymer or cell	Immunogenic targets
Tissue penetration	High	Low
Stability (pH, temperature)	High, possibility of renaturation	Low
Long-term availability	Unlimited shelf-life	Limited shelf-life
Circulating half-live	Susceptible to nucleases (limited by modified nucleotides) Eliminated by renal filtration (limited by bioconjugation)	Nuclease susceptibility absent and no elimination by renal filtration
Immunogenicity	No evidence	Significant
Production cost and scale-up	Cheaper and possible to scale-up	Expensive and low possibility to scale-up
Homogeneity batch	Uniform between batches	Activity varies between batches
Modifications	Wide variety of chemical modifications can be applied	Very limited modifications
Reversibility	Antidote can be produced	No method available

## 4.4 SELEX

Aptamers are selected through an *in vitro* interactive process called ‘selective evolution of ligands by exponential enrichment’ (SELEX) (Figure 15) (Zhou and Rossi, 2017).

SELEX was described simultaneously by 3 independent American teams. Gold team called SELEX to their process of RNA selection for T4 DNA polymerase ligands (Tuerk and Gold, 1990). An *in vitro* selection of organic colorants’ RNA was used by Ellington and Szostak (Ellington and Szostak, 1990). And, Joyce and Robertson selected the first artificial ribozyme (Robertson and Joyce, 1990).

In SELEX, a large library of around  $10^{14}$ – $10^{15}$  nucleic acid sequences (ssDNA or RNA) of 20–50 random and variable bases is put in contact with a given target. The SELEX process is composed of three steps: selection, partitioning and amplification. Upon selection, some of the nucleic acid sequences bind to the target, the others that did not bind are washed away during the partitioning step. Next, an amplification step is performed to enrich the candidates’ population. The variable nucleic acid sequences are flanked by primer-binding sequences, which allow by PCR (for ssDNA) or RT-PCR (for RNA) the amplification of the molecules. Upon PCR, double-stranded DNA molecules are separated to get the ssDNA sequences needed for DNA-SELEX, while for RNA an *in vitro* transcription is performed by a T7-RNA polymerase. It can be important to perform a negative selection to ensure binding selectivity and eliminate non-specific binding nucleic acids. The negative selection can be performed to environmental elements (filters or beads) and/or to target’s counterparts (related proteins or cells). Several rounds of selection are performed with progressively increased stringency, and under temperature and buffer conditions required, until molecules with a desired binding profile are obtained. The selected molecules are then cloned and sequenced (Mercier et al., 2017).

### 4.4.1 Protein-SELEX

Protein-SELEX is a common method where either full-length or truncated versions of proteins are used as targets. They are usually used as recombinant proteins conjugated to tags to facilitate their purification and selection on affinity columns (Mercier et al., 2017). Many proteins, in endogenous cellular-context, present post-translational modifications (phosphorylation, glycosylation, ubiquitination, methylation, myristoylation, acetylation...), different

conformations or lengths. That might be a reason why some aptamers selected by protein-SELEX failed to recognize their target in whole cells (Chauveau et al., 2007; Liu et al., 2009).

#### 4.4.2 Cell-SELEX

More complex SELEX processes have been developed to adapt to more complex targets, for example, in oncology. Identification of tumor biomarkers is needed for the performance of targeted-therapies and vectorization strategies. Cell surface targets are the 'sexiest' biomarkers for vectorization due to their easy access. Therefore, aptamers' selection against targets expressed at the surface of cells or tumor tissues have been performed using cell fragments, living cells or tumor tissues (Blank et al., 2001; Camorani et al., 2020; Fang and Tan, 2010; Mi et al., 2010). The so-called cell-SELEX, that uses whole living cells, allows the selection of functional cell surface molecules in their native conformation status, for example, with the presence of post-translational modifications or interacting with cofactors. Aptamers specific to tumor cells can also be used to identify new biomarkers of these tumors even if the aptamer target is not yet characterized as a biomarker. Another dimension of cell-SELEX is the internalized cell-SELEX, for which only aptamers that able to bind to cell-surface target and be internalized are selected (Mercier et al., 2017; Thiel et al., 2012; Wan et al., 2019). Cell-internalizing aptamers conjugated to therapeutic siRNA provided a strong RNAi response, which means that the cargo was delivered to the cytoplasm (Thiel et al., 2012). In this SELEX, the initial library was incubated with cells at 37°C to facilitate internalization. After, a stringent wash at high salt solution (0.5 M NaCl ± 0.2 N acetic wash) was performed to remove unbound and surface bound nucleic acids. The internalized nucleic acids were recovered using a trizol and then amplified (Hernandez et al., 2013). This technique allows the selection of internalized aptamers but not of aptamers that escape the endosomes and are found in the cytosol. Certain therapeutic uses of aptamer require the presence of aptamers in the cytosol. For example, aptamers conjugated to siRNAs need to escape from endosomal compartments before fusion with lysosomes, where the complex is destroyed by nucleases and acidity (Varkouhi et al., 2011). Therefore, addition of steps to cell-internalization SELEX like fractionation to separate endosome-bound and cytoplasmic nucleic acids sequences can be performed to recover more suitable aptamers (Hernandez et al., 2013). Both uptake kinetics and endosomal escape are still unknown for aptamers (Hernandez et al., 2013).

Selection can also be realized in more complex cellular environments. A selection of aptamers that are able to bind to cellular spheroids in 3D cell culture systems was described (Souza et al., 2016).

#### 4.4.3 Protein-SELEX versus cell-SELEX

Contrary to protein-SELEX, cell-SELEX does not need production and purification of targets, that can be advantageous if the target is difficult to be synthesized (Chen et al., 2016a). However, cell-SELEX is a complex process: (i) it needs the culture of stable cell lines, (ii) cell lines need often to be modified to change protein expression for positive and negative selections, (iii) cell-SELEX takes usually longer time than protein-SELEX, as it needs more rounds to improve aptamers' selectivity (Chen et al., 2016a).

#### 4.4.4 Other SELEX methodologies

Animal-SELEX can be useful in cancer or pathogen-infected mouse models. First of all, the initial nucleic acid library is injected to the mice and subsequently organs of interest are harvested for aptamer recovery. Then, aptamers are isolated and amplified. Negative selection can be made by using a healthy mouse. Using this technique, were identified aptamers able to penetrate the BBB (Cheng et al., 2013), to target bones in a prostate cancer bone metastasis model (Chen et al., 2019), or to target Toll-like receptor 4 (TLR4) blocking aptamers in acute stroke (Fernández et al., 2018). Finally, biomarker-aptamers for neurological disorders were discovered (Lecocq et al., 2018).

New biotechnology advances, such as capillary electrophoresis, microfluidics, flow cytometry and atomic force microscopy facilitate the selection of aptamers (Mayer et al., 2010; Mosing and Bowser, 2007; Mosing et al., 2005; Takenaka et al., 2017).

Moreover, advances are made on automate SELEX to reduce selection's time to only few days (Breuers et al., 2019; Eulberg et al., 2005; Hünninger et al., 2014).

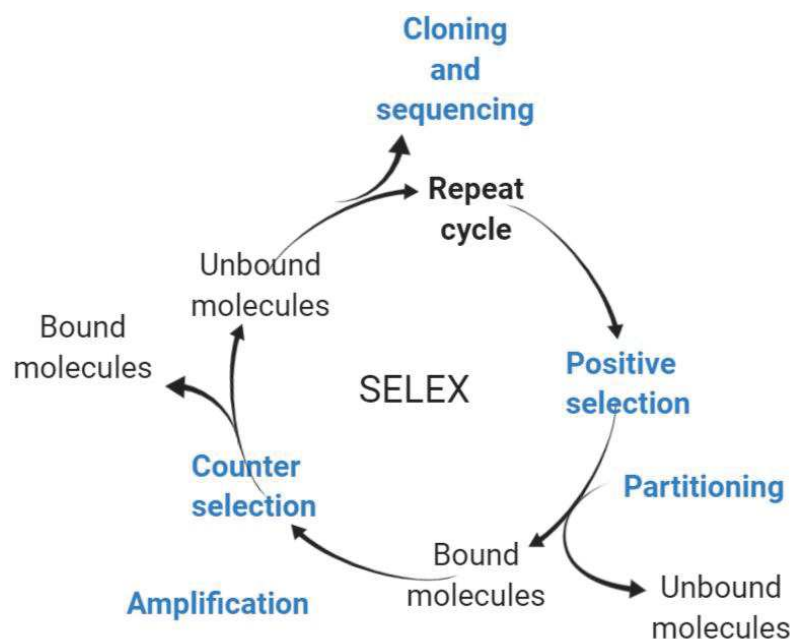


**Figure 15: SELEX.** SELEX is a molecular technique of aptamer selection. A library of nucleic acids is put in contact with a target (positive selection). All unbound sequences are eliminated. The bound molecules are amplified and enter in a counter selection, in contact with a random/negative target. The unbound sequences are retained to start a new cycle. In the end of several cycles with increasing stringency, the molecules selected are cloned and sequenced.

## 4.5 Applications of Aptamers

Aptamers have a large panel of different applications in molecular biology, biotechnology and biomedicine associated to their target-specificity, stability and chemical production. Aptamers have been used in diagnostics for the molecular recognition of their targets in pathogens, cancer or stem recognition, environmental protection, and food safety (Zhang et al., 2019).

SELEX has been used to generate aptamers for the detection of a number of pathogens such as bacteria, parasites and virus. In bacteria, aptamers were selected against outer membrane proteins of *enterotoxaemia E. coli* using FRET HTS (Bruno et al., 2010), surface proteins of *Campylobacter jejuni* (Bruno et al., 2009) and whole-bacterium for several other bacteria (Zhang et al., 2019) like some virulent strain as *Mycobacterium tuberculosis* (Chen et al., 2007).

For cancer recognition, aptamers have been developed against cancer cell-biomarkers (MUC1, HER2 for example) (Zhang et al., 2019) or tumor-related soluble biomarkers (carcinoembryonic antigen (CEA) and prostate specific antigen (PSA)) (Yang et al., 2015; Zhang et al., 2015a) and against cancer cells (like for leukemia CCRF-CEM cells) (Ye et al., 2015). Camorani et al demonstrated that EGFR-targeting aptamer CL4 was also able to bind mutant EGFRvIII. Moreover, the aptamer inhibits EGFRvIII activation (Camorani et al., 2015).

Aptamers were able to detect metastatic tumor tissues (Li et al., 2015a) and to perform *in vivo* imaging of different cancers (Wu et al., 2015).

In the clinic, aptamers can have a dual-performance: therapeutic and diagnostic. An aptamer against PDGFR $\beta$  blocked 3D cancer cell invasion and lung metastases formation on a triple-negative breast cancer mice model. The same aptamer conjugated to near-infrared fluorophore bound to triple-negative breast cancer subcutaneous xenografts and lung metastases (Camorani et al., 2018). There are only few aptamers for stem cell recognition, and they recognize biomarkers of cancer stem cells (epithelial cell adhesion molecule, CD133, CD117, and CD44) (Ababneh et al., 2013), and mouse embryonic stem cells (Iwagawa et al., 2012).

Environment can be contaminated by antibiotics, heavy metals, toxins, and pathogens that can be toxic to human health. Aptamers against antibiotics used for farm animals such as chloramphenicol (Burke et al., 1997) and tetracycline (Kim et al., 2010) were developed, and they determined if the antibiotics are accumulated in the animal tissues. Furthermore, aptamers have been also developed for environmental toxins, heavy metals, pesticides, herbicides and insecticides (Zhang et al., 2019).

Aptamers are more and more used as biosensors for different proposes. Biosensors are analytical devices that measure biological or chemical response by the generation of signals that are proportional to the concentration of the reaction's analyte (Bhalla et al., 2016). The biosensor capacity of aptamers can be enhanced by the use of nanomaterials, like ultrafine graphene (Yang et al., 2017), or the use of biomaterials, like antibodies to form a sandwich (Shui et al., 2018; Zhu et al., 2020). Electric and optic/fluorescent signals are used as methods of aptamer-biosensor signal detection.

#### 4.5.1 Aptamers as Therapeutics

Aptamers are promising therapeutics since they can activate target receptor functions upon binding, they can also compete with molecules and/or ligands to inhibit target activation, or they can be used as vectors for the delivery of therapeutic agents.

As written above aptamers have been selected for different targets, thus aptamers can be used as therapeutics in different fields. They might be used as agents against bacterial infection or as antiviral agent, in immune diseases and cancer.



Aptamers as antiviral agents have been described, such as RNA aptamers for human immunodeficiency virus-1 (HIV-1) (Mufhandu et al., 2012), Newcastle disease virus, vesicular stomatitis virus, influenza virus replication (Hwang et al., 2012) and hepatitis C virus (Nishikawa et al., 2003; Umehara et al., 2004). Anti-HIV-1 aptamer UCLA1 is able to inhibit HIV-1 entry in the cell by binding to a HIV-1 subtype gp120 (Mufhandu et al., 2012). Hepatitis C virus replication and proliferation need the non-structural protein 3 that is a bi-functional protein with protease and helicase actions. Individual aptamers against protease or helicase domains of the virus were obtained (Nishikawa et al., 2003). Then, bi-functional aptamers were constructed by conjugating protease and helicase aptamers via a spacer. They were more performant than aptamers in monomers (Mufhandu et al., 2012).

In cancer treatment, aptamers target different growth factors and their respective membrane receptors and the microenvironment. A DNA aptamer, called NAS-24, targets vimentin, a common ECM protein found in tumor microenvironment, and was described to lead mouse ascites adenocarcinoma cells to apoptosis in *in vitro* and *in vivo* models (Zamay et al., 2014). A novel therapeutic strategy of aptamers in cancer is bispecific antibody–aptamer conjugates. Passariello et al conjugated an anti-EGFR aptamer with an anti-PD-L1 immunomodulatory antibody. The complex decreased cancer cell survival and enhanced activation of T cells against cancer cells. In a co-culture of cancer cells with lymphocytes, the complex was able to increase levels of IL-2 and IFN- $\gamma$  in cell supernatants (Passariello et al., 2019).

Aptamer BC007 is a ssDNA against  $\beta$ 1-adrenoreceptor agonistic autoantibodies, activator of GPCR in cardiomyopathies. This aptamer can help the neutralization of autoantibodies while overcoming logistics problems of actual strategy, immunoadsorption (Wallukat et al., 2016).

#### 4.5.1.1 Aptamers used in clinical trials

Several clinical trials have been using aptamers for different pathologies as shown in table 5. Only two are in cancer treatment. This low use of aptamers in cancer can be due to tumor heterogeneity or to the microenvironment changes provoked by cancer cells. Even if aptamers are being tested in several clinical trials, to date only one aptamer reached the market. Macugen/Pegaptanib is a short RNA aptamer of 28 nucleotides against VEGF-165, used for neo-vascular age-related macular degeneration of the retina (NVAMD). The RNA molecule was submitted to modifications to improve its resistance to 3'-5' exonucleases (2'-modified pyrimidines and purines, addition of a 3'-3' inverted deoxythymidine) and was also conjugated

to PEG to enhance its pharmacokinetics. Macugen was approved by FDA in 2004 (Drolet et al., 2016; Ng et al., 2006). The same year a humanized monoclonal antibody, bevacizumab, was approved by FDA against the same target, VEGF, as a metastatic colorectal cancer treatment (Wang et al., 2004b). Later, bevacizumab was tested on NVAMD treatment and it showed improvement but unfortunately, it diffused through the retina. A modified version of bevacizumab, ranibizumab, was created and showed improvement in NVAMD treatment, so it was approved by FDA in 2006 (Kim and D'Amore, 2012).

➤ Macugen

Interestingly, Macugen was previously thought to target cancer cells but the movement towards eye degenerative diseases happened due to different factors: (i) VEGF was characterized to be an inducer of pathogenic angiogenesis in eyes, (ii) retina cells will continuously need VEGF while the dependency of cancer cells towards this growth factor can fade away (accumulation of mutations and signaling crosstalk), (iii) local administration in the eye compared to plasma will reduce possible undesirable reactions and lower the price of treatment (Drolet et al., 2016).

In 2014, the French *Haute Autorité de Santé* compared Macugen with other anti-VEGF molecules and concluded that Ranibizumab and Aflibercept (a recombinant fusion protein composed of fragments of the extracellular domains of human VEGFR types 1 and 2 fused to the Fc fragment of human IgG1) are more relevant with improved visual acuity while macugen just reduced the loss of visual acuity. Thus, Macugen was declared as not expected to benefit public health.

Aptamers also present limiting points that delay their use in clinics: few knowledge about their pharmacokinetics profile, their cost comparing to small molecules and the intellectual property exclusivity of SELEX.

➤ AS1411 aptamer

The first aptamer in clinical trials against cancer is a nucleolin DNA aptamer, AS1411, in phase II for acute myeloid leukemia. Nucleolin is a nuclear protein, but in several cancer cells nucleolin is present at cell surface (Chen and Xu, 2016; Hovanessian et al., 2010). AS1411 binds to cancer cell surface nucleolin and prevented tumor growth in over 80 cancer cell lines in lung, colorectal, breast and hepatocellular carcinoma cancer cells (Alibolandi et al., 2017; Bates et al., 2009; Cho et al., 2016; Wang et al., 2017b).

#### 4.5.1.2 Aptamer as therapeutic vector

Aptamer-based therapeutic delivery systems include aptamer-therapeutic oligonucleotide conjugates (Shu et al., 2015), aptamer-drug conjugates (Dou et al., 2018; Powell Gray et al., 2018), and aptamer-coupled to nanoparticles (Liang et al., 2015). A more thorough overview of the recent advances on aptamers-drug conjugates was reviewed by Zhu G et al (Zhu et al., 2015a). The use of vectors for drug delivery faces different challenges and issues to take into account: manufacture cost, therapeutic formulation, bio-stability, bio-availability, and pharmacokinetics. Aptamer-drug conjugates (AptDC) over their counterparts' antibody-drug conjugates (ADC) are easy and cost-effective produced and modified. Moreover, they present a higher homogeneity between batches of production that is essential for therapeutic use.

The efficiency of an aptamer-drug conjugate is dependent of various factors that need to be optimal to favor therapy efficiency. Aptamer binding to target, subsequent internalization of complex aptamer-target, fate of complex target in membrane trafficking and drug ability to act on their target (depending on drug availability on site of action, drug degradation and/or inhibition). After internalization, the complex aptamer-target is found inside intracellular endosomal compartments. Usually drugs conjugated to aptamers are chemotherapeutics, which targets are cytosolic or nuclear. The use of aptamers in therapy faces the challenge of its internalization and endosomal escape (Tawiah et al., 2017).

Table 5: Aptamers in clinical trials

	Name	Target	Type and modifications	Clinical Trial realized	Indication
<b>Macular degeneration</b>	Macugen Pegaptanib sodium	VEGF165	RNA (27nt) 2'-fluoropyrimidines 2'-O-methylpurines 3'-inverted dT 40kDa PEG	2 Phase I 1 Phase II 2 Phase II/III 1 Phase Iv	-Age-related macular degeneration (AMD) (FDA approval in 2004) -Diabetic macular edema -Proliferative diabetic retinopathy
	ARC1905	Human complement C5	RNA (38nt) 2'-fluoropyrimidines 2'-O-methylpurines 3'-inverted dT 40kDa PEG	2 Phase I 3 Phase II 1 Phase II/III	-AMD -Wet-AMD -Stargardt disease 1 -Idiopathic polypoidal choroidal vasculopathy -Geographic atrophy conditions
	E-100030	PDGF	DNA (29nt) 2'-O-methylpurines 3'-inverted dT 40kDa PEG	3 Phase I 1 Phase I/II 3 Phase II 3 Phase III	-AMD -Von Hippel-Lindau
<b>Coagulation</b>	REG1 (Drug:RB0006) (Antidote/Active control agente:RB0007)	Coagulation factor IXa (FIXa)	RB0006 RNA (31nt) 2'-fluoropyrimidines or 2'-ribo purine 3'-inverted dT 40kDa PEG RB0007 RNA (15-nt) 2'-O-methyl	2 Phase I 2 Phase II 1 Phase III	-Acute coronary syndrome -Coronary artery disease
	ARC1779	A1 domain of von Willebrand factor	DNA (39nt) 2'-O-methyl with a single phosphorothioate linkage	1 Phase I 5 Phase II	-von Willebrand disease and type 2b

			3'-inverted dT 20kDa PEG		thrombotic thrombocytopenic purpura -Percutaneous coronary intervention -Thrombosis
	NU172	Thrombin	DNA (26nt)	1 Phase II	-Heart disease
	ARC183	Thrombin	DNA (15nt)	1 Phase I	-Acute cardiovascular settings
	BX499 (previously known ARC19499)	Tissue Factor Pathway as Inhibitor (TFP1)	RNA (32nt) 2'-O- methylpurines 3'-inverted dT 40kDa PEG	1 Phase I	-Hemophilia
<b>Oncology</b>	AS1411	Nucleolin	DNA (26nt) PEG	1 Phase I 3 Phase II	-Acute myeloid leukemia -Metastatic renal cell carcinoma -Advanced solid tumor (renal, colon, pancreatic, lung, lymphoma, gastric, cervical, melanoma, prostate, synovial sarcoma, hemangiopericytoma) -Leukemia myeloid
	NOX-A12	CXCL12 (C-X- C Chemokine Ligand 12)	RNA spiegelmer (45 nt) L-ribonucleic acid 40 kDa PEG	2 Phase I 2 Phase I/II 2 Phase II	-Multiple myeloma -Non-Hodgkin lymphoma -Chronic lymphocytic leukemia -Autologous stem cell transplantation -Hematopoietic stem cell transplantation -Metastatic colorectal cancer -Metastatic pancreatic cancer -GBM

<b>Inflammation</b>	NOX-E36	CCL2 (C-C Chemokine Ligand 2)/MCP-1 (Monocyte chemoattractant protein 1)	RNA Spiegelmer (40 nt) L-ribonucleic acid 40 kDa PEG	2 Phase I 1 Phase I/II 1 Phase II	-Type 2 diabetes mellitus -Systemic Lupus erythematosus -Albuminuria -Renal impairment
	NOX-H94	Hepcidin peptide hormone	RNA Spiegelmer (44 nt) L-ribonucleic acid 40kDa PEG	2 Phase I 1 Phase I/II 1 Phase II 1 Phase II	-Anemia -End-stage renal disease -Inflammation

#### 4.5.1.3 Mechanisms of aptamer internalization

Several studies described two internalization mechanisms of aptamers, the receptor-mediated endocytosis and macropinocytosis (Figure 16) (Wan et al., 2019). The first mechanism is based on the ability of the aptamer to bind to membrane receptors and stay bound during all process of internalization of the target. This mechanism of internalization is the most commonly reported for aptamers, and it has been described to aptamers targeting transferrin, human protein tyrosine kinase-7, EGFR and prostate-specific membrane antigen (PSMA) (Chen et al., 2008; Wan et al., 2019). On the other hand, the macropinocytosis mechanism was described to be involved in nucleolin aptamer internalization (Reyes-Reyes et al., 2010). This entry pathway facilitates free shuttling between nucleus and cytoplasm, with any features of endosomal entrapment (Bates et al., 2017; Kotula et al., 2012). Under physiological conditions, macropinocytosis forms vacuoles of 10 µm of diameter by using lipid rafts, NA<sup>+</sup>/H<sup>+</sup> exchange pumps at the plasma membrane and actin filament polymerization (El-Sayed and Harashima, 2013). Several strategies have been used to better describe aptamer internalization pathway, the use of chemical inhibitors (for macropinocytosis, amiloride, for clathrin-dependent, Pitstop2, and for dynamin-dependent one dynasore or dyngo-4a) or the expression modulation of key proteins on each mechanism (Reyes-Reyes et al., 2010; Wan et al., 2019). The interference with a determinate pathway, can improve also the selection of aptamers in cell-internalization SELEX, since macropinocytosis is not the most common way of internalization but the one with more advances for therapy cytosolic delivery.

#### 4.5.1.4 Overcoming endosomal escape

Several techniques have been implemented to improve endosomal escape: pore formation in the endosomal membrane, pH-buffering effect of protonable groups and fusion into the lipid bilayer of endosomes (Varkouhi et al., 2011). Conjugation of cationic amphiphilic peptide-tag to aptamers can help disrupting endosomal membrane, leading to release of aptamer in the cytosol (Aaldering et al., 2015). These peptides after binding to endosomal lipid bilayer induce tension on the internal membrane that is strong enough to create pores (Huang et al., 2004; Varkouhi et al., 2011). Proton sponge effect is mediated by agents that protonate at low pH and thus increase inflow of ions and water, resulting in osmotic swelling and endosomal membrane disruption (Varkouhi et al., 2011). Fusogenic peptides, often found in viruses, undergo a conformational change upon pH change, being able to fuse with the lipid bilayer (Varkouhi et al., 2011).

Besides all the challenges associated to the use of aptamers for vectorization of therapeutic agents, these nucleic acids molecules are promising agents for cancer therapy and also diagnostics.

#### 4.5.2 Aptamers as diagnostic tools

Aptamers can be used as diagnostic tools for cell detection, staining of *ex vivo* tissue samples and as non-invasive *in vivo* imaging-probes for tumor assessment (Cerchia, 2018; Sun et al., 2016).

Aptamers can be used to detect and image specific tumor cells. Several aptamers targeting GBM cells were selected and can be used as imaging tools or even to isolate tumor cells from biopsies (Delač et al., 2015).

## Macropinocytosis

## Receptor-mediated endocytosis

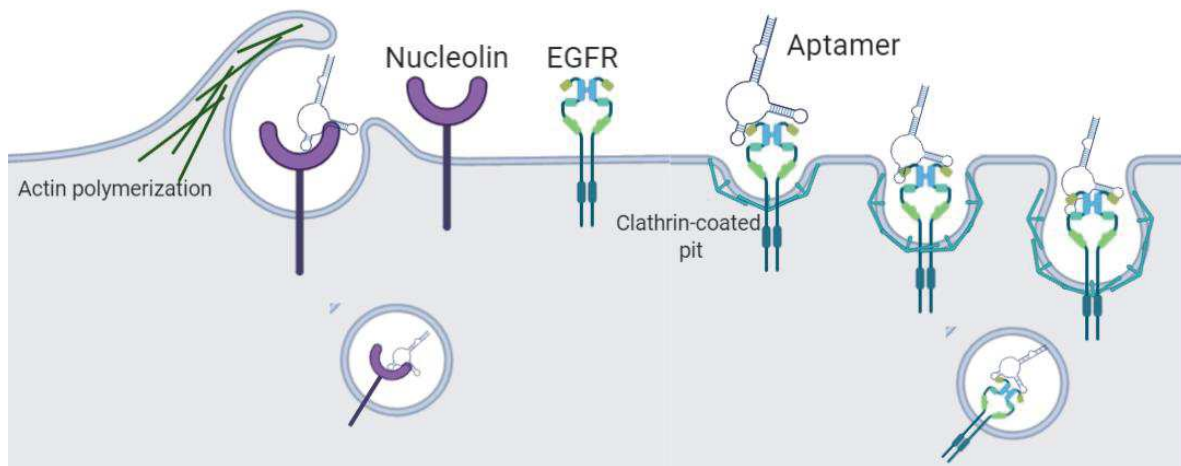


**Figure 16: Aptamer-internalization mechanisms.** The majority of aptamers against cell surface receptors are internalized upon binding to their target. Most of this receptor-mediated endocytosis is clathrin-dependent, and involves creation of a vesicle, pinch from the plasma membrane and release of vesicle into the cytoplasm. The amount of receptor internalized will depend on the internalization rate of the receptor. Interestingly, aptamers against nucleolin can also be internalized through macropinocytosis process. This mechanism involves actin polymerization to create an extension of the plasma membrane ruffle that will incorporate nucleolin-aptamer complex. The retraction of this membrane creates large intracellular vacuoles called macropinosomes. Both mechanisms will lead aptamers to intracellular trafficking.

Moreover, aptamers have been tested to detect circulating cancer cells. For example, Zhao et al created an activable aptamer to a simultaneous detection of multiple tumor biomarkers (MUC1, estrogen receptor (ER) and HER2 in breast cancer). The aptamer probe is composed by an aptamer targeting a tumor biomarker, a fluorophore and a quencher. In the absence of biomarker, fluorophore and quencher are in close proximity and signal is quenched by fluorescent resonance energy transfer. Upon binding of aptamer to the tumor biomarker, aptamer suffers a conformational change, physical separation of fluorophore and quencher, and thus fluorescence signal is observed. Simultaneous multi-detection can be achieved with different activable aptamer conjugated to various fluorophore/quencher arrangements (Zhao et al., 2015).

Studies comparing antibodies and aptamers in the gold standard of cancer diagnosis, the histochemistry, showed several advantages of nucleic acid probes.

First, aptamers need to be functionalized through conjugation with biotin or fluorophores. Aptamers-biotin conjugates can interact with streptavidin conjugated with horseradish peroxidase (HRP). Upon addition of a substrate for the HRP, a classical brown precipitate will



be generated (Bukari et al., 2017; Camorani et al., 2020). Aptamer-fluorophores conjugates allow fluorescence studies in tissues with uni- or multi-detections.

Simpler conditions are required to perform an appropriate aptamer histo-labelling. For example, lower temperature (37° versus 96 °C for antibody) can be used for antigen retrieval, and also less probing times (20 versus 90 min for antibody) (Zeng et al., 2010). The reason for lower temperature for antigen retrieval in aptahistochemistry can be explained by the higher permeability of an aptamer compared to an antibody, and thus aptamer can penetrate the spaces between the cross-links without complete reversal. In the same study, differences staining patterns were observed probably due to recognition of different epitopes and/or easier aptamer access to deeper targets. Moreover, aptamer labelling exhibited less background staining in necrotic areas (Zeng et al., 2010).

Aptamer for tumor imaging have been developed using fluorescence, positron emission tomography (PET), single-photon emission computed tomography (SPECT), and magnetic resonance imaging (MRI).

PET and SPECT are highly sensible techniques for *in vivo* tumor progression imaging. Aptamers were conjugated to radionuclides to improve tumor-specificity of these techniques. For example, aptamer-targeting EGFRvIII in GBM cells was conjugated to <sup>188</sup>Re and used for SPECT imaging on GBM xenografts (Wu et al., 2014).

For MRI, aptamers were conjugated to magnetic nanoparticles. For angiogenesis detection on GBM, an aptamer against VEGFR2 was added to a magnetic nanocrystal. In *in vivo* tests, the aptamer-probe was injected in the tail vein, and it successfully targeted VEGFR2 and produced sensitive MRI images of GBM orthotropic tumors with no cytotoxicity (Kim et al., 2013).

The advantages of aptamers as diagnostic tools and their future use in research and hospital routine are reinforced by the label WHO's "ASSURED" (affordable, sensitive, specific, user-friendly, robust) of several aptamer-based diagnostic assays (Dhiman et al., 2017).

*Other aptamers applications and functionalities might still be unexplored. We believe that aptamers will acquire more and more importance as tools for innovative academic and industrial research.*

## 5. Objectives

GBM is the most frequent and aggressive brain tumor. GBM is extremely refractive to radiotherapy, chemotherapy and targeted therapies. This aggressiveness can be explained by the overexpression of cell surface receptors promoting tumor cell survival, growth and invasion. EGFR, a member of HER tyrosine kinase receptor family, is overexpressed in around 50% of GBM cases. Another cell surface receptor overexpressed in GBM is  $\alpha 5\beta 1$  integrin, a member of ECM receptor family. Remarkably,  $\alpha 5\beta 1$  integrin crosstalks with EGFR leads to increased EGFR oncogenic signalling and resistance to EGFR targeted therapy. These two receptors share the common feature of being spatio-temporally regulated by their endocytosis and membrane trafficking.  $\alpha 5\beta 1$  has been described in EGFR endocytosis and recycling to the surface. Expression level of endocytosis proteins is often altered in GBMs, which contributes to the enhanced oncogenic activity of EGFR and foster GBM progression and aggressiveness. Even though, EGFR and integrin are pertinent therapeutic targets in GBM, targeted therapies failed in GBM clinical trials. Despite numerous studies, many questions remain about the behaviors of these 2 receptors during tumor progression and therapeutic treatments and new therapeutic tools, such as aptamers, might be needed to target EGFR and integrin.

My PhD research followed two main objectives:

- I first seek to characterize the effect of EGFR tyrosine kinase inhibitors in EGFR trafficking in GBM-derived cells. We showed that gefitinib induce ligand-independent EGFR and integrin endocytosis, and identified 3 endocytosis proteins which contribute to this effect. Moreover, we found that repression of endocytosis protects GBM cells from gefitinib-induced inhibition of GBM cell dissemination. Articles 1 and 2 (Blandin, Cruz da Silva et al, 2020; Cruz da Silva et al, under writing).
- I participate to the characterization of a new aptamer targeting  $\alpha 5$  integrin and in the validation of aptamers targeting integrin or EGFR and other RTK, as alternative to antibodies, for receptor detection in glioma cells and in human tissue samples. We further analyzed the effect of gefitinib treatment in aptamer internalization in glioma cells, exploring new opportunities for aptamers as vectorization agents (Articles 3 (Fechter, Cruz da Silva et al., 2019) and recent results.

In parallel, I also participated in the redaction of two reviews; one is presented as a draft (still in writing process) in Annex 1 and another (Annex 2), already published (Cruz da Silva et al., 2019). These manuscripts are about the role of integrin in resistance to growth factor receptors targeted therapies, and a systematic review on GBM clinical trials using targeted therapies. Moreover, I collaborated in the characterization of gold particles conjugated to EGFR antibody cetuximab, which may ameliorate targeted-radiotherapy (Groysbeck et al., 2019), in Annex 3.

# Material and Methods

Table 6, 7, 8 and 9 describe the dilution of antibodies used in this manuscript, the concentration of inhibitors, the characteristics and culture conditions of the cell lines used, and the nature and sequences of aptamers, respectively.

**Table 6: Dilutions of antibodies used**

Application	Protein	Antibody Reference	Company	Dilution
WB	DNM2	G-4	Santa Cruz	1-1000
	EGFR	D38B1	Cell signalling	1-1000
	GAPDH	6C5	Millipore	1-5000
	Integrin $\alpha$ 5	H104	Santa Cruz	1-1000
	LRP-1	PPR3724	Abcam	1-1000
	Rab5	D-11	Santa Cruz	1-1000
	Sortilin	16640	Abcam	1-1000
IF (cells)	CD63			1-50
	EEA1	610457	BD Transductions	1-1000
	EGFR	D1D4J	Cell signalling	1-200
	Integrin $\alpha$ 5 (active)	SNAKA		1-100
	Integrin $\alpha$ 5 (inactive)	IIA1	BD Transductions	1-100
	Integrin $\beta$ 1 (active and inactive)	TSC2/16	BioLegend	1-100
	LAMP1			1-50
	LRP-1	8G1	GeneTex	1-1000
	Rab5	C8B1	Cell signalling	1-200
IF (tissues)	Integrin $\alpha$ 5	AB 1928	Millipore	1-200

**Table 7: Concentration of inhibitors used**

Target	Drug name	Stock concentration	Working concentration	Company	Reference
DNM2	Dyngo-4a	10 mM	12 $\mu$ M	Selleckchem	S7163
	Dynasore	10 mM	10 $\mu$ M		S8047
EGFR	Gefitinib	20 mM	5-20 $\mu$ M	Chemitek	CT-GF001
	Lapatinib	10 mM	10 $\mu$ M		CT-LP002
	Erlotinib	10 mM	10 $\mu$ M		CT-EL002
	Afatinib	10 mM	5 $\mu$ M		CT-BW2992
LRP-1	RAP	2.65 ng/nl	500 nM	Provided by Prof. Stéphane Dedieu	(Perrot et al., 2012)

Table 8: Cell lines used

Type of tumor	Cell lines	Origin	Characteristics	Medium	
GBM	U87 ATCC	Obtained from ATCC (Molsheim, France)	Glioblastoma with PTEN mutated (splice deletion of exon 3, intron 3 and codon 54), homozygous deletions in the p16 and p14ARF genes, TP53 and EGFR WT.	EMEM 10% FBS 1% Non-essential amino acids 1% sodium pyruvate	
	U87 shRNA $\alpha 5$		U87 cell line modified by shRNA against mRNA of $\alpha 5$ integrin		
	U87 EGFR WT	Provided by Professor Furnari (California, USA)	U87 cell line modified by transfection with pcDNA3.1 plasmid containing coding sequence of EGFR		
	U87 D4	Obtained from ATCC (Molsheim, France)	U87 cell line modified by shRNA against mRNA of $\alpha 5$ integrin	EMEM 10% FBS	
	U87 F8		U87 cell line modified by transfection with pcDNA3.1 plasmid containing coding sequence of $\alpha 5$ integrin		
	LN443	Provided by Professor Hegi (Lausanne, Switzerland)	Glioblastoma with PTEN mutated (splice deletion exon 5), homozygous deletions in the p16 and p14ARF genes and TP53 WT.		
	LNZ308		Glioblastoma with deleted TP53, and mutated PTEN (splice deletion of exon 6), and EGFR WT.		
	LN319		Human astrocytoma with mutated TP53 (codon 175 CGC(Arg)→CAC(His)) and mutated PTEN (codon 15 AGA (Arg) → AGT (Ile)).		
	T98	Obtained from EACC (Saint Quentin Fallavier, France)	Glioblastoma with mutated TP53 (codon 237 ATG(Met)→ATA(Ile)), homozygous deletions in		EMEM 10% FBS 1% Non-essential amino acids

			the p16 and p14ARF genes, PTEN deleted and EGFR amplified.	1% sodium pyruvate
Breast cancer	MCF7	Provided by IGBMC collaborators Origin unknown.	Luminal A breast cancer with estrogen and progesterone receptor expression, EGFR and HER expression. Homozygous deletion in CDKN2A and TP53 WT.	DMEM (1g/L glucose) 10% FBS 0.6 µg/ml Insuline 40 µg/ml gentamicine
	MDA-MB-231	Provided by IGBMC Origin ATCC	Triple negative breast cancer type. EGFR and BRCA1 WT, p16 and p14ARF mutated. Homozygotic deletion CDKN2A, homozygotic TP53 mutation Arg280Lys, heterozygotic BRAF mutation Gly464Val, heterozygotic KRAS mutation Gly13Asp	RPMI 1640 without HEPES 10% FBS 40 µg/ml gentamicine
Skin squamous cell carcinoma	A-431	Provided by IGBMC Origin Dr. B. Magun (Oregon University, USA)	Epidermoid carcinoma with oncogenic gene fusion EGFR-PPARGC1A and mutated TP53 Arg273His	DMEM (1g/L glucose) 10% FBS 40 µg/ml gentamicine
Melanoma	MDA-MB-435	Provided by IGBMC Origin Frederick Cancer Center DCTD Tumor Repository, USA	Melanoma cell line previously described as breast cancer cell line. Heterozygous BRAF Val600G, TP53 Gly266Glu. EGFR negative	RPMI 1640 10% FBS 40 µg/ml gentamicine

**Table 9: Sequences of aptamers used**

Target	Aptamer	Type	Sequence (from 5' to 3')
Integrin $\alpha 5$	H02-2'F-Cy5	RNA	GGUUAACCAGCCUUCACUGCGGACGGACAGAGAGUGCAACCUGCCGUGCCGCACCACGGUCGGUCACAC(CY5)
EGFR	Cy5-E07	RNA 2' fluoro	(CY5)GGACGGAUUUAAUCGCCGUAGAAAAGCAUGUCAAAAGCCGGAACCGUCC
	Alexa 488-E07	RNA 2' fluoro	(A1488)GGACGGAUUUAAUCGCCGUAGAAAAGCAUGUCAAAAGCCGGAACCGUCC
	Anti-human EGFR aptamer Janellia Fluor 646 conjugate	ssDNA	Commercial aptamer - No information available
c-MET	Alexa 568-SL1	ssDNA	(A1568)ATCAGGCTGGATGGTAGCTCGGTCGGGGTGGGTGGGTTGGCAAGTCTGAT

## Reagents

The primary antibodies used for immunostaining are described in table 6. Fluorescently labeled secondary antibodies were purchased from Invitrogen (AlexaFluor –488; –568; –647). DAPI was purchased from Santa Cruz Biotechnology. Phalloidin-Atto 488 was purchased from Sigma-Aldrich. The primary antibodies used for immunoblot are described in table 6. HRP-conjugated secondary antibodies were purchased from Invitrogen. Cell culture medium and reagents were from Lonza. Tyrosine kinase inhibitors, dynasore and dyngo-4a were obtained from ChemiTek. His-tagged RAP was purified by gravity-flow chromatography using a nickel-charged resin as described previously (Perrot et al., 2012). Detailed information concerning drug concentrations are in table 7. Aptamers and chemicals were purchased from IBA (Goettingen, Germany), Eurogentec (Liège, Belgium) and Sigma-Aldrich (Hamburg, Germany), respectively, unless otherwise stated. The sequences of aptamers used on this study are described in Table 9. All other reagents were of molecular biology quality.

## Cell culture

The human glioblastoma cell line U87 was obtained from ATCC. The human glioblastoma cell line U87 EGFR WT cells were kindly provided by Prof. Furnani (California, USA). U87 cells were maintained in Eagle's minimum essential medium (EMEM) supplemented with 10%



foetal bovine serum (FBS), 1% sodium pyruvate and 1% nonessential amino-acid, in a 37 °C humidified incubator with 5% CO<sub>2</sub>. U87 cells were transfected by a specific shRNA targeting  $\alpha 5$ mRNA and considered as U87 cells expressing  $\alpha 5$ -shRNA as low  $\alpha 5$  expressing (U87 $\alpha 5^-$ ) (Blandin et al., 2016). LN443, T98 and LN308 cells were cultured as described in (Renner et al., 2016a). LN319 cells were kindly provided by Prof. Monika Hegi (Lausanne, Switzerland). Cells were maintained in Eagle's minimum essential medium (EMEM) supplemented with 10% FBS in a 37 °C humidified incubator with 5% CO<sub>2</sub>. A-431, MCF-7, MDA-MB-435 and MDA-MB-231 were obtained from UMR 7104. A-431 and MCF-7 were maintained in Dulbecco modified Eagle's minimum essential medium (1g/L glucose) supplemented with 10 % FBS and 40  $\mu$ g/ml of gentamicine. MCF-7 medium also contained 0.6 $\mu$ g/ml of insulin. MDA-MB-435 and MDA-MB-231 were maintained in Roswell Park Memorial Institute medium (RPMI) 1640 medium supplemented with 10 % FBS and 40  $\mu$ g/ml of gentamicine. Detailed information concerning cell lines are in table 8.

## Plasmid amplification

Competent bacteria DH5 $\alpha$  (One Shot™ TOP10 Chemically Competent E. coli) (Invitrogen) were used for bacterial transformation by heat-shock method. Bacteria suspension was thaw on ice. 100ng of plasmid was added and incubated during 30 min on ice. Membrane pores to allow plasmid entry were made by an exposition to 42°C during 30 sec and closure of pores was obtain by placement on ice during 2 min. Lysogeny-Broth (LB) medium was added and bacteria placed at 37°C during one hour with agitation. Different dilutions were scrap on warmed previously made agar plates with respective antibiotic. Plates were left overnight at 37°C. Isolated colonies were selected and put in 2ml of LB medium at 37°C during 8 hours with agitation. Then bacterial solution was added to 250ml LB and left overnight at 37°C with agitation. Suspension was centrifuged at 4°C and plasmid was purified from the bacterial pellet using NucleoBond® Xtra Midi kit (Macherey-Nagel®). Plasmid concentration was determined at 260nm on Nanodrop.

## Plasmid transfection

Plasmid  $\alpha 5$ -GFP was kindly provided by Dr. Alan Horwitz (University of Virginia, USA), pEYFP-Rab5a (kindly provided Dr. Marino Zerial (MaxPlanck Institut, Germany)), GFP-Rab5S324N (Addgene #35141) and GFP-Rab5Q79L (Addgene #35140), siGENOMETM Non-

targeting siRNA pools (Dharmacon D-001206-14-05), siRNA-DNM2 (Dharmacon M-004007-03-0005), siRNA-LRP-1 (Dharmacon M-004721-01-0005) plasmids were used. A total of  $0.25 \times 10^6$  cells was used for each transient transfection using 1.5  $\mu\text{g}$  for expression plasmid or 50 nM for siRNA using JetPrime® (PolyPlus-Transfection) following the manufacturer's instructions. Fusion protein expression was confirmed by fluorescent microscopy the day after and downregulation of DNM2 or LRP-1 was assessed by immunoblot 72h after siRNA transfection.

## Confocal microscopy and Image Analysis

Coverslips were coated with fibronectin ( $20 \mu\text{g.mL}^{-1}$  in DPBS). 15 000 cells were seeded in serum containing medium and cultured for 24 hours before TKI treatment. Alternatively, two-day-old U87 cell spheroids were seeded in complete medium in presence or absence of TKIs. Cells were then fixed in 3.7% (v/v) paraformaldehyde during 10 minutes, and permeabilized with 0.1% Triton-X100 for 2 min. After a 60-minutes blocking step using PBS-BSA 3% solution, cells were incubated with primary antibodies O/N at 4 °C ( $2 \mu\text{g.mL}^{-1}$  each in PBS-BSA 3%). Cells were rinsed in PBS and incubated with appropriate secondary antibodies ( $1 \mu\text{g.mL}^{-1}$  in PBS-BSA 3%) and DAPI for 45 min. Samples were mounted on microscope slides using fluorescence mounting medium (Dako). Images were acquired using a confocal microscope (LEICA TCS SPE II, 60 $\times$  magnification oil-immersion, N/A 1.3). For each experiment, identical background subtraction and scaling was applied to all images. Pearson correlation coefficient from 10-12 images (4-5 cells per images) from 3 independent experiments were calculated using JACoP plugin or Colocalization Finder ImageJ softwares. 3D reconstruction corresponds to confocal images Z-stacks obtained using stacks of 300 nm. 3D image reconstruction was performed using IMARIS software.

## EGF endocytosis and uptake quantification

EGF coupled to AlexaFluor488 (Molecular Probes, Invitrogen) was used to study the ligand-induced EGFR internalization. To this end, cells were plated on coverslips previously coated with fibronectin ( $20 \mu\text{g.mL}^{-1}$  in DPBS). Cells were starved in OptiMEM (Gibco) for 1h at 37 °C. Cells were first washed in ice-cold DPBS and then incubated on ice in OptiMEM medium containing  $100 \text{ ng.mL}^{-1}$  AlexaFluor488–EGF. After incubation on ice for 30 min, cells were gently washed in ice-cold DPBS. Cells fixed at this step were used as negative control.

Otherwise, cells were incubated with pre-warmed complete medium at 37°C during 1h in presence of gefitinib as indicated. Non-internalized EGF was strip by incubating the cells with a solution of sodium acetate 0.2M pH 2.7 for 5 min on ice. After washing, cells were fixed and stained with DAPI. Images were acquired using a confocal microscope. The analysis was performed after a threshold (identical for all conditions) applied to eliminate background. The integrated fluorescence intensity of EGF-Alexa488 was determined in each cell. Image analysis was performed using ImageJ in between 20-30 cells per condition on 3 independent experiments.

## STORM imaging and analysis

Samples were prepared as previously described for confocal microscopy, except that cells were incubated with quantum dots 655 (Invitrogen). Super-resolution imaging was performed on an inverted microscope Nikon Eclipse Ti-E (Nikon) equipped with 100x, 1.49 N.A. oil-immersion objective. Fluorescence signal was collected with an EM-CCD camera (Hamamatsu) using a previously optimized protocol (Glushonkov et al., 2018). Image reconstruction was performed using Thunderstorm, QDs were used for drift correction of both channels. The reference image with TetraSpek beads (ThermoFischer) was acquired to correct the lateral shift and chromatic aberrations (UnwarpJ plugin, ImageJ) between the two channels.

## Aptafluorescence on cells

U87  $\alpha 5^+$  (F8) and U87  $\alpha 5^-$  (D4) were plated on sterile glass slides for one night at 37°C in culture medium, washed three times with washing buffer (DPBS, 1 mM MgCl<sub>2</sub> and 0.5 mM CaCl<sub>2</sub>) and then saturated for 1 h at RT in washing buffer containing 2% BSA. Cy5-labeled aptamers (sequence table 9) were denatured at 95°C for 3 min and incubated on ice for 5 min and then on cells in washing buffer for 30 min at 37°C at different concentrations dependent on the assay (5, 2.5, 1.25, 0.6, or 0.3  $\mu$ M). Cells were then washed, fixed for 10 min in 4% PFA, washed, permeabilized for 1 min with 0.1% Triton-X, and washed again. Incubation with primary antibodies was made overnight at 4°C. After washing, secondary antibody at a 2  $\mu$ g/mL final concentration was added with DAPI (for nuclear labelling) for 1 h at RT. F-actin was labelled by Phalloidin-ATTO 488 (Sigma) at 1/4,000. Washing steps preceded mounting using fluorescent mounting medium. Images were acquired using a confocal microscope (Leica TCS SPE II, 63 $\times$  magnification, oil immersion). For all magnifications, an initial background

subtraction equal to all conditions was performed on immunofluorescence images to enhance intracellular immunolabelling. Mean fluorescence intensity on cells was measured using ImageJ software. Statistical analysis of data was performed with Student's t test. Data were analyzed with GraphPad Prism version 5.04 and are represented as mean  $\pm$  SEM.

## Aptahistochemistry

GBM patients' histologic tissues were obtained from the the CRB (Centre de Ressources Biologiques, CHRU Hautepierre, Strasbourg) tumor bank. Integrin  $\alpha 5$  and EGFR were apta- and immuno-stained using formalin-fixed paraffin-embedded tissues mounted on glass slides. Sections were deparaffinized with a 6 minutes bath on Roti-Histol (ROTH) at room temperature (RT). Sections were further rehydrated with a decreasing scale of ethanol containing two baths of absolute ethanol, two of 95% ethanol, one at 70% ethanol and finally one of H<sub>2</sub>O. Sections were subjected to an antigen unmasking protocol. Briefly, sections were boiled at 100°C for 10 min in target retrieval solution (pH 9) (S2367, DAKO) in the micro-wave, cooled down to RT for 20–40 min, and rinsed in H<sub>2</sub>O. For aptafluorescence, slides were rinsed for 5 min in washing buffer (DPBS, 1 mM MgCl<sub>2</sub> and 0.5 mM CaCl<sub>2</sub>), dried, incubated in blocking buffer (2% BSA in washing buffer) for 1 h at RT, rinsed in washing buffer, and dried. Aptamers were denatured at 95°C for 3 min and incubated on ice for 5 min before dilution in washing buffer to a final concentration of 1  $\mu$ M for integrin  $\alpha 5$  aptamer or 500 nM, for EGFR and c-MET aptamer. Aptamers were incubated on tumor sections for 1 h at RT in a humid chamber, washed in washing buffer, dried, fixed in 4% PFA for 8 minutes, and then washed three times in PBS. DAPI (10  $\mu$ g. mL<sup>-1</sup>) staining for 30 min at RT was performed to visualize cell nuclei. The stained samples were then washed in PBS for 5 minutes, and coverslips were mounted onto tissue sections using fluorescent mounting medium (S3023, Dako). For immunofluorescence of integrin  $\alpha 5$ , slides were rinsed in PBS, followed by 5 minutes in PBS-T (0.1% Tween-20 PBS) and incubation in blocking buffer (5% goat serum in PBS-0.1% Triton X-100) for 1h at RT. After drying, slides were incubated with primary antibody at 4°C overnight on a humid chamber. Slides were rinsed three times for 3 minutes in PBS-T, dried, incubated with secondary antibody diluted on blocking buffer during 2h at RT, and then washed three times for 3 minutes in PBS-T. DAPI (10 mg.mL<sup>-1</sup>) staining for 30 min at RT was performed to visualize cell nuclei. The stained samples were then washed in PBS for 5 minutes, and coverslips were mounted onto tissue sections using fluorescent mounting medium (S3023, Dako). Images were acquired using NANOZOOMER S60.

## Methylcellulose solution

Six grams of methylcellulose are dissolved in 250 ml of EMEM medium without FBS. Then the solution is heated at 60°C for one hour. 250 ml of EMEM medium supplemented with 20% of FBS, 2% of sodium pyruvate and 2% non-essential amino acids are added. The solution was mixed overnight at 4°C. The solution was centrifuged at 5000g for two hours. The supernatant is aliquoted and conserved at 4°C. Methylcellulose solution was made as previously described (Blandin et al., 2016).

## Spheroid migration assays

Single cell suspension was mixed in EMEM/10% FBS containing 10% of methylcellulose. All the spheroids were made with 1000 cells by hanging drop method in a 20 µL drop as previously described (Blandin et al., 2016). Tissue culture plates were coated with fibronectin (20 µg.ml<sup>-1</sup> in DPBS solution) for 2 h at 37 °C. Two-day-old spheroids were allowed to adhere and migrate in complete medium (EMEM, 10% FBS). Twenty-four hours later, cells were fixed with paraformaldehyde 3.7% (Electron Microscopy Sciences) and stained with DAPI. Nucleus were pictured under the objective 5x in the fluorescence microscope ZEISS-Axio (ZEISS). Image analysis to evaluate the number of cells that migrated out of the spheroid was performed with ImageJ software using a homemade plugin (Blandin et al., 2016). Phase-contrast images (EVOS X1, Core5× magnification, Thermo Scientific) were acquired. For 3D evasion assays, collagen/fibronectin gels were made as described (Thuault et al., 2013) except that fibronectin (20µg.ml<sup>-1</sup>) was added to the collagen solution prior polymerization.

## Flow cytometry

Flow cytometry was performed with individual aptamers directly coupled to Cy5 at their 3' end. For determination of equilibrium binding affinities of different aptamers to GBM EGFR positive and negative cells, aptamer E07 and aptamer anti-EGFR Janellia 646 conjugate were used at the concentrations indicated. After detachment with EDTA (0.2 M), 300,000 cells were incubated for 30 min at 4°C with Cy5-labeled aptamers. As a control, cells were incubated with 1µg.ml<sup>-1</sup> of an anti-EGFR antibody (cetuximab-Cy5) for 30 min. After washing, cells were analyzed using a FACSCalibur flow cytometer (Becton Dickinson), and the mean fluorescence intensity (counting 10 000 events) was measured using Flowing software 2.5.1. For  $K_D$

determination, experiments were repeated three times, and data were evaluated using GraphPad Prism.

## Immunoblot

Proteins were separated on precast gradient 4-20% SDS-PAGE gels (Bio-Rad) and transferred to PVDF membrane (GE Healthcare). Membranes were probed with primary antibodies at 1 $\mu$ g/ml (with the exception of anti-GAPDH at 0.2 $\mu$ g/ml) in blocking solution (TBS- 5% non-fat dry milk). Immunological complexes were revealed with anti-rabbit or anti-mouse IgG coupled peroxidase antibodies using chemoluminescence (ECL, Bio-Rad) and visualized with LAS4000 image analyser (GE Healthcare). GAPDH was used as the loading control for all samples.

## Statistical analysis

Data are reported as Tukey's box and whiskers or mean  $\pm$  95% confidence interval histograms, unless otherwise stated. Statistical analysis between samples was done by one-way analysis of the variance (ANOVA) corrected by Bonferroni post-test with the GraphPad Prism program. Significance level is controlled by 95% confidence interval, unless otherwise stated. Different statistical analysis is stated on respective legends.

# Results

## Introduction Articles 1 and 2

Molecular characterization of GBM demonstrate the importance of Epidermal growth factor receptor, EGFR, on tumor progression. The signaling of this receptor tyrosine kinase enhances GBM growth, survival, invasion and therapy resistance (An et al., 2018). Several clinical trials in GBM used EGFR-targeting therapies efficient in other solid tumors, nevertheless, no therapeutic improvement was obtained (Taylor et al., 2012). Several mechanisms were explored to uncover GBM resistance to EGFR targeting without any clinically relevant results. Better understanding of EGFR biology in tumor setting and its relationship with targeted therapy may help to identify new avenues for therapy improvement. EGFR and integrins are partners in crime during cancer progression and resistance to therapy (Silva, 2019). In particular, the fibronectin receptor  $\alpha5\beta1$  integrin has been shown to regulate EGFR activity to promote cancer cell invasion. This integrin is of a particular interest, described by our team and others as promising therapeutic target in GBM (Schaffner et al., 2013).

Endocytosis and membrane trafficking are now considered as fundamental regulators of cell surface receptor oncosignalling. During the last decade, EGFR and integrin membrane trafficking deregulation in GBM emerged as key contributors to tumor progression and resistance to therapy (Al-Akhrass et al., 2017; Kondapalli et al., 2015; Kurata et al., 2019; Walsh et al., 2015; Wang et al., 2019c; Ying et al., 2010). Moreover, several studies showed that therapeutic agents trigger stress-induced endocytosis of EGFR in cancer cells (Cao et al., 2011; Dittmann et al., 2005; Tan et al., 2016).

Concerning gefitinib, studies reported somehow confusing and conflicting data. Gefitinib can suppress ligand-induced EGFR endocytosis in lung cancer cells (Nishimura et al., 2007) and in squamous carcinoma cells xenografted in mice (Pinilla-Macua et al., 2017). However, another study showed an increased radiolabeled human EGF uptake in HNSCC, NSCLC and colon carcinoma cells (He and Li, 2013), suggesting an increase in endocytosis. Gefitinib has been shown to initiate autophagy in a EGFR-dependant, way in mammary carcinoma cells (Tan et al., 2015) or glioma cells (Chang et al., 2014; Liu et al., 2020). Kinase independent accumulation of EGFR in autophagic compartments upon gefitinib treatment was also observed in carcinoma cells (Tan et al., 2015). Of note autophagy and endocytosis are intimately interconnected (Birgisdottir and Johansen, 2020). Finally, downregulation of endocytic pathway is often observed in gefitinib-resistant cancer cells (Cui et al., 2015; Nishimura et al., 2008).



In front of the lack of experimental *in vitro* data, I aimed to explore in detail the impact of gefitinib in EGFR and integrin trafficking in glioma, in hope to find new clues to improve TKI-based therapy on GBM.

Using GBM cell lines, we showed that gefitinib induced a ligand-independent and massive EGFR endocytosis, assessed by a fluorescent EGF-uptake assay, endocytosis assay of cell-surface biotinylated EGFR, and EGFR immunolabelling. Process we named 'gefitinib-mediated endocytosis' (GME). In a dose-dependent way, gefitinib caused EGF internalization and EGFR co-localization in enlarged EEA1-positive early-endosomes. GME led to the accumulation for hours of fluorescent EGF, whereas in untreated cells, a slow decrease of intracellular fluorescent EGF occurred, suggesting receptor degradation. Results were confirmed by a biochemical technique of biotinylation endocytosis. GME increased around 25% of EGFR internalized. GME was observed in 4 different GBM cell lines presenting various level of EGFR expression (article 1). Gefitinib induced EGFR endocytosis occurred via a DNM2 and Rab5 dependent mechanism (article 2) and promoted EGFR transport into integrin  $\alpha 5\beta 1$  positive (article 1) and LRP-1 positive (article 2) endosomes. Close proximity between receptors was established by PALM-STORM imaging and suggested a potential functional link. Functional studies confirmed that expression of integrin and LRP-1 are also involved in GME (article 1 and 2 respectively). Finally, we evaluated the importance of endocytosis in gefitinib anti-tumoral activity, in cell evasion assay from 3D spheroids. Blocking of DNM2 and LRP-1 dependent GME protected the cells from treatment (article 2). However, integrin  $\alpha 5$  depletion sensitizes cells to gefitinib treatment (article 1).

Overall this work reveals that EGFR and integrin endocytosis plays an unexpected role in gefitinib action and that expression level of endocytosis proteins such as DNM2, LRP-1 or Rab5 could be relevant biomarkers to predict TKI efficiency in limiting invasion of GBM cells.



## Gefitinib induces EGFR and $\alpha 5 \beta 1$ integrin co-endocytosis in glioblastoma cells

Anne-Florence Blandin<sup>1</sup> · Elisabete Cruz Da Silva<sup>2</sup> · Marie-Cécile Mercier<sup>2</sup> · Oleksandr Glushonkov<sup>2</sup> · Pascal Didier<sup>2</sup> · Stéphane Dedieu<sup>4</sup> · Christophe Schneider<sup>4</sup> · Jessica Devy<sup>4</sup> · Nelly Etienne-Selloum<sup>2,3</sup> · Monique Dontenwill<sup>2</sup> · Laurence Chouliet<sup>2</sup> · Maxime Lehmann<sup>2</sup>

Received: 2 March 2020 / Revised: 8 September 2020 / Accepted: 16 October 2020  
© Springer Nature Switzerland AG 2020

### Abstract

Overexpression of EGFR drives glioblastomas (GBM) cell invasion but these tumours remain resistant to EGFR-targeted therapies such as tyrosine kinase inhibitors (TKIs). Endocytosis, an important modulator of EGFR function, is often dysregulated in glioma cells and is associated with therapy resistance. However, the impact of TKIs on EGFR endocytosis has never been examined in GBM cells. In the present study, we showed that gefitinib and other tyrosine kinase inhibitors induced EGFR accumulation in early-endosomes as a result of an increased endocytosis. Moreover, TKIs trigger early-endosome re-localization of another membrane receptor, the fibronectin receptor  $\alpha 5 \beta 1$  integrin, a promising therapeutic target in GBM that regulates physiological EGFR endocytosis and recycling in cancer cells. Super-resolution dSTORM imaging showed a close-proximity between  $\beta 1$  integrin and EGFR in intracellular membrane compartments of gefitinib-treated cells, suggesting their potential interaction. Interestingly, integrin depletion delayed gefitinib-mediated EGFR endocytosis. Co-endocytosis of EGFR and  $\alpha 5 \beta 1$  integrin may alter glioma cell response to gefitinib. Using an in vitro model of glioma cell dissemination from spheroid, we showed that  $\alpha 5$  integrin-depleted cells were more sensitive to TKIs than  $\alpha 5$ -expressing cells. This work provides evidence for the first time that EGFR TKIs can trigger massive EGFR and  $\alpha 5 \beta 1$  integrin co-endocytosis, which may modulate glioma cell invasiveness under therapeutic treatment.

**Keywords** Adhesion receptors · Cell migration · Growth factors receptors · Brain cancer · Membrane trafficking

---

Anne-Florence Blandin, Elisabete Cruz Da Silva contributed equally to this work.

---

**Electronic supplementary material** The online version of this article (<https://doi.org/10.1007/s00018-020-03686-6>) contains supplementary material, which is available to authorized users.

✉ Anne-Florence Blandin  
anne-florence\_blandin@dfci.harvard.edu

✉ Maxime Lehmann  
maxime.lehmann@unistra.fr

<sup>1</sup> Department of Oncologic Pathology, Dana Farber Cancer Institute, 450 Brookline Avenue, Boston, MA 02215, USA

<sup>2</sup> UMR 7021, Laboratoire de Bioimagerie et Pathologies, Faculté de Pharmacie, CNRS, Université de Strasbourg, 67401 Illkirch, France

<sup>3</sup> Département de Pharmacie, Centre de Lutte Contre le Cancer Paul Strauss, 67000 Strasbourg, France

<sup>4</sup> UMR CNRS 7369, Matrice Extracellulaire et Dynamique Cellulaire (MEDyC), Université de Reims Champagne Ardenne (URCA), Reims, France

### Introduction

Glioblastomas (GBM), a subgroup of the diffuse astrocytic and oligodendroglial tumours [1], are the most frequent and aggressive brain tumours. GBM are characterized by an inter- and intra-tumoral heterogeneity and a highly invasive phenotype. Overexpression or mutations of Epidermal Growth Factor Receptor (EGFR, HER1, ErbB1) are recurrent molecular alterations in GBM, associated with an unfavourable prognosis [2]. EGFR, a transmembrane receptor tyrosine kinase which belongs to the ERBB family, is responsible for glioma cell proliferation, survival, invasiveness and stemness regulation [3]. Although EGFR is an attractive therapeutic target in GBM, targeted therapies using EGFR-tyrosine kinase inhibitors (TKIs) failed to improve patient care [4, 5]. Following ligand binding and internalization, EGFR is either transported to lysosomes for degradation or recycled to the plasma membrane [6]. Many studies have shown that EGFR can trigger a wide

range of signalling pathways from both cell surface and the endosomal compartment [7, 8] and that spatial regulation of EGFR signalling closely regulates its oncogenic activity [9]. The overexpression of Sprouty2 or Golgi phosphoprotein 3 (GOLPH3), two proteins that prevent EGFR endocytosis, promotes the tumorigenic potential of glioma cells in vitro and in vivo [7, 10, 12–15]. Sortilin, a member of the vacuolar protein sorting 10 (VPS10), binds to normal EGFR, promoting receptor internalization [16] and intracellular trafficking to degradation or exosome secretion pathway [17]. In contrast with GOLPH3, sortilin overexpression reduces tumour growth in lung cancer [16]. The Na<sup>+</sup>/H<sup>+</sup> exchanger NHE9 limits EGFR turnover in endolysosomal compartment by inhibiting luminal acidification. EGFR downstream signalling pathways are thus sustained in NHE9 overexpressing glioma cells to promote tumour growth and cell invasion [18, 19]. EGFR interaction with Mig-6 (mitogen-inducible gene 6), a tumour suppressor gene, has been shown to inhibit EGFR signalling in cancer cells [11, 20, 21]. In GBM, Mig-6 drives EGFR trafficking to late endosome and to lysosomal degradation by linking EGFR to the SNARE protein (soluble N-ethylmaleimide-sensitive-factor attachment protein receptor protein) syntaxin 8 [22, 23]. Loss of Mig-6 in GBM amplifies EGFR oncogenic activity by altering receptor trafficking [22].

By organizing signalling platform called adhesome [24], integrins, a family of cell adhesion receptors, cooperate with several growth factor receptors (GFRs) including EGFR to drive tumour progression and aggressiveness [25]. Integrins also play a key role in resistance to GFR-targeted therapies [26, 27]. Moreover, recent publications revealed that integrins orchestrate GFRs endocytic pathway [25, 28]. For instance, the fibronectin receptor, integrin  $\alpha 5 \beta 1$  drives EGFR recycling from endosomes to the plasma membrane by promoting the interaction of the Rab-coupling protein to EGFR. Coordinate recycling of  $\alpha 5 \beta 1$  integrin and EGFR leads to an increase in EGFR downstream signalling and promotes carcinoma cell invasion [29]. Genome-wide RNA interference screening identified integrins  $\alpha 5 \beta 1$  and  $\alpha 2 \beta 1$  as potential regulators of EGFR endocytosis [30]. We and others previously showed that the fibronectin receptor, is a pertinent therapeutic target in GBM [31–34] but the role of  $\alpha 5 \beta 1$  in EGFR trafficking in GBM has not been examined so far.

The aberrant expression of proteins regulating EGFR membrane trafficking promotes glioma cell invasion and tumour progression [15, 16, 18, 35, 36]. However, the impact of TKIs on EGFR trafficking has not been studied in GBM cells. Conflicting results have been published in other solid tumour models. Gefitinib, an EGFR-TKI, could either induce EGFR endocytosis in mammary cancer cells [37] or limit EGFR internalization in lung carcinoma cells [38, 39].

The objective of our work was to evaluate the impact of clinically approved-TKIs on EGFR distribution in GBM cellular models. We showed that gefitinib strongly altered EGFR and integrin trafficking and promoted their endocytosis. Importantly,  $\alpha 5 \beta 1$  integrin silencing delays gefitinib-mediated EGF endocytosis. Furthermore, depletion of the  $\alpha 5 \beta 1$  integrin increased gefitinib efficacy to inhibit cell dissemination from GBM spheroids. Our findings uncover TKIs as key regulators of EGFR intracellular trafficking and highlight the complex relationship between EGFR and  $\alpha 5 \beta 1$  integrin during GBM cell dissemination.

## Material and methods

### Reagents

Anti-EGFR antibody (D1D4J) and anti-Rab5 (C8B1) were from Cell Signaling. Anti- $\alpha 5$  integrin (IIA1) and anti-EEA1 (610,457) were from BD Transductions. Anti- $\beta 1$  integrin (TS2/16) was from BioLegend. Fluorescently labelled secondary antibodies were purchased from Invitrogen (Alexa Fluor – 488; – 568; – 647). DAPI was purchased from Santa Cruz Biotechnology. Phalloidin-Atto 488 was purchased from Sigma-Aldrich. Following antibodies were used for immunoblot. Anti-EGFR antibody (D38B1) was from Cell Signaling, anti- $\alpha 5$  integrin (H104) from Santa Cruz and GAPDH from Millipore. HRP-conjugated secondary antibodies were purchased from Invitrogen. Cell culture medium and reagents were from Lonza. Tyrosine kinase inhibitors were obtained from ChemiTek. All other reagents were of molecular biology quality.

### Cell culture

The human glioblastoma cell line U87MG was obtained from ATCC. T98G cells were purchased from ECACC (European Collection of Authenticated Cell Cultures, Sigma). LN443, LN18, and LN308 cells were kindly provided by Prof. Monika Hegi (Lausanne, Switzerland). GBM cells were maintained in Eagle's minimum essential medium (EMEM) supplemented with 10% foetal bovine serum (FBS), 1% sodium pyruvate and 1% nonessential amino-acid, in a 37 °C humidified incubator with 5% CO<sub>2</sub>. U87 cells were transfected by a specific shRNA targeting  $\alpha 5$ mRNA. U87 cells expressing  $\alpha 5$ -shRNA are considered as low  $\alpha 5$  expressing cells (U87 $\alpha 5$ -) [40]. Plasmid encoding Rab5a-eYFP was kindly provided by Dr. Marino Zerial (MaxPlanck Institut, Germany) and plasmid containing  $\alpha 5$ -GFP was kindly provided by Dr. Alan Horwitz (University of Virginia, USA). Cells were transfected with 1.5  $\mu$ g

of DNA using Lipofectamine™ 2000 (Invitrogen) following the manufacturer's instructions. Fluorescent protein expression was confirmed the day after.

### Cell growth

**2D cell growth-** Cells were plated (1000 cells/well) onto a 96-well plate in EMEM supplemented with 10% FBS. Cell viability was determined using a tetrazolium compound [3-(4,5-dimethyl-2-yl)-5-(3-carboxymethoxyphenyl)-2-(4-sulfophenyl)-2H-tetrazolium, inner salt (MTS assay—CellTiter 96 AQueous One Solution Cell proliferation assay from Promega) at the indicated time. **3D cell growth-** Single-cell suspension was mixed in EMEM/10% FBS containing 10% of methylcellulose [40]. All the spheroids were made on a U-bottom 96 well plate (Greiner Cellstar U-bottom culture plate) (100  $\mu$ L, 2000 cells). Sphere growth was monitored for 8 days by phase-contrast microscopy (EVOS xl Core, 20 $\times$  magnification). Sphere area was measured using ImageJ software.

### Soft agar assay for colony formation and cell survival

Assays of colony formation in soft agar were performed essentially as described previously. Briefly, 1-ml underlayers of 0.5% agar medium were prepared in 35-mm dishes by combining equal volumes of 1% agar solution and 2 $\times$ EMEM with 20% fetal bovine serum. U87 cells were trypsinized, centrifuged, and resuspended. Cells were further filtered through sterile cell strainers (Corning).  $10^4$  single cells were plated in 0.3% agar medium. Growth medium was added to the top of the agar gel. When indicated gefitinib or DMSO were added in all step of soft agar preparation at the indicated final concentration. After 15 days, formed colonies were stained with 0.005% crystal violet solution for 1 h, and counted. Results are expressed as percentage colonies formed in presence of gefitinib versus solvent.

### Confocal microscopy and image analysis

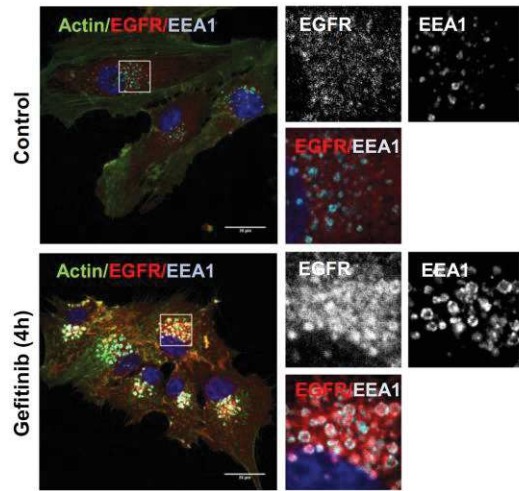
Coverslips were coated with fibronectin (20  $\mu$ g.mL<sup>-1</sup> in DPBS). 15 000 cells were seeded in serum-containing medium and cultured for 24 h before TKI treatment. Alternatively, two-day-old U87 cell spheroids were seeded in complete medium in the presence or absence of TKIs. Cells were then fixed in 3.7% (v/v) paraformaldehyde during 10 min, and permeabilized with 0.1% Triton-X100 for 2 min. After a 60-min blocking step using PBS-BSA 3% solution, cells were incubated with primary antibodies O/N at 4 °C (2  $\mu$ g.mL<sup>-1</sup> each in PBS-BSA 3%). Cells were rinsed in PBS and incubated with appropriate secondary antibodies (1  $\mu$ g.mL<sup>-1</sup> in PBS-BSA 3%) and DAPI for 45 min. Samples

were mounted on microscope slides using fluorescence mounting medium (Dako). Images were acquired using a confocal microscope (LEICA TCS SPE II, 60 $\times$  magnification oil-immersion, N/A 1.3). For each experiment, identical background subtraction and scaling were applied to all images. Pearson correlation and Mender's coefficients from 10–12 images (4–5 cells per images) from 3 independent experiments were calculated using JACoP plugin ImageJ software [41]. Quantification of the colocalized pixels in the cell periphery or in the perinuclear region (Fig. 2b and supplemental Fig. 5b) were performed using home-made Image J plugin. Briefly, using segmentation tools, a first region of interest (ROI) "total cell" corresponding to the cell contour is previously defined. A second ROI "cell periphery" is then defined as a regular inner region of 13 pixels following the cell contour. The third ROI "perinuclear region" is derived from the subtraction of the first two and the elimination of an ROI corresponding to the nucleus (DAPI labelling). Integrin/EGFR colocalized pixels are determined on each image using the scatter plot thanks to the Colocalization Finder plugin (<https://imagej.nih.gov/ij/plugins/colocalization-finder.html>). After binarisation of the colocalized pixel channel, the obtained image is used to quantify the number of colocalized pixels in each ROI, cell by cell. The results are expressed as (number of colocalized pixel in ROI "cell periphery" or "perinuclear"/number of colocalized pixel in ROI "total cell").

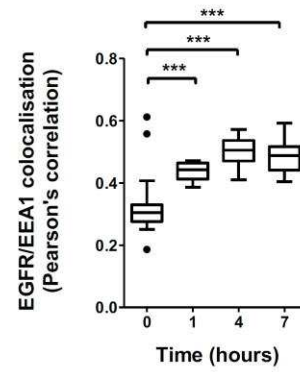
### EGF endocytosis and uptake quantification

EGF coupled to AlexaFluor488 (Molecular Probes, Invitrogen) was used to study the ligand-induced EGFR internalization. To this end, cells were plated on coverslips previously coated with fibronectin (20  $\mu$ g.mL<sup>-1</sup> in DPBS). Cells were starved in OptiMEM (Gibco) for 1 h at 37 °C. Cells were first washed in ice-cold DPBS and then incubated on ice in OptiMEM medium containing 100 ng.mL<sup>-1</sup> AlexaFluor488-EGF. After incubation on ice for 30 min, cells were gently washed in ice-cold DPBS. Cells kept at 4 °C were used as a negative control. Otherwise, cells were incubated with pre-warmed complete medium at 37 °C during 1 h in presence of gefitinib as indicated. Remaining cell surface EGF was removed by acid wash (sodium acetate 0.2M pH 2.7 for 5 min on ice), cells were fixed and nucleus stained with DAPI. Images were acquired using a confocal microscope. The analysis was performed after a threshold (identical for all conditions) applied to eliminate the background. The integrated fluorescence intensity of EGF-Alexa488 was determined in each cell. Image analysis was performed using ImageJ in between 20–30 cells per condition on 3 independent experiments.

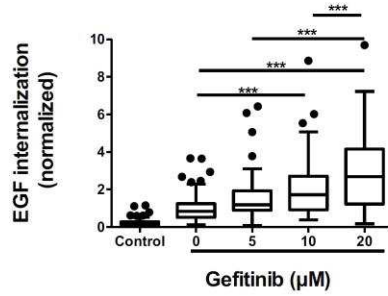
**A EGFR internalization in early endosomes**



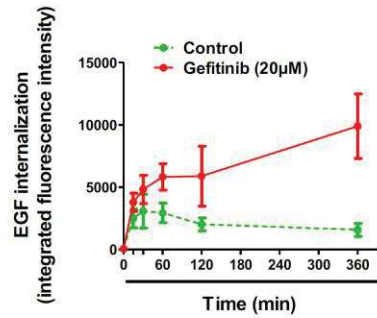
**B EGFR/EEA1 colocalization**



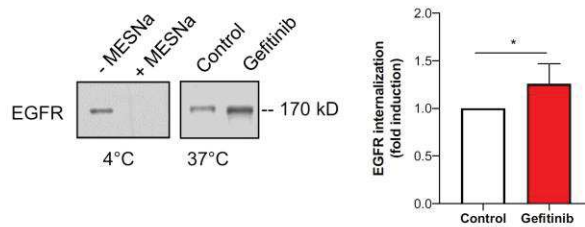
**C EGF internalization (1h treatment)**



**D Kinetics of EGF internalization**



**E Endocytosis of cell-surface biotinylated EGFR**



**F EGFR expression**

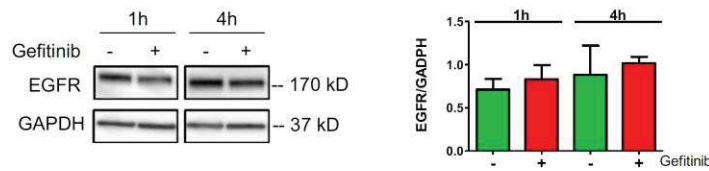


**Fig. 1** Gefitinib provokes EGFR endocytosis in U87 cells. **a** Immunodetection of actin (green), EGFR (red) and the endosomal marker EEA1 (cyan) after 4 h treatment with DMSO (control cells) or gefitinib (20  $\mu\text{M}$ ). Magnified images are from the inserts to the perinuclear area. Scale bar=20  $\mu\text{m}$ . **b** EGFR/EEA1 colocalization following gefitinib treatment. We collected 10–12 images from 3 independent experiments.  $***p < 0.001$ . **c–d** EGF-Alexa488 internalization in U87 cells. Following serum-starvation and EGF-Alexa488 binding to the cell surface, cells were replaced in complete medium at 37  $^{\circ}\text{C}$  to allow internalization of the ligand, in presence of the indicated concentration of gefitinib. The internalization was measured by integrated fluorescence density of 20–30 cells from 3 independent experiments. **c** Cells were treated with different concentrations of gefitinib (5–20  $\mu\text{M}$ ) for 1 h at 37  $^{\circ}\text{C}$  incubation.  $***p < 0.001$ . **d** Cells were treated with 20  $\mu\text{M}$  of gefitinib for 15 min to 6 h. Data are represented as mean  $\pm$  s.d. **e** Left panel: Immunoblot showing the endocytosis of biotinylated EGFR. Following cell-surface biotinylation, cells were incubated in complete media (with or without 15  $\mu\text{M}$  gefitinib) for 3 h. Cells were treated with MESNa agent to remove biotin present on cell-surface proteins. After purification, biotinylated proteins were then subjected EGFR immunoblot. Right panel: Quantification of EGFR protein bands (mean of 4 independent experiment).  $*p < 0.05$ . **f** Left panel: Immunoblot showing similar EGFR protein expression in gefitinib-treated and untreated cells. Right panel: Quantification of EGFR/GAPDH protein ratio (mean of 3 independent experiments)

### Endocytosis of biotinylated cell-surface EGFR

Subconfluent cells were placed on ice during the following steps to prevent internalization. Cells were washed with ice-cold Hank's Balanced Salt Solution containing 0.5 mM  $\text{MgCl}_2$  and 1.26 mM  $\text{CaCl}_2$  (Ca/Mg-HBSS) adjusted to pH 8, followed by incubation with 1 mg/ml EZ-Link Sulfo-NHS-LC-Biotin (Thermo Fisher Scientific) in Ca/Mg-HBSS for 30 min, and washed with ice-cold Ca/Mg-HBSS. Free biotin was quenched with 20 mM glycine in Ca/Mg-HBSS for 15 min, then cells were washed with Ca/Mg-HBSS before internalization assays.

Following cell-surface biotinylation, cells were incubated 2 h at 37  $^{\circ}\text{C}$  in 10% FBS-containing medium (with or without 15  $\mu\text{M}$  Gefitinib), to allow endocytosis. Cells were quickly replaced on ice, washed three times with ice-cold Ca/Mg-HBSS, then washed twice with 300 mM MESNa in the appropriate buffer (Tris 50 mM pH 8.6, NaCl 100 mM, EDTA 1 mM, BSA 0.2%) in the dark, for 15 min to remove biotin to cell-surface proteins. Cells were rinsed twice with Ca/Mg-HBSS, incubated with iodoacetamide (5 mg/ml) in Ca/Mg-HBSS for 10 min in dark, and subsequently washed with Ca/Mg-HBSS. To determine the total amount of surface biotinylation and to serve as a control, one dish was kept on ice after biotin labeling and preserved from MESNa treatment. Whole-cells extracts were prepared as described above and biotinylated proteins were recovered from 100  $\mu\text{g}$  of cell lysate by using avidin protein immobilized on agarose beads, subjected to SDS-PAGE, and revealed by immunoblotting with the anti-EGFR antibody.

### STORM imaging and analysis

Samples were prepared as previously described for confocal microscopy, except that cells were incubated with quantum dot 655 (Invitrogen). Super-resolution imaging was performed on an inverted microscope Nikon Eclipse Ti-E (Nikon) equipped with 100 $\times$ , 1.49 N.A. oil-immersion objective. Fluorescence signal was collected with an EM-CCD camera (Hamamatsu) using a previously optimized protocol [42]. Image reconstruction was performed using Thunderstorm, quantum dots were used for drift correction of both channels. The reference image with TetraSpek beads (ThermoFischer) was acquired to correct the lateral shift and chromatic aberrations (UnwarpJ plugin, ImageJ) between the two channels.

### Spheroid migration assays

Single-cell suspension was mixed in EMEM/10% FBS containing 10% of methylcellulose. All the spheroids were made with 1000 cells by hanging drop method in a 20  $\mu\text{L}$  drop as previously described [40]. Tissue culture plates were coated with fibronectin (20  $\mu\text{g}\cdot\text{mL}^{-1}$  in DPBS solution) for 2 h at 37  $^{\circ}\text{C}$ . Two-day-old spheroids were allowed to adhere and migrate in complete medium  $\pm$  gefitinib (EMEM, 10% FBS). Twenty-four hours later, cells were fixed with paraformaldehyde 3.7% and stained with DAPI. Nucleus were pictured under the 5 $\times$  objective a Zeiss-Axio fluorescence microscope. Image analysis to evaluate the number of cells that migrated out of the spheroid was performed with ImageJ software using a homemade plugin [40]. Alternatively, phase-contrast time-lapse images were acquired using a Leica DMIR2 microscope (5 $\times$ NPlan 0.25NA objective) equipped with a 37  $^{\circ}\text{C}$  5%  $\text{CO}_2$  control system (Life imaging Services) with Leica DCF350FX CCD camera piloted by the FW4000 software (1 image every 10 min.). Thirty randomly chosen cells per spheroids using (4–5 spheroids per assays) were tracked using MTrackJ plugin [43], average speed and average directionality (average ratio of the distance to the origin) were quantified. Phase-contrast images (EVOS XI, Core5 $\times$  magnification, Thermo Scientific) were acquired. For 3D evasion assays, collagen/fibronectin gels were made as described [44] except that fibronectin (20  $\mu\text{g}\cdot\text{mL}^{-1}$ ) was added to the collagen solution prior polymerization.

### Immunoblot

Equivalent amounts of proteins were separated on precast gradient 4–20% SDS-PAGE gels (Bio-Rad) and transferred to PVDF membrane (GE Healthcare). Membranes were probed with primary antibodies; anti-EGFR antibody (D38B1), anti- $\alpha 5$  integrin (H104) at 1  $\mu\text{g}/\text{ml}$  and anti-GAPDH at 0.2  $\mu\text{g}/\text{ml}$  in blocking solution (PBS- 5% non-fat

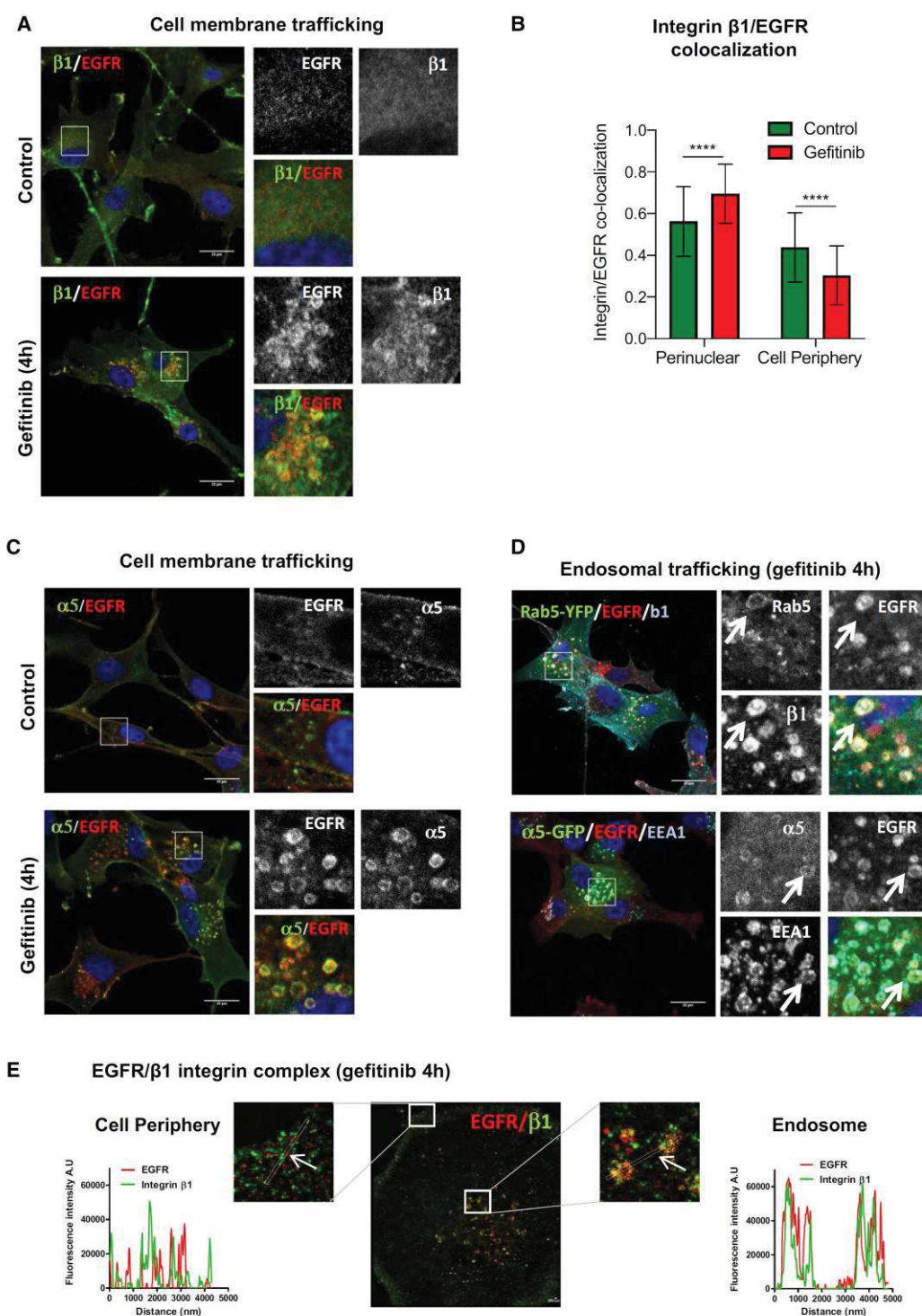


**Fig. 2** Gefitinib provokes the co-endocytosis of EGFR and  $\alpha 5\beta 1$  integrin. **a–c** Confocal images of U87 cells treated with vehicle (control) or gefitinib. Immunodetection of EGFR and  $\beta 1$  (**a**) or  $\alpha 5$  (**c**) integrin subunits by confocal microscopy. Scale bar = 20  $\mu\text{m}$ . **b** Quantification of the ratio  $\beta 1$  integrin/EGFR colocalized pixels in the perinuclear compartments compared to the cell periphery. The degree of colocalization between the  $\beta 1$  integrin and EGFR was quantified using a home-made plugin with the ImageJ software. **d** Confocal images of U87 cells expressing Rab5-YFP or  $\alpha 5$ -eGFP and treated with 20  $\mu\text{M}$  of gefitinib. High magnification images of the inserts at the perinuclear area. Arrows highlight vesicles that are labelled with both EGFR, integrin and early-endosome marker. Scale bar = 20  $\mu\text{m}$ . **e** Two-color dSTORM images of gefitinib-treated cells showing EGFR/ $\beta 1$  integrin complex at the cell periphery and endosomes. High magnification images of the inserts at the cell periphery and endosomes are shown. Plot profiles of pixel intensity of EGFR (red) and  $\beta 1$  integrin (green) corresponding to the region marked with white arrows. Scale bar = 200 nm

dry milk). Immunological complexes were revealed with anti-rabbit or anti-mouse IgG coupled peroxidase antibodies using chemoluminescence (ECL, Bio-Rad) and visualized with LAS4000 image analyser (GE Healthcare). Quantification of non-saturated images was performed with ImageJ software. GAPDH was used as the loading control for all samples.

### Statistical analysis

Data are reported as Tukey's box and whiskers unless otherwise stated. Statistical analysis between samples was done by one-way analysis of the variance (ANOVA) corrected by Bonferroni post-test with the GraphPad Prism program unless otherwise stated. Significance level is controlled by a 95% confidence interval.

## Results

### Gefitinib provokes EGFR endocytosis

EGFR trafficking dysregulation participates to GBM progression and aggressiveness. However, the significance and the role of TKIs on EGFR trafficking remain unclear [38, 45]. To address this question, we treated U87 GBM cells with gefitinib and examined EGFR localization by confocal microscopy (Fig. 1a). In untreated control cells, EGFR labelling was diffused and poorly localized in early endosome antigen-1 (EEA1)-positive endosomes. Remarkably, after 4 h of treatment, gefitinib provoked a massive relocalization of EGFR in EEA1-positive endosomes. These

endosomes were enlarged compared to control cells suggesting endosomes fusion and/or endosomal arrest. Gefitinib-mediated EGFR re-localization to early endosomes was observed at gefitinib concentrations ranging from 5  $\mu\text{M}$  to 20  $\mu\text{M}$  (data not shown). Quantification of EEA1/EGFR co-localization revealed that EGFR distribution in early endosomes increased after 1 h of treatment (Fig. 1b).

Using an EGF-internalization fluorescent assay, we showed that gefitinib strongly increased EGF endocytosis from the cell surface in a dose-dependent manner (Fig. 1c). Time-course experiments confirmed that gefitinib increased EGFR endocytosis within 30 min after treatment initiation. Moreover, fluorescent EGF accumulated for hours in gefitinib-treated cells, whereas in untreated cells, we measured a slow decrease of intracellular fluorescent EGF (Fig. 1d). To confirm these results, we conducted endocytosis assays of cell-surface biotinylated EGFR (Fig. 1e). Densitometric quantification of EGFR immunoblot revealed a 25% increase of internalized EGFR. Importantly, short-term gefitinib treatment had no impact on total EGFR expression level in U87 cells (Fig. 1f). Considering glioblastoma heterogeneity, we analysed the effect of gefitinib on EGFR distribution in 3 other cell lines presenting a various level of EGFR expression (Supplemental Fig. 1e). We showed that gefitinib increased EEA1/EGFR colocalization in T98G and LN443 cells (Supplemental Fig. 1a, b) and EGF endocytosis in LN443, T98 and LN443 cells (Supplemental Fig. 1c, d). These experiments indicated that *in vitro*, gefitinib led to massive EGFR endocytosis in GBM cells.

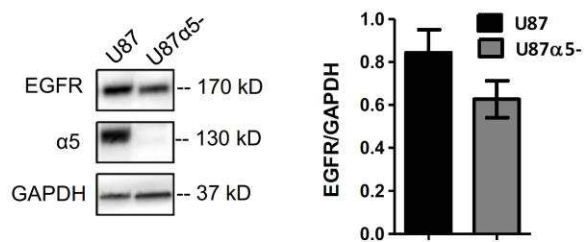
### Integrin and EGFR are co-recruited to early-endosomes by gefitinib treatment

Our previous experiments clearly showed that gefitinib strikingly increased EGFR endocytosis rate. Integrin  $\alpha 5\beta 1$  promotes EGFR recycling [29] and a genome-wide gene screening identified  $\alpha 5\beta 1$  integrin as a strong promoter of EGFR endocytosis [30]. We thus hypothesized that  $\alpha 5\beta 1$  integrin, a potential therapeutic target in GBM [32, 34] may have an impact on gefitinib-mediated EGFR endocytosis.

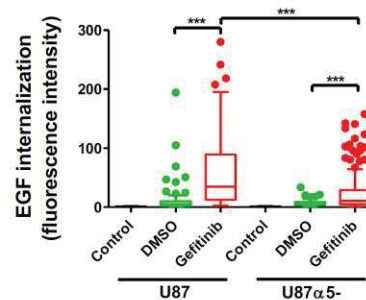
We first examined the impact of gefitinib on  $\alpha 5\beta 1$  integrin localization. Integrin/Rab5 colocalization was examined by immunofluorescence and confocal microscopy. As shown in Supplemental Fig. 2a, b, gefitinib triggered  $\beta 1$  integrin relocalization in Rab5-positive early endosomes. We next examined whether EGFR and integrin are transported to the same endosomes. In untreated cells,  $\alpha 5\beta 1$  integrin and EGFR were detected at the plasma membrane or as punctate intracellular staining (Fig. 2a). Surprisingly, upon short-term gefitinib treatment,  $\alpha 5\beta 1$  integrin was clearly redistributed into large EGFR-positive endosomes (Fig. 2a–c). As cells presented a dense EGFR and integrin co-labelling at the level of the plasma membrane (mainly due to membrane ruffling), we



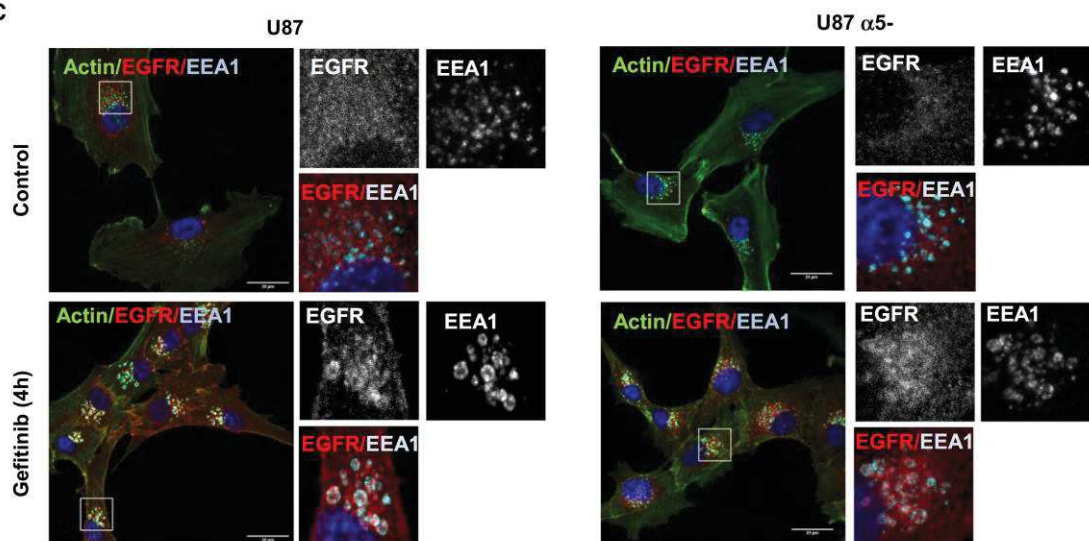
**A EGFR expression in U87 cells**



**B EGF internalization (1h treatment)**



**C**



**D EGFR/EEA1 colocalization**

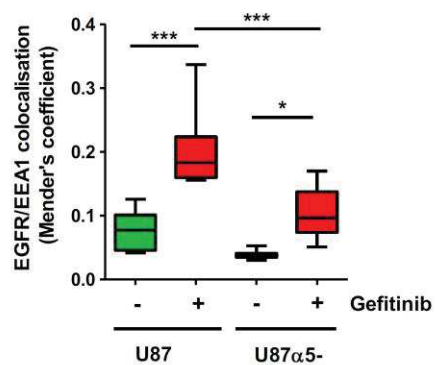


**Fig. 3** Silencing of  $\alpha 5\beta 1$  integrin delayed gefitinib-mediated EGFR endocytosis. **a** Left panel: U87 and U87 $\alpha 5^-$  cell lysates were immunoblotted to detect EGFR,  $\alpha 5$  integrin and GAPDH. Right panel: densitometric analysis. **b** EGF-Alexa488 internalization assays in U87 cells and U87 $\alpha 5^-$ . Following serum-starvation and EGF-Alexa488 binding to the cell surface, cells were replaced in complete medium at 37 °C to allow internalization of the ligand in presence of gefitinib (20  $\mu$ M) or DMSO. The internalization was measured by integrated fluorescence density on 20–30 cells/experiment of 3 independent experiments and reported in the histogram by arbitrary units of fluorescence (AUF). \*\*\* $p < 0.001$ . **c** Confocal microscopy detection of actin filaments (green), EGFR (red) and EEA1 (cyan) in U87 and U87 $\alpha 5^-$  cells treated with vehicle (control) or gefitinib (20  $\mu$ M, 4 hours). High-magnification images are from the inserts into the perinuclear area. Scale bar=20  $\mu$ m. **d** EGFR/EEA1 colocalization using Mander's coefficient. Confocal images from 3 independent experiments were analyzed with JACOBS plugin of ImageJ software

quantified the integrin/EGFR colocalized pixels ratio at the cell periphery or in the endosomes enriched perinuclear region. As shown in Fig. 2b, gefitinib treatment increased integrin/EGFR colocalization in the perinuclear region compared to untreated condition, indicating a recruitment of both receptors in the same endosomes. We next performed immunolabeling and confocal analysis of U87 cells that transiently expressed either  $\alpha 5$ -GFP or Rab5-YFP. Upon gefitinib treatment, integrin  $\beta 1$  and EGFR were both localized in Rab5-positive early-endosomes (Fig. 2d). Similarly, EGFR and  $\alpha 5$ -GFP were both found in EEA1-positive early-endosomes (Fig. 2d). We next performed 2-color dSTORM super-resolution microscopy to confirm a potential interaction between the integrin and EGFR in early-endosomes (Fig. 2e). In gefitinib-treated cells, plot profile views revealed a strong overlay of EGFR and integrin  $\beta 1$  labelling in endosome-like structures but not at the cell periphery, suggesting that these two receptors are more likely to interact in endosomes than at the plasma membrane (Fig. 2e). Additionally, we showed that not only first-class reversible TKI (erlotinib) but also second-generation irreversible TKIs which covalently bind to EGFR (lapatinib, afatinib, dacomitinib) provoked EGFR/ $\beta 1$  integrin co-redistribution in endosomal compartments (Supplemental Fig. 3a). Finally, upon gefitinib treatment, we observed endosomal integrin/EGFR co-labelling in three additional GBM lines (LN443, LN2308 and T98) (Supplemental Fig. 4).

Taken together, these data showed for the first time that EGFR TKIs increased EGFR endocytosis and  $\alpha 5\beta 1$  integrin co-accumulation in early endosomes of GBM cells.

### Knock-down of $\alpha 5\beta 1$ integrin reduced gefitinib-mediated EGFR endocytosis

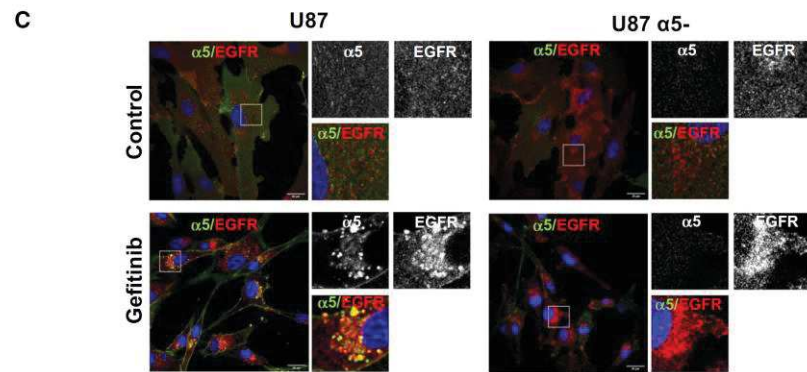
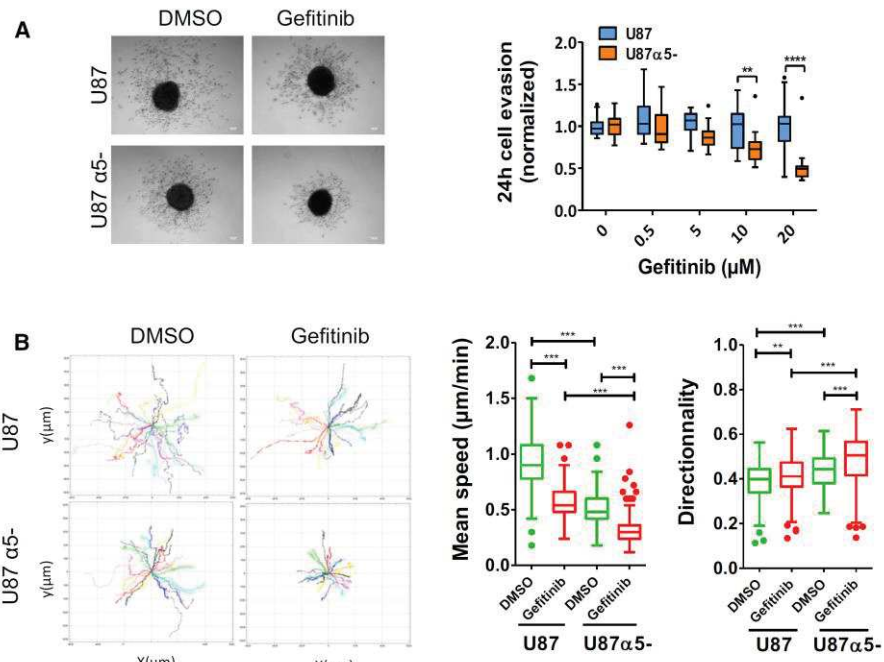
We next examined whether integrin  $\alpha 5$  gene silencing may affect gefitinib-mediated EGFR endocytosis. We first controlled by immunoblot, that loss of  $\alpha 5$  expression did not change EGFR expression level (Fig. 3a) and that EGFR

expression was not altered by gefitinib treatment in both cell lines (Supplemental Fig. 5a). Similarly, we showed that the effect of gefitinib on cell proliferation and cell survival was not dependant on  $\alpha 5$  expression in U87 cells (Supplemental Fig. 6). By contrast, EGF internalization assays showed that EGFR endocytosis was significantly reduced in  $\alpha 5$ -negative cells (U87  $\alpha 5^-$ ) (Fig. 3b). Analysis of EGFR/EEA1 colocalization by confocal images revealed that loss of  $\alpha 5$  expression limited the internalization and accumulation of EGFR in early-endosomes during short-term gefitinib treatment (Fig. 3c, d). These data support the hypothesis of a functional relationship between integrin  $\alpha 5\beta 1$  and EGFR and suggest that  $\alpha 5\beta 1$  integrin expression may contribute to gefitinib-mediated EGFR endocytosis.

### $\alpha 5\beta 1$ integrin expression decreases EGFR-TKIs efficacy during cell dissemination from GBM spheroid

In ovarian cancer cells, the co- trafficking of  $\alpha 5\beta 1$  integrin and EGFR is critical for cell migration and invasion [46, 47]. We thus hypothesized that the potential interaction between EGFR and  $\alpha 5\beta 1$  in early-endosomes of gefitinib-treated cells may impact on glioma cell migration and invasion. Tumour spheroids are reliable models of solid tumours and are increasingly used to decipher molecular mechanisms of cancer cell migration and resistance to therapy [40]. We thus compared the role of gefitinib on cell evasion from spheroids in  $\alpha 5$ -expressing and  $\alpha 5$ -depleted cells (Fig. 4). Phase-contrast microscopy indicated that in presence of gefitinib U87 $\alpha 5^-$  cells poorly escape from spheroids compared to control cells (Fig. 4a). Quantification of the number of evading cells, showed that gefitinib decreased the number of evaded cells from U87 $\alpha 5^-$  spheroids in a dose dependent way, but did not significantly affect evasion of U87 parental cells (Fig. 4a). Using video microscopy, we analysed the trajectories of individual cells migrating away from the spheroids. Figure 4b showed that in all experimental conditions, cells migrated radially from the spheroids. We also noticed that loss of  $\alpha 5$  integrin as well as gefitinib treatment slightly increased cell directionality, suggesting changes in direction sensing or planar polarity. As expected,  $\alpha 5\beta 1$  expression enhanced cell speed both in control and gefitinib-treated cells (Fig. 4b). However, we described that gefitinib significantly reduced both U87 and U87 $\alpha 5^-$  cell speed (Fig. 4b). We then analysed EGFR and integrin localization in cells migrating at long distance from the spheroids. In U87 parental cells, EGFR was found in  $\alpha 5\beta 1$ -positive endosomes, which is consistent with a co-trafficking of both receptors during cell migration (Fig. 4c-left panel). This result highlights that gefitinib had long term effect on EGFR and integrin co-trafficking. Interestingly, in  $\alpha 5$ -depleted glioma cells (Fig. 4c-right panel), we also observed enhanced EGFR

2D cell migration (24h)



3D cell invasion (24h)

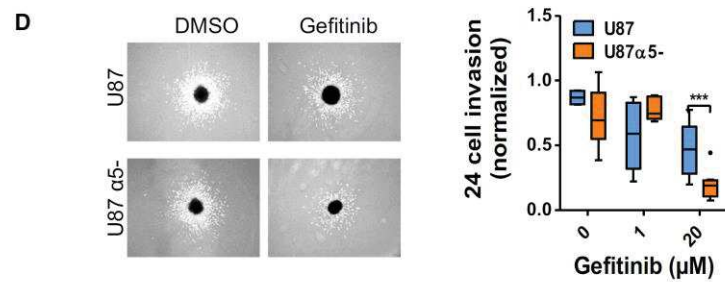


**Fig. 4** Silencing of  $\alpha 5\beta 1$  integrin sensitizes GBM cells to gefitinib treatment during GBM cell evasion in 2D and 3D environment. **a** Phase-contrast image of representative spheroids after 24 h of migration in the presence of DMSO or gefitinib (20  $\mu\text{M}$ ). Scale bar=100  $\mu\text{m}$ . After DAPI staining, the number of evading cells were quantified by automated counting of nuclei using an ImageJ homemade plugin.  $**p < 0.01$ ,  $***p < 0.001$ . **b** Left panels show the migratory tracks of individual cells. Right panels: Mean speed and directionality of DMSO or gefitinib-treated escaping cells (30 cells/spheroids, 5 spheroids/experiment, 3 independent experiments).  $**p < 0.05$ ,  $***p < 0.001$ . **c** EGFR and  $\alpha 5$  integrin are co-distributed in intracellular compartment of cells migrating at long distance during 24 h of gefitinib treatment. Confocal microscopy detection of EGFR and  $\alpha 5$  integrin in cells treated with DMSO (control) or gefitinib. High magnification images are from the inserts into the peri-nuclear area. Scale bar=20  $\mu\text{m}$ . **d** Left panel: Phase-contrast image of representative spheroids embedded in collagen/fibronectin 3D matrix after 24 h of invasion in the presence of DMSO or gefitinib (20  $\mu\text{M}$ ). Scale bar=100  $\mu\text{m}$ . Right panel: Curve-dose effect of gefitinib on cell invasion was quantified using ImageJ. Quantification of 15 spheroids from 3 independent experiments, normalized to the control cells.  $***p < 0.001$

internalization in gefitinib-treated cells compared to control cells, indicating that loss of  $\alpha 5$ -integrin expression reduced but did not suppress gefitinib-mediated endocytosis. Confocal images analysis confirmed that  $\alpha 5$ -integrin silencing reduced the number of  $\beta 1$  integrin/EGFR colocalized pixels in perinuclear region of migrating cells (Supplemental Fig. 5). We then compared the efficacy of 4 TKIs and confirmed that  $\alpha 5\beta 1$  integrin expression may trigger resistance to EGFR TKIs during U87 cell evasion from tumour spheres (Supplemental Fig. 3b). Finally, experiments performed with spheroids embedded in collagen/fibronectin matrix showed that  $\alpha 5\beta 1$ -depleted U87 cells were more sensitive to gefitinib treatment than parental  $\alpha 5\beta 1$ -expressing cells in 3D environment (Fig. 4d). In conclusion, we showed that EGFR-targeting TKIs induced EGFR/integrin co-endocytosis and trafficking, and that  $\alpha 5\beta 1$  expression stimulated evasion of TKIs-treated cell.

## Discussion

Gefitinib is a potent tyrosine kinase inhibitor of EGFR, used in cancer treatment. Despite the key role of EGFR in glioblastoma aggressiveness and progression, gefitinib did not improve the management of patients with a brain tumour [4, 5]. As membrane trafficking is a key regulator of EGFR function in cancer cells [6], and is often altered in GBM cells [12, 18, 22], we seek to study the impact of gefitinib treatment on EGFR trafficking. In this study, we showed that in a glioma cellular model, acute gefitinib treatment induced an intense EGFR endocytosis, a process we called gefitinib-mediated endocytosis (GME). GME is not specific to EGFR, as we observed a strong re-localization of the fibronectin receptor  $\alpha 5\beta 1$  integrin in EGFR-positive early endosome

and a co-trafficking of both receptors under gefitinib treatment (Fig. 5). Moreover, we suggest that  $\alpha 5\beta 1$  integrin may play a role in this process as shRNA-mediated depletion of  $\alpha 5$  integrin reduced EGFR GME. We showed that integrin expression is associated with a reduced gefitinib potency to inhibit cell dissemination from tumour spheroids. This suggests that in gefitinib-treated glioma cells, proteins involved in GME and in this altered EGFR trafficking, may affect cell response to gefitinib. The presence of integrin in EGFR-positive endosomes may modulate cell sensitivity to TKI during cell invasion. Our work underlines new properties of TKIs that need to be further investigated to improve cancer cell response to treatment.

Here, we clearly established that gefitinib treatment provoked endosomal accumulation of EGFR, partially due to a strong increase in endocytosis. Indeed, we cannot completely rule out that EGFR accumulation in endosomes can also be the consequence of a dysregulated trafficking of neo-synthesized EGFR. Altered EGFR trafficking is sustained as observed on the immunofluorescence images of migrating cells that were treated with gefitinib for 24 h. While surprising, our data are in agreement with a recent study showing that gefitinib can trigger EGFR accumulation in endosomes of breast cancer cells [37]. While physiological EGFR endocytosis upon ligand-binding is well characterized [48], we still don't know the driven mechanism of GME. Because gefitinib inhibits EGFR tyrosine kinase activity, we speculate that GME occurs independently of EGFR activity. Moreover, we observed that both ligand-bound and ligand-free EGFR (i.e. in serum-free medium, data not shown) were susceptible to GME. Stress-mediated by chemotherapeutic drugs elicits non-physiological EGFR endocytic trafficking dependant on p38-MAPK (mitogen-activated protein kinase) activity [37, 45, 49–52]. In agreement to our own observations, in these processes, EGFR re-localization into intracellular compartments can occur independently of EGF binding [37, 51] or tyrosine-kinase domain activation [37]. Indeed, p38-MAPK can trigger Rab5 pathway activation to promote EGFR endocytosis [53, 54]. Rab5 activation by off-target effect seems to be a common mechanism for drug-induced EGFR endocytosis [55]. Future experiments will determine if Rab5 or p38-MAPK are involved in GME of EGFR and integrin.

In addition to a potential stress-induced endocytosis of EGFR and integrin in gefitinib treated cells, it has been observed that lipophilic drug with a weak basic moiety, such as gefitinib, can become protonated and trapped within acidic intracellular compartment such as lysosomes. Gefitinib lysosomotropism has already been described in normal cells [56, 57]. Furthermore, lysosomal sequestration of gefitinib and other TKI has been reported in cancer cells derived from lung, colon, breast or ovarian carcinomas [58–60]. Whereas these works described that drug retention

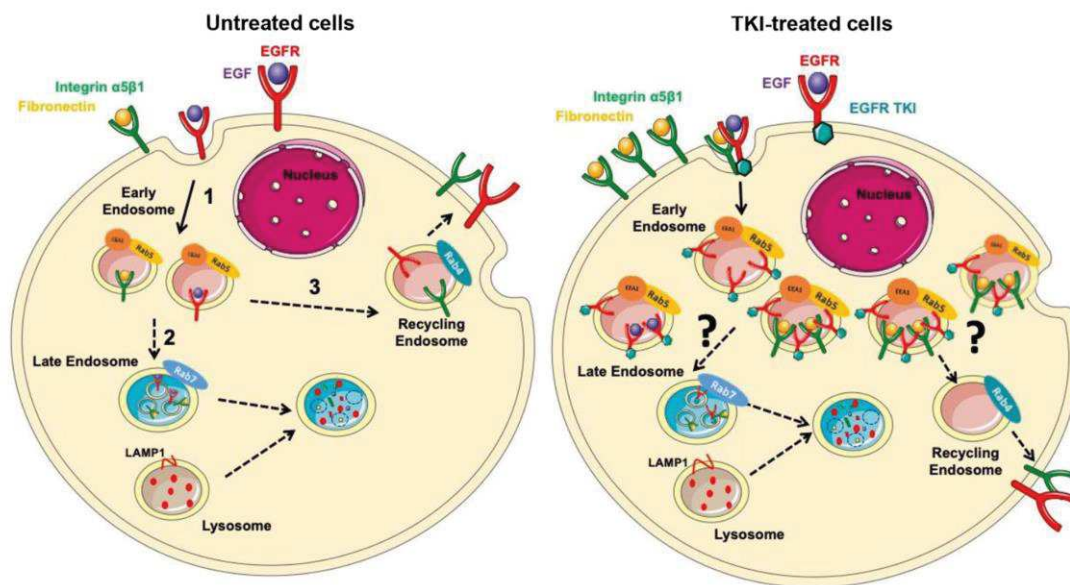


**Fig. 5** Proposed mechanism of gefitinib-mediated endocytosis of EGFR and  $\alpha 5\beta 1$  integrin in glioma cells. In untreated cells, upon ligand-binding, EGFR is internalized into early endosomes (1). EGFR receptors are sorted to different fates, either degradation (2) or recycling (3), according to receptor-ligand dissociation. Ligand-bound receptors are led to degradation by the maturation of early-to-late endosomes and further fusion with lysosomes (2). Otherwise, EGFR can be recycled back to the plasma membrane (3). Upon treatment

with an EGFR-tyrosine kinase inhibitor (TKI), EGFR is massively internalized into enlarged and abundant early endosomes (4). This massive internalization seems to happen to both bound and unbound EGFR. Moreover, TKI treatment also caused internalization of other membrane receptor such as the  $\alpha 5\beta 1$  integrin. EGFR and integrin were found together in early endosomes (5). After endocytosis, the journey of integrin and EGFR remains to be clarified and might modulate invasive behaviour of glioma cells under treatment

in lysosomes is associated with therapeutic resistance of cancer cell, a more recent study indicates that lysosomal sequestration of TKIs does not affect their cytosolic and extracellular concentrations, which is not in a favour for a role of TKI accumulation in an acidic compartment in drug resistance [61]. Interestingly, hydrophobic weak base therapeutic drugs increase lysosomal activity in a breast cancer cell line [59]. Moreover, proteomic analysis revealed that gefitinib treatment of lung cancer cells increased the expression or the ubiquitination level of numerous proteins involved in lysosomal and endocytic pathways [62]. Therefore, it will be interesting to determine in the future whether GME of EGFR and  $\alpha 5\beta 1$  integrin described herein might be the consequence of an alteration of the endocytic pathway triggers by TKI sequestration in the acidic compartment.

In summary, this study described a novel role of TKIs in EGFR/ $\alpha 5\beta 1$  integrin endocytosis and membrane trafficking. As these receptors play a critical function in cancer cell invasion and dissemination, future challenges would evaluate TKIs impact on integrin biological functions and how integrin/EGFR altered endocytosis in TKIs-treated cells may contribute to GBM cell evasion. Finally, a recent

report highlighted the underestimated importance of the off-target cytotoxicity of targeted therapies [63]. This work emphasized the need to better understand drug mechanisms to identify appropriate biomarkers predicting drug efficacy. Thus, it will be important in the future to depict the impact of drugs such as gefitinib on endosomal trafficking and uncover molecules involved in these mechanisms. This may provide rationales for novel treatment protocols and improve precision medicine approach for brain tumours.

**Acknowledgements** This research was funded by Ligue Contre le Cancer, Région Grand-Est, programme-inter region (No S17R417B). Elisabete Cruz Da Silva and Anne-Florence Blandin were PhD students funded by the University of Strasbourg. Marie-Cécile Mercier was a pharmacy intern funded by ARS Grand Est (regional health agency). We thank Romain Vauchelles and the PIQ platform (IBiSa Quest imaging facility) for their assistance in image quantification.

**Author contribution** Participated in research design: ML, MD, LC, PD. Conducted experiments: AFB, ECS, MCM, OG, NES, SD, CS, JD. Performed data analysis: AFB, ECS, MCM, SD, CS, JD. Wrote or contributed to the writing of the manuscript: AFB, ECS, SD, LC, ML. All of the authors reviewed the manuscript and approved the final version.

## Compliance with ethical standards

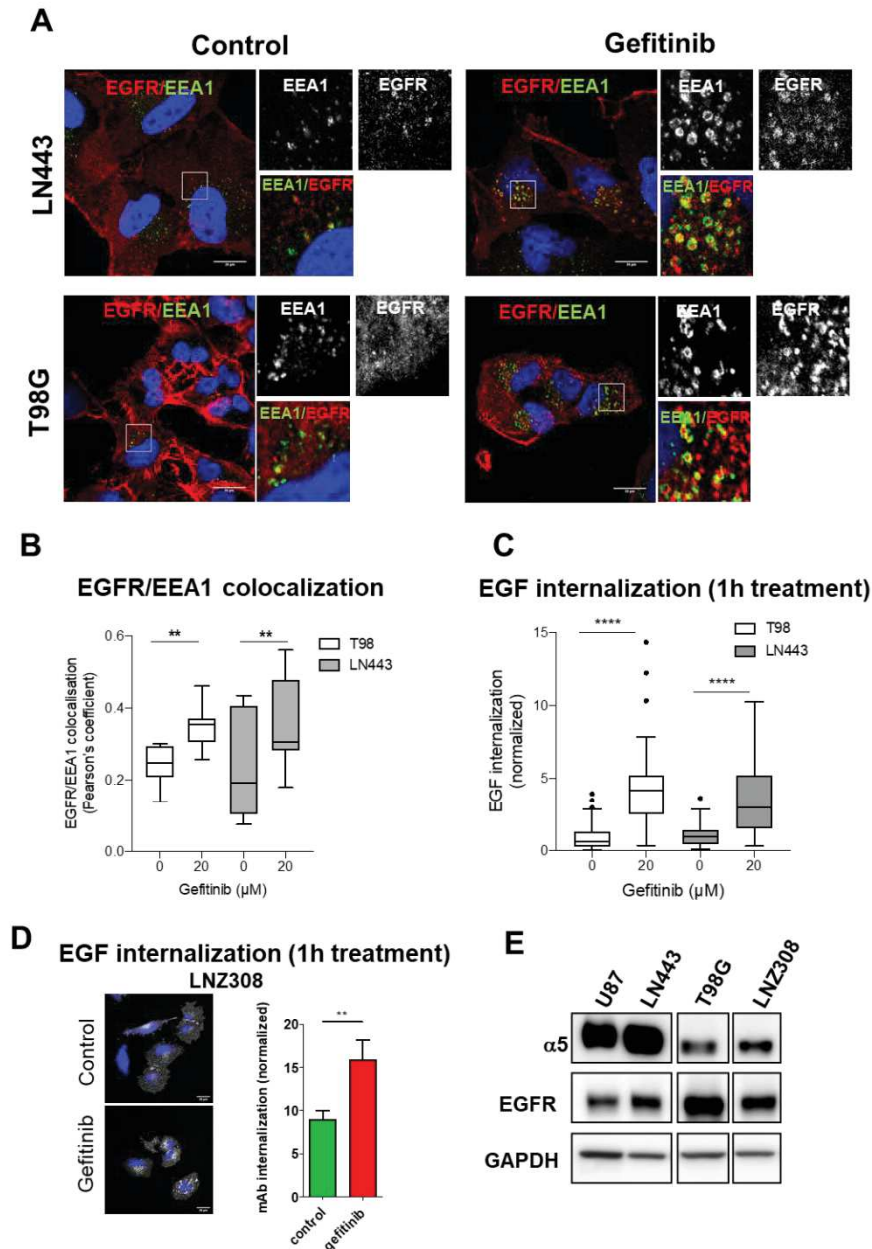
**Conflict of interest** The authors disclose no conflicts.

## References

- Louis DN, Perry A, Reifenberger G et al (2016) The 2016 World Health Organization classification of tumors of the central nervous system: a summary. *Acta Neuropathol* 131:803–820. <https://doi.org/10.1007/s00401-016-1545-1>
- Brennan CW, Verhaak RGW, McKenna A et al (2013) The somatic genomic landscape of glioblastoma. *Cell* 155:462–477. <https://doi.org/10.1016/j.cell.2013.09.034>
- An Z, Aksoy O, Zheng T et al (2018) Epidermal growth factor receptor (EGFR) and EGFRvIII in glioblastoma (GBM): signaling pathways and targeted therapies. *Oncogene* 37:1561–1575. <https://doi.org/10.1038/s41388-017-0045-7>
- Taylor TE, Furnari FB, Cavenee WK (2012) Targeting EGFR for treatment of glioblastoma: molecular basis to overcome resistance. *Curr Cancer Drug Targets* 12:197–209
- Mellinghoff IK, Cloughesy TF, Mischel PS (2007) PTEN-mediated resistance to epidermal growth factor receptor kinase inhibitors. *Clin Cancer Res* 13:378–381. <https://doi.org/10.1158/1078-0432.CCR-06-1992>
- Tomas A, Futter CE, Eden ER (2014) EGF receptor trafficking: consequences for signaling and cancer. *Trends Cell Biol* 24:26–34. <https://doi.org/10.1016/j.tcb.2013.11.002>
- Kim HJ, Taylor LJ, Bar-Sagi D (2007) Spatial regulation of EGFR signaling by Sprouty2. *Curr Biol* 17:455–461. <https://doi.org/10.1016/j.cub.2007.01.059>
- Sousa LP, Lax I, Shen H et al (2012) Suppression of EGFR endocytosis by dynamin depletion reveals that EGFR signaling occurs primarily at the plasma membrane. *Proc Natl Acad Sci U S A* 109:4419–4424. <https://doi.org/10.1073/pnas.1200164109>
- Sigismund S, Avanzato D, Lanzetti L (2018) Emerging functions of the EGFR in cancer. *Mol Oncol* 12:3–20. <https://doi.org/10.1002/1878-0261.12155>
- Wong ESM, Fong CW, Lim J et al (2002) Sprouty2 attenuates epidermal growth factor receptor ubiquitylation and endocytosis, and consequently enhances Ras/ERK signalling. *EMBO J* 21:4796–4808. <https://doi.org/10.1093/emboj/cdf493>
- Walsh AM, Lazzara MJ (2013) Regulation of EGFR trafficking and cell signaling by Sprouty2 and MIG6 in lung cancer cells. *J Cell Sci* 126:4339–4348. <https://doi.org/10.1242/jcs.123208>
- Zhou X, Xie S, Wu S et al (2017) Golgi phosphoprotein 3 promotes glioma progression via inhibiting Rab5-mediated endocytosis and degradation of epidermal growth factor receptor. *Neuro Oncol* 19:1628–1639. <https://doi.org/10.1093/neuonc/nox104>
- Wu S, Fu J, Dong Y et al (2018) GOLPH3 promotes glioma progression via facilitating JAK2–STAT3 pathway activation. *J Neurooncol* 139:269–279. <https://doi.org/10.1007/s11060-018-2884-7>
- Park J-W, Wollmann G, Urbiola C et al (2018) Sprouty2 enhances the tumorigenic potential of glioblastoma cells. *Neuro Oncol* 20:1044–1054. <https://doi.org/10.1093/neuonc/noy028>
- Walsh AM, Kapoor GS, Buonato JM et al (2015) Sprouty2 drives drug resistance and proliferation in glioblastoma. *Mol Cancer Res* 13:1227–1237. <https://doi.org/10.1158/1541-7786.MCR-14-0183-T>
- Al-Akhrass H, Naves T, Vincent F et al (2017) Sortilin limits EGFR signaling by promoting its internalization in lung cancer. *Nat Commun* 8:1182. <https://doi.org/10.1038/s41467-017-01172-5>
- Wilson CM, Naves T, Vincent F et al (2014) Sortilin mediates the release and transfer of exosomes in concert with two tyrosine kinase receptors. *J Cell Sci* 127:3983–3997. <https://doi.org/10.1242/jcs.149336>
- Kondapalli KC, Llongueras JP, Capilla-González V et al (2015) A leak pathway for luminal protons in endosomes drives oncogenic signalling in glioblastoma. *Nat Commun* 6:6289. <https://doi.org/10.1038/ncomms7289>
- Gomez Zubieta DM, Hamood MA, Beydoun R et al (2017) MicroRNA-135a regulates NHE9 to inhibit proliferation and migration of glioblastoma cells. *Cell Commun Signal* 15:55. <https://doi.org/10.1186/s12964-017-0209-7>
- Zhang X, Pickin KA, Bose R et al (2007) Inhibition of the EGF receptor by binding of MIG6 to an activating kinase domain interface. *Nature* 450:741–744. <https://doi.org/10.1038/nature05998>
- Ferby I, Reschke M, Kudlacek O et al (2006) Mig6 is a negative regulator of EGF receptor-mediated skin morphogenesis and tumor formation. *Nat Med* 12:568–573. <https://doi.org/10.1038/nm1401>
- Ying H, Zheng H, Scott K et al (2010) Mig-6 controls EGFR trafficking and suppresses gliomagenesis. *Proc Natl Acad Sci U S A* 107:6912–6917. <https://doi.org/10.1073/pnas.0914930107>
- Kim J, Zhang Y, Skalski M et al (2014) microRNA-148a is a prognostic oncomiR that targets MIG6 and BIM to regulate EGFR and apoptosis in glioblastoma. *Cancer Res* 74:1541–1553. <https://doi.org/10.1158/0008-5472.CAN-13-1449>
- Zaidel-Bar R, ItzkovitzMa'ayan SA et al (2007) Functional atlas of the integrin adhesome. *Nat Cell Biol* 9:858–867. <https://doi.org/10.1038/ncb0807-858>
- Ivaska J, Heino J (2011) Cooperation between integrins and growth factor receptors in signaling and endocytosis. *Annu Rev Cell Dev Biol* 27:291–320. <https://doi.org/10.1146/annurev-cellbio-092910-154017>
- Cruz da Silva E, Dontenwill M, Choulier L, Lehmann M (2019) Role of integrins in resistance to therapies targeting growth factor receptors in cancer. *Cancers*. <https://doi.org/10.3390/cancers11050692>
- Seguin L, Kato S, Franovic A et al (2014) An integrin  $\beta 3$ -KRAS-RalB complex drives tumour stemness and resistance to EGFR inhibition. *Nat Cell Biol* 16:457–468. <https://doi.org/10.1038/ncb2953>
- Barrow-McGee R, Kishi N, Joffe C et al (2016) Beta 1-integrin-c-Met cooperation reveals an inside-in survival signalling on autophagy-related endomembranes. *Nat Commun* 7:11942. <https://doi.org/10.1038/ncomms11942>
- Caswell PT, Chan M, Lindsay AJ et al (2008a) Rab-coupling protein coordinates recycling of alpha5beta1 integrin and EGFR1 to promote cell migration in 3D microenvironments. *J Cell Biol* 183:143–155. <https://doi.org/10.1083/jcb.200804140>
- Collinet C, Stöter M, Bradshaw CR et al (2010) Systems survey of endocytosis by multiparametric image analysis. *Nature* 464:243–249. <https://doi.org/10.1038/nature08779>
- Schaffner F, Ray AM, Dontenwill M (2013) Integrin  $\alpha 5\beta 1$ , the fibronectin receptor, as a pertinent therapeutic target in solid tumors. *Cancers* 5:27–47. <https://doi.org/10.3390/cancers5010027>
- Janouskova H, Maglott A, Leger DY et al (2012) Integrin  $\alpha 5\beta 1$  plays a critical role in resistance to temozolomide by interfering with the p53 pathway in high-grade glioma. *Cancer Res* 72:3463–3470. <https://doi.org/10.1158/0008-5472.CAN-11-4199>
- Renner G, Janouskova H, Noulet F et al (2016) Integrin  $\alpha 5\beta 1$  and p53 convergent pathways in the control of anti-apoptotic proteins PEA-15 and survivin in high-grade glioma. *Cell Death Differ* 23:640–653. <https://doi.org/10.1038/cdd.2015.131>
- Maglott A, Bartik P, Cosgun S et al (2006) The small alpha5beta1 integrin antagonist, SJ749, reduces proliferation and clonogenicity

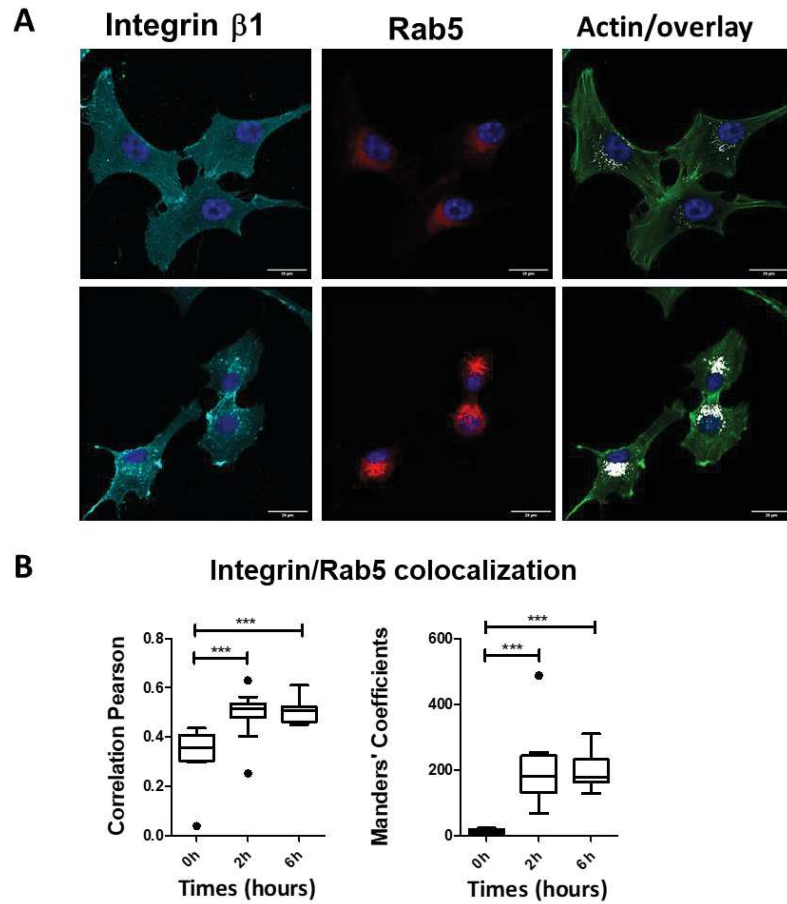
- of human astrocytoma cells. *Cancer Res* 66:6002–6007. <https://doi.org/10.1158/0008-5472.CAN-05-4105>
35. Wang X, Wang Z, Zhang Y et al (2019) Golgi phosphoprotein 3 sensitizes the tumour suppression effect of gefitinib on gliomas. *Cell Prolif* 52:e12636. <https://doi.org/10.1111/cpr.12636>
  36. Li Z-X, Qu L-Y, Wen H et al (2014) Mig-6 overcomes gefitinib resistance by inhibiting EGFR/ERK pathway in non-small cell lung cancer cell lines. *Int J Clin Exp Pathol* 7:7304–7311
  37. Tan X, Thapa N, Sun Y, Anderson RA (2015) A kinase-independent role for EGF receptor in autophagy initiation. *Cell* 160:145–160. <https://doi.org/10.1016/j.cell.2014.12.006>
  38. Jo U, Park KH, Whang YM et al (2014) EGFR endocytosis is a novel therapeutic target in lung cancer with wild-type EGFR. *Oncotarget* 5:1265–1278
  39. Nishimura Y, Bereczky B, Ono M (2007) The EGFR inhibitor gefitinib suppresses ligand-stimulated endocytosis of EGFR via the early/late endocytic pathway in non-small cell lung cancer cell lines. *Histochem Cell Biol* 127:541–553. <https://doi.org/10.1007/s00418-007-0281-y>
  40. Blandin A-F, Noulet F, Renner G et al (2016) Glioma cell dispersion is driven by  $\alpha 5$  integrin-mediated cell–matrix and cell–cell interactions. *Cancer Lett* 376:328–338. <https://doi.org/10.1016/j.canlet.2016.04.007>
  41. Bolte S, Cordelières FP (2006) A guided tour into subcellular colocalization analysis in light microscopy. *J Microsc* 224:213–232. <https://doi.org/10.1111/j.1365-2818.2006.01706.x>
  42. Glushonkov O, Réal E, Boutant E et al (2018) Optimized protocol for combined PALM-dSTORM imaging. *Sci Rep*. <https://doi.org/10.1038/s41598-018-27059-z>
  43. Meijering E, Dzyubachyk O, Smal I (2012) Methods for cell and particle tracking. In: *Methods in enzymology*. Elsevier, pp 183–200
  44. Thuault S, Hayashi S, Lagirand-Cantaloube J et al (2013) P-cadherin is a direct PAX3–FOXO1A target involved in alveolar rhabdomyosarcoma aggressiveness. *Oncogene* 32:1876–1887. <https://doi.org/10.1038/onc.2012.217>
  45. Tan X, Lambert PF, Rappaegeer AC, Anderson RA (2016) Stress-induced EGFR trafficking: mechanisms, functions, and therapeutic implications. *Trends Cell Biol* 26:352–366. <https://doi.org/10.1016/j.tcb.2015.12.006>
  46. Caswell PT, Chan M, Lindsay AJ et al (2008b) Rab-coupling protein coordinates recycling of  $\alpha 5 \beta 1$  integrin and EGFR1 to promote cell migration in 3D microenvironments. *J Cell Biol* 183:143–155. <https://doi.org/10.1083/jcb.200804140>
  47. Muller PAJ, Caswell PT, Doyle B et al (2009) Mutant p53 drives invasion by promoting integrin recycling. *Cell* 139:1327–1341. <https://doi.org/10.1016/j.cell.2009.11.026>
  48. Caldieri G, Barbieri E, Nappo G et al (2017) Reticulon 3–dependent ER-PM contact sites control EGFR nonclathrin endocytosis. *Science* 356:617–624. <https://doi.org/10.1126/science.aah6152>
  49. Zwang Y, Yarden Y (2006) p38 MAP kinase mediates stress-induced internalization of EGFR: implications for cancer chemotherapy. *EMBO J* 25:4195–4206. <https://doi.org/10.1038/sj.emboj.7601297>
  50. Oksvold MP, Huitfeldt HS, Østfold AC, Skarpen E (2002) UV induces tyrosine kinase-independent internalisation and endosome arrest of the EGF receptor. *J Cell Sci* 115:793–803
  51. Tomas A, Vaughan SO, Burgoyne T et al (2015) WASH and Tsg101/ALIX-dependent diversion of stress-internalized EGFR from the canonical endocytic pathway. *Nat Commun*. <https://doi.org/10.1038/ncomms8324>
  52. Cao X, Zhu H, Ali-Osman F, Lo H-W (2011) EGFR and EGFRvIII undergo stress- and EGFR kinase inhibitor-induced mitochondrial translocation: a potential mechanism of EGFR-driven antagonism of apoptosis. *Mol Cancer* 10:26. <https://doi.org/10.1186/1476-4598-10-26>
  53. Cavalli V, Vilbois F, Corti M et al (2001) The stress-induced MAP kinase p38 regulates endocytic trafficking via the GDI:Rab5 complex. *Mol Cell* 7:421–432. [https://doi.org/10.1016/S1097-2765\(01\)00189-7](https://doi.org/10.1016/S1097-2765(01)00189-7)
  54. Macé G, Miaczynska M, Zerial M, Nebreda AR (2005) Phosphorylation of EEA1 by p38 MAP kinase regulates  $\mu$  opioid receptor endocytosis. *EMBO J* 24:3235–3246. <https://doi.org/10.1038/sj.emboj.7600799>
  55. Chen X, Wang Z (2001) Regulation of epidermal growth factor receptor endocytosis by wortmannin through activation of Rab5 rather than inhibition of phosphatidylinositol 3-kinase. *EMBO Rep* 2:842–849. <https://doi.org/10.1093/embo-reports/kve179>
  56. Nadanaciva S, Lu S, Gebhard DF et al (2011) A high content screening assay for identifying lysosomotropic compounds. *Toxicol Vitro* 25:715–723. <https://doi.org/10.1016/j.tiv.2010.12.010>
  57. Kazmi F, Hensley T, Pope C et al (2013) Lysosomal sequestration (Trapping) of lipophilic amine (Cationic Amphiphilic) drugs in immortalized human hepatocytes (Fa2N-4 Cells). *Drug Metab Dispos* 41:897–905. <https://doi.org/10.1124/dmd.112.050054>
  58. Englinger B, Kallus S, Senkiv J et al (2018) Lysosomal sequestration impairs the activity of the preclinical FGFR inhibitor PD173074. *Cells*. <https://doi.org/10.3390/cells7120259>
  59. Zhitomirsky B, Assaraf YG (2014) Lysosomal sequestration of hydrophobic weak base chemotherapeutics triggers lysosomal biogenesis and lysosome-dependent cancer multidrug resistance. *Oncotarget* 6:1143–1156
  60. Gotink KJ, Broxterman HJ, Labots M et al (2011) Lysosomal sequestration of sunitinib: a novel mechanism of drug resistance. *Clin Cancer Res* 17:7337–7346. <https://doi.org/10.1158/1078-0432.CCR-11-1667>
  61. Ruzickova E, Skoupa N, Dolezel P et al (2019) The lysosomal sequestration of tyrosine kinase inhibitors and drug resistance. *Biomolecules*. <https://doi.org/10.3390/biom9110675>
  62. Li W, Wang H, Yang Y et al (2018) Integrative analysis of proteome and ubiquitylome reveals unique features of lysosomal and endocytic pathways in gefitinib-resistant non-small cell lung cancer cells. *Proteomics* 18:1700388. <https://doi.org/10.1002/pmic.201700388>
  63. Lin A, Giuliano CJ, Palladino A et al (2019) Off-target toxicity is a common mechanism of action of cancer drugs undergoing clinical trials. *Sci Transl Med* 11:eaaw8412. <https://doi.org/10.1126/scitranslmed.aaw8412>

**Publisher's Note** Springer Nature remains neutral with regard to jurisdictional claims in published maps and institutional affiliations.

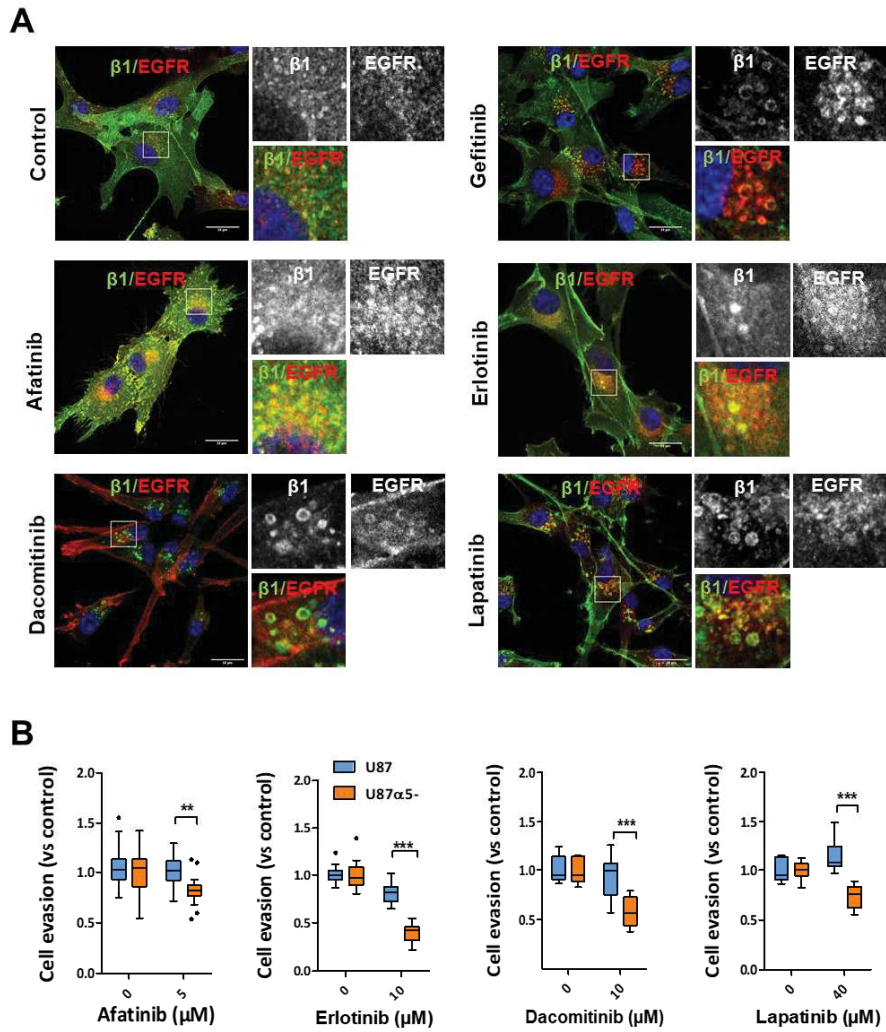


**Supplemental Figure 1: Gefitinib provokes EGFR endocytosis in GBM cells.** (A) Immunodetection of EGFR (red) and the endosomal marker EEA1 (green) after 4h treatment with DMSO (control) or gefitinib in LN443 and T98G GBM cells. Magnified images are from the inserts to the peri-nuclear area. Scale bar = 20 μm. (B) Quantification of EGFR/EEA1 colocalization following gefitinib treatment from 10–12 images (3 independent experiments). \*\*\* $p < 0.001$ . (C–D) Endocytosis assays of EGF-Alexa488 was performed on LN443, T98G and LNZ308 cells during 1h in presence of gefitinib (20μM). The internalization was measured by integrating fluorescence density of 20–30 cells from 3 independent experiments. \*\*\*\* $p < 0.0001$ . (E) Immunoblot showing α5 integrin and EGFR expression in the 4 cell lines used in this study.

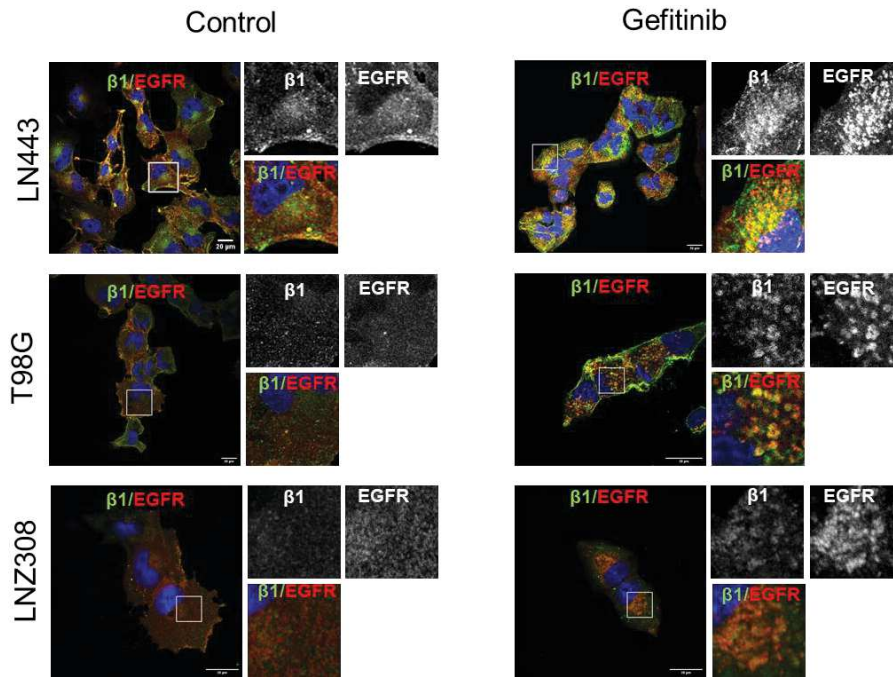




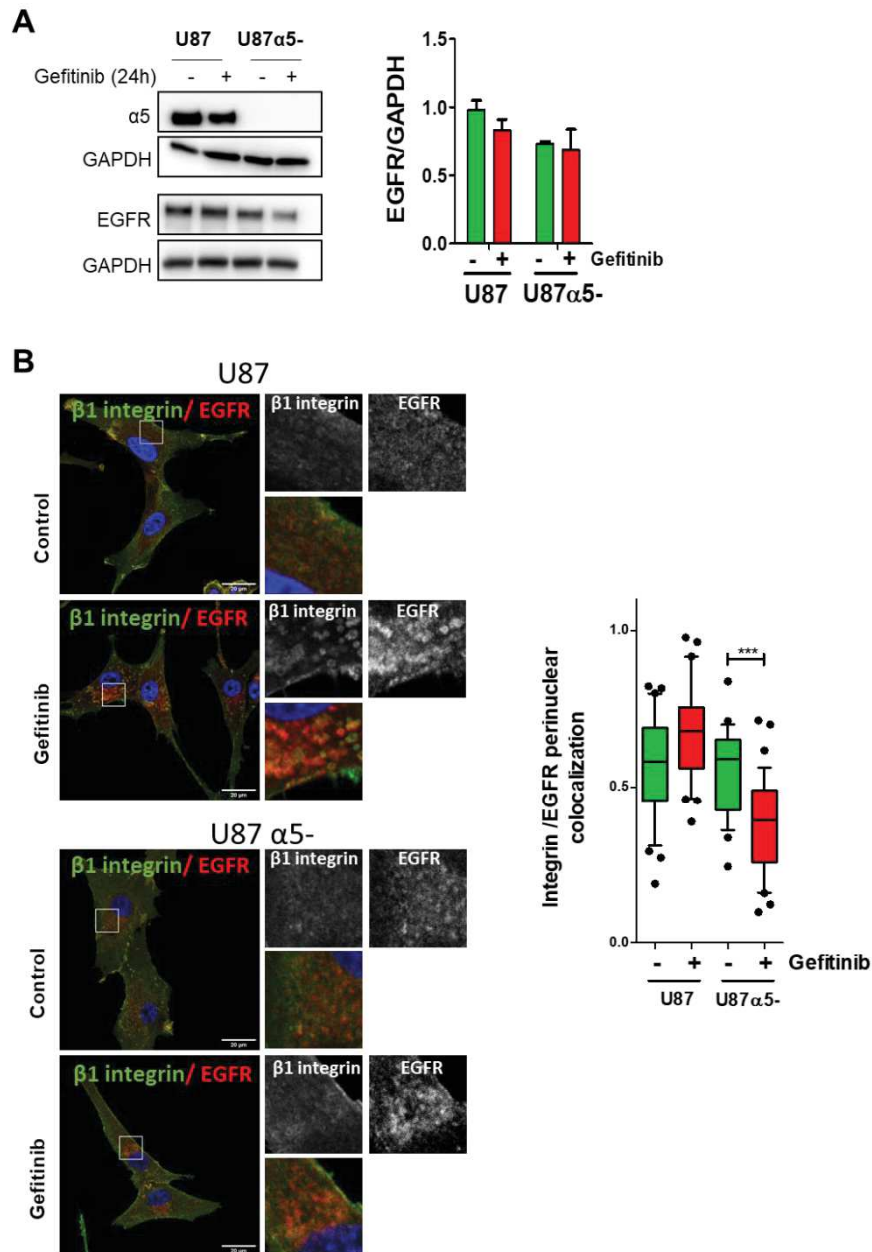
**Supplemental Figure 2: Gefitinib provokes integrin re-localization in early endosomes.** (A) Fluorescence microscopy images of U87 cells treated with gefitinib showing peri-nuclear co-localization of the  $\beta$ 1 integrin (cyan) and the early-endosome marker Rab5 (red). (B) The Pearson correlation and Mander's coefficient were used to quantify the degree of colocalization between the  $\beta$ 1 integrin and Rab5. \*\*\* $p < 0.001$ .



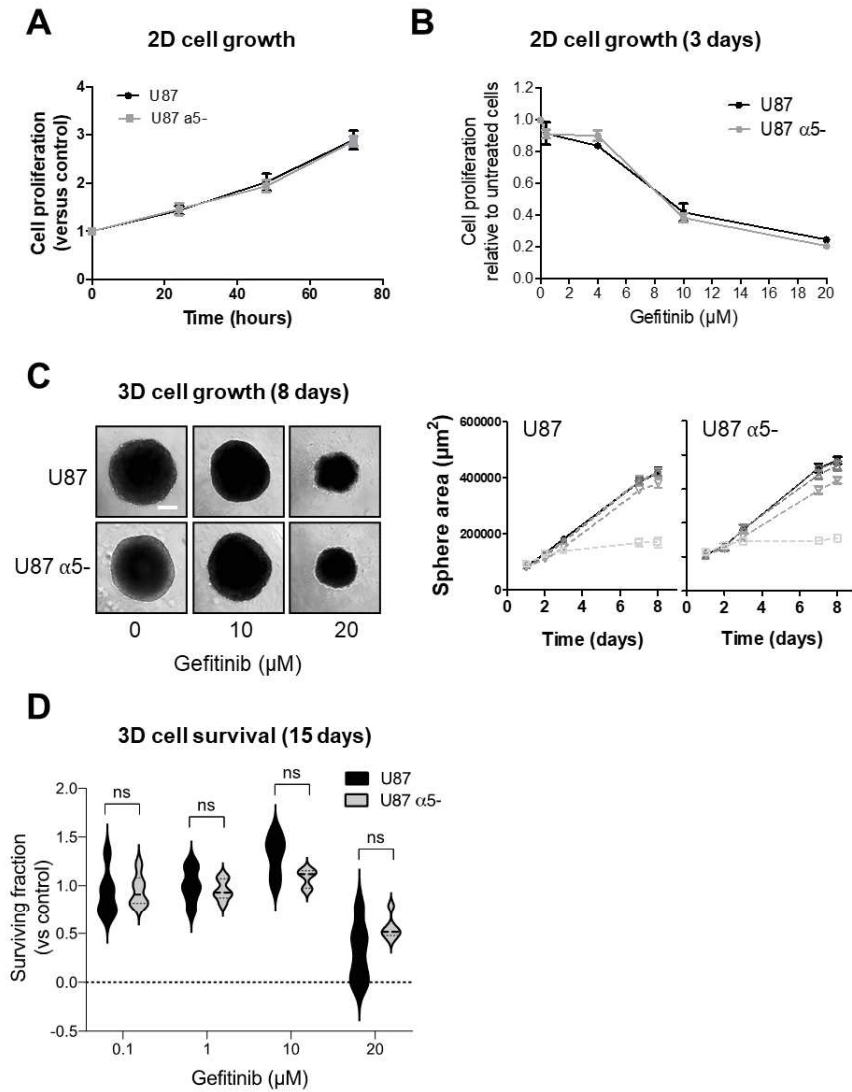
Supplemental Figure 3: Second and third-generation TKIs also induce co-internalization of  $\alpha 5\beta 1$  integrin and EGFR during U87 GBM cell evasion. (A) Confocal images of U87 cells treated with vehicle (control) or TKIs gefitinib (20  $\mu\text{M}$ ), afatinib (5  $\mu\text{M}$ ), erlotinib (10  $\mu\text{M}$ ), dacomitinib (10  $\mu\text{M}$ ) or lapatinib (10  $\mu\text{M}$ ). Images are representative of 3 independent experiments. High-magnification images are from the inserts into the peri-nuclear area. Scale bar = 20  $\mu\text{m}$ . (B) Quantification of the number of evading cells from U87 and U87 $\alpha 5$ - treated spheroids. Spheroids were incubated for 24 hours in the presence of DMSO or different TKIs (erlotinib, dacomitinib, lapatinib and afatinib) at the indicated concentrations. Nuclei were stained with DAPI and the number of evading cells was quantified using an ImageJ homemade plugin. Mean of 15 spheroids from 3 independent experiments. \*\* $p < 0.05$ , \*\*\* $p < 0.001$ .



**Supplemental Figure 4: Gefitinib treatment provokes integrin/EGFR relocation in endosomal compartments of GBM cell lines.** Confocal images showing the intracellular locations (perinuclear region enriched in endomembrane) of EGFR and  $\beta 1$  integrin in LN443, T98G and LNZ308 gefitinib-treated cells.



**Supplemental Figure 5: Gefitinib treatment does not affect the expression of total EGFR in U87 cells.** Left panel: (A) Protein expression of EGFR and  $\alpha$ 5 integrin in U87 GBM cells and U87 $\alpha$ 5- cells after 24h treatment with DMSO (-) or gefitinib 20 $\mu$ M (+). GAPDH was used as loading control. Right panel: Histogram showing the quantification of GAPDH-normalized EGFR level of 3 independent experiments. Data represented are the mean  $\pm$  s.e.m. (B) Quantification of the ratio integrin/EGFR colocalized pixels in the perinuclear compartments of U87 or U87 $\alpha$ 5- cells that migrated at distance from spheroids after 24 hours of incubation in presence of 20 $\mu$ M gefitinib or DMSO (control). The degree of colocalization between the integrin  $\beta$ 1 and EGFR was quantified using an home-made plugin with the ImageJ software. Data expressed as box and whiskers are from at least 30 cells from 10 different fields.



**Supplemental Figure 6:  $\alpha 5$  expression does not affect U87 cell sensitivity to gefitinib in cell growth and cell survival experiments.** (A) Comparative time course of U87 and U87 $\alpha 5^-$  cells 2D growth in serum-containing medium. (B) Dose-response curve of gefitinib on 2D cell growth after 3 days of treatment. (C) Left panel: phase contrast images of spheroids after 8 days of treatment with indicated concentration of gefitinib. Right panel: dose-response curves of gefitinib on spheroid growth. (D) Clonogenic assay in soft agar comparing U87 and U87 $\alpha 5^-$  cell survival in presence of the indicated concentrations of gefitinib.

## Article 2

### Role of endocytosis proteins in gefitinib-mediated EGFR internalization in gliomas cells.

**Authors:** E. Cruz Da Silva<sup>1</sup>, L. Choulier<sup>1</sup>, J. Thevenard-Devy<sup>2</sup>, C. Schneider<sup>2</sup>, M. Dontenwill<sup>1</sup>, S Dedieu<sup>2</sup>, M. Lehmann<sup>1</sup>.

1-University of Strasbourg, Laboratory of Bioimaging and Pathologies – UMR CNRS 7021, Illkirch, France

2- UMR CNRS 7369, Matrice Extracellulaire et Dynamique Cellulaire (MEDyC), Université de Reims Champagne Ardenne (URCA), Reims, France.

#### Abstract

EGFR (epidermal growth factor receptor), a member of the ErbB tyrosine kinase receptor family, is a clinical therapeutic target in numerous solid tumors. EGFR overexpression in glioblastoma (GBM) drives cell invasion and tumor progression. However, clinical trials were disappointing, and we are still missing a molecular basis to explain these poor results. EGFR endocytosis and membrane trafficking which tightly regulates EGFR oncosignaling are often dysregulated in glioma. In a previous work, we showed that EGFR tyrosine kinase inhibitors, like gefitinib, lead to a massive and ligand-independent EGFR endocytosis into fused early-endosomes. Here, using pharmacological inhibitors, siRNA-mediated silencing, or expression of mutant proteins we showed that in glioma cells dynamin 2 (DNM2), the small GTPase Rab5 and the endocytosis receptor LDL receptor-related protein 1 (LRP-1) contribute significantly in gefitinib-mediated EGFR endocytosis. Importantly, we showed that DNM2 or LRP-1 targeting inhibited gefitinib-mediated endocytosis and decreased glioma cell responsiveness to gefitinib during cell evasion from tumor spheroids. By highlighting the contribution of endocytosis proteins in the activity of gefitinib on glioma cells, this study suggests that endocytosis and membrane trafficking might be an attractive therapeutic target to improve GBM treatment.

## Introduction

EGFR (epidermal growth factor receptor), a member of the ErbB tyrosine kinase receptor family, is commonly found amplified and/or mutated in near 60% of glioblastoma (GBM), the most aggressive brain tumor. In GBM, activated EGFR promotes PI3K/Akt (Phosphatidylinositol-Kinase/Akt), MAPK/ERK (mitogen-activated protein kinases/ extracellular signal-regulated kinases), signal transducer and activator of transcription 3 (STAT3), and phospholipase C gamma signalling cascades. These EGFR transduced signals promote GBM cell proliferation and invasion, and tumor progression (An et al., 2018; Eskilsson et al., 2018)

EGFR signalling function is tightly regulated by endocytosis and membrane trafficking. Physiological EGFR endocytosis can occur through different pathways such as clathrin-mediated endocytosis and non-clathrin endocytic pathway, depending on the nature and concentration of the ligand. Upon-vesicle formation, dynamin-2 (DNM2), a GTPase protein, is recruited to pinch the vesicle from the plasma membrane (Henriksen et al., 2013; Sigismund et al., 2008) giving rise to early endosomes (EE). In the EE, EGFR fate is decided, where the receptor is either transported to lysosomes for degradation or recycled back to the plasma membrane (Tomas et al., 2014). A critical group of endocytic regulators are the Ras-associated binding (Rab) proteins. In EE, Rab5 is responsible for cargo entry from the plasma membrane to the EE, generation of phosphatidylinositol-3-phosphate (PtdIns(3)P) lipid, homotypic fusion and actin/microtubules motility of EE and activation of endosomal signalling pathways (Jovic et al., 2010).

In GBM, altered expression of EGFR membrane trafficking regulators, resulting in aberrant EGFR localization, has been associated with tumor progression and therapy resistance to EGFR-targeted therapies (Al-Akhrass et al., 2017; Kondapalli et al., 2015; Walsh et al., 2015; Wang et al., 2019; Ying et al., 2010). Dysregulation of EGFR trafficking also occurs upon receptor mutation. For instance, EGFRvIII, the most common EGFR mutant in GBM, is inefficiently degraded as a consequence of a high rate of recycling to the plasma membrane (Grandal et al., 2007) or its translocation to the mitochondria wherein it triggers resistance to apoptosis (Cao et al., 2011).

Other studies have shown that EGFR trafficking is altered during therapeutic interventions and enlighten that this process may have important impact on patient therapeutic responses (Tan et al., 2016). Compared to physiological situation, under therapeutic stress, EGFR follows distinct

endocytosis and trafficking routes in a ligand- and tyrosine kinase- independent way (Tan et al., 2015; Tomas et al., 2015). For instance, *in vitro* studies indicate that X-ray irradiation of human bronchial carcinoma cells promotes caveolin1-mediated EGFR internalization, in a Src (Proto-oncogene tyrosine-protein kinase) kinase activity dependent. After being internalized, EGFR is transported to the nucleus where it activates DNA-PK (Deoxyribonucleic acid-dependent protein kinase) phosphorylation and enhances double strand breaks repair (Dittmann et al., 2005). Moreover, cisplatin treatment induces EGFR endocytosis and its accumulation into multivesicular bodies (MVB), through the activation of the stress-induced p38-MAPK pathway (Tan et al., 2016; Tomas et al., 2015; Zwang and Yarden, 2006). EGFR accumulation in MVB activates ERK pathway to delay apoptosis and to promote chemoresistance (Tomas et al., 2015). It has also been shown that EGFR-targeting antibodies used in clinic or ongoing clinical development are able to induce EGFR internalization (Jones et al., 2020; Keir et al., 2018; Liao and Carpenter, 2009). Additionally, it has been shown that EGFR-targeting tyrosine kinase inhibitors (TKIs) also disturb EGFR trafficking in GBM cells and various other cancer cell types. TKI can trigger EGFR translocation, in autophagy compartment (Tan et al., 2016), in mitochondria (Cao et al., 2011) or in nucleuses (Dittmann et al., 2005).

Dysregulation of EGFR trafficking play an essential role in cancer progression and response to anti-EGFR therapies. In a previous work, we showed that gefitinib and others TKIs promote massive EGFR endocytosis and EGFR accumulation in fused early endosomes (Blandin et al., 2020). The aim of the present work was to identify key proteins that contribute to gefitinib-mediated EGFR endocytosis. In the present study, we identified the contribution of 3 endocytic proteins DNM2, Rab5 and the LDL receptor-related protein 1 (LRP-1) in this process. Importantly, inhibiting endocytosis by targeting DNM2 or LRP-1 protects glioma cells against TKI treatment during cell dissemination from tumor spheroids. The present study enlightens the importance of endocytosis proteins in gefitinib anti-tumoral effects on glioma cells.

## **Material and methods**

### Reagents

Following antibodies were used for immunostaining. Anti-EGFR antibody (D1D4J) was from Cell Signaling. Anti-EEA1 (610457) was from BD Transductions. Anti-LRP-1 (8G1) was from Genetex. Fluorescently labeled secondary antibodies were purchased from Invitrogen (AlexaFluor -488; -568; -647). DAPI was purchased from Santa Cruz Biotechnology.



Following antibodies were used for immunoblot. Anti-EGFR antibody (D38B1) were from Cell Signaling, anti-LRP-1 (PPR3724) from Abcam, anti-DNM2 (G-4) and anti-Rab5 (D-11) were from Santa Cruz and GAPDH from Millipore. HRP-conjugated secondary antibodies were purchased from Invitrogen. Cell culture medium and reagents were from Lonza. Tyrosine kinase inhibitors, dynasore and dyngo-4a were obtained from ChemiTek. His-tagged RAP was purified by gravity-flow chromatography using a nickel-charged resin as described previously (Perrot et al., 2012). All other reagents were of molecular biology quality.

### Cell culture

The human glioblastoma cell line U87 was obtained from ATCC, T98 cells were from ECACC (European Collection of Authenticated Cell Cultures, Sigma). LN443 cells were kindly provided by Prof. Monika Hegi (Lausanne, Switzerland). GBM cells were maintained in Eagle's minimum essential medium (EMEM) supplemented with 10% fetal bovine serum (FBS), 1% sodium pyruvate and 1% nonessential amino acid, in a 37 °C humidified incubator with 5% CO<sub>2</sub>.

### Plasmid transfection

YFP-Rab5 (kindly provided Dr. Marino Zerial (MaxPlanck Institut, Germany)), GFP-Rab5S34N (Addgene #35141) and GFP-Rab5Q79L (Addgene #35140), siGENOMETM Non-targeting siRNA pools (Dharmacon D-001206-14-05), siRNA-DNM2 (Dharmacon M-004007-03-0005), siRNA-LRP-1 (Dharmacon M-004721-01-0005) plasmids were used. A total of  $0.25 \times 10^6$  cells was used for each transient transfection using 1.5 µg for expression plasmid or 50 nM for siRNA using JetPrime® (PolyPlus-Transfection) following the manufacturer's instructions. Fusion protein expression was confirmed by fluorescent microscopy the day after and downregulation of DNM2 or LRP-1 was assessed by immunoblot 72h after siRNA transfection.

### EGF endocytosis and uptake quantification

EGF coupled to AlexaFluor 488 (Molecular Probes, Invitrogen) was used for studying the ligand-induced EGFR endocytosis. For EGF uptake, cells were plated on coverslips previously coated with Collagen-I (20 µg. ml<sup>-1</sup> in DPBS) (Advanced BioMatrix). Cells were serum starved for 1h at 37 °C. Cells were first washed in ice-cold DPBS and then incubated on ice in serum-free culture medium containing 100 ng.ml<sup>-1</sup> AlexaFluor 488-EGF. After incubation on

ice for 30 min, cells were briefly washed with ice-cold DPBS. Cells fixed at this step were used as negative control. Otherwise, cells were incubated with pre-warmed complete medium at 37°C for 1h in the presence of 20  $\mu$ M gefitinib and pharmacological inhibitors as indicated. Non-internalized EGF was strip by incubating the cells with a solution of sodium acetate 0.2M pH 2.7 for 5 min on ice. After washing, cells were fixed and stained with DAPI. Images were acquired using a confocal microscope. The analysis was performed after a threshold (identical for all conditions) applied to eliminate background. The integrated fluorescence intensity of EGF-Alexa488 was determined in each cell. Image analysis was performed using ImageJ in between 20 cells per condition on 3 independent experiments.

#### Cell-surface EGFR endocytosis assay

Subconfluent cells were placed at 4°C to prevent internalization, washed twice with ice-cold Hank's Balanced Salt Solution containing 0.5 mM MgCl<sub>2</sub> and 1.26 mM CaCl<sub>2</sub> (Ca/Mg-HBSS) adjusted to pH 8, then incubated for 30 min with 1 mg.ml<sup>-1</sup> EZ-Link Sulfo-NHS-LC-Biotin in Ca/Mg-HBSS. After washing with ice-cold Ca/Mg-HBSS, free biotin was quenched with 20 mM glycine in Ca/Mg-HBSS. Following cell-surface biotinylation, cells were incubated 2 hours at 37°C in complete medium (w/wo gefitinib and/or RAP), to allow endocytosis. Cells were quickly replaced on ice, washed thrice with ice-cold Ca/Mg-HBSS, then washed twice to remove biotin to cell-surface proteins with 300 mM Mesna in buffer composed of Tris 50 mM pH 8,6, NaCl 100 mM, EDTA 1 mM, BSA 0,2%. Cells were rinsed twice with Ca/Mg-HBSS, incubated with iodoacetamide (5 mg ml) in Ca/Mg-HBSS, then washed with Ca/Mg-HBSS. To determine the total amount of surface biotinylation and to serve as a control, dishes were kept on ice after biotin labeling and protected from MesnNa treatment. Whole-cells extracts were prepared, and biotinylated proteins were recovered from 100  $\mu$ g of cell lysate by using avidin protein immobilized on agarose beads, subjected to SDS-PAGE, and revealed by immunoblotting with anti-EGFR.

#### Immunoblot

Proteins were separated on precast gradient 4-20% SDS-PAGE gels (Bio-Rad) and transferred to PVDF membrane (GE Healthcare). Membranes were probed with primary antibodies: anti-EGFR antibody, anti-DNM2, anti-Rab5 and anti-LRP-1 at 1 $\mu$ g.ml<sup>-1</sup> and anti-GAPDH at 0.2 $\mu$ g.ml<sup>-1</sup> in blocking solution (TBS- 5% non-fat dry milk). Immunological complexes were revealed with anti-rabbit or anti-mouse IgG coupled peroxidase antibodies using

chemoluminescence (ECL, Bio-Rad) and visualized with LAS4000 image analyser (GE Healthcare). GAPDH was used as the loading control for all samples.

### Confocal microscopy and Image Analysis

Coverslips were coated with Collagen-I (20  $\mu\text{g. ml}^{-1}$  in DPBS). 20 000 cells were seeded in serum containing medium and cultured for twenty-four hours before TKI treatment. Alternatively, two-day-old spheroids were seeded in complete medium and treated with 20  $\mu\text{M}$  of gefitinib. Cells were fixed in 3.7% (v/v) paraformaldehyde (Electron Microscopy Sciences) during 20 min, permeabilized with 0.1% Triton-X100 for maximum 5 min. After 3 hours blocking step using PBS-BSA 3% solution, cells were incubated with primary antibodies O/N at 4 °C (2  $\mu\text{g. ml}^{-1}$  each in PBS-BSA 3%). Cells were rinsed in PBS 1X and incubated with appropriate secondary antibodies (1  $\mu\text{g. ml}^{-1}$  in PBS-BSA 3%) and DAPI for 2 hours. Samples were mounted on microscope slides using fluorescence mounting medium (Dako). Images were acquired using a confocal microscope (LEICA TCS SPE II, 60 $\times$  magnification oil-immersion). For each experiment, identical background subtraction was applied to all images. Pearson correlation coefficient from 8 images (2-4 cells per images) from 3 independent experiments were calculated using Colocalization\_Finder ImageJ software. 3D reconstruction corresponds to confocal images Z-stacks obtained using stacks of 350 nm. 3D image reconstruction was performed using IMARIS software.

### Spheroid migration assays

Methylcellulose solution was made as previously described (Blandin et al., 2016). Single cell suspension was mixed in EMEM/10%FBS containing 10% of methylcellulose. All the spheroids were made with 1000 cells by hanging drop methods in a 20  $\mu\text{L}$  drop (Blandin et al., 2016). Tissue culture plastic dishes were previously coated with 10  $\mu\text{g.ml}^{-1}$  of Collagen-I in DPBS solution for 2 h at 37 °C. Two-day-old spheroids were allowed to adhere and migrate in complete medium (EMEM, 10% FBS). Twenty-four hours later, cells were fixed with paraformaldehyde 3.7% and nucleus were stained with DAPI. Nucleus were picturized under the objective 5x in the fluorescence microscope ZEISS-Axio (ZEISS). Image analysis to evaluate the number of cells that migrated out of the spheroid was performed with ImageJ software using a homemade plugin.

### Statistical analysis

Data are reported as mean  $\pm$  95% confidence interval column histograms unless otherwise stated. Statistical analysis between samples was done by one-way analysis of the variance (ANOVA) followed by Bonferroni post-test with the GraphPad Prism program, unless otherwise stated. Significance level is controlled by 95% confidence interval.

## Results

### Knock-down of DNM2 decreases gefitinib-mediated EGF endocytosis

We have previously shown that in U87, T98 and LN443 GBM cells, cytostatic concentrations of gefitinib lead to the accumulation of EGFR in enlarged early-endosomes and promote a massive increase in EGF endocytosis, a phenomenon we called gefitinib-mediated endocytosis (GME) (Blandin et al., 2020). To better characterize the molecular mechanisms underlying GME, we first seek to determine the potential involvement of DNM2 which is critical in physiological EGFR endocytosis (Sousa et al., 2012). As shown by immunoblot experiments, DNM2 is expressed in the three GBM cell lines used in this study (Figure S1). We firstly examined the effect of dynasore and dyngo-4A, two potent pharmacological inhibitors of DNM2 GTPase activity (Kirchhausen et al., 2008; Robertson et al., 2014), on EGF-Alexa488 endocytosis in U87 cells. As previously described (Blandin et al., 2020), compared to physiological untreated-conditions, gefitinib addition in the culture medium of U87 cells increased EGF endocytosis as shown by its strong intracellular accumulation (Figure 1A). Importantly, addition of dynasore in culture medium clearly decreased intracellular EGF endocytosis in both control (DMSO-treated) or gefitinib-treated cells. Quantification of integrated fluorescence in each cell confirmed, as expected, that dynasore (12 $\mu$ M) and dyngo-4A (10 $\mu$ M) were able to inhibit physiological EGF endocytosis by 86% and 49% respectively, which is in agreement with the established role of DNM2 in EGFR ligand-endocytosis (Sousa, PNAS 2012). As already been published, gefitinib (20 $\mu$ M) increased by 3- fold EGF endocytosis. Interestingly, dynamin inhibitors significantly inhibited GME of EGFR (96% for dynasore and 53% for dyngo4A) (Figure 1A-right panel). As shown in Figure 1B, dynasore and dyngo-4a inhibited GME in both T98 and LN443 cell lines, confirming data obtained with U87 cells. To further confirm the involvement of DNM2 in gefitinib-mediated EGF endocytosis, we silenced DNM2 expression in U87 cells using siRNA strategy. SiRNA-DNM2 efficiently repressed DNM2 expression and had no impact on EGFR expression (Figure 1C). DNM2 downregulation inhibited physiological EGF-Alexa448 endocytosis. Of note, siRNA-DNM2

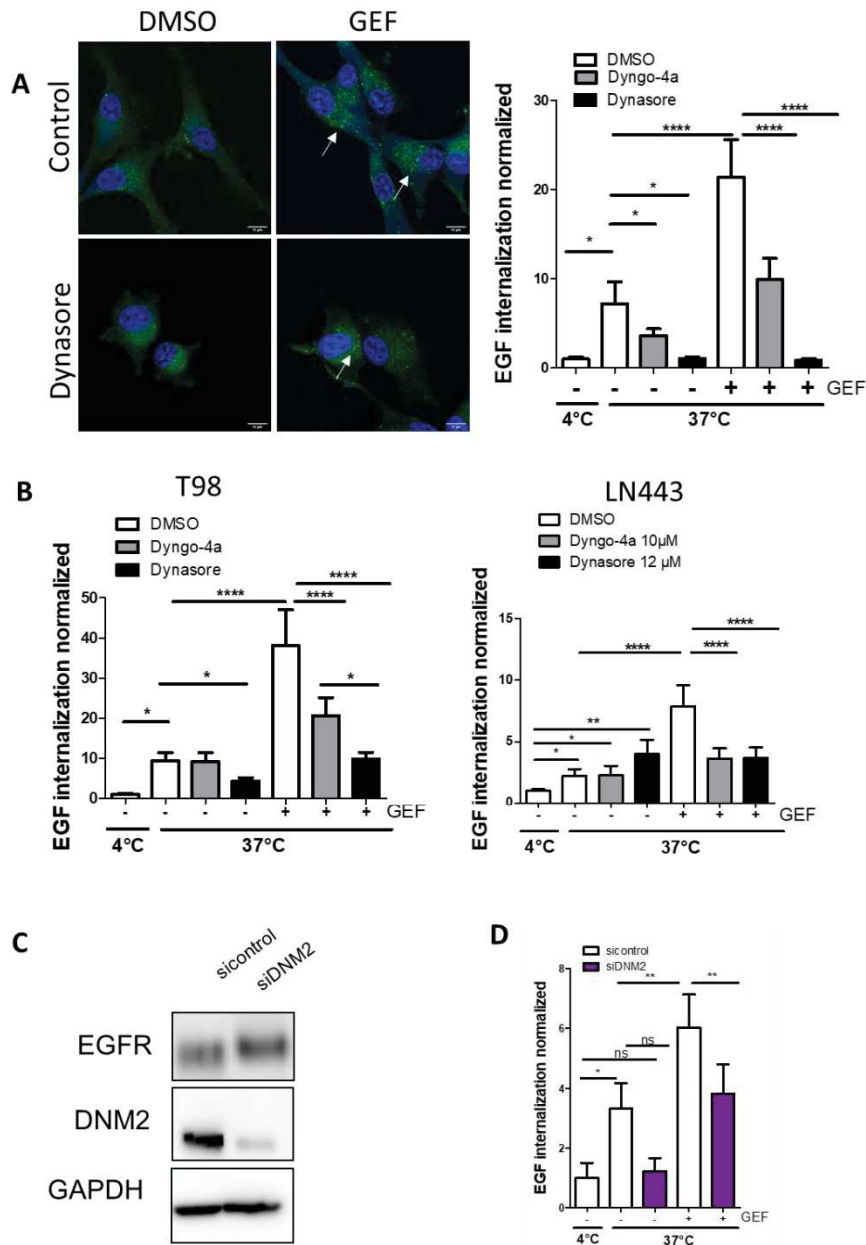


**Figure 1- Gefitinib-mediated EGF internalisation is dependent of DNM2.** EGF-internalization assays were performed in the presence gefitinib (20µM) during 1 hour. **(A, B)** DNM2 GTPase activity was inhibited by either dynasore (12µM) or dyngo-4a (10µM) **(A) Left panel:** confocal images of control and dynasore-treated cells, showing, in green, fluorescence internalized EGF-Alexa 488 upon incubation at 37°C. Arrows enlighten internalized EGF. Scale bar = 12µm **Right panel:** the internalization was quantified by integrated fluorescence density on 20 cells of 3 independent experiments. Data are reported in columns histograms. \*\*\*\*p < 0.0001. **(B)** Results were confirmed in other GBM cell lines. EGF-internalization assay was performed in T98 and LN443 cells using dynasore and dyngo-4a. \*\*\*\*p < 0.0001. **(C)** Downregulation of DNM2 expression was obtained by 50 nM of siRNA transiently transfected using JetPrime®. DNM2 silencing was confirmed by immunoblot after 72h. EGFR protein level was also immunoblotted and remained constant in both conditions. GAPDH was used as loading control. **(D)** EGF-internalization assay was performed on U87 cells transfected with siRNA-control or U87 siRNA-DNM2. \*\*p < 0.01.

also dampened EGF internalisation of gefitinib treated cells (Figure 1D), confirming that GME is dependent of DNM2 expression and function.

### **Gefitinib-mediated EGFR endocytosis requires Rab5 activation**

The monomeric GTPase Rab5 has been shown to play an essential function during EGFR endocytosis (Barbieri et al., 2000; Chen et al., 2009; Dinneen and Ceresa, 2004). Notably, overactivation of Rab5 leads to EGFR accumulation in large, fused endosomes (Ceresa et al., 2001; Chen and Wang, 2001; Dinneen and Ceresa, 2004). In the first few hours of gefitinib treatment, GME is also characterized by the formation of enlarged early-endosomes that accumulates EGFR (Blandin et al., 2020). Thus, we seek to determine the potential role of Rab5 in GME. First, we transiently expressed a recombinant wild-type Rab5 (YFP-Rab5) or a constitutively active Rab5 mutant (GFP-Rab5-Q79L) in U87 cells. In line with data from Ceresa's studies, we observed that overexpression of GFP-Rab5-Q79L, and to a lesser extent YFP-Rab5, triggered an accumulation of EGFR into enlarged early endosome antigen 1 (EEA1)-positive early endosomes (Figure 2A). Quantification of EGFR/EEA1 co-localization was performed in each cell expressing or not GFP-Rab5-Q79L (Figure 2B). As expected, EGFR/EEA1 co-localization was increased in cells expressing constitutively active Rab5 compared to non-expressing cells. We next assessed whether Rab5 activation is required for GME. For this purpose, we analysed EGFR recruitment into early endosomes in U87 cells that transiently expressed the dominant-negative (DN) Rab5 mutant (GFP-Rab5-S34N) compared to non-expressing cells. As shown in Figures 2C and 2D, after 2h of gefitinib treatment, DN-Rab5 null cells were sensitive to TKI, and presented a significant increase in EGFR/EEA1 colocalization. By contrast, in GFP-Rab5-S34N expressing U87 cells, EGFR was barely found in EEA1-positive endosome after gefitinib treatment (Figure 2C) and image quantification showed that gefitinib failed to promote EGFR/EEA1 co-localization (Figure 2D). These data showed that GME requires Rab5 activation and suggest that gefitinib may activate Rab5 by a still unknown mechanism. Furthermore, these results enlighten that GME shares common features with physiological endocytosis of EGFR

### **LRP-1 and EGFR are co-endocytosed upon gefitinib treatment**

Global endocytosis processes appear to be affected by gefitinib treatment thus opening up the possibility that, like Rab5 or DNM2, other endocytosis proteins may be involved in GME. The low-density lipoprotein receptor-related protein-1 (LRP-1) is a large multifunctional endocytic

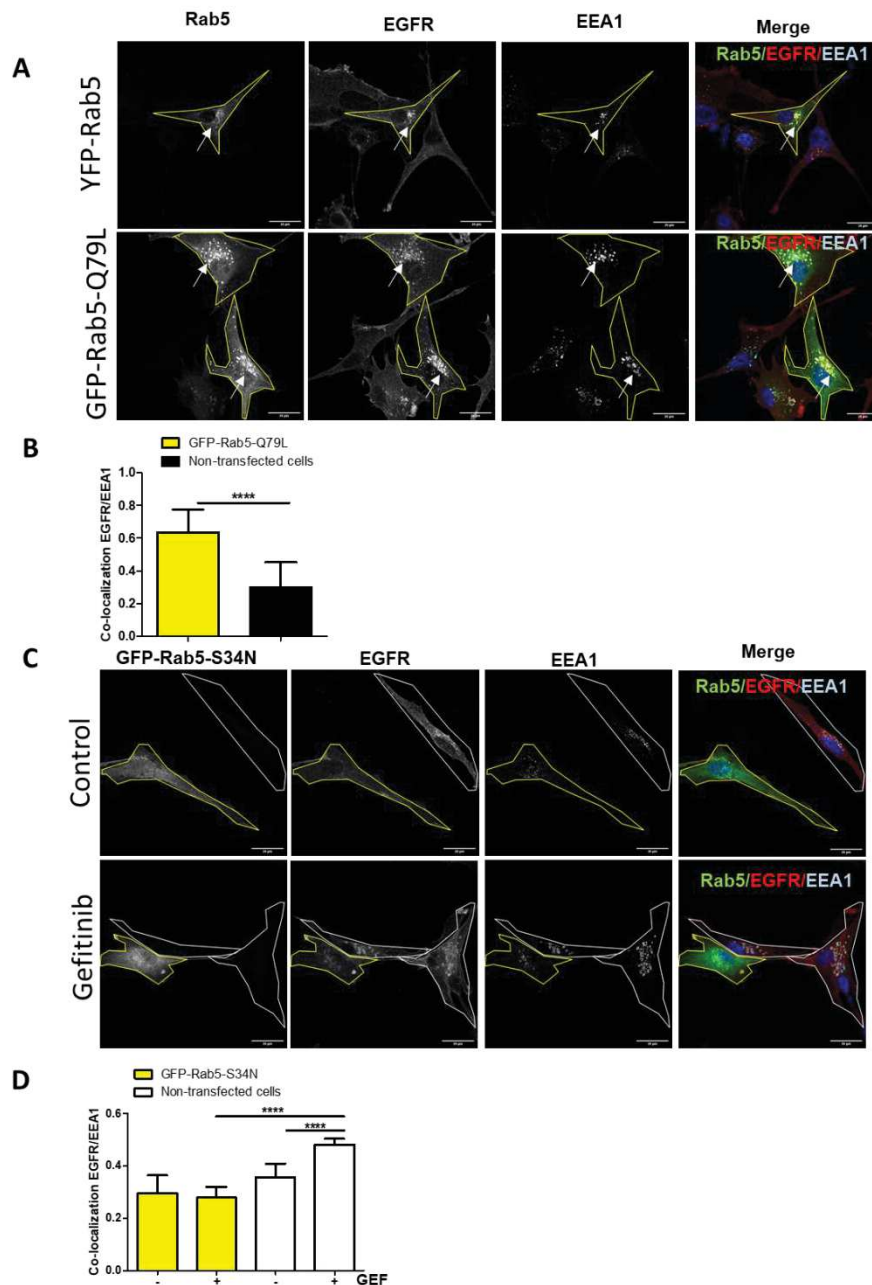


**Figure 2- EGFR GME requires Rab5 activation.** (A) U87 cells that transiently expresses a recombinant wild-type Rab5 (YFP-Rab5) (green) or a constitutively active Rab5 mutant (GFP-Rab5-Q79L) (green) were seeded on glass coverslips. Cells were fixed, then EGFR (red) and EEA1 (cyan) were immunodetected and analyzed by confocal imaging. Single or merge channel images are represented. Transfected cells are delimited in yellow in all images. Arrows enlighten internalized EGFR. Scale bar = 20  $\mu$ m. (B) EGFR/EEA1 co-localization on cells transfected with GFP-Rab5-Q79L (yellow) and no transfected cells (black) was evaluated using Pearson's correlation coefficient from 10 images (2-4 cells per images). Data are reported in column histogram. \*\*\*\* $p < 0.0001$ . (C) U87 cells that transiently expresses a dominant negative Rab5 mutant (GFP-Rab5-S34N) (green) were seeded on glass coverslips. After 4 hours of treatment with 20  $\mu$ M of gefitinib, cells were fixed, then EGFR (red) and EEA1 (cyan) were immunodetected and analyzed by confocal imaging. Single or merge channel images are represented. Positive cells for GFP-Rab5-S34N are delimited in yellow and no transfected cells in white. Arrows enlighten GME internalized EGFR. Scale bar = 20  $\mu$ m. (D) EGFR/EEA1 co-localization upon gefitinib treatment in each cell negative (white bars) and positive (yellow bars) for GFP-Rab5-S34N was evaluated using Pearson's correlation coefficient from 8 images (2-4 cells per images) from 3 independent experiments. Data are reported in column histogram. \*\*\*\* $p < 0.0001$ .

receptor belonging to the low-density lipoprotein receptor family. LRP-1 is a transmembrane receptor involved in the endocytosis of more than 30 different ligands including growth factor receptors, however, no functional interaction with EGFR has been yet established (Etique et al., 2013). Data depicted in Figure S1 indicates that LRP-1 was expressed in the three GBM cell lines studied. We then analysed the impact of gefitinib on LRP-1 and EGFR localization in cells that were treated for 24h with gefitinib (Figure 3). Confocal imaging and 3D reconstructed images revealed that in U87 control cells EGFR was mainly present at the cell-surface level and that LRP-1 was distributed in small intracellular vesicles and at the plasma membrane (Figure 3A-left panel and online movie 1). Upon gefitinib-treatment, EGFR was massively translocated in large LRP-1-positive endosomes, suggesting a co-trafficking of both receptors (Figure 3A-right panel and online movie 2). We obtained similar results on T98 and LN443 cell lines (Figure 3B). Image analysis showed that gefitinib treatment significantly increased EGFR/LRP-1 co-localization in the three GBM cell lines (Figure 3C). These data enlighten that gefitinib triggered EGFR and LRP-1 co-endocytosis and trafficking.

### **LRP-1 is involved in gefitinib-mediated EGFR endocytosis**

We then sought to determine whether LRP-1 may have any impact on gefitinib-mediated EGFR endocytosis. To this end, we first used the recombinant protein RAP (receptor-associated protein) an endogenous competitive antagonist of LRP-1 binding to extracellular ligands (Bu and Schwartz, 1998; Bu et al., 1995). Confocal images in Figure 4A showed that addition of RAP decreased fluorescent EGF accumulation in intracellular vesicles upon gefitinib treatment. Quantification of integrated fluorescence in individual cells, showed that RAP had limited impact on physiological EGFR endocytosis but significantly inhibited gefitinib-mediated EGF endocytosis on U87 cells (Figure 4A-right panel). To confirm these data, we directly monitored EGFR endocytosis by cell surface biotinylation and confirmed that LRP-1 inhibition by RAP decreased EGFR internalization mediated by gefitinib (Figure 4B). To better demonstrate the role of LRP-1 in GME, we next used siRNA-mediated LRP-1 silencing in U87 cells. As depicted in Figure 4C, LRP-1 expression was efficiently downregulated by siRNA-LRP-1, while EGFR expression remained intact. EGF endocytosis assays revealed that LRP-1 knockdown inhibited gefitinib-induced EGF internalization in a similar extent compared to RAP treatment (Figures 4C and 4A). As observed on U87 cells, in T98 and LN443 cells, LRP-1 inhibition by RAP efficiently overrode the stimulation of EGF internalization by gefitinib but not the physiological endocytosis (Figure 4D and 4E). Endocytosis of cell surface biotinylated-



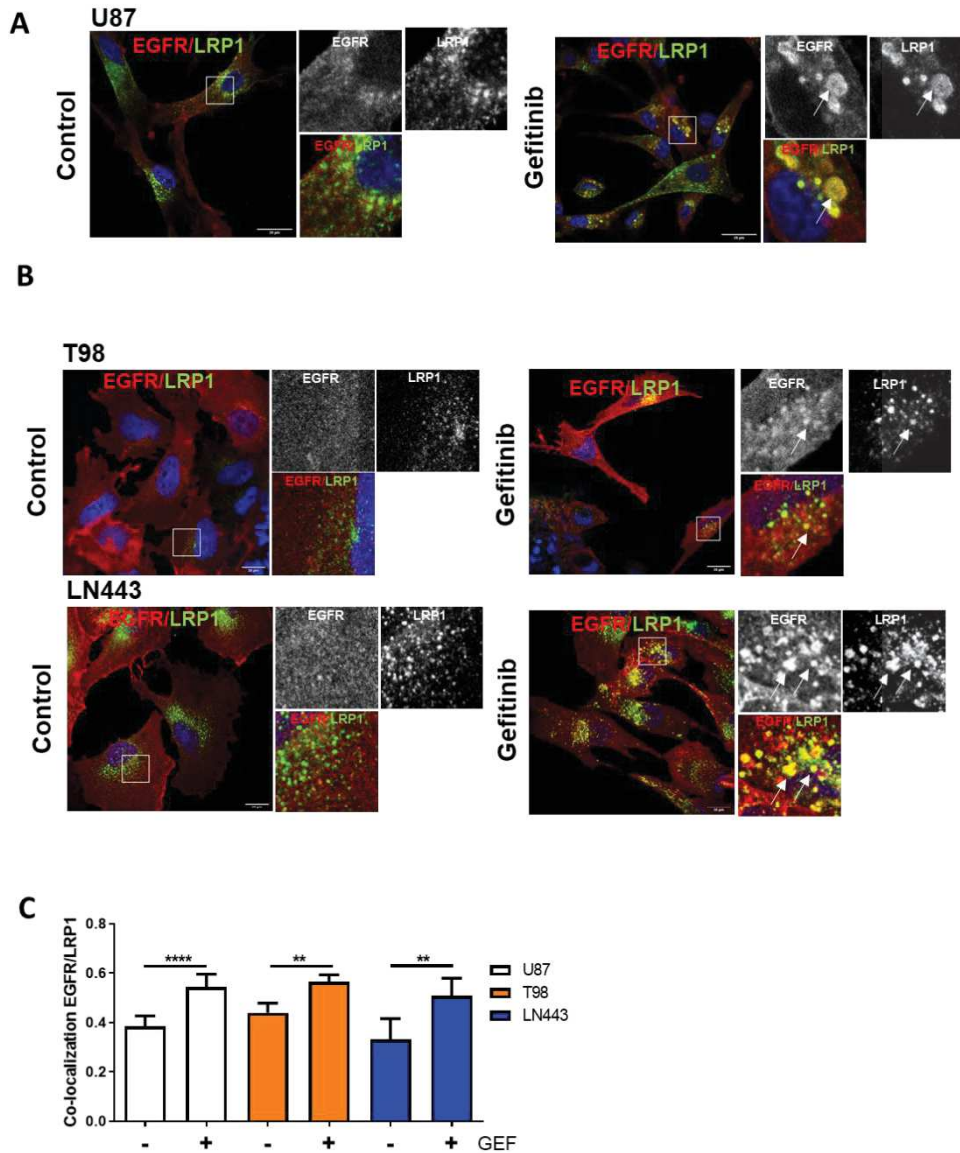


**Figure 3 – Gefitinib re-localizes EGFR on LRP-1-positive endosomes.** U87 (A), T98 and LN443 (B) two-days old spheroids were seeded on collagen-I-coated (20  $\mu\text{g.mL}^{-1}$ ) glass coverslips. After 24 hours of treatment with vehicle DMSO (Control) or 20  $\mu\text{M}$  of gefitinib (Gefitinib), spheroids were fixed, EGFR (red) and LRP-1 (green) were immunodetected and analysed by confocal microscopy. Magnified images are from the inserts into the peri-nuclear area, either in single channel or in merge. Arrows enlighten GME co-internalized EGFR and LRP-1. Scale bar = 20  $\mu\text{m}$ . (C) EGFR/EEA1 co-localization upon gefitinib treatment was determined using Pearson's correlation coefficient from 8 images (2-4 cells per images) from 3 independent experiments. Data are reported in column histogram. \*\* $p < 0.01$ , \*\*\*\* $p < 0.0001$ .

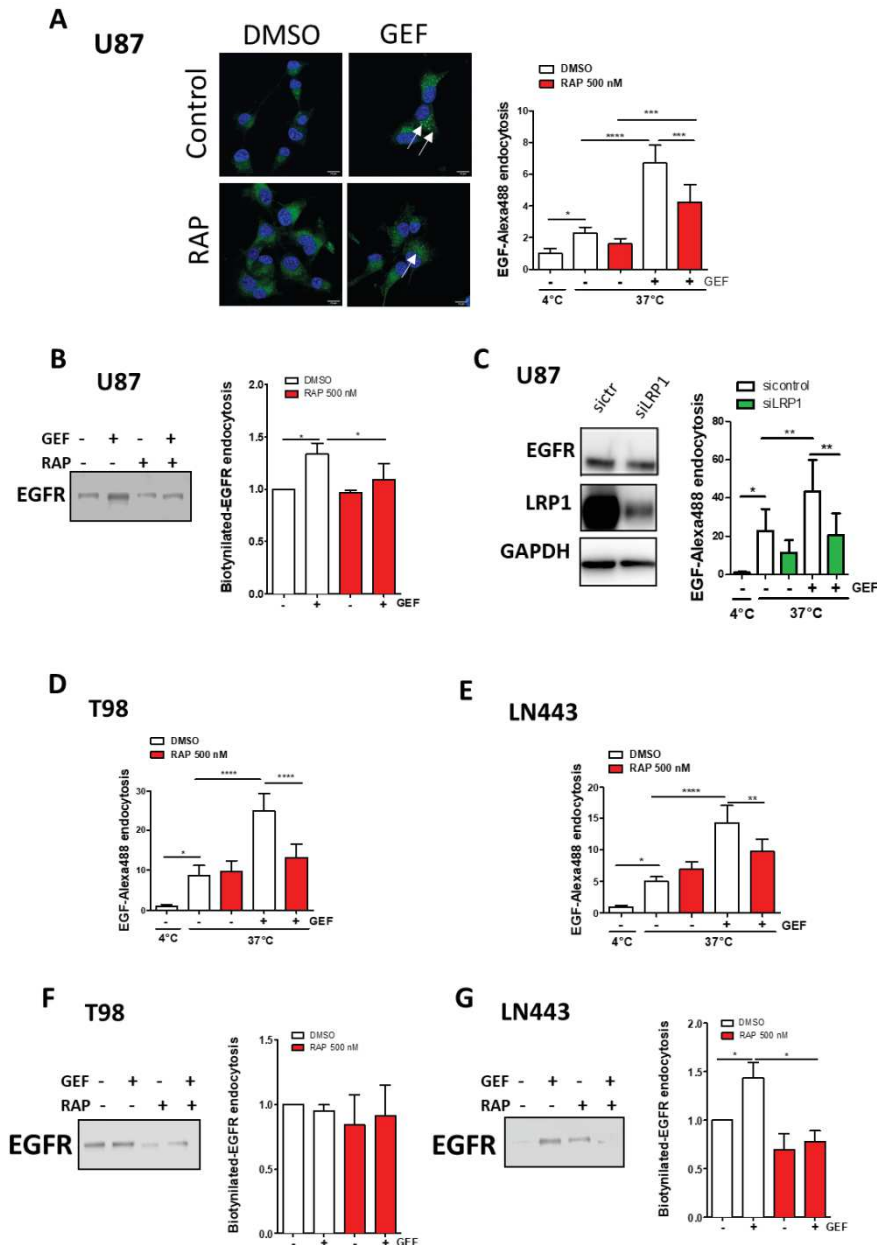


**Figure 4- Inhibition of LRP-1-mediated endocytosis decreases GME. (A)** After 30 min starvation, U87 cells were incubated 30 min at 4°C with 100 ng.mL<sup>-1</sup> EGF-Alexa 488 for EGF-internalization assay. The cells were replaced again in complete medium at 37°C for 1 hour to allow internalization of the ligand, in presence of 20 μM of gefitinib and/or 500nM of RAP for LRP-1 inhibition. Remaining cell surface EGF was removed by acid wash, cells were fixed, and nucleus stained with DAPI. Left panel: Confocal images of Control and RAP-treated conditions, showing in green EGF-Alexa 488 internalized upon incubation at 37°C. Arrows enlighten internalized EGF. Scale bar = 12μm. Right panel: The internalization was measured by integrated fluorescence density on 20 cells of 3 independent experiments. Data are reported in columns histograms. \*p < 0.5, \*\*\*p < 0.001, \*\*\*\*p < 0.0001. **(B)** EGFR internalization assay. Left panel: Immunoblot showing the endocytosis of biotinylated EGFR. Following cell-surface biotinylation, cells were incubated in complete media (with or without 15 μM gefitinib and with or without RAP) for 3 hours. Cells were treated with MESNa agent to remove biotin present on cell-surface proteins. After purification, biotinylated proteins were then subjected to EGFR immunoblot. Right panel: Quantification of EGFR protein bands (mean of 4 independent experiment). \*p < 0.05. **(C)** Left panel: Downregulation of LRP-1 expression was obtained by 50 nm of siRNA-LRP-1 transiently transfected using JetPrime®. LRP-1 silencing was confirmed by immunoblot 72h after transfection. EGFR protein level was controlled and remained constant in both conditions. GAPDH was used as loading control. Right panel: EGF-internalization assay was further performed on U87 transfected with siRNA-control (white bars) and siRNA-LRP-1 (green bars). \*p < 0.5\*\*p < 0.01. **(D-E)** EGF-internalization assay was performed in T98 **(D)** and LN443 **(E)** cells as described in A. \*p < 0.5, \*\*p < 0.01, \*\*\*\*p < 0.0001. **(F-G)** EGFR-internalization assay was performed in T98 **(F)** and LN443 **(G)** cells as described in B. \*p < 0.5

EGFR experiments unexpectedly failed to reveal an increase in EGFR internalization by gefitinib in T98 cells (Figure 4F), but confirmed the results obtained on U87 in LN443 cells (Figure 4G). Together, our results highlight the contribution of LRP-1 in GME and shed light on the first ever functional interplay between LRP-1 and EGFR.

### **Endocytosis is critical for gefitinib-mediated inhibition of GBM cell dissemination from 3D spheroids**

Endocytosis and membrane trafficking play important role in tumor cell migration and invasion (Díaz et al., 2014; Maritzen et al., 2015; Wilson et al., 2018) and EGFR trafficking dysregulation has been associated with an invasive profile on glioma cells (Kondapalli et al., 2015). It thus appears important to determine whether GME may have an impact in gefitinib-mediated inhibition on glioma cell invasion. We showed using cell evasion from 3D tumor spheroid assays (Blandin et al., 2016), as already been shown (Blandin et al., 2020), that gefitinib reduced by almost 50% the number of evading cells. In a first series of experiments, cell evasion of GBM cells was quantify in presence of dynasore or dyngo-4 to inhibit DNM2 or RAP to inhibit LRP-1 (Figure 5). In the absence of gefitinib, DNM2 inhibitors had no little impact on cell evasion, but were able to restore efficient cell evasion in gefitinib-treated GBM cells (Figures 5A, C and E). On the other hand, LRP-1 inhibition increased the number of evading cells upon gefitinib treatment in U87 and LN443 cells by 1.8 fold and 1.5 fold, respectively (Figure 5B and 5F). However, the effect of RAP was not significant in T98 cells (Figure 5D), even though it seems to have a tendency to increase the number of evading cells compared to gefitinib treatment alone. To confirm the protective role of DNM2 or LRP-1 inhibition, prior to spheroid formation, we transfected U87 cells with siRNA targeting either DMN2 or LRP-1. Figure 6A depicted fluorescent microscopy images of DAPI-labelled cells that escaped from a spheroid 24h after seeding on a collagen coated substratum. It can be observed that neither siRNA-DNM2 nor siRNA-LRP-1 had noticeable impact on the capability of the cell to escape from the spheroid (Figure 6A), which was confirmed by the quantification of the number of evading cells (Figure 6B). Gefitinib inhibited by 82% the number of evading cells that were transfected with siRNA-control. Importantly, both silencing of DNM2 and LRP-1 significantly increased by more than two-fold the cell evasion of gefitinib-treated spheroids. In conclusion, we identified two endocytosis proteins involved in GME whose expression level and function participated to GBM cell response to TKI treatment.

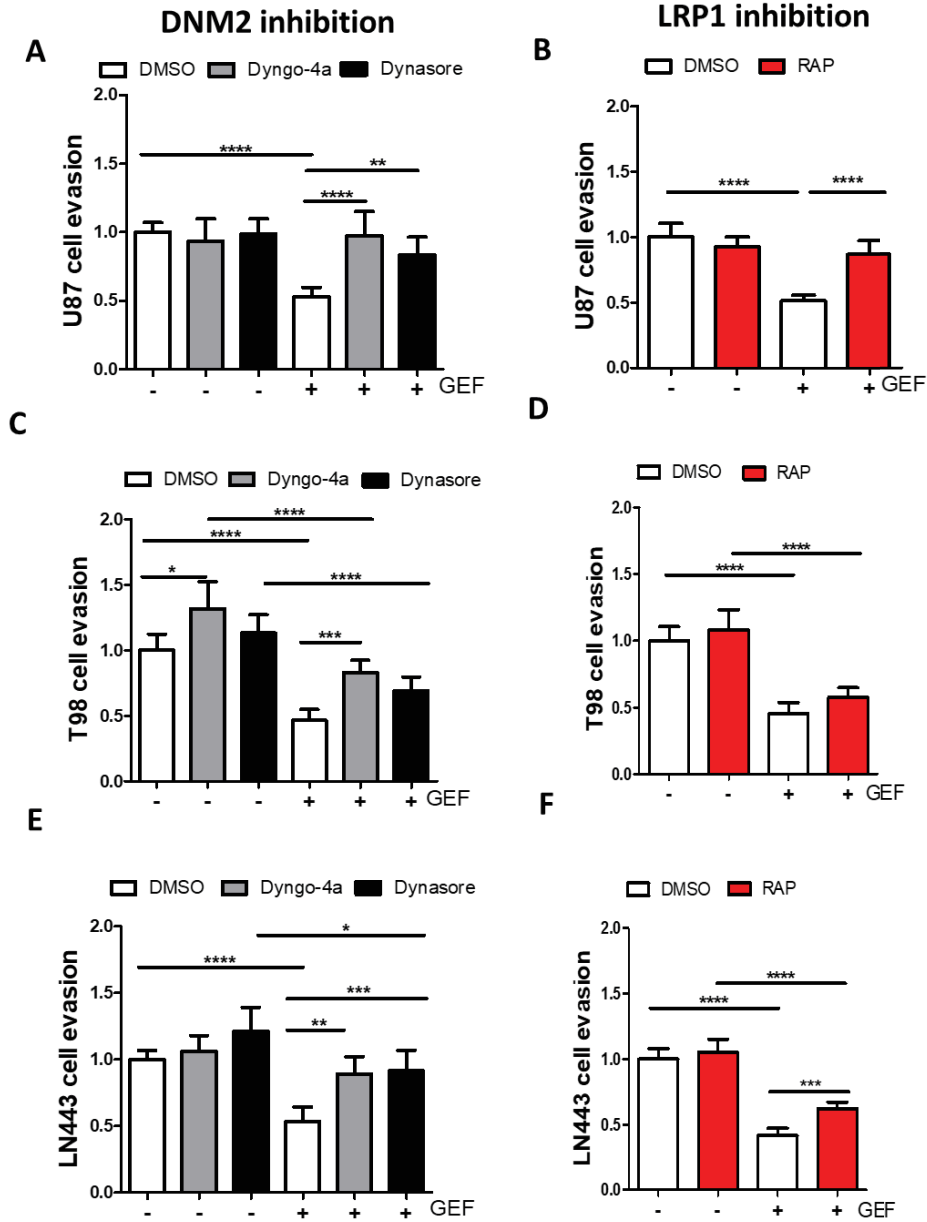


**Figure 5 - GME inhibition decreases gefitinib efficacy on cell evasion.** (A) U87 two-days old spheroids were plated onto collagen-I-coated (10  $\mu\text{g.mL}^{-1}$ ) plastic dishes. Spheroids were treated with DNM2 GTPase activity inhibitors (10  $\mu\text{M}$  of dyngo-4a or 12  $\mu\text{M}$  of dynasore) and/or 20 $\mu\text{M}$  of gefitinib. After DAPI staining, the number of evading cells were quantified by automated counting of nuclei using an ImageJ homemade plugin. Data is represented in column histograms. (B) U87 two-days old spheroids were plated as described above and treated with LRP-1 antagonist RAP (500nM) and/or 20 $\mu\text{M}$  of gefitinib. (C-D) Cell evasion assays from 3D tumor spheroids using dynasore or dyngo-4a (C) or RAP (D) were performed with T98 gefitinib-treated cells. (E-F) Cell evasion assays from 3D tumor spheroids using dynasore or dyngo-4a (E) or RAP (F) were performed with LN443 gefitinib-treated cells. \* $p < 0.5$ , \*\* $p < 0.05$  \*\*\* $p < 0.001$ , \*\*\*\* $p < 0.0001$ .

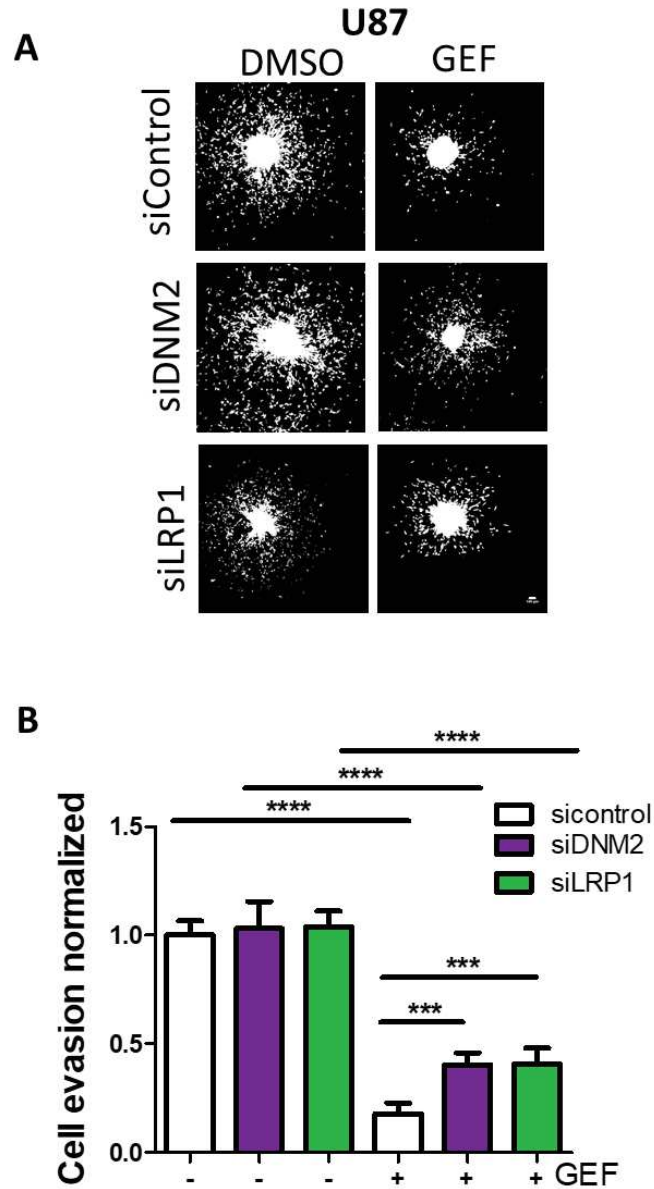


**Figure 6 - DN2 and LRP-1 silencing decreases gefitinib efficacy on cell evasion.** (A) U87 transfected with siRNA-control or siRNA targeting DN2 or LRP-1 two-days old spheroids were plated onto collagen-I-coated (10  $\mu\text{g}\cdot\text{mL}^{-1}$ ) plastic dishes. After 24h of gefitinib treatment, spheroids were fixed, and nucleus were labelled by DAPI staining. Fluorescent microscopy image of representative spheroid after 24 hours of migration were taken. Scale bar: 100  $\mu\text{m}$  (B) After DAPI staining, the number of evading cells were quantified by automated counting of nuclei using a previously validated ImageJ homemade plugin. Data is represented in column histograms. \*\*\* $p < 0.001$ , \*\*\*\* $p < 0.0001$ .

## Discussion

We recently showed that in various GBM cells, gefitinib and other TKI targeting EGFR induce its endocytosis and its massive accumulation in early-endosomes (Blandin et al., 2020). In the present *in vitro* study based on 3 different GBM cells, we have identified 3 endocytosis proteins, DNM2, Rab5 and LRP-1 as key regulators of gefitinib-mediated EGFR internalization (Figure 7). Using pharmacological and siRNA-mediated approach, we showed that DNM2 inhibition or downregulation efficiently counteracted gefitinib-mediated EGFR endocytosis. We expressed a dominant-negative mutant form of Rab5 to demonstrate that GME is dependent of the small GTPase function. Confocal images revealed that EGFR is localized in LRP-1-rich endosomes upon gefitinib treatment. Functional inhibition and silencing showed that LRP-1 was not involved in conventional EGFR endocytosis but played an important role in gefitinib-mediated EGFR endocytosis. Several studies have shown that change in level of expression of proteins regulating EGFR trafficking affect cancer cell sensitivity to targeted therapies (Al-Akhrass et al., 2017; Kondapalli et al., 2015; Wang et al., 2019). Using cell dissemination from spheroids, we showed that inhibition of DNM2 or LRP-1 confers greater resistance to gefitinib (Figure 7). Our results reveal that endocytosis plays an unexpected role in gefitinib action and that expression level of endocytosis proteins such as DNM2, LRP-1 or Rab5 could be relevant biomarkers to predict TKI efficiency in limiting invasion of GBM cells.

DNM2, a large GTPase protein in charge of the endocytic fusion of clathrin coated pits, has been shown to play a significant role in EGFR endocytosis (Sousa et al., 2012). Here, using pharmacological inhibitors dynasore and dyngo-4A and by siRNA-mediated silencing, we showed that DNM2 plays a significant role in GME of EGFR and that its inhibition increased the invasive potential of gefitinib-treated GBM cells. The role of DNM2 in cancer cell migration and invasion is matter of debate. Some reports indicate that DNM2 stimulates migration and invasion of cancer cell, including glioma (Eppinga et al., 2012; Feng et al., 2012). DNM2 has been shown to activate RAC1 and lamellipodia formation (Razidlo et al., 2013), to stabilize F-actin and filopodia (Yamada et al., 2016), and to promote invadopodia invasive function (Destaing et al., 2013). Others have shown that DNM2 downregulation promotes EGFR signalling and cancer cell motility (Gong et al., 2015; Khan et al., 2019). In our experimental setup, DNM2 inhibition or repression had no impact in evasion of controlled cells indicating that DNM2 may not play an important function in the capacity of GBM cells to detach from tumor spheroids and to migrate. These results also suggest that dynasore and

dyngo-4A or siRNA increased the evasion of gefitinib-treated cells, most likely by blocking GME rather than by stimulating cell migration.

The contribution of Rab5 in GME of EGFR was highlighted by the inhibition of EGFR recruitment to early endosomes in DN-Rab5 gefitinib-treated cells. Moreover, gefitinib treatment phenocopy Rab5-Q79L expression characterized by a massive distribution of EGFR into fused early-endosomes (Dinneen and Ceresa, 2004). The role of Rab5 in glioma progression and resistance to anti-EGFR therapy is still a matter of debate. Indeed, a recent study reported that in human, Rab5 is overexpressed in glioma tissue compared to normal brain and that overexpression of Rab5 lead to enhanced proliferation and migration, which can be reversed by knockout of Rab5 (Jian et al., 2020). By contrast, it has been shown that Rab5 inhibition sustains aberrant oncogenic EGFR signalling. For instance, Golgi phosphoprotein 3 (GOLPH3), a protein implicated in multiple cellular functions, was reported to promote glioma progression by inhibiting Rab5-dependent EGFR endocytosis (Zhou et al., 2017). Conversely, the tumor suppressors CMTM3 and CMTM7 (chemokine-like factor-like MARVEL transmembrane domain-containing 3 and 7) inhibit EGFR-mediated tumorigenicity and EGFR-dependent cell migration by stimulating Rab5 activity, in gastric and lung carcinomas, respectively (Liu et al., 2015; Yuan et al., 2017). Further studies are therefore required to delineate the role of Rab5 in glioma progression. An intriguing possibility to explain our results is that gefitinib activates Rab5 to increase EGFR endocytosis. Although we did not test this hypothesis, this would mean that in line with results obtained on DNM2 or LRP-1, Rab5 inhibition would hamper gefitinib anti-invasive function. This possibility was indirectly investigated in 2 recent studies which reported conflicting results. GOLPH3 has been reported to enhance the anti-tumoral activity of gefitinib in GBM cell lines (Wang et al., 2019), suggesting that Rab5 inhibition would sensitize cells to gefitinib. By contrast, compared to monotherapies co-delivery of siRNA targeting GOLPH3 and gefitinib in brain tumors reduces cancer progression and improves mice survival (Ye et al., 2019). The molecular mechanism by which gefitinib would activate Rab5 has not be investigated, yet. An attractive hypothesis would be that like cisplatin, UV radiation or anisomycin, gefitinib may accelerate ligand-independent EGFR endocytosis by stimulating the stress-activated p38-MAPK (MAPK14) (Cavalli et al., 2001; Macé et al., 2005; Peng et al., 2016; Tomas et al., 2015, 2017; Vergarajauregui et al., 2006; Zwang and Yarden, 2006). Several mechanisms have been proposed, stress-activated p38 can directly phosphorylate EGFR on Ser1015 in lung cancer cells (Tanaka et al., 2018). Alternatively, p38 has been shown to be a major regulator of Rab5

activity. P38 can either phosphorylate EEA1 and rabenosin, two effectors of Rab5 (Macé et al., 2005) or phosphorylate the GDP dissociation factor, which releases inactive Rab5-GDP from the endosomal membrane and allows the maintenance of Rab5 in the cytoplasm for its subsequent activation (Cavalli et al., 2001). P38 was shown to promote EGFR endocytosis, and its pharmacological inhibition lead to sustained EGFR expression in glioma stem cells (Soeda et al., 2017). We thus speculate once more that targeting endocytosis by p38 inhibition would reduce Rab5-mediated EGFR endocytosis and increase glioma cell resistance to gefitinib as it has been found in the case of cisplatin treatment of U87 cells (Baldwin et al., 2006).

Membrane trafficking is often deregulated in cancer and contributes significantly to the antitumor activity of gefitinib. Therefore, therapeutic manipulation of endocytosis may represent an interesting strategy to increase the potency of EGFR TKI. The present work and other studies (Al-Akhrass et al., 2017; Kondapalli et al., 2015; Llongueras et al., 2014; Wang et al., 2019) have shown that intensive endocytosis is associated with increased sensitivity of glioma cells to TKI treatment. Predictably, *in vivo* targeting of proteins inhibiting endocytosis such as GOLPH3 or the Na<sup>+</sup>/H<sup>+</sup> exchanger NHE9 represent an attractive therapeutic strategy to limit EGFR oncogenic activity and to increase cancer cell responsiveness to TKI (Kondapalli et al., 2015; Ye et al., 2019). A milestone was achieved by Simpson group's who recently revealed that tumors can be classified based on EGF endocytosis profile from an *ex vivo* EGF endocytosis assay to predict antibody-based anti-EGFR therapy efficacy (Chew et al., 2020; Joseph et al., 2019). In the end, the analysis of protein expression levels alone does not always provide sufficient information to predict the clinical benefits of a targeted therapy or to stratify patients for personalized medicine. Thus, the molecular characterization of tumors must enter a new era including functional studies of proteins such as endocytosis and membrane trafficking.



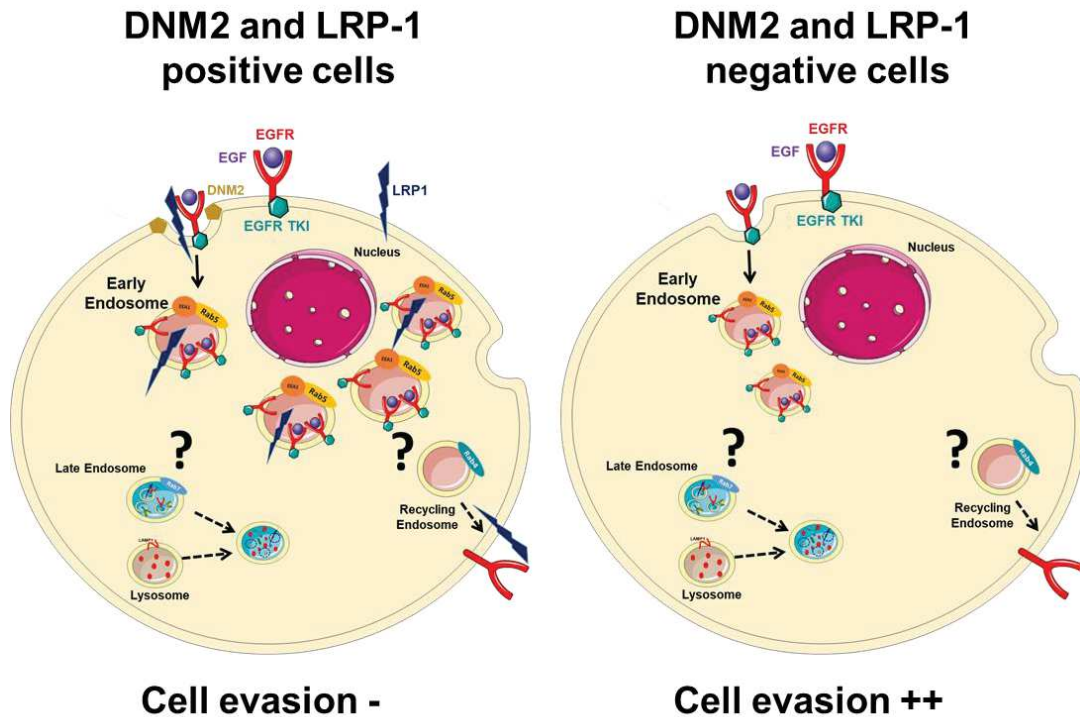


**Figure 7 – Schematic of DNM2 and LRP-1 involvement in GME and gefitinib-cell evasion inhibition.** (Left panel) In GBM cells expressing DNM2 and LRP-1, treatment with a EGFR-tyrosine kinase inhibitor (TKI) provokes a massive EGFR internalization into enlarged and abundant early endosomes that we called gefitinib-mediated endocytosis (GME). Moreover, TKI treatment was also able to internalized EGFR in LRP-1 positive endosomes. Furthermore, the fate of these receptors remains unknown. Possible recycling or degradation can occur. (Right panel) The absence of DNM2 and LRP-1 reduces GME and increased cell evasion from a 3D tumor spheroid compared to condition represented in the left panel. GME can thus be important for gefitinib efficiency in inhibiting GBM cell evasion.

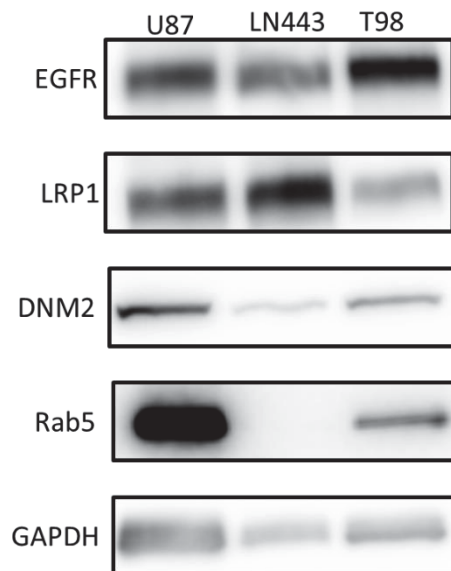


**Figure S1 – Protein expression profile of the 3 GBM cell lines studied.** Protein expression of EGFR, LRP-1, DNM2 and Rab5 in U87, LN443 and T98 GBM cells was studied by immunoblot. GAPDH was used as loading control.

## References

- Al-Akhrass, H., Naves, T., Vincent, F., Magnaudeix, A., Durand, K., Bertin, F., Melloni, B., Jauberteau, M.-O., and Lalloué, F. (2017). Sortilin limits EGFR signaling by promoting its internalization in lung cancer. *Nat. Commun.* 8.
- An, Z., Aksoy, O., Zheng, T., Fan, Q.-W., and Weiss, W.A. (2018). Epidermal growth factor receptor (EGFR) and EGFRvIII in glioblastoma (GBM): signaling pathways and targeted therapies. *Oncogene* 37, 1561–1575.
- Baldwin, R.M., Garratt-Lalonde, M., Parolin, D. a. E., Krzyzanowski, P.M., Andrade, M.A., and Lorimer, I. a. J. (2006). Protection of glioblastoma cells from cisplatin cytotoxicity via protein kinase C  $\iota$ -mediated attenuation of p38 MAP kinase signaling. *Oncogene* 25, 2909–2919.
- Barbieri, M.A., Roberts, R.L., Gumusboga, A., Highfield, H., Alvarez-Dominguez, C., Wells, A., and Stahl, P.D. (2000). Epidermal Growth Factor and Membrane Trafficking. *J. Cell Biol.* 151, 539–550.
- Blandin, A.-F., Noulet, F., Renner, G., Mercier, M.-C., Choulier, L., Vauchelles, R., Ronde, P., Carreiras, F., Etienne-Selloum, N., Vereb, G., et al. (2016). Glioma cell dispersion is driven by  $\alpha 5$  integrin-mediated cell–matrix and cell–cell interactions. *Cancer Lett.* 376, 328–338.
- Blandin, A.-F\*, Cruz Da Silva, E\*, Mercier, M.-C., Glushonkov, O., Didier, P., Dedieu, S., Schneider, C., Devy, J., Etienne-Selloum, N., Dontenwill, M., et al. (2020). Gefitinib induces EGFR and  $\alpha 5\beta 1$  integrin co-endocytosis in glioblastoma cells. *Cell. Mol. Life Sci. CMLS.*
- Bu, G., and Schwartz, A.L. (1998). RAP, a novel type of ER chaperone. *Trends Cell Biol.* 8, 272–276.
- Bu, G., Geuze, H.J., Strous, G.J., and Schwartz, A.L. (1995). 39 kDa receptor-associated protein is an ER resident protein and molecular chaperone for LDL receptor-related protein. *EMBO J.* 14, 2269–2280.
- Cao, X., Zhu, H., Ali-Osman, F., and Lo, H.-W. (2011). EGFR and EGFRvIII undergo stress- and EGFR kinase inhibitor-induced mitochondrial translocation: A potential mechanism of EGFR-driven antagonism of apoptosis. *Mol. Cancer* 10, 26.
- Cavalli, V., Vilbois, F., Corti, M., Marcote, M.J., Tamura, K., Karin, M., Arkinstall, S., and Gruenberg, J. (2001). The stress-induced MAP kinase p38 regulates endocytic trafficking via the GDI:Rab5 complex. *Mol. Cell* 7, 421–432.
- Ceresa, B., Lotscher, M., and Schmid, S. (2001). Receptor and Membrane Recycling Can Occur with Unaltered Efficiency Despite Dramatic Rab5(Q79L)-induced Changes in Endosome Geometry. *J. Biol. Chem.* 276, 9649–9654.
- Chen, X., and Wang, Z. (2001). Regulation of epidermal growth factor receptor endocytosis by wortmannin through activation of Rab5 rather than inhibition of phosphatidylinositol 3-kinase. *EMBO Rep.* 2, 842–849.
- Chen, P.-I., Kong, C., Su, X., and Stahl, P.D. (2009). Rab5 Isoforms Differentially Regulate the Trafficking and Degradation of Epidermal Growth Factor Receptors. *J. Biol. Chem.* 284, 30328–30338.
- Chew, H.Y., De Lima, P.O., Gonzalez Cruz, J.L., Banushi, B., Echejoh, G., Hu, L., Joseph, S.R., Lum, B., Rae, J., O'Donnell, J.S., et al. (2020). Endocytosis Inhibition in Humans to Improve Responses to ADCC-Mediating Antibodies. *Cell* 180, 895-914.e27.
- Destaing, O., Ferguson, S.M., Grichine, A., Oddou, C., Camilli, P.D., Albiges-Rizo, C., and Baron, R. (2013). Essential Function of Dynamin in the Invasive Properties and Actin Architecture of v-Src Induced Podosomes/Invadosomes. *PLOS ONE* 8, e77956.
- Díaz, J., Mendoza, P., Ortiz, R., Díaz, N., Leyton, L., Stupack, D., Quest, A.F.G., and Torres, V.A. (2014). Rab5 is required in metastatic cancer cells for Caveolin-1-enhanced Rac1 activation, migration and invasion. *J. Cell Sci.* 127, 2401–2406.
- Dinneen, J.L., and Ceresa, B.P. (2004). Continual expression of Rab5(Q79L) causes a ligand-independent EGFR internalization and diminishes EGFR activity. *Traffic Cph. Den.* 5, 606–615.
- Dittmann, K., Mayer, C., Fehrenbacher, B., Schaller, M., Raju, U., Milas, L., Chen, D.J., Kehlbach, R., and Rodemann, H.P. (2005). Radiation-induced Epidermal Growth Factor Receptor Nuclear Import Is Linked to Activation of DNA-dependent Protein Kinase. *J. Biol. Chem.* 280, 31182–31189.
- Eppinga, R.D., Krueger, E.W., Weller, S.G., Zhang, L., Cao, H., and McNiven, M.A. (2012). Increased expression of the large GTPase dynamin 2 potentiates metastatic migration and invasion of pancreatic ductal carcinoma. *Oncogene* 31, 1228–1241.
- Eskilsson, E., Røslund, G.V., Solecki, G., Wang, Q., Harter, P.N., Graziani, G., Verhaak, R.G.W., Winkler, F., Bjerkvig, R., and Miletic, H. (2018). EGFR heterogeneity and implications for therapeutic intervention in glioblastoma. *Neuro-Oncol.* 20, 743–752.
- Etique, N., Verzeaux, L., Dedieu, S., and Emonard, H. (2013). LRP-1: a checkpoint for the extracellular matrix proteolysis. *BioMed Res. Int.* 2013, 152163.
- Feng, H., Liu, K., Guo, P., Zhang, P., Cheng, T., McNiven, M., Johnson, G., Hu, B., and Cheng, S. (2012). Dynamin 2 Mediates PDGFR $\alpha$ -SHP-2-Promoted Glioblastoma Growth and Invasion. *Oncogene* 31, 2691–2702.

Gong, C., Zhang, J., Zhang, L., Wang, Y., Ma, H., Wu, W., Cui, J., Wang, Y., and Ren, Z. (2015). Dynamin2 downregulation delays EGFR endocytic trafficking and promotes EGFR signaling and invasion in hepatocellular carcinoma. *Am. J. Cancer Res.* 5, 702–713.

Grandal, M.V., Zandi, R., Pedersen, M.W., Willumsen, B.M., van Deurs, B., and Poulsen, H.S. (2007). EGFRvIII escapes down-regulation due to impaired internalization and sorting to lysosomes. *Carcinogenesis* 28, 1408–1417.

Henriksen, L., Grandal, M.V., Knudsen, S.L.J., van Deurs, B., and Grøvdal, L.M. (2013). Internalization Mechanisms of the Epidermal Growth Factor Receptor after Activation with Different Ligands. *PLoS ONE* 8.

Jian, Z., Zhang, L., Jin, L., Lan, W., Zhang, W., and Gao, G. (2020). Rab5 regulates the proliferation, migration and invasion of glioma cells via cyclin E. *Oncol. Lett.* 20, 1055–1062.

Jones, S., King, P.J., Antonescu, C.N., Sugiyama, M.G., Bhamra, A., Surinova, S., Angelopoulos, N., Kragh, M., Pedersen, M.W., Hartley, J.A., et al. (2020). Targeting of EGFR by a combination of antibodies mediates unconventional EGFR trafficking and degradation. *Sci. Rep.* 10, 1–19.

Joseph, S.R., Gaffney, D., Barry, R., Hu, L., Banushi, B., Wells, J.W., Lambie, D., Stratton, G., Porceddu, S.V., Burmeister, B., et al. (2019). An Ex Vivo Human Tumor Assay Shows Distinct Patterns of EGFR Trafficking in Squamous Cell Carcinoma Correlating to Therapeutic Outcomes. *J. Invest. Dermatol.* 139, 213–223.

Jovic, M., Sharma, M., Rahajeng, J., and Caplan, S. (2010). The early endosome: a busy sorting station for proteins at the crossroads. *Histol. Histopathol.* 25, 99–112.

Keir, S.T., Chandramohan, V., Hemphill, C.D., Grandal, M.M., Melander, M.C., Pedersen, M.W., Horak, I.D., Kragh, M., Desjardins, A., Friedman, H.S., et al. (2018). Sym004-induced EGFR elimination is associated with profound anti-tumor activity in EGFRvIII patient-derived glioblastoma models. *J. Neurooncol.* 138, 489–498.

Khan, I., Gril, B., and Steeg, P.S. (2019). Metastasis Suppressors NME1 and NME2 Promote Dynamin 2 Oligomerization and Regulate Tumor Cell Endocytosis, Motility, and Metastasis. *Cancer Res.* 79, 4689–4702.

Kirchhausen, T., Macia, E., and Pelish, H.E. (2008). Use of dynasore, the small molecule inhibitor of dynamin, in the regulation of endocytosis. *Methods Enzymol.* 438, 77–93.

Kondapalli, K.C., Llongueras, J.P., Capilla-González, V., Prasad, H., Hack, A., Smith, C., Guerrero-Cázares, H., Quiñones-Hinojosa, A., and Rao, R. (2015). A leak pathway for luminal protons in endosomes drives oncogenic signalling in glioblastoma. *Nat. Commun.* 6, 6289.

Liao, H.-J., and Carpenter, G. (2009). Cetuximab/C225-Induced Intracellular Trafficking of Epidermal Growth Factor Receptor. *Cancer Res.*

Liu, B., Su, Y., Li, T., Yuan, W., Mo, X., Li, H., He, Q., Ma, D., and Han, W. (2015). CMTM7 knockdown increases tumorigenicity of human non-small cell lung cancer cells and EGFR-AKT signaling by reducing Rab5 activation. *Oncotarget* 6, 41092–41107.

Llongueras, J., Kondapalli, K., Hack, A., Capilla-González, V., Smith, C., Guerrero-Cazares, H., Quiñones-Hinojosa, A., and Rao, R. (2014). Na<sup>+</sup>/H<sup>+</sup> exchanger NHE9 affects tumor progression of human glioblastomas by altering endosomal pH (893.34). *FASEB J.* 28, 893.34.

Macé, G., Miaczynska, M., Zerial, M., and Nebreda, A.R. (2005). Phosphorylation of EEA1 by p38 MAP kinase regulates  $\mu$  opioid receptor endocytosis. *EMBO J.* 24, 3235–3246.

Maritzen, T., Schachner, H., and Legler, D.F. (2015). On the move: endocytic trafficking in cell migration. *Cell. Mol. Life Sci. CMLS* 72, 2119–2134.

Peng, K., Dai, Q., Wei, J., Shao, G., Sun, A., Yang, W., and Lin, Q. (2016). Stress-induced endocytosis and degradation of epidermal growth factor receptor are two independent processes. *Cancer Cell Int.* 16, 25.

Perrot, G., Langlois, B., Devy, J., Jeanne, A., Verzeaux, L., Almagro, S., Sartelet, H., Hachet, C., Schneider, C., Sick, E., et al. (2012). LRP-1--CD44, a new cell surface complex regulating tumor cell adhesion. *Mol. Cell. Biol.* 32, 3293–3307.

Razidlo, G.L., Wang, Y., Chen, J., Krueger, E.W., Billadeau, D.D., and McNiven, M.A. (2013). Dynamin 2 Potentiates Invasive Migration of Pancreatic Tumor Cells through Stabilization of the Rac1 GEF Vav1. *Dev. Cell* 24, 573–585.

Robertson, M.J., Deane, F.M., Robinson, P.J., and McCluskey, A. (2014). Synthesis of Dynole 34-2, Dynole 2-24 and Dynole 4a for investigating dynamin GTPase. *Nat. Protoc.* 9, 851–870.

Sigismund, S., Argenzio, E., Tosoni, D., Cavallaro, E., Polo, S., and Di Fiore, P.P. (2008). Clathrin-Mediated Internalization Is Essential for Sustained EGFR Signaling but Dispensable for Degradation. *Dev. Cell* 15, 209–219.

Soeda, A., Lathia, J., Williams, B.J., Wu, Q., Gallagher, J., Androutsellis-Theotokis, A., Giles, A.J., Yang, C., Zhuang, Z., Gilbert, M.R., et al. (2017). The p38 signaling pathway mediates quiescence of glioma stem cells by regulating epidermal growth factor receptor trafficking. *Oncotarget* 5.

Sousa, L.P., Lax, I., Shen, H., Ferguson, S.M., De Camilli, P., and Schlessinger, J. (2012). Suppression of EGFR endocytosis by dynamin depletion reveals that EGFR signaling occurs primarily at the plasma membrane. *Proc. Natl. Acad. Sci. U. S. A.* 109, 4419–4424.

Tan, X., Thapa, N., Sun, Y., and Anderson, R.A. (2015). A Kinase-Independent Role for EGF Receptor in Autophagy Initiation. *Cell* 160, 145–160.

Tan, X., Lambert, P.F., Rapraeger, A.C., and Anderson, R.A. (2016). Stress-Induced EGFR Trafficking: Mechanisms, Functions, and Therapeutic Implications. *Trends Cell Biol.* 26, 352–366.

Tanaka, T., Ozawa, T., Oga, E., Muraguchi, A., and Sakurai, H. (2018). Cisplatin-induced non-canonical endocytosis of EGFR via p38 phosphorylation of the C-terminal region containing Ser-1015 in non-small cell lung cancer cells. *Oncol. Lett.* 15, 9251–9256.

Tomas, A., Futter, C.E., and Eden, E.R. (2014). EGF receptor trafficking: consequences for signaling and cancer. *Trends Cell Biol.* 24, 26–34.

Tomas, A., Vaughan, S.O., Burgoyne, T., Sorkin, A., Hartley, J.A., Hochhauser, D., and Futter, C.E. (2015). WASH and Tsg101/ALIX-dependent diversion of stress-internalized EGFR from the canonical endocytic pathway. *Nat. Commun.* 6, 7324.

Tomas, A., Jones, S., Vaughan, S.O., Hochhauser, D., and Futter, C.E. (2017). Stress-specific p38 MAPK activation is sufficient to drive EGFR endocytosis but not its nuclear translocation. *J. Cell Sci.* 130, 2481–2490.

Vergarajauregui, S., Miguel, A.S., and Puertollano, R. (2006). Activation of p38 Mitogen-Activated Protein Kinase Promotes Epidermal Growth Factor Receptor Internalization. *Traffic Cph. Den.* 7, 686–698.

Walsh, A.M., Kapoor, G.S., Buonato, J.M., Mathew, L.K., Bi, Y., Davuluri, R.V., Martinez-Lage, M., Simon, M.C., O'Rourke, D.M., and Lazzara, M.J. (2015). Sprouty2 Drives Drug Resistance and Proliferation in Glioblastoma. *Mol. Cancer Res. MCR* 13, 1227–1237.

Wang, X., Wang, Z., Zhang, Y., Wang, Y., Zhang, H., Xie, S., Xie, P., Yu, R., and Zhou, X. (2019). Golgi phosphoprotein 3 sensitizes the tumor suppression effect of gefitinib on gliomas. *Cell Prolif.* 52, e12636.

Wilson, B.J., Allen, J.L., and Caswell, P.T. (2018). Vesicle trafficking pathways that direct cell migration in 3D matrices and in vivo. *Traffic Cph. Den.* 19, 899–909.

Yamada, H., Takeda, T., Michiue, H., Abe, T., and Takei, K. (2016). Actin bundling by dynamin 2 and cortactin is implicated in cell migration by stabilizing filopodia in human non-small cell lung carcinoma cells. *Int. J. Oncol.* 49, 877–886.

Ye, C., Pan, B., Xu, H., Zhao, Z., Shen, J., Lu, J., Yu, R., and Liu, H. (2019). Co-delivery of GOLPH3 siRNA and gefitinib by cationic lipid-PLGA nanoparticles improves EGFR-targeted therapy for glioma. *J. Mol. Med. Berl. Ger.*

Ying, H., Zheng, H., Scott, K., Wiedemeyer, R., Yan, H., Lim, C., Huang, J., Dhakal, S., Ivanova, E., Xiao, Y., et al. (2010). Mig-6 controls EGFR trafficking and suppresses gliomagenesis. *Proc. Natl. Acad. Sci. U. S. A.* 107, 6912–6917.

Yuan, W., Liu, B., Wang, X., Li, T., Xue, H., Mo, X., Yang, S., Ding, S., and Han, W. (2017). CMTM3 decreases EGFR expression and EGF-mediated tumorigenicity by promoting Rab5 activity in gastric cancer. *Cancer Lett.* 386, 77–86.

Zhou, X., Xie, S., Wu, S., Qi, Y., Wang, Z., Zhang, H., Lu, D., Wang, X., Dong, Y., Liu, G., et al. (2017). Golgi phosphoprotein 3 promotes glioma progression via inhibiting Rab5-mediated endocytosis and degradation of epidermal growth factor receptor. *Neuro-Oncol.* 19, 1628–1639.

Zwang, Y., and Yarden, Y. (2006). p38 MAP kinase mediates stress-induced internalization of EGFR: implications for cancer chemotherapy. *EMBO J.* 25, 4195–4206.

## General conclusions of Articles 1 and 2

- Gefitinib provoked stress-induced receptor endocytosis in fused endosomes.
- Gefitinib promoted EGFR and  $\alpha 5\beta 1$  integrin co-endocytosis
- We have identified 3 endocytosis proteins, DNM2, Rab5 and LRP-1 as key regulators of gefitinib-mediated EGFR internalization
- Modulation of endocytosis changes glioma cell response to gefitinib treatment.

In the first article, we described in four different glioma cell lines that gefitinib and other TKIs mediated a stress-induced, ligand-independent endocytosis of EGFR. We also described that GME is not restrictive to EGFR, as we showed a co-localization of EGFR with integrin  $\alpha 5\beta 1$  in early endosomes upon gefitinib treatment. Gefitinib increased integrin/EGFR co-localization in perinuclear vesicles compared to untreated condition. Using super-resolution PALM-STORM microscopy, we verified the close proximity between EGFR and integrin  $\beta 1$ , suggesting a potential functional interaction. To explore integrin involvement in GME, integrin  $\alpha 5$  was depleted on U87 cells using shRNA technology. Integrin  $\alpha 5\beta 1$  depletion reduced GME and limited EGFR accumulation in early endosomes during short-term treatment. We next assess if GME impacts on glioma cell response to treatment. Since GBM is a highly invasive tumor, we decided to evaluate the role of trafficking dysregulation in cell evasion from 3D tumor spheroids. Gefitinib treatment decreased the number of evaded cells from U87 $\alpha 5$ - spheroids in a dose dependent way. However, no significant gefitinib impact occurred in cell evasion of integrin  $\alpha 5$  positive cells.

In the second article, we tried to better elucidate the molecular mechanisms inherent to GME. First, we studied the role of 2 proteins normally associated to ligand-induced EGFR endocytosis, DNM2 and Rab5. Using pharmacological inhibitors and siRNA-mediated depletion we showed that GME was DNM2-dependent. We also showed that GME required Rab5 activity. Constitutively active mutant of Rab5 produced enlarged early endosomes similar to GME. Also, dominant-negative of Rab5 mutant reduces EGFR localization in EEA1-positive

early endosomes upon gefitinib treatment. We next examined the potential role of LRP-1, an endocytosis receptor. GME on U87 cells induced EGFR re-localization in LRP-1-positive endosomes. Next, LRP-1 role in GME was studied using siRNA-depletion methodology and pharmacological inhibition by receptor-associated receptor (RAP). Interestingly, we found that LRP-1 is not involved in ligand-induced EGFR endocytosis but contribute significantly to gefitinib-mediated EGFR endocytosis. GME inhibition by blocking DNM2 and LRP-1 significantly increased the cell dissemination of gefitinib-treated cells, protecting cells from TKI treatment.

In summary, we showed that in glioma cells, TKI elicited a complex EGFR endocytosis mechanism. Moreover, we demonstrated for the first time a link functional between LRP-1 and EGFR endocytosis and a novel role of TKIs in EGFR and  $\alpha 5\beta 1$  integrin endocytosis. We determined that expression level and function of proteins involved in GME may modulate GBM cell responses to TKI treatment. However, future challenges will be to evaluate TKIs impact on integrin function and if its cooperation with EGFR during membrane trafficking change GBM cell evasion. Finally, this work has highlighted the need to better understand the mechanisms of drugs, and not just their presumed properties. This could lead to the identification of appropriate biomarkers predicting drug efficacy and thus improve the accuracy of drug therapies.

## Introduction to Article 3 and to recent results

Several membrane receptors, like EGFR are overexpressed in GBM to promote glioma cell survival, growth and migration (An et al., 2018). The team 'Integrins and cancers' from UMR 7021 demonstrated the potential of integrin  $\alpha 5\beta 1$  as therapeutic target on GBM (Janouskova et al., 2012). Its natural ligand is fibronectin, an extracellular matrix protein overexpressed in GBM tumor microenvironment (Lal et al., 1999). Biomarkers like integrin  $\alpha 5\beta 1$ , have great potential in clinics in the future as diagnosis (elevated expression in high grade glioma compared to low grade and normal tissue), prognosis (high expression associated with lower patient survival), and predictive (high expression associated with resistance to TMZ) markers. EGFR/  $\beta 1$  integrin interaction in patient tissues was demonstrated using proximity ligation assay (Petrás et al., 2013). In GBM patient tumors, a strong inter and intra heterogeneity is observed (Eskilsson et al., 2018; Janouskova et al., 2012; Szerlip et al., 2012). Another interesting therapeutic target in GBM is c-MET and its ligand, the hepatocyte growth factor (HGF). C-MET/HGF signaling pathway is dysregulated in GBM and involved in glioma cell proliferation, survival, invasion, angiogenesis, stem cell profile, therapeutic resistance and GBM recurrence (Cheng and Guo, 2019). C-MET expression was associated with an unfavorable prognostic in GBM patients (Pettersson et al., 2015). A study of immunohistochemistry of GBM tissue samples showed c-MET localization in tumor cells, blood vessels, and peri-necrotic areas (Pettersson et al., 2015). Interestingly, EGFR and c-Met were found co-localized in GBM cell and tissue samples, suggesting a crosstalk between both receptors (Velpula et al., 2012). A dual-inhibition of EGFR and c-MET overcome TMZ resistance in GBM cells and reduced tumor growth in *in vivo* GBM models (Meng et al., 2020).

This highly aggressive and resistance tumor has been studied in more than 1519 clinical trials, in which 259 are targeted-therapies. The majority of them do not improve patient progression-free survival and overall survival. The GBM heterogeneity is one of the main reasons for therapy resistance and tumor recurrence. Knowing the expression status of different biomarkers might be used to stratify patients in clinical trials to better select patients and/or adjust treatment plan. Therefore, the possibility of simultaneously staining different proteins on the same GBM tissue would facilitate therapeutic decisions.

Ligands of these therapeutic targets may therefore be interesting tools. They need to be accurate and of rapid use to better evaluate the membrane receptor expression, at the protein level, in GBM tumor sections. Usual immunohistochemistry (IHC) protocol uses indirect method with a first incubation of tissues with an unconjugated primary antibody specific to the biomarker of interest, followed by a second incubation with a conjugated antibody able to identify first antibody species. This indirect method of detection increases the sensibility since secondary antibodies can bind to two antigenic sites of the primary antibody. The drawback of this method of detection is due to non-specific binding of secondary antibodies. A direct detection allows a fast protocol since only one incubation time is needed. Direct detection methodologies are probably more reliable for multiplexing since there is no risk of cross-species reaction (by using dye directly conjugated antibodies) (Odell and Cook, 2013). But, direct labelling of antibodies is complex. To covalently couple a fluorophore to a recombinant protein, such as an antibody or antibody fragment, the procedure most commonly used consists of substituting an identified amino acid with a cysteine and coupling the fluorophore to its thiol group. This method requires the production and purification of large quantities of recombinant proteins. In addition, this method is relatively complicated. Indeed, mutations and/or couplings might (i) decrease the protein expression level, (ii) decrease or inhibit the binding, (iii) cause a loss of stability or the aggregation of the protein, or (iv) induce an absence of fluorescence signal. The fluorophore occasionally may even be coupled to the lysine side chains.

Antibody homogeneity from batch to batch might be low, representing a huge disadvantage in reproducibility (Zhou and Rossi, 2017). For multiplex immune-detection, several antibodies of different specificities, coupled to different reporter molecules are needed, which enhance these difficulties. These problems might be solved by the use of other molecules, chemically synthesized, in large quantities, and more stable, such as peptides, small chemical compounds, or aptamers (Hori et al., 2018; Musumeci et al., 2017).

In oncology, aptamers, the so-called chemical antibodies, are emerging tools as potential diagnostic and therapeutic (direct binding to their targets or for drug vectorization) tools. Aptamers are single-stranded DNA or RNA molecules that bind to their target with high affinity and specificity, such as antibodies. Aptamers have advantages over antibodies: their smaller size, thermal stability, lack of immunogenicity and toxicity, and chemical synthesis (Mercier et al., 2017; Zhou and Rossi, 2017). Moreover, aptamers penetrate deeper in tissues compared to antibodies due to their smaller size (Xiang et al., 2015). The selection of aptamers is made



through an *in vitro* process called SELEX (selective evolution of ligands by exponential enrichment) (Ellington and Szostak, 1990; Tuerk and Gold, 1990). Aptamers might be used as diagnostic and/or therapeutic tools against identified therapeutic targets like membrane receptors, interesting targets because of their accessibility at the cell surface.

During my thesis, we used aptamers targeting EGFR, integrin  $\alpha 5$  and c-MET in GBM cell lines and patient tissue samples. EGFR aptamers (E07 and anti-EGFR janellia 646 conjugate) and c-MET (SL1) were already described in literature (Kratschmer and Levy, 2018; Li et al., 2011; Ray et al., 2012; Zhang et al., 2018), and integrin  $\alpha 5$  aptamer H02 was identified and characterized in the laboratory (Article 3).

## Article 3

### Identification and characterization of aptamer H02 targeting integrin $\alpha 5\beta 1$

An original selection process, combining cell- and protein SELEX, was performed in the laboratory to identify aptamer as new ligands able to bind to GBM cells and tissues expressing integrin  $\alpha 5\beta 1$ . The selection, identification and characterization of the aptamer, named H02, are described in the manuscript (Fechter, Cruz da Silva et al., 2019).

- The sequence of the aptamer H02 has been patented (EP18306664.6 ‘Aptamer and use thereof’). Integrin  $\alpha 5\beta 1$  was validated as the target of H02 aptamer using surface plasmon resonance, in which human integrin  $\alpha v\beta 3$  was used as a negative control.
- The equilibrium affinity ( $K_D$ ) of the interaction between aptamer H02 and U87 cells overexpressing  $\alpha 5$  was determined using flow cytometry. Binding events between the aptamer and cells were quantified by a fluorescent signal associated to the aptamer-fluorophore conjugate tested at different concentrations. A  $K_D$  of  $277.8 \pm 51.8$  nM was determined.
- Furthermore,  $\alpha 5\beta 1$  integrin aptamer H02 were able to identify different GBM cell lines according to their integrin  $\alpha 5\beta 1$  expression level.
- At  $4^\circ\text{C}$ , aptamer H02 was able to detect integrin  $\alpha 5\beta 1$  present at the plasma membrane and at cell-cell junctions. At  $37^\circ\text{C}$ , the H02 aptamer was internalized after binding to integrin  $\alpha 5\beta 1$  and found in EEA1-positive early endosomes.

# RNA Aptamers Targeting Integrin $\alpha 5 \beta 1$ as Probes for Cyto- and Histofluorescence in Glioblastoma

Pierre Fechter,<sup>1,6</sup> Elisabete Cruz Da Silva,<sup>2,6</sup> Marie-Cécile Mercier,<sup>2</sup> Fanny Noulet,<sup>2</sup> Nelly Etienne-Seloum,<sup>2,3</sup> Dominique Guenot,<sup>4</sup> Maxime Lehmann,<sup>2</sup> Romain Vauchelles,<sup>2</sup> Sophie Martin,<sup>2</sup> Isabelle Lelong-Rebel,<sup>2</sup> Anne-Marie Ray,<sup>2</sup> Cendrine Seguin,<sup>5</sup> Monique Dontenwill,<sup>2</sup> and Laurence Choulier<sup>2</sup>

<sup>1</sup>CNRS, UMR 7242, Biotechnologie et Signalisation Cellulaire, Institut de Recherche de l'École de Biotechnologie de Strasbourg, Université de Strasbourg, 67400 Illkirch-Graffenstaden, France; <sup>2</sup>CNRS, UMR 7021, Laboratoire de Bioimagerie et Pathologies, Tumoral Signaling and Therapeutic Targets, Faculté de Pharmacie, Université de Strasbourg, 67401 Illkirch, France; <sup>3</sup>Département de Pharmacie, Centre de Lutte Contre le Cancer Paul Strauss, 67000 Strasbourg, France; <sup>4</sup>EA 3430, Progression Tumorale et Micro-environnement, Approches Translationnelles et Épidémiologie, Université de Strasbourg, 67000 Strasbourg, France; <sup>5</sup>CNRS, UMR 7199, Laboratoire de Conception et Application de Molécules Bioactives, Faculté de Pharmacie, Université de Strasbourg, 67401 Illkirch, France

**Nucleic acid aptamers are often referred to as chemical antibodies. Because they possess several advantages, like their smaller size, temperature stability, ease of chemical modification, lack of immunogenicity and toxicity, and lower cost of production, aptamers are promising tools for clinical applications. Aptamers against cell surface protein biomarkers are of particular interest for cancer diagnosis and targeted therapy. In this study, we identified and characterized RNA aptamers targeting cells expressing integrin  $\alpha 5 \beta 1$ . This  $\alpha \beta$  heterodimeric cell surface receptor is implicated in tumor angiogenesis and solid tumor aggressiveness. In glioblastoma, integrin  $\alpha 5 \beta 1$  expression is associated with an aggressive phenotype and a decrease in patient survival. We used a complex and original hybrid SELEX (selective evolution of ligands by exponential enrichment) strategy combining protein-SELEX cycles on the recombinant  $\alpha 5 \beta 1$  protein, surrounded by cell-SELEX cycles using two different cell lines. We identified aptamer H02, able to differentiate, in cyto- and histofluorescence assays, glioblastoma cell lines, and tissues from patient-derived tumor xenografts according to their  $\alpha 5$  expression levels. Aptamer H02 is therefore an interesting tool for glioblastoma tumor characterization.**

## INTRODUCTION

Glioblastoma (GBM), the highest-grade glioma tumor (grade IV), is the most aggressive and the most common malignant form of astrocytoma. Standard therapy consists of surgical resection to an extent that is safely feasible, followed by radiotherapy and concomitant chemotherapy with temozolomide (Stupp protocol).<sup>1</sup> Despite these therapies, patients with GBM rarely live longer than 2 years.<sup>2</sup> Histological features that characterize GBM are the presence of necrosis and abnormal growth of blood vessels around the tumor. Defining molecular profiles aims to develop molecularly guided approaches for the treatment of patients. The 2016 World Health Organization (WHO) classification scheme<sup>3</sup> integrated phenotypic and genotypic parameters for CNS tumor classification. GBMs are divided into isocitrate dehydrogenase (IDH) 1 wild-type (about 90% of cases;

corresponds to the most frequent primary or *de novo* GBM) and IDH-mutant GBM (about 10% of cases; corresponds to secondary GBM). Some of the GBM biomarkers that have been and are being discovered<sup>4</sup> are cell surface protein biomarkers.<sup>5–8</sup> Expression of cell surface protein is often remodeled in cancers. Genetic and epigenetic features altered in cancer<sup>8</sup> include modification of copy number (under- or overexpression), truncations, mutations, and post-translational modifications. These modified proteins are major clinical targets for diagnosis and therapies, considering their accessibility for pharmacological compounds.

Tumor-specific tools such as aptamers can be used as recognition ligands to discriminate a tumor cell from another cell, as agonists or antagonists, or as carriers to deliver therapeutic payloads to targeted tumor cells.<sup>9–13</sup> Aptamers are single-stranded DNA or RNA molecules that constitute an alternative class of molecules emerging as cancer-specific therapeutic, diagnostic, and theranostic tools.<sup>9,10,14–18</sup> They are selected through an *in vitro* selection process, published for the first time in 1990 by three independent research groups,<sup>19–21</sup> known as SELEX (selective evolution of ligands by exponential enrichment).<sup>20</sup> Aptamers<sup>19</sup> from the Latin *aptāre* (to fit) and from the ancient Greek *meros* (part) are often referred to as chemical antibodies<sup>13</sup> because they bind to their specific targets with high affinity and specificity. Aptamers possess numerous advantages over antibodies, like smaller size, temperature stability, self-refolding, fewer side effects for immunotherapy, lack of immunogenicity and toxicity, more efficient penetration into biological compartments, chemical synthesis with high batch fidelity, and the option of site-specific and flexible introduction of linkers, reporters, functional groups,

Received 17 July 2018; accepted 3 May 2019;  
<https://doi.org/10.1016/j.omtn.2019.05.006>

<sup>6</sup>These authors contributed equally to this work

**Correspondence:** L. Choulier, CNRS, UMR 7021, Laboratoire de Bioimagerie et Pathologies, Tumoral Signaling and Therapeutic Targets, Faculté de Pharmacie, Université de Strasbourg, 67401 Illkirch, France.

**E-mail:** [laurence.choulier@unistra.fr](mailto:laurence.choulier@unistra.fr)



small interfering RNA (siRNA), nanoparticles, drugs, and so forth.<sup>10,11,14</sup> Aptamers toward a wide variety of targets have been identified, the most common ones remaining proteins. We recently reviewed aptamers to more than 30 different tumor cell surface protein biomarkers,<sup>22</sup> a few of them being heterodimeric receptors, such as tyrosine kinase receptors and cell adhesion molecules. However, selection of aptamers to cell surface proteins remains a complex process.

Among cell surface biomarkers, integrins are heterodimeric cell surface receptors for cell migration, differentiation, and survival,<sup>23</sup> composed of  $\alpha$  and  $\beta$  subunits; their deregulation leads to cancer progression and therapy resistance.<sup>24</sup> In mammals, 24 distinct integrins are formed by the combination of 18  $\alpha$  and 8  $\beta$  subunits. Specific heterodimers preferentially bind to distinct extracellular matrix proteins. Integrin  $\alpha 5\beta 1$ , the fibronectin receptor, belongs to the arginine, glycine, and aspartate (RGD)-binding integrin family. Overexpressed on tumor neovessels and on solid tumor cells, integrin  $\alpha 5\beta 1$  is implicated in tumor angiogenesis and solid tumor aggressiveness. We and others have shown that  $\alpha 5\beta 1$  integrin is a pertinent therapeutic target for GBM<sup>25</sup> through its active role in tumor proliferation, migration, invasion, and resistance to chemotherapy.<sup>26–30</sup> At the mRNA level, high  $\alpha 5\beta 1$  integrin expression is associated with more aggressive tumors in patients with glioma.<sup>26</sup> At the protein level, to date, only a few *in situ* analyses of GBM tumor section have been described.<sup>31,32</sup> Further investigation of  $\alpha 5\beta 1$  expression in GBM tumor cells as a potential prognostic factor and/or biomarker for diagnosis requires rapid and accurate tools.

In our study, aptamers to integrin  $\alpha 5\beta 1$ -expressing cells were selected by an original and complex hybrid SELEX process. This SELEX combines three rounds of protein-SELEX surrounded by 15 rounds of cell-SELEX on two different cell lines genetically modified to overexpress integrin  $\alpha 5$ , the human GBM U87MG cell line, and the Chinese hamster ovaries CHO-B2 cell line. Counterselection steps were performed on isogenic cell lines underexpressing  $\alpha 5$  for U87MG or ones that do not express  $\alpha 5$  for CHO-B2. We identified and characterized an aptamer named H02. Directly coupled to the cyanine 5 fluorophore, aptamer H02 was able to discriminate between 10 GBM cell lines expressing high and low levels of integrin  $\alpha 5$ . Aptamer H02 is internalized at 37°C. As a proof of concept, we also demonstrated that aptamer H02 is very efficient in apta-fluorescence assays to distinguish GBM tumor tissues from patient-derived tumor xenografts expressing high levels of  $\alpha 5$  from GBM tumor tissues expressing low levels of  $\alpha 5$ .

## RESULTS

### Selection Strategy Combining Cell-SELEX on Two Cell Lines Expressing Integrin $\alpha 5\beta 1$ and Protein-SELEX on the Recombinant $\alpha 5\beta 1$ Integrin

To guide the selection toward  $\alpha 5\beta 1$ , we used an original hybrid SELEX strategy that alternates protein and cell-SELEX. Our strategy is divided into three steps, symbolized by three circles in Figure 1A, using two different cell lines (Figure 1B) and a recombinant  $\alpha 5\beta 1$  pro-

tein (Figure 1C). The first seven rounds of cell-SELEX were performed on human GBM U87MG cells overexpressing the  $\alpha 5$  subunit (U87MG  $\alpha 5+$ ).<sup>26</sup> An RNA library comprising  $10^{14}$  different molecules was incubated with U87MG  $\alpha 5+$  cells plated in a cell culture dish. Isogenic U87MG cells modified to underexpress the  $\alpha 5$  subunit (U87MG  $\alpha 5-$ )<sup>26</sup> were used for counterselection steps. Although the  $\alpha 5$  subunit has never been detected by western blot (Figure 1B) in these cells, to avoid any loss of potential  $\alpha 5$  binders, counterselection steps were not introduced before the fourth round of selection and were performed only during rounds 4–6. The next three rounds of selection were performed by a protein-based SELEX process (rounds 8–10) on the protein A-purified form of integrin  $\alpha 5\beta 1$ . The recombinant protein  $\alpha 5$ (E<sub>951</sub>)  $\beta 1$ (D<sub>708</sub>)-Fc ( $\alpha 5\beta 1$ -Fc) is composed of human  $\alpha 5$  and  $\beta 1$  ectodomains fused to Fc $\gamma 1$  knobs mutated into their CH3 domains to increase the likelihood of heterodimerization between  $\alpha 5$  and  $\beta 1$  chains.<sup>33</sup> Negative and counterselection steps preceding positive selection steps were performed on protein A-Sepharose beads (rounds 8–10) and on an antibody presenting the same  $\gamma 1$  isotype as the Fc fused to  $\alpha 5\beta 1$  ectodomains (rounds 9 and 10). Finally, cell-SELEX rounds were implemented on two different cell lines: on U87MG cells (round 11, as for rounds 1–7) and CHO-B2 cells (rounds 12–18). CHO-B2 cells, which do not naturally express  $\alpha 5$ ,<sup>34</sup> were used for counterselection. For positive selection, CHO-B2 cells were manipulated to generate positive  $\alpha 5$  cells by overexpressing human ITGA5. During the course of the SELEX process, the stringency was progressively increased by decreasing and increasing the incubation time for positive and counterselection, respectively by introducing competitor yeast tRNAs and increasing the number of washes (Table S1). Enrichment of RNA pools during selection was followed by qRT-PCR. The RNA pool at round 18 showed significant amplification compared with pools of preceding rounds (Figure S1) and was cloned. Of 82 sequenced molecules, five aptamers, named H02, H03, G10, B03, and G11, were selected for further characterization.

### Identification of Aptamers Binding to $\alpha 5$ -Expressing Cells

Aptamer H02 was the most frequently represented over all sequences (6 times over 82 sequences, 7.3%). Aptamers H03, G10, and G11 represented 3.7% of all sequenced molecules and aptamer B03 1.2%. The predicted secondary structures of the five aptamers (H02, G11, B03, G10, and H03) are shown in Figure 2A. Fixed regions (shown in dark red in Figure 2A) were designed to display partial complementarity and pre-organize aptamers in hairpin structures.<sup>35</sup> The secondary structure predictions of aptamers H02, G11, and B03 are highly similar and very different from those of G10 and H03.

Identification of  $\alpha 5\beta 1$ -binding aptamers was performed using confocal fluorescence microscopy by incubating cyanine-5 (Cy5)-labeled aptamers at 4°C with the cells used for the cell-SELEX process. None of the five aptamers binds to U87MG  $\alpha 5-$  and CHO-B2 cells used for the counterselection steps (Figures S2A and S2B). Only aptamer H02 binds to the U87MG  $\alpha 5+$  and CHO-B2  $\alpha 5+$  cells used for positive selection steps (Figures 2B and 2C). We next checked

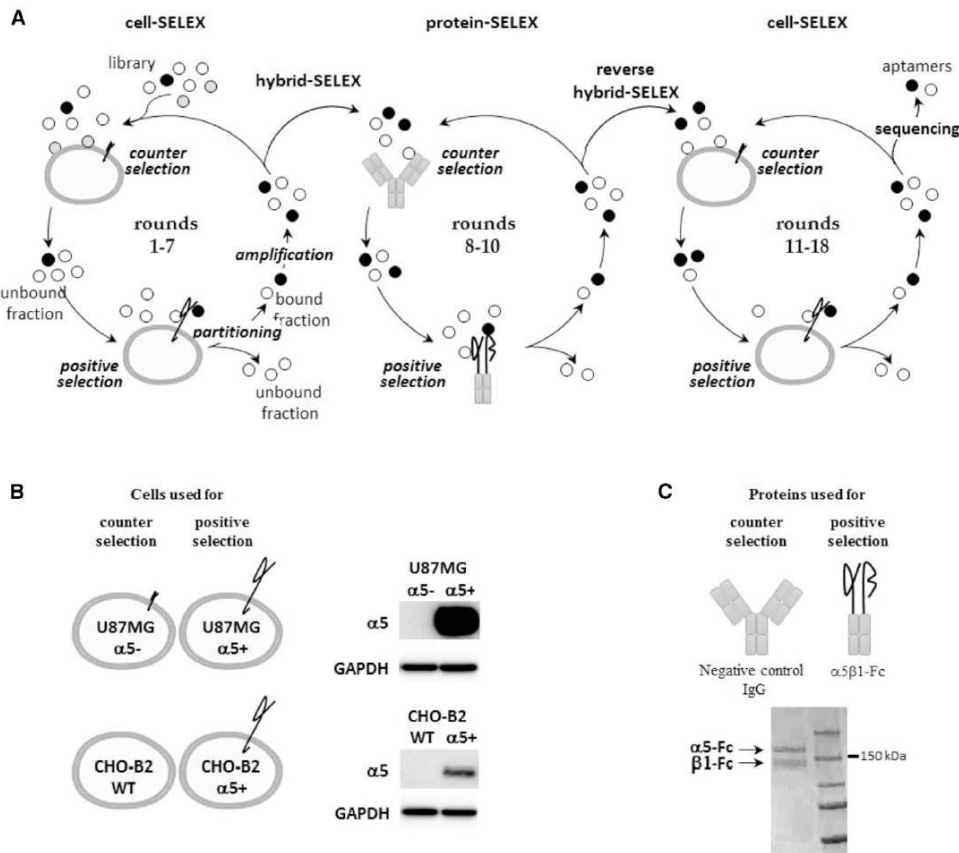


**Figure 1. SELEX Strategy**

(A) Scheme of the cell- and protein-based SELEX strategy used for aptamer selection. Briefly, one round of SELEX first involves a selection step. The nucleic acid library is incubated with a target (positive selection), which can be preceded by counterselection to remove non-specific nucleic acid molecules. During the partitioning step, bound and unbound fractions are separated. The bound fraction is amplified to obtain an enriched pool for the next round of selection. First, cell-SELEX processes were performed (rounds 1–7), followed by protein-SELEX (rounds 8–10) and then by cell-SELEX (rounds 11–18). The combination of cell- and protein-based SELEX is called hybrid SELEX and reverse hybrid SELEX. At the end of selection, nucleic acid molecules were cloned and sequenced. Individual sequences are aptamers. (B) Description of cells used for counterselection and positive selection (rounds 1–7 and 11–18). On the right, western blots show the level of expression of  $\alpha 5$  in the different cell lines used for the SELEX strategy. (C) Description of proteins used for counterselection and positive selection (rounds 8–10). Counterselection was also performed on protein-A Sepharose beads alone in rounds 8–10. Shown below is a denaturing SDS polyacrylamide gel loaded with the protein A-purified recombinant  $\alpha 5\beta 1$ -Fc protein and Coomassie blue stained.

whether, under the same methodological conditions, these aptamers were able to bind to U87MG cells at 37°C, the temperature used for the cell-SELEX process. H02, G11, B03, G10, and B03 did not bind to U87MG  $\alpha 5^-$  cells (Figure 3A). On U87MG  $\alpha 5^+$  cells, we observed strong binding not only of aptamer H02 but also, to a lesser extent, of aptamer G11 (Figure 3B). Because of its binding to U87MG  $\alpha 5^+$  cells at 4°C and at 37°C, subsequent analyses were performed using aptamer H02.

**Validation of Integrin  $\alpha 5\beta 1$  as the Target of Aptamer H02**

The SELEX process was performed to guide the selection toward integrin  $\alpha 5\beta 1$ . However, cell-SELEX-based strategies have already led

to the selection of aptamers against “undesirable targets,” meaning other proteins than the expected pre-identified targets.<sup>36,37</sup>

To validate integrin  $\alpha 5\beta 1$  as the target of our SELEX process, surface plasmon resonance (SPR) experiments were performed on a Biacore T200 instrument. Figure 4A shows the experimental scheme. Aptamer H02, with 2'-fluoro pyrimidines to increase its stability in SPR experiments, was captured on a CAP sensor chip via a biotin at its 5' extremity. The aptamer was captured on a biotin CAPture reagent. Integrins were injected at concentrations ranging from 8–130 nM. We tested human integrins  $\alpha 5\beta 1$  and  $\alpha v\beta 3$  to check the H02 aptamer's specificity. The surface was then

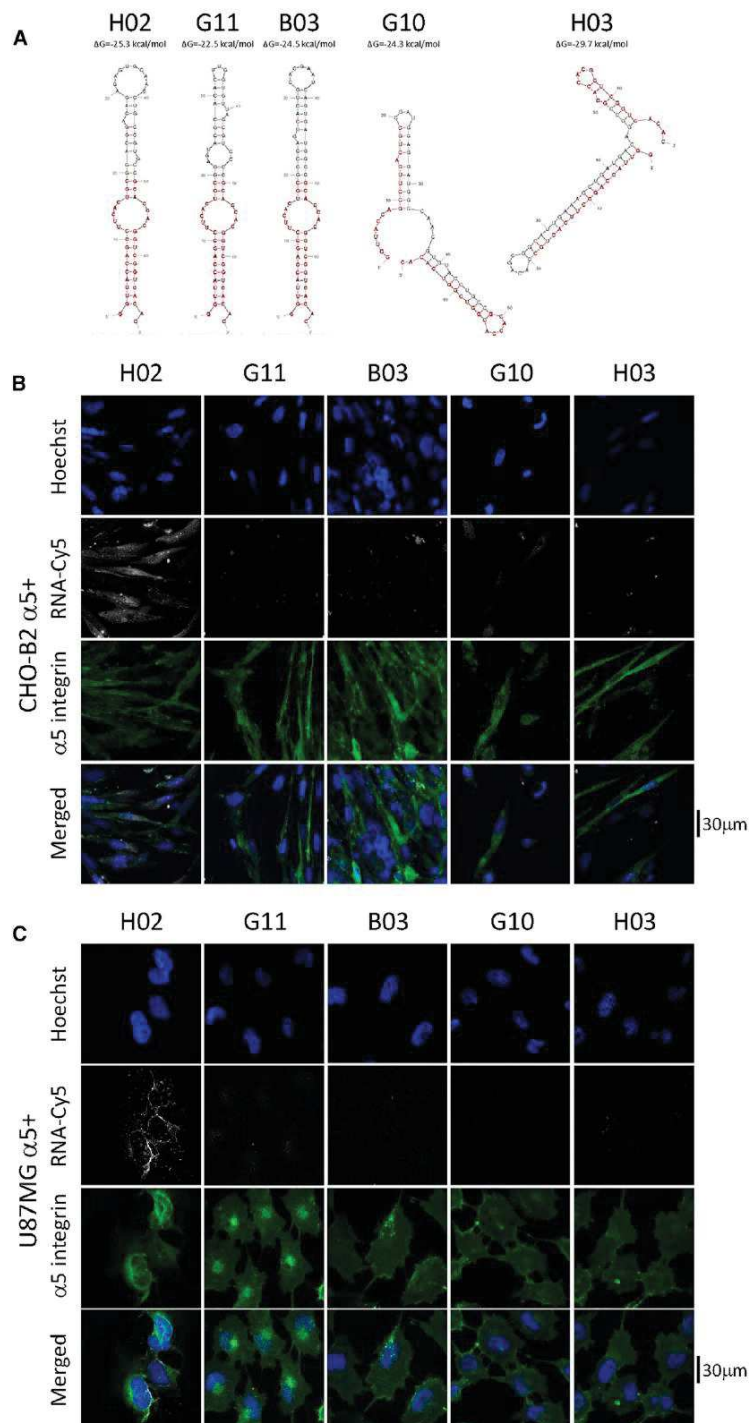
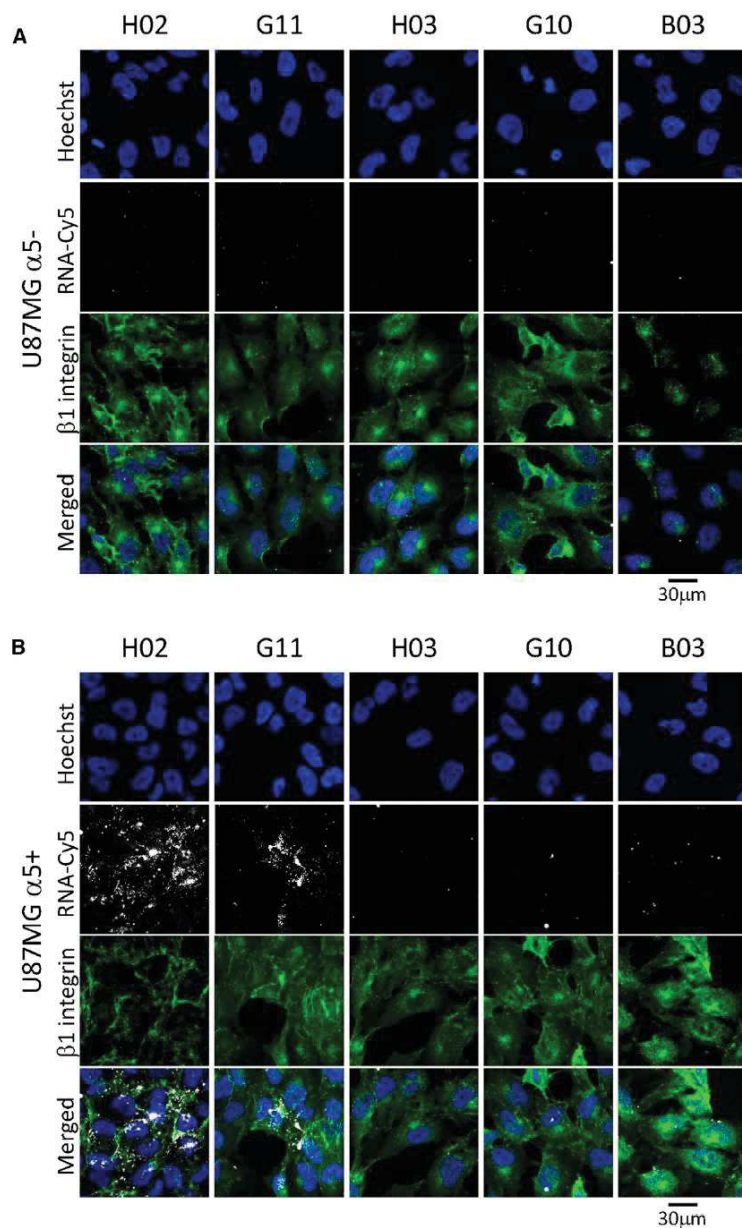


**Figure 2. Aptamers Predicted Secondary Structures and Binding to  $\alpha 5$ -Expressing Cells**

(A) Predicted secondary structure of aptamers H02, G11, B03, G10, and H03. Structures were predicted using the mfold web server.<sup>67</sup> Nucleotides 1–19 and 50–68 correspond to fixed flanks of the candidate sequences. They are shown in dark red.  $\Delta G$  values are noted above the structures. (B and C) Monitoring of the binding of five Cy5-labeled aptamers (H02, G11, B03, G10, and H03) at 5  $\mu$ M on CHO-B2 and U87MG cell lines at 4 $^{\circ}$ C using confocal microscopy. Nuclei, counterstained with Hoechst, are shown in royal blue. Aptamers, coupled to Cy5, are shown in white. (B) Binding on CHO-B2  $\alpha 5+$ .  $\alpha 5$  integrin is visualized, using the GFP-fused protein, in green. (C) Binding on U87MG  $\alpha 5+$ .  $\alpha 5$  integrin was labeled with the IIA1 antibody and is shown in green. Images were captured at the same setting to allow direct comparison of staining patterns.



regenerated. CAP chips are designed to capture biotinylated molecules reversibly on the sensor surface, facilitating its regeneration.<sup>38</sup> An SPR cycle thus consisted of injections of biotin CAPture reagent, biotinylated aptamer, integrin, and regeneration solution. Successive cycles were repeated, changing the integrin nature and concentration at each cycle (Figure S3A). Because of 2'-fluoro modifications, aptamer H02 was resistant to degradation over time, and aptamer

10% fetal bovine serum (FBS) (Figure S4A). If this aptamer had to be used under more complex conditions than in a simple buffer, then it would have to be modified to increase its nuclease sensitivity. For example the 2'-fluoro-modified H02 aptamer is very stable in contact with cells at 4°C and at 37°C as it is not degraded in the selection buffer and in a complex medium for at least 1 h (Figure S4B).

### Figure 3. Binding of Aptamers to U87MG Cells

(A and B) Monitoring the binding of five Cy5-labeled aptamers (H02, G11, B03, G10, and H03; 5  $\mu$ M) at 37°C, using confocal microscopy, on U87MG  $\alpha$ 5- (A) and U87MG  $\alpha$ 5+ cells (B). Nuclei, counterstained with Hoechst, are shown in royal blue. Aptamers, coupled to Cy5, are shown in white. The anti- $\beta$ 1 TS2/16 antibody (Ab) labeling is shown in green. Merged images are shown. Images were captured at the same setting to allow direct comparison of staining patterns.

injections were highly reproducible. The biotinylated aptamer reached the same level at each cycle with as low as 2% variation in responses over 20 cycles (Figure S3A). Therefore, the surface has the same properties during all experiments.

Figures 4B and 4C show the sensorgrams obtained for integrins  $\alpha$ 5 $\beta$ 1 and  $\alpha$ v $\beta$ 3, respectively, after double referencing (subtraction of reference channel and buffer injection). The sensorgrams show that, even when responses are low, aptamer H02 bound specifically to integrin  $\alpha$ 5 $\beta$ 1 in a dose-dependent manner but failed to interact with integrin  $\alpha$ v $\beta$ 3. The equilibrium affinity parameter ( $K_D$ ) of the interaction between integrin  $\alpha$ 5 $\beta$ 1 and aptamer H02 was  $72 \pm 11$  nM. To ensure that integrin was active, positive controls were used. Figure S3B shows binding by SPR of integrin  $\alpha$ 5 $\beta$ 1 to its natural ligand, fibronectin. We also demonstrated that only aptamer H02 was an  $\alpha$ 5 $\beta$ 1 binder (but not, for example, aptamer B03; Figure S3C).

### H02 Aptamer Stability, Specificity and Affinity for U87MG $\alpha$ 5+ Cells

Because aptamer H02 is a non-modified RNA molecule, we tested its stability in the presence of cells at 4°C and 37°C in the buffer used for selection. The results (Figure S4A) confirmed that incubation on cells for 1 h, which corresponds to the maximum contact time of RNAs with cells during different assays, does not induce aptamer H02 degradation. However, this aptamer is extremely rapidly degraded when incubated on cells in a culture medium supplemented with

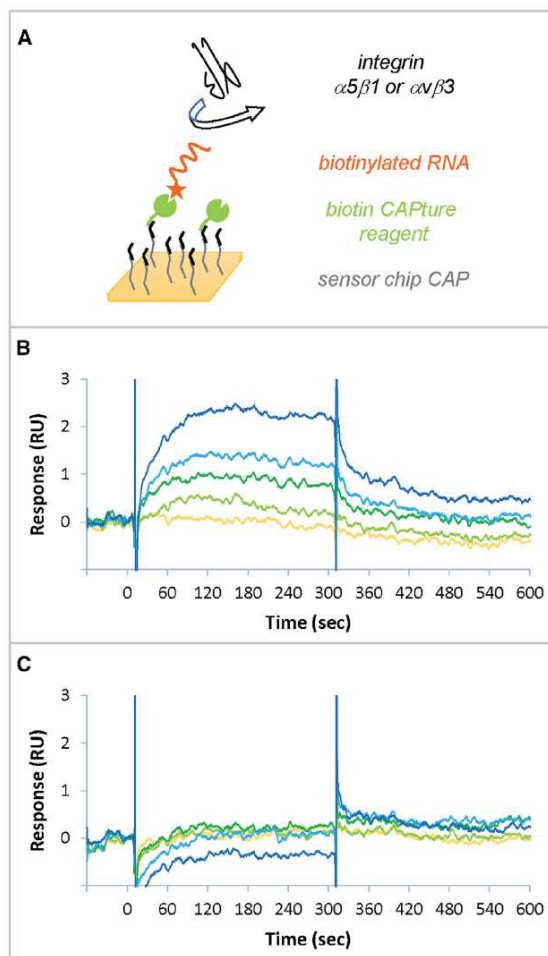


**Figure 4. Surface Plasmon Resonance Experiments for Target Validation** (A) Experimental scheme. The biotin CAPture reagent (green), composed of streptavidin conjugated with an oligonucleotide, is stably hybridized to a complementary sequence immobilized on the sensor chip (black). The biotinylated aptamer (orange) is captured to the biotin CAPture reagent. Integrins are used as analytes (black). The interaction between integrins and the captured aptamer is studied. The surface is then regenerated and rebuilt with new biotin CAPture reagent in the next cycle. (B and C). SPR sensorgrams obtained for the injections of integrins  $\alpha 5\beta 1$  (B) and  $\alpha 5\beta 3$  (C) at 8.1 nM (yellow), 16.2 nM (light green), 32.5 nM (dark green), 65 nM (light blue), and 130 nM (dark blue).

The specificity of aptamer H02 for  $\alpha 5$ -overexpressing cells was confirmed by flow cytometry at 4°C by incubation of Cy5-coupled aptamers B03 and H02 at 500 nM for 1 h with detached CHO-B2 cells (Figure 5A) and by incubation of Cy5-coupled aptamers G11 and H02 at concentrations ranging from 0.15–5  $\mu\text{M}$  with detached CHO-B2  $\alpha 5$ + cells (Figure S5). Although no shift in fluorescence was detected for CHO-B2 cells after incubation with

the two Cy5-labeled H02 and B03 aptamers, a shift was detected for CHO-B2  $\alpha 5$ + cells with aptamer H02 but not with aptamer B03. Figure S5 also confirmed that aptamer H02 was our best hit from SELEX because it binds much better to  $\alpha 5$ -expressing cells than aptamer G11.

The equilibrium affinity parameter  $K_D$  of the interaction between aptamer H02 and U87MG  $\alpha 5$ + cells was determined using flow cytometry (Figure 5B). Binding events associated with the fluorescence signal of different concentrations of aptamer, ranging from 0.15–5  $\mu\text{M}$ , to a constant number of cells were measured. A  $K_D$  of  $277.8 \pm 51.8$  nM was determined by plotting the mean fluorescence of U87MG  $\alpha 5$ + cells against the concentration of the H02 aptamer.

#### H02 Aptamer Localization in U87MG $\alpha 5$ + Cells

The localization of aptamer H02 on GBM U87MG  $\alpha 5$ + cells was analyzed by confocal microscopy at 4°C and 37°C. Cells were incubated with the Cy5-labeled aptamer H02 and with the anti- $\alpha 5$  IIA1 antibody, followed by incubation of a secondary antibody labeled with Alexa 546. Spots of co-localization were detected between Alexa 546 and Cy5, which reflect spatial proximity between the  $\alpha 5$  subunit and the aptamer H02, at 4°C and, to a lesser extent, at 37°C (Figures 6A and 6B). Aptamer H02 detected  $\alpha 5\beta 1$  mostly at the plasma membrane and at cell-cell junctions at 4°C, whereas punctuate labeling suggested internalized molecules at 37°C. The weaker co-localization observed with anti- $\beta 1$  antibody and aptamer H02 (Figure 3B) is explained as the  $\beta 1$  subunit associates with different  $\alpha$  subunits to form different integrins, whereas the  $\alpha 5$  subunit associates only with the  $\beta 1$  subunit to form the fibronectin receptor.

We next wanted to confirm the internalization of aptamer H02 in  $\alpha 5$ -expressing cells at 37°C. To this end, adherent U87MG  $\alpha 5$ + cells were labeled for 30 min with the Cy5-coupled aptamer H02 at five different concentrations (5, 2.5, 1.25, 0.6, and 0.3  $\mu\text{M}$ ). After cell fixation, cells were immunolabeled with the anti-EEA1 antibody to detect early endosomes and then analyzed by confocal microscopy. Figure 6C shows clear co-localization of aptamer H02 at 5, 2.5, and 1.25  $\mu\text{M}$  with the anti-EEA1 antibody in U87MG  $\alpha 5$ + cytoplasm, suggesting aptamer H02 endocytosis. A 3D reconstruction of whole z stacks is shown in Video S1.

Fluorescently labeled aptamers were not detected at lower concentrations (0.6 and 0.3  $\mu\text{M}$ ). The lower concentration limit of 1.25  $\mu\text{M}$  corresponds to 4.5-fold the  $K_D$  of the H02-cell interaction and, theoretically, to 82% receptor occupancy, governed by concentration and affinity. At 4°C, aptamers were not detected at concentrations lower than 5  $\mu\text{M}$  (Figure S6), suggesting a different binding mechanism at 4°C and at 37°C. Figures 5A and S5 show that, in flow cytometry experiments, a difference could be detected at 4°C between H02 and aptamers B03 and G11 at concentrations lower than 1  $\mu\text{M}$ . This difference may be due to the differences inherent to the two different techniques (flow cytometry versus confocal microscopy).<sup>39</sup>



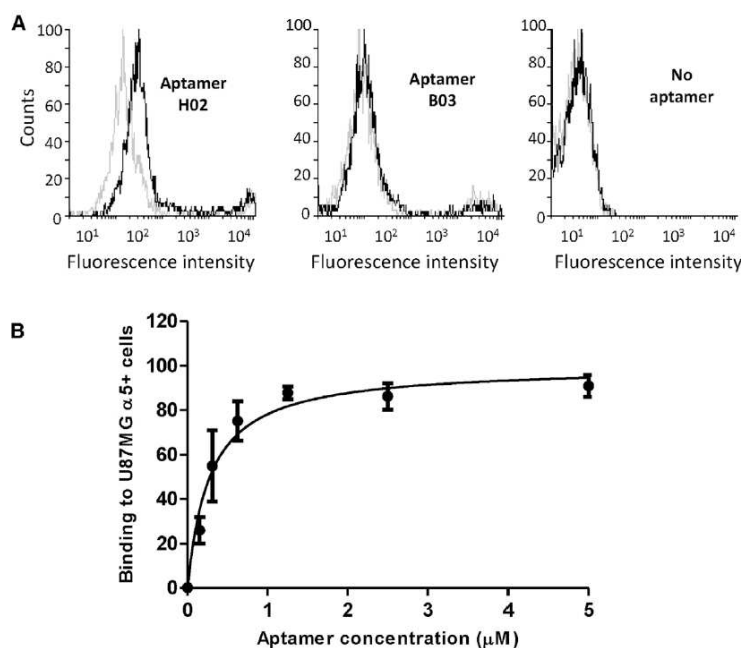


**Figure 5. Flow Cytometry Binding of Aptamers**

(A) Comparison of the binding profiles of aptamers H02 (left) and B03 (center) on CHO-B2 cells (gray lines) and CHO-B2  $\alpha 5+$  cells (black lines) at 4°C. Profiles without aptamer labeling are shown on the right. (B) Titration of aptamer H02 resulted in determination of the equilibrium affinity parameter  $K_D$  for the interaction between U87MG  $\alpha 5+$  cells and aptamers H02 ( $277.8 \pm 51.8$  nM). Cy5-aptamer H02 at concentrations of 0.15, 0.3, 0.6, 1.25, 2.5, and 5  $\mu$ M was incubated on ice with a constant amount of cells and analyzed by flow cytometry.

#### Cyto- and Histofluorescence with Aptamer H02 on Different GBM Cell Lines and on Patient-Derived GBM Xenografts

Aptamer molecules have the potential to revolutionize the field of diagnostics for the detection of cell-specific biomarkers.<sup>40</sup> We evaluated the capacity of aptamer H02 to be a new tool for the characterization of GBM  $\alpha 5$ -expressing cells and tissues. We first characterized the ability of aptamer H02 to distinguish between 10 human GBM cell lines expressing different levels of the  $\alpha 5$  subunit (Figure 7A). Among those are U87MG  $\alpha 5+$  and U87MG  $\alpha 5-$ , used for cell-SELEX, and eight GBM cell lines, LN319, LN229, SF763, LN18, LNZ308, U373, T98G, and LN443. For aptacytochemical assays, confluent adherent cells were stained with the Cy5-labeled aptamer H02 at 4°C at 5  $\mu$ M for 30 min. After cell fixation with paraformaldehyde, cells were immunolabeled with an anti- $\alpha 5$  primary antibody and a secondary antibody labeled with Alexa 546. Quantification of apta- and immunostaining of the different cell lines is shown in Figure 7B. A correlation coefficient of 0.78 has been determined between apta- and immunofluorescence. Integrin  $\alpha 5\beta 1$  expression in GBM cell lines can therefore be monitored in cytofluorescence with the Cy5-labeled aptamer H02.

Histochemical assays were performed on two patient-derived GBM xenografts, TC22 and TC7. These two tumors present a 7.6-fold difference in mRNA ITGA5 levels, with the TC7 level higher than that of TC22. These tissue sections, embedded in paraffin, were first deparaffinized and subjected to an antigen unmasking protocol. Histofluorescence analysis was performed on the two tissue sections to quantify the protein level of integrin  $\alpha 5$  in both tumors and to compare immun- and aptahistochemistry assays. For immunostaining, the indi-

rect assay consisted of successive incubation of an anti- $\alpha 5$  antibody and a secondary fluorescent antibody. Immunohistochemical assays showed that the TC7 tumor presented a higher integrin  $\alpha 5$  expression level than the TC22 tumor (Figures 7C and 7D, top panels), in accordance with the mRNA levels. Aptahistochemical assays were performed by incubation of tumor sections with the Cy5-labeled aptamers H02 and G11 at the lower concentration limit of 1  $\mu$ M, as outlined in H02 Aptamer Localization in U87MG  $\alpha 5+$  Cells (Figures 7C and 7D, bottom panels). With aptamer

H02, the fluorescence intensity is 4-fold higher on TC7 than on TC22. Under the conditions used for these histochemical experiments, the TC7 versus TC22 discrimination capacity was better with aptamer H02 than with the anti- $\alpha 5$  antibody. Aptamer G11 was also able to discriminate between both tissue sections, but to a much lesser extent than aptamer H02 (difference of 1.6-fold).

Aptamer H02 is therefore an interesting and promising new tool to differentiate cells according to their  $\alpha 5$  subunit expression levels in cyto- and histofluorescence experiments.

#### DISCUSSION

Biomarkers are indicators used to establish a diagnosis and prognosis and predict susceptibility to targeted therapies. GBM is the most aggressive form of brain tumors in adults. Despite intensive treatments, the prognosis of GBM patients remains poor. There is an urgent need to incorporate known biomarkers into clinical trials and routine clinical practice, which may assist not only with patient selection but also with adjustment of the treatment schedule based on patient-specific biology.<sup>41</sup> Because differential expression of cell surface proteins often occurs in tumor cells, and considering their accessibility to extracellular ligands, these proteins provide biomarkers of interest in oncology. The identification of molecular probes specific for cell surface protein biomarkers is of great importance.<sup>22</sup> Because of their high affinity and specificity toward their targets, aptamers are attractive and promising tools, alternatives to antibodies for clinical applications. In this study, using a complex and highly stringent SELEX strategy, we showed that it was possible to select an RNA aptamer specific to a pre-identified heterodimeric

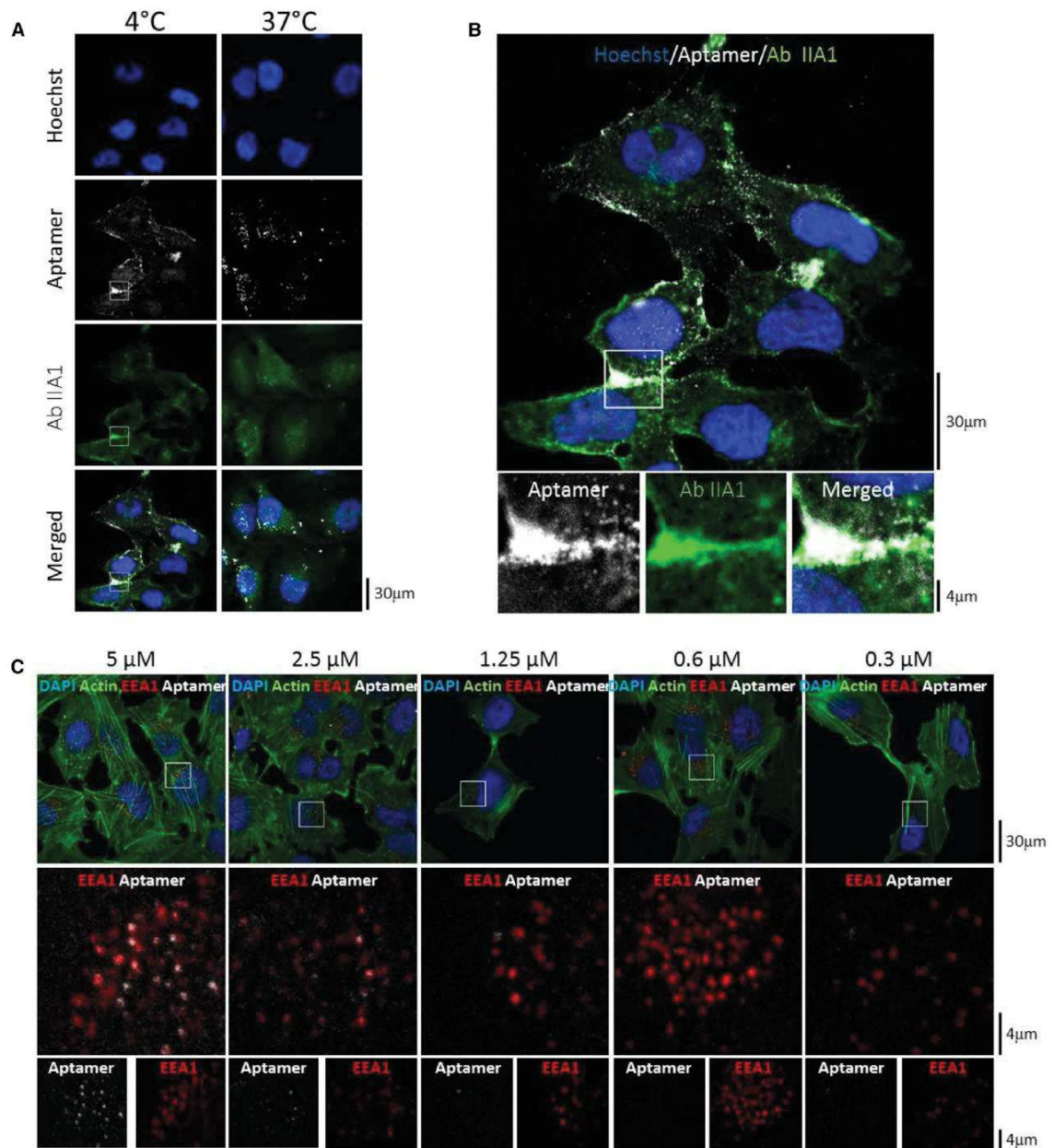


**Figure 6. Confocal Microscopy Analysis of Aptamer H02 on U87MG  $\alpha$ 5+**

(A) Confocal microscopy analysis with aptamer H02 at 5  $\mu$ M and the anti- $\alpha$ 5 antibody IIA1 on U87MG  $\alpha$ 5+ cells at 4°C and 37°C. The aptamer is labeled with Cy5 (white). Incubation of antibody IIA1 was followed by incubation with a secondary antibody labeled with Alexa 546 (green). Nuclei are stained with Hoechst (blue). (B) Top: enlargement of the merged image in (A) at 4°C. Bottom: magnified images acquired by zooming in on the indicated areas of the parental image. Scale bars are shown in the lower right corners of the images. (C) Co-localization of aptamer H02 and the endocytosis marker EEA1. Shown are confocal images of U87MG  $\alpha$ 5+ cells incubated at 37°C with the

(legend continued on next page)

cell surface protein embedded in its natural environment. Integrin  $\alpha 5\beta 1$  is a GBM cell surface biomarker.<sup>26</sup> Aptamer H02 was able to differentiate between high and low expression of the  $\alpha 5$  integrin on cells and tissues. This aptamer is suitable for tumor characterization.

Two main processes have been developed to select aptamers specific for pre-determined cell surface proteins: protein- and cell-based SELEX.<sup>22</sup> In protein-based SELEX, a purified protein is used as target, usually full-length or truncated (generally recombinant ectodomains). The major issues with the protein-based SELEX process are that purification of membrane proteins is not easy and that purified proteins may not adopt the same conformational state as in their endogenous cellular environment. Some aptamers identified through protein-based SELEX failed to recognize their target when embedded in whole living cells.<sup>42,43</sup> In cell-based SELEX, targets are cell surface proteins in their cellular environment. This process is much more complex than protein-based SELEX. Modification of cell lines is often required to guide the selection toward the desired target, like over- and/or underexpression of the protein target for positive- and/or counterselection, respectively. Cell-SELEX generally employs cells genetically modified to overexpress a defined cell surface target for positive selection and mock cells for counterselection or mock cells for positive selection and isogenic cells underexpressing the cell surface target for counterselection.<sup>22</sup> Cancer cell lines have been used for the cell-based SELEX process,<sup>9,44</sup> both for therapy and diagnostic purposes.

Only three integrins ( $\beta 2$ ,  $\alpha v\beta 3$ , and  $\alpha 6\beta 4$ ) have so far been used as pre-identified targets for the SELEX processes. Blind et al.<sup>45</sup> selected, by protein-SELEX, RNA aptamers targeting a 46-mer peptide corresponding to the complete cytoplasmic domain of the  $\beta 2$  subunit of integrin  $\alpha L\beta 2$ . Cells infected with vaccinia viruses encoding  $\beta 2$ -specific aptamers enabled high-level cytoplasmic expression of RNA aptamers. Intracellular integrin-binding aptamers reduced inducible cell adhesion to the intercellular adhesion molecule 1 (ICAM-1). To target integrin  $\alpha v\beta 3$ , two different protein-based SELEX processes and a cell-based SELEX were used to identify 2'-fluoropyrimidine RNA aptamers. The 2'-fluoropyrimidine modification confers increased nuclease resistance to RNA molecules. Aptamer Apt- $\alpha v\beta 3$ , selected on  $\alpha v\beta 3$  purified by immunoaffinity chromatography, was able to bind  $\alpha v\beta 3$  integrin expressed on the surface of live cells and to impair endothelial cell growth and survival.<sup>46,47</sup> To select aptamers specific to homodimer  $\alpha v$  and  $\beta 3$ , Gong et al.<sup>48</sup> developed a strategy called multivalent aptamer isolation (MAI)-SELEX. Two distinct selection stages were employed, the first being a classical affinity selection on the purified full-length  $\alpha v\beta 3$  integrin. The second, for specificity, leads selection to  $\beta 3$  because integrin  $\alpha IIb\beta 3$  served as a protein decoy. Two aptamers specific for  $\alpha v$  and  $\beta 3$  were identified

with affinities in the low nanomolar range. Takahashi et al.<sup>49</sup> applied a process they called isogenic cell (Icell)-SELEX to identify RNA aptamers targeting  $\alpha v$  integrins (integrin alpha subunit [ITGAV]), in which isogenic HEK293 cell lines were manipulated for counterselection by microRNA-mediated silencing and for positive selection by overexpression of target proteins. Integrin  $\alpha 6\beta 4$  has recently been the target of hybrid SELEX,<sup>50,51</sup> a combination of protein- and cell-based SELEX processes, for which five rounds of cell-SELEX on PC-3 cells were followed by 7 rounds of protein-based SELEX on a recombinant  $\alpha 6\beta 4$  protein.<sup>52</sup> In this last study, despite introduction of counterselection on PC-3  $\beta 4$  integrin (ITGB4) knockdown cells to deplete single-stranded DNA (ssDNA) aptamers specific for cell surface markers other than the  $\beta 4$  subunit, the cell-SELEX process alone was not sufficient to prevent enrichment of non-target-specific aptamers.

To allow discovery of highly selective but also conformation-dependent aptamers and to guide the selection toward  $\alpha 5\beta 1$  integrin, the complex SELEX strategy we adopted presents two originalities compared with other SELEX strategies toward cell surface biomarkers. In our study, a hybrid SELEX combining successive rounds of cell-SELEX, protein-SELEX, and then again cell-SELEX was performed. Usually, in hybrid SELEX, the first rounds of selection are performed by cell-SELEX, and then rounds of selection are performed on the same version of the target in its purified form by protein-based SELEX.<sup>50,52</sup> A reverse hybrid SELEX combines protein-SELEX followed by cell-SELEX.<sup>51,53,54</sup> Consequently, our strategy combines hybrid SELEX and reverse hybrid SELEX (Figure 1). The second originality is that two different cell lines were used compared with one in previous studies. These two cell lines were the human GBM U87MG and the hamster CHO-B2 cell lines. Both cell lines were genetically transformed to express high levels of the human  $\alpha 5$  subunit for positive selection rounds. These two cell lines do not express the same level of the  $\alpha 5$  subunit (Figure 1). The first rounds of selection were performed on the U87MG  $\alpha 5+$  cells to guide the selection toward cells highly expressing the  $\alpha 5$  subunit. The last rounds of cell-SELEX were performed on CHO-B2  $\alpha 5+$  cells, a cell line expressing  $\alpha 5$  levels similar to  $\alpha 5$  expression of the wild-type GBM cell line U373, to guide the selection to a more natural expression and, probably, a more natural conformation and environment of the target. For counterselection rounds, the ideal cell line was CHO-B2 because it does not express the  $\alpha 5$  subunit at all. U87MG  $\alpha 5-$  cells were stably transfected to repress the human  $\alpha 5$  gene by transfecting a pSM2 plasmid coding for a short hairpin RNA (shRNA) targeting the  $\alpha 5$  mRNA.<sup>26</sup> Despite the fact that U87MG  $\alpha 5-$  cells were probably not fully depleted in  $\alpha 5$ , we showed that the differential expression level of  $\alpha 5$  between U87MG  $\alpha 5+$  and U87MG  $\alpha 5-$  cells (not detected in western blots) was high enough to permit a differential binding pattern of aptamer H02 (Figure 3B). The keys to this successful complex SELEX are the

Cy5-labeled aptamer H02 at five different concentrations (5, 2.5, 1.25, 0.6, and 0.3  $\mu$ M). After aptamer labeling (shown in white), cells were fixed, permeabilized, and then labeled to detect nuclei (DAPI, blue), actin (Phalloidin-Atto 488, green), and early endosome EEA1 (EEA1 immunolabeling, red). Shown in the first row are merged images. Shown in the second row are magnified images of selected areas (white squares) of the parental images. These images show co-labeling of EEA1 and aptamer H02. Shown in the third row are separate EEA1 and aptamer labeling. Images were captured at the same setting to allow direct comparison of staining patterns.

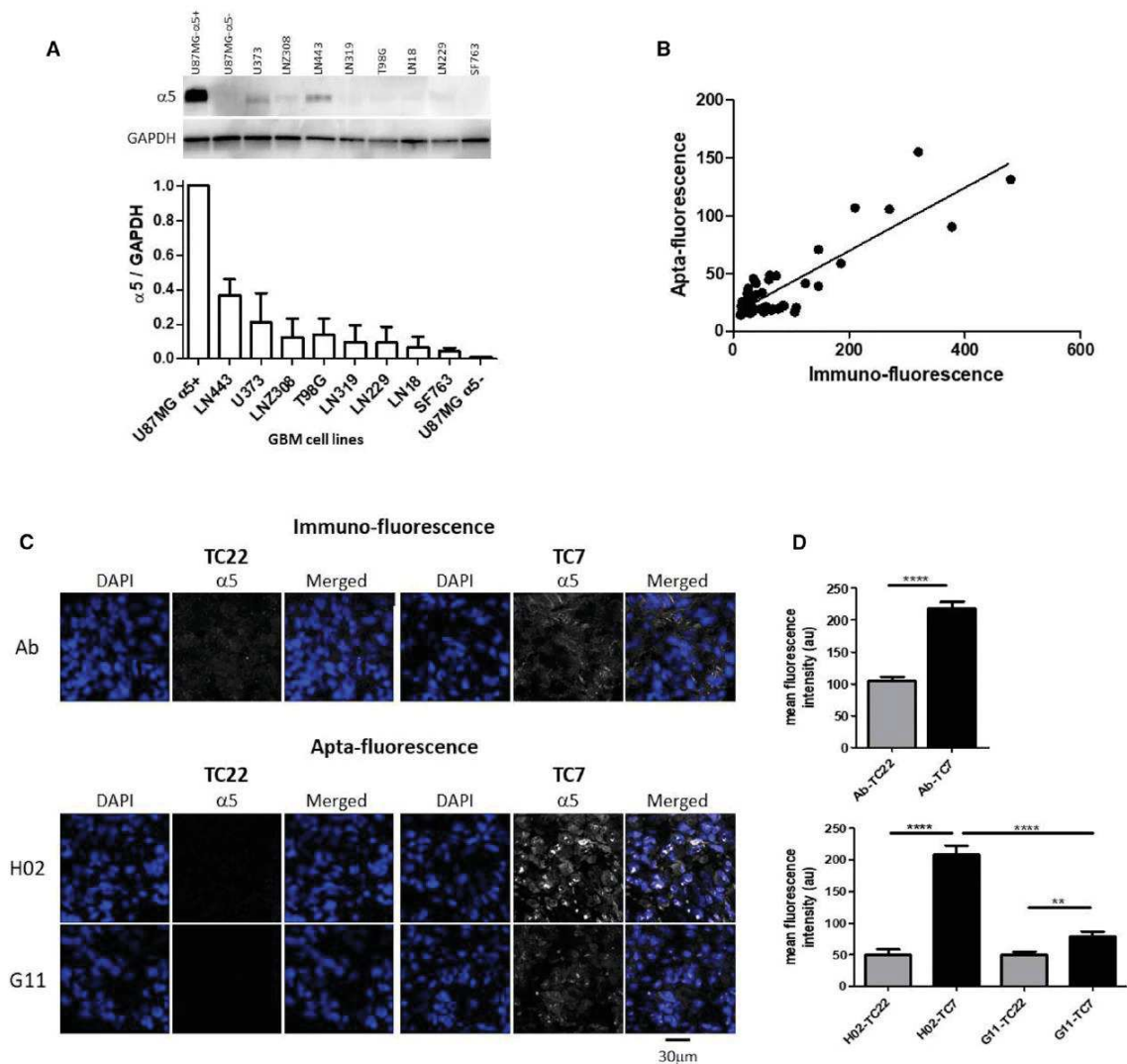


**Figure 7. Aptafluorescence on GBM Cells and Tissues**

(A–D) Aptafluorescence on GBM cells (A and B) and tissues (C and D). (A) Western blot analysis. One representative western blot of the GBM cell lines (U87MG  $\alpha 5+$ , U87MG  $\alpha 5-$ , LN319, LN229, SF763, LN18, LN2308, U373, LN443, and T98G) used in this study is shown at the top. Histograms, at the bottom, show the quantification of  $\alpha 5$  integrin expression normalized to GAPDH levels (mean  $\pm$  SEM of 3 independent experiments). GAPDH was used as a loading control. (B) Immuno-quantification versus apta-quantification of confocal fluorescence experiments on ten GBM cell lines. Immuno-quantification was performed with an anti- $\alpha 5$  antibody, followed by a secondary antibody coupled to Alexa 546. Aptafluorescence was performed with the Cy5-labeled aptamer H02. Quantification of mean fluorescence intensity (a.u.) was performed on at least 5 randomly selected images per cell line. The correlation coefficient is 0.78, with  $p < 0.0001$ . (C) Immunofluorescence (top panel) and apta-fluorescence (bottom panel) of patient-derived tumor xenografts TC7 and TC22, showing high and low levels of  $\alpha 5$  integrins, respectively. For immunofluorescence, detection of  $\alpha 5$  (white) was performed with an antibody, followed by a secondary antibody coupled to Alexa 647. For aptafluorescence, detection of  $\alpha 5$  (in white) was performed with the Cy5-labeled aptamers H02 and G11. DAPI staining is shown in blue. Images were captured at the same setting to allow direct comparison of staining patterns. One representative image per condition is shown. (D) Quantification of immuno-fluorescence (top panel) and apta-fluorescence (bottom panel) by confocal microscopy. Histograms show quantification of 10 to 26 different images per condition. Statistical analyses were done with Student's t test (\*\*\*\* $p < 0.0001$  and \*\* $p < 0.003$ ).

use of alternative rounds of cell- and protein-SELEX rounds, the use of at least two different cell lines to remove unspecific binding, and the high differential expression of the target expressed on cells used for positive selection compared with cells used for counterselection.

Aptamer H02 was selected after 18 rounds of a stringent SELEX process. This aptamer was the most represented sequence. It is not degraded in contact with cells under the conditions used for the experiments. As for aptamers G11 and B03, the predicted secondary structure of aptamer H02 is highly stable in imperfect hairpins. Using label-free SPR experiments, integrin  $\alpha 5\beta 1$  was validated as the target of aptamer H02 (Figure 4B). Aptamer H02 was also identified as a binder of  $\alpha 5$ -expressing cells on cells used for positive selection or on other GBM cells in aptacytochemistry assays (Figures 6, 7A, and 7B). U87MG  $\alpha 5+$  cells incubated with aptamer H02 allowed internalization of aptamer H02 at 37°C by endocytosis of the  $\alpha 5\beta 1$  cell surface receptor. A  $K_D$  value of  $277.8 \pm 51.8$  nM was determined for the interaction between aptamer H02 and U87MG  $\alpha 5+$  cells. This affinity value is of the same order of magnitude than the 100–400 nM that have been determined for aptamers characterized toward other integrins by cell- or hybrid SELEX.<sup>49,52</sup> By SPR, a  $K_D$  of 72 nM was determined for the interaction between aptamer H02-2'F and integrin  $\alpha 5\beta 1$ . The 3.8-fold difference in binding affinity between the aptamer-recombinant protein and aptamer-cell interaction can certainly be explained by the different techniques used (flow cytometry versus SPR) and by conformational differences between cell surface proteins and soluble recombinant proteins. However, it is not due to the use of the H02-2'F aptamer in SPR versus the non-modified aptamer in flow cytometry because the H02-2'F and non-modified H02 aptamers have the same affinity for U87MG  $\alpha 5+$  cells (data not shown). Only a few studies compared aptamer binding with isolated proteins and with tumor cell surface protein biomarkers.<sup>22</sup> The 5-fold difference, which is of the same order of magnitude than the difference observed in our study, has been described for the OX40-aptamer interaction and can be explained by conformational differences.<sup>55</sup>

In the field of precision oncology, histological detection of specific biomarkers is a crucial diagnostic tool. Immunohistochemistry is a cheap, easy method for detection of tumor biomarkers. Aptahistochemistry is a new option, still rarely described, for which aptamers, as a new class of probes, are used instead of antibodies. In our study, we used aptamer H02 directly end-labeled with a single cyanine 5 fluorescent dye. Aptamer H02 was able to specifically interact with  $\alpha 5$ -overexpressing tumor tissues from patient-derived xenografts (Figures 7C and 7D) because it efficiently differentiates TC7 (tissue with high  $\alpha 5$  expression) from TC22 (tissue with low  $\alpha 5$  expression). Aptamer H02 is an effective molecular probe for labeling histological tissue sections and detection of the  $\alpha 5\beta 1$  biomarker on tumor cells. Aptamer probes may become powerful tools for pathologists to characterize tumor tissues because the protocols are simple to implement, straightforward to automate, and can be applied to paraffin-embedded cancer tissue as well as to frozen tumor tissues.<sup>56–58</sup> Aptahistochemistry could certainly be easily extrapolated to biomarker multiplexing detection<sup>59</sup> to assess co-localization of different markers

on the same tumor section. Aptamer H02 targeting integrin  $\alpha 5\beta 1$  as well as other aptamers targeting other GBM biomarkers might therefore help to better characterize GBM inter-tumoral as well as intra-tumoral heterogeneity, which would have implications for personalized targeted therapies. A recent review describes the technicalities of the current applications of aptahistochemistry.<sup>60</sup> Aptafluorescence will probably reduce the cost, time, and cross-reactivity concerns compared with indirect immunofluorescence approaches generally based on primary and then secondary antibodies. Conjugation of dye on aptamers is easy and reduces the risk of disrupting the aptamer structure compared with antibodies generally labeled with multiple tags. Compared with an antibody, the aptamer's smaller size (10-fold reduction in size) allows better penetration in tissues,<sup>61,62</sup> particularly in applications for which epitope accessibility is reduced, such as in fixed tissues. A further advantage of aptamers is that the target of interest is not limited to molecules that produce an immune response in the host animal, as for antibodies.<sup>40</sup> Chemical synthesis of aptamers virtually eliminates the issue of batch-to-batch variation.

### Conclusion

In conclusion, we characterized a new, original, and powerful aptamer tool to detect GBM tumoral cells and tissues expressing integrin  $\alpha 5\beta 1$ . These detections might be extended for use in other cancers where  $\alpha 5\beta 1$  has proven to be a therapeutic target, such as colon cancer, ovarian cancer, breast cancer, lung tumors, and melanoma.<sup>25</sup> For clinical translation, the structure of aptamer H02 will have to be confirmed, and aptamer H02 will be improved further by truncations to obtain the minimal active fraction and by increasing its resistance toward nucleases via modifications of its nucleic acid backbone and extremities.<sup>63</sup> Internalized, an aptamer targeting integrin  $\alpha 5\beta 1$  might open roads for  $\alpha 5\beta 1$ -specific therapeutic payload delivery. Endocytosis may be crucial for targeting and increasing the therapeutic efficacy of GBM drugs. Linked to a cytotoxic agent, an aptamer to integrin  $\alpha 5\beta 1$  could serve as a carrier for targeted therapeutic delivery. Such aptamers were very recently called "charomers."<sup>64</sup> Charomers internalized with integrin  $\alpha 5\beta 1$  would be very powerful carriers to deliver therapeutic agents into targeted cells.

## MATERIALS AND METHODS

### Materials

The ssDNA library was synthesized and purified by Eurogentec (Seraing, Belgium). All RNA aptamers and chemicals were purchased from IBA and Sigma-Aldrich (Hamburg, Germany), respectively, unless otherwise stated. The sequences of all primers, the library, and aptamers from this study are described in Table S2.

### Cell Culture and Transfection

Cell culture medium and reagents were from Lonza (Basel, Switzerland) or Gibco (Thermo Fisher Scientific, Waltham, MA, USA). U87MG cells were from the ATCC. U373MG and T98G cells were from ECACC (European Collection of Authenticated Cell Cultures, Sigma). LN319, LN229, LN443, LN18, and LN2308 cells were kindly provided by Prof. Monika Hegi (Lausanne, Switzerland), SF763 by Frédéric André (Marseille, France), and CHO-B2 by

Wolfram Ruf (La Jolla, CA, USA). All GBM cells were routinely cultured in Eagle's minimum essential medium (EMEM), 10% heat-inactivated FBS, and 2 mM glutamine. For U373MG and T98G, 1% non-essential amino acids and 1 mM sodium pyruvate were added to the medium. For CHO-B2 cells, EMEM was substituted for DMEM (high glucose). U87MG cells were stably transfected to over-express (U87MG  $\alpha 5+$ ) and repress (U87MG  $\alpha 5-$ ) the human  $\alpha 5$  gene, as described previously.<sup>26</sup> CHO-B2 cells lacked the  $\alpha 5$  subunit. They were stably transfected by a pcDNA3.1 plasmid provided by Dr. Ruoshlati (La Jolla, CA, USA) to overexpress the human  $\alpha 5$  integrin gene in fusion with the gene for GFP by using jetPRIME (Polyplus transfection) according to the manufacturer's instructions and named CHO-B2  $\alpha 5+$  cells.

#### Expression and Purification of $\alpha 5\beta 1$ -Fc

The recombinant soluble human  $\alpha 5\beta 1$ -Fc integrin (a gift from Martin Humphries, Manchester, UK) was produced from NSO culture supernatant and purified via the Fc domain on protein A-Sepharose as described previously.<sup>33</sup> The purity of the protein was verified by Coomassie staining of SDS-polyacrylamide gels.

#### SELEX Strategy

The RNA library was obtained by transcription from a starting ssDNA library (Eurogentec) containing 30 random nucleotides (N30) and flanked by primer annealing sites: 5'-GTGTGACCGACCGTGGTGC-N30-GCAGTGAAGGCTGGTAACC-3'. Two primers, P3' (5'-GTGTGACCGACCGTGGTGC-3') and P5' (5'-TAATACGACTCACTATAGGTTACCAGCCTTCACTGC-3'), containing the T7 transcription promoter (underlined) were used for PCR amplification as described previously.<sup>35</sup> Synthesis of the RNA library and transcription followed by DNase I (Roche) treatment have been described previously.<sup>65</sup> The RNA pool was gel purified by denaturing (7 M urea) gel electrophoresis on an 8% polyacrylamide gel. The band corresponding to the RNA was visualized by UV shadowing and cut out for overnight extraction (500 mM  $\text{NH}_4\text{OAc}$ , 1 mM EDTA, and 20% phenol) at 4°C. The RNAs were then purified by phenol-chloroform extraction and ethanol precipitation. Prior to each round, the RNA pool was heated at 80°C for 2 min, immediately cooled down on ice for 5 min, and then kept at room temperature (RT) for 10 min to allow formation of the optimal conformation in selection buffer composed of 1 mM  $\text{MgCl}_2$  and 0.5 mM  $\text{CaCl}_2$  in PBS (pH 7.4). For cell-SELEX, adherent cells at confluency were washed 3 times in PBS and 3 times in selection buffer before incubation with the starting RNA library (1 nmol) at 37°C for 30 min under slow agitation (75 rpm). Cells were then washed once for 5 min and detached with a cell scraper. Binding RNA molecules were detached from cells by heating at 95°C for 2 min. Eluted RNA pools were extracted by phenol-chloroform and ethanol precipitated. They were then amplified by reverse transcription prior amplification.<sup>65</sup> The dsDNA pool was then transcribed as described above. For the next rounds of selection, the number of washes was modified compared with the first round as described in Table S1. From the fourth round to the sixth round, the RNA pool was first incubated with cells used for counterselection, and unbound sequences were then incubated

with cells used for positive selection (Figure 1). A protein-based SELEX process was applied during rounds 8–10. The recombinant  $\alpha 5\beta 1$ -Fc integrin was coupled to protein A-Sepharose 4B conjugate (Invitrogen), ahead washed 3 times with selection buffer. We employed a negative selection step in which the RNA pools were pre-incubated with protein A-Sepharose beads alone prior to positive selection. Unbound sequences were incubated under agitation on  $\alpha 5\beta 1$ -Fc-loaded beads for 20 mins. Eluted RNA was recovered, reverse transcribed, PCR amplified, and transcribed back into RNA for the subsequent round as described above. For rounds 9 and 10, counterselection was also performed on negative control immunoglobulin G (IgG; cetuximab, Merck Serono). Beginning with round 11, another cell-SELEX process was performed as described above. Cells for counterselection and positive selection and SELEX conditions are described in Figure 1 and Table S1. After the 14<sup>th</sup> round of selection, competitor yeast tRNA was added (Table S1). At the end of SELEX, the sequences of the 18<sup>th</sup> pools were cloned with the TOPO-TA cloning kit (Invitrogen Life Technologies) before sequencing. The sequences were compared by MultAlin.<sup>66</sup> Prediction of secondary structure was obtained using the mfold software.<sup>67</sup>

#### Flow Cytometry

Flow cytometry was performed with individual aptamers directly coupled to Cy5 at their 3' end. For comparison of the binding profile of different aptamers to cells, aptamers were used at a final concentration of 500 nM. For determination of equilibrium binding affinities, aptamer H02 was used at concentrations of 0.15, 0.3, 0.6, 1.25, 2.5, and 5  $\mu\text{M}$ . After detachment with EDTA (0.2 M), 300,000 cells were incubated for 30 min at 4°C with Cy5-labeled aptamers. As a control, cells were incubated with a 1/100 dilution of an anti- $\alpha 5$  antibody (mouse anti-human CD49e, IIA1 antibody, BD Chemigen) for 30 min, followed by 30-min incubation with Alexa 647-conjugated affine pure goat anti-mouse IgG (Jackson ImmunoResearch) at 10  $\mu\text{g}/\text{mL}$ . After washing, cells were analyzed using a FACSCalibur flow cytometer (Becton Dickinson), and the mean fluorescence intensity (counting 10 000 events) was measured using Flowing software 2.5.1. For  $K_D$  determination, experiments were repeated three times, and data were evaluated using GraphPad Prism (version 5.04).

#### SPR Analyses of Aptamer H02-Integrin Interactions on a CAP Sensor Chip

All experiments were performed on a Biacore T200 instrument (GE Healthcare) at 25°C. The sensor surface and other Biacore consumables were purchased from GE Healthcare. Integrins  $\alpha 5\beta 1$  and  $\alpha v\beta 3$  were from R&D Systems. Running buffer was composed of PBS (10 mM), NaCl (150 mM), and  $\text{MgCl}_2$  (1 mM), filtered through a 0.22- $\mu\text{m}$  membrane, and supplemented with surfactant P20 (0.005% v/v). The biotin CAPture reagent, composed of streptavidin conjugated with an oligonucleotide, was stably hybridized to the complementary sequence of a CAP sensor chip following the biotin CAPture kit instructions (GE Healthcare). The biotinylated aptamer was denatured at 95°C for 3 min, incubated on ice, and then injected onto the biotin CAP reagent at 100 nM for 5 min at a flow rate of

10  $\mu\text{L}/\text{min}$ . Five different concentrations of integrin (ranging from 8–130 nM) were injected into the flow cells at 10 or 30  $\mu\text{L}/\text{min}$  for 300 s. Dissociation followed for 300 s. After each measurement, the sensor chip was washed with an injection of 6 M guanidine hydrochloride in 0.25 M NaOH as recommended by the manufacturer. The reference surface was treated similarly except that aptamer injection was omitted. Binding curves were double-reference-subtracted from the buffer blank and reference flow cell (without the aptamer). The equilibrium response was recorded 5 s before the end of integrin injection. The  $K_D$  was determined by fitting the equilibrium response versus the [integrin] curve to a simple 1:1 interaction model with the Biacore T200 evaluation software (GE Healthcare).

#### Western Blot

Cells were lysed (1% Triton X-100, NaF [100 mmol/L], NaPPi [10 mmol/L], and  $\text{Na}_3\text{VO}_4$  [1 mmol/L] in PBS, supplemented with complete anti-protease cocktail; Roche), and 10  $\mu\text{g}$  of protein was separated by SDS-PAGE (Bio-Rad) and transferred to polyvinylidene fluoride (PVDF) membranes (Amersham). Blots were probed with antibodies to  $\alpha 5$  integrin (H104, Santa Cruz Biotechnology) and to glyceraldehyde 3-phosphate dehydrogenase (GAPDH; Millipore). Horseradish peroxidase (HRP)-coupled secondary antibodies were from Promega. Proteins were visualized with enhanced chemiluminescence using the LAS4000 imager, and densitometry analysis was performed using the ImageJ software (GE Healthcare). GAPDH was used as housekeeping protein to serve as the loading control for cell lysate samples. Analyses were performed on three independent experiments.

#### Fluorescence-Based Assays on Cell Lines

The adherent CHO-B2 and GBM cell lines (U87MG  $\alpha 5+$ , U87MG  $\alpha 5-$ , LN319, LN229, LN443, SF763, LN18, LN2308, U373, and T98G) were plated on sterile glass slides for one night at 37°C in culture medium, washed three times, and then saturated for 1 h at RT in selection buffer containing 2% BSA. Cy5-labeled aptamers were denatured at 95°C for 3 min and incubated on ice for 5 min and then on cells in selection buffer for 30 min on ice or at 37°C at concentrations dependent on the assay (5, 2.5, 1.25, 0.6, or 0.3  $\mu\text{M}$ ). Cells were then washed in selection buffer, fixed for 8 min in 4% paraformaldehyde (PFA), permeabilized for 2 min with 0.2% Triton, and washed again. Sequentially, when immunocytochemistry was performed, the primary antibodies used were the anti- $\alpha 5$  antibody (mouse anti-human CD49e, IIA1 antibody, BD Chemigen, 1/200), the anti- $\beta 1$  antibody (mouse anti-human CD29 antibody, clone TS2/16, BioLegend, 1/500), or the anti-EEA1 (early endosome antigen 1) antibody (anti-mouse clone 14/EEA1, BD Transduction Laboratories, 1/1,000). Primary antibodies were added for 1 h at RT or overnight (O/N) at 4°C, followed by a secondary antibody coupled to Alexa 546 or 568 (Life Technology) at a 2  $\mu\text{g}/\text{mL}$  final concentration. Hoechst or DAPI were added at 1/1,000 for 1 h at RT to visualize the nucleus. F-actin identification was performed using Phalloidin-ATTO 488 (Sigma) at 1/4,000. Washing steps were performed before mounting using fluorescent mounting medium (S3023, Dako).

#### Fluorescence-Based Histochemical Assays of Patient-Derived Xenografts

Two patient-derived heterotopic xenografts (PDXs) were selected for *in vivo* analysis.<sup>68</sup> TC7 and TC22 GBM-PDXs presented high and low levels of  $\alpha 5$  integrins, respectively. PDX mouse models were established using tissues surgically removed from patients as described previously.<sup>69,70</sup> Integrin  $\alpha 5$  was apta- and immunostained using formalin-fixed paraffin-embedded xenografts mounted on glass slides. Sections were deparaffinized, rehydrated, and subjected to an antigen unmasking protocol. Briefly, sections were boiled at 100°C for 10 min in target retrieval solution (pH 9) (S2367, Dako), cooled down to RT for 20–40 min, and rinsed in  $\text{H}_2\text{O}$ . For aptafluorescence, slides were rinsed for 5 min in selection buffer, dried, incubated in blocking buffer (2% BSA in selection buffer) for 1 h at RT, rinsed in  $\text{H}_2\text{O}$  and then in selection buffer, and dried. RNA molecules were denatured at 95°C for 3 min and incubated on ice for 5 min before dilution in selection buffer to a 1  $\mu\text{M}$  final concentration. Aptamers were incubated on tumor sections for 1 h at RT in a humid chamber, washed in selection buffer, dried, fixed in 4% PFA, and then washed three times in PBS. For immunofluorescence, slides were rinsed for 5 min in PBS-T (0.1% Tween 20 in PBS), dried, and then incubated in blocking buffer BB-I (5% goat serum in PBS-T) for 1 h at RT in a humid chamber. Overnight incubation with anti-integrin  $\alpha 5$  mAb 1928 (6B8516, Millipore, 1/200) in BB-I was followed by a 5-min wash in PBS-T and by an incubation step with a 1/100 dilution of the goat anti-rabbit secondary antibody coupled to Alexa Fluor 647 (A21245, Life Technologies). Immuno- and apta staining was followed by DAPI (10  $\mu\text{g}/\text{mL}$ ) staining for 30 min at RT to visualize cell nuclei. The stained samples were then washed in PBS, and coverslips were mounted onto tissue sections using fluorescent mounting medium (S3023, Dako).

#### Confocal Imaging

Images were acquired using a confocal microscope (Leica TCS SPE II, 63 $\times$  magnification, oil immersion).

Mean fluorescence intensity on cells and tissues was measured using ImageJ software. Statistical analysis of data was performed with Student's t test. Data were analyzed with GraphPad Prism version 5.04 and are represented as mean  $\pm$  SEM.

#### SUPPLEMENTAL INFORMATION

Supplemental Information can be found online at <https://doi.org/10.1016/j.omtn.2019.05.006>.

#### AUTHOR CONTRIBUTIONS

Research was performed by P.F., A.-M.R. (aptamer identification), E.C.D.S. (apta- and immuno-fluorescence), and M.-C.M., F.N., C.S. (flow cytometry). D.G. and I.L.-R. provided useful reagents. P.F., E.C.D.S., M.D., and L.C. analyzed the data. P.F., M.L., R.V., N.E.-S., S.M., and M.D. provided expertise. L.C. designed, coordinated, and performed research and wrote the manuscript.

## CONFLICTS OF INTEREST

The authors declare no competing interests.

## ACKNOWLEDGMENTS

We thank Martin Humphries (Manchester, UK) for the gift of NS0 cells expressing  $\alpha 5\beta 1$ -Fc integrin and Julie Hémart and Antoine Schillinger for technical assistance. This work was supported by two contracts from the SATT Conectus Alsace (I14-057/01 and I18-020/01), a grant from the PEPS-IDEX program of the Université de Strasbourg (W15RPE24), the Ligue contre le cancer CCIR-Est (S19R417C), and the INTEGLIO program of the Cancéropôle Grand-Est.

## REFERENCES

- Stupp, R., Mason, W.P., van den Bent, M.J., Weller, M., Fisher, B., Taphoorn, M.J.B., Belanger, K., Brandes, A.A., Marosi, C., Bogdahn, U., et al.; European Organisation for Research and Treatment of Cancer Brain Tumor and Radiotherapy Groups; National Cancer Institute of Canada Clinical Trials Group (2005). Radiotherapy plus concomitant and adjuvant temozolomide for glioblastoma. *N. Engl. J. Med.* 352, 987–996.
- Woodworth, G.F., Dunn, G.P., Nance, E.A., Hanes, J., and Brem, H. (2014). Emerging insights into barriers to effective brain tumor therapeutics. *Front. Oncol.* 4, 126.
- Louis, D.N., Perry, A., Reifenberger, G., von Deimling, A., Figarella-Branger, D., Cavenee, W.K., Ohgaki, H., Wiestler, O.D., Kleihues, P., and Ellison, D.W. (2016). The 2016 World Health Organization Classification of Tumors of the Central Nervous System: a summary. *Acta Neuropathol.* 131, 803–820.
- Hung, A.L., Garzon-Muvdi, T., and Lim, M. (2017). Biomarkers and Immunotherapeutic Targets in Glioblastoma. *World Neurosurg.* 102, 494–506.
- Cloughesy, T.F., Cavenee, W.K., and Mischel, P.S. (2014). Glioblastoma: from molecular pathology to targeted treatment. *Annu. Rev. Pathol.* 9, 1–25.
- Wadajkar, A.S., Dancy, J.G., Hersh, D.S., Anastasiadis, P., Tran, N.L., Woodworth, G.F., Winkles, J.A., and Kim, A.J. (2017). Tumor-targeted nanotherapeutics: overcoming treatment barriers for glioblastoma. *Wiley Interdiscip. Rev. Nanomed. Nanobiotechnol.* Published online November 4, 2016. <https://doi.org/10.1002/wnan.1439>.
- Jacobi, N., Seeboeck, R., Hofmann, E., and Eger, A. (2017). ErbB Family Signalling: A Paradigm for Oncogene Addiction and Personalized Oncology. *Cancers (Basel)* 9, 33.
- Ciriello, G., Miller, M.L., Aksoy, B.A., Senbabaoglu, Y., Schultz, N., and Sander, C. (2013). Emerging landscape of oncogenic signatures across human cancers. *Nat. Genet.* 45, 1127–1133.
- Chen, M., Yu, Y., Jiang, F., Zhou, J., Li, Y., Liang, C., Dang, L., Lu, A., and Zhang, G. (2016). Development of Cell-SELEX Technology and Its Application in Cancer Diagnosis and Therapy. *Int. J. Mol. Sci.* 17, E2079.
- Yoon, S., and Rossi, J.J. (2017). Emerging cancer-specific therapeutic aptamers. *Curr. Opin. Oncol.* 29, 366–374.
- Pastor, F. (2016). Aptamers: A New Technological Platform in Cancer Immunotherapy. *Pharmaceuticals (Basel)* 9, E64.
- Zhu, G., and Chen, X. (2018). Aptamer-based targeted therapy. *Adv. Drug Deliv. Rev.* 134, 65–78.
- Pastor, F., Berraondo, P., Etxebarria, I., Frederick, J., Sahin, U., Gilboa, E., and Melero, I. (2018). An RNA toolbox for cancer immunotherapy. *Nat. Rev. Drug Discov.* 17, 751–767.
- Zhou, J., and Rossi, J. (2017). Aptamers as targeted therapeutics: current potential and challenges. *Nat. Rev. Drug Discov.* 16, 181–202.
- Kaur, H., Bruno, J.G., Kumar, A., and Sharma, T.K. (2018). Aptamers in the Therapeutics and Diagnostics Pipelines. *Theranostics* 8, 4016–4032.
- Ruiz Ciancio, D., Vargas, M.R., Thiel, W.H., Bruno, M.A., Giangrande, P.H., and Mestre, M.B. (2018). Aptamers as Diagnostic Tools in Cancer. *Pharmaceuticals (Basel)* 11, 86.
- Bouvier-Müller, A., and Ducongé, F. (2018). Application of aptamers for in vivo molecular imaging and theranostics. *Adv. Drug Deliv. Rev.* 134, 94–106.
- Kim, M., Kim, D.M., Kim, K.S., Jung, W., and Kim, D.E. (2018). Applications of Cancer Cell-Specific Aptamers in Targeted Delivery of Anticancer Therapeutic Agents. *Molecules* 23, 830.
- Ellington, A.D., and Szostak, J.W. (1990). In vitro selection of RNA molecules that bind specific ligands. *Nature* 346, 818–822.
- Tuerk, C., and Gold, L. (1990). Systematic evolution of ligands by exponential enrichment: RNA ligands to bacteriophage T4 DNA polymerase. *Science* 249, 505–510.
- Robertson, D.L., and Joyce, G.F. (1990). Selection in vitro of an RNA enzyme that specifically cleaves single-stranded DNA. *Nature* 344, 467–468.
- Mercier, M.-C., Dontenwill, M., and Choulier, L. (2017). Selection of Nucleic Acid Aptamers Targeting Tumor Cell-Surface Protein Biomarkers. *Cancers (Basel)* 9, E69.
- Hynes, R.O. (2002). Integrins: bidirectional, allosteric signaling machines. *Cell* 110, 673–687.
- Desgrosellier, J.S., and Cheresch, D.A. (2010). Integrins in cancer: biological implications and therapeutic opportunities. *Nat. Rev. Cancer* 10, 9–22.
- Schaffner, F., Ray, A.M., and Dontenwill, M. (2013). Integrin  $\alpha 5\beta 1$ , the Fibronectin Receptor, as a Pertinent Therapeutic Target in Solid Tumors. *Cancers (Basel)* 5, 27–47.
- Janouskova, H., Maglott, A., Leger, D.Y., Bossert, C., Noulet, F., Guerin, E., Guenot, D., Pinel, S., Chastagner, P., Plenat, F., et al. (2012). Integrin  $\alpha 5\beta 1$  plays a critical role in resistance to temozolomide by interfering with the p53 pathway in high-grade glioma. *Cancer Res.* 72, 3463–3470.
- Maglott, A., Bartik, P., Cosgun, S., Klotz, P., Rondé, P., Fuhrmann, G., Takeda, K., Martin, S., and Dontenwill, M. (2006). The small  $\alpha 5\beta 1$  integrin antagonist, SJ749, reduces proliferation and clonogenicity of human astrocytoma cells. *Cancer Res.* 66, 6002–6007.
- Martin, S., Cosset, E.C., Terrand, J., Maglott, A., Takeda, K., and Dontenwill, M. (2009). Caveolin-1 regulates glioblastoma aggressiveness through the control of  $\alpha(5)\beta(1)$  integrin expression and modulates glioblastoma responsiveness to SJ749, an  $\alpha(5)\beta(1)$  integrin antagonist. *Biochim. Biophys. Acta* 1793, 354–367.
- Freije, W.A., Castro-Vargas, F.E., Fang, Z., Horvath, S., Cloughesy, T., Liu, L.M., Mischel, P.S., and Nelson, S.F. (2004). Gene expression profiling of gliomas strongly predicts survival. *Cancer Res.* 64, 6503–6510.
- Phillips, H.S., Kharbanda, S., Chen, R., Forrester, W.F., Soriano, R.H., Wu, T.D., Misra, A., Nigro, J.M., Colman, H., Soroceanu, L., et al. (2006). Molecular subclasses of high-grade glioma predict prognosis, delineate a pattern of disease progression, and resemble stages in neurogenesis. *Cancer Cell* 9, 157–173.
- Riemenschnieder, M.J., Mueller, W., Betensky, R.A., Mohapatra, G., and Louis, D.N. (2005). In situ analysis of integrin and growth factor receptor signaling pathways in human glioblastomas suggests overlapping relationships with focal adhesion kinase activation. *Am. J. Pathol.* 167, 1379–1387.
- Cosset, E.C., Godet, J., Entz-Werlé, N., Guérin, E., Guenot, D., Froelich, S., Bonnet, D., Pinel, S., Plenat, F., Chastagner, P., et al. (2012). Involvement of the TGF $\beta$  pathway in the regulation of  $\alpha 5\beta 1$  integrins by caveolin-1 in human glioblastoma. *Int. J. Cancer* 131, 601–611.
- Coe, A.P., Askari, J.A., Kline, A.D., Robinson, M.K., Kirby, H., Stephens, P.E., and Humphries, M.J. (2001). Generation of a minimal  $\alpha 5\beta 1$  integrin-Fc fragment. *J. Biol. Chem.* 276, 35854–35866.
- Schreiner, C.L., Bauer, J.S., Danilov, Y.N., Hussein, S., Szczek, M.M., and Juliano, R.L. (1989). Isolation and characterization of Chinese hamster ovary cell variants deficient in the expression of fibronectin receptor. *J. Cell Biol.* 109, 3157–3167.
- Da Rocha Gomes, S., Miguel, J., Azéma, L., Eimer, S., Ries, C., Dausse, E., Loiseau, H., Allard, M., and Toulmé, J.J. (2012).  $(^{99m}\text{Tc})\text{-MAG3}$ -aptamer for imaging human tumors associated with high level of matrix metalloproteinase-9. *Bioconjug. Chem.* 23, 2192–2200.
- Cibiel, A., Quang, N.N., Gombert, K., Thézé, B., Garofalakis, A., and Ducongé, F. (2014). From ugly duckling to swan: unexpected identification from cell-SELEX of an anti-Annexin A2 aptamer targeting tumors. *PLoS ONE* 9, e87002.



37. Xu, L., Zhang, Z., Zhao, Z., Liu, Q., Tan, W., and Fang, X. (2013). Cellular Internalization and Cytotoxicity of Aptamers Selected from Lung Cancer Cell. *Am. J. Biomed. Sci.* 5, 47–58.
38. Suenaga, E., Mizuno, H., and Penmetcha, K.K.R. (2012). Monitoring influenza hemagglutinin and glycan interactions using surface plasmon resonance. *Biosens. Bioelectron.* 32, 195–201.
39. Basiji, D.A., Ortyu, W.E., Liang, L., Venkatachalam, V., and Morrissey, P. (2007). Cellular image analysis and imaging by flow cytometry. *Clin. Lab. Med.* 27, 653–670, viii.
40. Bauer, M., Macdonald, J., Henri, J., Duan, W., and Shigdar, S. (2016). The Application of Aptamers for Immunohistochemistry. *Nucleic Acid Ther.* 26, 120–126.
41. Szopa, W., Burley, T.A., Kramer-Marek, G., and Kaspara, W. (2017). Diagnostic and Therapeutic Biomarkers in Glioblastoma: Current Status and Future Perspectives. *BioMed Res. Int.* 2017, 8013575.
42. Liu, Y., Kuan, C.-T., Mi, J., Zhang, X., Clary, B.M., Bigner, D.D., and Sullenger, B.A. (2009). Aptamers selected against the glycosylated EGFRvIII ectodomain and delivered intracellularly reduce membrane-bound EGFRvIII and induce apoptosis. *Biol. Chem.* 390, 137–144.
43. Chauveau, F., Aissouni, Y., Hamm, J., Boutin, H., Libri, D., Ducongé, F., and Tavitian, B. (2007). Binding of an aptamer to the N-terminal fragment of VCAM-1. *Bioorg. Med. Chem. Lett.* 17, 6119–6122.
44. Ohuchi, S. (2012). Cell-SELEX Technology. *BioRes. J.* 265–272, Open Access.
45. Blind, M., Kolanus, W., and Famulok, M. (1999). Cytoplasmic RNA modulators of an inside-out signal-transduction cascade. *Proc. Natl. Acad. Sci. USA* 96, 3606–3610.
46. Mi, J., Zhang, X., Giangrande, P.H., McNamara, J.O., 2nd, Nimjee, S.M., Sarraf-Yazdi, S., Sullenger, B.A., and Clary, B.M. (2005). Targeted inhibition of alphavbeta3 integrin with an RNA aptamer impairs endothelial cell growth and survival. *Biochem. Biophys. Res. Commun.* 338, 956–963.
47. Ruckman, J., Gold, L., Stephens, A., and Janjic, N. (2001). Nucleic acid ligands to integrins. US patent US7094535 B2, filed December 18, 2001, and granted August 22, 2006.
48. Gong, Q., Wang, J., Ahmad, K.M., Csordas, A.T., Zhou, J., Nie, J., Stewart, R., Thomson, J.A., Rossi, J.J., and Soh, H.T. (2012). Selection strategy to generate aptamer pairs that bind to distinct sites on protein targets. *Anal. Chem.* 84, 5365–5371.
49. Takahashi, M., Sakota, E., and Nakamura, Y. (2016). The efficient cell-SELEX strategy, Icell-SELEX, using isogenic cell lines for selection and counter-selection to generate RNA aptamers to cell surface proteins. *Biochimie* 131, 77–84.
50. Pestourie, C., Cerchia, L., Gombert, K., Aissouni, Y., Boulay, J., De Franciscis, V., Libri, D., Tavitian, B., and Ducongé, F. (2006). Comparison of different strategies to select aptamers against a transmembrane protein target. *Oligonucleotides* 16, 323–335.
51. Zhu, G., Zhang, H., Jacobson, O., Wang, Z., Chen, H., Yang, X., Niu, G., and Chen, X. (2017). Combinatorial Screening of DNA Aptamers for Molecular Imaging of HER2 in Cancer. *Bioconjug. Chem.* 28, 1068–1075.
52. Berg, K., Lange, T., Mittelberger, F., Schumacher, U., and Hahn, U. (2016). Selection and Characterization of an  $\alpha 6 \beta 4$  Integrin blocking DNA Aptamer. *Mol. Ther. Nucleic Acids* 5, e294.
53. Wilner, S.E., Wengerter, B., Maier, K., de Lourdes Borba Magalhães, M., Del Amo, D.S., Pai, S., Opazo, F., Rizzoli, S.O., Yan, A., and Levy, M. (2012). An RNA alternative to human transferrin: a new tool for targeting human cells. *Mol. Ther. Nucleic Acids* 1, e21.
54. Boltz, A., Piater, B., Toleikis, L., Guenther, R., Kolmar, H., and Hock, B. (2011). Bisppecific aptamers mediating tumor cell lysis. *J. Biol. Chem.* 286, 21896–21905.
55. Pratico, E.D., Sullenger, B.A., and Nair, S.K. (2013). Identification and characterization of an agonistic aptamer against the T cell costimulatory receptor, OX40. *Nucleic Acid Ther.* 23, 35–43.
56. Zamay, G.S., Ivanchenko, T.I., Zamay, T.N., Grigorieva, V.L., Glazyrin, Y.E., Kolovskaya, O.S., Garanzha, I.V., Barinov, A.A., Krat, A.V., Mironov, G.G., et al. (2017). DNA Aptamers for the Characterization of Histological Structure of Lung Adenocarcinoma. *Mol. Ther. Nucleic Acids* 6, 150–162.
57. Pu, Y., Liu, Z., Lu, Y., Yuan, P., Liu, J., Yu, B., Wang, G., Yang, C.J., Liu, H., and Tan, W. (2015). Using DNA aptamer probe for immunostaining of cancer frozen tissues. *Anal. Chem.* 87, 1919–1924.
58. Zeng, Z., Zhang, P., Zhao, N., Sheehan, A.M., Tung, C.-H., Chang, C.-C., and Zu, Y. (2010). Using oligonucleotide aptamer probes for immunostaining of formalin-fixed and paraffin-embedded tissues. *Mod. Pathol.* 23, 1553–1558.
59. Blom, S., Paavolainen, L., Bychkov, D., Turkki, R., Mäki-Teeri, P., Hemmes, A., Välimäki, K., Lundin, J., Kallioniemi, O., and Pellinen, T. (2017). Systems pathology by multiplexed immunohistochemistry and whole-slide digital image analysis. *Sci. Rep.* 7, 15580.
60. Bukari, B.A., Citartan, M., Ch'ng, E.S., Bilibana, M.P., Rozhdstvensky, T., and Tang, T.-H. (2017). Aptahistochemistry in diagnostic pathology: technical scrutiny and feasibility. *Histochem. Cell Biol.* 147, 545–553.
61. Xiang, D., Zheng, C., Zhou, S.-F., Qiao, S., Tran, P.H.-L., Pu, C., Li, Y., Kong, L., Kouzani, A.Z., Lin, J., et al. (2015). Superior Performance of Aptamer in Tumor Penetration over Antibody: Implication of Aptamer-Based Theranostics in Solid Tumors. *Theranostics* 5, 1083–1097.
62. Sun, H., Tan, W., and Zu, Y. (2016). Aptamers: versatile molecular recognition probes for cancer detection. *Analyst (Lond.)* 141, 403–415.
63. Wang, T., Chen, C., Larcher, L.M., Barrero, R.A., and Veedu, R.N. (2019). Three decades of nucleic acid aptamer technologies: Lessons learned, progress and opportunities on aptamer development. *Biotechnol. Adv.* 37, 28–50.
64. Hahn, U. (2017). Charomers-Interleukin-6 Receptor Specific Aptamers for Cellular Internalization and Targeted Drug Delivery. *Int. J. Mol. Sci.* 18, E2641.
65. Dausse, E., Cazenave, C., Rayner, B., and Toulmé, J.-J. (2005). In vitro selection procedures for identifying DNA and RNA aptamers targeted to nucleic acids and proteins. *Methods Mol. Biol.* 288, 391–410.
66. Corpet, F. (1988). Multiple sequence alignment with hierarchical clustering. *Nucleic Acids Res.* 16, 10881–10890.
67. Zuker, M. (2003). Mfold web server for nucleic acid folding and hybridization prediction. *Nucleic Acids Res.* 31, 3406–3415.
68. Blandin, A.-F., Noulet, F., Renner, G., Mercier, M.-C., Choulier, L., Vauchelles, R., Ronde, P., Carreiras, F., Etienne-Selloum, N., Vereb, G., et al. (2016). Glioma cell dispersion is driven by  $\alpha 5$  integrin-mediated cell-matrix and cell-cell interactions. *Cancer Lett.* 376, 328–338.
69. Leuraud, P., Taillandier, L., Medioni, J., Aguirre-Cruz, L., Crinière, E., Marie, Y., Kujas, M., Golmard, J.L., Duprez, A., Delattre, J.Y., et al. (2004). Distinct responses of xenografted gliomas to different alkylating agents are related to histology and genetic alterations. *Cancer Res.* 64, 4648–4653.
70. Pinel, S., Mriouah, J., Vandamme, M., Chateau, A., Plénat, F., Guérin, E., Taillandier, L., Bernier-Chastagner, V., Merlin, J.L., and Chastagner, P. (2013). Synergistic anti-tumor effect between gefitinib and fractionated irradiation in anaplastic oligodendrogliomas cannot be predicted by the Egfr signaling activity. *PLoS ONE* 8, e68333.

# Recent results on aptamers targeting different cell-surface receptors, biomarkers of GBM

During the last year of my Ph.D., I focused, not only on aptamer H02, but also on three other aptamers targeting two other membrane receptors. Recent data were acquired by using aptamers:

- E07 and the Janellia 646 conjugate targeting EGFR
- SL1 targeting c-MET

Sequences of aptamers are presented in Table 9 in section Material and Methods.

## A. Cell-binding assays

### A1. Flow cytometry assays

Flow cytometry experiments were performed with aptamers E07 and Janellia on GBM cells with different levels of EGFR expression (Figure 1). We first characterized the EGFR protein expression levels by Western blot (Figure 1), in different cell lines: GBM (U87 EGFR WT and LN319), breast cancer (MCF-7 and MDA-MB-231) and skin cancer (A-431 and MDA-MB-435). EGFR is expressed U87 EGFR WT and MDA-MB-231 but absent in the other cell lines.

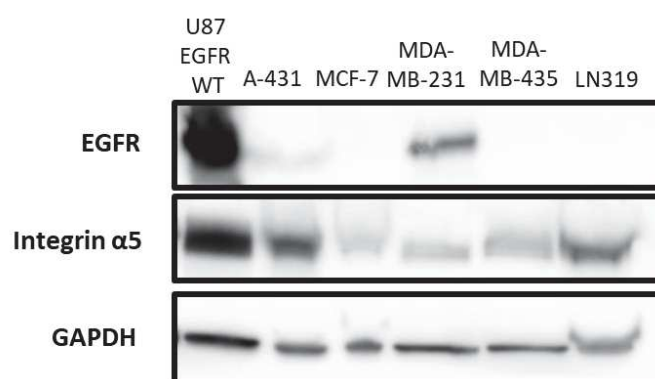


**Figure 1 – Immunoblot of protein expression profiles on different cell lines.** Protein expression of EGFR and integrin  $\alpha5\beta1$  in U87 EGFR WT, A-431, MCF-7, MDA-MB-231, MDA-MB-435, LN319 cells was studied by immunoblot. GAPDH was used as loading control.

EGFR expression was controlled by flow cytometry in cell lines U87 EGFR WT and LN319 using an anti-EGFR antibody (cetuximab) conjugated to Cy5 (Figure 2A). A shift can be

observed to the left with LN319, compared to U87 EGFR WT, confirming different expression levels of EGFR on these two cell lines.

Aptamers E07 (Figure 2B-C) and Janellia (Figure 2E-F) were tested on U87 EGFR WT and LN319 cells by flow cytometry. The shift observed with cetuximab on the two cell lines was also observed with aptamer E07 (Figure 2B) and with Aptamer-conjugated to Janellia 646 (Figure 2E). The equilibrium affinity parameter  $K_D$  of the interaction between EGFR-targeting aptamers and EGFR-overexpressing cells was determined by flow cytometry at 4°C by incubation of labelled aptamers with different concentrations of aptamers for 1 h. A  $K_D$  of  $208.7 \pm 45.57$  nM was determined by plotting the mean fluorescence of U87 EGFR WT cells against the concentration of aptamer E07 (Figure 2D), and a  $K_D$  of  $370 \pm 162.9$  nM for Janellia 646 conjugate aptamer (Figure 2G).

Concerning aptamer SL1, the affinity for multiple myeloma cells was determined by Zhang et al., (2018) using flow cytometry. SL1 has a  $K_D$  of 135.6 nM towards MM.1S cells and 237.1 nM towards ARP-1 cells (Zhang et al., 2018).

$K_D$ s determined for the interaction of aptamers targeting integrin  $\alpha 5\beta 1$ , EGFR and c-MET are summarized in Table 1.

## A2. Confocal imaging

### *EGFR-aptamers bind to EGFR-positive GBM cell lines*

For confocal aptacytochemical assays, confluent adherent cells were stained with the Cy5-labeled aptamer E07 and Janellia 646 conjugate aptamer at 37°C for 30 min. After cell fixation, cells were immunolabeled with an anti-EGFR primary antibody and a secondary antibody labelled with Alexa 568. At 37°C, aptamers E07 and Janellia presented plasma membrane labelling and punctuated intracellular labelling of U87 EGFR WT. In LN319 cells, almost no unspecific labelling of EGFR-aptamers is detected (Figure 3). Aptamer E07 was also tested on other cell lines (A-431, MCF-7, MDA-MB-231 and MDA-MB-435). Figure 4 shows that, among these cell lines, only the EGFR-positive MDA-MB-231 cell line was labelled with aptamer E07.

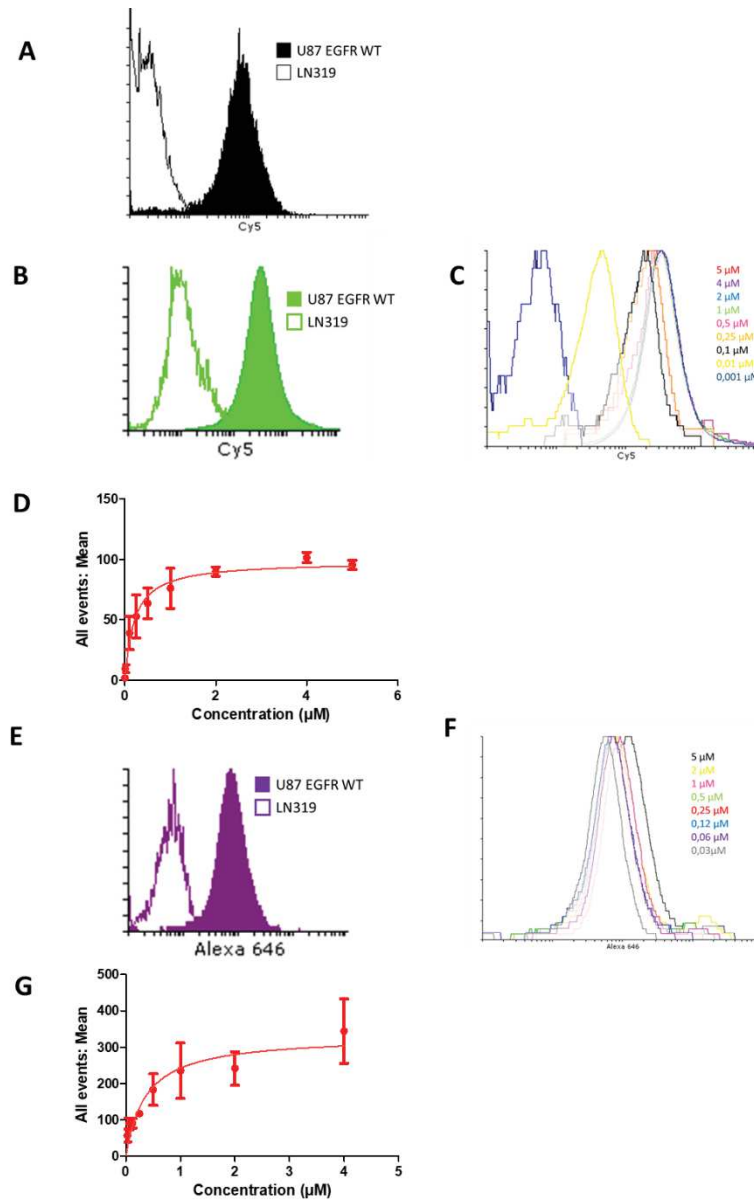


**Figure 2: EGFR-aptamers binding profiles by flow cytometry.** (A) Positive control of EGFR-expression by binding of EGFR-antibody Cetuximab-conjugated to Cy5 on U87 EGFR WT (fill black) and LN319 cells (black line). (B) Comparison of the binding profiles of aptamer E07 conjugated to Cy5 at 1  $\mu\text{M}$  on U87 EGFR WT cells (fill green) and LN319 cells (green line) at 4°C. (C) Different concentrations of E07 aptamer (0.001, 0.01, 0.1, 0.25, 0.5, 1, 2, 4 and 5  $\mu\text{M}$ ) were incubated on ice with a constant amount of U87 EGFR WT cells and analysed by flow cytometry. (D) Titration of aptamer E07 resulted in determination of the equilibrium affinity parameter  $K_D$  for the interaction between U87 EGFR WT cells and aptamer E07. A  $K_D$  of  $208.7 \pm 45.57$  nM was determined. (E) Comparison of the binding profiles of aptamer conjugated to Janellia 646 at 1  $\mu\text{M}$  on U87 EGFR WT cells (fill purple) and LN319 cells (purple line) at 4°C. (F) Different concentrations of Janellia aptamer (0.03, 0.06, 0.12, 0.25, 0.5, 1, 2 and 5  $\mu\text{M}$ ) cells were incubated on ice with a constant amount of U87 EGFR WT cells and analysed by flow cytometry. (G) Titration of aptamer Janellia resulted in determination of the equilibrium affinity parameter  $K_D$  for the interaction between U87 EGFR WT cells and aptamer Janellia ( $370 \pm 162.9$  nM).

**Table 1: Equilibrium affinity of the interaction between aptamers and cells**

Aptamer	Cell line	K <sub>D</sub>
H02	U87MG overexpressing $\alpha 5$ integrin	277.8 $\pm$ 51.8 nM
E07	U87 EGFR WT	208.7 $\pm$ 45.57 nM
Janellia 646 conjugate aptamer		370 $\pm$ 162.9 nM
SL1	MM.1S	135.6 nM
	ARP-1	237.1 nM

Experiments of the same type were realized in the literature with aptamer SL1: aptamer SL1 was able to identify multiple myeloma cells positives to c-MET, and no binding to c-MET negative B cells was detected (Zhang et al., 2018).

#### *EGFR aptamers are internalized in U87 EGFR WT cells*

Aptamers targeting cell surface receptors tend to be internalized upon binding to receptors. We wonder if EGFR-targeting aptamers were also internalized at 37°C. To verify the internalization of EGFR-targeting aptamers, we used aptamers E07 coupled to cyanine 5 or aptamer conjugated to Janellia 646 and a primary antibody targeting EEA1 and a secondary antibody labelled with Alexa 488.

Figures 5 and 6 show co-localization of EGFR-targeting aptamer E07 and Janellia, respectively, with the anti-EEA1 antibody in the cytoplasm of GBM cells, suggesting aptamer endocytosis upon receptor binding. We also demonstrated an increased EGFR internalization induced by treatment with EGFR-TKI (gefitinib). In this study, aptamer E07 was found in EEA1 positive endosomes in control and upon TKI treatment (Figure 5A). Aptamer conjugated to Janellia was less internalized in control cells but aptamer internalization increased as well upon TKI treatment (Figure 6A). Aptamer labelling intensity was quantified in individualized cells (Figure 5B and 6B). Aptamer signal was doubled upon TKI treatment for both aptamers in U87 EGFR WT.

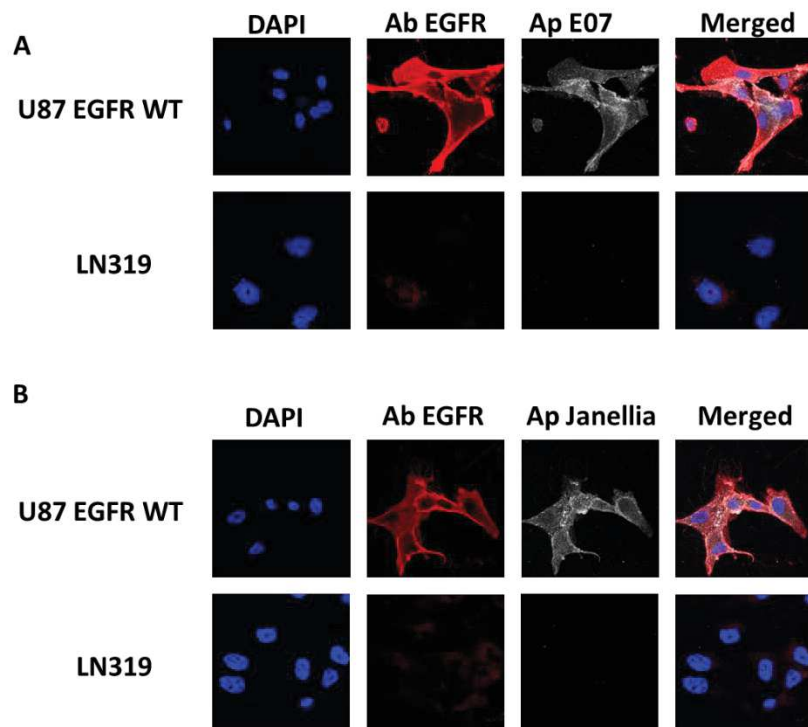


**Figure 3: Confocal imaging on U87 EGFR WT and LN 319 cell lines.** GBM cells were seeded in coverslips and incubated with 100 nM of aptamer E07-Cy5 (A) or Aptamer conjugated Janellia 646 (B) for 30 minutes. Aptamer labelling is represented in white. Incubation of antibody anti-EGFR was followed by incubation with a secondary antibody labelled with Alexa 568 (red). Nuclei are stained with DAPI (blue).

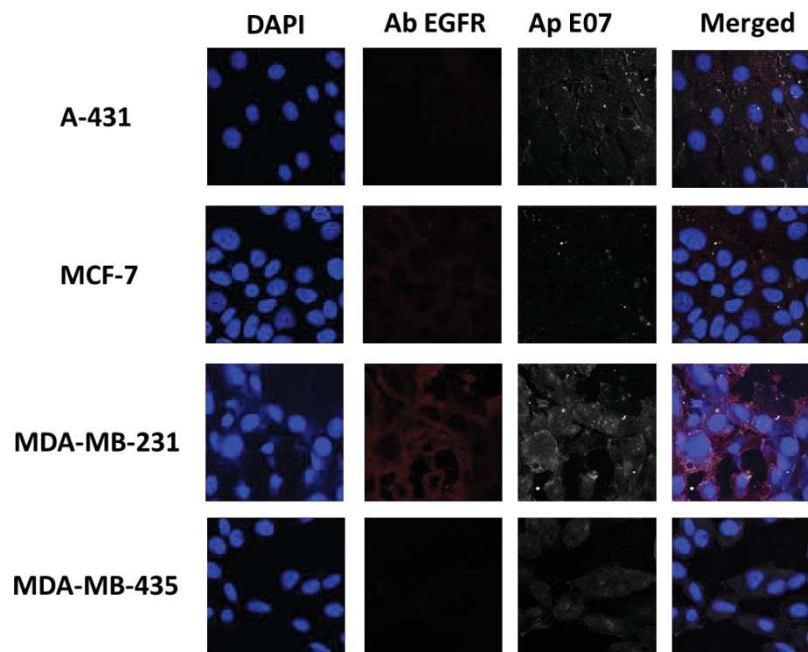


**Figure 4: Confocal imaging on cell lines A-431, MCF-7, MDA-MB-231 and MDA-MB-435.** Cells were seeded in coverslips and incubated with 100 nM of aptamer E07 for 30 minutes. The aptamer is labeled with Cy5 (white). Incubation of antibody anti-EGFR was followed by incubation with a secondary antibody labelled with Alexa 568 (red). Nuclei are stained with DAPI (blue).

We showed that EGFR-aptamers are co-localized with EEA1. We believe that aptamers are internalized via internalization of their respective receptors. Very interestingly, aptamer internalization was increased upon gefitinib treatment, which might open roads for combination strategies, using aptamers for drug vectorization in cancer treatment. However, further studies are needed to determine aptamer trafficking and aptamer cytosolic release, in order to better exploit aptamers as vectors for therapeutic use.

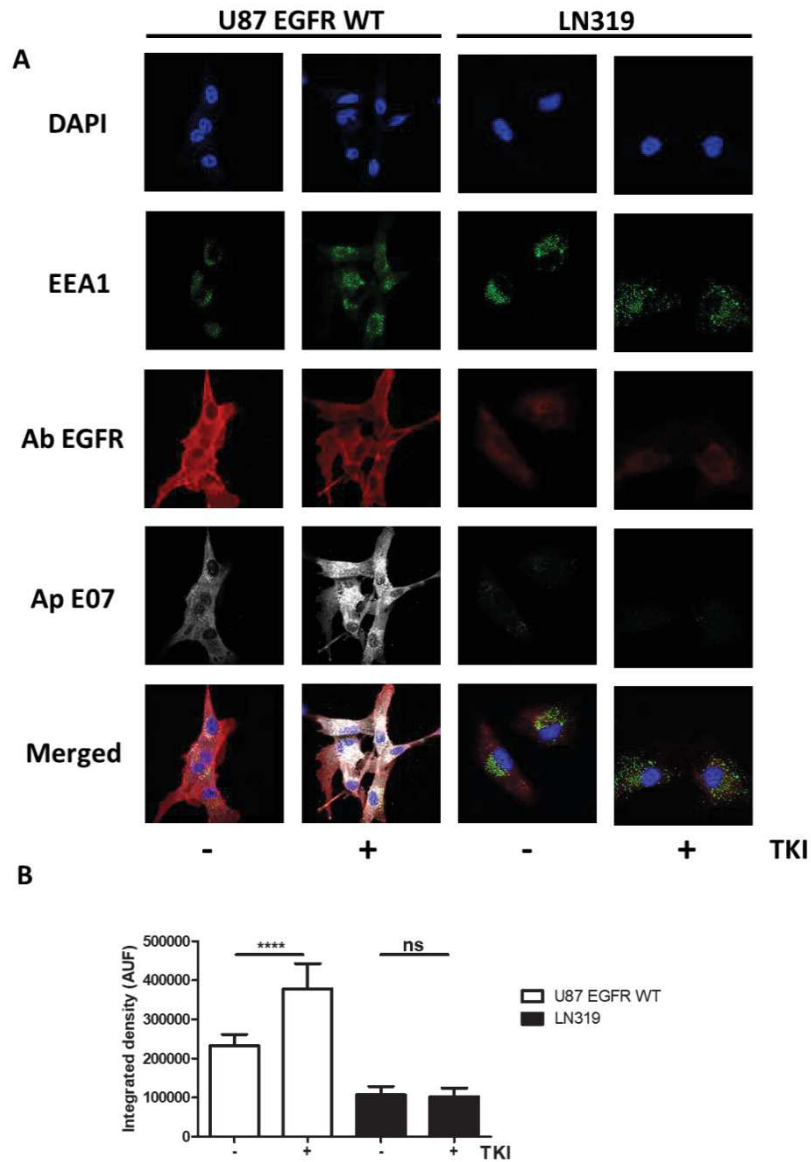


**Figure 5: Confocal imaging of E07 aptamer internalization in U87 EGFR WT and LN319 cells. (A)** GBM cells were seeded in coverslips and incubated with 100 nM of aptamer E07 and treated with DMSO (TKI minus) or 20  $\mu$ M of gefitinib (TKI plus) for 30 minutes at 37°C. The aptamer, labeled with Cy5, is shown in white. Incubation of the anti-EEA1 antibody was followed by incubation with a secondary antibody labelled with Alexa 488 (represented in green). Incubation of antibody anti-EGFR was followed by incubation with a secondary antibody labelled with Alexa 568 (represented in red). Nuclei are stained with DAPI (blue). **(B)** Integrated density of aptamer signal in individualized cells was quantified (3-4 cells / image and 30 images analysed) and is represented in the histogram. \*\*\*\* $p < 0.0001$

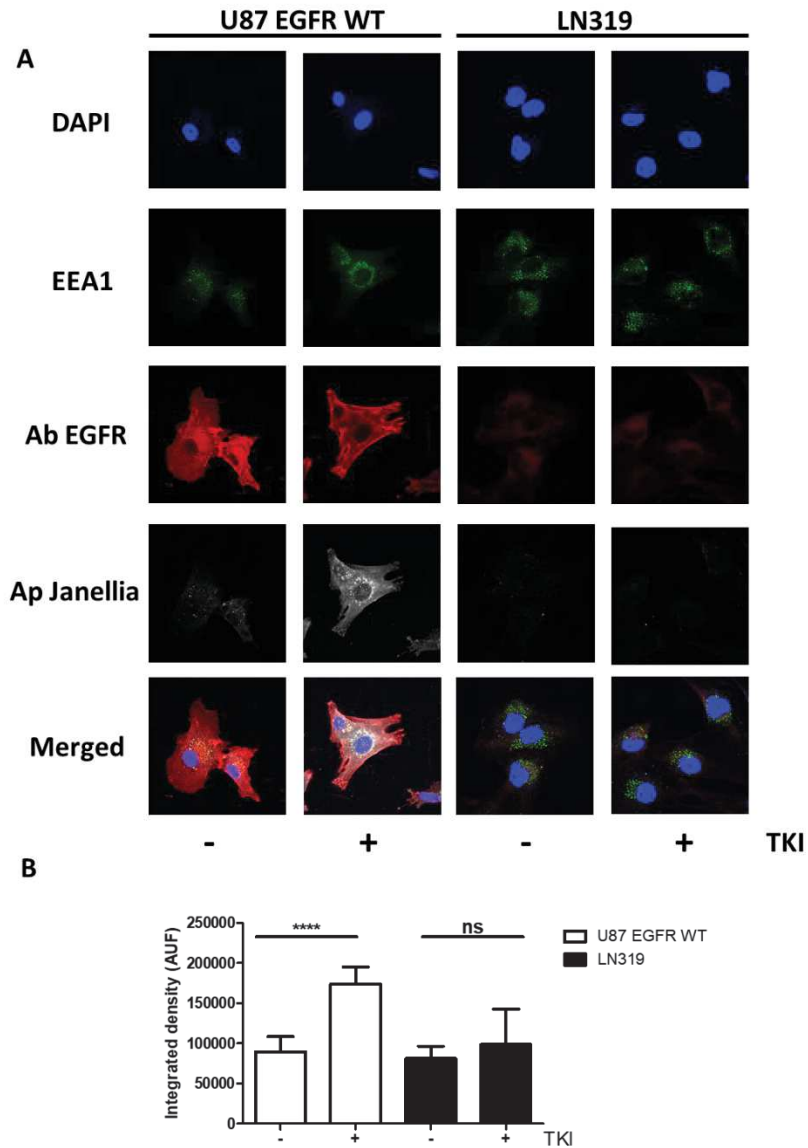


**Figure 6: Confocal imaging of the internalization of the Janellia 646 aptamer in U87 EGFR WT and LN319 cells.** The legend is the same than in Figure 5, except that aptamer Janellia 646 was used instead of Aptamer E07.

## B. Tissue-binding assays

Routine diagnostics usually uses histological tissues for anatomopathological visualization. The most common reporting process in histological routine diagnostics is chemical, using HRP for example. Chromogenic signal is resistant to photobleaching and lasts long. However, it is difficult to distinguish mixed colors, determine co-localization, and perform multiplexing. Fluorescent detection allows easier multiplexing due to larger color choices and better co-localization analysis. However, fluorescent signal can be decreased and even lost by



photobleaching. Moreover, fluorescent detection in diagnostic routine needs a fluorescent microscope (Odell and Cook, 2013).

In order to perform multiplexing we used fluorescent fluorophores conjugated to aptamers, and performed a type of detection called aptahistochemistry, AHC (Bukari et al., 2017). Several studies already reported the use of aptamers as diagnostics tools for cancer cell detection and aptahistochemistry (Gupta et al., 2011; Pu et al., 2015; Zamaç et al., 2017; Zeng et al., 2010).

In our study (Fechter, Cruz da Silva et al., 2019, Article 3), we demonstrated that aptamer H02 was able to detect a human GBM xenograft tissue positive for integrin  $\alpha 5\beta 1$  expression. We wonder whether aptamer H02 might detect integrin  $\alpha 5\beta 1$  in human GBM tissues and not only in xenografts, since mouse component can induce off target bindings. The objective of these studies were also to test different aptamers labelled with different fluorophores on the same GBM patient tissue. In this perspective, were assayed, separately and then together, aptamers H02, E07 and SL1, targeting integrin  $\alpha 5\beta 1$ , EGFR and c-MET, respectively.

We used the slides reader Nanozoomer (Hamamatsu) that allows fast acquisition from histological slides in bright field and in fluorescence. Nanozoomer allows increased magnification until 40x without losing resolution properties.

Data presented below are still preliminary results which will be completed and which need in-depth image analysis.

### *1. Haematoxylin-eosin versus aptahistochemistry (for integrin $\alpha 5\beta 1$ detection)*

Haematoxylin-eosin (H&E) labelling was performed to distinguish between normal and tumoral tissues areas on tissues from four patients (Figure 7 left panel).

AHC was performed on the same GBM patient tissues. The tumor tissue sections, embedded in paraffin, were first deparaffinised and subjected to an antigen unmasking protocol. Figure 7 right panel shows AHC with aptamer H02.

Interestingly, in some tissue areas, like for example the area on tissue section 16T0042 highlighted with an arrow, a more intensed color seem to show areas positive for  $\alpha 5\beta 1$  integrin. We will need the hand of an anathomopathologist and deeper image analysis to understand if such tumor areas are tumoral or necrotic zones.

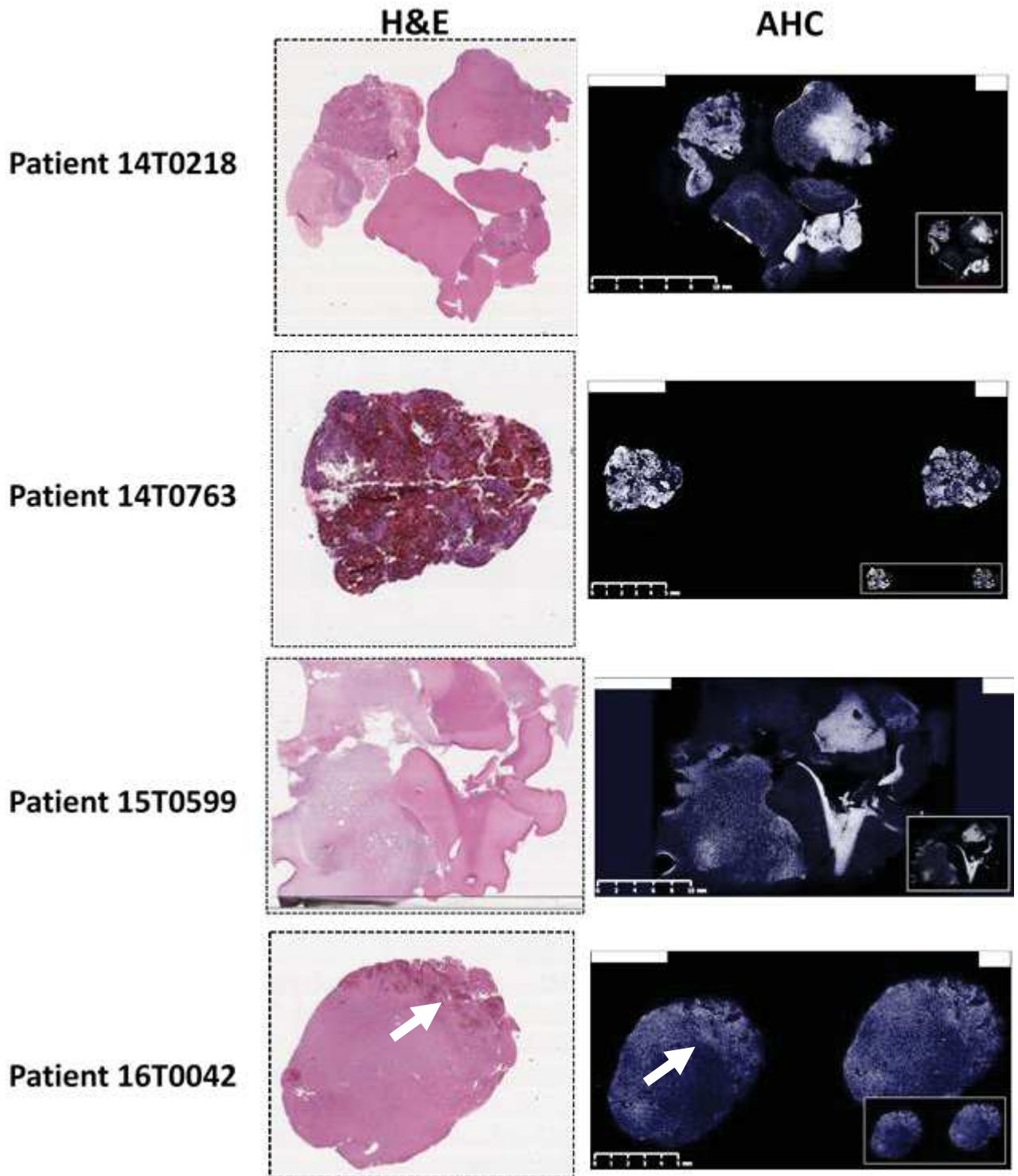


**Figure 7: Haematoxylin-Eosin staining and aptahistochemistry of  $\alpha 5$  integrin on GBM Tissues.** H&E (left panel) and AHC (right panel) of GBM patient tissues. For AHC, detection of  $\alpha 5$  (in white) was performed with the Cy5-labeled aptamer H02. DAPI staining is shown in blue. AHC images were captured at the same setting in Nanozoomer.

## 2. Aptamers versus Antibody (for integrin $\alpha 5\beta 1$ detection)

For immunohistochemistry (IHC), the indirect method that we used, consisted of the incubation of the anti- $\alpha 5$  integrin AB 1928 antibody and secondary antibody anti-Rabbit conjugated to Alexa 647. AHC was performed with the Cy5-labeled aptamers H02 (Figure 8) at  $1\mu\text{M}$ . Aptamer H02 and the anti- $\alpha 5$  antibody allowed to differentiate two different areas, but the contrast between these two areas is higher with less background in AHC compared to IHC. We still need to determine whether these two areas correspond to tumor versus normal tissues or to two tumor areas with different  $\alpha 5\beta 1$  expression levels. In that last option, it would mean that aptamer H02 is able to detect intra-tumoral heterogeneity. Moreover, it would be interesting to determine  $\alpha 5$  integrin mRNA expression levels in order to exclude any off target bindings.

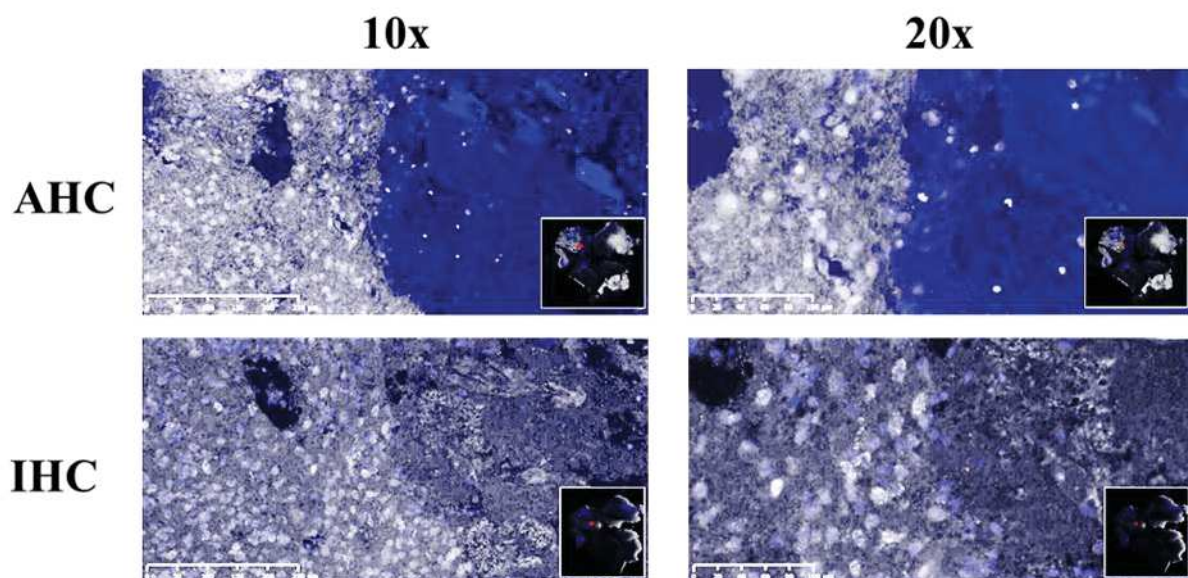


**Figure 8: Comparison between apta- and immuno- histochemistry.** For AHC, detection of  $\alpha 5$  (in white) was performed with the Cy5-labeled aptamer H02 at  $1\mu\text{M}$ . For IHC, detection of  $\alpha 5$  (white) was performed with antibody AB 1928 at  $1/200$ , followed by a secondary antibody coupled to Alexa 647. DAPI staining is shown in blue. Images were captured at the same settings to allow direct comparison of staining patterns on Nanozoomer. Images shows different magnificence (10x on left panel and 20x on right panel).

## 3. Multiplexing

We also wished to perform multiplexing on GBM tissue samples by using on the same GBM tissue section, aptamers H02 (targeting integrin  $\alpha 5\beta 1$ ), E07 (targeting EGFR) and SL1 (targeting c-MET), labeled with fluorophores Cy5, Alexa 488 and Alexa 568, respectively. First, a double-AHC labelling was performed on three tumor sections, using aptamer H02 and E07 (Figure 9). We can clearly observe areas positive for integrin  $\alpha 5\beta 1$  or for EGFR or for both receptors.

To detect c-MET (in addition to integrin  $\alpha 5\beta 1$  and EGFR), from now, we just realized AHC using the SL1 aptamer coupled to Alexa-Fluor 568 (Figure 10). The SL1 aptamer seems to highlight heterogeneous c-MET expression levels, and might label invading cells and tumor blood vessels. Aptamer SL1 might therefore be of interest in AHC.

*In a future series of experiments, we will perform triple multiplexing using aptamers targeting  $\alpha 5$  integrin, EGFR and c-MET. We wish to know whether GBM tumor inter- and intra-heterogeneity can be highlighted thanks to aptamers targeting cell-surface receptors and whether aptahistochemistry might be useful for tumor characterization.*

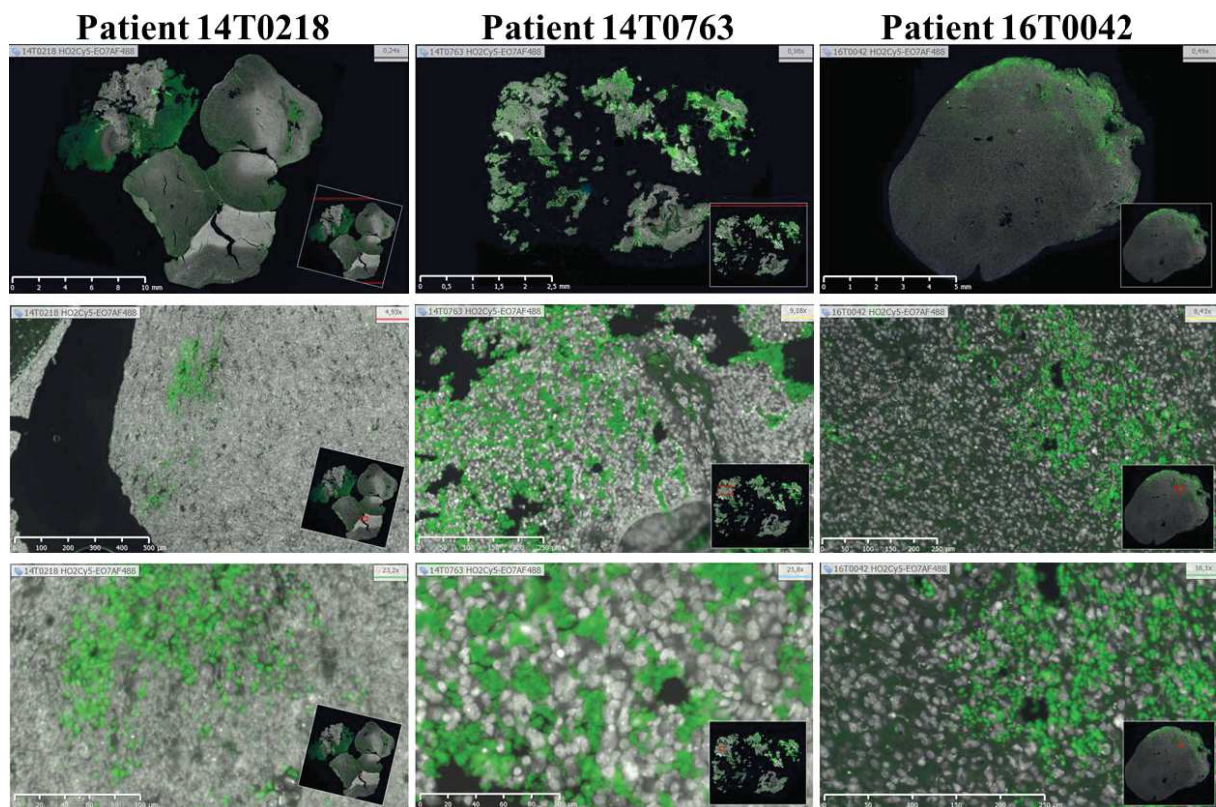


**Figure 9: Apta-labelling of integrin  $\alpha 5$  and EGFR on GBM tissues from three patients (14T0218, 14T0763 and 16T0042).** For AHC, detection of  $\alpha 5$  (in white) and EGFR (in green) were performed with the Cy5-labeled aptamer H02 at  $1 \mu\text{M}$  and the Alexa-Fluor 488-labeled aptamer E07 at  $500 \text{ nM}$ , respectively. Images were captured at the same settings to allow direct comparison of staining patterns in Nanozoomer. Images from the top to the bottom show different magnification (1x, 10x and 20x)

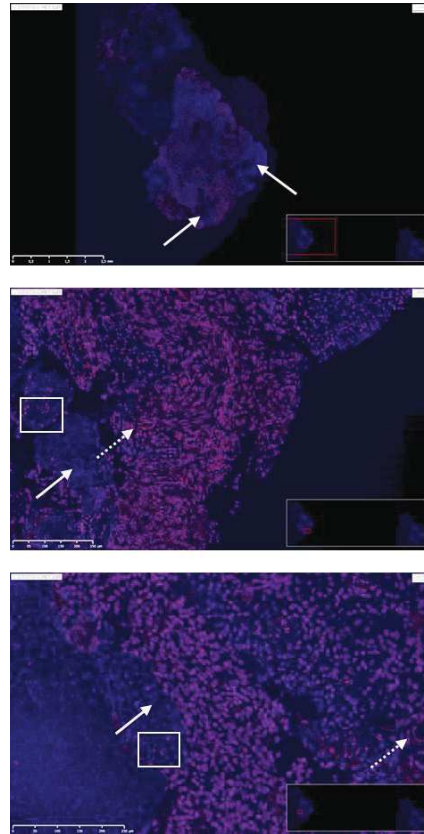


**Figure 10: c-MET aptafluorescence on one GBM tissue.** For AHC, detection of c-MET (in pink) was performed with the Alexa-Fluo 568-labeled aptamer SL1. DAPI staining is shown in blue. Images were captured at the same setting to allow direct comparison of staining patterns in Nanozoomer. Full arrows show c-MET negative zones. Discontinuous arrows might show c-MET labelling of tumor blood vessels. The white squares might show c-MET positive cells invading c-MET negative zones.

## General conclusions

- Aptamer H02 identified  $\alpha 5\beta 1$  integrin in glioma cells and human tissues samples.
- EGFR-aptamers identified EGFR expression in cells and human tissue samples.
- Gefitinib increased EGFR-aptamers internalization.
- Aptahistochemistry using simultaneously aptamer H02 and an EGFR-aptamer may highlight GBM heterogeneity.

In the first article, we described a new aptamer, H02, targeting  $\alpha 5\beta 1$  integrin. H02 was able to recognize  $\alpha 5$ -positive GBM cells and tumor xenografts. H02 was internalized in EEA1-positive early endosomes at 37°C.

In the second part, we characterized EGFR-targeting aptamers in cell-based assays. EGFR-aptamers were able to recognize EGFR-positive GBM cells. The aptamers were internalized at 37°C, and this internalization was enhanced upon treatment with gefitinib.

Next, we start characterizing aptahistochemistry using aptamers targeting  $\alpha 5$  integrin, EGFR and c-MET receptors.

Aptamer targeting  $\alpha 5$  integrin provided integrin detection with less background compared to antibody labelling. Interestingly, dual detection of integrin  $\alpha 5$  and EGFR using aptamers might be of interest to demonstrate GBM intra-tumoral heterogeneity. On going studies will provide evidence with a triple labelling of GBM tissues using aptamers against three membrane receptors.

Finally, this work highlighted the potential use of aptamers as cancer detection tools. Further work is necessary to really access their interest as vectorization tools by exploiting the fact that aptamers are internalized at 37°C.

# Conclusion

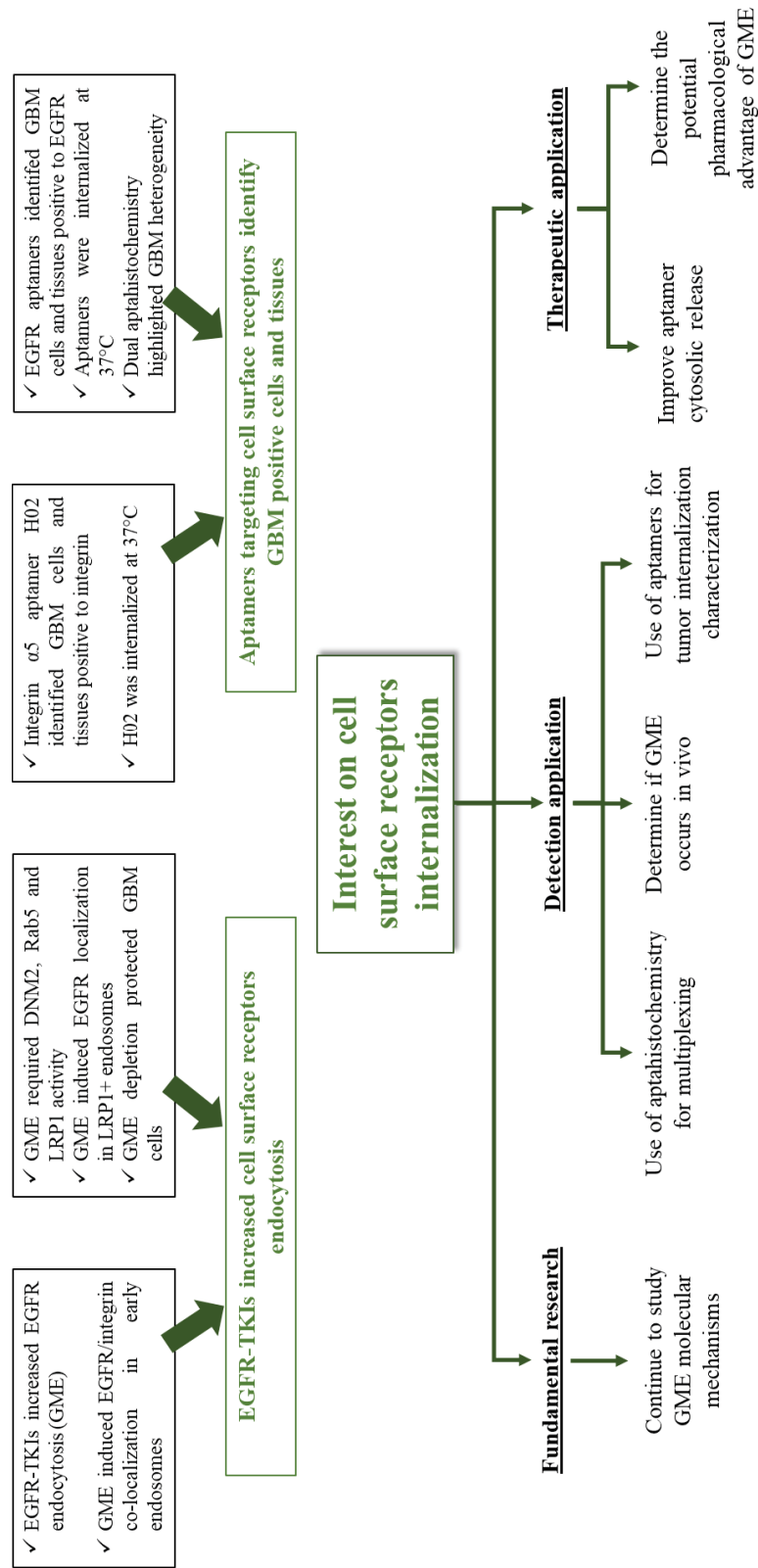


Figure 17: Perspectives of the present work.



### *Perspectives for fundamental research*

Certain studies showed the impact of gefitinib treatment in membrane trafficking. Studies showed that gefitinib suppresses ligand-induced EGFR endocytosis in *in vitro* sensitive cells (Nishimura et al., 2007) and in *in vivo* tumor xenografts (Pinilla-Macua et al., 2017). However, another study was in agreement with our results since gefitinib increased radiolabeled human EGF uptake in HNSCC, NSCLC and colon carcinoma cells (He and Li, 2013). In this work we demonstrated that in glioma cells, EGFR-TKI gefitinib increase EGFR endocytosis in a process we called gefitinib-mediated endocytosis (GME). A better understanding of GME molecular mechanisms is needed in order to correctly explore this gefitinib activity for therapeutic purposes. In our study, we described the endocytosis proteins DNM2, Rab5, integrin  $\alpha 5\beta 1$  and LRP-1 as molecular regulators of GME since their blockage reduces EGFR endocytosis and/or EGFR localization in EEA1-positive early endosomes.

How gefitinib may promote endocytosis is an intriguing question emerging from our results. A recent study highlighted a frequent off-target cytotoxicity of targeted therapies (Lin et al., 2019). Using CRISPR-Cas9, authors studied targeted-therapies present in clinical trials. Contrarily to RNA interference and small-molecule inhibitors, CRISPR-Cas9 deletion of the target gene demonstrated that drugs still have anti-proliferative effects. This study demonstrated that in most targeted-therapies studied, effect is mainly off-target derived. Thus, it would be interesting to verify the importance of EGFR and its TK domain necessity to GME mechanism. Several lines of evidence are in favor of off-target effect of gefitinib. Previous evidences showed that gefitinib can trigger stress-induced alterations of membrane trafficking (Tomas et al., 2014). Furthermore, using *in vitro* kinome studies, gefitinib and the other TKIs we used were shown to inhibit numerous others tyrosine kinases (Table 10) (Kitagawa et al., 2013; Verma et al., 2016). Lysotrophism of gefitinib has been evoked as potential mechanism to perturb overall membrane trafficking (Li et al., 2018). Finally, GME may be related to a kinase-independent function of EGFR as it has been shown in the initiation of autophagy by serum starvation (Tan et al., 2015). We never observed neither endosomal enlargement/fusion in GBM in cells treated with EGFR siRNA. Similarly, serum-starvation did not provoke EGFR endocytosis and allow efficient GME (data not shown). It will be thus important to determine if GME is dependent or not of EGFR. One way will be to study integrin and LRP-1 endocytosis in EGFR-null cells (depletion of EGFR by siRNA or CRISPR-Cas9 or using the LN319 cell line).

**Table 10: Target affinity of EGFR-TKIs.** Adapted from HMS LINCS Database Kinome SCAN small molecules

Target affinity	Gefitinib	Erlotinib	Lapatinib	Afatinib	Dacomitinib
$K_D < 100 \text{ nM}$	<i>EGFR, GAK, IRAK1</i>	<i>ABL1, EGFR, ERBB3, GAK, MAP2K5, MAP3K19, SLK, STK10</i>	<i>EGFR, ERBB2, ERBB4, Tuba1a</i>	<i>EGFR, ERBB2, ERBB4, GAK</i>	<i>EGFR, ERBB2, ERBB4</i>
$100 \text{ nM} \leq K_D < 1 \mu\text{M}$	<i>ERBB2, ERBB3, ERBB4, plus other 20</i>	<i>ERBB2, ERBB4, plus other 30</i>	<i>PI4KB, PIK3C2B, RAF1</i>	<i>ABL1, BLK, DYRK1A, EPHA6, HIPK4, IRAK1, LCK, PHKG2</i>	No data available
$1 \mu\text{M} \leq K_D < 10 \mu\text{M}$	More than 20	More than 20	More than 20	More than 20	No data available

Molecular mechanisms of GME are not yet totally clear. Further studies are needed to better understand how gefitinib can dysregulate membrane trafficking. We demonstrated that EGFR localization in EEA1-positive early endosomes upon gefitinib treatment is reduced with a dominant negative of Rab5. However, we still need to determine if gefitinib is able to activate Rab5 and how it happens. First, Rab5-GTP pull-down assays in control and gefitinib-treated cells would show if gefitinib activates this GTPase. Next, we might study the impact of gefitinib in Rab5 interaction with guanine nucleotide-exchange factors (GEFs). For example, SPIN90, an adaptor protein, was shown to affect Rab5 interaction with one GEF, promoting its activation (Kim et al., 2019). It will also be interesting to study other molecules described to participate in EGFR trafficking dysregulation, for example, p-38-MAPK that is involved in almost all mechanisms of stress-induced EGFR internalization (Cavalli et al., 2001; Tomas et al., 2017; Zwang and Yarden, 2006), and described to activate Rab5 (Cavalli et al., 2001).

Data on the invasive properties of glioma cells suggest that reduced endocytosis, for example by inhibition of DNM2, turned glioma cells to a more resistant phenotype. In line with our results, gefitinib-resistant tumor cells present dysregulated trafficking (Al-Akhrass et al., 2017; Kondapalli et al., 2015; Wang et al., 2019c). Impairment of EGFR internalization and entrapment of internalized EGFR in early endosomes with sorting nexin 1, leads to uncontrolled signaling in gefitinib resistant cells (Nishimura and Itoh, 2019; Nishimura et al., 2008). Also, hypophosphorylation of Y1045 in EGFRvIII leads to defective Cbl recruitment, receptor ubiquitination and degradation in gefitinib-resistant cells (Han et al., 2006). Co-treatment with TKIs and 1,3,4-O-Bu<sub>3</sub>ManNAc showed efficient synergy in pancreatic cells. 1,3,4-O-

Bu3ManNAc increased EGFR internalization via non-clathrin mediated endocytosis that favors receptor degradation and impairs EGFR endosomal signaling (Mathew et al., 2016). However, a different study in NSCLC cells showed the opposite since gefitinib-resistant cells presented an increased EGFR endocytosis and degradation (Yamaoka et al., 2004).

Moreover, it is well established that cancer cell migration is mediated by cellular trafficking. Rab5 influences cell migration through its control of integrin endocytosis, for instance. Rab5 interacts with focal adhesion proteins, promotes integrin endocytosis and cell migration (Mendoza et al., 2013). Moreover, overexpression of Rab5 increased glioma cell migration and invasion (Jian et al., 2020). DNM2 also facilitates cell migration and invasion. DNM2 interacts with FAK at focal adhesions. DNM2 blockage inhibits focal adhesion disassembly and reduced cell migration (Ezratty et al., 2005). In lung cancer cells, DNM2 stabilizes F-actin bundles in filopodia, promoting cell migration and thus tumor progression (Yamada et al., 2016). Additionally, DNM2 promotes actin polymerization at cell edges allowing actomyosin-mediated force transmission to ECM and 3D cell migration (Lees et al., 2015). Interestingly, our results showed that DNM2 inhibition significantly increased cell evasion of gefitinib-treated spheroids but had no impact on the number of cells evading from the spheroid in control condition. At this step, we still don't know how endocytosis inhibition can promote cell invasion in gefitinib-treated cells. We can imagine that EGFR interactions with other receptors at the plasma membrane can stimulate cell migration even though EGFR-kinase domain are blocked by gefitinib. EGFR-kinase independent interactions at the plasma membrane facilitate cancer cell survival (Hanabata et al., 2012; Weihua et al., 2008).

One evident partner of EGFR function and trafficking is the  $\alpha 5\beta 1$  integrin. Our study showed that as an endocytosis protein,  $\alpha 5\beta 1$  integrin contributed to GME. However, compared with classical endocytosis proteins, inhibition of integrin expression leads to decrease in cell resistance to TKI. This can be explained by the direct influence of integrin in cell evasion (Blandin et al., 2016) and cell migration (Paul et al., 2015). In this context, endosomal signalling of  $\beta 1$  integrins contributes to cancer cell anchorage-independent growth and invasion via FAK activation (Alanko et al., 2015), recruitment and activation of mTOR to late endosomes (Rainero et al., 2015) or co-signalling with c-MET (Barrow-McGee et al., 2016). Furthermore, several reports demonstrated the importance of integrin and EGFR recycling for cancer progression and invasion (Caswell et al., 2008; Lakoduk et al., 2019; Muller et al., 2009). Thus, in gefitinib-treated cells,  $\alpha 5\beta 1$  integrin may promote cell evasion, by endosomal signalling or

regulation of EGFR recycling. It will be interesting to compare integrin and EGFR interactome and signalling either at the plasma membrane level or in the endosomes, in function of gefitinib treatment. Another point of interest would be to examine in detail the impact of gefitinib in EGFR and  $\alpha 5\beta 1$  integrin journey inside the cell. We know that integrin trafficking depends on their conformational status (Arjonen et al., 2012). In article 1, to detect  $\alpha 5\beta 1$  integrin we used a monoclonal antibody (clone IIA1) that selectively recognizes the inactive bent form of the receptor. However, during my thesis, I wondered whether gefitinib would also impact on active form of integrin. To this end, I performed preliminary experiments using anti- $\alpha 5$  monoclonal antibody (clone SNAKA51, Millipore) which binds to an epitope only accessible in ligand-bound and active  $\alpha 5\beta 1$  integrin (Figures 18 and 19). First, we can observe that gefitinib also induced endosomal accumulation of ligand-bound active  $\alpha 5\beta 1$ , and that EGFR and active integrin co-labelled the same endosome. This is an important information as it suggests that during GME,  $\alpha 5\beta 1$  integrin might remain competent for endosomal co-signalling with EGFR. However, upon gefitinib treatment the kinetics of active and inactive  $\alpha 5\beta 1$  integrin trafficking were clearly different, suggesting that as in physiological endocytosis and trafficking, they may take different routes in GME. Obviously, more studies are needed to determine the respective endosomal compartments where each of these conformations are and their fate.

We assume that GME relies on general perturbation of membrane trafficking and we need to take into account the complexity of the cellular context to better understand the potential therapeutic significance of GME.

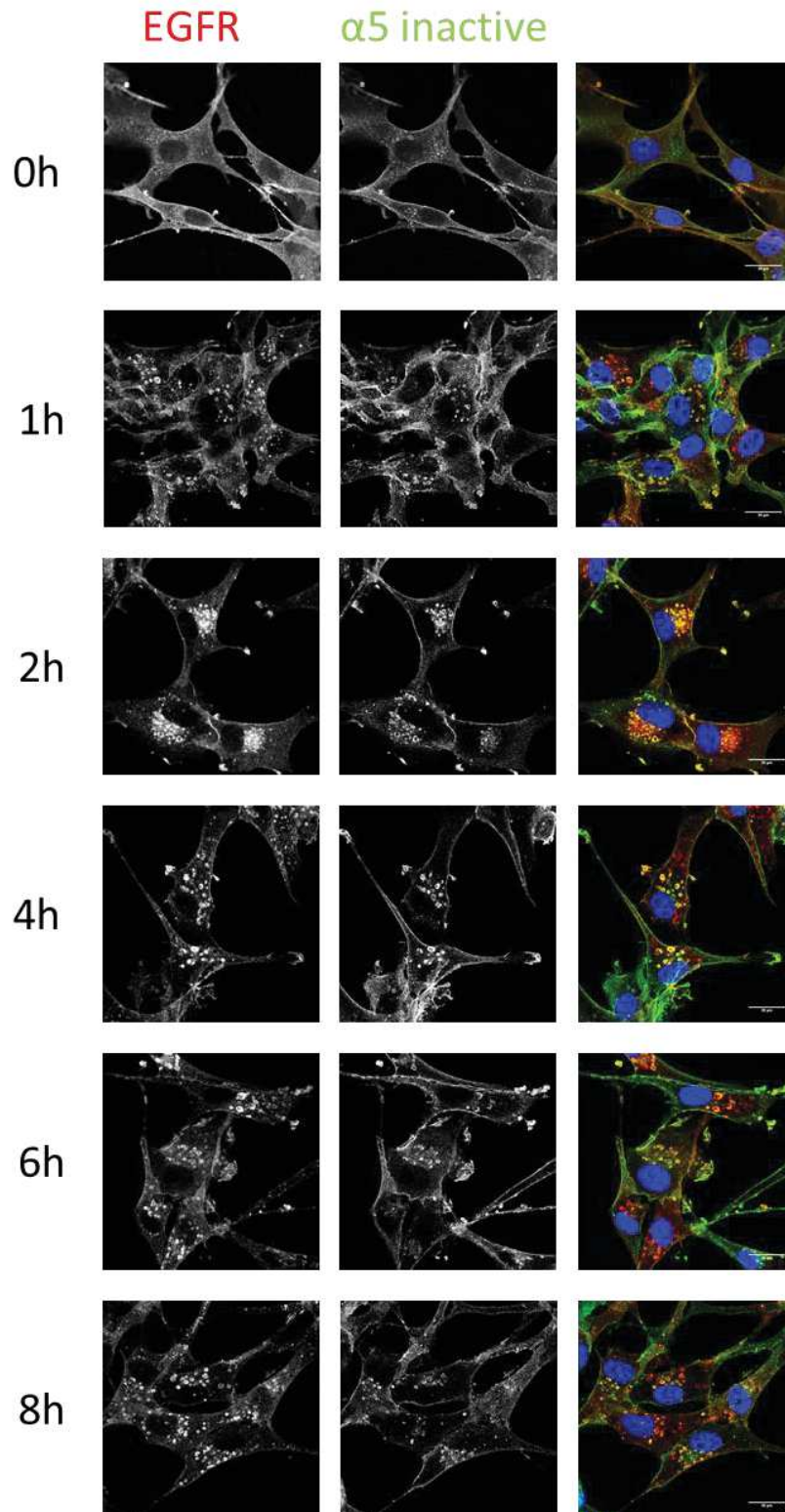


**Figure 18: GME effect on inactive integrin trafficking.** U87 were treated with 20 $\mu$ M of gefitinib for different period of time (1, 2, 4, 6 and 8 hours). Cells were fixed, inactive  $\alpha 5$  integrin and EGFR were immunolabelled. Scale-bar: 20 $\mu$ m

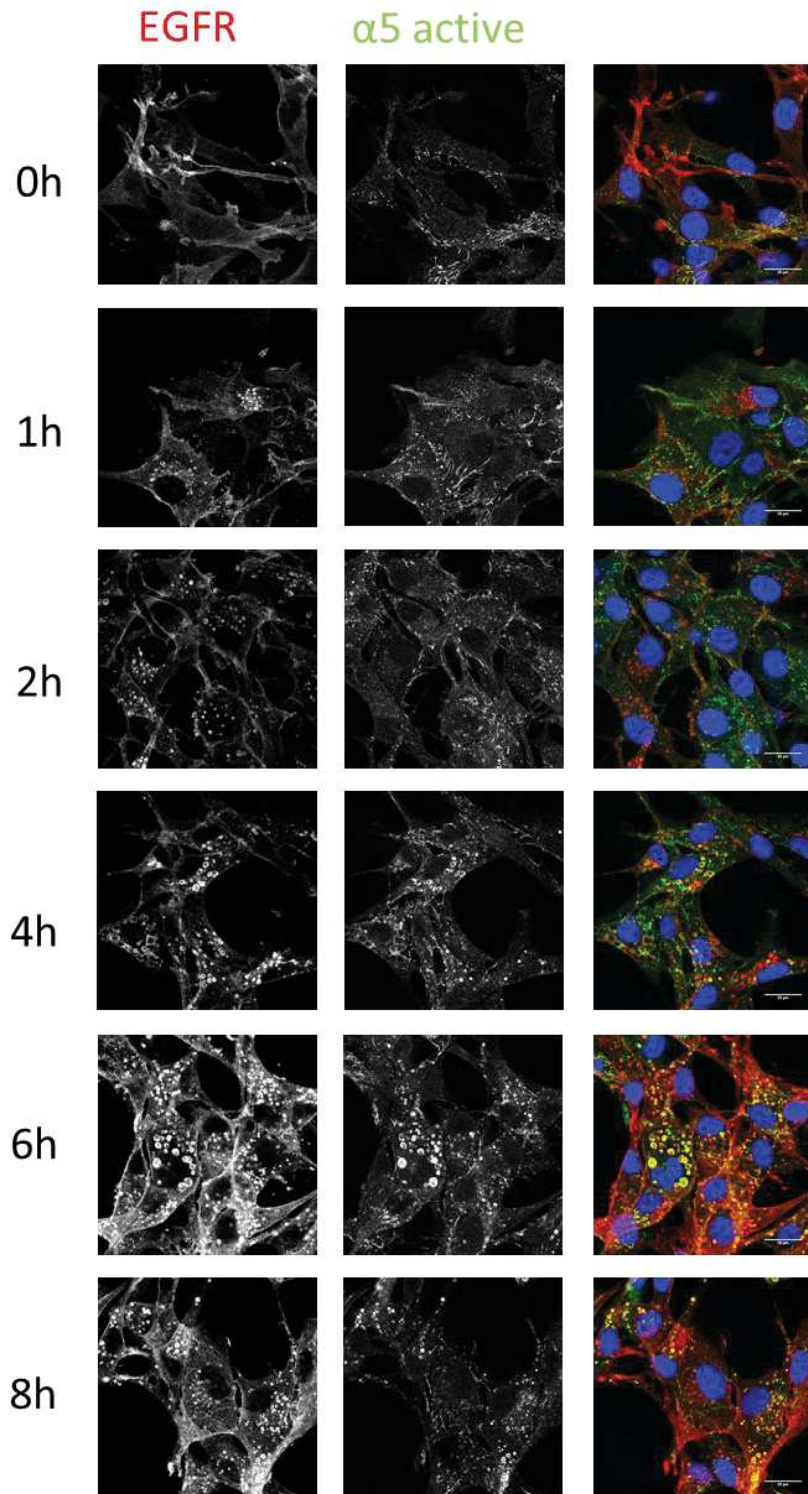


**Figure 19: GME effect on active integrin trafficking.** U87 cells were treated with 20 $\mu$ M of gefitinib for different period of time (1, 2, 4, 6 and 8 hours). Cells were fixed, active  $\alpha 5$  integrin and EGFR were immunolabelled. Scale-bar: 20 $\mu$ m

## Perspectives for clinical applications

### A. GME as a new therapeutic rationale

An exciting avenue, is that GME might be used in a new therapeutic scheme in order to increase internalization of therapeutic agents or vectors.

During my thesis, I challenged the proof of concept of this hypothesis. Using GBM cellular models, we demonstrated that gefitinib treatment is able to increase EGFR targeting aptamers (recent results section) and antibodies (Figure 20) endocytosis.

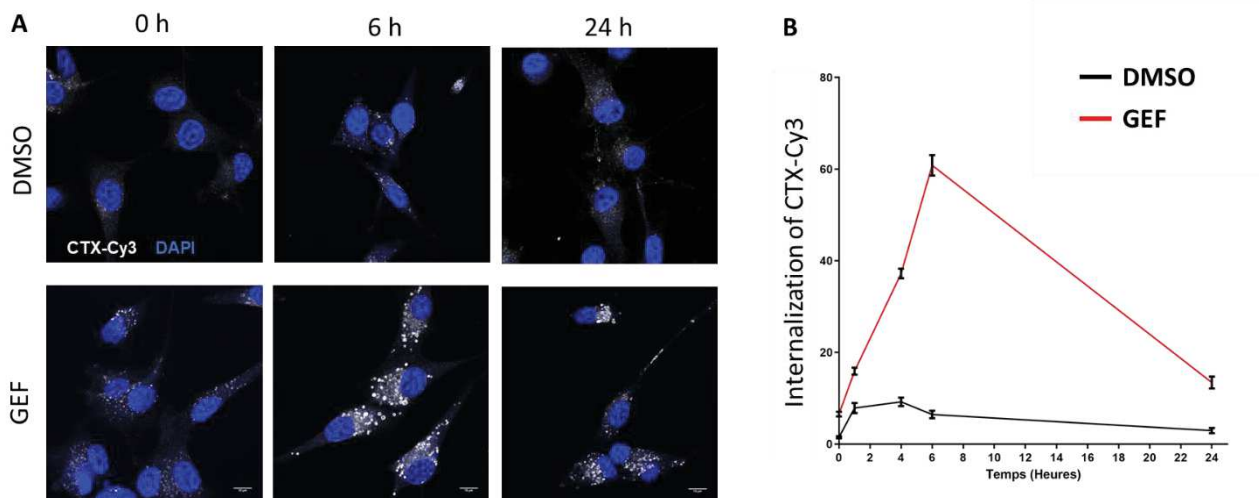


**Figure 20: Gefitinib effect on cetuximab (CTX) internalization.** U87 cells were pre-incubated with CTX-Cy3 at 4°C, then placed at 37°C in the presence of DMSO or gefitinib (20µM). After fixation, CTX-Cy3 localization was analysed and quantified by confocal microscopy. **(A)** Confocal images of U87 cells showing an increase of CTX-Cy3 internalization after 6h of gefitinib. Upon 24h of incubation, this signal decreased. **(B)** Quantification of fluorescence associated to internalized CTX-Cy3 demonstrated clear differences in treatment kinetics between control cells (DMSO-black) and gefitinib-treated cells (GEF-red). Results represented by mean ± s.d. of 30 cells of 3 independent experiences.

Increased anti-EGFR antibody endocytosis should boost the cytotoxic activity of anti-EGFR ADC. To test this hypothesis, we selected depatuzumab-mafatodin (ABT-414), an ADC developed by AbbVie and tested in clinical trials for the treatment of GBM (Van Den Bent et al., 2020). ABT-414 is an ADC composed of an EGFR targeting-monoclonal antibody whose cysteine residues are conjugated to a microtubule inhibitor, monomethyl auristatin F (MMAF), via a stable maleimidocaproyl linker. Auristatin targets the vinca alkaloid site of microtubules (Chen et al., 2017). To improve its cytotoxic effect, auristatin gave origin to monomethyl auristatin-E (MMAE) and MMAF. Both are stable in the plasma and in the lysosome. There is an advantage of MMAF for bioconjugation with non-cleavable linkers, since it retains potency

when linked to a simple alkyl chain while MMAE is potent in native form (Doronina et al., 2006).

After endocytosis of EGFR, the lysosomal degradation of the antibody allows the release of Cys-mcMMAF that can cross alone the endosome membrane to reach cytosol and its target. Drug will be released attached to the linker that carries an amino acid from the antibody. The majority of these structures attach the linker-drug directly to a cysteine group of the antibody, through a reaction between maleimide group and sulfhydryl groups. This reaction in pH between 6.5 and 7.5 results in a non-reversible link (Jain et al., 2015).

Preliminary pharmacological studies on U87 cells demonstrated that association of gefitinib with ABT-414 decreased by 10 000 fold the cytotoxic concentration of ABT-414 compared to ADC alone (Figure 21).

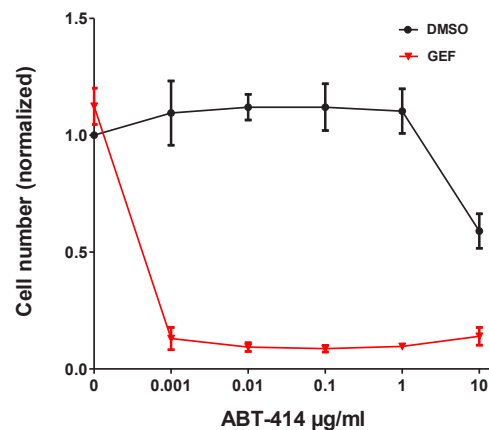


**Figure 21: Gefitinib increases ABT-414 efficiency.** U87 cells were cultured during 3 days in the presence of gefitinib at a low cytotoxic concentration ( $10\mu\text{g}\cdot\text{ml}^{-1}$ ) and variable concentrations of the ADC. Number of cells is quantified by crystal violet staining after fixation ( $n=3$ , 6 wells/condition). Black line represents cell treatment with different concentrations of ABT-414. Red line represents co-treatment with  $10\mu\text{g}\cdot\text{ml}^{-1}$  of gefitinib with different concentrations of ABT-414.

These promising results need to be validated in other GBM models and with the other controls (for example the separated use of antibody and cytotoxic drug), before moving into mice models. In order to establish a correlation between antibody/ADC internalization with the effectiveness of the therapeutic combination we could decrease GME by blocking DNM2 and determine the impact of therapeutic synergy. It will be interesting to evaluate the intracellular localization of the antibody to verify if gefitinib can promote its localization in lysosomal compartments, using immunolabelling of LAMP1 for example. We could also quantify through cell fractionation followed by mass spectrometry analysis if gefitinib can increase the cytosolic concentration of cys-mcMMAF.



*This work might create new opportunities to improve GBM therapeutic approaches, either by facilitating tumor characterization using aptamers targeting cell surface receptors for studying receptor expression and trafficking, or by proposing a new purpose for EGFR-TKIs as an enhancer of therapeutic agents' entry in cancer cells.*

B. Aptamers targeting cell surface protein biomarkers: towards diagnostic and targeted delivery tools

My experience with aptamers targeting integrin  $\alpha 5\beta 1$ , EGFR (and to a lesser extent c-MET) is motivated by a desire to understand the mechanism of action of aptamers targeting cellular receptors, so that in the future, they can find clinical applications, particularly in diagnostics and towards targeted therapies (Figure 22).

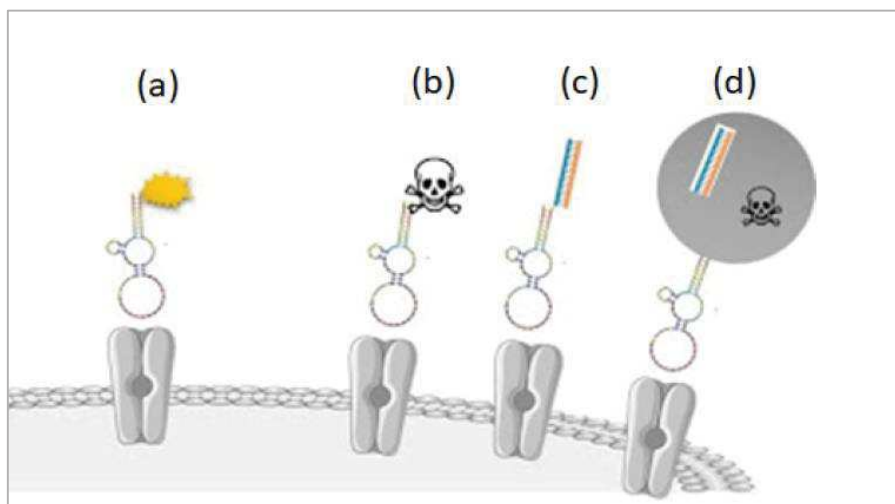


**Figure 22: Illustration of clinical applications of aptamers targeting GBM cell-surface biomarkers.** In clinical perspectives, an aptamer targeting a cell-surface GBM biomarker might be coupled with different molecules such as (a) a fluorophore or a radioactive element for imaging/diagnostic purposes; (b) a cytotoxic agent (AptDC) or (c) a siRNA (aptamer-siRNA conjugate, AsiC) in therapeutic targeting. The coupling could be direct (b, c) or via a nanoparticle (d).

Our studies highlighted the potential use of aptamers as detection tools.

Integrin  $\alpha 5$  and EGFR aptamers were able to identify GBM cells and tissues expressing their respective targets. We still have to complete the studies initiated during my PhD, notably by a multiplexing approach on GBM tissues with aptamers targeting integrin  $\alpha 5\beta 1$ , EGFR and c-MET (as already mentioned in the Result section).

Moreover, aptamers can be used to study cell surface receptor endocytosis features in *ex vivo* tumor samples. An interesting study demonstrated a correlation between dysregulated EGFR endocytosis and anti-EGFR monoclonal antibody therapy outcomes (Joseph et al., 2019). Aptamers can play a role in studying receptor endocytosis in *ex vivo* samples and consequently in patient stratification and predictive outcome.

Another perspective will be to use aptamers as a non-invasive molecular imaging tools to visualise brain tumours expressing cell-surface biomarkers of interest and to monitor tumour progression in mouse xenograft models. EGFR aptamers coupled with radio isotope were already used for in *in vivo* imaging of GBM tumor cells in mouse xenografts (Wu et al., 2014). It will be thus interesting to image aptamers targeting other cell-surface biomarkers (such as integrin  $\alpha 5\beta 1$  and c-MET). The evolution of tumour progression of GBM xenografts will be followed longitudinally, *in vivo*, in Positron Emission Tomography (PET) imaging. The Cyr c platform's TR24 cyclotron will be used for the production of Fluor-18. Radiolabelling will be carried out using click chemistry between the modified aptamer and a Fluor-18 labelled prosthetic group (Hassanzadeh et al., 2018).

Our studies also highlighted the potential use of aptamers as targeted delivery tools.

Aptamers might have an advantage over antibodies for vectorization, as they are produced chemically and thus are easy to be modified, allowing a more controlled and precise bioconjugation. For AptDC, only one cytotoxic payload can be conjugated to one aptamer, whereas antibody-bioconjugation can occur on different and multiple residues. It is therefore difficult to obtain a homogeneous and batch-reproducible drug-antibody ratio (DAR). Even though aptamer used as vectorization it is still in its infancy compared to studies with antibodies, promising results were obtained with two prostate-specific membrane antigen targeting 2'-F-Py-RNA aptamers (A9 and A10) used to deliver siRNA, nanoparticles, quantum dots and toxins to prostate cancer cells (Cerchia and de Franciscis, 2010).

Interestingly, our study demonstrated that aptamers were internalized at 37 C upon binding to cell surface receptors. This property might be exploited to follow cell surface receptor internalization in cells. Better knowledge on aptamer cytosolic release might improve efficiency of aptamer application in vectorization approaches. Aptamers entry in cells is well known, however, few knowledge about aptamers intracellular trafficking and cytosolic release exists. Aptamer endosomal escape rate is lower than 0.01% (Tawiah et al., 2017), even though

this is an essential step for therapy efficiency. For aptamer-siRNA conjugates (AsiC, Figure 23), for example, it would be interesting to improve aptamer cytosolic release.

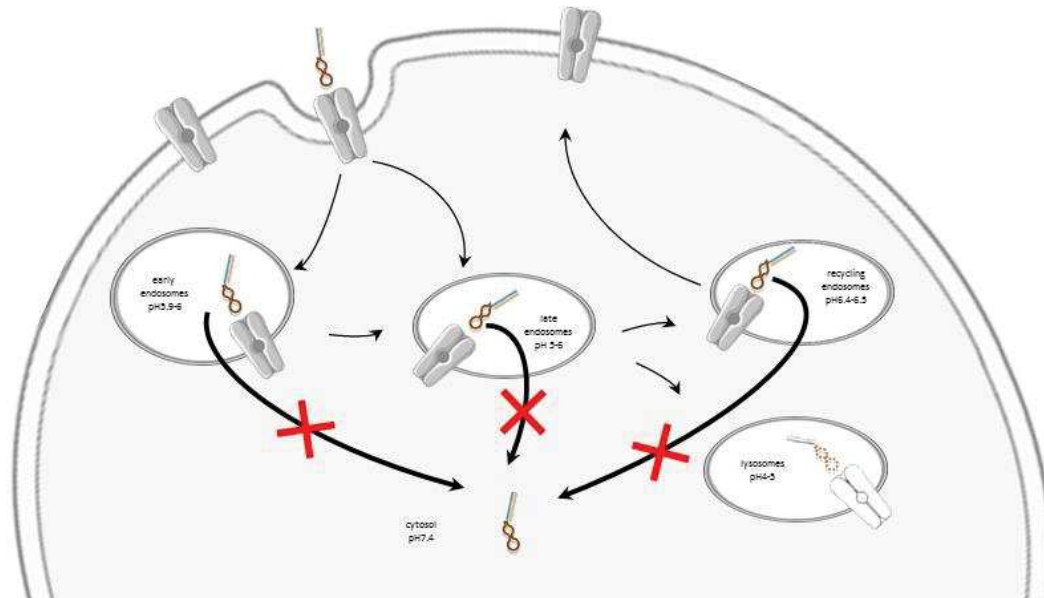


**Figure 23: Illustration of the putative intracellular trafficking, by RME ('receptor mediated endocytosis'), of aptamers targeting cellular receptors and conjugated to siRNAs.** After binding to the cell-surface biomarker, the AsiC might be internalised in early endosomes. Then its intracellular traffic is rather unknown. It might follow the same intracellular traffic routes as the receptor, through different compartments. Indeed, it might be found in the late endosomes and then in the recycling endosomes, or in the lysosomes. The aptamer might also dissociate from the receptor. However, its endosomal escape from the intracellular compartments to access the cytosol is unknown (symbolised by red crosses).

In order to better assess this issue, we first need to establish techniques to determine and quantify cytosolic release events. Studies on aptamer intracellular trafficking will give insights about the subcellular localization of aptamers. Intracellular trafficking of aptamers will be monitored by microscopy techniques such as confocal microscopy, TIRF and two-photon laser scanning. The aptamers will be coupled with pH sensitive fluorophores (1 fluorophore/aptamer) (Li et al., 2015b). Thanks to its ratiometric properties and its pKa (6.2), it will emit at a different wavelength when the aptamers are in the cytosol (pH 7.4) compared to the acid compartments (early endosomes: pH 5.9-6.0; late endosomes: pH 5-6; lysosomes: pH 4-5; recycling endosomes: pH 6.4-6.5). Using fluorescence microscopy, aptamers conjugated to fluorophores can be spotted in different endolysosomal compartments identified by specific markers (Rab5 and EEA1 for early endosomes, Rab11 and Rab4 for recycling endosomes, Rab7 and CD63 for late endosomes, and finally LAMP1 and LysoTracker® for lysosomes). Quantitative evaluation of aptamer cytosolic release might be performed by cytosol recovery through cell fractioning (separation of cytosol/nucleus/other sub-cellular compartments) followed by aptamer

quantification by Real-time Quantitative Polymerase Chain Reaction (qPCR). qPCR is known for detecting very small amounts of DNA. Using a standard curve, we might be able to calculate the initial quantity of target DNA (Santos et al., 2019). It would also be interesting to perform a cell internalization-SELEX to collect only internalized aptamers (Mercier et al., 2017; Thiel et al., 2012; Wan et al., 2019). In that case, steps of cytosol recovery could be added to the SELEX cycles in order to specifically select aptamers able to be released in the cytosol.

If the sub-cellular escape of aptamers were optimised, aptamers could be very efficient vehicles for drug delivery. It might be possible to perturb membrane trafficking to increase the time spent by aptamers in endosomal compartments in order to favour their release (Dowdy, 2017; Tawiah et al., 2017). For example, BafilomycinA that blocks endosome acidification. Another possibility would be to induce endosomal disruption via a proton-sponge effect using cationic polymer polyethylenimine (PEI) (Liang and Lam, 2012), for example. And, definitely, the studies of gefitinib on aptamer internalization will be further exploited. Before applying GME for pharmacological purposes, we need to determine if gefitinib induces cell surface receptors internalization in *in vivo* models. Intravital multiphoton imaging allowed to follow endogenous EGFR tagged with fluorophore and injected fluorescent-EGF internalization in mouse xenografts models (Pinilla-Macua et al., 2017). It would be interesting to use aptamers to follow EGFR upon gefitinib treatment *in vivo*.

*My Ph.D. project proposes an open door towards the application of aptamers in in vivo molecular imaging. It establishes the basis for the use of aptamers for the detection of tumors and could open up prospects for the study of tumor growth and for the use of aptamer-conjugates in therapy. It might promote the development of targeted drug delivery systems, probably in combination with molecules favoring sub-cellular escape.*

*Vectorization tools are aimed to deliver highly toxic chemotherapeutics or therapeutic siRNA selectively to tumor cells with low toxic effects on non-tumoral cells. Vectors can be antibodies conjugated with drugs (ADC, antibody-drug conjugate) or with gold nano-particules that enhanced chemo- and radio-therapy potency (Groysbeck et al., 2019) (annex 3). Aptamers constitute another class of promising vectorization agents to deliver either drugs (aptamer-drug conjugate, AptDC) or siRNA (aptamer-siRNA chimera, AsiC) (Cerchia et al., 2011). Besides the challenge of bioconjugation of vector to therapeutic agents, another challenge is the complex internalization and intracellular trafficking. Association of these vectors with gefitinib or other TKI might be beneficial to patient by increasing vector endocytosis.*

# References

- Aaldering, L.J., Tayeb, H., Krishnan, S., Fletcher, S., Wilton, S.D., and Veedu, R.N. (2015). Smart functional nucleic acid chimeras: enabling tissue specific RNA targeting therapy. *RNA Biol.* *12*, 412–425.
- Ababneh, N., Alshaer, W., Allozi, O., Mahafzah, A., El-Khateeb, M., Hillaireau, H., Noiray, M., Fattal, E., and Ismail, S. (2013). In vitro selection of modified RNA aptamers against CD44 cancer stem cell marker. *Nucleic Acid Ther.* *23*, 401–407.
- Agarwala, S.S., and Kirkwood, J.M. (2000). Temozolomide, a novel alkylating agent with activity in the central nervous system, may improve the treatment of advanced metastatic melanoma. *The Oncologist* *5*, 144–151.
- Al-Akhrass, H., Naves, T., Vincent, F., Magnaudeix, A., Durand, K., Bertin, F., Melloni, B., Jauberteau, M.-O., and Lalloué, F. (2017). Sortilin limits EGFR signaling by promoting its internalization in lung cancer. *Nat. Commun.* *8*.
- Alanko, J., Mai, A., Jacquemet, G., Schauer, K., Kaukonen, R., Saari, M., Goud, B., and Ivaska, J. (2015). Integrin endosomal signalling suppresses anoikis. *Nat. Cell Biol.* *17*, 1412–1421.
- Alibolandi, M., Taghdisi, S.M., Ramezani, P., Hosseini Shamili, F., Farzad, S.A., Abnous, K., and Ramezani, M. (2017). Smart AS1411-aptamer conjugated pegylated PAMAM dendrimer for the superior delivery of camptothecin to colon adenocarcinoma in vitro and in vivo. *Int. J. Pharm.* *519*, 352–364.
- Allaire, P.D., Seyed Sadr, M., Chaineau, M., Seyed Sadr, E., Konefal, S., Fotouhi, M., Maret, D., Ritter, B., Del Maestro, R.F., and McPherson, P.S. (2013). Interplay between Rab35 and Arf6 controls cargo recycling to coordinate cell adhesion and migration. *J. Cell Sci.* *126*, 722–731.
- Almeida, K.H., and Sobol, R.W. (2007). A unified view of base excision repair: lesion-dependent protein complexes regulated by post-translational modification. *DNA Repair* *6*, 695–711.
- Alves, T.R., Lima, F.R.S., Kahn, S.A., Lobo, D., Dubois, L.G.F., Soletti, R., Borges, H., and Neto, V.M. (2011). Glioblastoma cells: a heterogeneous and fatal tumor interacting with the parenchyma. *Life Sci.* *89*, 532–539.
- An, Z., Aksoy, O., Zheng, T., Fan, Q.-W., and Weiss, W.A. (2018). Epidermal growth factor receptor (EGFR) and EGFRvIII in glioblastoma (GBM): signaling pathways and targeted therapies. *Oncogene* *37*, 1561–1575.
- Anderson, N.G., Ahmad, T., Chan, K., Dobson, R., and Bundred, N.J. (2001). ZD1839 (Iressa), a novel epidermal growth factor receptor (EGFR) tyrosine kinase inhibitor, potently inhibits the growth of EGFR-positive cancer cell lines with or without erbB2 overexpression. *Int. J. Cancer* *94*, 774–782.
- Aoudjit, F., and Vuori, K. (2001). Integrin signaling inhibits paclitaxel-induced apoptosis in breast cancer cells. *Oncogene* *20*, 4995–5004.
- Arjonen, A., Alanko, J., Veltel, S., and Ivaska, J. (2012). Distinct Recycling of Active and Inactive  $\beta$ 1 Integrins. *Traffic Cph. Den.* *13*, 610–625.

Arcscott, W.T., Tandle, A.T., Zhao, S., Shabason, J.E., Gordon, I.K., Schlaff, C.D., Zhang, G., Tofilon, P.J., and Camphausen, K.A. (2013). Ionizing Radiation and Glioblastoma Exosomes: Implications in Tumor Biology and Cell Migration. *Transl. Oncol.* 6, 638–648.

Arteaga, C.L., and Johnson, D.H. (2001). Tyrosine kinase inhibitors-ZD1839 (Iressa). *Curr. Opin. Oncol.* 13, 491–498.

Askari, J.A., Buckley, P.A., Mould, A.P., and Humphries, M.J. (2009). Linking integrin conformation to function. *J. Cell Sci.* 122, 165–170.

Avraamides, C.J., Garmy-Susini, B., and Varner, J.A. (2008). Integrins in angiogenesis and lymphangiogenesis. *Nat. Rev. Cancer* 8, 604–617.

Baarlink, C., Wang, H., and Grosse, R. (2013). Nuclear actin network assembly by formins regulates the SRF coactivator MAL. *Science* 340, 864–867.

Badiga, A.V., Chetty, C., Kesanakurti, D., Are, D., Gujrati, M., Klopfenstein, J.D., Dinh, D.H., and Rao, J.S. (2011). MMP-2 siRNA inhibits radiation-enhanced invasiveness in glioma cells. *PLoS One* 6, e20614.

Barazzuol, L., Jena, R., Burnet, N.G., Meira, L.B., Jeynes, J.C.G., Kirkby, K.J., and Kirkby, N.F. (2013). Evaluation of poly (ADP-ribose) polymerase inhibitor ABT-888 combined with radiotherapy and temozolomide in glioblastoma. *Radiat. Oncol. Lond. Engl.* 8, 65.

Barczyk, M., Carracedo, S., and Gullberg, D. (2010). Integrins. *Cell Tissue Res.* 339, 269–280.

Barrow-McGee, R., Kishi, N., Joffre, C., Ménard, L., Hervieu, A., Bakhouché, B.A., Noval, A.J., Mai, A., Guzmán, C., Robbez-Masson, L., et al. (2016). Beta 1-integrin–c-Met cooperation reveals an inside-in survival signalling on autophagy-related endomembranes. *Nat. Commun.* 7, 11942.

Bates, P.J., Laber, D.A., Miller, D.M., Thomas, S.D., and Trent, J.O. (2009). Discovery and development of the G-rich oligonucleotide AS1411 as a novel treatment for cancer. *Exp. Mol. Pathol.* 86, 151–164.

Bates, P.J., Reyes-Reyes, E.M., Malik, M.T., Murphy, E.M., O’Toole, M.G., and Trent, J.O. (2017). G-quadruplex oligonucleotide AS1411 as a cancer-targeting agent: Uses and mechanisms. *Biochim. Biophys. Acta Gen. Subj.* 1861, 1414–1428.

Batzer, A.G., Rotin, D., Ureña, J.M., Skolnik, E.Y., and Schlessinger, J. (1994). Hierarchy of binding sites for Grb2 and Shc on the epidermal growth factor receptor. *Mol. Cell. Biol.* 14, 5192–5201.

Behin, A., Hoang-Xuan, K., Carpentier, A.F., and Delattre, J.-Y. (2003). Primary brain tumours in adults. *The Lancet* 361, 323–331.

Bell, A.W., Ward, M.A., Blackstock, W.P., Freeman, H.N., Choudhary, J.S., Lewis, A.P., Chotai, D., Fazel, A., Gushue, J.N., Paiement, J., et al. (2001). Proteomics characterization of abundant Golgi membrane proteins. *J. Biol. Chem.* 276, 5152–5165.

Bell-McGuinn, K.M., Matthews, C.M., Ho, S.N., Barve, M., Gilbert, L., Penson, R.T., Lengyel, E., Palaparthi, R., Gilder, K., Vassos, A., et al. (2011). A phase II, single-arm study of the anti-



$\alpha 5\beta 1$  integrin antibody volociximab as monotherapy in patients with platinum-resistant advanced epithelial ovarian or primary peritoneal cancer. *Gynecol. Oncol.* *121*, 273–279.

Bello, L., Francolini, M., Marthyn, P., Zhang, J., Carroll, R.S., Nikas, D.C., Strasser, J.F., Villani, R., Cheresch, D.A., and Black, P.M. (2001). Alpha(v)beta3 and alpha(v)beta5 integrin expression in glioma periphery. *Neurosurgery* *49*, 380–389; discussion 390.

Berasain, C., and Avila, M.A. (2014). The EGFR signalling system in the liver: from hepatoprotection to hepatocarcinogenesis. *J. Gastroenterol.* *49*, 9–23.

van Bergen en Henegouwen, P.M. (2009). Eps15: a multifunctional adaptor protein regulating intracellular trafficking. *Cell Commun. Signal. CCS* *7*, 24.

Besse, B., Tsao, L.C., Chao, D.T., Fang, Y., Soria, J.-C., Almokadem, S., and Belani, C.P. (2013). Phase Ib safety and pharmacokinetic study of volociximab, an anti- $\alpha 5\beta 1$  integrin antibody, in combination with carboplatin and paclitaxel in advanced non-small-cell lung cancer. *Ann. Oncol. Off. J. Eur. Soc. Med. Oncol.* *24*, 90–96.

Bhalla, N., Jolly, P., Formisano, N., and Estrela, P. (2016). Introduction to biosensors. *Essays Biochem.* *60*, 1.

Bhat, K.P.L., Balasubramaniyan, V., Vaillant, B., Ezhilarasan, R., Hummelink, K., Hollingsworth, F., Wani, K., Heathcock, L., James, J.D., Goodman, L.D., et al. (2013). Mesenchymal differentiation mediated by NF- $\kappa$ B promotes radiation resistance in glioblastoma. *Cancer Cell* *24*, 331–346.

Birgisdottir, Á.B., and Johansen, T. (2020). Autophagy and endocytosis – interconnections and interdependencies. *J. Cell Sci.* *133*.

Blakeley, J.O., Grossman, S.A., Mikkelsen, T., Rosenfeld, M.R., Peereboom, D., Nabors, L.B., Chi, A.S., Emmons, G., Ribas, I.G., Supko, J.G., et al. (2015). Phase I study of iniparib concurrent with monthly or continuous temozolomide dosing schedules in patients with newly diagnosed malignant gliomas. *J. Neurooncol.* *125*, 123–131.

Blandin, A.-F., Renner, G., Lehmann, M., Lelong-Rebel, I., Martin, S., and Dontenwill, M. (2015).  $\beta 1$  Integrins as Therapeutic Targets to Disrupt Hallmarks of Cancer. *Front. Pharmacol.* *6*.

Blandin, A.-F., Noulet, F., Renner, G., Mercier, M.-C., Choulier, L., Vauchelles, R., Ronde, P., Carreiras, F., Etienne-Selloum, N., Vereb, G., et al. (2016). Glioma cell dispersion is driven by  $\alpha 5$  integrin-mediated cell–matrix and cell–cell interactions. *Cancer Lett.* *376*, 328–338.

Blank, M., Weinschenk, T., Priemer, M., and Schluesener, H. (2001). Systematic evolution of a DNA aptamer binding to rat brain tumor microvessels. selective targeting of endothelial regulatory protein pigen. *J. Biol. Chem.* *276*, 16464–16468.

Bonavia, R., Inda, M.-M., Cavenee, W.K., and Furnari, F.B. (2011). Heterogeneity maintenance in glioblastoma: a social network. *Cancer Res.* *71*, 4055–4060.

Bonavia, R., Inda, M.M., Vandenberg, S., Cheng, S.-Y., Nagane, M., Hadwiger, P., Tan, P., Sah, D.W.Y., Cavenee, W.K., and Furnari, F.B. (2012). EGFRvIII promotes glioma angiogenesis and growth through the NF- $\kappa$ B, interleukin-8 pathway. *Oncogene* *31*, 4054–4066.

- Bondy, M.L., Scheurer, M.E., Malmer, B., Barnholtz-Sloan, J.S., Davis, F.G., Il'yasova, D., Kruchko, C., McCarthy, B.J., Rajaraman, P., Schwartzbaum, J.A., et al. (2008). Brain Tumor Epidemiology: Consensus from the Brain Tumor Epidemiology Consortium (BTEC). *Cancer* *113*, 1953–1968.
- Breuers, S., Bryant, L.L., Legen, T., and Mayer, G. (2019). Robotic assisted generation of 2'-deoxy-2'-fluoro-modified RNA aptamers – High performance enabling strategies in aptamer selection. *Methods* *161*, 3–9.
- Brooks, P.C., Montgomery, A.M., Rosenfeld, M., Reisfeld, R.A., Hu, T., Klier, G., and Cheresch, D.A. (1994). Integrin alpha v beta 3 antagonists promote tumor regression by inducing apoptosis of angiogenic blood vessels. *Cell* *79*, 1157–1164.
- Bruno, J.G., Phillips, T., Carrillo, M.P., and Crowell, R. (2009). Plastic-adherent DNA aptamer-magnetic bead and quantum dot sandwich assay for *Campylobacter* detection. *J. Fluoresc.* *19*, 427–435.
- Bruno, J.G., Carrillo, M.P., Phillips, T., and Andrews, C.J. (2010). A novel screening method for competitive FRET-aptamers applied to *E. coli* assay development. *J. Fluoresc.* *20*, 1211–1223.
- Bukari, B.A., Citartan, M., Ch'ng, E.S., Bilibana, M.P., Rozhdestvensky, T., and Tang, T.-H. (2017). Aptahistochemistry in diagnostic pathology: technical scrutiny and feasibility. *Histochem. Cell Biol.* *147*, 545–553.
- Burke, D.H., Hoffman, D.C., Brown, A., Hansen, M., Pardi, A., and Gold, L. (1997). RNA aptamers to the peptidyl transferase inhibitor chloramphenicol. *Chem. Biol.* *4*, 833–843.
- Buruiană, A., Florian, Ștefan I., Florian, A.I., Timiș, T.-L., Mișu, C.M., Miclăuș, M., Oșan, S., Hrapșa, I., Cataniciu, R.C., Farcaș, M., et al. (2020). The Roles of miRNA in Glioblastoma Tumor Cell Communication: Diplomatic and Aggressive Negotiations. *Int. J. Mol. Sci.* *21*.
- Calderwood, D.A., Fujioka, Y., de Pereda, J.M., García-Alvarez, B., Nakamoto, T., Margolis, B., McGlade, C.J., Liddington, R.C., and Ginsberg, M.H. (2003). Integrin beta cytoplasmic domain interactions with phosphotyrosine-binding domains: a structural prototype for diversity in integrin signaling. *Proc. Natl. Acad. Sci. U. S. A.* *100*, 2272–2277.
- Caldieri, G., Malabarba, M.G., Di Fiore, P.P., and Sigismund, S. (2018). EGFR Trafficking in Physiology and Cancer. *Prog. Mol. Subcell. Biol.* *57*, 235–272.
- Camorani, S., Crescenzi, E., Colecchia, D., Carpentieri, A., Amoresano, A., Fedele, M., Chiariello, M., and Cerchia, L. (2015). Aptamer targeting EGFRvIII mutant hampers its constitutive autophosphorylation and affects migration, invasion and proliferation of glioblastoma cells. *Oncotarget* *6*, 37570–37587.
- Camorani, S., Hill, B.S., Collina, F., Gargiulo, S., Napolitano, M., Cantile, M., Di Bonito, M., Botti, G., Fedele, M., Zannetti, A., et al. (2018). Targeted imaging and inhibition of triple-negative breast cancer metastases by a PDGFR $\beta$  aptamer. *Theranostics* *8*, 5178–5199.

- Camorani, S., Granata, I., Collina, F., Leonetti, F., Cantile, M., Botti, G., Fedele, M., Guarracino, M.R., and Cerchia, L. (2020). Novel Aptamers Selected on Living Cells for Specific Recognition of Triple-Negative Breast Cancer. *IScience* 23.
- Campbell, I.D., and Humphries, M.J. (2011). Integrin Structure, Activation, and Interactions. *Cold Spring Harb. Perspect. Biol.* 3.
- Campbell, R.M., Anderson, B.D., Brooks, N.A., Brooks, H.B., Chan, E.M., De Dios, A., Gilmour, R., Graff, J.R., Jambrina, E., Mader, M., et al. (2014). Characterization of LY2228820 dimesylate, a potent and selective inhibitor of p38 MAPK with antitumor activity. *Mol. Cancer Ther.* 13, 364–374.
- Cao, X., Zhu, H., Ali-Osman, F., and Lo, H.-W. (2011). EGFR and EGFRvIII undergo stress- and EGFR kinase inhibitor-induced mitochondrial translocation: A potential mechanism of EGFR-driven antagonism of apoptosis. *Mol. Cancer* 10, 26.
- Carpenter, C.L., Duckworth, B.C., Auger, K.R., Cohen, B., Schaffhausen, B.S., and Cantley, L.C. (1990). Purification and characterization of phosphoinositide 3-kinase from rat liver. *J. Biol. Chem.* 265, 19704–19711.
- Caswell, P.T., Spence, H.J., Parsons, M., White, D.P., Clark, K., Cheng, K.W., Mills, G.B., Humphries, M.J., Messent, A.J., Anderson, K.I., et al. (2007). Rab25 associates with alpha5beta1 integrin to promote invasive migration in 3D microenvironments. *Dev. Cell* 13, 496–510.
- Caswell, P.T., Chan, M., Lindsay, A.J., McCaffrey, M.W., Boettiger, D., and Norman, J.C. (2008). Rab-coupling protein coordinates recycling of alpha5beta1 integrin and EGFR1 to promote cell migration in 3D microenvironments. *J. Cell Biol.* 183, 143–155.
- Cavalli, V., Vilbois, F., Corti, M., Marcote, M.J., Tamura, K., Karin, M., Arkinstall, S., and Gruenberg, J. (2001). The stress-induced MAP kinase p38 regulates endocytic trafficking via the GDI:Rab5 complex. *Mol. Cell* 7, 421–432.
- Ceccarelli, M., Barthel, F.P., Malta, T.M., Sabedot, T.S., Salama, S.R., Murray, B.A., Morozova, O., Newton, Y., Radenbaugh, A., Pagnotta, S.M., et al. (2016). Molecular Profiling Reveals Biologically Discrete Subsets and Pathways of Progression in Diffuse Glioma. *Cell* 164, 550–563.
- Cerchia, L. (2018). Aptamers: Promising Tools for Cancer Diagnosis and Therapy. *Cancers* 10.
- Cerchia, L., and de Franciscis, V. (2010). Targeting cancer cells with nucleic acid aptamers. *Trends Biotechnol.* 28, 517–525.
- Cerchia, L., Esposito, C.L., Camorani, S., Catuogno, S., and de Franciscis, V. (2011). Coupling Aptamers to Short Interfering RNAs as Therapeutics. *Pharmaceuticals* 4, 1434–1449.
- Ceresa, B.P., and Bahr, S.J. (2006). rab7 activity affects epidermal growth factor:epidermal growth factor receptor degradation by regulating endocytic trafficking from the late endosome. *J. Biol. Chem.* 281, 1099–1106.
- Cersosimo, R.J. (2004). Gefitinib: a new antineoplastic for advanced non-small-cell lung cancer. *Am. J. Health-Syst. Pharm. AJHP Off. J. Am. Soc. Health-Syst. Pharm.* 61, 889–898.

- Cha, J., Kang, S.-G., and Kim, P. (2016). Strategies of Mesenchymal Invasion of Patient-derived Brain Tumors: Microenvironmental Adaptation. *Sci. Rep.* *6*, 24912.
- Chagoya, G., Kwatra, S.G., Nanni, C.W., Roberts, C.M., Phillips, S.M., Nullmeyergh, S., Gilmore, S.P., Spasojevic, I., Corcoran, D.L., Young, C.C., et al. (2020). Efficacy of osimertinib against EGFRvIII+ glioblastoma. *Oncotarget* *11*, 2074–2082.
- Chakravarti, A., Noll, E., Black, P.M., Finkelstein, D.F., Finkelstein, D.M., Dyson, N.J., and Loeffler, J.S. (2002). Quantitatively Determined Survivin Expression Levels Are of Prognostic Value in Human Gliomas. *J. Clin. Oncol.* *20*, 1063–1068.
- Chang, C.-Y., Kuan, Y.-H., Ou, Y.-C., Li, J.-R., Wu, C.-C., Pan, P.-H., Chen, W.-Y., Huang, H.-Y., and Chen, C.-J. (2014). Autophagy contributes to gefitinib-induced glioma cell growth inhibition. *Exp. Cell Res.* *327*, 102–112.
- Chang, Y.S., Choi, C.-M., and Lee, J.C. (2016). Mechanisms of Epidermal Growth Factor Receptor Tyrosine Kinase Inhibitor Resistance and Strategies to Overcome Resistance in Lung Adenocarcinoma. *Tuberc. Respir. Dis.* *79*, 248–256.
- Chauveau, F., Aissouni, Y., Hamm, J., Boutin, H., Libri, D., Ducongé, F., and Tavitian, B. (2007). Binding of an aptamer to the N-terminal fragment of VCAM-1. *Bioorg. Med. Chem. Lett.* *17*, 6119–6122.
- Chen, Z., and Xu, X. (2016). Roles of nucleolin. *Saudi Med. J.* *37*, 1312–1318.
- Chen, C.B., Dellamaggiore, K.R., Ouellette, C.P., Sedano, C.D., Lizadjohry, M., Chernis, G.A., Gonzales, M., Baltasar, F.E., Fan, A.L., Myerowitz, R., et al. (2008). Aptamer-based endocytosis of a lysosomal enzyme. *Proc. Natl. Acad. Sci. U. S. A.* *105*, 15908–15913.
- Chen, F., Zhou, J., Luo, F., Mohammed, A.-B., and Zhang, X.-L. (2007). Aptamer from whole-bacterium SELEX as new therapeutic reagent against virulent *Mycobacterium tuberculosis*. *Biochem. Biophys. Res. Commun.* *357*, 743–748.
- Chen, H., Lin, Z., Arnst, K.E., Miller, D.D., and Li, W. (2017). Tubulin Inhibitor-Based Antibody-Drug Conjugates for Cancer Therapy. *Mol. J. Synth. Chem. Nat. Prod. Chem.* *22*.
- Chen, L., He, W., Jiang, H., Wu, L., Xiong, W., Li, B., Zhou, Z., and Qian, Y. (2019). In vivo SELEX of bone targeting aptamer in prostate cancer bone metastasis model. *Int. J. Nanomedicine* *14*, 149–159.
- Chen, M., Yu, Y., Jiang, F., Zhou, J., Li, Y., Liang, C., Dang, L., Lu, A., and Zhang, G. (2016a). Development of Cell-SELEX Technology and Its Application in Cancer Diagnosis and Therapy. *Int. J. Mol. Sci.* *17*.
- Chen, W., Xia, T., Wang, D., Huang, B., Zhao, P., Wang, J., Qu, X., and Li, X. (2016b). Human astrocytes secrete IL-6 to promote glioma migration and invasion through upregulation of cytomembrane MMP14. *Oncotarget* *7*, 62425–62438.
- Cheng, F., and Guo, D. (2019). MET in glioma: signaling pathways and targeted therapies. *J. Exp. Clin. Cancer Res.* *38*, 270.

- Cheng, C., Chen, Y.H., Lennox, K.A., Behlke, M.A., and Davidson, B.L. (2013). In vivo SELEX for Identification of Brain-penetrating Aptamers. *Mol. Ther. Nucleic Acids* 2, e67.
- Chew, H.Y., De Lima, P.O., Gonzalez Cruz, J.L., Banushi, B., Echejoh, G., Hu, L., Joseph, S.R., Lum, B., Rae, J., O'Donnell, J.S., et al. (2020). Endocytosis Inhibition in Humans to Improve Responses to ADCC-Mediating Antibodies. *Cell* 180, 895-914.e27.
- Chi, S., Cao, H., Wang, Y., and McNiven, M.A. (2011). Recycling of the Epidermal Growth Factor Receptor Is Mediated by a Novel Form of the Clathrin Adaptor Protein Eps15. *J. Biol. Chem.* 286, 35196–35208.
- Cho, Y., Lee, Y.B., Lee, J.-H., Lee, D.H., Cho, E.J., Yu, S.J., Kim, Y.J., Kim, J.I., Im, J.H., Lee, J.H., et al. (2016). Modified AS1411 Aptamer Suppresses Hepatocellular Carcinoma by Up-Regulating Galectin-14. *PloS One* 11, e0160822.
- Christoforides, C., Rainero, E., Brown, K.K., Norman, J.C., and Toker, A. (2012). PKD Controls  $\alpha\beta 3$  Integrin Recycling and Tumor Cell Invasive Migration through Its Substrate Rabaptin-5. *Dev. Cell* 23, 560–572.
- Cianfrocca, M.E., Kimmel, K.A., Gallo, J., Cardoso, T., Brown, M.M., Hudes, G., Lewis, N., Weiner, L., Lam, G.N., Brown, S.C., et al. (2006). Phase 1 trial of the antiangiogenic peptide ATN-161 (Ac-PHSCN-NH(2)), a beta integrin antagonist, in patients with solid tumours. *Br. J. Cancer* 94, 1621–1626.
- Clare, C.E., Brassington, A.H., Kwong, W.Y., and Sinclair, K.D. (2019). One-Carbon Metabolism: Linking Nutritional Biochemistry to Epigenetic Programming of Long-Term Development. *Annu. Rev. Anim. Biosci.* 7, 263–287.
- Clark, P.A., Iida, M., Treisman, D.M., Kalluri, H., Ezhilan, S., Zorniak, M., Wheeler, D.L., and Kuo, J.S. (2012). Activation of multiple ERBB family receptors mediates glioblastoma cancer stem-like cell resistance to EGFR-targeted inhibition. *Neoplasia* N. Y. N 14, 420–428.
- Cohen, A., Holmen, S., and Colman, H. (2013). IDH1 and IDH2 Mutations in Gliomas. *Curr. Neurol. Neurosci. Rep.* 13, 345.
- Cohen, A.S., Geng, L., Zhao, P., Fu, A., Schulte, M.L., Graves-Deal, R., Washington, M.K., Berlin, J., Coffey, R.J., and Manning, H.C. (2020). Combined blockade of EGFR and glutamine metabolism in preclinical models of colorectal cancer. *Transl. Oncol.* 13.
- Cohen, S., Carpenter, G., and King, L. (1980). Epidermal growth factor-receptor-protein kinase interactions. Co-purification of receptor and epidermal growth factor-enhanced phosphorylation activity. *J. Biol. Chem.* 255, 4834–4842.
- Combs, S.E., Schulz-Ertner, D., Hartmann, C., Welzel, T., Timke, C., Herfarth, K., von Deimling, A., Edler, L., Platten, M., Wick, W., et al. (2008). Phase I/II study of cetuximab plus temozolomide as radiochemotherapy for primary glioblastoma (GERT)—Eudract number 2005–003911–63; NCT00311857. *J. Clin. Oncol.* 26, 2077–2077.
- Cormier, A., Campbell, M.G., Ito, S., Wu, S., Lou, J., Marks, J., Baron, J., Nishimura, S.L., and Cheng, Y. (2018). Cryo-EM structure of the  $\alpha\beta 8$  integrin reveals a mechanism for stabilizing integrin extension. *Nat. Struct. Mol. Biol.* 25, 698–704.

- Cosset, É., Ilmjärv, S., Dutoit, V., Elliott, K., von Schalscha, T., Camargo, M.F., Reiss, A., Moroishi, T., Seguin, L., Gomez, G., et al. (2017). Glut3 Addiction Is a Druggable Vulnerability for a Molecularly Defined Subpopulation of Glioblastoma. *Cancer Cell* *32*, 856-868.e5.
- Cox, T.R., Bird, D., Baker, A.-M., Barker, H.E., Ho, M.W.-Y., Lang, G., and Erler, J.T. (2013). LOX-mediated collagen crosslinking is responsible for fibrosis-enhanced metastasis. *Cancer Res.* *73*, 1721–1732.
- Cruz da Silva, E., Dontenwill, M., Choulier, L., and Lehmann, M. (2019). Role of Integrins in Resistance to Therapies Targeting Growth Factor Receptors in Cancer. *Cancers* *11*, 692.
- Cui, G., Cui, M., Li, Y., Liang, Y., Li, W., Guo, H., and Zhao, S. (2015). Galectin-3 knockdown increases gefitinib sensitivity to the inhibition of EGFR endocytosis in gefitinib-insensitive esophageal squamous cancer cells. *Med. Oncol. Northwood Lond. Engl.* *32*, 124.
- Dang, L., White, D.W., Gross, S., Bennett, B.D., Bittinger, M.A., Driggers, E.M., Fantin, V.R., Jang, H.G., Jin, S., Keenan, M.C., et al. (2009). Cancer-associated IDH1 mutations produce 2-hydroxyglutarate. *Nature* *462*, 739.
- Day, E.K., Sosale, N.G., Xiao, A., Zhong, Q., Purow, B., and Lazzara, M.J. (2020). Glioblastoma Cell Resistance to EGFR and MET Inhibition Can Be Overcome via Blockade of FGFR-SPRY2 Bypass Signaling. *Cell Rep.* *30*, 3383-3396.e7.
- De Franceschi, N., Arjonen, A., Elkhatib, N., Denessiouk, K., Wrobel, A.G., Wilson, T.A., Pouwels, J., Montagnac, G., Owen, D.J., and Ivaska, J. (2016). Selective integrin endocytosis is driven by interactions between the integrin  $\alpha$ -chain and AP2. *Nat. Struct. Mol. Biol.* *23*, 172–179.
- DeAngelis, L.M. (2001). Brain Tumors. *N. Engl. J. Med.* *344*, 114–123.
- Delač, M., Motaln, H., Ulrich, H., and Lah, T.T. (2015). Aptamer for imaging and therapeutic targeting of brain tumor glioblastoma. *Cytom. Part J. Int. Soc. Anal. Cytol.* *87*, 806–816.
- DeLay, M., Jahangiri, A., Carbonell, W.S., Hu, Y.-L., Tsao, S., Tom, M.W., Paquette, J., Tokuyasu, T.A., and Aghi, M.K. (2012). Microarray analysis verifies two distinct phenotypes of glioblastomas resistant to antiangiogenic therapy. *Clin. Cancer Res. Off. J. Am. Assoc. Cancer Res.* *18*, 2930–2942.
- Deluche, E., Bessette, B., Durand, S., Caire, F., Rigau, V., Robert, S., Chaunavel, A., Forestier, L., Labrousse, F., Jauberteau, M.-O., et al. (2019). CHI3L1, NTRK2, 1p/19q and IDH Status Predicts Prognosis in Glioma. *Cancers* *11*.
- Deng, Q.-F., Su, B.O., Zhao, Y.-M., Tang, L., Zhang, J., and Zhou, C.-C. (2016). Integrin  $\beta$ 1-mediated acquired gefitinib resistance in non-small cell lung cancer cells occurs via the phosphoinositide 3-kinase-dependent pathway. *Oncol. Lett.* *11*, 535–542.
- Deryugina, E.I., and Quigley, J.P. (2012). Cell Surface Remodeling by Plasmin: A New Function for an Old Enzyme. *J. Biomed. Biotechnol.* *2012*.
- Desgrosellier, J.S., and Chersesh, D.A. (2010). Integrins in cancer: biological implications and therapeutic opportunities. *Nat. Rev. Cancer* *10*, 9–22.

- Dhiman, A., Kalra, P., Bansal, V., Bruno, J.G., and Sharma, T.K. (2017). Aptamer-based point-of-care diagnostic platforms. *Sens. Actuators B Chem.* *246*, 535–553.
- Diggins, N.L., Kang, H., Weaver, A., and Webb, D.J. (2018).  $\alpha 5\beta 1$  integrin trafficking and Rac activation are regulated by APPL1 in a Rab5-dependent manner to inhibit cell migration. *J. Cell Sci.* *131*.
- Dinneen, J.L., and Ceresa, B.P. (2004). Continual expression of Rab5(Q79L) causes a ligand-independent EGFR internalization and diminishes EGFR activity. *Traffic Cph. Den.* *5*, 606–615.
- Dippold, H.C., Ng, M.M., Farber-Katz, S.E., Lee, S.-K., Kerr, M.L., Peterman, M.C., Sim, R., Wiharto, P.A., Galbraith, K.A., Madhavarapu, S., et al. (2009). GOLPH3 Bridges Phosphatidylinositol-4- Phosphate and Actomyosin to Stretch and Shape the Golgi to Promote Budding. *Cell* *139*, 337–351.
- Dittmann, K., Mayer, C., Fehrenbacher, B., Schaller, M., Raju, U., Milas, L., Chen, D.J., Kehlbach, R., and Rodemann, H.P. (2005). Radiation-induced Epidermal Growth Factor Receptor Nuclear Import Is Linked to Activation of DNA-dependent Protein Kinase. *J. Biol. Chem.* *280*, 31182–31189.
- Dong, J., Opresko, L.K., Chrisler, W., Orr, G., Quesenberry, R.D., Lauffenburger, D.A., and Wiley, H.S. (2005). The Membrane-anchoring Domain of Epidermal Growth Factor Receptor Ligands Dictates Their Ability to Operate in Juxtacrine Mode. *Mol. Biol. Cell* *16*, 2984–2998.
- Doronina, S.O., Mendelsohn, B.A., Bovee, T.D., Cervený, C.G., Alley, S.C., Meyer, D.L., Oflazoglu, E., Toki, B.E., Sanderson, R.J., Zabinski, R.F., et al. (2006). Enhanced activity of monomethylauristatin F through monoclonal antibody delivery: effects of linker technology on efficacy and toxicity. *Bioconjug. Chem.* *17*, 114–124.
- Dou, X.-Q., Wang, H., Zhang, J., Wang, F., Xu, G.-L., Xu, C.-C., Xu, H.-H., Xiang, S.-S., Fu, J., and Song, H.-F. (2018). Aptamer-drug conjugate: targeted delivery of doxorubicin in a HER3 aptamer-functionalized liposomal delivery system reduces cardiotoxicity. *Int. J. Nanomedicine* *13*, 763–776.
- Dowdy, S.F. (2017). Overcoming cellular barriers for RNA therapeutics. *Nat. Biotechnol.* *35*, 222–229.
- Dozynkiewicz, M.A., Jamieson, N.B., Macpherson, I., Grindlay, J., van den Berghe, P.V.E., von Thun, A., Morton, J.P., Gourley, C., Timpson, P., Nixon, C., et al. (2012). Rab25 and CLIC3 collaborate to promote integrin recycling from late endosomes/lysosomes and drive cancer progression. *Dev. Cell* *22*, 131–145.
- Drolet, D.W., Green, L.S., Gold, L., and Janjic, N. (2016). Fit for the Eye: Aptamers in Ocular Disorders. *Nucleic Acid Ther.* *26*, 127–146.
- Du, X.-J., Li, X.-M., Cai, L.-B., Sun, J.-C., Wang, S.-Y., Wang, X.-C., Pang, X.-L., Deng, M.-L., Chen, F.-F., Wang, Z.-Q., et al. (2019). Efficacy and safety of nimotuzumab in addition to radiotherapy and temozolomide for cerebral glioblastoma: a phase II multicenter clinical trial. *J. Cancer* *10*, 3214–3223.

- Dudvarski Stanković, N., Bicker, F., Keller, S., Jones, D.T., Harter, P.N., Kienzle, A., Gillmann, C., Arnold, P., Golebiewska, A., Keunen, O., et al. (2018). EGFL7 enhances surface expression of integrin  $\alpha 5\beta 1$  to promote angiogenesis in malignant brain tumors. *EMBO Mol. Med.* *10*.
- Duleh, S.N., and Welch, M.D. (2010). WASH and the Arp2/3 complex regulate endosome shape and trafficking. *Cytoskelet. Hoboken NJ* *67*, 193–206.
- Dunty, J.M., Gabarra-Niecko, V., King, M.L., Ceccarelli, D.F.J., Eck, M.J., and Schaller, M.D. (2004). FERM Domain Interaction Promotes FAK Signaling. *Mol. Cell. Biol.* *24*, 5353–5368.
- Durrant, T.N., van den Bosch, M.T., and Hers, I. (2017). Integrin  $\alpha IIb\beta 3$  outside-in signaling. *Blood* *130*, 1607–1619.
- Eke, I., Storch, K., Krause, M., and Cordes, N. (2013). Cetuximab attenuates its cytotoxic and radiosensitizing potential by inducing fibronectin biosynthesis. *Cancer Res.* *73*, 5869–5879.
- Eke, I., Zscheppang, K., Dickreuter, E., Hickmann, L., Mazzeo, E., Unger, K., Krause, M., and Cordes, N. (2015). Simultaneous  $\beta 1$  integrin-EGFR targeting and radiosensitization of human head and neck cancer. *J. Natl. Cancer Inst.* *107*.
- Eller, J.L., Longo, S.L., Kyle, M.M., Bassano, D., Hicklin, D.J., and Canute, G.W. (2005). Anti-epidermal growth factor receptor monoclonal antibody cetuximab augments radiation effects in glioblastoma multiforme in vitro and in vivo. *Neurosurgery* *56*, 155–162; discussion 162.
- Ellington, A.D., and Szostak, J.W. (1990). In vitro selection of RNA molecules that bind specific ligands. *Nature* *346*, 818–822.
- El-Sayed, A., and Harashima, H. (2013). Endocytosis of gene delivery vectors: from clathrin-dependent to lipid raft-mediated endocytosis. *Mol. Ther. J. Am. Soc. Gene Ther.* *21*, 1118–1130.
- Eskilsson, E., Røsland, G.V., Solecki, G., Wang, Q., Harter, P.N., Graziani, G., Verhaak, R.G.W., Winkler, F., Bjerkvig, R., and Miletic, H. (2018). EGFR heterogeneity and implications for therapeutic intervention in glioblastoma. *Neuro-Oncol.* *20*, 743–752.
- Esnault, C., Stewart, A., Gualdrini, F., East, P., Horswell, S., Matthews, N., and Treisman, R. (2014). Rho-actin signaling to the MRTF coactivators dominates the immediate transcriptional response to serum in fibroblasts. *Genes Dev.* *28*, 943–958.
- Eulberg, D., Buchner, K., Maasch, C., and Klussmann, S. (2005). Development of an automated in vitro selection protocol to obtain RNA-based aptamers: identification of a biostable substance P antagonist. *Nucleic Acids Res.* *33*, e45.
- Ezratty, E.J., Partridge, M.A., and Gundersen, G.G. (2005). Microtubule-induced focal adhesion disassembly is mediated by dynamin and focal adhesion kinase. *Nat. Cell Biol.* *7*, 581–590.
- Fan, Q., Aksoy, O., Wong, R.A., Ilkhanizadeh, S., Novotny, C.J., Gustafson, W.C., Truong, A.Y.-Q., Cayanan, G., Simonds, E.F., Haas-Kogan, D., et al. (2017). A Kinase Inhibitor Targeted to mTORC1 Drives Regression in Glioblastoma. *Cancer Cell* *31*, 424–435.



Fan, Q.-W., Cheng, C.K., Gustafson, W.C., Charron, E., Zipper, P., Wong, R.A., Chen, J., Lau, J., Knobbe-Thomsen, C., Weller, M., et al. (2013). EGFR phosphorylates tumor-derived EGFRvIII driving STAT3/5 and progression in glioblastoma. *Cancer Cell* 24, 438–449.

Fang, X., and Tan, W. (2010). Aptamers generated from cell-SELEX for molecular medicine: a chemical biology approach. *Acc. Chem. Res.* 43, 48–57.

Färber, K., Synowitz, M., Zahn, G., Vossmeier, D., Stragies, R., van Rooijen, N., and Kettenmann, H. (2008). An alpha5beta1 integrin inhibitor attenuates glioma growth. *Mol. Cell. Neurosci.* 39, 579–585.

Fechter, P., Silva, E.C.D., Mercier, M.-C., Noulet, F., Etienne-Seloum, N., Guenot, D., Lehmann, M., Vauchelles, R., Martin, S., Lelong-Rebel, I., et al. (2019). RNA Aptamers Targeting Integrin  $\alpha 5 \beta 1$  as Probes for Cyto- and Histofluorescence in Glioblastoma. *Mol. Ther. - Nucleic Acids* 17, 63–77.

Ferguson, S.M., and De Camilli, P. (2012). Dynamin, a membrane remodelling GTPase. *Nat. Rev. Mol. Cell Biol.* 13, 75–88.

Fernández, G., Moraga, A., Cuartero, M.I., García-Culebras, A., Peña-Martínez, C., Pradillo, J.M., Hernández-Jiménez, M., Sacristán, S., Ayuso, M.I., Gonzalo-Gobernado, R., et al. (2018). TLR4-Binding DNA Aptamers Show a Protective Effect against Acute Stroke in Animal Models. *Mol. Ther. J. Am. Soc. Gene Ther.* 26, 2047–2059.

Ferraro, N., Barbarite, E., Albert, T.R., Berchmans, E., Shah, A.H., Bregy, A., Ivan, M.E., Brown, T., and Komotar, R.J. (2016). The role of 5-aminolevulinic acid in brain tumor surgery: a systematic review. *Neurosurg. Rev.* 39, 545–555.

Frankel, E.B., and Audhya, A. (2018). ESCRT-dependent cargo sorting at multivesicular endosomes. *Semin. Cell Dev. Biol.* 74, 4–10.

Frederick, L., Wang, X.Y., Eley, G., and James, C.D. (2000). Diversity and frequency of epidermal growth factor receptor mutations in human glioblastomas. *Cancer Res.* 60, 1383–1387.

Friedlander, M., Brooks, P.C., Shaffer, R.W., Kincaid, C.M., Varner, J.A., and Cheresch, D.A. (1995). Definition of two angiogenic pathways by distinct alpha v integrins. *Science* 270, 1500–1502.

Friess, H., Langrehr, J.M., Oettle, H., Raedle, J., Niedergethmann, M., Dittrich, C., Hossfeld, D.K., Stöger, H., Neyns, B., Herzog, P., et al. (2006). A randomized multi-center phase II trial of the angiogenesis inhibitor Cilengitide (EMD 121974) and gemcitabine compared with gemcitabine alone in advanced unresectable pancreatic cancer. *BMC Cancer* 6, 285.

Ganson, N.J., Povsic, T.J., Sullenger, B.A., Alexander, J.H., Zelenkofske, S.L., Sailstad, J.M., Rusconi, C.P., and Hershfield, M.S. (2016). Pre-existing anti-polyethylene glycol antibody linked to first-exposure allergic reactions to pegnivacogin, a PEGylated RNA aptamer. *J. Allergy Clin. Immunol.* 137, 1610-1613.e7.

Gao, A.E., Sullivan, K.E., and Black, L.D. (2016). Lysyl oxidase expression in cardiac fibroblasts is regulated by  $\alpha 2\beta 1$  integrin interactions with the cellular microenvironment. *Biochem. Biophys. Res. Commun.* 475, 70–75.

Gao, X., Sanderson, S.M., Dai, Z., Reid, M.A., Cooper, D.E., Lu, M., Richie, J.P., Ciccarella, A., Calcagnotto, A., Mikhael, P.G., et al. (2019). Dietary methionine influences therapy in mouse cancer models and alters human metabolism. *Nature* 572, 397–401.

Garrido, G., Tikhomirov, I.A., Rabasa, A., Yang, E., Gracia, E., Iznaga, N., Fernández, L.E., Crombet, T., Kerbel, R.S., and Pérez, R. (2011). Bivalent binding by intermediate affinity of nimotuzumab: a contribution to explain antibody clinical profile. *Cancer Biol. Ther.* 11, 373–382.

Giese, A., and Westphal, M. (1996). Glioma invasion in the central nervous system. *Neurosurgery* 39, 235–250; discussion 250-252.

Gingras, M.C., Roussel, E., Bruner, J.M., Branch, C.D., and Moser, R.P. (1995). Comparison of cell adhesion molecule expression between glioblastoma multiforme and autologous normal brain tissue. *J. Neuroimmunol.* 57, 143–153.

Gladson, C.L. (1996). Expression of Integrin  $\alpha v\beta 3$  in Small Blood Vessels of Glioblastoma Tumors. *J. Neuropathol. Exp. Neurol.* 55, 1143–1149.

Glushonkov, O., Réal, E., Boutant, E., Mély, Y., and Didier, P. (2018). Optimized protocol for combined PALM-dSTORM imaging. *Sci. Rep.* 8, 8749.

Goetz, J.G., Minguet, S., Navarro-Lérida, I., Lazcano, J.J., Samaniego, R., Calvo, E., Tello, M., Osteso-Ibáñez, T., Pellinen, T., Echarri, A., et al. (2011). Biomechanical Remodeling of the Microenvironment by Stromal Caveolin-1 Favors Tumor Invasion and Metastasis. *Cell* 146, 148–163.

Gomez Zubieta, D.M., Hamood, M.A., Beydoun, R., Pall, A.E., and Kondapalli, K.C. (2017). MicroRNA-135a regulates NHE9 to inhibit proliferation and migration of glioblastoma cells. *Cell Commun. Signal. CCS* 15, 55.

Goodwin, C.R., Rath, P., Oyinlade, O., Lopez, H., Mughal, S., Xia, S., Li, Y., Kaur, H., Zhou, X., Ahmed, A.K., et al. (2018). Crizotinib and erlotinib inhibits growth of c-Met<sup>+</sup>/EGFR<sup>vIII</sup><sup>+</sup> primary human glioblastoma xenografts. *Clin. Neurol. Neurosurg.* 171, 26–33.

Graff, J.R., McNulty, A.M., Hanna, K.R., Konicek, B.W., Lynch, R.L., Bailey, S.N., Banks, C., Capen, A., Goode, R., Lewis, J.E., et al. (2005). The protein kinase C $\beta$ -selective inhibitor, Enzastaurin (LY317615.HCl), suppresses signaling through the AKT pathway, induces apoptosis, and suppresses growth of human colon cancer and glioblastoma xenografts. *Cancer Res.* 65, 7462–7469.

Grandal, M.V., Zandi, R., Pedersen, M.W., Willumsen, B.M., van Deurs, B., and Poulsen, H.S. (2007). EGFR<sup>vIII</sup> escapes down-regulation due to impaired internalization and sorting to lysosomes. *Carcinogenesis* 28, 1408–1417.

Grasset, E.M., Bertero, T., Bozec, A., Friard, J., Bourget, I., Pisano, S., Lecacheur, M., Maiel, M., Bailleux, C., Emelyanov, A., et al. (2018). Matrix Stiffening and EGFR Cooperate to Promote the Collective Invasion of Cancer Cells. *Cancer Res.* *78*, 5229–5242.

Griffero, F., Daga, A., Marubbi, D., Capra, M.C., Melotti, A., Pattarozzi, A., Gatti, M., Bajetto, A., Porcile, C., Barbieri, F., et al. (2009). Different response of human glioma tumor-initiating cells to epidermal growth factor receptor kinase inhibitors. *J. Biol. Chem.* *284*, 7138–7148.

Groysbeck, N., Stoessel, A., Donzeau, M., da Silva, E.C., Lehmann, M., Strub, J.-M., Cianferani, S., Dembélé, K., and Zuber, G. (2019). Synthesis and biological evaluation of 2.4 nm thiolate-protected gold nanoparticles conjugated to Cetuximab for targeting glioblastoma cancer cells via the EGFR. *Nanotechnology* *30*, 184005.

Guerrero, P.A., Tchaicha, J.H., Chen, Z., Morales, J.E., McCarty, N., Wang, Q., Sulman, E.P., Fuller, G., Lang, F.F., Rao, G., et al. (2017). Glioblastoma stem cells exploit the  $\alpha\beta 8$  integrin-TGF $\beta 1$  signaling axis to drive tumor initiation and progression. *Oncogene* *36*, 6568–6580.

Gujar, A.D., Le, S., Mao, D.D., Dadey, D.Y.A., Turski, A., Sasaki, Y., Aum, D., Luo, J., Dahiya, S., Yuan, L., et al. (2016). An NAD<sup>+</sup>-dependent transcriptional program governs self-renewal and radiation resistance in glioblastoma. *Proc. Natl. Acad. Sci. U. S. A.* *113*, E8247–E8256.

Gupta, S., Thirstrup, D., Jarvis, T.C., Schneider, D.J., Wilcox, S.K., Carter, J., Zhang, C., Gelinis, A., Weiss, A., Janjic, N., et al. (2011). Rapid histochemistry using slow off-rate modified aptamers with anionic competition. *Appl. Immunohistochem. Mol. Morphol. AIMM* *19*, 273–278.

Haas, T.L., Sciuto, M.R., Brunetto, L., Valvo, C., Signore, M., Fiori, M.E., di Martino, S., Giannetti, S., Morgante, L., Boe, A., et al. (2017). Integrin  $\alpha 7$  Is a Functional Marker and Potential Therapeutic Target in Glioblastoma. *Cell Stem Cell* *21*, 35-50.e9.

Haeger, A., Alexander, S., Vullings, M., Kaiser, F.M.P., Veelken, C., Flucke, U., Koehl, G.E., Hirschberg, M., Flentje, M., Hoffman, R.M., et al. (2020). Collective cancer invasion forms an integrin-dependent radioresistant niche. *J. Exp. Med.* *217*.

Hagemann, C., Anacker, J., Ernestus, R.-I., and Vince, G.H. (2012). A complete compilation of matrix metalloproteinase expression in human malignant gliomas. *World J. Clin. Oncol.* *3*, 67–79.

Hamblett, K.J., Kozlosky, C.J., Siu, S., Chang, W.S., Liu, H., Foltz, I.N., Trueblood, E.S., Meininger, D., Arora, T., Twomey, B., et al. (2015). AMG 595, an Anti-EGFRvIII Antibody-Drug Conjugate, Induces Potent Antitumor Activity against EGFRvIII-Expressing Glioblastoma. *Mol. Cancer Ther.* *14*, 1614–1624.

Han, W., Zhang, T., Yu, H., Foulke, J.G., and Tang, C.K. (2006). Hypophosphorylation of residue Y1045 leads to defective downregulation of EGFRvIII. *Cancer Biol. Ther.* *5*, 1361–1368.

Hanabata, Y., Nakajima, Y., Morita, K., Kayamori, K., and Omura, K. (2012). Coexpression of SGLT1 and EGFR is associated with tumor differentiation in oral squamous cell carcinoma. *Odontology* *100*, 156–163.

Hanahan, D., and Weinberg, R.A. (2011). Hallmarks of cancer: the next generation. *Cell* *144*, 646–674.

Hanif, F., Muzaffar, K., Perveen, K., Malhi, S.M., and Simjee, S.U. (2017). Glioblastoma Multiforme: A Review of its Epidemiology and Pathogenesis through Clinical Presentation and Treatment. *Asian Pac. J. Cancer Prev. APJCP* *18*, 3–9.

Harari, P.M. (2004). Epidermal growth factor receptor inhibition strategies in oncology. *Endocr. Relat. Cancer* *11*, 689–708.

Harburger, D.S., and Calderwood, D.A. (2009). Integrin signalling at a glance. *J. Cell Sci.* *122*, 159–163.

Hartmann, T.N., Burger, J.A., Glodek, A., Fujii, N., and Burger, M. (2005). CXCR4 chemokine receptor and integrin signaling co-operate in mediating adhesion and chemoresistance in small cell lung cancer (SCLC) cells. *Oncogene* *24*, 4462–4471.

Hasegawa, H., Savory, N., Abe, K., and Ikebukuro, K. (2016). Methods for Improving Aptamer Binding Affinity. *Molecules* *21*.

Hassanzadeh, L., Chen, S., and Veedu, R.N. (2018). Radiolabeling of Nucleic Acid Aptamers for Highly Sensitive Disease-Specific Molecular Imaging. *Pharmaceuticals* *11*.

Hasselbalch, B., Lassen, U., Hansen, S., Holmberg, M., Sørensen, M., Kosteljanetz, M., Broholm, H., Stockhausen, M.-T., and Poulsen, H.S. (2010). Cetuximab, bevacizumab, and irinotecan for patients with primary glioblastoma and progression after radiation therapy and temozolomide: a phase II trial. *Neuro-Oncol.* *12*, 508–516.

Hatanpaa, K.J., Burma, S., Zhao, D., and Habib, A.A. (2010). Epidermal Growth Factor Receptor in Glioma: Signal Transduction, Neuropathology, Imaging, and Radioresistance. *Neoplasia* *12*, 675–684.

He, P., and Li, G. (2013). Significant increase in hEGF uptake is correlated with formation of EGFR dimers induced by the EGFR tyrosine kinase inhibitor gefitinib. *Cancer Chemother. Pharmacol.* *72*, 341–348.

He, X., Zhang, S., Chen, J., and Li, D. (2019). Increased LGALS3 expression independently predicts shorter overall survival in patients with the proneural subtype of glioblastoma. *Cancer Med.* *8*, 2031–2040.

Healy, J.M., Lewis, S.D., Kurz, M., Boomer, R.M., Thompson, K.M., Wilson, C., and McCauley, T.G. (2004). Pharmacokinetics and biodistribution of novel aptamer compositions. *Pharm. Res.* *21*, 2234–2246.

Heckmann, D., Meyer, A., Laufer, B., Zahn, G., Stragies, R., and Kessler, H. (2008). Rational Design of Highly Active and Selective Ligands for the  $\alpha 5\beta 1$  Integrin Receptor. *ChemBioChem* *9*, 1397–1407.

Heimberger, A.B., Crotty, L.E., Archer, G.E., Hess, K.R., Wikstrand, C.J., Friedman, A.H., Friedman, H.S., Bigner, D.D., and Sampson, J.H. (2003). Epidermal growth factor receptor VIII peptide vaccination is efficacious against established intracerebral tumors. *Clin. Cancer Res. Off. J. Am. Assoc. Cancer Res.* *9*, 4247–4254.

- Henriksen, L., Grandal, M.V., Knudsen, S.L.J., van Deurs, B., and Grøvdal, L.M. (2013). Internalization Mechanisms of the Epidermal Growth Factor Receptor after Activation with Different Ligands. *PLoS ONE* 8.
- Heppner, D.E., Hristova, M., Dustin, C.M., Danyal, K., Habibovic, A., and Vliet, A. van der (2016). The NADPH Oxidases DUOX1 and NOX2 Play Distinct Roles in Redox Regulation of Epidermal Growth Factor Receptor Signaling. *J. Biol. Chem.* 291, 23282–23293.
- Hernandez, L.I., Flenker, K.S., Hernandez, F.J., Klingelutz, A.J., II, J.O.M., and Giangrande, P.H. (2013). Methods for Evaluating Cell-Specific, Cell-Internalizing RNA Aptamers. *Pharmaceuticals* 6, 295–319.
- Herrmann, A., Lahtz, C., Song, J., Aftabizadeh, M., Cherryholmes, G.A., Xin, H., Adamus, T., Lee, H., Grunert, D., Armstrong, B., et al. (2020). Integrin  $\alpha 6$  signaling induces STAT3-TET3-mediated hydroxymethylation of genes critical for maintenance of glioma stem cells. *Oncogene* 39, 2156–2169.
- Hirata, E., Yukinaga, H., Kamioka, Y., Arakawa, Y., Miyamoto, S., Okada, T., Sahai, E., and Matsuda, M. (2012). In vivo fluorescence resonance energy transfer imaging reveals differential activation of Rho-family GTPases in glioblastoma cell invasion. *J. Cell Sci.* 125, 858–868.
- Holland, E.C. (2000). Glioblastoma multiforme: The terminator. *Proc. Natl. Acad. Sci. U. S. A.* 97, 6242–6244.
- Hori, S.-I., Herrera, A., Rossi, J.J., and Zhou, J. (2018). Current Advances in Aptamers for Cancer Diagnosis and Therapy. *Cancers* 10.
- Horton, E.R., Byron, A., Askari, J.A., Ng, D.H.J., Millon-Frémillon, A., Robertson, J., Koper, E.J., Paul, N.R., Warwood, S., Knight, D., et al. (2015). Definition of a consensus integrin adhesome and its dynamics during adhesion complex assembly and disassembly. *Nat. Cell Biol.* 17, 1577–1587.
- Hoshino, A., Costa-Silva, B., Shen, T.-L., Rodrigues, G., Hashimoto, A., Tesic Mark, M., Molina, H., Kohsaka, S., Di Giannatale, A., Ceder, S., et al. (2015). Tumour exosome integrins determine organotropic metastasis. *Nature* 527, 329–335.
- Hovanessian, A.G., Soundaramourty, C., Khoury, D.E., Nondier, I., Svab, J., and Krust, B. (2010). Surface Expressed Nucleolin Is Constantly Induced in Tumor Cells to Mediate Calcium-Dependent Ligand Internalization. *PLoS ONE* 5.
- Howe, E.N., Burnette, M.D., Justice, M.E., Schnepf, P.M., Hedrick, V., Clancy, J.W., Guldner, I.H., Lamere, A.T., Li, J., Aryal, U.K., et al. (2020). Rab11b-mediated integrin recycling promotes brain metastatic adaptation and outgrowth. *Nat. Commun.* 11, 3017.
- Huang, H.W., Chen, F.-Y., and Lee, M.-T. (2004). Molecular mechanism of Peptide-induced pores in membranes. *Phys. Rev. Lett.* 92, 198304.
- Huang, J., DeWees, T., Campian, J.L., Chheda, M.G., Ansstas, G., Tsien, C., Zipfel, G.J., Dunn, G.P., Ippolito, J.E., Cairncross, J.G., et al. (2019a). A TITE-CRM phase I/II study of disulfiram

and copper with concurrent radiation therapy and temozolomide for newly diagnosed glioblastoma. *J. Clin. Oncol.* *37*, 2033–2033.

Huang, J., Li, X., Shi, X., Zhu, M., Wang, J., Huang, S., Huang, X., Wang, H., Li, L., Deng, H., et al. (2019b). Platelet integrin  $\alpha\text{IIb}\beta\text{3}$ : signal transduction, regulation, and its therapeutic targeting. *J. Hematol. Oncol.* *12*.

Huang, P.H., Xu, A.M., and White, F.M. (2009). Oncogenic EGFR signaling networks in glioma. *Sci. Signal.* *2*, re6.

Hünniger, T., Wessels, H., Fischer, C., Paschke-Kratzin, A., and Fischer, M. (2014). Just in time-selection: A rapid semiautomated SELEX of DNA aptamers using magnetic separation and BEAMing. *Anal. Chem.* *86*, 10940–10947.

Hwang, S.-Y., Sun, H.-Y., Lee, K.-H., Oh, B.-H., Cha, Y.J., Kim, B.H., and Yoo, J.-Y. (2012). 5'-Triphosphate-RNA-independent activation of RIG-I via RNA aptamer with enhanced antiviral activity. *Nucleic Acids Res.* *40*, 2724–2733.

Iida, M., Brand, T.M., Starr, M.M., Huppert, E.J., Luthar, N., Bahrar, H., Coan, J.P., Pearson, H.E., Salgia, R., and Wheeler, D.L. (2014). Overcoming acquired resistance to cetuximab by dual targeting HER family receptors with antibody-based therapy. *Mol. Cancer* *13*, 242.

Iida, M., Brand, T., Starr, M., Li, C., Huppert, E.J., Luthar, N., Pedersen, M.W., Horak, I.D., Kragh, M., and Wheeler, D.L. (2013). Sym004, a novel EGFR antibody mixture, can overcome acquired resistance to cetuximab. *Neoplasia N. Y. N* *15*, 1196–1206.

Inda, M.-M., Bonavia, R., Mukasa, A., Narita, Y., Sah, D.W.Y., Vandenberg, S., Brennan, C., Johns, T.G., Bachoo, R., Hadwiger, P., et al. (2010). Tumor heterogeneity is an active process maintained by a mutant EGFR-induced cytokine circuit in glioblastoma. *Genes Dev.* *24*, 1731–1745.

Ito, K., and Hataji, O. (2018). Osimertinib therapy as first-line treatment before acquiring T790M mutation: from AURA1 trial. *J. Thorac. Dis.* *10*, S3071–S3077.

Ivaska, J. (2011). Cooperation Between Integrins and Growth Factor Receptors in Signaling and Endocytosis. *Annu. Rev. Cell Dev. Biol.* *27*, 291–320.

Iwagawa, T., Ohuchi, S.P., Watanabe, S., and Nakamura, Y. (2012). Selection of RNA aptamers against mouse embryonic stem cells. *Biochimie* *94*, 250–257.

Jahangiri, A., Aghi, M.K., and Carbonell, W.S. (2014).  $\beta\text{1}$  integrin: Critical path to antiangiogenic therapy resistance and beyond. *Cancer Res.* *74*, 3–7.

Jahangiri, A., Nguyen, A., Chandra, A., Sidorov, M.K., Yagnik, G., Rick, J., Han, S.W., Chen, W., Flanigan, P.M., Schneidman-Duhovny, D., et al. (2017). Cross-activating c-Met/ $\beta\text{1}$  integrin complex drives metastasis and invasive resistance in cancer. *Proc. Natl. Acad. Sci. U. S. A.* *114*, E8685–E8694.

Jain, N., Smith, S.W., Ghone, S., and Tomczuk, B. (2015). Current ADC Linker Chemistry. *Pharm. Res.* *32*, 3526–3540.

- JAMA Onc (2017). Association Between Telomere Length and Risk of Cancer and Non-Neoplastic Diseases: A Mendelian Randomization Study. *JAMA Oncol.* 3, 636–651.
- Jang, I., and Beningo, K.A. (2019). Integrins, CAFs and Mechanical Forces in the Progression of Cancer. *Cancers* 11.
- Janouskova, H., Maglott, A., Leger, D.Y., Bossert, C., Noulet, F., Guerin, E., Guenot, D., Pinel, S., Chastagner, P., Plenat, F., et al. (2012). Integrin  $\alpha 5\beta 1$  Plays a Critical Role in Resistance to Temozolomide by Interfering with the p53 Pathway in High-Grade Glioma. *Cancer Res.* 72, 3463–3470.
- Jayasena, S.D. (1999). Aptamers: an emerging class of molecules that rival antibodies in diagnostics. *Clin. Chem.* 45, 1628–1650.
- Jian, Z., Zhang, L., Jin, L., Lan, W., Zhang, W., and Gao, G. (2020). Rab5 regulates the proliferation, migration and invasion of glioma cells via cyclin E. *Oncol. Lett.* 20, 1055–1062.
- Jo, M.-Y., Kim, Y.G., Kim, Y., Lee, S.J., Kim, M.H., Joo, K.M., Kim, H.H., and Nam, D.-H. (2012). Combined therapy of temozolomide and ZD6474 (vandetanib) effectively reduces glioblastoma tumor volume through anti-angiogenic and anti-proliferative mechanisms. *Mol. Med. Rep.* 6, 88–92.
- Jones, S., and Rappoport, J.Z. (2014). Interdependent epidermal growth factor receptor signalling and trafficking. *Int. J. Biochem. Cell Biol.* 51, 23–28.
- Jorissen, R.N., Walker, F., Pouliot, N., Garrett, T.P.J., Ward, C.W., and Burgess, A.W. (2003). Epidermal growth factor receptor: mechanisms of activation and signalling. *Exp. Cell Res.* 284, 31–53.
- Joseph, S.R., Gaffney, D., Barry, R., Hu, L., Banushi, B., Wells, J.W., Lambie, D., Strutton, G., Porceddu, S.V., Burmeister, B., et al. (2019). An Ex Vivo Human Tumor Assay Shows Distinct Patterns of EGFR Trafficking in Squamous Cell Carcinoma Correlating to Therapeutic Outcomes. *J. Invest. Dermatol.* 139, 213–223.
- Jovic, M., Sharma, M., Rahajeng, J., and Caplan, S. (2010). The early endosome: a busy sorting station for proteins at the crossroads. *Histol. Histopathol.* 25, 99–112.
- Ju, L., Zhou, C., Li, W., and Yan, L. (2010). Integrin beta1 over-expression associates with resistance to tyrosine kinase inhibitor gefitinib in non-small cell lung cancer. *J. Cell. Biochem.* 111, 1565–1574.
- Kaminska, B., Czapski, B., Guzik, R., Król, S.K., and Gielniewski, B. (2019). Consequences of IDH1/2 Mutations in Gliomas and an Assessment of Inhibitors Targeting Mutated IDH Proteins. *Molecules* 24.
- Kanda, R., Kawahara, A., Watari, K., Murakami, Y., Sonoda, K., Maeda, M., Fujita, H., Kage, M., Uramoto, H., Costa, C., et al. (2013). Erlotinib resistance in lung cancer cells mediated by integrin  $\beta 1$ /Src/Akt-driven bypass signaling. *Cancer Res.* 73, 6243–6253.
- Kazandjian, D., Blumenthal, G.M., Yuan, W., He, K., Keegan, P., and Pazdur, R. (2016). FDA Approval of Gefitinib for the Treatment of Patients with Metastatic EGFR Mutation-Positive

Non-Small Cell Lung Cancer. *Clin. Cancer Res. Off. J. Am. Assoc. Cancer Res.* 22, 1307–1312.

Keefe, A.D., Pai, S., and Ellington, A. (2010). Aptamers as therapeutics. *Nat. Rev. Drug Discov.* 9, 537–550.

Kesanakurti, D., Chetty, C., Rajasekhar Maddirela, D., Gujrati, M., and Rao, J.S. (2012). Functional cooperativity by direct interaction between PAK4 and MMP-2 in the regulation of anoikis resistance, migration and invasion in glioma. *Cell Death Dis.* 3, e445.

Kesanakurti, D., Chetty, C., Dinh, D.H., Gujrati, M., and Rao, J.S. (2013). Role of MMP-2 in the regulation of IL-6/Stat3 survival signaling via interaction with  $\alpha 5\beta 1$  integrin in glioma. *Oncogene* 32, 327–340.

Khan, Z., and Marshall, J.F. (2016). The role of integrins in TGF $\beta$  activation in the tumour stroma. *Cell Tissue Res.* 365, 657–673.

Kiema, T., Lad, Y., Jiang, P., Oxley, C.L., Baldassarre, M., Wegener, K.L., Campbell, I.D., Ylänne, J., and Calderwood, D.A. (2006). The molecular basis of filamin binding to integrins and competition with talin. *Mol. Cell* 21, 337–347.

Kim, L.A., and D'Amore, P.A. (2012). A Brief History of Anti-VEGF for the Treatment of Ocular Angiogenesis. *Am. J. Pathol.* 181, 376–379.

Kim, B., Yang, J., Hwang, M., Choi, J., Kim, H.-O., Jang, E., Lee, J.H., Ryu, S.-H., Suh, J.-S., Huh, Y.-M., et al. (2013). Aptamer-modified magnetic nanoprobe for molecular MR imaging of VEGFR2 on angiogenic vasculature. *Nanoscale Res. Lett.* 8, 399.

Kim, H., Oh, H., Oh, Y.S., Bae, J., Hong, N.H., Park, S.J., Ahn, S., Lee, M., Rhee, S., Lee, S.H., et al. (2019). SPIN90, an adaptor protein, alters the proximity between Rab5 and Gapex5 and facilitates Rab5 activation during EGF endocytosis. *Exp. Mol. Med.* 51, 85.

Kim, J., Zhang, Y., Skalski, M., Hayes, J., Kefas, B., Schiff, D., Purow, B., Parsons, S., Lawler, S., and Abounader, R. (2014). microRNA-148a is a prognostic oncomiR that targets MIG6 and BIM to regulate EGFR and apoptosis in glioblastoma. *Cancer Res.* 74, 1541–1553.

Kim, J., Lee, I.-H., Cho, H.J., Park, C.-K., Jung, Y.-S., Kim, Y., Nam, S.H., Kim, B.S., Johnson, M.D., Kong, D.-S., et al. (2015). Spatiotemporal Evolution of the Primary Glioblastoma Genome. *Cancer Cell* 28, 318–328.

Kim, K.B., Prieto, V., Joseph, R.W., Diwan, A.H., Gallick, G.E., Papadopoulos, N.E., Bedikian, A.Y., Camacho, L.H., Hwu, P., Ng, C.S., et al. (2012). A randomized phase II study of cilengitide (EMD 121974) in patients with metastatic melanoma. *Melanoma Res.* 22, 294–301.

Kim, M.-Y., Cho, W.-D., Hong, K.P., Choi, D.B., Hong, J.W., Kim, S., Moon, Y.R., Son, S.-M., Lee, O.-J., Lee, H.-C., et al. (2016). Novel monoclonal antibody against beta 1 integrin enhances cisplatin efficacy in human lung adenocarcinoma cells. *J. Biomed. Res.* 30, 217–224.

Kim, S., Bell, K., Mousa, S.A., and Varner, J.A. (2000). Regulation of angiogenesis in vivo by ligation of integrin  $\alpha 5\beta 1$  with the central cell-binding domain of fibronectin. *Am. J. Pathol.* 156, 1345–1362.



- Kim, Y.-J., Kim, Y.S., Niazi, J.H., and Gu, M.B. (2010). Electrochemical aptasensor for tetracycline detection. *Bioprocess Biosyst. Eng.* *33*, 31–37.
- Kim, Y.-J., Jung, K., Baek, D.-S., Hong, S.-S., and Kim, Y.-S. (2017). Co-targeting of EGF receptor and neuropilin-1 overcomes cetuximab resistance in pancreatic ductal adenocarcinoma with integrin  $\beta$ 1-driven Src-Akt bypass signaling. *Oncogene* *36*, 2543–2552.
- Kimura, H., Sakai, K., Arao, T., Shimoyama, T., Tamura, T., and Nishio, K. (2007). Antibody-dependent cellular cytotoxicity of cetuximab against tumor cells with wild-type or mutant epidermal growth factor receptor. *Cancer Sci.* *98*, 1275–1280.
- Kinnersley, B., Houlston, R.S., and Bondy, M.L. (2018). Genome-wide association studies in glioma. *Cancer Epidemiol. Prev. Biomark.*
- Kitagawa, D., Yokota, K., Gouda, M., Narumi, Y., Ohmoto, H., Nishiwaki, E., Akita, K., and Kirii, Y. (2013). Activity-based kinase profiling of approved tyrosine kinase inhibitors. *Genes Cells* *18*, 110–122.
- Knight, Z.A., Gonzalez, B., Feldman, M.E., Zunder, E.R., Goldenberg, D.D., Williams, O., Loewith, R., Stokoe, D., Balla, A., Toth, B., et al. (2006). A Pharmacological Map of the PI3-K Family Defines a Role for p110 $\alpha$  in Insulin Signaling. *Cell* *125*, 733–747.
- Komada, M., and Soriano, P. (1999). Hrs, a FYVE finger protein localized to early endosomes, is implicated in vesicular traffic and required for ventral folding morphogenesis. *Genes Dev.* *13*, 1475–1485.
- Kondapalli, K.C., Hack, A., Schushan, M., Landau, M., Ben-Tal, N., and Rao, R. (2013). Functional evaluation of autism-associated mutations in NHE9. *Nat. Commun.* *4*, 2510.
- Kondapalli, K.C., Prasad, H., and Rao, R. (2014). An inside job: how endosomal Na<sup>+</sup>/H<sup>+</sup> exchangers link to autism and neurological disease. *Front. Cell. Neurosci.* *8*.
- Kondapalli, K.C., Llongueras, J.P., Capilla-González, V., Prasad, H., Hack, A., Smith, C., Guerrero-Cázares, H., Quiñones-Hinojosa, A., and Rao, R. (2015). A leak pathway for luminal protons in endosomes drives oncogenic signalling in glioblastoma. *Nat. Commun.* *6*, 6289.
- Korolchuk, V.I., Schütz, M.M., Gómez-Llorente, C., Rocha, J., Lansu, N.R., Collins, S.M., Wairkar, Y.P., Robinson, I.M., and O’Kane, C.J. (2007). *Drosophila* Vps35 function is necessary for normal endocytic trafficking and actin cytoskeleton organisation. *J. Cell Sci.* *120*, 4367–4376.
- Kotula, J.W., Pratico, E.D., Ming, X., Nakagawa, O., Juliano, R.L., and Sullenger, B.A. (2012). Aptamer-mediated delivery of splice-switching oligonucleotides to the nuclei of cancer cells. *Nucleic Acid Ther.* *22*, 187–195.
- Kratschmer, C., and Levy, M. (2018). Targeted Delivery of Auristatin-Modified Toxins to Pancreatic Cancer Using Aptamers. *Mol. Ther. Nucleic Acids* *10*, 227–236.
- Kryukov, G.V., Wilson, F.H., Ruth, J.R., Paulk, J., Tsherniak, A., Marlow, S.E., Vazquez, F., Weir, B.A., Fitzgerald, M.E., Tanaka, M., et al. (2016). MTAP deletion confers enhanced dependency on the PRMT5 arginine methyltransferase in cancer cells. *Science* *351*, 1214–1218.

- Kurata, T., Rajendran, V., Fan, S., Ohta, T., Numata, M., and Fushida, S. (2019). NHE5 regulates growth factor signaling, integrin trafficking, and degradation in glioma cells. *Clin. Exp. Metastasis*.
- Kwan, B.H., Zhu, E.F., Tzeng, A., Sugito, H.R., Eltahir, A.A., Ma, B., Delaney, M.K., Murphy, P.A., Kauke, M.J., Angelini, A., et al. (2017). Integrin-targeted cancer immunotherapy elicits protective adaptive immune responses. *J. Exp. Med.* *214*, 1679–1690.
- Lakhin, A.V., Tarantul, V.Z., and Gening, L.V. (2013). Aptamers: Problems, Solutions and Prospects. *Acta Naturae* *5*, 34–43.
- Lakoduk, A.M., Roudot, P., Mettlen, M., Grossman, H.M., Schmid, S.L., and Chen, P.-H. (2019). Mutant p53 amplifies a dynamin-1/APPL1 endosome feedback loop that regulates recycling and migration. *J. Cell Biol.* *218*, 1928–1942.
- Lal, A., Lash, A.E., Altschul, S.F., Velculescu, V., Zhang, L., McLendon, R.E., Marra, M.A., Prange, C., Morin, P.J., Polyak, K., et al. (1999). A Public Database for Gene Expression in Human Cancers. *Cancer Res.* *59*, 5403–5407.
- Lal, A., Glazer, C.A., Martinson, H.M., Friedman, H.S., Archer, G.E., Sampson, J.H., and Riggins, G.J. (2002). Mutant Epidermal Growth Factor Receptor Up-Regulates Molecular Effectors of Tumor Invasion. *Cancer Res.* *62*, 3335–3339.
- Lathia, J.D., Li, M., Sinyuk, M., Alvarado, A.G., Flavahan, W.A., Stoltz, K., Rosager, A.M., Hale, J., Hitomi, M., Gallagher, J., et al. (2014). High-throughput flow cytometry screening reveals a role for junctional adhesion molecule a as a cancer stem cell maintenance factor. *Cell Rep.* *6*, 117–129.
- Lavacchi, D., Mazzoni, F., and Giaccone, G. (2019). Clinical evaluation of dacomitinib for the treatment of metastatic non-small cell lung cancer (NSCLC): current perspectives. *Drug Des. Devel. Ther.* *13*, 3187–3198.
- Le, D.M., Besson, A., Fogg, D.K., Choi, K.-S., Waisman, D.M., Goodyer, C.G., Rewcastle, B., and Yong, V.W. (2003). Exploitation of Astrocytes by Glioma Cells to Facilitate Invasiveness: A Mechanism Involving Matrix Metalloproteinase-2 and the Urokinase-Type Plasminogen Activator–Plasmin Cascade. *J. Neurosci.* *23*, 4034–4043.
- Lecocq, S., Spinella, K., Dubois, B., Lista, S., Hampel, H., and Penner, G. (2018). Aptamers as biomarkers for neurological disorders. Proof of concept in transgenic mice. *PloS One* *13*, e0190212.
- Lees, J.G., Gorgani, N.N., Ammit, A.J., McCluskey, A., Robinson, P.J., and O’Neill, G.M. (2015). Role of dynamin in elongated cell migration in a 3D matrix. *Biochim. Biophys. Acta BBA - Mol. Cell Res.* *1853*, 611–618.
- Lefranc, F., Le Rhun, E., Kiss, R., and Weller, M. (2018). Glioblastoma quo vadis: Will migration and invasiveness reemerge as therapeutic targets? *Cancer Treat. Rev.* *68*, 145–154.
- Leitinger, M., Varosanec, M.V., Pikija, S., Wass, R.E., Bandke, D., Weis, S., Studnicka, M., Grinzinger, S., McCoy, M.R., Hauer, L., et al. (2018). Fatal Necrotizing Encephalopathy after

- Treatment with Nivolumab for Squamous Non-Small Cell Lung Cancer: Case Report and Review of the Literature. *Front. Immunol.* *9*, 108.
- Lemée, J.-M., Clavreul, A., and Menei, P. (2015). Intratumoral heterogeneity in glioblastoma: don't forget the peritumoral brain zone. *Neuro-Oncol.* *17*, 1322–1332.
- Lherbette, M., Redlingshöfer, L., Brodsky, F.M., Schaap, I.A.T., and Dannhauser, P.N. (2019). The AP2 adaptor enhances clathrin coat stiffness. *FEBS J.* *286*, 4074–4085.
- Li, L., Welser-Alves, J., van der Flier, A., Boroujerdi, A., Hynes, R.O., and Milner, R. (2012). An angiogenic role for the  $\alpha 5\beta 1$  integrin in promoting endothelial cell proliferation during cerebral hypoxia. *Exp. Neurol.* *237*, 46–54.
- Li, N., Nguyen, H.H., Byrom, M., and Ellington, A.D. (2011). Inhibition of Cell Proliferation by an Anti-EGFR Aptamer. *PLOS ONE* *6*, e20299.
- Li, W., Wang, H., Yang, Y., Zhao, T., Zhang, Z., Tian, Y., Shi, Z., Peng, X., Li, F., Feng, Y., et al. (2018). Integrative Analysis of Proteome and Ubiquitylome Reveals Unique Features of Lysosomal and Endocytic Pathways in Gefitinib-Resistant Non-Small Cell Lung Cancer Cells. *Proteomics* *18*, e1700388.
- Li, X., An, Y., Jin, J., Zhu, Z., Hao, L., Liu, L., Shi, Y., Fan, D., Ji, T., and Yang, C.J. (2015a). Evolution of DNA aptamers through in vitro metastatic-cell-based systematic evolution of ligands by exponential enrichment for metastatic cancer recognition and imaging. *Anal. Chem.* *87*, 4941–4948.
- Li, Y., Wang, Y., Yang, S., Zhao, Y., Yuan, L., Zheng, J., and Yang, R. (2015b). Hemicyanine-based High Resolution Ratiometric near-Infrared Fluorescent Probe for Monitoring pH Changes in Vivo. *Anal. Chem.* *87*, 2495–2503.
- Liang, W., and Lam, J.K.W. (2012). Endosomal Escape Pathways for Non-Viral Nucleic Acid Delivery Systems. *Mol. Regul. Endocytosis*.
- Liang, C., Guo, B., Wu, H., Shao, N., Li, D., Liu, J., Dang, L., Wang, C., Li, H., Li, S., et al. (2015). Aptamer-functionalized lipid nanoparticles targeting osteoblasts as a novel RNA interference-based bone anabolic strategy. *Nat. Med.* *21*, 288–294.
- Liao, J., Gallas, M., Pegram, M., and Slingerland, J. (2010). Lapatinib: new opportunities for management of breast cancer. *Breast Cancer Targets Ther.* *2*, 79–91.
- Lièvre, A., Bachet, J.-B., Corre, D.L., Boige, V., Landi, B., Emile, J.-F., Côté, J.-F., Tomasic, G., Penna, C., Ducreux, M., et al. (2006). KRAS Mutation Status Is Predictive of Response to Cetuximab Therapy in Colorectal Cancer. *Cancer Res.* *66*, 3992–3995.
- Lim, E.-J., Kim, S., Oh, Y., Suh, Y., Kaushik, N., Lee, J.-H., Lee, H.-J., Kim, M.-J., Park, M.-J., Kim, R.-K., et al. (2020). Crosstalk between GBM cells and mesenchymal stem-like cells promotes the invasiveness of GBM through the C5a/p38/ZEB1 axis. *Neuro-Oncol.*
- Lin, J.H., and Lu, A.Y. (2001). Interindividual variability in inhibition and induction of cytochrome P450 enzymes. *Annu. Rev. Pharmacol. Toxicol.* *41*, 535–567.

Lin, A., Giuliano, C.J., Palladino, A., John, K.M., Abramowicz, C., Yuan, M.L., Sausville, E.L., Lukow, D.A., Liu, L., Chait, A.R., et al. (2019). Off-target toxicity is a common mechanism of action of cancer drugs undergoing clinical trials. *Sci. Transl. Med.* *11*.

Lincoff, A.M., Mehran, R., Povsic, T.J., Zelenkofske, S.L., Huang, Z., Armstrong, P.W., Steg, P.G., Bode, C., Cohen, M.G., Buller, C., et al. (2016). Effect of the REG1 anticoagulation system versus bivalirudin on outcomes after percutaneous coronary intervention (REGULATE-PCI): a randomised clinical trial. *Lancet Lond. Engl.* *387*, 349–356.

Lissitzky, J.C., Luis, J., Munzer, J.S., Benjannet, S., Parat, F., Chrétien, M., Marvaldi, J., and Seidah, N.G. (2000). Endoproteolytic processing of integrin pro-alpha subunits involves the redundant function of furin and proprotein convertase (PC) 5A, but not paired basic amino acid converting enzyme (PACE) 4, PC5B or PC7. *Biochem. J.* *346 Pt 1*, 133–138.

Little, S.E., Popov, S., Jury, A., Bax, D.A., Doey, L., Al-Sarraj, S., Jurgensmeier, J.M., and Jones, C. (2012). Receptor Tyrosine Kinase Genes Amplified in Glioblastoma Exhibit a Mutual Exclusivity in Variable Proportions Reflective of Individual Tumor Heterogeneity. *Cancer Res.* *72*, 1614–1620.

Liu, W., Hsu, D.K., Chen, H.-Y., Yang, R.-Y., Carraway, K.L., Isseroff, R.R., and Liu, F.-T. (2012). Galectin-3 regulates intracellular trafficking of EGFR through Alix and promotes keratinocyte migration. *J. Invest. Dermatol.* *132*, 2828–2837.

Liu, X., Lin, P., Perrett, I., Lin, J., Liao, Y.-P., Chang, C.H., Jiang, J., Wu, N., Donahue, T., Wainberg, Z., et al. (2017). Tumor-penetrating peptide enhances transcytosis of silicasome-based chemotherapy for pancreatic cancer. *J. Clin. Invest.* *127*, 2007–2018.

Liu, Y., Kuan, C.-T., Mi, J., Zhang, X., Clary, B.M., Bigner, D.D., and Sullenger, B.A. (2009). Aptamers selected against the unglycosylated EGFRvIII ectodomain and delivered intracellularly reduce membrane-bound EGFRvIII and induce apoptosis. *Biol. Chem.* *390*, 137–144.

Liu, Y., Yang, L., Liao, F., Wang, W., and Wang, Z.-F. (2020). MiR-450a-5p strengthens the drug sensitivity of gefitinib in glioma chemotherapy via regulating autophagy by targeting EGFR. *Oncogene*.

Ljubimova, J.Y., Fujita, M., Khazenzon, N.M., Ljubimov, A.V., and Black, K.L. (2006). CHANGES IN LAMININ ISOFORMS ASSOCIATED WITH BRAIN TUMOR INVASION AND ANGIOGENESIS. *Front. Biosci. J. Virtual Libr.* *11*, 81–88.

Longva, K.E., Blystad, F.D., Stang, E., Larsen, A.M., Johannessen, L.E., and Madshus, I.H. (2002). Ubiquitination and proteasomal activity is required for transport of the EGF receptor to inner membranes of multivesicular bodies. *J. Cell Biol.* *156*, 843–854.

Louis, D.N., Ohgaki, H., Wiestler, O.D., Cavenee, W.K., Burger, P.C., Jouvet, A., Scheithauer, B.W., and Kleihues, P. (2007). The 2007 WHO Classification of Tumours of the Central Nervous System. *Acta Neuropathol. (Berl.)* *114*, 97–109.

Louis, D.N., Perry, A., Reifenberger, G., Deimling, A. von, Figarella-Branger, D., Cavenee, W.K., Ohgaki, H., Wiestler, O.D., Kleihues, P., and Ellison, D.W. (2016). The 2016 World

Health Organization Classification of Tumors of the Central Nervous System: a summary. *Acta Neuropathol. (Berl.)* 131, 803–820.

Lowell, C.A., and Mayadas, T.N. (2012). Overview-studying integrins in vivo. *Methods Mol. Biol. Clifton NJ* 757, 369–397.

Lu, H., Lu, Y., Xie, Y., Qiu, S., Li, X., and Fan, Z. (2019). Rational combination with PDK1 inhibition overcomes cetuximab resistance in head and neck squamous cell carcinoma. *JCI Insight* 4.

Lu, J., Zheng, X., Li, F., Yu, Y., Chen, Z., Liu, Z., Wang, Z., Xu, H., and Yang, W. (2017). Tunneling nanotubes promote intercellular mitochondria transfer followed by increased invasiveness in bladder cancer cells. *Oncotarget* 8, 15539–15552.

Lugano, R., Vemuri, K., Yu, D., Bergqvist, M., Smits, A., Essand, M., Johansson, S., Dejana, E., and Dimberg, A. (2018). CD93 promotes  $\beta$ 1 integrin activation and fibronectin fibrillogenesis during tumor angiogenesis. *J. Clin. Invest.* 128, 3280–3297.

Ma, S., Li, X., Wang, X., Cheng, L., Li, Z., Zhang, C., Ye, Z., and Qian, Q. (2019). Current Progress in CAR-T Cell Therapy for Solid Tumors. *Int. J. Biol. Sci.* 15, 2548–2560.

Madala, H.R., Punganuru, S.R., Arutla, V., Misra, S., Thomas, T.J., and Srivenugopal, K.S. (2018). Beyond Brooding on Oncometabolic Havoc in IDH-Mutant Gliomas and AML: Current and Future Therapeutic Strategies. *Cancers* 10.

Madshus, I.H., and Stang, E. (2009). Internalization and intracellular sorting of the EGF receptor: a model for understanding the mechanisms of receptor trafficking. *J. Cell Sci.* 122, 3433–3439.

Mahabeleshwar, G.H., Chen, J., Feng, W., Somanath, P.R., Razorenova, O.V., and Byzova, T.V. (2008). Integrin affinity modulation in angiogenesis. *Cell Cycle Georget. Tex* 7, 335–347.

Mai, A., Muharram, G., Barrow-McGee, R., Baghirov, H., Rantala, J., Kermorgant, S., and Ivaska, J. (2014). Distinct c-Met activation mechanisms induce cell rounding or invasion through pathways involving integrins, RhoA and HIP1. *J. Cell Sci.* 127, 1938–1952.

Maier, A.-K.B., Kociok, N., Zahn, G., Vossmeier, D., Stragies, R., Muether, P.S., and Jousen, A.M. (2007). Modulation of hypoxia-induced neovascularization by JSM6427, an integrin  $\alpha$ 5 $\beta$ 1 inhibiting molecule. *Curr. Eye Res.* 32, 801–812.

Majem, M., and Remon, J. (2013). Tumor heterogeneity: evolution through space and time in EGFR mutant non small cell lung cancer patients. *Transl. Lung Cancer Res.* 2, 226–237.

Mallawaarachy, D.M., Buckland, M.E., McDonald, K.L., Li, C.C.Y., Ly, L., Sykes, E.K., Christopherson, R.I., and Kaufman, K.L. (2015). Membrane Proteome Analysis of Glioblastoma Cell Invasion. *J. Neuropathol. Exp. Neurol.* 74, 425–441.

Malric, L., Monferran, S., Gilhodes, J., Boyrie, S., Dahan, P., Skuli, N., Sesen, J., Filleron, T., Kowalski-Chauvel, A., Cohen-Jonathan Moyal, E., et al. (2017). Interest of integrins targeting in glioblastoma according to tumor heterogeneity and cancer stem cell paradigm: an update. *Oncotarget* 8, 86947–86968.

- Malric, L., Monferran, S., Delmas, C., Arnauduc, F., Dahan, P., Boyrie, S., Deshors, P., Lubrano, V., Da Mota, D.F., Gilhodes, J., et al. (2019). Inhibiting Integrin  $\beta 8$  to Differentiate and Radiosensitize Glioblastoma-Initiating Cells. *Mol. Cancer Res. MCR* *17*, 384–397.
- Mamidi, A., Prawiro, C., Seymour, P.A., de Lichtenberg, K.H., Jackson, A., Serup, P., and Semb, H. (2018). Mechanosignalling via integrins directs fate decisions of pancreatic progenitors. *Nature* *564*, 114–118.
- Mammoto, T., Jiang, A., Jiang, E., Panigrahy, D., Kieran, M.W., and Mammoto, A. (2013). Role of Collagen Matrix in Tumor Angiogenesis and Glioblastoma Multiforme Progression. *Am. J. Pathol.* *183*, 1293–1305.
- Marcusson, E.G., Horazdovsky, B.F., Cereghino, J.L., Gharakhanian, E., and Emr, S.D. (1994). The sorting receptor for yeast vacuolar carboxypeptidase Y is encoded by the VPS10 gene. *Cell* *77*, 579–586.
- Martinkova, E., Maglott, A., Leger, D.Y., Bonnet, D., Stiborova, M., Takeda, K., Martin, S., and Dontenwill, M. (2010).  $\alpha 5\beta 1$  integrin antagonists reduce chemotherapy-induced premature senescence and facilitate apoptosis in human glioblastoma cells. *Int. J. Cancer* *127*, 1240–1248.
- Mas-Moruno, C., Rechenmacher, F., and Kessler, H. (2010). Cilengitide: The First Anti-Angiogenic Small Molecule Drug Candidate. Design, Synthesis and Clinical Evaluation. *Anticancer Agents Med. Chem.* *10*, 753–768.
- Mathew, M.P., Tan, E., Saeui, C.T., Bovonratwet, P., Sklar, S., Bhattacharya, R., and Yarema, K.J. (2016). Metabolic flux-driven sialylation alters internalization, recycling, and drug sensitivity of the epidermal growth factor receptor (EGFR) in SW1990 pancreatic cancer cells. *Oncotarget* *7*, 66491–66511.
- Mayer, G., Ahmed, M.-S.L., Dolf, A., Endl, E., Knolle, P.A., and Famulok, M. (2010). Fluorescence-activated cell sorting for aptamer SELEX with cell mixtures. *Nat. Protoc.* *5*, 1993–2004.
- Mazor, G., Levin, L., Picard, D., Ahmadov, U., Carén, H., Borkhardt, A., Reifenberger, G., Leprivier, G., Remke, M., and Rotblat, B. (2019). The lncRNA TP73-AS1 is linked to aggressiveness in glioblastoma and promotes temozolomide resistance in glioblastoma cancer stem cells. *Cell Death Dis.* *10*, 1–14.
- McBrayer, S.K., Mayers, J.R., DiNatale, G.J., Shi, D.D., Khanal, J., Chakraborty, A.A., Sarosiek, K.A., Briggs, K.J., Robbins, A.K., Sewastianik, T., et al. (2018). Transaminase Inhibition by 2-Hydroxyglutarate Impairs Glutamate Biosynthesis and Redox Homeostasis in Glioma. *Cell* *175*, 101-116.e25.
- McCaffrey, M.W., Bielli, A., Cantalupo, G., Mora, S., Roberti, V., Santillo, M., Drummond, F., and Bucci, C. (2001). Rab4 affects both recycling and degradative endosomal trafficking. *FEBS Lett.* *495*, 21–30.
- McCoy, M.G., Nyanyo, D., Hung, C.K., Goerger, J.P., R Zipfel, W., Williams, R.M., Nishimura, N., and Fischbach, C. (2019). Endothelial cells promote 3D invasion of GBM by IL-8-dependent induction of cancer stem cell properties. *Sci. Rep.* *9*, 9069.

- McGranahan, T., Therkelsen, K.E., Ahmad, S., and Nagpal, S. (2019). Current State of Immunotherapy for Treatment of Glioblastoma. *Curr. Treat. Options Oncol.* *20*, 24.
- Mendoza, P., Ortiz, R., Díaz, J., Quest, A.F.G., Leyton, L., Stupack, D., and Torres, V.A. (2013). Rab5 activation promotes focal adhesion disassembly, migration and invasiveness in tumor cells. *J. Cell Sci.* *126*, 3835–3847.
- Meng, X., Zhao, Y., Han, B., Zha, C., Zhang, Y., Li, Z., Wu, P., Qi, T., Jiang, C., Liu, Y., et al. (2020). Dual functionalized brain-targeting nanoinhibitors restrain temozolomide-resistant glioma via attenuating EGFR and MET signaling pathways. *Nat. Commun.* *11*, 594.
- Mercier, M.-C., Dontenwill, M., and Choulier, L. (2017). Selection of Nucleic Acid Aptamers Targeting Tumor Cell-Surface Protein Biomarkers. *Cancers* *9*.
- Mi, J., Liu, Y., Rabbani, Z.N., Yang, Z., Urban, J.H., Sullenger, B.A., and Clary, B.M. (2010). In vivo selection of tumor-targeting RNA motifs. *Nat. Chem. Biol.* *6*, 22–24.
- Mikkelsen, T., Brodie, C., Finniss, S., Berens, M.E., Rennert, J.L., Nelson, K., Lemke, N., Brown, S.L., Hahn, D., Neuteboom, B., et al. (2009). Radiation sensitization of glioblastoma by cilengitide has unanticipated schedule-dependency. *Int. J. Cancer* *124*, 2719–2727.
- Miliotou, A.N., and Papadopoulou, L.C. (2018). CAR T-cell Therapy: A New Era in Cancer Immunotherapy. *Curr. Pharm. Biotechnol.* *19*, 5–18.
- Miranda-Filho, A., Piñeros, M., Soerjomataram, I., Deltour, I., and Bray, F. (2017). Cancers of the brain and CNS: global patterns and trends in incidence. *Neuro-Oncol.* *19*, 270–280.
- Mirimanoff, R.-O., Gorlia, T., Mason, W., Van den Bent, M.J., Kortmann, R.-D., Fisher, B., Reni, M., Brandes, A.A., Curschmann, J., Villa, S., et al. (2006). Radiotherapy and Temozolomide for Newly Diagnosed Glioblastoma: Recursive Partitioning Analysis of the EORTC 26981/22981-NCIC CE3 Phase III Randomized Trial. *J. Clin. Oncol.* *24*, 2563–2569.
- Mitra, A.K., Sawada, K., Tiwari, P., Mui, K., Gwin, K., and Lengyel, E. (2011). Ligand-independent activation of c-Met by fibronectin and  $\alpha(5)\beta(1)$ -integrin regulates ovarian cancer invasion and metastasis. *Oncogene* *30*, 1566–1576.
- Miyazaki, N., Iwasaki, K., and Takagi, J. (2018). A systematic survey of conformational states in  $\beta 1$  and  $\beta 4$  integrins using negative-stain electron microscopy. *J. Cell Sci.* *131*.
- Mohanam, S., Jasti, S.L., Kondraganti, S.R., Chandrasekar, N., Lakka, S.S., Kin, Y., Fuller, G.N., Yung, A.W., Kyritsis, A.P., Dinh, D.H., et al. (2001). Down-regulation of cathepsin B expression impairs the invasive and tumorigenic potential of human glioblastoma cells. *Oncogene* *20*, 3665–3673.
- Momcilovic, M., Bailey, S.T., Lee, J.T., Fishbein, M.C., Magyar, C., Braas, D., Graeber, T., Jackson, N.J., Czernin, J., Emberley, E., et al. (2017). Targeted inhibition of EGFR and glutaminase induces metabolic crisis in EGFR mutant lung cancer. *Cell Rep.* *18*, 601–610.
- Monferran, S., Skuli, N., Delmas, C., Favre, G., Bonnet, J., Cohen-Jonathan-Moyal, E., and Toulas, C. (2008).  $\alpha 3\beta 1$  and  $\alpha 5\beta 1$  integrins control glioma cell response to ionising radiation through ILK and RhoB. *Int. J. Cancer* *123*, 357–364.

- Morello, V., Cabodi, S., Sigismund, S., Camacho-Leal, M.P., Repetto, D., Volante, M., Papotti, M., Turco, E., and Defilippi, P. (2011).  $\beta 1$  integrin controls EGFR signaling and tumorigenic properties of lung cancer cells. *Oncogene* *30*, 4087–4096.
- Moreno-Layseca, P., Icha, J., Hamidi, H., and Ivaska, J. (2019). Integrin trafficking in cells and tissues. *Nat. Cell Biol.* *21*, 122–132.
- Morgan, M.R., Hamidi, H., Bass, M.D., Warwood, S., Ballestrem, C., and Humphries, M.J. (2013). Syndecan-4 Phosphorylation Is a Control Point for Integrin Recycling. *Dev. Cell* *24*, 472–485.
- Morozevich, G.E., Kozlova, N.I., Ushakova, N.A., Preobrazhenskaya, M.E., and Berman, A.E. (2012). Integrin  $\alpha 5\beta 1$  simultaneously controls EGFR-dependent proliferation and Akt-dependent pro-survival signaling in epidermoid carcinoma cells. *Aging* *4*, 368–374.
- Mosing, R.K., and Bowser, M.T. (2007). Microfluidic selection and applications of aptamers. *J. Sep. Sci.* *30*, 1420–1426.
- Mosing, R.K., Mendonsa, S.D., and Bowser, M.T. (2005). Capillary electrophoresis-SELEX selection of aptamers with affinity for HIV-1 reverse transcriptase. *Anal. Chem.* *77*, 6107–6112.
- Mufhandu, H.T., Gray, E.S., Madiga, M.C., Tumba, N., Alexandre, K.B., Khoza, T., Wibmer, C.K., Moore, P.L., Morris, L., and Khati, M. (2012). UCLA1, a synthetic derivative of a gp120 RNA aptamer, inhibits entry of human immunodeficiency virus type 1 subtype C. *J. Virol.* *86*, 4989–4999.
- Muller, P. a. J., Trinidad, A.G., Timpson, P., Morton, J.P., Zanivan, S., van den Berghe, P.V.E., Nixon, C., Karim, S.A., Caswell, P.T., Noll, J.E., et al. (2013). Mutant p53 enhances MET trafficking and signalling to drive cell scattering and invasion. *Oncogene* *32*, 1252–1265.
- Muller, P.A.J., Caswell, P.T., Doyle, B., Iwanicki, M.P., Tan, E.H., Karim, S., Lukashchuk, N., Gillespie, D.A., Ludwig, R.L., Gosselin, P., et al. (2009). Mutant p53 drives invasion by promoting integrin recycling. *Cell* *139*, 1327–1341.
- Munksgaard Thorén, M., Chmielarska Masoumi, K., Krona, C., Huang, X., Kundu, S., Schmidt, L., Forsberg-Nilsson, K., Floyd Keep, M., Englund, E., Nelander, S., et al. (2019). Integrin  $\alpha 10$ , a Novel Therapeutic Target in Glioblastoma, Regulates Cell Migration, Proliferation, and Survival. *Cancers* *11*.
- Musumeci, D., Platella, C., Riccardi, C., Moccia, F., and Montesarchio, D. (2017). Fluorescence Sensing Using DNA Aptamers in Cancer Research and Clinical Diagnostics. *Cancers* *9*.
- Nabors, L.B., Fink, K.L., Mikkelsen, T., Grujicic, D., Tarnawski, R., Nam, D.H., Mazurkiewicz, M., Salacz, M., Ashby, L., Zagonel, V., et al. (2015). Two cilengitide regimens in combination with standard treatment for patients with newly diagnosed glioblastoma and unmethylated MGMT gene promoter: results of the open-label, controlled, randomized phase II CORE study. *Neuro-Oncol.* *17*, 708–717.
- Narita, Y., Muragaki, Y., Maruyama, T., Kagawa, N., Asai, K., Kuroda, J., Kurozumi, K., Nagane, M., Matsuda, M., Ueki, K., et al. (2019). Phase I/II study of depatuxizumab mafodotin



- (ABT-414) monotherapy or combination with temozolomide in Japanese patients with/without EGFR-amplified recurrent glioblastoma. *J. Clin. Oncol.* *37*, 2065–2065.
- Neftel, C., Laffy, J., Filbin, M.G., Hara, T., Shore, M.E., Rahme, G.J., Richman, A.R., Silverbush, D., Shaw, M.L., Hebert, C.M., et al. (2019). An Integrative Model of Cellular States, Plasticity, and Genetics for Glioblastoma. *Cell* *178*, 835-849.e21.
- Newlands, E.S., Blackledge, G.R., Slack, J.A., Rustin, G.J., Smith, D.B., Stuart, N.S., Quarterman, C.P., Hoffman, R., Stevens, M.F., and Brampton, M.H. (1992). Phase I trial of temozolomide (CCRG 81045; M&B 39831; NSC 362856). *Br. J. Cancer* *65*, 287–291.
- Newlands, E.S., Stevens, M.F., Wedge, S.R., Wheelhouse, R.T., and Brock, C. (1997). Temozolomide: a review of its discovery, chemical properties, pre-clinical development and clinical trials. *Cancer Treat. Rev.* *23*, 35–61.
- Newton, H. (2006). Innovative Approaches to Chemotherapy Delivery. In *Handbook of Brain Tumor Chemotherapy*, (California: Academic Press), p.
- Ng, E.W.M., Shima, D.T., Calias, P., Cunningham, E.T., Guyer, D.R., and Adamis, A.P. (2006). Pegaptanib, a targeted anti-VEGF aptamer for ocular vascular disease. *Nat. Rev. Drug Discov.* *5*, 123–132.
- Ni, S., Yao, H., Wang, L., Lu, J., Jiang, F., Lu, A., and Zhang, G. (2017). Chemical Modifications of Nucleic Acid Aptamers for Therapeutic Purposes. *Int. J. Mol. Sci.* *18*.
- van Niftherik, K.A., van den Berg, J., Stalpers, L.J.A., Lafleur, M.V.M., Leenstra, S., Slotman, B.J., Hulsebos, T.J.M., and Sminia, P. (2007). Differential radiosensitizing potential of temozolomide in MGMT promoter methylated glioblastoma multiforme cell lines. *Int. J. Radiat. Oncol. Biol. Phys.* *69*, 1246–1253.
- Nimjee, S.M., White, R.R., Becker, R.C., and Sullenger, B.A. (2017). Aptamers as Therapeutics. *Annu. Rev. Pharmacol. Toxicol.* *57*, 61–79.
- Nishikawa, F., Kakiuchi, N., Funaji, K., Fukuda, K., Sekiya, S., and Nishikawa, S. (2003). Inhibition of HCV NS3 protease by RNA aptamers in cells. *Nucleic Acids Res.* *31*, 1935–1943.
- Nishimura, Y., and Itoh, K. (2019). Involvement of SNX1 in regulating EGFR endocytosis in a gefitinib-resistant NSCLC cell lines. *Cancer Drug Resist.* *2*, 539–549.
- Nishimura, Y., Berezky, B., and Ono, M. (2007). The EGFR inhibitor gefitinib suppresses ligand-stimulated endocytosis of EGFR via the early/late endocytic pathway in non-small cell lung cancer cell lines. *Histochem. Cell Biol.* *127*, 541–553.
- Nishimura, Y., Yoshioka, K., Berezky, B., and Itoh, K. (2008). Evidence for efficient phosphorylation of EGFR and rapid endocytosis of phosphorylated EGFR via the early/late endocytic pathway in a gefitinib-sensitive non-small cell lung cancer cell line. *Mol. Cancer* *7*, 42.
- Normanno, N., De Luca, A., Bianco, C., Strizzi, L., Mancino, M., Maiello, M.R., Carotenuto, A., De Feo, G., Caponigro, F., and Salomon, D.S. (2006). Epidermal growth factor receptor (EGFR) signaling in cancer. *Gene* *366*, 2–16.

- Noushmehr, H., Weisenberger, D.J., Diefes, K., Phillips, H.S., Pujara, K., Berman, B.P., Pan, F., Pelloski, C.E., Sulman, E.P., Bhat, K.P., et al. (2010). Identification of a CpG island methylator phenotype that defines a distinct subgroup of glioma. *Cancer Cell* 17, 510–522.
- Odell, I.D., and Cook, D. (2013). Immunofluorescence Techniques. *J. Invest. Dermatol.* 133, 1–4.
- O'Donnell, P.H., Undevia, S.D., Stadler, W.M., Karrison, T.M., Nicholas, M.K., Janisch, L., and Ratain, M.J. (2012). A phase I study of continuous infusion cilengitide in patients with solid tumors. *Invest. New Drugs* 30, 604–610.
- Okada, Y., Hurwitz, E.E., Esposito, J.M., Brower, M.A., Nutt, C.L., and Louis, D.N. (2003). Selection pressures of TP53 mutation and microenvironmental location influence epidermal growth factor receptor gene amplification in human glioblastomas. *Cancer Res.* 63, 413–416.
- Oksvold, M.P., Huitfeldt, H.S., Østvold, A.C., and Skarpen, E. (2002). UV induces tyrosine kinase-independent internalisation and endosome arrest of the EGF receptor. *J. Cell Sci.* 115, 793–803.
- Oksvold, M.P., Thien, C.B.F., Widerberg, J., Chantry, A., Huitfeldt, H.S., and Langdon, W.Y. (2004). UV-radiation-induced internalization of the epidermal growth factor receptor requires distinct serine and tyrosine residues in the cytoplasmic carboxy-terminal domain. *Radiat. Res.* 161, 685–691.
- Olayioye, M.A., Neve, R.M., Lane, H.A., and Hynes, N.E. (2000). The ErbB signaling network: receptor heterodimerization in development and cancer. *EMBO J.* 19, 3159–3167.
- OncoSynergy (2019). FDA Acceptance of IND Application for Phase I Trial of OS2966 in Patients with Recurrent Glioblastoma.
- Oroudjev, E., Lopus, M., Wilson, L., Audette, C., Provenzano, C., Erickson, H., Kovtun, Y., Chari, R., and Jordan, M.A. (2010). Maytansinoid-Antibody Conjugates Induce Mitotic Arrest by Suppressing Microtubule Dynamic Instability. *Mol. Cancer Ther.* 9, 2700–2713.
- Osswald, M., Jung, E., Sahm, F., Solecki, G., Venkataramani, V., Blaes, J., Weil, S., Horstmann, H., Wiestler, B., Syed, M., et al. (2015). Brain tumour cells interconnect to a functional and resistant network. *Nature* 528, 93–98.
- Ou, J., Luan, W., Deng, J., Sa, R., and Liang, H. (2012).  $\alpha$ V Integrin Induces Multicellular Radioresistance in Human Nasopharyngeal Carcinoma via Activating SAPK/JNK Pathway. *PLOS ONE* 7, e38737.
- Ozawa, T., Riester, M., Cheng, Y.-K., Huse, J.T., Squatrito, M., Helmy, K., Charles, N., Michor, F., and Holland, E.C. (2014). Most human non-GCIMP glioblastoma subtypes evolve from a common proneural-like precursor glioma. *Cancer Cell* 26, 288–300.
- Palmieri, D., Bouadis, A., Ronchetti, R., Merino, M.J., and Steeg, P.S. (2005). The protein trafficking Rab-GTPase, Rab11a, modulates EGFR recycling and motility in MCF10A human breast epithelial cells. *Cancer Res.* 65, 54–54.
- Paolillo, M., and Schinelli, S. (2019). Extracellular Matrix Alterations in Metastatic Processes. *Int. J. Mol. Sci.* 20.

- Parachoniak, C.A., and Park, M. (2009). Distinct Recruitment of Eps15 via Its Coiled-coil Domain Is Required For Efficient Down-regulation of the Met Receptor Tyrosine Kinase. *J. Biol. Chem.* *284*, 8382–8394.
- Parisi, S., Corsa, P., Raguso, A., Perrone, A., Cossa, S., Munafò, T., Sanpaolo, G., Donno, E., Clemente, M.A., Piombino, M., et al. (2015). Temozolomide and Radiotherapy versus Radiotherapy Alone in High Grade Gliomas: A Very Long Term Comparative Study and Literature Review. *BioMed Res. Int.* *2015*.
- Parker, J.J., Dionne, K.R., Massarwa, R., Klaassen, M., Foreman, N.K., Niswander, L., Canoll, P., Kleinschmidt-DeMasters, B.K., and Waziri, A. (2013). Gefitinib selectively inhibits tumor cell migration in EGFR-amplified human glioblastoma. *Neuro-Oncol.* *15*, 1048–1057.
- Parker, N.R., Khong, P., Parkinson, J.F., Howell, V.M., and Wheeler, H.R. (2015). Molecular heterogeneity in glioblastoma: potential clinical implications. *Front. Oncol.* *5*, 55.
- Passariello, M., Camorani, S., Vetrei, C., Cerchia, L., and De Lorenzo, C. (2019). Novel Human Bispecific Aptamer-Antibody Conjugates for Efficient Cancer Cell Killing. *Cancers* *11*.
- Patel, A.P., Tirosh, I., Trombetta, J.J., Shalek, A.K., Gillespie, S.M., Wakimoto, H., Cahill, D.P., Nahed, B.V., Curry, W.T., Martuza, R.L., et al. (2014). Single-cell RNA-seq highlights intratumoral heterogeneity in primary glioblastoma. *Science* *344*, 1396–1401.
- Patel, A.P., Fisher, J.L., Nichols, E., Abd-Allah, F., Abdela, J., Abdelalim, A., Abraha, H.N., Agius, D., Alahdab, F., Alam, T., et al. (2019). Global, regional, and national burden of brain and other CNS cancer, 1990–2016: a systematic analysis for the Global Burden of Disease Study 2016. *Lancet Neurol.* *18*, 376–393.
- Patil, S.S., Railkar, R., Swain, M., Atreya, H.S., Dighe, R.R., and Kondaiah, P. (2015). Novel anti IGFBP2 single chain variable fragment inhibits glioma cell migration and invasion. *J. Neurooncol.* *123*, 225–235.
- Paul, N.R., Jacquemet, G., and Caswell, P.T. (2015). Endocytic Trafficking of Integrins in Cell Migration. *Curr. Biol. CB* *25*, R1092-1105.
- Peereboom, D., Nabors, L.B., Kumthekar, P., Badruddoja, M., Fink, K., Lieberman, F., Phuphanich, S., Dunbar, E., Walbert, T., Schiff, D., et al. (2018). ATIM-06. PHASE 2 TRIAL OF SL-701 + BEVACIZUMAB IN PATIENTS WITH PREVIOUSLY TREATED GLIOBLASTOMA (GBM) MEETS PRIMARY ENDPOINT OF OS-12, WITH PRELIMINARY CORRELATION BETWEEN LONG-TERM SURVIVAL AND TARGET-SPECIFIC CD8+ T CELL IMMUNE RESPONSE. *Neuro-Oncol.* *20*, vi2–vi2.
- Pelicci, G., Lanfrancone, L., Grignani, F., McGlade, J., Cavallo, F., Forni, G., Nicoletti, I., Grignani, F., Pawson, T., and Pelicci, P.G. (1992). A novel transforming protein (SHC) with an SH2 domain is implicated in mitogenic signal transduction. *Cell* *70*, 93–104.
- Peng, K., Dai, Q., Wei, J., Shao, G., Sun, A., Yang, W., and Lin, Q. (2016). Stress-induced endocytosis and degradation of epidermal growth factor receptor are two independent processes. *Cancer Cell Int.* *16*, 25.

- Perrot, G., Langlois, B., Devy, J., Jeanne, A., Verzeaux, L., Almagro, S., Sartelet, H., Hachet, C., Schneider, C., Sick, E., et al. (2012). LRP-1--CD44, a new cell surface complex regulating tumor cell adhesion. *Mol. Cell. Biol.* *32*, 3293–3307.
- Petrás, M., Lajtos, T., Friedländer, E., Klekner, A., Pintye, E., Feuerstein, B.G., Szölloosi, J., and Vereb, G. (2013). Molecular interactions of ErbB1 (EGFR) and integrin- $\beta$ 1 in astrocytoma frozen sections predict clinical outcome and correlate with Akt-mediated in vitro radioresistance. *Neuro-Oncol.* *15*, 1027–1040.
- Petterson, S.A., Dahlrot, R.H., Hermansen, S.K., K A Munthe, S., Gundesen, M.T., Wohlleben, H., Rasmussen, T., Beier, C.P., Hansen, S., and Kristensen, B.W. (2015). High levels of c-Met is associated with poor prognosis in glioblastoma. *J. Neurooncol.* *122*, 517–527.
- Phillips, A.C., Boghaert, E.R., Vaidya, K.S., Mitten, M.J., Norvell, S., Falls, H.D., DeVries, P.J., Cheng, D., Meulbroek, J.A., Buchanan, F.G., et al. (2016). ABT-414, an Antibody-Drug Conjugate Targeting a Tumor-Selective EGFR Epitope. *Mol. Cancer Ther.* *15*, 661–669.
- Piao, Y., Lu, L., and de Groot, J. (2009). AMPA receptors promote perivascular glioma invasion via  $\beta$ 1 integrin-dependent adhesion to the extracellular matrix. *Neuro-Oncol.* *11*, 260–273.
- Piccirillo, S.G., Spiteri, I., Sottoriva, A., Touloumis, A., Ber, S., Price, S.J., Heywood, R., Francis, N.-J., Howarth, K.D., Collins, V.P., et al. (2015). Contributions to drug resistance in glioblastoma derived from malignant cells in the sub-ependymal zone. *Cancer Res.* *75*, 194–202.
- Pinilla-Macua, I., Grassart, A., Duvvuri, U., Watkins, S.C., and Sorkin, A. (2017). EGF receptor signaling, phosphorylation, ubiquitylation and endocytosis in tumors in vivo. *ELife* *6*, e31993.
- Platten, M., Schilling, D., Bunse, L., Wick, A., Bunse, T., Riehl, D., Green, E., Sanghvi, K., Karapanagiotou-Schenkel, I., Harting, I., et al. (2018). ATIM-33. NOA-16: A FIRST-IN-MAN MULTICENTER PHASE I CLINICAL TRIAL OF THE GERMAN NEUROONCOLOGY WORKING GROUP EVALUATING A MUTATION-SPECIFIC PEPTIDE VACCINE TARGETING IDH1R132H IN PATIENTS WITH NEWLY DIAGNOSED MALIGNANT ASTROCYTOMAS. *Neuro-Oncol.* *20*, vi8–vi9.
- Pointer, K.B., Clark, P.A., Schroeder, A.B., Salamat, M.S., Eliceiri, K.W., and Kuo, J.S. (2017). Association of collagen architecture with glioblastoma patient survival. *J. Neurosurg.* *126*, 1812–1821.
- Polakis, P. (2016). Antibody Drug Conjugates for Cancer Therapy. *Pharmacol. Rev.* *68*, 3–19.
- Poltavets, V., Kochetkova, M., Pitson, S.M., and Samuel, M.S. (2018). The Role of the Extracellular Matrix and Its Molecular and Cellular Regulators in Cancer Cell Plasticity. *Front. Oncol.* *8*.
- Poschau, M., Dickreuter, E., Singh-Müller, J., Zscheppang, K., Eke, I., Liersch, T., and Cordes, N. (2015). EGFR and  $\beta$ 1-integrin targeting differentially affect colorectal carcinoma cell radiosensitivity and invasion. *Radiother. Oncol. J. Eur. Soc. Ther. Radiol. Oncol.* *116*, 510–516.

Powell Gray, B., Kelly, L., Ahrens, D.P., Barry, A.P., Kratschmer, C., Levy, M., and Sullenger, B.A. (2018). Tunable cytotoxic aptamer–drug conjugates for the treatment of prostate cancer. *Proc. Natl. Acad. Sci. U. S. A.* *115*, 4761–4766.

Prager-Khoutorsky, M., Lichtenstein, A., Krishnan, R., Rajendran, K., Mayo, A., Kam, Z., Geiger, B., and Bershadsky, A.D. (2011). Fibroblast polarization is a matrix-rigidity-dependent process controlled by focal adhesion mechanosensing. *Nat. Cell Biol.* *13*, 1457–1465.

Pu, Y., Liu, Z., Lu, Y., Yuan, P., Liu, J., Yu, B., Wang, G., Yang, C.J., Liu, H., and Tan, W. (2015). Using DNA Aptamer Probe for Immunostaining of Cancer Frozen Tissues. *Anal. Chem.* *87*, 1919–1924.

Raab-Westphal, S., Marshall, J., and Goodman, S. (2017). Integrins as Therapeutic Targets: Successes and Cancers. *Cancers* *9*, 110.

Rahman, M., Deleyrolle, L., Vedam-Mai, V., Azari, H., Abd-El-Barr, M., and Reynolds, B.A. (2011). The cancer stem cell hypothesis: failures and pitfalls. *Neurosurgery* *68*, 531–545; discussion 545.

Rainero, E., Howe, J.D., Caswell, P.T., Jamieson, N.B., Anderson, K., Critchley, D.R., Machesky, L., and Norman, J.C. (2015). Ligand-Occupied Integrin Internalization Links Nutrient Signaling to Invasive Migration. *Cell Rep.* *10*, 398–413.

Ramakrishnan, M.S., Eswaraiyah, A., Crombet, T., Piedra, P., Saurez, G., Iyer, H., and Arvind, A. (2009). Nimotuzumab, a promising therapeutic monoclonal for treatment of tumors of epithelial origin. *MAbs* *1*, 41–48.

Rangel, A.E., Chen, Z., Ayele, T.M., and Heemstra, J.M. (2018). In vitro selection of an XNA aptamer capable of small-molecule recognition. *Nucleic Acids Res.* *46*, 8057–8068.

Rape, A., Ananthanarayanan, B., and Kumar, S. (2014). Engineering strategies to mimic the glioblastoma microenvironment. *Adv. Drug Deliv. Rev.* *79–80*, 172–183.

Ray, A.-M., Schaffner, F., Janouskova, H., Noulet, F., Rognan, D., Lelong-Rebel, I., Choulier, L., Blandin, A.-F., Lehmann, M., Martin, S., et al. (2014). Single cell tracking assay reveals an opposite effect of selective small non-peptidic  $\alpha 5\beta 1$  or  $\alpha v\beta 3/\beta 5$  integrin antagonists in U87MG glioma cells. *Biochim. Biophys. Acta* *1840*, 2978–2987.

Ray, P., Cheek, M.A., Sharaf, M.L., Li, N., Ellington, A.D., Sullenger, B.A., Shaw, B.R., and White, R.R. (2012). Aptamer-mediated delivery of chemotherapy to pancreatic cancer cells. *Nucleic Acid Ther.* *22*, 295–305.

Reardon, D.A., Desjardins, A., Vredenburgh, J.J., O'Rourke, D.M., Tran, D.D., Fink, K.L., Nabors, L.B., Li, G., Bota, D.A., Lukas, R.V., et al. (2020). Rindopepimut with Bevacizumab for Patients with Relapsed EGFRvIII-Expressing Glioblastoma (ReACT): Results of a Double-Blind Randomized Phase II Trial. *Clin. Cancer Res.* *26*, 1586–1594.

Rechenmacher, F., Neubauer, S., Polleux, J., Mas-Moruno, C., De Simone, M., Cavalcanti-Adam, E.A., Spatz, J.P., Fässler, R., and Kessler, H. (2013). Functionalizing  $\alpha v\beta 3$ - or  $\alpha 5\beta 1$ -Selective Integrin Antagonists for Surface Coating: A Method To Discriminate Integrin Subtypes In Vitro. *Angew. Chem. Int. Ed.* *52*, 1572–1575.

- Renner, G., Janouskova, H., Noulet, F., Koenig, V., Guerin, E., Bär, S., Nuesch, J., Rechenmacher, F., Neubauer, S., Kessler, H., et al. (2016a). Integrin  $\alpha 5\beta 1$  and p53 convergent pathways in the control of anti-apoptotic proteins PEA-15 and survivin in high-grade glioma. *Cell Death Differ.* *23*, 640–653.
- Renner, G., Noulet, F., Mercier, M.-C., Choulier, L., Etienne-Selloum, N., Gies, J.-P., Lehmann, M., Lelong-Rebel, I., Martin, S., and Dontenwill, M. (2016b). Expression/activation of  $\alpha 5\beta 1$  integrin is linked to the  $\beta$ -catenin signaling pathway to drive migration in glioma cells. *Oncotarget* *7*, 62194–62207.
- Reyes, S.B., Narayanan, A.S., Lee, H.S., Tchaicha, J.H., Aldape, K.D., Lang, F.F., Tolias, K.F., and McCarty, J.H. (2013).  $\alpha v\beta 8$  integrin interacts with RhoGDI1 to regulate Rac1 and Cdc42 activation and drive glioblastoma cell invasion. *Mol. Biol. Cell* *24*, 474–482.
- Reyes-Reyes, E.M., Teng, Y., and Bates, P.J. (2010). A new paradigm for aptamer therapeutic AS1411 action: uptake by macropinocytosis and its stimulation by a nucleolin-dependent mechanism. *Cancer Res.* *70*, 8617–8629.
- Reynolds, A.R., Hart, I.R., Watson, A.R., Welti, J.C., Silva, R.G., Robinson, S.D., Da Violante, G., Gourlaouen, M., Salih, M., Jones, M.C., et al. (2009). Stimulation of tumor growth and angiogenesis by low concentrations of RGD-mimetic integrin inhibitors. *Nat. Med.* *15*, 392–400.
- Reynolds, L.E., Wyder, L., Lively, J.C., Taverna, D., Robinson, S.D., Huang, X., Sheppard, D., Hynes, R.O., and Hodivala-Dilke, K.M. (2002). Enhanced pathological angiogenesis in mice lacking beta3 integrin or beta3 and beta5 integrins. *Nat. Med.* *8*, 27–34.
- Ricciuti, B., Baglivo, S., De Giglio, A., and Chiari, R. (2018). Afatinib in the first-line treatment of patients with non-small cell lung cancer: clinical evidence and experience. *Ther. Adv. Respir. Dis.* *12*.
- Robertson, D.L., and Joyce, G.F. (1990). Selection in vitro of an RNA enzyme that specifically cleaves single-stranded DNA. *Nature* *344*, 467–468.
- Robertson, J., Humphries, J.D., Paul, N.R., Warwood, S., Knight, D., Byron, A., and Humphries, M.J. (2017). Characterization of the Phospho-Adhesome by Mass Spectrometry-Based Proteomics. *Methods Mol. Biol. Clifton NJ* *1636*, 235–251.
- Rocha-Lima, C.M., and Raez, L.E. (2009). Erlotinib (Tarceva) for the Treatment of Non-Small-Cell Lung Cancer and Pancreatic Cancer. *Pharm. Ther.* *34*, 554–564.
- Rohle, D., Popovici-Muller, J., Palaskas, N., Turcan, S., Grommes, C., Campos, C., Tsoi, J., Clark, O., Oldrini, B., Komisopoulou, E., et al. (2013). An inhibitor of mutant IDH1 delays growth and promotes differentiation of glioma cells. *Science* *340*, 626–630.
- Roskoski, R. (2014). The ErbB/HER family of protein-tyrosine kinases and cancer. *Pharmacol. Res.* *79*, 34–74.
- Roxrud, I., Raiborg, C., Pedersen, N.M., Stang, E., and Stenmark, H. (2008). An endosomally localized isoform of Eps15 interacts with Hrs to mediate degradation of epidermal growth factor receptor. *J. Cell Biol.* *180*, 1205–1218.

- Rozakis-Adcock, M., McGlade, J., Mbamalu, G., Pelicci, G., Daly, R., Li, W., Batzer, A., Thomas, S., Brugge, J., Pelicci, P.G., et al. (1992). Association of the Shc and Grb2/Sem5 SH2-containing proteins is implicated in activation of the Ras pathway by tyrosine kinases. *Nature* 360, 689–692.
- Ruckman, J., Green, L.S., Beeson, J., Waugh, S., Gillette, W.L., Henninger, D.D., Claesson-Welsh, L., and Janjić, N. (1998). 2'-Fluoropyrimidine RNA-based aptamers to the 165-amino acid form of vascular endothelial growth factor (VEGF165). Inhibition of receptor binding and VEGF-induced vascular permeability through interactions requiring the exon 7-encoded domain. *J. Biol. Chem.* 273, 20556–20567.
- Ruscito, A., and DeRosa, M.C. (2016). Small-Molecule Binding Aptamers: Selection Strategies, Characterization, and Applications. *Front. Chem.* 4.
- Russo, A.L., Kwon, H.-C., Burgan, W.E., Carter, D., Beam, K., Weizheng, X., Zhang, J., Slusher, B.S., Chakravarti, A., Tofilon, P.J., et al. (2009). In vitro and In vivo Radiosensitization of Glioblastoma Cells by the Poly (ADP-Ribose) Polymerase Inhibitor E7016. *Clin. Cancer Res. Off. J. Am. Assoc. Cancer Res.* 15, 607–612.
- Ryman, J.T., and Meibohm, B. (2017). Pharmacokinetics of Monoclonal Antibodies. *CPT Pharmacomet. Syst. Pharmacol.* 6, 576–588.
- Safaeian, M., Rajaraman, P., Hartge, P., Yeager, M., Linet, M., Butler, M.A., Ruder, A.M., Purdue, M.P., Hsing, A., Beane-Freeman, L., et al. (2013). Joint effects between five identified risk variants, allergy, and autoimmune conditions on glioma risk. *Cancer Causes Control CCC* 24, 1885–1891.
- Samarelli, A.V., Ziegler, T., Meves, A., Fässler, R., and Böttcher, R.T. (2020). Rabgap1 promotes recycling of active  $\beta 1$  integrins to support effective cell migration. *J. Cell Sci.*
- Sampath, D., Zabka, T.S., Misner, D.L., O'Brien, T., and Dragovich, P.S. (2015). Inhibition of nicotinamide phosphoribosyltransferase (NAMPT) as a therapeutic strategy in cancer. *Pharmacol. Ther.* 151, 16–31.
- Sangpairoj, K., Vivithanaporn, P., Apisawetakan, S., Chongthammakun, S., Sobhon, P., and Chaithirayanon, K. (2016). RUNX1 Regulates Migration, Invasion, and Angiogenesis via p38 MAPK Pathway in Human Glioblastoma. *Cell. Mol. Neurobiol.*
- Santos, V.C.F. dos, Almeida, N.B.F., Sousa, T.A.S.L. de, Araujo, E.N.D., Andrade, A.S.R. de, and Plentz, F. (2019). Real-time PCR for direct aptamer quantification on functionalized graphene surfaces. *Sci. Rep.* 9, 1–8.
- Schaffner, F., Ray, A.M., and Dontenwill, M. (2013). Integrin  $\alpha 5\beta 1$ , the Fibronectin Receptor, as a Pertinent Therapeutic Target in Solid Tumors. *Cancers* 5, 27–47.
- Schittenhelm, J., Schwab, E.I., Sperveslage, J., Tatagiba, M., Meyermann, R., Fend, F., Goodman, S.L., and Sipos, B. (2013). Longitudinal expression analysis of  $\alpha v$  integrins in human gliomas reveals upregulation of integrin  $\alpha v\beta 3$  as a negative prognostic factor. *J. Neuropathol. Exp. Neurol.* 72, 194–210.

- Schlaepfer, D.D., Broome, M.A., and Hunter, T. (1997). Fibronectin-stimulated signaling from a focal adhesion kinase-c-Src complex: involvement of the Grb2, p130cas, and Nck adaptor proteins. *Mol. Cell. Biol.* *17*, 1702–1713.
- Schmidt, M.H.H., Furnari, F.B., Cavenee, W.K., and Bögl, O. (2003). Epidermal growth factor receptor signaling intensity determines intracellular protein interactions, ubiquitination, and internalization. *Proc. Natl. Acad. Sci.* *100*, 6505–6510.
- Schnell, O., Krebs, B., Wagner, E., Romagna, A., Beer, A.J., Grau, S.J., Thon, N., Goetz, C., Kretzschmar, H.A., Tonn, J.-C., et al. (2008). Expression of integrin  $\alpha$ v $\beta$ 3 in gliomas correlates with tumor grade and is not restricted to tumor vasculature. *Brain Pathol. Zurich Switz.* *18*, 378–386.
- Sebastian, S., Settleman, J., Reshkin, S.J., Azzariti, A., Bellizzi, A., and Paradiso, A. (2006). The complexity of targeting EGFR signalling in cancer: From expression to turnover. *Biochim. Biophys. Acta BBA - Rev. Cancer* *1766*, 120–139.
- Sechi, S., Frappaolo, A., Belloni, G., Colotti, G., and Giansanti, M.G. (2015). The multiple cellular functions of the oncoprotein Golgi phosphoprotein 3. *Oncotarget* *6*, 3493–3506.
- Seymour, T., Nowak, A., and Kakulas, F. (2015). Targeting Aggressive Cancer Stem Cells in Glioblastoma. *Front. Oncol.* *5*.
- Sheng, Q., and Liu, J. (2011). The therapeutic potential of targeting the EGFR family in epithelial ovarian cancer. *Br. J. Cancer* *104*, 1241–1245.
- Shu, D., Li, H., Shu, Y., Xiong, G., Carson, W.E., Haque, F., Xu, R., and Guo, P. (2015). Systemic Delivery of Anti-miRNA for Suppression of Triple Negative Breast Cancer Utilizing RNA Nanotechnology. *ACS Nano* *9*, 9731–9740.
- Shui, B., Tao, D., Cheng, J., Mei, Y., Jaffrezic-Renault, N., and Guo, Z. (2018). A novel electrochemical aptamer–antibody sandwich assay for the detection of tau-381 in human serum. *Analyst* *143*, 3549–3554.
- Sigismund, S., Woelk, T., Puri, C., Maspero, E., Tacchetti, C., Transidico, P., Di Fiore, P.P., and Polo, S. (2005). Clathrin-independent endocytosis of ubiquitinated cargos. *Proc. Natl. Acad. Sci. U. S. A.* *102*, 2760–2765.
- Sigismund, S., Argenzio, E., Tosoni, D., Cavallaro, E., Polo, S., and Di Fiore, P.P. (2008). Clathrin-Mediated Internalization Is Essential for Sustained EGFR Signaling but Dispensable for Degradation. *Dev. Cell* *15*, 209–219.
- Simmons, M.L., Lamborn, K.R., Takahashi, M., Chen, P., Israel, M.A., Berger, M.S., Godfrey, T., Nigro, J., Prados, M., Chang, S., et al. (2001). Analysis of complex relationships between age, p53, epidermal growth factor receptor, and survival in glioblastoma patients. *Cancer Res.* *61*, 1122–1128.
- Singh, S.K., Hawkins, C., Clarke, I.D., Squire, J.A., Bayani, J., Hide, T., Henkelman, R.M., Cusimano, M.D., and Dirks, P.B. (2004). Identification of human brain tumour initiating cells. *Nature* *432*, 396–401.



Siwak, D.R., Carey, M., Hennessy, B.T., Nguyen, C.T., McGahren Murray, M.J., Nolden, L., and Mills, G.B. (2010). Targeting the Epidermal Growth Factor Receptor in Epithelial Ovarian Cancer: Current Knowledge and Future Challenges. *J. Oncol.* 2010.

Smolková, K., and Ježek, P. (2012). The Role of Mitochondrial NADPH-Dependent Isocitrate Dehydrogenase in Cancer Cells. *Int. J. Cell Biol.* 2012.

Snuderl, M., Fazlollahi, L., Le, L.P., Nitta, M., Zhelyazkova, B.H., Davidson, C.J., Akhavanfard, S., Cahill, D.P., Aldape, K.D., Betensky, R.A., et al. (2011). Mosaic Amplification of Multiple Receptor Tyrosine Kinase Genes in Glioblastoma. *Cancer Cell* 20, 810–817.

Solomón, M.T., Selva, J.C., Figueredo, J., Vaquer, J., Toledo, C., Quintanal, N., Salva, S., Domínguez, R., Alert, J., Marinello, J.J., et al. (2013). Radiotherapy plus nimotuzumab or placebo in the treatment of high grade glioma patients: results from a randomized, double blind trial. *BMC Cancer* 13, 299.

Soria, J.-C., Felip, E., Cobo, M., Lu, S., Syrigos, K., Lee, K.H., Göker, E., Georgoulas, V., Li, W., Isla, D., et al. (2015). Afatinib versus erlotinib as second-line treatment of patients with advanced squamous cell carcinoma of the lung (LUX-Lung 8): an open-label randomised controlled phase 3 trial. *Lancet Oncol.* 16, 897–907.

Sorkin, A., and Goh, L.K. (2008). Endocytosis and intracellular trafficking of ErbBs. *Exp. Cell Res.* 314, 3093–3106.

Sottoriva, A., Spiteri, I., Piccirillo, S.G.M., Touloumis, A., Collins, V.P., Marioni, J.C., Curtis, C., Watts, C., and Tavaré, S. (2013). Intratumor heterogeneity in human glioblastoma reflects cancer evolutionary dynamics. *Proc. Natl. Acad. Sci. U. S. A.* 110, 4009–4014.

Sousa, L.P., Lax, I., Shen, H., Ferguson, S.M., De Camilli, P., and Schlessinger, J. (2012). Suppression of EGFR endocytosis by dynamin depletion reveals that EGFR signaling occurs primarily at the plasma membrane. *Proc. Natl. Acad. Sci. U. S. A.* 109, 4419–4424.

Souza, A.G., Marangoni, K., Fujimura, P.T., Alves, P.T., Silva, M.J., Bastos, V.A.F., Goulart, L.R., and Goulart, V.A. (2016). 3D Cell-SELEX: Development of RNA aptamers as molecular probes for PC-3 tumor cell line. *Exp. Cell Res.* 341, 147–156.

Stevens, L.E., Cheung, W.K.C., Adua, S.J., Arnal-Estapé, A., Zhao, M., Liu, Z., Brewer, K., Herbst, R.S., and Nguyen, D.X. (2017). Extracellular Matrix Receptor Expression in Subtypes of Lung Adenocarcinoma Potentiates Outgrowth of Micrometastases. *Cancer Res.* 77, 1905–1917.

Stupack, D.G., and Cheresch, D.A. (2003). Apoptotic cues from the extracellular matrix: regulators of angiogenesis. *Oncogene* 22, 9022–9029.

Stupp, R., Mason, W.P., van den Bent, M.J., Weller, M., Fisher, B., Taphoorn, M.J.B., Belanger, K., Brandes, A.A., Marosi, C., Bogdahn, U., et al. (2005). Radiotherapy plus Concomitant and Adjuvant Temozolomide for Glioblastoma. *N. Engl. J. Med.* 352, 987–996.

Stupp, R., Hegi, M.E., Neyns, B., Goldbrunner, R., Schlegel, U., Clement, P.M.J., Grabenbauer, G.G., Oehsenbein, A.F., Simon, M., Dietrich, P.-Y., et al. (2010). Phase I/IIa study of

cilengitide and temozolomide with concomitant radiotherapy followed by cilengitide and temozolomide maintenance therapy in patients with newly diagnosed glioblastoma. *J. Clin. Oncol. Off. J. Am. Soc. Clin. Oncol.* *28*, 2712–2718.

Stupp, R., Hegi, M.E., Gorlia, T., Erridge, S.C., Perry, J., Hong, Y.-K., Aldape, K.D., Lhermitte, B., Pietsch, T., Grujicic, D., et al. (2014). Cilengitide combined with standard treatment for patients with newly diagnosed glioblastoma with methylated MGMT promoter (CENTRIC EORTC 26071-22072 study): a multicentre, randomised, open-label, phase 3 trial. *Lancet Oncol.* *15*, 1100–1108.

Sun, H., Tan, W., and Zu, Y. (2016). Aptamers: versatile molecular recognition probes for cancer detection. *The Analyst* *141*, 403–415.

Sun, J., Wang, X.-Y., Lv, P.-C., and Zhu, H.-L. (2015). Discovery of a series of novel phenylpiperazine derivatives as EGFR TK inhibitors. *Sci. Rep.* *5*.

Sun, L., Xu, X., Chen, Y., Zhou, Y., Tan, R., Qiu, H., Jin, L., Zhang, W., Fan, R., Hong, W., et al. (2018). Rab34 regulates adhesion, migration, and invasion of breast cancer cells. *Oncogene* *37*, 3698–3714.

Sun, Z., Costell, M., and Fässler, R. (2019). Integrin activation by talin, kindlin and mechanical forces. *Nat. Cell Biol.* *21*, 25–31.

Sundborger, A.C., and Hinshaw, J.E. (2014). Regulating dynamin dynamics during endocytosis. *F1000Prime Rep.* *6*.

Szerlip, N.J., Pedraza, A., Chakravarty, D., Azim, M., McGuire, J., Fang, Y., Ozawa, T., Holland, E.C., Huse, J.T., Jhanwar, S., et al. (2012). Intratumoral heterogeneity of receptor tyrosine kinases EGFR and PDGFRA amplification in glioblastoma defines subpopulations with distinct growth factor response. *Proc. Natl. Acad. Sci.* *109*, 3041–3046.

Takada, Y., Ye, X., and Simon, S. (2007). The integrins. *Genome Biol.* *8*, 215.

Takenaka, M., Okumura, Y., Amino, T., Miyachi, Y., Ogino, C., and Kondo, A. (2017). DNA-duplex linker for AFM-SELEX of DNA aptamer against human serum albumin. *Bioorg. Med. Chem. Lett.* *27*, 954–957.

Tamimi, A.F., and Juweid, M. (2017). Epidemiology and Outcome of Glioblastoma. In *Glioblastoma*, S. De Vleeschouwer, ed. (Brisbane (AU): Codon Publications), p.

Tan, W., and Fang, X. (2015). *Aptamers Selected by Cell-SELEX for Theranostics* (Springer).

Tan, X., Thapa, N., Sun, Y., and Anderson, R.A. (2015). A Kinase-Independent Role for EGF Receptor in Autophagy Initiation. *Cell* *160*, 145–160.

Tan, X., Lambert, P.F., Rapraeger, A.C., and Anderson, R.A. (2016). Stress-Induced EGFR Trafficking: Mechanisms, Functions, and Therapeutic Implications. *Trends Cell Biol.* *26*, 352–366.

Tarone, G., Hirsch, E., Brancaccio, M., De Acetis, M., Barberis, L., Balzac, F., Retta, S.F., Botta, C., Altruda, F., Silengo, L., et al. (2000). Integrin function and regulation in development. *Int. J. Dev. Biol.* *44*, 725–731.

- Tawiah, K.D., Porciani, D., and Burke, D.H. (2017). Toward the Selection of Cell Targeting Aptamers with Extended Biological Functionalities to Facilitate Endosomal Escape of Cargoes. *Biomedicines* 5.
- Taylor, T.E., Furnari, F.B., and Cavenee, W.K. (2012). Targeting EGFR for treatment of glioblastoma: molecular basis to overcome resistance. *Curr. Cancer Drug Targets* 12, 197–209.
- Thakkar, J.P., Dolecek, T.A., Horbinski, C., Ostrom, Q.T., Lightner, D.D., Barnholtz-Sloan, J.S., and Villano, J.L. (2014). Epidemiologic and Molecular Prognostic Review of Glioblastoma. *Cancer Epidemiol. Biomark. Prev. Publ. Am. Assoc. Cancer Res. Cosponsored Am. Soc. Prev. Oncol.* 23, 1985–1996.
- Theret, L., Jeanne, A., Langlois, B., Hachet, C., David, M., Khrestchatisky, M., Devy, J., Hervé, E., Almagro, S., and Dedieu, S. (2017). Identification of LRP-1 as an endocytosis and recycling receptor for  $\beta$ 1-integrin in thyroid cancer cells. *Oncotarget* 8, 78614–78632.
- Thiel, K.W., Hernandez, L.I., Dassie, J.P., Thiel, W.H., Liu, X., Stockdale, K.R., Rothman, A.M., Hernandez, F.J., McNamara, J.O., and Giangrande, P.H. (2012). Delivery of chemosensitizing siRNAs to HER2+ breast cancer cells using RNA aptamers. *Nucleic Acids Res.* 40, 6319–6337.
- Thompson, D.M., and Gill, G.N. (1985). The EGF receptor: structure, regulation and potential role in malignancy. *Cancer Surv.* 4, 767–788.
- Thuault, S., Hayashi, S., Lagirand-Cantaloube, J., Plutoni, C., Comunale, F., Delattre, O., Relaix, F., and Gauthier-Rouvière, C. (2013). P-cadherin is a direct PAX3-FOXO1A target involved in alveolar rhabdomyosarcoma aggressiveness. *Oncogene* 32, 1876–1887.
- Tomas, A., Futter, C.E., and Eden, E.R. (2014). EGF receptor trafficking: consequences for signaling and cancer. *Trends Cell Biol.* 24, 26–34.
- Tomas, A., Vaughan, S.O., Burgoyne, T., Sorkin, A., Hartley, J.A., Hochhauser, D., and Futter, C.E. (2015). WASH and Tsg101/ALIX-dependent diversion of stress-internalized EGFR from the canonical endocytic pathway. *Nat. Commun.* 6, 7324.
- Tomas, A., Jones, S., Vaughan, S.O., Hochhauser, D., and Futter, C.E. (2017). Stress-specific p38 MAPK activation is sufficient to drive EGFR endocytosis but not its nuclear translocation. *J. Cell Sci.* 130, 2481–2490.
- Tong, X., Yang, P., Wang, K., Liu, Y., Liu, X., Shan, X., Huang, R., Zhang, K., and Wang, J. (2019). Survivin is a prognostic indicator in glioblastoma and may be a target of microRNA-218. *Oncol. Lett.* 18, 359–367.
- Totaro, A., Panciera, T., and Piccolo, S. (2018). YAP/TAZ upstream signals and downstream responses. *Nat. Cell Biol.* 20, 888–899.
- Tubbesing, K., Ward, J., Abini-Agbomson, R., Malhotra, A., Rudkouskaya, A., Warren, J., Lamar, J., Martino, N., Adam, A.P., and Barroso, M. (2020). Complex Rab4-Mediated Regulation of Endosomal Size and EGFR Activation. *Mol. Cancer Res.* 18, 757–773.
- Tuerk, C., and Gold, L. (1990). Systematic evolution of ligands by exponential enrichment: RNA ligands to bacteriophage T4 DNA polymerase. *Science* 249, 505–510.

- Umehara, T., Fukuda, K., Nishikawa, F., Sekiya, S., Kohara, M., Hasegawa, T., and Nishikawa, S. (2004). Designing and analysis of a potent bi-functional aptamers that inhibit protease and helicase activities of HCV NS3. *Nucleic Acids Symp. Ser.* 2004 195–196.
- Valente, P., Fassina, G., Melchiori, A., Masiello, L., Cilli, M., Vacca, A., Onisto, M., Santi, L., Stetler-Stevenson, W.G., and Albini, A. (1998). TIMP-2 over-expression reduces invasion and angiogenesis and protects B16F10 melanoma cells from apoptosis. *Int. J. Cancer* 75, 246–253.
- Van Den Bent, M., Eoli, M., Sepulveda, J.M., Smits, M., Walenkamp, A., Frenel, J.-S., Franceschi, E., Clement, P.M., Chinot, O., De Vos, F., et al. (2020). INTELLANCE 2/EORTC 1410 randomized phase II study of Depatux-M alone and with temozolomide vs temozolomide or lomustine in recurrent EGFR amplified glioblastoma. *Neuro-Oncol.* 22, 684–693.
- Vanhaesebroeck, B., Stephens, L., and Hawkins, P. (2012). PI3K signalling: the path to discovery and understanding. *Nat. Rev. Mol. Cell Biol.* 13, 195–203.
- Vanlandingham, P.A., and Ceresa, B.P. (2009). Rab7 regulates late endocytic trafficking downstream of multivesicular body biogenesis and cargo sequestration. *J. Biol. Chem.* 284, 12110–12124.
- Varkouhi, A.K., Scholte, M., Storm, G., and Haisma, H.J. (2011). Endosomal escape pathways for delivery of biologicals. *J. Control. Release Off. J. Control. Release Soc.* 151, 220–228.
- Vater, A., and Klussmann, S. (2015). Turning mirror-image oligonucleotides into drugs: the evolution of Spiegelmer(®) therapeutics. *Drug Discov. Today* 20, 147–155.
- Vehlow, A., and Cordes, N. (2013). Invasion as target for therapy of glioblastoma multiforme. *Biochim. Biophys. Acta* 1836, 236–244.
- Velpula, K.K., Dasari, V.R., Asuthkar, S., Gorantla, B., and Tsung, A.J. (2012). EGFR and c-Met Cross Talk in Glioblastoma and Its Regulation by Human Cord Blood Stem Cells. *Transl. Oncol.* 5, 379-IN18.
- Verhaak, R.G.W., Hoadley, K.A., Purdom, E., Wang, V., Qi, Y., Wilkerson, M.D., Miller, C.R., Ding, L., Golub, T., Mesirov, J.P., et al. (2010). Integrated genomic analysis identifies clinically relevant subtypes of glioblastoma characterized by abnormalities in PDGFRA, IDH1, EGFR, and NF1. *Cancer Cell* 17, 98–110.
- Verma, N., Rai, A.K., Kaushik, V., Brünnert, D., Chahar, K.R., Pandey, J., and Goyal, P. (2016). Identification of gefitinib off-targets using a structure-based systems biology approach; their validation with reverse docking and retrospective data mining. *Sci. Rep.* 6, 33949.
- Wakeling, A.E., Guy, S.P., Woodburn, J.R., Ashton, S.E., Curry, B.J., Barker, A.J., and Gibson, K.H. (2002). ZD1839 (Iressa): An Orally Active Inhibitor of Epidermal Growth Factor Signaling with Potential for Cancer Therapy. *Cancer Res.* 62, 5749–5754.
- Wallukat, G., Müller, J., Haberland, A., Berg, S., Schulz, A., Freyse, E.-J., Vetter, R., Salzsieder, E., Kreutz, R., and Schimke, I. (2016). Aptamer BC007 for neutralization of pathogenic autoantibodies directed against G-protein coupled receptors: A vision of future treatment of patients with cardiomyopathies and positivity for those autoantibodies. *Atherosclerosis* 244, 44–47.

- Walsh, A.M., and Lazzara, M.J. (2013). Regulation of EGFR trafficking and cell signaling by Sprouty2 and MIG6 in lung cancer cells. *J. Cell Sci.* *126*, 4339–4348.
- Walsh, A.M., Kapoor, G.S., Buonato, J.M., Mathew, L.K., Bi, Y., Davuluri, R.V., Martinez-Lage, M., Simon, M.C., O'Rourke, D.M., and Lazzara, M.J. (2015). Sprouty2 Drives Drug Resistance and Proliferation in Glioblastoma. *Mol. Cancer Res. MCR* *13*, 1227–1237.
- Wan, L.-Y., Yuan, W.-F., Ai, W.-B., Ai, Y.-W., Wang, J.-J., Chu, L.-Y., Zhang, Y.-Q., and Wu, J.-F. (2019). An exploration of aptamer internalization mechanisms and their applications in drug delivery. *Expert Opin. Drug Deliv.* *16*, 207–218.
- Wang, X., and Gerdes, H.-H. (2015). Transfer of mitochondria via tunneling nanotubes rescues apoptotic PC12 cells. *Cell Death Differ.* *22*, 1181–1191.
- Wang, H., Wang, H., Zhang, W., Huang, H.J., Liao, W.S.L., and Fuller, G.N. (2004a). Analysis of the activation status of Akt, NFkappaB, and Stat3 in human diffuse gliomas. *Lab. Investig. J. Tech. Methods Pathol.* *84*, 941–951.
- Wang, H., Song, X., Huang, Q., Xu, T., Yun, D., Wang, Y., Hu, L., Yan, Y., Chen, H., Lu, D., et al. (2019a). LGALS3 Promotes Treatment Resistance in Glioblastoma and Is Associated with Tumor Risk and Prognosis. *Cancer Epidemiol. Prev. Biomark.* *28*, 760–769.
- Wang, J., Zhou, P., Wang, X., Yu, Y., Zhu, G., Zheng, L., Xu, Z., Li, F., You, Q., Yang, Q., et al. (2019b). Rab25 promotes erlotinib resistance by activating the  $\beta 1$  integrin/AKT/ $\beta$ -catenin pathway in NSCLC. *Cell Prolif.* e12592.
- Wang, Q., Hu, B., Hu, X., Kim, H., Squatrito, M., Scarpace, L., deCarvalho, A.C., Lyu, S., Li, P., Li, Y., et al. (2017a). Tumor evolution of glioma intrinsic gene expression subtype associates with immunological changes in the microenvironment. *Cancer Cell* *32*, 42-56.e6.
- Wang, S., Cang, S., and Liu, D. (2016). Third-generation inhibitors targeting EGFR T790M mutation in advanced non-small cell lung cancer. *J. Hematol. Oncol. J Hematol Oncol* *9*.
- Wang, X., Wang, Z., Zhang, Y., Wang, Y., Zhang, H., Xie, S., Xie, P., Yu, R., and Zhou, X. (2019c). Golgi phosphoprotein 3 sensitizes the tumour suppression effect of gefitinib on gliomas. *Cell Prolif.* *52*, e12636.
- Wang, Y., Pennock, S., Chen, X., and Wang, Z. (2002). Endosomal Signaling of Epidermal Growth Factor Receptor Stimulates Signal Transduction Pathways Leading to Cell Survival. *Mol. Cell. Biol.* *22*, 7279–7290.
- Wang, Y., Fei, D., Vanderlaan, M., and Song, A. (2004b). Biological activity of bevacizumab, a humanized anti-VEGF antibody in vitro. *Angiogenesis* *7*, 335–345.
- Wang, Y., Arjonen, A., Pouwels, J., Ta, H., Pausch, P., Bange, G., Engel, U., Pan, X., Fackler, O.T., Ivaska, J., et al. (2015). Formin-like 2 Promotes  $\beta 1$ -Integrin Trafficking and Invasive Motility Downstream of PKC $\alpha$ . *Dev. Cell* *34*, 475–483.
- Wang, Y., Chen, X., Tian, B., Liu, J., Yang, L., Zeng, L., Chen, T., Hong, A., and Wang, X. (2017b). Nucleolin-targeted Extracellular Vesicles as a Versatile Platform for Biologics Delivery to Breast Cancer. *Theranostics* *7*, 1360–1372.

- Weihua, Z., Tsan, R., Huang, W.-C., Wu, Q., Chiu, C.-H., Fidler, I.J., and Hung, M.-C. (2008). Survival of cancer cells is maintained by EGFR independent of its kinase activity. *Cancer Cell* *13*, 385–393.
- Weil, S., Osswald, M., Solecki, G., Grosch, J., Jung, E., Lemke, D., Ratliff, M., Hänggi, D., Wick, W., and Winkler, F. (2017). Tumor microtubules convey resistance to surgical lesions and chemotherapy in gliomas. *Neuro-Oncol.* *19*, 1316–1326.
- Weller, M., Nabors, L.B., Gorlia, T., Leske, H., Rushing, E., Bady, P., Hicking, C., Perry, J., Hong, Y.-K., Roth, P., et al. (2016). Cilengitide in newly diagnosed glioblastoma: biomarker expression and outcome. *Oncotarget* *7*, 15018–15032.
- Weller, M., Butowski, N., Tran, D.D., Recht, L.D., Lim, M., Hirte, H., Ashby, L., Mechtler, L., Goldlust, S.A., Iwamoto, F., et al. (2017). Rindopepimut with temozolomide for patients with newly diagnosed, EGFRvIII-expressing glioblastoma (ACT IV): a randomised, double-blind, international phase 3 trial. *Lancet Oncol.* *18*, 1373–1385.
- Westphal, M., Heese, O., Steinbach, J.P., Schnell, O., Schackert, G., Mehdorn, M., Schulz, D., Simon, M., Schlegel, U., Senft, C., et al. (2015). A randomised, open label phase III trial with nimotuzumab, an anti-epidermal growth factor receptor monoclonal antibody in the treatment of newly diagnosed adult glioblastoma. *Eur. J. Cancer Oxf. Engl.* *1990* *51*, 522–532.
- Wheeler, D.B., Zoncu, R., Root, D.E., Sabatini, D.M., and Sawyers, C.L. (2015). Identification of an oncogenic RAB protein. *Science* *350*, 211–217.
- Whitman, M., Downes, C.P., Keeler, M., Keller, T., and Cantley, L. (1988). Type I phosphatidylinositol kinase makes a novel inositol phospholipid, phosphatidylinositol-3-phosphate. *Nature* *332*, 644–646.
- Wick, W., Platten, M., and Weller, M. (2009). New (alternative) temozolomide regimens for the treatment of glioma. *Neuro-Oncol.* *11*, 69–79.
- Wick, W., Puduvalli, V.K., Chamberlain, M.C., van den Bent, M.J., Carpentier, A.F., Cher, L.M., Mason, W., Weller, M., Hong, S., Musib, L., et al. (2010). Phase III study of enzastaurin compared with lomustine in the treatment of recurrent intracranial glioblastoma. *J. Clin. Oncol. Off. J. Am. Soc. Clin. Oncol.* *28*, 1168–1174.
- Wieduwilt, M.J., and Moasser, M.M. (2008). The epidermal growth factor receptor family: Biology driving targeted therapeutics. *Cell. Mol. Life Sci.* *65*, 1566–1584.
- Williams, K.C., and Coppolino, M.G. (2014). SNARE-dependent interaction of Src, EGFR and  $\beta$ 1 integrin regulates invadopodia formation and tumor cell invasion. *J. Cell Sci.* *127*, 1712–1725.
- Williams, R.L., and Urbé, S. (2007). The emerging shape of the ESCRT machinery. *Nat. Rev. Mol. Cell Biol.* *8*, 355–368.
- Winograd-Katz, S.E., and Levitzki, A. (2006). Cisplatin induces PKB/Akt activation and p38 MAPK phosphorylation of the EGF receptor. *Oncogene* *25*, 7381–7390.
- Winograd-Katz, S.E., Fässler, R., Geiger, B., and Legate, K.R. (2014). The integrin adhesome: from genes and proteins to human disease. *Nat. Rev. Mol. Cell Biol.* *15*, 273–288.

- Wu, X., Liang, H., Tan, Y., Yuan, C., Li, S., Li, X., Li, G., Shi, Y., and Zhang, X. (2014). Cell-SELEX Aptamer for Highly Specific Radionuclide Molecular Imaging of Glioblastoma In Vivo. *PLoS ONE* 9.
- Wu, X., Zhao, Z., Bai, H., Fu, T., Yang, C., Hu, X., Liu, Q., Champanhac, C., Teng, I.-T., Ye, M., et al. (2015). DNA Aptamer Selected against Pancreatic Ductal Adenocarcinoma for in vivo Imaging and Clinical Tissue Recognition. *Theranostics* 5, 985–994.
- Xiang, D., Zheng, C., Zhou, S.-F., Qiao, S., Tran, P.H.-L., Pu, C., Li, Y., Kong, L., Kouzani, A.Z., Lin, J., et al. (2015). Superior Performance of Aptamer in Tumor Penetration over Antibody: Implication of Aptamer-Based Theranostics in Solid Tumors. *Theranostics* 5, 1083–1097.
- Xiao, T., Takagi, J., Collier, B.S., Wang, J.-H., and Springer, T.A. (2004). Structural basis for allostery in integrins and binding to fibrinogen-mimetic therapeutics. *Nature* 432, 59–67.
- Xiong, J., Zhou, L., Yang, M., Lim, Y., Zhu, Y., Fu, D., Li, Z., Zhong, J., Xiao, Z., and Zhou, X.-F. (2013). ProBDNF and its receptors are upregulated in glioma and inhibit the growth of glioma cells in vitro. *Neuro-Oncol.* 15, 990–1007.
- Xiong, J.P., Stehle, T., Diefenbach, B., Zhang, R., Dunker, R., Scott, D.L., Joachimiak, A., Goodman, S.L., and Arnaout, M.A. (2001). Crystal structure of the extracellular segment of integrin alpha Vbeta3. *Science* 294, 339–345.
- Xiong, J.-P., Stehle, T., Zhang, R., Joachimiak, A., Frech, M., Goodman, S.L., and Arnaout, M.A. (2002). Crystal structure of the extracellular segment of integrin alpha Vbeta3 in complex with an Arg-Gly-Asp ligand. *Science* 296, 151–155.
- Xu, H., Zong, H., Ma, C., Ming, X., Shang, M., Li, K., He, X., Du, H., and Cao, L. (2017a). Epidermal growth factor receptor in glioblastoma. *Oncol. Lett.* 14, 512–516.
- Xu, M.J., Johnson, D.E., and Grandis, J.R. (2017b). EGFR-targeted therapies in the post-genomic era. *Cancer Metastasis Rev.* 36, 463–473.
- Yamada, H., Takeda, T., Michiue, H., Abe, T., and Takei, K. (2016). Actin bundling by dynamin 2 and cortactin is implicated in cell migration by stabilizing filopodia in human non-small cell lung carcinoma cells. *Int. J. Oncol.* 49, 877–886.
- Yamada, S., Bu, X.-Y., Khankaldyyan, V., Gonzales-Gomez, I., McComb, J.G., and Laug, W.E. (2006). Effect of the angiogenesis inhibitor Cilengitide (EMD 121974) on glioblastoma growth in nude mice. *Neurosurgery* 59, 1304–1312; discussion 1312.
- Yamaoka, T., Ohmori, T., Inoue, F., Kadofuku, T., Ando, K., Ishida, H., Hosaka, T., Shirai, T., Matsuda, M., Noda, M., et al. (2004). Enhancement of Epidermal Growth Factor Receptor-degradation Pathway in Acquired Gefitinib-resistant Human Non-small Cell Lung Cancer Cell Lines. *Showa Univ. J. Med. Sci.* 16, 147–159.
- Yang, R., Li, X., Wu, Y., Zhang, G., Liu, X., Li, Y., Bao, Y., Yang, W., and Cui, H. (2020). EGFR activates GDH1 transcription to promote glutamine metabolism through MEK/ERK/ELK1 pathway in glioblastoma. *Oncogene* 39, 2975–2986.

Yang, W., Wu, P., Ma, J., Liao, M., Wang, X., Xu, L., Xu, M., and Yi, L. (2019). Sortilin promotes glioblastoma invasion and mesenchymal transition through GSK-3 $\beta$ / $\beta$ -catenin/twist pathway. *Cell Death Dis.* *10*.

Yang, X., Zhuo, Y., Zhu, S., Luo, Y., Feng, Y., and Xu, Y. (2015). Selectively assaying CEA based on a creative strategy of gold nanoparticles enhancing silver nanoclusters' fluorescence. *Biosens. Bioelectron.* *64*, 345–351.

Yang, Y., Guo, Q., Chen, X., Zhang, J., Guo, H., Qian, W., Hou, S., Dai, J., Li, B., Guo, Y., et al. (2016). Preclinical studies of a Pro-antibody-drug conjugate designed to selectively target EGFR-overexpressing tumors with improved therapeutic efficacy. *MAbs* *8*, 405–413.

Yang, Y., Yang, X., Zou, X., Wu, S., Wan, D., Cao, A., Liao, L., Yuan, Q., and Duan, X. (2017). Ultrafine Graphene Nanomesh with Large On/Off Ratio for High-Performance Flexible Biosensors. *Adv. Funct. Mater.* *27*, 1604096.

Ye, B., Duan, B., Deng, W., Wang, Y., Chen, Y., Cui, J., Sun, S., Zhang, Y., Du, J., Gu, L., et al. (2018). EGF Stimulates Rab35 Activation and Gastric Cancer Cell Migration by Regulating DENND1A-Grb2 Complex Formation. *Front. Pharmacol.* *9*.

Ye, C., Pan, B., Xu, H., Zhao, Z., Shen, J., Lu, J., Yu, R., and Liu, H. (2019). Co-delivery of GOLPH3 siRNA and gefitinib by cationic lipid-PLGA nanoparticles improves EGFR-targeted therapy for glioma. *J. Mol. Med. Berl. Ger.*

Ye, X., Shi, H., He, X., Wang, K., He, D., Yan, L., Xu, F., Lei, Y., Tang, J., and Yu, Y. (2015). Iodide-Responsive Cu–Au Nanoparticle-Based Colorimetric Platform for Ultrasensitive Detection of Target Cancer Cells. *Anal. Chem.* *87*, 7141–7147.

Yeh, Y.-C., Ling, J.-Y., Chen, W.-C., Lin, H.-H., and Tang, M.-J. (2017). Mechanotransduction of matrix stiffness in regulation of focal adhesion size and number: reciprocal regulation of caveolin-1 and  $\beta$ 1 integrin. *Sci. Rep.* *7*, 1–14.

Ying, H., Zheng, H., Scott, K., Wiedemeyer, R., Yan, H., Lim, C., Huang, J., Dhakal, S., Ivanova, E., Xiao, Y., et al. (2010). Mig-6 controls EGFR trafficking and suppresses gliomagenesis. *Proc. Natl. Acad. Sci. U. S. A.* *107*, 6912–6917.

Yu, W., Zhang, L., Wei, Q., and Shao, A. (2020). O6-Methylguanine-DNA Methyltransferase (MGMT): Challenges and New Opportunities in Glioma Chemotherapy. *Front. Oncol.* *9*.

Zahonero, C., Aguilera, P., Ramírez-Castillejo, C., Pajares, M., Bolós, M.V., Cantero, D., Perez-Nuñez, A., Hernández-Lain, A., Sánchez-Gómez, P., and Sepúlveda, J.M. (2015). Preclinical Test of Dacomitinib, an Irreversible EGFR Inhibitor, Confirms Its Effectiveness for Glioblastoma. *Mol. Cancer Ther.* *14*, 1548–1558.

Zaidel-Bar, R., and Geiger, B. (2010). The switchable integrin adhesome. *J. Cell Sci.* *123*, 1385–1388.

Zaidel-Bar, R., Itzkovitz, S., Ma'ayan, A., Iyengar, R., and Geiger, B. (2007). Functional atlas of the integrin adhesome. *Nat. Cell Biol.* *9*, 858–867.

Zamay, G.S., Ivanchenko, T.I., Zamay, T.N., Grigorieva, V.L., Glazyrin, Y.E., Kolovskaya, O.S., Garanzha, I.V., Barinov, A.A., Krat, A.V., Mironov, G.G., et al. (2017). DNA Aptamers



for the Characterization of Histological Structure of Lung Adenocarcinoma. *Mol. Ther. Nucleic Acids* 6, 150–162.

Zamay, T.N., Kolovskaya, O.S., Glazyrin, Y.E., Zamay, G.S., Kuznetsova, S.A., Spivak, E.A., Wehbe, M., Savitskaya, A.G., Zubkova, O.A., Kadkina, A., et al. (2014). DNA-aptamer targeting vimentin for tumor therapy in vivo. *Nucleic Acid Ther.* 24, 160–170.

Zeng, Z., Zhang, P., Zhao, N., Sheehan, A.M., Tung, C.-H., Chang, C.-C., and Zu, Y. (2010). Using oligonucleotide aptamer probes for immunostaining of formalin-fixed and paraffin-embedded tissues. *Mod. Pathol. Off. J. U. S. Can. Acad. Pathol. Inc* 23, 1553–1558.

Zhang, K., and Chen, J. (2012). The regulation of integrin function by divalent cations. *Cell Adhes. Migr.* 6, 20–29.

Zhang, F., Li, S., Cao, K., Wang, P., Su, Y., Zhu, X., and Wan, Y. (2015a). A Microfluidic Love-Wave Biosensing Device for PSA Detection Based on an Aptamer Beacon Probe. *Sensors* 15, 13839–13850.

Zhang, H., Zhou, Y., Cui, B., Liu, Z., and Shen, H. (2020a). Novel insights into astrocyte-mediated signaling of proliferation, invasion and tumor immune microenvironment in glioblastoma. *Biomed. Pharmacother.* 126, 110086.

Zhang, J.G., Eguchi, J., Kruse, C.A., Gomez, G.G., Fakhrai, H., Schroter, S., Ma, W., Hoa, N., Minev, B., Delgado, C., et al. (2007a). Antigenic profiling of glioma cells to generate allogeneic vaccines or dendritic cell-based therapeutics. *Clin. Cancer Res. Off. J. Am. Assoc. Cancer Res.* 13, 566–575.

Zhang, L., Xie, B., Qiu, Y., Jing, D., Zhang, J., Duan, Y., Li, Z., Fan, M., He, J., Qiu, Y., et al. (2020b). Rab25-Mediated EGFR Recycling Causes Tumor Acquired Radioresistance. *IScience* 23.

Zhang, X., Ding, Z., Mo, J., Sang, B., Shi, Q., Hu, J., Xie, S., Zhan, W., Lu, D., Yang, M., et al. (2015b). GOLPH3 promotes glioblastoma cell migration and invasion via the mTOR-YB1 pathway in vitro. *Mol. Carcinog.* 54, 1252–1263.

Zhang, Y., Gao, H., Zhou, W., Sun, S., Zeng, Y., Zhang, H., Liang, L., Xiao, X., Song, J., Ye, M., et al. (2018). Targeting c-met receptor tyrosine kinase by the DNA aptamer SL1 as a potential novel therapeutic option for myeloma. *J. Cell. Mol. Med.* 22, 5978–5990.

Zhang, Y., Lai, B.S., and Juhas, M. (2019). Recent Advances in Aptamer Discovery and Applications. *Mol. Basel Switz.* 24.

Zhang, Y.-W., Staal, B., Su, Y., Swiatek, P., Zhao, P., Cao, B., Resau, J., Sigler, R., Bronson, R., and Vande Woude, G.F. (2007b). Evidence that MIG-6 is a tumor-suppressor gene. *Oncogene* 26, 269–276.

Zhao, B., Wu, P., Zhang, H., and Cai, C. (2015). Designing activatable aptamer probes for simultaneous detection of multiple tumor-related proteins in living cancer cells. *Biosens. Bioelectron.* 68, 763–770.

Zheng, J., Duan, B., Sun, S., Cui, J., Du, J., and Zhang, Y. (2017). Folliculin Interacts with Rab35 to Regulate EGF-Induced EGFR Degradation. *Front. Pharmacol.* 8.

Zhou, J., and Rossi, J. (2017). Aptamers as targeted therapeutics: current potential and challenges. *Nat. Rev. Drug Discov.* *16*, 181–202.

Zhou, W., and Wahl, D.R. (2019). Metabolic Abnormalities in Glioblastoma and Metabolic Strategies to Overcome Treatment Resistance. *Cancers* *11*.

Zhou, X., Xie, S., Wu, S., Qi, Y., Wang, Z., Zhang, H., Lu, D., Wang, X., Dong, Y., Liu, G., et al. (2017). Golgi phosphoprotein 3 promotes glioma progression via inhibiting Rab5-mediated endocytosis and degradation of epidermal growth factor receptor. *Neuro-Oncol.* *19*, 1628–1639.

Zhu, Z. (2007). Targeted cancer therapies based on antibodies directed against epidermal growth factor receptor: status and perspectives. *Acta Pharmacol. Sin.* *28*, 1476–1493.

Zhu, G., and Chen, X. (2018). Aptamer-based targeted therapy. *Adv. Drug Deliv. Rev.* *134*, 65–78.

Zhu, G., Niu, G., and Chen, X. (2015a). Aptamer-Drug Conjugates. *Bioconjug. Chem.* *26*, 2186–2197.

Zhu, Q., Liu, G., and Kai, M. (2015b). DNA Aptamers in the Diagnosis and Treatment of Human Diseases. *Molecules* *20*, 20979–20997.

Zhu, W., Zhou, L., Qian, J.-Q., Qiu, T.-Z., Shu, Y.-Q., and Liu, P. (2014). Temozolomide for treatment of brain metastases: A review of 21 clinical trials. *World J. Clin. Oncol.* *5*, 19–27.

Zhu, Y., Xu, Z., Gao, J., Ji, W., and Zhang, J. (2020). An antibody-aptamer sandwich cathodic photoelectrochemical biosensor for the detection of progesterone. *Biosens. Bioelectron.* *160*, 112210.

Zscheppang, K., Kurth, I., Wachtel, N., Dubrovskaja, A., Kunz-Schughart, L.A., and Cordes, N. (2016). Efficacy of Beta1 Integrin and EGFR Targeting in Sphere-Forming Human Head and Neck Cancer Cells. *J. Cancer* *7*, 736–745.

Zwang, Y., and Yarden, Y. (2006). p38 MAP kinase mediates stress-induced internalization of EGFR: implications for cancer chemotherapy. *EMBO J.* *25*, 4195–4206.

# Résumé

## Synopsis

Ce manuscrit de thèse, intitulé "Stratégies de l'endocytose non physiologique de l'EGFR et de vectorisation par des aptamères", est présenté ainsi :

### Introduction :

Les caractéristiques des glioblastomes (GBM) et ses principaux challenges thérapeutiques sont présentés, puis deux cibles thérapeutiques des GBM sont décrites : l'EGFR (Epidermal Growth Factor Receptor) et l'intégrine  $\alpha 5\beta 1$ . Enfin, les aptamères, petites molécules d'acides nucléiques, également appelés anticorps chimiques, sont décrits en tant qu'alternative aux anticorps comme outils de vectorisation et de détection.

### Matériel et Méthodes :

Une partie méthodologie montre les expériences réalisées durant mon doctorat.

### Résultats :

Les résultats sont présentés sous la forme de trois articles scientifiques, 2 publiés et 1 soumis et d'une section de résultats non publiés. Les deux objectifs principaux de mon doctorat sont :

(1) la description de l'effet des inhibiteurs de l'activité tyrosine kinase (TKI) de l'EGFR, utilisés en clinique, sur l'endocytose de deux cibles thérapeutiques dans des modèles cellulaires de GBM. Nous avons d'abord décrit que les TKI de l'EGFR déclenchent une endocytose non-physiologique de l'EGFR et de l'intégrine  $\alpha 5\beta 1$ , qui peut moduler l'invasion des cellules de gliome sous traitement thérapeutique (Blandin, Cruz da Silva et al., 2020). Afin de mieux comprendre le mécanisme moléculaire, nous avons identifié plusieurs protéines impliquées dans cette endocytose non physiologique (Cruz da Silva et al, soumis à FASEB J).

(2) la validation d'aptamères ciblant l'intégrine  $\alpha 5\beta 1$  ou l'EGFR pour le diagnostic et la délivrance intracellulaire d'agents cytotoxiques. Nous avons d'abord décrit et caractérisé l'aptamère H02, un nouvel aptamère ciblant l'intégrine  $\alpha 5$ . Son affinité et sa spécificité vis-à-vis des cellules GBM et des tissus tumoraux exprimant l'intégrine  $\alpha 5$  ont été déterminées (Fechter, Cruz Da Silva et al, 2019). Les aptamères ciblant l'EGFR sont décrits et étudiés dans la 4e section. Les aptamères ciblant l'intégrine  $\alpha 5$  ou l'EGFR ont été utilisés en aptafluorescence sur cellules et tissus de GBM (Cruz da Silva, en cours de rédaction).

## Discussion

Enfin, une discussion critique sur les principaux résultats expérimentaux de ma thèse est présentée. Quelques résultats préliminaires et perspectives d'avenir sont également avancés.

## Annexes

L'annexe 1 présente un projet de revue sur les thérapies moléculaires ciblées pour le glioblastome en phases II, III, IV (Cruz da Silva et al., en cours de rédaction).

L'annexe 2 présente une revue sur le rôle des intégrines dans la résistance aux thérapies ciblées sur les récepteurs de tyrosine kinase dans le cancer (Cruz da Silva et al., 2019).

L'annexe 3 présente un article scientifique caractérisant la conjugaison des particules d'or au cétuximab, un anticorps anti-EGFR. Ce travail est le résultat d'une collaboration avec l'équipe du Dr Guy Zuber (UMR 7242).

# Introduction

## 1. Glioblastome

### **Definition**

Le glioblastome (GBM) est la tumeur cérébrale la plus fréquente et la plus agressive. Le GBM représente 60% de tous les cas de cancer du cerveau chez les adultes. Cette tumeur se caractérise par sa forte résistance à la radiothérapie et à la chimiothérapie, ainsi qu'aux thérapies ciblées (Thakkar et al., 2014). La survie médiane est de 15 mois. Le traitement standard des GBM repose sur une résection chirurgicale suivie d'une radiothérapie et d'une chimiothérapie concomitante pendant 6 semaines. La chimiothérapie est ensuite poursuivie seule toutes les quatre semaines (Stupp et al., 2005). La chimiothérapie utilisée est le temozolomide (TMZ), un agent alkylant qui provoque des dommages à l'ADN, un arrêt du cycle cellulaire et l'apoptose des cellules (Agarwala and Kirkwood, 2000).

### **Caractérisation moléculaire des GBM**

La classification de l'Organisation Mondiale de la Santé (OMS) datant de 2007 décrit 3 grands groupes de tumeurs cérébrales non-neuronales : l'astrocytome (grade I à IV), l'oligodendrogliome (grade II à III) et l'oligoastrocytome (grade II à III). Les tumeurs cérébrales ont été classées en fonction de leurs caractéristiques anatomopathologiques (Louis et al., 2007). En 2016, une nouvelle classification est proposée, basée sur un diagnostic intégré avec des caractéristiques phénotypiques et génotypiques (Louis et al., 2016). Les GBM sont maintenant classées comme des tumeurs astrocytaires et oligodendrocytaires diffuses de grade IV. Ces tumeurs font l'objet d'une ségrégation supplémentaire en fonction du statut du gène isocitrate déshydrogénase (IDH). 90 % des GBM expriment un gène IDH de type sauvage et les 10 % restants expriment des formes mutantes (Cohen et al., 2013).

La classification moléculaire actuelle de l'OMS ne représente pas l'hétérogénéité moléculaire des GBM.

Le groupe de Verhaak a réalisé des analyses transcriptomiques de 200 biopsies de GBM humains, démontre pour la première fois une hétérogénéité moléculaire inter-tumorale. Cette classification divise les GBM en 4 groupes en fonction de leur profil moléculaire : classique, mésoenchymateux, proneural et neural (Verhaak et al., 2010). Le GBM classique se caractérise

par des niveaux élevés du gène *erbB1* (codant pour l'EGFR) et est plus sensible au traitement. Les tumeurs de type mésenchymateux présentent une forte expression des gènes de remodelage de la matrice extracellulaire (CHI3L1, c-MET et CD44). Le sous-type proneural est caractérisé par des altérations dans le PDGFRA, des mutations ponctuelles des gènes IDH1 et TP53, et est corrélé avec un pronostic de survie plus défavorable. Enfin, le sous-type neuronal est caractérisé par l'expression de marqueurs neuronaux tels que NEFL, GABRA1, SYT1 et SLC12A5 (Verhaak et al., 2010). Plus récemment, ce sous-groupe a été identifié comme pouvant être des cellules neuronales normales (Wang et al., 2017a).

L'hétérogénéité intra-tumorale des GBM a été démontré en utilisant la technique d'hybridation *in-situ* par fluorescence (FISH). Snuderl et al. ont décrit une amplification en mosaïque des différents récepteurs tyrosine kinase (Epidermal Growth Factor Receptor (EGFR), c-MET, PDGFRA) dans des cellules de GBM (Snuderl et al., 2011). De plus, le séquençage du génome au niveau de la cellule unique de 28 tumeurs a montré que les GBM présentent une hétérogénéité intra-tumorale complexe et dynamique. Quatre sous-types de cellules de GBM ont été ainsi identifiés, chacun étant caractérisé par des altérations génétiques spécifiques (CDK4, EGFR, PDGFRA, NF1). Les génotype des cellules de GBM est fortement influencé par le microenvironnement de la tumeur, et présentent une plasticité forte puisqu'une seule cellule peut générer les quatre sous-types avec de multiples transitions possibles (Nefel et al., 2019).

## 2. Epidermal Growth Factor Receptor

### **EGFR comme cible thérapeutique dans le GBM**

Dans le GBM, *erbB*, le gène codant pour l'EGFR est amplifié dans 40 à 60 % des cas suite à un réarrangement des gènes et/ou à l'amplification focale. Cette amplification est souvent associée à des mutations (Frederick et al., 2000). La mutation de l'EGFR la plus courante, EGFRvIII (représente plus de 50 % des mutations) correspond à une perte des exons 2-7 aboutissant à une délétion de 801 paires de bases (Huang et al., 2009). Les acides aminés 6 à 273 sont remplacés par un résidu glycine. La glycoprotéine qui en résulte est plus courte (145 kDa au lieu de 175 kDa), et est activée de manière constitutive indépendamment du ligand. L'activation constitutive est potentialisée par l'interaction réduite avec la E3-ligase Cbl, ce qui entraîne une dégradation réduite du récepteur (Normanno et al., 2006).

Des études histologiques ont montré une distribution hétérogène de l'EGFR dans les tissus de GBM. L'expression de l'EGFR est diffuse dans la masse de la tumeur (Hatanpaa et al., 2010), ou plus focalisée aux limites de la tumeur (Okada et al., 2003), étant associée à l'invasion tumorale.

### **Activité oncogénique de l'EGFR dans le GBM**

La liaison d'un de ces ligands, comme l'EGF, sur le récepteur, provoque la dimérisation de l'EGFR et l'activation de son activité tyrosine kinase intrinsèque. Il s'en suit une transphosphorylation de résidus de tyrosine, qui servent de site de recrutement de protéine de signalisation. La surexpression de l'EGFR active des voies de signalisation stimulant la prolifération, la migration et l'invasion des cellules de GBM (An et al., 2018). La voie de signalisation PI3K est amplifiée par la surexpression de l'EGFR mais aussi par la perte de son régulateur négatif PTEN observé dans 45 % des GBM. De plus, des mutations activatrices de PI3K ont été trouvées dans le domaine de régulation (Wang et al., 2004a). En outre, le ciblage de la voie de signalisation PI3K par l'inhibition de mTOR provoque une régression tumorale (Fan et al., 2017; Zhang et al., 2015b). Cependant, l'efficacité clinique de la rapamycine (inhibiteur de mTOR) et de ses analogues n'a eu que peu de bénéfices cliniques (Xu et al., 2017a). L'inhibition de la voie PKC/PI3K/AKT par l'enzastaurine provoque l'apoptose des cellules de gliome, supprime la prolifération dans la lignée cellulaire U87 MG, et réduit la croissance tumorale et l'angiogenèse dans des xénogreffes de souris (Graff et al., 2005).



L'enzastaurine a été évaluée dans un essai clinique de phase III sur le GBM en monothérapie (Wick et al., 2010). Même si l'enzastaurine est bien tolérée et est moins toxique que la chimiothérapie avec la lomustine, elle n'a pas démontré de bénéfice pour les patients (Wick et al., 2010). Une autre voie de signalisation suractivée par l'EGFR dans le GBM est la voie des MAPK, elle est impliquée dans l'invasion tumorale et dans la néo-angiogenèse (Sangpairoj et al., 2016). L'inhibition de cette voie diminue la croissance des tumeurs dans des xénogreffes de gliome (Campbell et al., 2014). Enfin, l'EGFR activé peut recruter STAT3 et favoriser sa dimérisation. STAT3 est transporté dans le noyau où il agit comme un facteur de transcription pour réguler la prolifération, la différenciation, la survie et l'apoptose cellulaire (Jorissen et al., 2003). Dans le GBM, l'EGFR peut phosphoryler l'EGFRvIII, favorisant sa translocation nucléaire où il peut interagir avec STAT3, augmentant ainsi l'agressivité de la tumeur (Fan et al., 2013).

### **Thérapies ciblant l'EGFR**

Différentes thérapies ciblant l'EGFR sont déjà utilisées en clinique comme l'utilisation d'anticorps monoclonaux antagonistes (mAbs) ou d'inhibiteurs de l'activité tyrosine kinase (TKI). L'utilisation de mAbs ou de TKI a pour objectif l'inhibition des cascades de signalisation induites par l'EGFR et ainsi un ralentissement de la prolifération cellulaire et une induction de l'apoptose des cellules cancéreuses ) (Xu et al., 2017b).

Les mAbs antagonistes de l'EGFR développés se lient au domaine extracellulaire du récepteur, empêchent la fixation du ligand et provoquent ainsi l'inactivation de la cascade de signalisation. De plus, la région Fc des mAbs permet l'activation d'une cytotoxicité cellulaire dépendante de l'anticorps (ADCC) (Kimura et al., 2007).

Les TKI sont de petites molécules structurellement analogues de l'ATP qui entrent en compétition avec l'ATP au niveau du domaine catalytique de la tyrosine kinase, conduisant à une inhibition de l'activation de la tyrosine kinase, l'autophosphorylation de l'EGFR et l'interruption de la cascade de signalisation (Sun et al., 2015). Le géfitinib est un TKI de première génération qui prévient la liaison de l'ATP au domaine catalytique et bloque la transphosphorylation du récepteur.

## Résistance aux thérapies ciblant l'EGFR

Malgré de nombreux essais, les thérapies ciblant l'EGFR ont malheureusement échouées en clinique (Taylor et al., 2012). De nombreuses études ont exploré les différents mécanismes moléculaires possibles favorisant la résistance à ce traitement. Dans le cadre de cette thèse, je développerais deux mécanismes de résistance innovant potentiellement intéressants.

### Dérégulation du trafic membranaire de l'EGFR dans le GBM

Différentes études ont montré que le trafic membranaire de l'EGFR est fréquemment altéré dans les tumeurs, y compris dans le GBM, ce qui contribue ainsi à la progression tumorale. NHE9 est un canal  $Na^+/H^+$ , identifié pour la première fois dans l'autisme où il induit une hyperacidification des endosomes et par conséquent des défauts dans le trafic vésiculaire (Kondapalli et al., 2013). NHE9 est fortement exprimé dans les tissus cérébraux (Kondapalli et al., 2014). Dans le GBM, la surexpression de NHE9 favorise l'invasion tumorale en stimulant le recyclage à la membrane plasmique de l'EGFR, potentialisant ainsi sa signalisation. La présence plus élevée de l'EGFR au niveau de la membrane plasmique, favorisée par la surexpression de NHE9, rend le GBM plus résistant aux traitements aux TKIs (Kondapalli et al., 2015). D'autre part, le trafic membranaire de l'EGFR WT et de l'EGFRvIII n'est pas le même. L'EGFRvIII est peu internalisé et plus fréquemment recyclé que dégradé. La présence prolongée de l'EGFRvIII à la membrane plasmique maintient une voie de signalisation différente de celle de l'EGFR WT. Cette dégradation déficiente est le résultat d'une ubiquitination insuffisante du récepteur par le Cbl (Grandal et al., 2007 ; Han et al., 2006 ; Schmidt et al., 2003). L'importance de l'endocytose de l'EGFR dans la réponse thérapeutique a été souligné par deux récentes études montrant que l'endocytose de l'EGFR peut être utilisée comme biomarqueur moléculaire prédictif et aussi comme un outil thérapeutique *in vivo* et en clinique (Chew et al., 2020 ; Joseph et al., 2019 ; Ye et al., 2019).

Certains traitements ont également été décrits comme des déclencheurs d'une endocytose induite par le stress. Des études réalisées sur des cellules HeLa et sur des cellules cancéreuses de la tête et du cou ont démontré que des stimuli de stress tels que les rayonnements (UVB et UVC) ou la chimiothérapie peuvent affecter le trafic de l'EGFR et jouer un rôle dans la progression tumorale indépendamment des lésions sur l'ADN (Tomas et al., 2017). La cisplatine induit l'internalisation de l'EGFR d'une façon dépendante de la p38 MAPK et provoque aussi une résistance à la thérapie dans les cellules cancéreuses du sein (Winograd-Katz and Levitzki,

2006). Le p38-MAPK peut activer Rab5 en phosphorylant ses effecteurs EEA1 et GDI, favorisant ainsi l'internalisation de l'EGFR et la fusion des endosomes (Cavalli, 2001). Après un stress, l'EGFR est activé suite son internalisation et sa rétention dans les endosomes (Tomas et al., 2015). La signalisation de l'EGFR à partir de ces compartiments péri nucléaires retarde l'apoptose induite par les UVC ou la cisplatine, mais la mort cellulaire se produit, peut-être en raison de la signalisation prolongée de la p38-MAPK (Tomas et al., 2017).

#### Interaction avec des autres récepteurs membranaires

De nombreuses études décrivent une étroite coopération entre les récepteurs à tyrosine kinase, comme l'EGFR, avec les intégrines. Cette coopération amplifie l'activité oncogénique de l'EGFR et est à l'origine de mécanismes de résistance aux thérapies ciblées (Cruz da Silva et al., 2019 ; Ivaska, 2011). Ces résultats sont décrits en détail dans la revue ajoutée à l'annexe 2 de la thèse (Cruz da Silva et al., 2019), Par exemple, la résistance aux TKI ciblant l'EGFR dans les cellules de poumon a été corrélée avec une augmentation de l'expression de l'intégrine  $\beta 1$  (Deng et al., 2016 ; Ju et al., 2010 ; Kanda et al., 2013). De plus, l'inhibition de l'intégrine  $\beta 1$  sensibilise ces cellules aux traitements avec les TKI *in vitro* et *in vivo* (Deng et al., 2016 ; Kanda et al., 2013 ; Morello et al., 2011).

### 3. Intégrines

#### **Famille des intégrines**

A l'instar de l'EGFR et des autres récepteurs à activité tyrosine kinase, la surexpression des intégrines, des récepteurs de la matrice extracellulaire, joue un rôle majeur dans la progression tumorale. Les intégrines sont une famille de glycoprotéines hétérodimériques transmembranaires, composées de deux sous-unités,  $\alpha$  et  $\beta$ . On dénombre chez les mammifères 24 intégrines, représentées par 18 sous-unités  $\alpha$  et 8 sous-unités  $\beta$ . Dans le GBM, la surexpression des intégrines conduit à l'activation de l'invasion tumorale et à des mécanismes de résistance aux thérapies (Janouskova et al., 2012; Martinkova et al., 2010) et est clairement associée à un mauvais pronostic.

#### **Intégrine $\alpha 5\beta 1$ dans le GBM**

Notre équipe et d'autres ont démontré que l'une d'entre elle, l'intégrine  $\alpha 5\beta 1$ , récepteur de la fibronectine est une cible d'intérêt thérapeutique dans le GBM.

L'intégrine  $\alpha 5\beta 1$ , présente des niveaux d'expression plus élevés dans le GBM par rapport aux parenchyme cérébrale sain (Gingras et al., 1995; Janouskova et al., 2012). Cette surexpression est associée à un mauvais pronostic pour les patients (Janouskova et al., 2012; Lathia et al., 2014). Des données précliniques ont démontré le rôle de l'intégrine  $\alpha 5\beta 1$  dans la croissance et la survie des cellules de gliome (Färber et al., 2008; Kesanakurti et al., 2013), la motilité cellulaire (Blandin et al., 2016; Mallawaarachy et al., 2015; Patil et al., 2015) et la résistance à la chimiothérapie (Janouskova et al., 2012; Martinkova et al., 2010; Renner et al., 2016a). L'inhibition de l'intégrine  $\alpha 5\beta 1$  réduit la prolifération cellulaire *in vitro* et la taille des tumeurs *in vivo* (Färber et al., 2008). L'intégrine  $\alpha 5\beta 1$  active la voie de la  $\beta$ -caténine pour stimuler la migration des cellules de GBM (Ray et al., 2014; Renner et al., 2016b). L'inhibition de l'intégrine  $\alpha 5\beta 1$  favorise l'activation de p53 et sensibilise les cellules de GBM au TMZ (Janouskova et al., 2012; Renner et al., 2016a). De plus, l'intégrine  $\alpha 5\beta 1$  inhibe l'apoptose induite par le TMZ et stimule la sénescence des cellules, induisant une résistance à la chimiothérapie (Martinkova et al., 2010). L'inhibition des complexes intégrine  $\beta 1$ /EGFR sensibilise les cellules cancéreuses à la radiothérapie (Eke et al., 2013, 2015). De plus, l'intégrine  $\alpha 5\beta 1$  est impliquée dans l'angiogenèse tumorale (Dudvarski Stanković et al., 2018; Li et al., 2012; Lugano et al., 2018). L'intégrine  $\alpha 5\beta 1$  favorise la prolifération des cellules

endothéliales du cerveau en réponse à l'hypoxie, ce qui démontre l'intérêt de cibler cette intégrine comme thérapie anti-angiogénique (Li et al., 2012). L'expression de l'intégrine  $\alpha 5\beta 1$  sur les cellules endothéliales stimule la vascularisation des GBM dans des modèles *in vivo*. La fibrillogenèse de la fibronectine médiée par l'intégrine  $\beta 1$  dans les cellules endothéliales favorise la vascularisation *in vivo* des tumeurs de GBM (Li et al., 2012).

Plusieurs inhibiteurs de l'intégrine  $\alpha 5\beta 1$  ont été testés dans d'autres tumeurs solides ou maladies angiogéniques. En ce qui concerne le GBM, seules des études cliniques de phase I et II ont été réalisées. D'autres études sont nécessaires pour mieux évaluer l'efficacité de ces thérapies ciblées.

#### 4. Aptamères comme alternative aux anticorps

**Les aptamères sont des oligonucléotides ADN simple brin ou ARN capables de se lier avec une grande affinité et spécificité à leur cible.**

Les aptamères présentent plusieurs avantages par rapport aux anticorps. Les aptamères sont plus petits que les anticorps (5-25 kDa versus 150 kDa) et sont thermostables. Comme les aptamères sont synthétisés chimiquement, ils peuvent être facilement modifiés, et présentent moins de variabilité entre batch que des protéines. De plus, les aptamères semblent non immunogènes et peu toxiques. Cependant, les aptamères présentent également des désavantages. Ils sont soumis à l'action des nucléases et sont plus facilement éliminés par les reins, ce qui diminue leur demi-vie. Pour rendre les aptamères plus résistants à l'action des nucléases, plusieurs chimies peuvent être envisagées, telles que la modification du groupement 2'OH des riboses des chaînes d'ARN par un groupement 2'Fluoro. Le couplage des aptamères à des groupements polyéthylène glycol (PEG) augmente leur poids et diminue leur élimination rénale.

#### **SELEX**

Les aptamères sont sélectionnés par un processus de sélection *in vitro* appelé SELEX (Selective evolution of ligands by exponential enrichment) (Ellington and Szostak, 1990; Tuerk and Gold, 1990).

#### **Applications des aptamères**

Une fois sélectionnés et caractérisés, les aptamères peuvent être utilisés dans de nombreuses applications, notamment diagnostiques et thérapeutiques.

#### Applications thérapeutiques des aptamères

Les aptamères pourraient avoir des applications thérapeutiques intéressantes. Ils peuvent entraîner une modification de fonction des récepteurs lors de la liaison. Ils peuvent également entrer en compétition avec des molécules et/ou des ligands pour inhiber l'activation de la cible, ou ils peuvent être utilisés comme vecteurs pour l'administration d'agents thérapeutiques.

Des aptamères ciblant différents facteurs de croissance et leurs récepteurs membranaires respectifs ainsi que le microenvironnement tumoral ont été décrits. Un aptamère à base d'ADN,

appelé NAS-24, cible la vimentine, une protéine de la matrice extracellulaire présente dans le microenvironnement tumoral. Cet aptamère induit l'apoptose *in vitro* et *in vivo* des cellules d'adénocarcinome (Zamay et al., 2014). Une nouvelle stratégie thérapeutique antitumorale des aptamères consiste à utiliser des conjugués anticorps-aptamères bispécifiques. Passariello et al ont conjugué un aptamère anti-EGFR avec un anticorps immunomodulateur anti-PD-L1. Ce complexe permet de diminuer la survie des cellules cancéreuses et de renforcer l'activation des cellules T. Dans une co-culture de cellules cancéreuses avec des lymphocytes, le complexe a permis d'augmenter les niveaux d'IL-2 et d'IFN- $\gamma$  dans les surnageants cellulaires (Passariello et al., 2019).

### Applications diagnostiques des aptamères

Les aptamères peuvent être aussi utilisés comme outils de diagnostic pour la détection des cellules, la coloration des échantillons de tissus *ex vivo* et comme des sondes d'imagerie non invasives *in vivo* pour suivre la progression tumorale (Cerchia, 2018; Sun et al., 2016). L'utilisation des aptamères en clinique est prometteuse, mais n'en est encore qu'à ses prémices.

## Objectifs de mon doctorat

Le GBM est la tumeur cérébrale primaire la plus fréquente et la plus agressive. Le GBM est extrêmement résistant à la radiothérapie et à la chimiothérapie, ainsi qu'aux thérapies ciblées. L'agressivité du GBM s'explique en partie par la surexpression de protéines pro-tumorales qui dynamisent la croissance et l'invasion tumorale. Ainsi, le gène *erbB1*, codant pour l'EGFR est amplifié dans plus de 50 % des tumeurs. Un autre récepteur de surface cellulaire surexprimé dans GBM est l'intégrine  $\alpha5\beta1$ , un membre de la famille des récepteurs de la matrice extracellulaire. La surexpression des intégrines est associée à un mauvais pronostic. Les intégrines peuvent coopérer avec les récepteurs aux facteurs de croissance, comme l'EGFR, et ainsi amplifier leur potentiel oncogénique. Ces deux récepteurs sont régulés par leur endocytose et leur trafic membranaire. L'expression des protéines impliquées dans l'endocytose est souvent modifiée dans les cellules de GBM, ce qui contribue au potentiel oncogénique de l'EGFR et favorise la progression tumorale et la résistance aux thérapies ciblées. Malheureusement, le ciblage de l'EGFR et des intégrines a échoué dans les essais cliniques sur des patients atteints de GBM.

Mon doctorat porte principalement sur ces deux récepteurs de surface cellulaire, et a deux objectifs principaux :

- 1) La première partie de mon doctorat porte sur l'étude de l'impact des thérapies ciblées, plus concrètement des inhibiteurs de la tyrosine kinase de l'EGFR, comme le géfitinib, dans le trafic membranaire de l'EGFR dans les cellules de GBM. Nous avons montré que le géfitinib induit une endocytose de l'EGFR et de l'intégrine  $\alpha5\beta1$ , indépendante du ligand, et nous avons identifié trois protéines d'endocytose qui contribuent à cet effet. De plus, nous avons découvert que la répression de l'endocytose protège les cellules de GBM de l'inhibition induite par le géfitinib. Articles 1 et 2 (Blandin, Cruz da Silva et al, CMLS, 2020 ; Cruz da Silva et al, en cours de rédaction).
- 2) La deuxième partie porte sur la caractérisation d'aptamères (molécules également nommées anticorps chimiques) ciblant l'intégrine  $\alpha5\beta1$  et l'EGFR dans l'objectif de développer des stratégies de détection des récepteurs dans les cellules de gliome et dans les échantillons de tissus humains. Nous avons également analysé l'effet du traitement au géfitinib sur l'internalisation des aptamères dans les cellules de gliome, en explorant de nouvelles possibilités pour les aptamères comme agents alternatifs de vectorisation



(de siRNA par exemple) (articles 3 (Fechter, Cruz da Silva et al., 2019) et résultats récents.

En parallèle, j'ai également participé à la rédaction de deux revues bibliographiques : l'une est en cours de rédaction (annexe 1) et l'autre (annexe 2) est publiée (Cruz da Silva et al., 2019). La première est une revue systématique des essais cliniques sur les GBM utilisant des thérapies ciblées. La deuxième porte sur le rôle de l'intégrine dans la résistance aux thérapies ciblées sur les récepteurs des facteurs de croissance. De plus, j'ai collaboré à la caractérisation de particules d'or conjuguées à l'anticorps ciblant l'EGFR, cétuximab, qui peuvent améliorer la radiothérapie ciblée (Groysbeck et al., 2019), présent dans l'annexe 3.

## Résultats

### Introduction aux Articles 1 et 2

La caractérisation moléculaire des GBM démontre l'importance de l'EGFR sur la progression tumorale. La signalisation de ce récepteur tyrosine kinase augmente la croissance, la survie, l'invasion et la résistance aux traitements du GBM (An et al., 2018). Plusieurs essais cliniques utilisent des thérapies ciblant l'EGFR, efficaces dans d'autres tumeurs solides, mais aucune amélioration thérapeutique n'a été obtenue dans le cas des GBM (Taylor et al., 2012). Plusieurs mécanismes ont été explorés pour justifier cette résistance mais aucun résultat n'est jusqu'alors cliniquement pertinent. L'EGFR et les intégrines sont partenaires lors de la progression tumorale et la résistance à des thérapies (Silva, 2019). En particulier, il a été démontré que le récepteur de la fibronectine, l'intégrine  $\alpha 5\beta 1$ , régule l'activité de l'EGFR pour favoriser l'invasion des cellules cancéreuses. Cette intégrine, d'un intérêt clinique particulier, a été décrite par notre équipe et d'autres comme une cible thérapeutique prometteuse dans le GBM (Schaffner et al., 2013).

L'endocytose et le trafic membranaire sont désormais considérés comme des régulateurs fondamentaux de la signalisation tumorale des récepteurs de surface cellulaire. Au cours de la dernière décennie, la dérégulation du trafic membranaire de l'EGFR dans le GBM est décrite comme un facteur clé pour la progression tumorale et la résistance aux thérapies (Al-Akhrass et al., 2017 ; Kondapalli et al., 2015 ; Kurata et al., 2019 ; Walsh et al., 2015 ; Wang et al., 2019c ; Ying et al., 2010). Par ailleurs, plusieurs études ont montré que les agents thérapeutiques déclenchent une endocytose de l'EGFR induite par le stress dans les cellules cancéreuses (Cao et al., 2011 ; Dittmann et al., 2005 ; Tan et al., 2016).

En ce qui concerne le géfitinib, les études sont contradictoires. Le géfitinib peut supprimer l'endocytose de l'EGFR induite par son ligand dans les cellules cancéreuses du poumon (Nishimura et al., 2007) et dans les cellules de carcinome épidermoïde (Pinilla-Macua et al., 2017). Cependant, une autre étude a montré une augmentation de l'absorption d'EGF humain marqué avec un radio-isotope dans des cellules de carcinome du côlon, de NSCLC et de HNSCC (He et Li, 2013), ce qui suggère une augmentation de l'endocytose. Il a été également démontré que le géfitinib initie l'autophagie de manière dépendante de l'EGFR dans les cellules de carcinome mammaire (Tan et al., 2015) ou les cellules de gliome (Chang et al., 2014 ; Liu et al., 2020). Une accumulation de l'EGFR, indépendante de leur activité tyrosine kinase, dans les compartiments autophagiques lors du traitement au géfitinib a également été observée dans

les cellules cancéreuses (Tan et al., 2015). Il convient de noter que l'autophagie et l'endocytose sont moléculairement liées (Birgisdottir et Johansen, 2020). Enfin, la dérégulation de l'endocytose est souvent observée dans les cellules cancéreuses résistantes au géfitinib (Cui et al., 2015 ; Nishimura et al., 2008).

**Nous avons exploré en détail l'impact du géfitinib sur le trafic de l'EGFR et des intégrines dans les cellules de GBM, dans l'espoir de trouver de nouvelles pistes pour améliorer les thérapies ciblant l'EGFR dans le traitement du GBM.**

En utilisant des lignées cellulaires de GBM, nous avons montré que le géfitinib induit une endocytose massive de l'EGFR, indépendante de la liaison du ligand. L'endocytose a été évaluée par des tests d'absorption de l'EGF fluorescent, des tests d'endocytose de l'EGFR après marquage de surface par la biotine et par immunomarquage de l'EGFR et des endosomes précoces et analyse en microscopie confocale. Nous avons appelé ce phénomène "endocytose médiée par le géfitinib" (GME). De manière dose-dépendante, le géfitinib provoque l'internalisation de l'EGF et la co-localisation de l'EGFR dans les endosomes précoces. La GME conduit à l'accumulation prolongée de l'EGF fluorescent, alors que dans les cellules non traitées une diminution de l'EGF fluorescent intracellulaire se produit au fil du temps, suggérant une dégradation du récepteur. La GME augmente d'environ 25 % l'internalisation de l'EGFR. La GME a été observée dans 4 lignées cellulaires de GBM différentes, toutes exprimant l'EGFR (article 1). L'endocytose de l'EGFR induite par le traitement au géfitinib est dépendante des protéines DNM2 et Rab5 (article 2) et favorise le transport de l'EGFR dans des endosomes positifs pour l'intégrine  $\alpha 5 \beta 1$  (article 1) et un autre récepteur de surface cellulaire, LRP-1 (article 2). La proximité entre ces récepteurs a été établie par imagerie et suggère un lien fonctionnel. Des études fonctionnelles ont confirmé que l'expression de l'intégrine et de LRP-1 est également impliquée dans la GME (article 1 et 2, respectivement). Enfin, nous avons évalué l'importance de l'endocytose dans l'activité anti-tumorale du géfitinib, au travers de tests d'évasion cellulaire des sphéroïdes 3D. L'inhibition de la GME protège les cellules contre le traitement au géfitinib (article 2). Cependant, la déplétion de l'intégrine  $\alpha 5$  sensibilise les cellules au traitement par le géfitinib (article 1).

Brièvement, ces travaux révèlent que l'endocytose de l'EGFR et des intégrines joue un rôle inattendu dans l'action du géfitinib et que le niveau d'expression des protéines de l'endocytose telles que la DNM2, le LRP-1 ou le Rab5 pourraient être des biomarqueurs pertinents pour prédire l'efficacité des TKI à limiter l'invasion des cellules GBM.

## Conclusions générales des articles 1 et 2

- Le géfitinib provoque une endocytose des récepteurs dans des endosomes.
- Le géfitinib favorise la co-endocytose de l'EGFR et de l'intégrine  $\alpha 5\beta 1$ .
- Nous avons identifié 3 protéines impliquées dans l'endocytose, DNM2, Rab5 et LRP-1, comme régulateurs clés de l'internalisation de l'EGFR induite par le géfitinib.
- La modulation de l'endocytose modifie la réponse des cellules de gliome au traitement par le géfitinib.

Dans le premier article, nous avons décrit, dans quatre lignées cellulaires différentes de GBM, que le géfitinib et d'autres TKI sont des inducteurs d'une endocytose de l'EGFR en réponse au stress et indépendamment du ligand. Nous avons également décrit que la GME ne se limite pas à l'EGFR. Nous avons montré une co-localisation de l'EGFR avec l'intégrine  $\alpha 5\beta 1$  dans les endosomes précoces lors du traitement au géfitinib. Le géfitinib augmente la co-localisation intégrine/EGFR dans les vésicules périnucléaires par rapport à des cellules non traitées. En utilisant une technique de microscopie à super-résolution PALM-STORM, nous avons vérifié la proximité physique entre l'EGFR et l'intégrine  $\beta 1$ , suggérant une interaction fonctionnelle potentielle. Pour explorer l'implication de l'intégrine dans la GME, l'intégrine  $\alpha 5$  a été défectée dans des cellules de GBM U87 en utilisant la technique de l'ARNsh. La délétion de l'intégrine  $\alpha 5\beta 1$  limite l'accumulation de l'EGFR dans les endosomes précoces après un traitement court de géfitinib. Nous avons également évalué quel est l'impact de cette endocytose dans la réponse des cellules de gliome au traitement par le géfitinib. Comme le GBM est une tumeur très invasive, nous avons décidé d'évaluer le rôle de la dérégulation du trafic dans l'évasion des cellules des sphéroïdes tumorales 3D. Le traitement au géfitinib réduit le nombre de cellules qui s'échappent des sphéroïdes U87  $\alpha 5^-$  (qui sous-expriment l'intégrine  $\alpha 5$ ) en fonction de la dose. Cependant, le géfitinib n'a pas d'impact significatif sur l'évasion cellulaire des cellules U87  $\alpha 5^+$  (qui sur-expriment l'intégrine  $\alpha 5$ ).

Dans le deuxième article, nous avons essayé de mieux comprendre les mécanismes moléculaires de la GME. Tout d'abord, nous avons étudié le rôle de deux protéines habituellement associées à l'endocytose de l'EGFR induite par un ligand, la DNM2 et le Rab5. En utilisant des inhibiteurs pharmacologiques et la déplétion médiée par un siRNA, nous avons montré que la GME était dépendante de la DNM2. Nous avons également montré que la GME

nécessitait l'activation de Rab5. Un mutant constitutivement actif de Rab5 produit de grands endosomes précoces similaires à ceux induits par la GME. De plus, le mutant dominant-négatif de Rab5 réduit la co-localisation de l'EGFR dans les endosomes précoces lors du traitement au géfitinib. Nous avons ensuite examiné le rôle potentiel du LRP-1, un récepteur d'endocytose. La GME sur les cellules U87 induit la relocalisation de l'EGFR dans les endosomes positifs au LRP-1. Ensuite, le rôle de LRP-1 dans la GME a été étudié en utilisant des techniques similaires à celles utilisées pour la protéine Rab5. Nous avons montré que LRP-1 n'est pas impliqué dans l'endocytose de l'EGF induite par un ligand, mais qu'il contribue de manière significative à l'endocytose de l'EGF médiée par le géfitinib. L'inhibition de la GME par le blocage de DNM2 et de LRP-1 augmente de manière significative la dissémination des cellules traitées au géfitinib.

En résumé, nous avons montré que dans les cellules de gliome, les différents TKI (géfitinib, mais aussi d'autres TKI) ciblant l'EGFR déclenchent un mécanisme complexe d'endocytose du récepteur. En outre, nous avons démontré pour la première fois un lien fonctionnel entre le LRP-1 et l'endocytose de l'EGFR. Nous avons déterminé que le niveau d'expression et la fonction des protéines impliquées dans la GME peuvent moduler les réponses des cellules de GBM au traitement aux TKIs.

Les défis futurs consisteront à évaluer l'impact des TKIs sur la fonction des intégrines et à déterminer si leur coopération avec l'EGFR pendant le trafic membranaire modifie l'évasion des cellules de GBM. Enfin, ces travaux ont mis en évidence la nécessité de mieux comprendre les mécanismes d'action des agents thérapeutiques, et pas seulement leurs propriétés présumées. Cela pourrait conduire à l'identification de biomarqueurs appropriés pour améliorer la prédiction de leur efficacité.

## Introduction à l'article 3

L'équipe "Intégrines et cancers" de l'UMR 7021 a démontré le potentiel de l'intégrine  $\alpha 5\beta 1$  comme cible thérapeutique sur le GBM (Janouskova et al., 2012). Son ligand naturel est la fibronectine, une protéine de la matrice extracellulaire surexprimée dans le microenvironnement tumoral du GBM (Lal et al., 1999). Les biomarqueurs, comme l'intégrine  $\alpha 5\beta 1$ , ont un grand potentiel clinique en tant que marqueurs de diagnostic (expression élevée dans les gliomes de haut grade par rapport aux tissus normaux et tumoraux de bas grade), de pronostic (expression élevée associée à une survie diminuée des patients), et de prédiction (expression élevée associée à la résistance au TMZ).

En oncologie, les aptamères, appelés aussi anticorps chimiques, sont des outils émergents de diagnostic et de thérapie (liaison directe avec leurs cibles ou pour la vectorisation d'agents thérapeutiques). Les aptamères sont des molécules d'ADN simple brin ou d'ARN qui se lient à leur cible avec une grande affinité et spécificité, comme les anticorps. Les aptamères présentent des avantages par rapport aux anticorps : leur taille réduite, leur stabilité thermique, leur absence d'immunogénicité et de toxicité, et leur synthèse chimique (Mercier et al., 2017 ; Zhou et Rossi, 2017). De plus, les aptamères pénètrent plus profondément les tissus que les anticorps en raison de leur taille plus petite (Xiang et al., 2015). La sélection des aptamères se fait par un processus *in vitro* appelé SELEX (Ellington et Szostak, 1990 ; Tuerk et Gold, 1990). Les aptamères peuvent être utilisés comme outils diagnostiques et/ou thérapeutiques contre des cibles thérapeutiques identifiées comme les récepteurs membranaires, qui sont des cibles intéressantes en raison de leur accessibilité à la surface des cellules.

Un processus de sélection original, combinant cell- et protein- SELEX, a été réalisé dans le laboratoire pour identifier les aptamères capables de se lier aux cellules et tissus de GBM exprimant l'intégrine  $\alpha 5\beta 1$ . La sélection, l'identification et la caractérisation d'un aptamère, appelé H02, sont décrites dans l'article 3 (Fechter, Cruz da Silva et al., 2019).

- L'intégrine  $\alpha 5\beta 1$  a été validée comme la cible de l'aptamère H02 en utilisant la résonance plasmonique de surface, dans laquelle l'intégrine humaine  $\alpha v\beta 3$  a été utilisée comme témoin négatif.
- L'affinité à l'équilibre ( $K_D$ ) de l'interaction entre l'aptamère H02 et les cellules U87 surexprimant  $\alpha 5$  a été déterminée par cytométrie de flux. La liaison entre l'aptamère et les cellules a été quantifiée au travers du signal fluorescent associé au conjugué aptamère-fluorophore testé à différentes concentrations. Un  $K_D$  de  $277,8 \pm 51,8$  nM a été déterminé.
- En outre, l'aptamère H02 permet d'identifier différentes lignées cellulaires de GBM en fonction de leur niveau d'expression de l'intégrine  $\alpha 5\beta 1$ .
- A  $4^\circ\text{C}$ , l'aptamère H02 permet de détecter l'intégrine  $\alpha 5\beta 1$  présente à la membrane plasmique et dans les jonctions cellules-cellules. À  $37^\circ\text{C}$ , l'aptamère H02 est internalisé après sa liaison à l'intégrine  $\alpha 5\beta 1$  et est localisé dans les endosomes précoces positifs à l'EEA1 (early endosome antigen 1).
- La séquence de l'aptamère H02 a été brevetée (EP18306664.6 "Aptamer and use thereof").

## Introduction aux résultats récents sur aptafluorescence

Plusieurs récepteurs membranaires, comme l'EGFR, sont surexprimés dans les cellules de GBM pour favoriser la survie, la croissance et la migration des cellules de gliome (An et al., 2018). Le GBM présente une forte hétérogénéité inter- et intra- tumorale (Eskilsson et al., 2018 ; Janouskova et al., 2012 ; Szerlip et al., 2012). Une autre cible thérapeutique intéressante dans le GBM est le c-MET et son ligand, le facteur de croissance des hépatocytes (HGF). La voie de signalisation c-MET/HGF est dérégulée dans le GBM et est impliquée dans la prolifération, la survie, l'invasion des cellules de gliome, l'angiogenèse, la résistance aux thérapies et la récurrence (Cheng et Guo, 2019). L'expression de c-MET a été associée à un pronostic défavorable chez les patients atteints de GBM (Petterson et al., 2015). Une étude d'immunohistochimie d'échantillons de tissus de GBM a montré une localisation de c-MET dans les cellules tumorales, les vaisseaux sanguins et les zones péri-nécrotiques (Petterson et al., 2015). Il est intéressant de noter que l'EGFR et le c-Met ont été trouvés co-localisés dans des échantillons de cellules et de tissus de GBM, ce qui suggère une coopération entre les deux récepteurs (Velpula et al., 2012). Une double inhibition de l'EGFR et du c-MET permet de surmonter la résistance au TMZ dans les cellules de GBM et de réduire la croissance des tumeurs dans les modèles *in vivo* (Meng et al., 2020).

Cette tumeur très agressive et résistante a fait l'objet de plus de 1519 essais cliniques, dont 259 utilisant des thérapies ciblées (Annexe 1). La majorité des essais ne permet pas d'améliorer la survie globale des patients. L'hétérogénéité du GBM est l'un des principaux facteurs de résistance aux thérapies et de récurrence tumorale. La connaissance du statut d'expression des différents biomarqueurs pourrait être utilisée pour stratifier les patients dans les essais cliniques afin de mieux sélectionner les patients et/ou d'ajuster la stratégie thérapeutique. Par conséquent, la possibilité d'identifier simultanément différentes protéines sur un même tissu de GBM faciliterait les décisions thérapeutiques.

Les ligands de ces cibles thérapeutiques peuvent donc être des outils diagnostiques et/ou thérapeutiques intéressants. Ils doivent être précis et rapides pour évaluer l'expression protéique des récepteurs membranaires dans les tissus tumoraux de GBM. Le protocole de routine d'immunohistochimie (IHC) utilise une méthode indirecte de marquage avec une première incubation avec un anticorps primaire spécifique au biomarqueur d'intérêt non conjugué, suivie d'une seconde incubation avec un anticorps conjugué capable d'identifier l'espèce du premier



anticorps. Cette méthode de détection indirecte augmente la sensibilité puisque les anticorps secondaires peuvent se lier à plusieurs sites antigéniques de l'anticorps primaire. Une détection directe est plus rapide puisqu'un seul temps d'incubation est nécessaire. Les méthodes de détection directe sont probablement plus fiables pour le multi marquage puisqu'il n'y a pas de risque de réaction inter-espèces (Odell et Cook, 2013). Mais le marquage direct des anticorps est complexe. Pour coupler par covalence un fluorochrome à une protéine recombinante, comme un anticorps ou un fragment d'anticorps, la procédure la plus couramment utilisée consiste à remplacer un acide aminé identifié par une cystéine et à coupler le fluorochrome à son groupe thiol. Cette méthode nécessite la production et la purification de grandes quantités de protéines recombinantes. En outre, cette méthode est relativement compliquée. En effet, les mutations et/ou les couplages peuvent (i) diminuer le niveau d'expression de la protéine, (ii) diminuer ou inhiber la liaison, (iii) provoquer une perte de stabilité ou l'agrégation de la protéine, ou (iv) induire une absence de signal de fluorescence. Le fluorochrome peut même parfois être couplé aux chaînes latérales de la lysine.

L'homogénéité des lots d'anticorps peut être faible, ce qui représente un énorme désavantage en termes de reproductibilité (Zhou et Rossi, 2017). Pour un multi marquage, il faut plusieurs anticorps de différentes spécificités, couplés à différents fluorochromes, ce qui accentue ces difficultés. Ces problèmes pourraient être résolus par l'utilisation d'autres molécules, synthétisées chimiquement, en grandes quantités et plus stables, telles que des peptides, de petits composés chimiques ou des aptamères (Hori et al., 2018 ; Musumeci et al., 2017).

Au cours de ma thèse, nous avons utilisé des aptamères ciblant l'EGFR, l'intégrine  $\alpha 5$  et le c-MET dans des lignées cellulaires de GBM et des tissus de patients. Les aptamères EGFR (E07 et conjugué anti-EGFR janellia 646) et c-MET (SL1) étaient déjà décrits dans la littérature (Kratschmer et Levy, 2018 ; Li et al., 2011 ; Ray et al., 2012 ; Zhang et al., 2018). Quant à l'aptamère H02 ciblant l'intégrine  $\alpha 5$ , il a été identifié et caractérisé au laboratoire (article 3).

## Conclusions générales de l'article 3 et des résultats récents

- L'aptamère H02 se lie à l'intégrine  $\alpha 5\beta 1$  dans des cellules et tissus humains de GBM.
- Les aptamères ciblant l'EGFR que nous avons utilisé permettent de détecter l'expression de l'EGFR dans des cellules et tissus humains.
- Le traitement au géfitinib augmente l'internalisation des aptamères ciblant l'EGFR.
- L'aptahistochimie en utilisant simultanément l'aptamère H02 et d'autres aptamères ciblant les récepteurs EGFR et c-Met pourraient être intéressants pour mettre en évidence l'hétérogénéité tumorale des GBM.

Dans l'article 3, nous avons décrit l'identification d'un nouvel aptamère, H02, ciblant l'intégrine  $\alpha 5\beta 1$ . H02 est capable de reconnaître les cellules de GBM et les xénogreffes de tumeurs positives pour l'intégrine  $\alpha 5$ . H02 est internalisé dans les endosomes précoces positifs à 37°C.

Dans la partie 'résultats récents', nous avons caractérisé deux aptamères ciblant l'EGFR. Ces aptamères sont capables de reconnaître les cellules de GBM positives pour l'EGFR. Ces aptamères sont internalisés à 37°C, et cette internalisation est augmentée lors du traitement au géfitinib.

Ensuite, nous avons réalisé des expériences pour détecter des biomarqueurs de GBM par aptahistochimie en utilisant des aptamères fluorescents ciblant les récepteurs intégrine  $\alpha 5$ , EGFR et c-MET.

L'aptamère ciblant l'intégrine  $\alpha 5$  a permis de détecter les intégrines avec moins de bruit de fond que le marquage avec des anticorps. Il est intéressant de noter que la double détection de l'intégrine  $\alpha 5$  et de l'EGFR avec des aptamères pourrait être intéressante pour démontrer l'hétérogénéité intra-tumorale des GBM. Des études en cours sont réalisées avec un triple marquage des tissus de GBM en utilisant simultanément des aptamères contre les trois récepteurs membranaires.

Mes travaux de thèse sur les aptamères ciblant des récepteurs de surface cellulaire ouvrent la voie à l'utilisation potentielle des aptamères comme outils diagnostics, mais aussi comme outils de vectorisation en exploitant le fait que les aptamères sont internalisés à 37°C.

## Conclusion

Les outils de vectorisation visent à délivrer des chimiothérapies hautement toxiques ou des siRNA thérapeutiques de manière sélective aux cellules tumorales avec de faibles effets toxiques sur les cellules non tumorales. Les vecteurs peuvent être des anticorps conjugués à des médicaments (ADC, *antibody-drug conjugate*) ou à des nano-particules d'or qui augmentent la puissance de la chimiothérapie et de la radiothérapie (Groysbeck et al., 2019) (annexe 3). Les aptamères constituent une autre classe d'agents de vectorisation prometteurs pour l'administration de médicaments (*aptamer-drug conjugate*, AptDC) ou de siRNA (*aptamer-siRNA chimera*, AsiC) (Cerchia et al., 2011). Au-delà du défi de la bioconjugaison du vecteur aux agents thérapeutiques, un autre défi est l'internalisation du complexe et leur trafic intracellulaire. L'association de ces vecteurs avec le géfitinib pourrait être bénéfique en augmentant l'endocytose du vecteur.

# Annexes

Annexe 1 Draft of Review: A systematic review of glioblastoma  
molecular targeted therapies in Phases II, III, IV clinical trials

# A systematic review of glioblastoma molecular targeted therapies in Phases II, III, IV clinical trials

Elisabete Cruz Da Silva<sup>1</sup>† , Marie-Cécile Mercier<sup>1</sup> , Nelly Etienne-Selloum<sup>1,2</sup> ,  
Monique Dontenwill<sup>1</sup> & Laurence Choulier<sup>1</sup>\*

<sup>1</sup>CNRS, UMR 7021, Laboratoire de Bioimagerie et Pathologies, Tumoral Signaling and Therapeutic Targets, Université de Strasbourg, Faculté de Pharmacie, 67401 Illkirch, France  
<sup>2</sup>Département de Pharmacie, Centre de Lutte Contre le Cancer Paul Strauss, 67000 Strasbourg, France

elisabete.silva@unistra.fr (E.C-S.) ; marie-cecile.mercier@unistra.fr (M.C.M.);  
nelly.etienneselloum@unistra.fr (N.E-S.); monique.dontenwill@unistra.fr (M.D.)  
\*Correspondence: laurence.choulier@unistra.fr (L.C.); Tel.: +33-36885-4114; Fax: +33-36885-4313

## ABSTRACT

Glioblastoma (GBM), the most frequent and aggressive glial tumor, is currently treated by the Stupp protocol, which combines surgery, radiotherapy and chemotherapy. Despite this heavy treatment, the mean survival of patients is under 18 months. Many clinical studies are underway. This systematic review lists targeted therapies in phases II-IV of 259 clinical trials on adults with newly diagnosed or recurrent GBMs. It does not involve targeted immunotherapies and therapies targeting tumor cell metabolism, that are well documented in other reviews. It focuses on drugs targeting the potential for unlimited replication, the growth autonomy and migration, the escape to cell death and angiogenesis.


**KEYWORDS** Clinical trials, Glioblastoma, targeted therapies, biomarkers

The review and respective tables can be access in their totality in two files shared in (<https://seafire.unistra.fr/d/a6a6133ad0ad4f52b8f3/>). Any problem found to open these files please contact the corresponding author.

## Annexe 2 Review: Role of Integrins in Resistance to Therapies Targeting Growth Factor Receptors in Cancer

Review

# Role of Integrins in Resistance to Therapies Targeting Growth Factor Receptors in Cancer

Elisabete Cruz da Silva, Monique Dontenwill, Laurence Choulier and Maxime Lehmann \* 

UMR 7021 CNRS, Laboratoire de Bioimagerie et Pathologies, Tumoral Signaling and Therapeutic Targets, Université de Strasbourg, Faculté de Pharmacie, 67401 Illkirch, France;

elisabete.cruz-da-silva@etu.unistra.fr (E.C.d.S.); monique.dontenwill@unistra.fr (M.D.);

laurence.choulier@unistra.fr (L.C.)

\* Correspondence: maxime.lehmann@unistra.fr; Tel.: +33-(0)3-68-85-41-92

Received: 15 April 2019; Accepted: 14 May 2019; Published: 17 May 2019



**Abstract:** Integrins contribute to cancer progression and aggressiveness by activating intracellular signal transduction pathways and transducing mechanical tension forces. Remarkably, these adhesion receptors share common signaling networks with receptor tyrosine kinases (RTKs) and support their oncogenic activity, thereby promoting cancer cell proliferation, survival and invasion. During the last decade, preclinical studies have revealed that integrins play an important role in resistance to therapies targeting RTKs and their downstream pathways. A remarkable feature of integrins is their wide-ranging interconnection with RTKs, which helps cancer cells to adapt and better survive therapeutic treatments. In this context, we should consider not only the integrins expressed in cancer cells but also those expressed in stromal cells, since these can mechanically increase the rigidity of the tumor microenvironment and confer resistance to treatment. This review presents some of these mechanisms and outlines new treatment options for improving the efficacy of therapies targeting RTK signaling.

**Keywords:** integrin; focal adhesion kinase; therapy resistance; tyrosine kinase inhibitors; cancer-associated fibroblasts; mechanotransduction; EGFR; c-MET

## 1. Introduction

Many tumors initially respond to targeted therapies before resistance appears. The mechanisms that sustain tumor cells between initial response and disease progression are not well understood. Understanding drug resistance is urgently needed in cancer therapy. The interaction between cancer cells and the microenvironment (the extracellular matrix (ECM), fibroblasts, endothelial cells, and immune cells) is essential to cell survival, proliferation and migration [1,2]. Be it through physiological mechanisms or remodeling after therapy, the tumor microenvironment provides a safe haven that promotes the emergence of resistance.

The ECM alone can induce tumor cell resistance to treatment [3]. Integrins, a family of cell surface receptors, play an important role in the interaction with the ECM. The integrin family comprises 24 different receptors made up of heterodimers of 18 alpha ( $\alpha$ ) and 8 beta ( $\beta$ ) subunits, each of which binds to one or more ECM ligands. Integrins are involved in cellular adhesion to the ECM and in intercellular cohesion. Integrin biochemical and mechanical signaling regulates cell survival, proliferation, differentiation, migration, adhesion, apoptosis, anoikis, polarity and stemness [4–6]. Since integrins do not have enzymatic activity, once they bind to a ligand, they recruit cytoplasmic kinases such as focal adhesion kinases (FAKs). These, once recruited, autophosphorylate and present a docking site for the proto-oncogene tyrosine-protein kinase Src [7]. The FAK/Src complex activates the NF- $\kappa$ B (nuclear factor- $\kappa$ B), MAPK (mitogen-activated protein kinase) and PI3K (phosphoinositide



3-kinases) pathways. These signaling pathways are redundant with the receptor tyrosine kinase (RTK) signaling pathways. RTKs are families of surface receptors with tyrosine kinase activity that bind to growth factors, cytokines and hormones. RTK signaling pathways regulate cell growth, differentiation, metabolism and apoptosis in response to growth factor stimulation of cross-activation by co-receptors such as integrins. In normal cells, RTK function is tightly regulated. However, in cancer, mutations, overexpression, autocrine/paracrine stimulation and aberrant degradation lead to RTK constitutive activation and consequently to tumor formation and progression [8,9].

Integrins cooperate with several RTKs, such as epidermal growth factor receptor (EGFR), c-Met, platelet-derived growth factor receptor (PDGFR), insulin-like growth factor receptor (IGFR) and vascular endothelial growth factor receptor (VEGFR). This cooperation promotes solid tumor progression and aggressiveness as well as contributing to therapy resistance, be it to chemotherapy, radiotherapy or targeted therapy. Integrin/RTK crosstalk has been well described in several reviews [4,5]. In recent decades, integrins have emerged as new players in resistance to RTK-targeted therapies. The purpose of this review is to present a synthesis of the literature and to explore the diversity of the mechanisms by which integrins are able to counteract RTK-targeted therapies (Table 1). New promising therapeutic approaches resulting from these discoveries will be also discussed.

**Table 1.** Cases of integrin-mediated resistance to RTK-targeted therapies cited in this review.

RTK	Therapies Targeting RTK	Type of Tumor	Experimental Model	Patient Data	Integrin Modulation	Mechanisms of Resistance	Ref
<b><math>\beta 1</math> integrin</b>							
EGFR	Cetuximab	Head and neck squamous cell carcinoma	A549 cells	-	Cetuximab-induced fibronectin overexpression. siRNA-mediated depletion of $\beta 1$ and $\alpha 5$	Cetuximab enhances p38/ATF2-dependent fibronectin production and the activation of the focal adhesion kinase (FAK)/Erk pathway. siRNA-mediated depletion of $\beta 1$ and $\alpha 5$ integrin decreases the cell survival of cetuximab-treated cells.	[10]
EGFR	Cetuximab	Pancreatic cancer	Miapaca-2, Capan-2, SW1990 AsPC-1, BXPc-3, PANC-1	-	-Endogenous overexpression of $\beta 1$ integrin in resistant cells -siRNA-mediated depletion of $\beta 1$	$\beta 1$ overexpression in resistant cells stimulates Src and Akt pathways. Extracellular matrix (ECM)-independent activation of $\beta 1$ is mediated by its interaction with neuropilin-1. siRNA-mediated depletion of $\beta 1$ or inhibition of $\beta 1$ /neuropilin-1 interaction increases cetuximab cell toxicity.	[11]
EGFR	mAb225	Colon cancer	Caco-2	-	Plasmid-induced $\alpha 5$ overexpression	Fibronectin stimulation of $\alpha 5$ -expressing cells overrides mAb225-mediated cell growth inhibition. Integrin activates epidermal growth factor receptor (EGFR) kinase and the mitogen-activated protein kinase (MAPK) pathway.	[12]
EGFR	Gefitinib Erlotinib	Lung cancer	PC-9 and 11-18	Patient samples	-Endogenous overexpression of $\beta 1$ integrin in resistant cells and tumors -siRNA-mediated depletion of $\beta 1$	siRNA-mediated silencing of $\beta 1$ restores Erlotinib potency to inhibit cell proliferation and the Src and Akt pathways.	[13]
EGFR	PD1530335 (AG1517)	Glioma	Glioma stem-like cells (GSCs) isolated from glioblastoma (G1BM) surgical pieces	-	Lentiviral-mediated $\beta 1$ overexpression	Delocalization of $\beta 1$ integrin from lipid raft sensitizes GSC to tyrosine kinase inhibitor (TKI)-induced apoptosis. $\beta 1$ overexpression protects GSC from apoptosis in a FAK-dependent manner.	[14]

Table 1. Cont.

RTK	Therapies Targeting RTK	Type of Tumor	Experimental Model	Patient Data	Integrin Modulation	Mechanisms of Resistance	Ref
HER2	Trastuzumab Lapatinib	Breast cancer	HER2+ cells (BT147, HCC1954)	-	-Endogenous overexpression of $\beta 1$ integrin in resistant cells. -shRNA-mediated depletion of $\beta 1$ and function-blocking mAb	Overexpression of $\beta 1$ enhances FAK and Src phosphorylation. Silencing or functional inhibition of $\beta 1$ integrin sensitizes cells to HER-2 inhibition (cell proliferation, apoptosis, clonogenic assays) in a FAK-dependent way.	[15]
HER2	TPB (trastuzumab + pertuzumab + burpatrisib)	Breast cancer	Tumors cells derived from HER2+/PIK3CAH <sup>187R</sup> mice, MDA-MB453, HCC1954 cell lines	Patient samples and data	-Endogenous overexpression of collagen II in resistant tumors - $\beta 1$ function-blocking mAb	Resistance to anti-HER2 tritherapy activates $\beta 1$ integrin and Src pathways. Inhibition of $\beta 1$ /Src blocks cell II-induced resistance to TPB (cell growth, cell survival)	[16]
VEGFR	Bevacizumab	Glioma	U87, bevacizumab-resistant cell lines derived from surgical pieces (in vitro and xenografts)	Patient samples and data	-Endogenous overexpression of $\beta 1$ integrin in resistant cells. -shRNA-mediated depletion of $\beta 1$ and function-blocking mAb	Bevacizumab induces hypoxia that is associated with increased $\beta 1$ and FAK expression. $\beta 1$ inhibition (function-blocking mAb) results in increased cell apoptosis and in disrupted tumor mass formation in the treated tumor	[17]
VEGFR	Bevacizumab	Glioblastoma breast cancer	PDX for bevacizumab-resistant human GBM and breast cancer cells	Patient samples	Increased $\beta 1$ /c-Met complex formation in bevacizumab-resistant tumors	Vascular endothelial growth factor receptor (VEGFR)-2 activation impedes $\beta 1$ /cMet complex formation. Resistance to antiangiogenic therapy increased $\beta 1$ /cMet complex formation and cross-activation of both receptors.	[18]
$\beta 3$ integrin							
EGFR	Erlotinib Lapatinib	Lung cancer	A549 and H23 xenograft	Patient samples	shRNA-mediated depletion of $\beta 3$	EGFR TKI treatment induces selection of $\beta 3$ -positive cancer stem cells. Integrin $\beta 3$ (in a ligand-independent way) interacts with galectin-3 to promote KRAS/RalB/NFKB activation, thereby promoting cell survival.	[19]

Table 1. Cont.

RTK	Therapies Targeting RTK	Type of Tumor	Experimental Model	Patient Data	Integrin Modulation	Mechanisms of Resistance	Ref
IGFR	Linsitinib	Pancreatic cancer	Panc-1 and FC xenograft	-	-Ergonomic silencing of $\beta 3$ -targeting miR-489-3p in resistance cells -Lentivirus-mediated expression of $\beta 3$ -Inhibitor or mimic of miR-489-3p	Hypermethylation of miR-489-3p in resistant cells activates the $\beta 3$ -dependent FAK/Erk pathway to promote cell survival and EMT	[20]
EGFR	Gefitinib	Lung cancer	HCC827	-	-	Upon cixutumumab treatment, insulin-like growth factor (IGF)-1 directly binds to integrin $\alpha v \beta 3$ , increasing Src/Akt-dependent proliferation and survival.	[21]
IGFR	Cixutumumab	Head and neck squamous cell carcinoma Lung cancer	Several cell lines 686LN, UMN5CC38, H2268, A549 in vitro and xenograft	Patient samples	shRNA-mediated depletion of $\beta 3$ and function-blocking mAb	Activation of $\beta 3$ /PI3K/Akt/GSK3 $\beta$ / $\beta$ -catenin pathway reduces apoptotic level and increases cell proliferation in resistant cells	[22]
PDGFR, VEGFR, FGFR	Sorafenib	Acute myeloid leukemia	MV4-11	Patient samples and data	-Endogenous overexpression of $\beta 3$ integrin in resistant cells - $\beta 3$ function-blocking mAb	Forced expression of galectin-1 elevates $\beta 3$ expression and activates the FAK/PI3K/Akt pathway to trigger EMT. This is correlated with an increased resistance to sorafenib in galectin-1 expressing cells.	[23]
PDGFR, VEGFR, FGFR	Sorafenib	Hepatic cancer	Huh7, Hep3B, SK-Hep-1, HepG2, PLC/PRF/5	-	-shRNA-mediated depletion of $\beta 3$		
<b><math>\beta 4</math> Integrin</b>							
HER2	Gefitinib	Breast cancer	Murine model mammary gland MMTV-Neu (YD)	-	-Forced expression of $\beta 4$ mutant (depleted from its signaling domain)	$\alpha 6 \beta 4$ /ErbB2 complex activates transcription factor STAT3 and c-Jun to promote cancer progression. The signaling domain of $\beta 4$ is required to trigger gefitinib resistance by an unknown mechanism, whereas ErbB2, C-Jun and STAT3 phosphorylation is still inhibited by gefitinib.	[24]
HER2	Trastuzumab Lapatinib	Breast cancer	BT474, ZR-75-1, SKBR3, MDAMB-435	-	shRNA-mediated depletion of $\alpha 6 \beta 4$ and function-blocking mAbs	Integrin-mediated adhesion to laminin-5 promotes resistance to anti-ERB2 therapies. Removal of CD151 (an integrin co-receptor) or FAK sensitizes cells to drugs (cell proliferation)	[25]
EGFR	Gefitinib	Gastric cancer	SGC7901	Patient samples	-Endogenous overexpression of $\alpha 6 \beta 4$ integrin in resistant cells -siRNA-mediated depletion of $\alpha 6 \beta 4$	Endogenous or forced expression of $\beta 4$ integrin promotes gefitinib resistance (cell proliferation and apoptosis). $\beta 4$ expression is correlated with a decrease in p-EGFR protein levels.	[26]
EGFR	Gefitinib	Hepatic cancer	HLE, Alexander, HepG2, Sk-Hep1	-	Laminin-332 expression	Lm-332-dependent activation of integrin dampens gefitinib effectiveness in cell proliferation survival and apoptosis assays. Lm-332 potentiates the activation of Akt in gefitinib-treated cells.	[27]

Table 1. Cont.

RTK	Therapies Targeting RTK	Type of Tumor	Experimental Model	Patient Data	Integrin Modulation	Mechanisms of Resistance	Ref
FAK							
EGFR	Erlotinib	Lung cancer	A549, H1299, H1975, HCC827, HCC4006 Xenograft of A549	-	FAK inhibitors	Combination of FAK inhibitors and erlotinib is more potent than a single agent to reduce cell viability (2D and 3D models), to increase the apoptosis pathway and cell cycle arrest in resistant cells, and to reduce tumor growth in vivo. The sensitization of erlotinib by FAK inhibitors is associated with a strong inhibition of Akt.	[28]
EGFR	Erlotinib Osimertinib	Lung cancer	PC-9, H1975, HCC827, HCC4006, H5255, 11-18 cell lines PC-9 xenografts	-	FAK inhibitor	Activation of FAK and Src family kinases (SFK) pathways attenuates the efficiency of EGFR therapies presumably via the sustained activation of MAPK and Akt pathways. Concomitant inhibition FAK, Src and EGFR inhibitors potentially inhibit MAPK and Akt pathways and cell proliferation.	[29]
EGFR	Atatinib Erlotinib Osimertinib	Lung cancer	PC-9, HCC827 Established TKI-resistant cells	-	siRNA-mediated depletion of FAK and inhibitor	Compensatory activation of SFKs, FAK and Akt is observed in TKI-resistant cells. FAK inhibition increased atatinib efficacy to inhibit cell survival and cell migration.	[30]
EGFR	Erlotinib	Lung cancer	H1299, H1650 cell lines H388 cell line and xenograft	-	siRNA-mediated depletion of FAK and inhibitor (PF-562271)	Mass spectrometry analysis revealed an aberrant phosphorylation of FAK in erlotinib-resistant cells. Inhibition of FAK led to a decrease in cell survival in erlotinib-treated cells.	[31]

## 2. $\beta$ 1 Integrins

$\beta$ 1 integrins form heterodimers with no less than 12 of the 18 known alpha subunits, and thus represent the largest integrin subgroup.  $\beta$ 1 integrins are overexpressed in solid tumors such as breast carcinoma, lung carcinoma and head and neck squamous cell carcinoma (HNSCC) [32–34]. In cancer cells,  $\beta$ 1 integrins are associated with proliferative signaling, trigger cell death resistance, induce angiogenesis and activate cell migration and the metastatic cascade [35–39].  $\beta$ 1 integrins contribute to chemotherapy resistance [38,40–50] and promote radiotherapy resistance in HNSCC [51–54], breast carcinoma [55,56], laryngeal carcinoma [57,58], and glioma [59,60]. Based on these observations,  $\beta$ 1 integrin antagonists such as small molecules (ATN-161, JSM6427) or function-blocking antibodies (volociximab, OS2966) have been considered as potential therapeutic approaches [32].

### 2.1. $\beta$ 1 Integrins Promote Resistance to EGFR-Targeted Therapies

#### 2.1.1. Cooperation between $\beta$ 1 Integrin and EGFR in Cancer Cells

EGFR was the first growth factor receptor reported as being activated in normal cells by  $\beta$ 1 integrin adhesion to fibronectin, with or without the presence of EGF [61,62]. In cancer cells,  $\beta$ 1 integrin potentiates EGF-mediated EGFR autophosphorylation in vitro and in vivo [38].  $\beta$ 1 integrin also regulates EGFR membrane trafficking and so modulates its oncogenic signaling activity [63]. In human ovarian carcinoma cells,  $\alpha$ 5 $\beta$ 1 coordinates EGFR recycling to the plasma membrane in a way that enhances EGFR-Tyr845 phosphorylation and the serine kinase Akt downstream pathway, thus promoting cell invasion [64]. In lung carcinoma cells, the level of  $\beta$ 1 integrin expression regulates the cell surface expression of EGFR and sustains its endocytic pathway [38]. It should be noted that although the literature has mostly described  $\beta$ 1 integrins as positive regulators of EGFR, the relationship between integrin and EGFR appears to be far more complex. For instance,  $\alpha$ 5 $\beta$ 1 has been described as restricting EGFR membrane localization and responsiveness to EGF stimulation [65], while  $\alpha$ 1 $\beta$ 1 inhibits EGFR signaling by activating the protein phosphatase TCPTP (T-cell protein tyrosine phosphatase) [66].  $\beta$ 1 integrin/EGFR interaction was initially suggested by co-immunoprecipitation and confocal experiments, and FRET analysis revealed potential direct physical interaction between  $\beta$ 1 integrin and either EGFR [59,67] or HER2 (ErbB2) [68]. Studies on  $\beta$ 1 integrin cooperation with EGFR have revealed new avenues for improving the effectiveness of radiotherapy. Indeed, EGFR/ $\beta$ 1 complex formation is a prognostic factor for radiotherapy resistance in glioma [59]. The importance of EGFR/ $\beta$ 1 integrin cooperation in radiotherapy resistance has been confirmed by experiments which have shown that co-targeting the two of them radiosensitizes cancer cells [10,53]. Whole exome analysis has identified mTOR and KEAP1 as potential genetic biomarkers and molecular targets for radiosensitizing HNSCC [69]. By contrast, concomitant inhibition of  $\beta$ 1 integrin and EGFR in HNSCC spheroids [70] and colon carcinoma [71] does not improve radiotherapy efficacy.

#### 2.1.2. Molecular Mechanism of $\beta$ 1 Integrin-Mediated Resistance to EGFR-Targeted Therapies

The most common type of lung cancer is non-small cell lung carcinoma (NSCLC), and it is characterized by EGFR overexpression. Several oral tyrosine kinase inhibitors (TKIs) targeting EGFR are used in clinical practice for treating NSCLC, including gefitinib, erlotinib, afatinib, dacomitinib and osimertinib. These drugs show some efficacy, but NSCLC eventually relapses. Resistance to treatment is caused either by T790M EGFR mutation, which impedes TKIs (except osimertinib) from binding to EGFR by increasing its affinity to ATP, or by the activation of alternative or downstream signaling pathways [72]. Several groups independently report that acquired resistance to gefitinib has correlated with  $\beta$ 1 integrin overexpression in NSCLC cells [13,73,74] or in lung tumor samples from patients refractory to gefitinib or erlotinib [13]. Interestingly, these studies revealed that  $\beta$ 1 integrin overexpression occurs in NSCLC cells that do or do not harbor EGFR T790M mutations, irrespective of EGFR-phosphorylation level. Both antibody-mediated functional inhibition and siRNA-mediated silencing of  $\beta$ 1 integrin sensitize

NSCLC to TKIs in vitro and in vivo [13,38,73], demonstrating that  $\beta 1$  integrin is instrumental in TKI resistance. Conversely, the vector-mediated overexpression of  $\beta 1$  integrin protects cancer cells from TKI-induced cell growth inhibition [14,38]. Downstream of the  $\beta 1$ /PI3K and  $\beta 1$ /Src/FAK pathways, the serine kinase Akt plays a pivotal role in resistance to gefitinib or erlotinib (Figure 1) [13,38,73,75]. FAK is an essential protein in integrin/growth factor receptor crosstalk and could be a valuable target for sensitizing cancer cells to TKIs [76]. Integrin-dependent FAK activation decreased cancer cells' sensitivity to anti-EGFR drugs [10,14]. A series of studies confirmed the importance of FAK signaling in resistance to first- (erlotinib), second- (afatinib) and third-generation (osimertinib) EGFR TKIs [28–31].

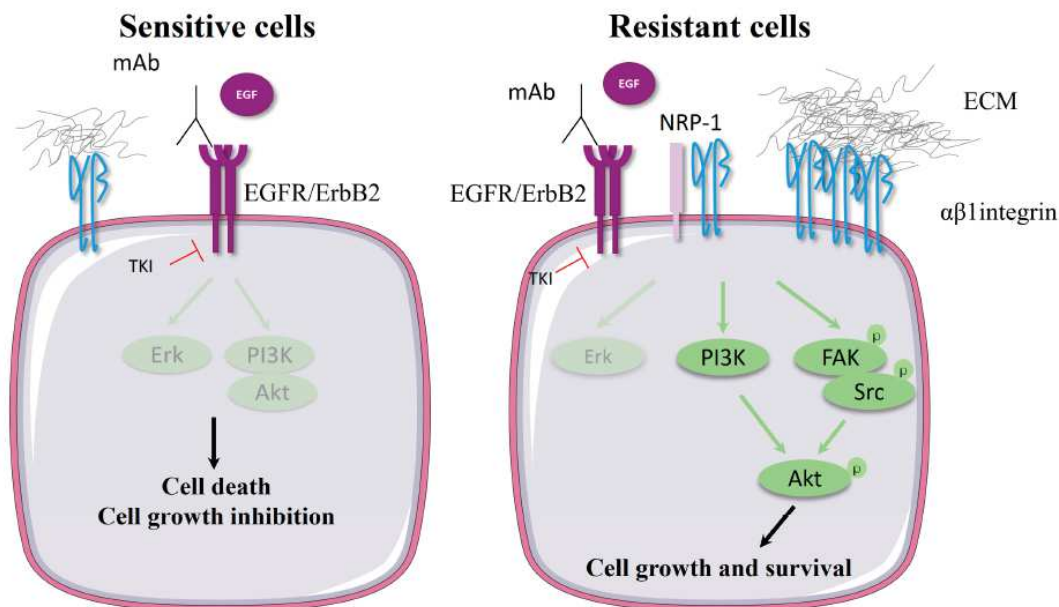


**Figure 1.**  $\beta 1$  integrin induces EGFR- or HER (ErbB2)-targeted therapy resistance. In sensitive cells, the inhibition of the ErbB receptor family by either antibodies or tyrosine kinase inhibitors (TKIs) blocks Erk and Akt pathway activation leading to cell death and cell growth inhibition. In resistant cells,  $\beta 1$  integrin or its associated extracellular matrix (ECM) proteins are often overexpressed, leading to the activation of  $\beta 1$ -downstream pathways such as PI3K or FAK/Src. These pathways converge to activate the serine kinase Akt that promotes cell survival and cell growth. Alternatively,  $\beta 1$  integrin can be activated by coreceptors such as neuropilin-1 (NRP-1) to trigger EGFR-targeted therapy resistance independently of integrin-mediated cell adhesion.

$\beta 1$  integrins can also trigger resistance to antibody-mediated EGFR inhibition. In colon carcinoma cells, the fibronectin/ $\alpha 5\beta 1$  axis overcomes the inhibition of EGFR-mediated cell growth by mAb225, the murine form of the chimeric anti-EGFR antibody cetuximab [12]. In lung carcinoma cells, cetuximab activates the p38/ATF2 pathway. This enhances fibronectin synthesis, which in turn dampens cetuximab's cytotoxic effect both in vitro and in xenografted mice.  $\alpha 5\beta 1$  integrin-silencing sensitized NSCLC cells to cetuximab monotherapy, showing that  $\alpha 5\beta 1$  integrin-mediated adhesion to fibronectin plays an essential role in reducing cetuximab activity in lung carcinoma cells [10,53]. In pancreatic ductal adenocarcinoma cells, the overexpression of  $\beta 1$  activates the FAK/Src/Akt pathway, triggering EGFR ligand-independent cell growth and thus bypassing cetuximab antagonist activity [11].

## 2.2. B1 Integrins Promote Resistance to Therapies Targeting HER2

HER2 (ErbB2) is another member of the EGFR family with intrinsic tyrosine kinase activity and is devoid of a ligand-binding domain. Overexpressed in nearly 30% of breast cancers, HER2 plays an important role in cancer progression. It is a highly attractive target for treatment with trastuzumab or pertuzumab, two humanized HER2- targeted antibodies, or for treatment with lapatinib, a TKI. Despite the radical improvement in the prognosis of HER2+ breast cancer brought about by these

drugs, most patients with HER2+ tumors relapse and progress within a few years [77]. Using a genetic approach in mice,  $\beta 1$  integrin expression has been shown to play a critical role in HER2- induced breast tumor progression but is not required for tumor formation [78]. An immunochemical analysis of clinical samples revealed that  $\beta 1$  integrin overexpression is a negative prognostic factor for patients with HER2+ breast cancer being treated with trastuzumab [68]. In vitro,  $\beta 1$  integrin is overexpressed in HER2+ breast tumor cells with de novo resistance to trastuzumab.  $\beta 1$  integrin knockdown by siRNA silencing or inhibition by function-blocking antibody therapy enhanced drug efficacy by inhibiting the Erk1,2 and Akt pathways [79]. In contrast, another report showed that HER2+ breast cancer cell lines with de novo resistance to trastuzumab were not sensitized by  $\beta 1$  integrin inhibition, presumably because they maintain HER2 hyperphosphorylation. However, in the same study,  $\beta 1$  integrin was shown to promote resistance to lapatinib/trastuzumab treatment via an upregulation of FAK and Src. In that setting, antibody-mediated inhibition of  $\beta 1$  integrin decreased the 3D-growth and survival of the resistant cells being treated [15]. HER3, a kinase-dead member of the EGFR family, regulates HER2 signaling by initiating ligand-induced HER2 activation in the HER2-HER3 heterodimer. Co-targeting HER3 (via siRNA-mediated silencing) and  $\beta 1$  integrin (via a function-blocking antibody) is more effective in controlling tumor growth in mice than the dual inhibition of HER2 (lapatinib) and  $\beta 1$  integrin (antibody) [80].

The tumor microenvironment may markedly affect the response to HER2- targeted therapy [3]. Laminin-332, a ligand of integrins  $\alpha 6\beta 4$ ,  $\alpha 6\beta 1$  and  $\alpha 3\beta 1$ , is lost during the malignant transformation of breast cancer but remains expressed by normal tissue and may thus support the initial transition to invasive cancer. Integrin-dependent adhesion to laminin-332 elicits lapatinib and trastuzumab resistance in HER2+ human breast tumor cell lines [25]. Recently, Hanker and colleagues used genetic engineering of HER2+/PIK3CA<sup>H1047R</sup> mice to generate tumors resistant to TPB treatment (trastuzumab + pertuzumab + burparlisib, a PI3K inhibitor). Whole genome sequencing did not reveal any acquired mutation that could explain the acquired resistance to TPB. RNA-seq analysis did reveal the upregulation of several ECM genes, including Col2a1, which codes for the collagen type II alpha 1 chain. Collagen II activates the  $\beta 1$  integrin/Src pathway, promoting tumor resistance to TPB. In clinical settings, collagen II expression on immunohistochemical analysis correlates with a poor response to HER2- targeted therapies [16]. Antibody-drug conjugates (ADCs) are a promising novel class of therapeutic agents that combine a cytotoxic agent with the antigenic selectivity of an antibody. Ado-trastuzumab emtansine (T-DM1) is an ADC consisting of trastuzumab and DM1, a microtubule inhibitor [81]. Despite a good initial response to the drug, most patients eventually relapse due to acquired resistance. Recent reports have documented alterations in the ECM/integrin pathway in T-DM1-resistant cancer cells [82,83], which represent promising new approaches to enhancing T-DM1 toxicity against cancer cells.

### 2.3. $\beta 1$ Integrin Expression Confers Resistance to Anti-Angiogenic Therapies Targeting VEGFR or c-Met

Tumor neo-angiogenesis is the formation of new blood vessels from those pre-existing in the tumor. Neo-angiogenesis is a critical step in tumor progression as it enhances tumor growth and cancer cell metastasis. The concept of anti-angiogenic therapy, i.e., inhibiting pro-angiogenic factors, has remained disappointing, in part due to acquired resistance [84]. The role of integrin in endothelial cell migration and survival and in angiogenesis has been widely described [85]. Several reports indicate that  $\beta 1$  integrin plays a part in anti-angiogenic therapy resistance [35,86]. Bevacizumab, a humanized antibody against VEGF-A, was the first anti-angiogenic drug used in clinical practice [87]. Micro-array analysis revealed that a subset of bevacizumab-resistant glioblastomas (GBMs) harbor  $\alpha 5$  integrin and fibronectin overexpression [88], likely due to hypoxia provoked by bevacizumab treatment [17]. The inhibition of  $\beta 1$  integrin could become a treatment avenue in the future, as  $\beta 1$  integrin knockdown in bevacizumab-resistant glioma cells prevents in vivo growth while OS2966, a  $\beta 1$  function-blocking antibody, potentiates bevacizumab therapy [17].



The hepatocyte growth factor (HGF)/c-Met pathway plays an important role in tumor angiogenesis as well as in the development of resistance to VEGFR inhibition by TKIs [89].  $\beta 1$  integrin and c-Met are able to form a complex and drive mutual ligand-independent cross-activation [18,90], indicating that  $\beta 1$  integrin and c-Met crosstalk may represent an adaptive mechanism to anti-angiogenic therapies. C-Met and  $\beta 1$  integrin membrane trafficking are closely related. In vascular endothelial cells, HGF stimulates  $\beta 1$  integrin recycling to promote cell spreading, focal adhesion formation, cell migration and tumor angiogenesis [91]. Moreover, c-Met can induce  $\beta 1$  integrin endocytosis [92], and integrin can transmit cell survival signaling from early endosomes [93]. The serine–threonine kinase MAP4K4 activates  $\beta 1$  integrin and mediates the accumulation of activated c-Met in cytosolic vesicles [94]. Thus,  $\beta 1$  integrin/c-Met ligand-independent cooperation is not restricted to the cell surface and can occur in autophagy-like endosomal compartments [95]. Because VEGFR-2 activation sequesters  $\beta 1$  integrin from c-Met in patients, the  $\beta 1$  integrin/c-Met complex is associated with bevacizumab resistance in GBM. It is interesting to note that OS2966 can reduce the formation of the  $\beta 1$  integrin/c-Met complex [18], which could explain its anti-angiogenic activity in bevacizumab-resistant tumors [17]. Targeting  $\beta 1$  integrin/c-Met complex formation may open up new treatment options for overriding resistance to targeted therapy and so limiting tumor angiogenesis as well as c-Met-mediated cell growth [75].

It seems clear that  $\beta 1$  integrins play a pivotal role in resistance to RTK-targeted therapies both in vitro and in vivo. The pharmacological manipulation of integrins [14,15,18,79,80] or downstream signaling molecules such as FAK or Akt [51–54,58–61] has shown some efficacy in preclinical models and may offer promising new avenues to sensitizing cancer cells to anti-RTK therapies.  $\beta 1$  integrin expression levels could also represent a potent biomarker for stratifying patients likely to derive greater benefit from anti-RTK therapy, but the search for a molecular complex such as  $\beta 1$ /EGFR,  $\beta 1$ /HER2 or  $\beta 1$ /c-Met could lead to even more promising strategies (Figure 2) [18,59,68].

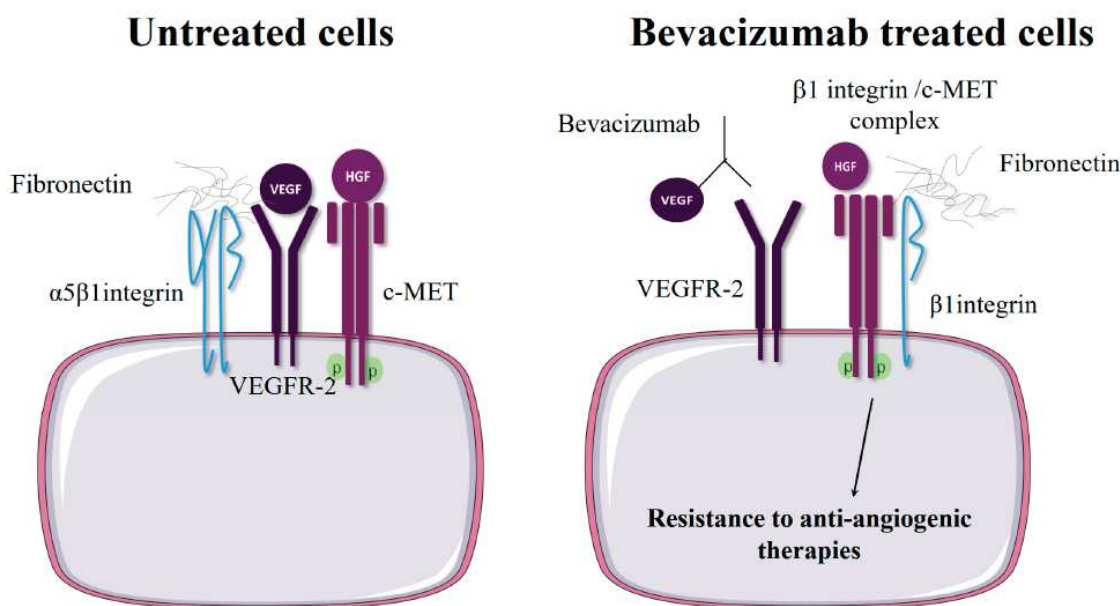


**Figure 2.** Hypothetical model presenting how  $\beta 1$ /c-MET molecular complexes provide cancer cell resistance to anti-angiogenic therapies. In untreated cells, ligand-activated VEGFR-2 engages both  $\alpha 5\beta 1$  integrin and c-MET, impeding their physical contact. In  $\alpha 5\beta 1$  integrin-expressing cells, anti-angiogenic therapeutic intervention with bevacizumab decreases VEGF/VEGFR-2 binding.  $\beta 1$ /c-MET complex formation is thus promoted, which leads to the cross-activation of both receptors and the activation of the downstream AKT signaling pathway (adapted from [18]).

In solid tumors, resistance to targeted therapies can be mediated by  $\beta 1$  integrin via a wide diversity of mechanisms that may require ligand-dependent or -independent integrin functions, or  $\beta 1$

integrin interaction with RTKs or with other co-receptors. The clinical relevance of the *in vitro* and *in vivo* studies was mainly evident in glioma and breast cancers. Even with the promising therapeutic role of  $\beta 1$  integrin, it is important to keep in mind the complexity of integrin functions and the fact that the  $\alpha$  subunits involved in the process remain indeterminate most of the time, although we know their importance in integrin function. The present data could also benefit from a patient stratification, allowing decreased doses of targeted therapy and consequently fewer secondary effects.

### 3. $\alpha v \beta$ Integrins

$\alpha v \beta$  integrins are a large family of integrins ( $\alpha v \beta 3$ ,  $\alpha v \beta 5$ ,  $\alpha v \beta 6$  and  $\alpha v \beta 8$ ).  $\alpha v$  integrins drive cancer progression and are upregulated either by cancer cells or endothelial cells in many solid tumors, including colon carcinoma, melanoma, and breast, lung, pancreatic and brain cancers.  $\alpha v \beta$  integrins are characterized by their capacity to recognize the RGD (arginine-glycine-aspartate) peptide sequence in a large variety of ligands (such as vitronectin, fibronectin and osteopontin) [96].  $\alpha v \beta$  integrin expression and activation drive the intracellular signaling that promotes cancer cell survival, invasion, metastasis, angiogenesis, and self-renewal [5,97], as well as chemotherapy resistance [98,99] and radiotherapy resistance [100–104]. Extensive preclinical studies have established  $\alpha v \beta 3$  inhibitors as potential new therapeutic tools [103,105–107], with several trials evaluating their efficacy in clinical settings as a result [108–110]. Cilengitide (EMD121974, Merck), a cyclic pentapeptide derived from the RGD sequence, was the most promising drug and was evaluated in clinical trials in newly diagnosed GBM. Unfortunately, these trials revealed that cilengitide did not improve the outcomes of patients receiving chemo- and radiotherapy [111–113], making it necessary to re-evaluate the treatment conditions or improve the molecular-based selection of patients who could benefit from cilengitide. Recently, Cosset and colleagues have shown that in GBM,  $\alpha v \beta 3$  integrin enhances the expression of the high-affinity glucose transporter GLUT3 via PAK4 (P21 Activated Kinase 4)/YAP (Yes-associated protein) pathway activation. The overexpression of GLUT3 increased tumor cell survival in a glucose-depleted environment. Furthermore, using genomic analysis the authors identified a subset of  $\alpha v \beta 3$ /GLUT3-expressing tumors that were addicted to GLUT3 as well as highly sensitive to cilengitide and function-blocking anti- $\alpha v$  antibodies [114].

#### 3.1. $\alpha v$ Integrin Triggers Resistance to Anti-EGFR Therapies

The work of Seguin and colleagues paved the way for the demonstration of a pivotal role for  $\alpha v \beta 3$  integrin in resistance to EGFR-targeted therapy [19]. They first established that  $\alpha v \beta 3$  integrin was selectively expressed by tumor-initiating cells from lung and pancreatic carcinoma patient-derived-xenografts (PDXs). More strikingly,  $\beta 3$  expression drove lung and pancreatic cancer cell resistance to TKIs targeting EGFR (erlotinib and lapatinib) both *in vitro* and *in mice*. Conversely, the short hairpin RNA-mediated depletion of  $\beta 3$  sensitized cells to the TKIs. In fact, TKI treatment of human PDX tumors led to the selection of  $\beta 3$ -positive cells that acquired stem cell-like and resistant phenotypes. Mechanistically,  $\beta 3$  integrin activates the KRAS (V-Ki-ras2 Kirsten rat sarcoma viral oncogene homolog)/RalB (Ras-like proto-oncogene B)/NF- $\kappa$ B pathway. It is important to note that the activation of this pathway is independent of the canonical FAK pathway and of integrin/ECM interaction. While this is surprising at first glance, the same group had already observed that  $\alpha v \beta 3$  integrin could promote tumor progression independently of ligand binding and FAK activation [115]. The authors discovered that the recruitment of KRAS and the consequent activation of RalB by  $\beta 3$  required  $\beta 3$  binding to galectin-3, a cell adhesion protein with a specific affinity for  $\beta$ -galactoside glycoconjugates (Figure 3).  $\beta 3$  integrin may also play a pivotal role in mutant KRAS oncogenic function [116]. In a subset of lung and pancreatic adenocarcinomas addicted to mutant KRAS, the disruption of galectin-3/ $\beta 3$  interaction by GCS-100, a galectin-3 antagonist currently under clinical development [117], released mutant KRAS from  $\beta 3$  and inhibited tumor growth in mice. While these results may suggest that GCS-100 could sensitize lung cancer cells to TKIs, the authors have not yet explored this possibility. A growing body of data indicates that microRNA (miRNA)

dysregulation modulates gefitinib resistance in lung carcinoma [118–124]. In gefitinib-resistant cells, a miRNA targeting the 3'-UTR of  $\beta 3$  integrin (miR-483-3p) is silenced by epigenetic methylation. The forced overexpression of  $\beta 3$  integrin can restore gefitinib resistance in miR-483-3p-expressing cells through the activation of a  $\beta 3$ /FAK/ERK pathway and epithelial to mesenchymal transition induction [20].

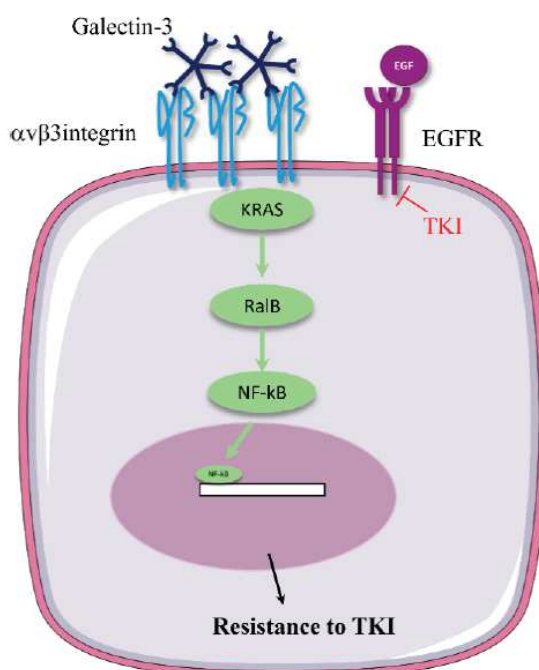


**Figure 3.**  $\beta 3$ /KRAS/RalB/NF $\kappa$ B pathway mediates EGFR-targeted therapy resistance. In EGFR TKI-treated tumors, cells overexpressing  $\alpha v \beta 3$  integrin are selected, leading to a resistant tumor. By binding to oligosaccharide moieties of  $\beta 3$  integrin, galectin-3 promotes integrin/KRAS interaction independently of integrin-mediated adhesion to ECM proteins. KRAS activates the downstream RalB/NF $\kappa$ B pathway that leads to therapy resistance by promoting a stem cell-like phenotype (adapted from [19]).

The role of  $\alpha v$  integrin in resistance to anti-EGFR therapy has been assessed in clinical settings. Cilengitide has been evaluated in combination with cetuximab in two phase II clinical trials on HNSCC and NSCLC [125]. Cilengitide did not improve patient outcomes. However, *ex vivo* experiments on patient-derived samples showed that a subset of sensitive tumors could be selected based on the inhibition of colony formation or cytokine release [126,127]. The phase I/II Poseidon trial explored the efficacy of a combination treatment using abituzumab, an  $\alpha v$  integrin inhibitor, and cetuximab in KRAS wild-type metastatic colorectal cancer. Again, the trial did not reach the primary phase II endpoint, but the authors did observe that patients overexpressing  $\alpha v \beta 6$  integrin might benefit from the abituzumab/cetuximab plus irinotecan combination treatment compared to cetuximab plus irinotecan alone [128]. In the future, therefore, reliable biomarkers may emerge for selecting patients likely to benefit from the synergy between  $\alpha v$  integrin and EGFR inhibition.

### 3.2. $\alpha v \beta 3$ Integrin Involvement in Resistance to Drugs Targeting Other RTKs

Insulin-like growth factors and their cognate receptors are important in cancer progression [129]. Antibody-based therapy against IGF-1R has shown limited efficacy in phase II/III clinical trials [130].  $\alpha v \beta 3$  integrin enhances IGF-1R signaling activity through the joint ligand-dependent activation of both receptors. However, another model of crosstalk has been proposed in which the IGF-1R ligand, IGF-1, directly binds to the  $\beta 3$  integrin subunit and promotes the anchorage-independent formation of a  $\beta 3$ /IGF-1/IGF-1R ternary complex [131–134].  $\alpha v \beta 3$  integrin significantly contributes to resistance to

IGF-1R-targeted TKIs [19]. In HNSCC and NSCLC, during treatment with cixutumumab, a humanized anti-IGF-1R antibody, the Src/Akt pathway is activated by IGF-1/ $\beta$ 3 integrin interaction independently of cell/ECM interaction. The molecular targeting of  $\beta$ 3 integrin increased cixutumumab's efficacy both in vitro and in mice [21]. While these preclinical data are encouraging, the role of the  $\beta$ 3/Src pathway in resistance to anti-IGFR treatment has not yet been evaluated in clinical settings.

Sorafenib is a multikinase inhibitor for treating hepatocellular, kidney and thyroid carcinomas [135]. According to KINOMEscan data from the Library of Integrated Network-based Cellular Signatures project (<http://lincs.hms.harvard.edu/>), among the numerous kinases inhibited by sorafenib are the receptors for PDGF, VEGF and fibroblast growth factor. In acute myeloid leukaemia,  $\alpha$ v $\beta$ 3 integrin expression is a negative prognostic factor and is associated with a decrease in sorafenib activity. Mechanistically,  $\alpha$ v $\beta$ 3 integrin is activated by osteopontin and stimulates the PI3K/Akt/GSK3 pathway [22]. In hepatocellular carcinoma, galectin-1, a  $\beta$ -galactoside-binding protein, is a negative prognostic factor [136], whose expression increases sorafenib resistance [23]. Galectin-1 stimulates  $\alpha$ v $\beta$ 3 expression and hyperactivation of the  $\beta$ 3/FAK/PI3K/Akt pathway to potentiate EMT, but a clear demonstration of a role of  $\beta$ 3 in resistance to sorafenib is missing in this study [23]. Galectin-1 has been shown to interact with other integrins, including  $\beta$ 1 [136–138]. Thus, given their ability to regulate both  $\beta$ 1 and  $\beta$ 3 integrin function, dysregulation of galectin-1 and galectin-3 expression in the tumor microenvironment may have a profound impact on the efficacy of therapies targeting RTKs.

In vitro and vivo data revealed that  $\alpha$ v $\beta$ 3 integrin may support resistance to therapies targeting several RTKs (EGFR, IGFR, PDGFR, FGFR, VEGFR). Furthermore, mechanisms of resistance to EGFR and IGFR TKIs have been identified and found to be independent of  $\alpha$ v $\beta$ 3 binding to ECM ligands, via recognition of the RGD sequence [19,21]. Given the clinical failure of cilengitide to improve the outcomes of cetuximab-treated patients [122,123], the time may have come for the development and use of integrin-targeted drugs that do not target integrin binding to ECM proteins such as RGD-derived peptide.

#### 4. $\alpha$ 6 $\beta$ 4 Integrins

As a nucleator of hemidesmosomes,  $\alpha$ 6 $\beta$ 4 integrin, a laminin-332 (also named laminin-5) receptor, is a master regulator of epithelium integrity and homeostasis. Hemidesmosomes are junctional structures that mediate the firm adhesion of epithelial cells to the basement membrane by linking intermediate filaments to laminin-332. Dysregulation of  $\alpha$ 6 $\beta$ 4 leads to aberrant hemidesmosomal and epithelial dysfunction [139,140]. It has been reported that hemidesmosomal  $\alpha$ 6 $\beta$ 4 integrin is not fully competent for signal transduction, suggesting that epithelium/basement membrane attachment remains its main function in healthy tissue [24,141].

##### 4.1. Crosstalk between $\alpha$ 6 $\beta$ 4 Integrin and Growth Factor Receptors

Hemidesmosomes are dynamic adhesive structures that must be dismantled to allow epithelial cell migration during wound healing.  $\alpha$ 6 $\beta$ 4 interaction with hemidesmosomal proteins is tightly regulated by EGFR signaling pathways [142–147]. EGFR activation promotes the phosphorylation of serine residues in the signaling domain of  $\beta$ 4, which disrupts its interaction with plectin, a linker between integrin and intermediate filaments. The phosphorylated  $\beta$ 4 cytoplasmic domain serves as a docking platform to stimulate signaling pathways (such as Src, PI3K, Rho GTPases) and synergize with RTKs. The clinical significance and roles of  $\alpha$ 6 $\beta$ 4 in carcinoma development and progression have been extensively reviewed [148,149]. In mice, the ablation of  $\alpha$ 6 integrin in intestinal epithelial cells has led to hemidesmosomal disruption and a loss of epithelial/basement membrane junction integrity. These mice spontaneously developed long-standing colitis and subsequent colorectal carcinoma [150]. This may suggest that  $\alpha$ 6 $\beta$ 4 acts as a tumor suppression gene. However, except in basal carcinoma and prostate carcinoma,  $\alpha$ 6 $\beta$ 4 is overexpressed in epithelial tumors and largely contributes to cancer progression and poor prognosis [148]. In these tumors, over-activation of the EGFR, HER2 or c-Met pathways disrupted plectin/ $\alpha$ 6 $\beta$ 4 integrin coupling and hemidesmosomal disassembly [151,152].  $\alpha$ 6 $\beta$ 4 becomes

fully competent for signal transduction and cooperation with RTKs [24,153], and can promote cancer cell proliferation and survival, tumor invasion, metastasis and angiogenesis [149].

#### 4.2. $\alpha 6\beta 4$ Integrin and Resistance to Anti-HER2 Therapies

Although  $\alpha 6\beta 4$  integrin is a pertinent therapeutic target in most forms of carcinoma, few studies have evaluated its potential to trigger RTK-targeted therapy resistance. Using an in vitro knock-in system, Guo and colleagues established a murine model in which endogenous  $\beta 4$  integrin was replaced by signaling-defective  $\beta 4$  integrin (lacking the carboxyterminal moiety of its intracellular domain) in the mammary gland of MMTV-Neu(YD) mice [24]. In this model, wild-type (WT)  $\beta 4$  integrin, but not the mutant form, synergized with HER2 to increase mammary carcinoma tumorigenicity. Interestingly, the therapeutic activity of gefitinib was dampened in WT- $\beta 4$  mice compared to mutant- $\beta 4$  mice, indicating that  $\beta 4$  signaling function can promote resistance to anti-HER2 drugs. The molecular pathway eliciting this resistance is independent of HER2 phosphorylation and remains unknown. Small molecules or antibodies capable of disrupting the integrin/HER2 heterocomplex may improve HER2-targeted therapies. In human breast cancer cells, the expression of laminin-332 or  $\alpha 6\beta 4$  integrin triggers a notable resistance to trastuzumab and lapatinib [25]. Gefitinib-mediated cell toxicity was substantially reduced when hepatocarcinoma cells were exposed to laminin-332 but not to other ECM proteins such as collagen or fibronectin [27]. More recently, high  $\beta 4$  integrin expression was associated with a gefitinib-resistant phenotype in gastric cancer cells [26]. The resistant phenotype could be reverted by RNA-mediated  $\beta 4$  silencing, whereas sensitive cells became more resistant to gefitinib after  $\beta 4$  overexpression. A clinical study in 38 patients has indicated some correlation between  $\beta 4$  expression and gefitinib resistance. However, given the small sample size, it is far too early to draw any conclusion about the potential repercussions of this observation [26]. Another clinical study showed that  $\beta 4$  integrin polymorphism expression was associated with resistance to therapy. The authors examined the expression level of three different  $\beta 4$  polymorphisms in HER3-negative/KRAS WT metastatic colorectal cancer from patients receiving irinotecan/cetuximab. Although conducted in a small cohort of patients, the study showed a significant decrease in progression-free survival and overall survival in patients harboring the  $\beta 4$  rs8669 G polymorphism [154].

It is clear that  $\alpha 6\beta 4$  can unleash the oncogenic potency of RTKs in cancer cells. Data obtained from cell lines, murine models and patient samples are the first insight into the role of  $\alpha 6\beta 4$  integrin in resistance mechanisms to TKIs and antibodies against members of the HER family. Further investigation is required to assess the clinical relevance of these observations. Targeting  $\alpha 6\beta 4$  integrin/RTK interaction could be a promising strategy for overcoming resistance. Another strategy could be to use integrin  $\beta 4$  expression and polymorphism to stratify patients to EGFR-targeted therapies.

### 5. Integrins and Carcinoma-Associated Fibroblasts

Tumor progression relies on close interaction and communication between cancer cells and cancer-associated fibroblasts (CAFs) through several mechanisms, including paracrine signals (transforming growth factor- $\beta$ , IGF-1, exosomes), cell-to-cell contact and ECM remodeling [155,156]. Emerging data indicating that CAFs can decrease therapeutic response (including to anti-RTK drugs) have been extensively reviewed [157]. We will restrict our analysis to research incriminating integrin involvement in CAF-mediated therapy resistance.

In breast cancer cells, physical interaction between cancer cells and stromal cells (mesenchymal stem cells or CAFs) strongly protects against lapatinib or trastuzumab [158,159]. In those two studies, no experimental data could attest to any role for integrin in CAF-mediated resistance. However, CAF/breast cancer cell interaction requires the synthesis of hyaluronic acid by CAFs [159]. Hyaluronic acid can bind to and activate CD44, a known partner and regulator of integrins [160]. Alternatively, integrin may also be involved in CAF/cancer cell interaction. For instance, we showed that  $\alpha 5\beta 1$  integrin can promote cell/cell interaction during tumor spheroid formation [161]. This particular

integrin can mediate CAF interaction with a highly aggressive subset of ovarian carcinoma cells. Heterotypic CAF/cancer cell spheroids promote the metastasis of ovarian cells in mice [162].

In vitro assays have revealed that collagen fiber synthesis and assembly by CAFs promote lung cancer cell resistance to gefitinib and osimertinib [163]. Another study showed that collagen-mediated resistance to TKIs requires the activation of the Akt/mTOR pathway [164]. Interestingly, the inhibition of collagen synthesis or  $\beta 1$  integrin function suppresses this resistance, offering new therapeutic options [163]. These observations may be clinically relevant as increased collagen deposition has been observed in erlotinib-resistant xenografts [163], and as progression-free survival has been seen to decrease in gefitinib-treated patients with collagen-rich lung tumors [164]. Another group used genetically modified mice expressing inducible RAF-driven tumors to model melanoma development in the ear. For the longitudinal monitoring of tumor development, the authors used intravital two-photon microscopy of fluorescently tagged melanoma cells. Upon MEK inhibition, the tumors transiently responded but returned to their original size after 12 weeks of treatment. It was noted that the cells that survived MEK inhibition co-localized with collagen bundles (imaged by second harmonic generation) [165].

Hirata and colleagues have shown that melanoma-associated fibroblasts can drive resistance to the BRAF (v-Raf murine sarcoma viral oncogene homolog B) inhibitor vemurafenib by stimulating fibronectin production and remodeling, and subsequently promoting  $\beta 1$ /Src/FAK pathway signaling in melanoma [166]. Another study confirmed the crucial role of fibronectin/ $\beta 1$  integrin signaling in melanoma adaptation to BRAF inhibition [167]. In both studies, following vemurafenib treatment, increases in fibrous ECM were observed in xenograft tumors and in several excised human melanomas. The concomitant inhibition of BRAF and FAK to suppress PDX growth in mice has been advanced as one way of improving therapy [166]. The efficacy of this therapeutic option was recently confirmed through the screening of a kinase inhibitor library [168]. Matrix stiffening generates mechanical forces that are transduced through the plasma membrane by integrin adhesome and stimulate YAP and TAZ (transcriptional coactivator with PDZ-binding motif) nuclear translocation and activation [169,170]. Cancer cells that express the activating mutant of Ras (RASG12D) are addicted to this oncogene. Studies from two different laboratories conjointly established that YAP and TAZ activation drive mutant KRAS-independent tumor growth and progression [171,172]. Therefore, increased matrix stiffness is sufficient to protect BRAF-mutant melanoma cells from BRAF inhibition [166], while YAP/TAZ activation induces resistance to therapy targeting the RAS/RAF pathway [173,174]. Additionally, several concurrent reports confirmed that matrix stiffening modulates cancer cell response to TKIs [175–177]. As mechanotransducers, integrin and FAK play key functions in tension generation by CAFs [178–182]. In turn, ECM stiffening enhances integrin signaling in cancer cells [183] and contributes to cancer progression [184]. Hence integrin mechanosensing plays multiple roles in the microenvironment (both in stromal and cancer cells) that promote tumor growth and therapy resistance [185,186]. It can be hypothesized that YAP/TAZ regulation by integrin mechanotransduction provides a safe haven that protects cells from therapies targeting the RTK pathway (Figure 4).

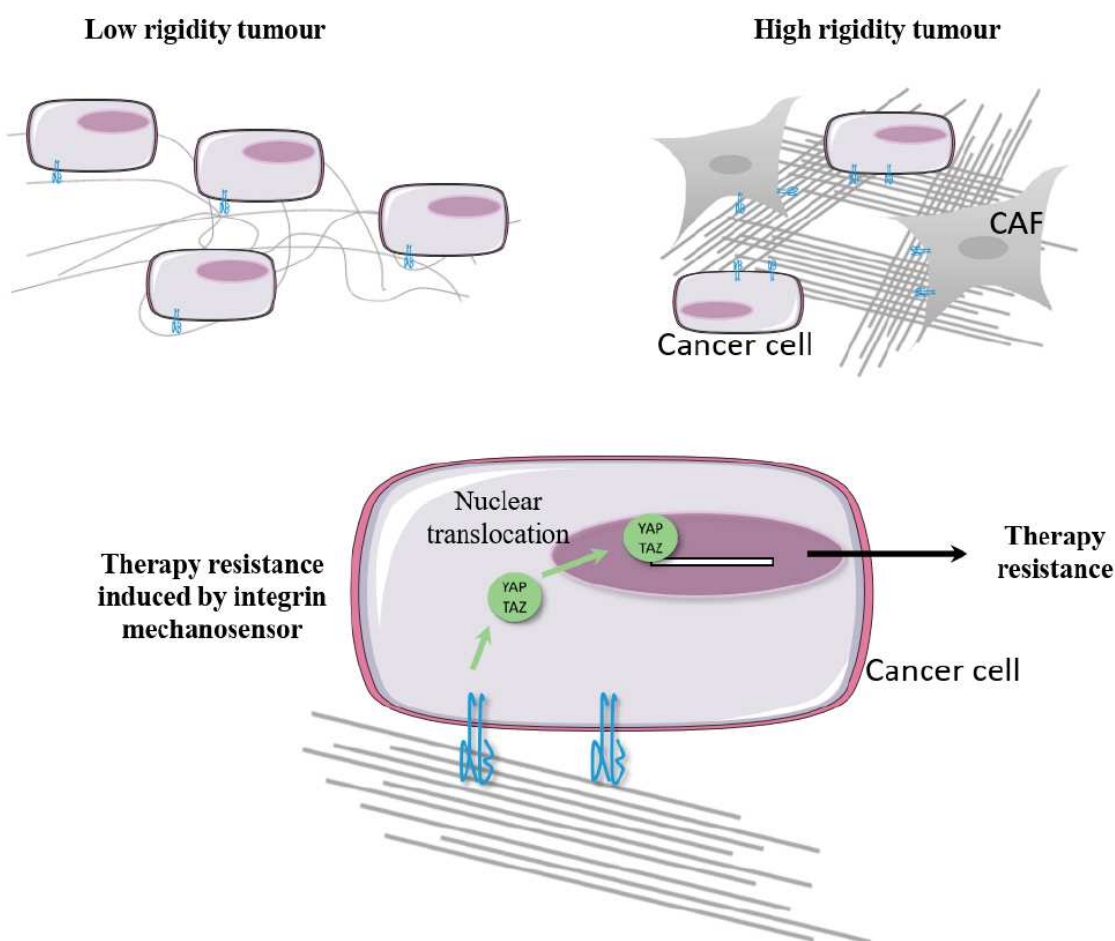


**Figure 4.** Hypothetic model showing how integrins may trigger therapy resistance in stiff micro-environmental niches. Therapy-resistant tumors are often characterized by an increase in matrix stiffness. Cancer-associated fibroblast (CAF) integrins (mainly  $\alpha 5\beta 1$  integrin) generate mechanical forces that increase ECM protein assembly and matrix rigidity. In cancer cells, the sensing of CAF-generated tension by integrins activates transcriptional co-regulators YAP and TAZ and their translocation to the nucleus. The transcriptional response leads to therapy resistance (adapted from [186]).

## 6. Conclusions

As shown in this review, integrin interacts with several RTKs such as the HER family, c-Met, PDGFR and others. These interactions can give cells an intrinsic ability to better adapt to and resist targeted therapies. Several integrin inhibitors were described and are being tested in clinical settings, albeit with no strong benefit, not even in combination with RTK inhibitors. It should be noted that, although in clinical practice integrin-targeted therapies are based on the inhibition of their adhesive function by small antagonist molecules or monoclonal antibodies, several studies have shown that integrin/RTK interactions and integrin-mediated resistance to therapies targeting RTK can be elicited by unbound integrins [19,95,115,153]. The ability of integrins to form functional molecular complexes with RTKs makes the situation much more difficult to understand. But it also makes new treatment approaches possible, be it predicting the efficacy of anti-RTK therapies in subpopulations of patients based on their level of heterocomplex expression [18,59] or developing treatments for disrupting integrin/RTK complex formation [17,18]. Aptamers, small nucleic acids used in treatment [187], can disrupt EGFR/ $\beta 3$  integrin interaction to inhibit tumor growth [188]. Meanwhile, targeting EGFR/uPAR using an integrin antagonist confers sensitivity to vemurafenib [189]. Finally, Kim and colleagues created an antibody that co-targets EGFR and neuropilin-1, a receptor that physically interacts with active  $\beta 1$  integrin. This antibody enhanced  $\beta 1$  integrin internalization and so led to the inhibition of  $\beta 1$  signaling,

reducing tumor volume in in vivo experiments [11]. All these examples illustrate the strong potential of this new therapeutic concept.

New functions of integrins are continually being discovered, proving their importance in therapy resistance. A better understanding of the molecular mechanisms underlying the integrin/RTK relationship could one day make it possible to improve the efficacy of therapies targeting RTKs.

**Funding:** This research was supported by the French research funding program Ligue contre le cancer—Appel d’offres 2017 CCIR Est—Projets de Recherche Interrégionaux Multicentriques. Elisabete Cruz Da Silva is a PhD student funded by the University of Strasbourg.

**Conflicts of Interest:** The authors declare no conflict of interest.

## References

- Hanahan, D.; Weinberg, R.A. Hallmarks of cancer: The next generation. *Cell* **2011**, *144*, 646–674. [[CrossRef](#)] [[PubMed](#)]
- Paraiso, K.H.T.; Smalley, K.S.M. Fibroblast-mediated drug resistance in cancer. *Biochem. Pharmacol.* **2013**, *85*, 1033–1041. [[CrossRef](#)]
- Zoeller, J.J.; Bronson, R.T.; Selfors, L.M.; Mills, G.B.; Brugge, J.S. Niche-localized tumor cells are protected from HER2-targeted therapy via upregulation of an anti-apoptotic program in vivo. *NPJ Breast Cancer* **2017**, *3*, 18. [[CrossRef](#)] [[PubMed](#)]
- Ivaska, J.; Heino, J. Cooperation between integrins and growth factor receptors in signaling and endocytosis. *Annu. Rev. Cell Dev. Biol.* **2011**, *27*, 291–320. [[CrossRef](#)] [[PubMed](#)]
- Desgrosellier, J.S.; Chersesh, D.A. Integrins in cancer: Biological implications and therapeutic opportunities. *Nat. Rev. Cancer* **2010**, *10*, 9–22. [[CrossRef](#)]
- Barczyk, M.; Carracedo, S.; Gullberg, D. Integrins. *Cell Tissue Res.* **2010**, *339*, 269–280. [[CrossRef](#)]
- Xing, Z.; Chen, H.C.; Nowlen, J.K.; Taylor, S.J.; Shalloway, D.; Guan, J.L. Direct interaction of v-Src with the focal adhesion kinase mediated by the Src SH2 domain. *Mol. Biol. Cell* **1994**, *5*, 413–421. [[CrossRef](#)]
- Paul, M.K.; Mukhopadhyay, A.K. Tyrosine kinase—Role and significance in Cancer. *Int. J. Med. Sci.* **2004**, *1*, 101–115. [[CrossRef](#)] [[PubMed](#)]
- Sangwan, V.; Park, M. Receptor tyrosine kinases: Role in cancer progression. *Curr. Oncol.* **2006**, *13*, 191–193.
- Eke, I.; Storch, K.; Krause, M.; Cordes, N. Cetuximab attenuates its cytotoxic and radiosensitizing potential by inducing fibronectin biosynthesis. *Cancer Res.* **2013**, *73*, 5869–5879. [[CrossRef](#)]
- Kim, Y.-J.; Jung, K.; Baek, D.-S.; Hong, S.-S.; Kim, Y.-S. Co-targeting of EGF receptor and neuropilin-1 overcomes cetuximab resistance in pancreatic ductal adenocarcinoma with integrin  $\beta$ 1-driven Src-Akt bypass signaling. *Oncogene* **2017**, *36*, 2543–2552. [[CrossRef](#)] [[PubMed](#)]
- Kuwada, S.K.; Li, X. Integrin  $\alpha$ 5/ $\beta$ 1 Mediates fibronectin-dependent epithelial cell proliferation through epidermal growth factor receptor activation. *Mol. Biol. Cell* **2000**, *11*, 2485–2496. [[CrossRef](#)] [[PubMed](#)]
- Kanda, R.; Kawahara, A.; Watari, K.; Murakami, Y.; Sonoda, K.; Maeda, M.; Fujita, H.; Kage, M.; Uramoto, H.; Costa, C.; et al. Erlotinib resistance in lung cancer cells mediated by integrin  $\beta$ 1/Src/Akt-driven bypass signaling. *Cancer Res.* **2013**, *73*, 6243–6253. [[CrossRef](#)] [[PubMed](#)]
- Srikanth, M.; Das, S.; Berns, E.J.; Kim, J.; Stupp, S.I.; Kessler, J.A. Nanofiber-mediated inhibition of focal adhesion kinase sensitizes glioma stemlike cells to epidermal growth factor receptor inhibition. *Neuro. Oncol.* **2013**, *15*, 319–329. [[CrossRef](#)]
- Huang, C.; Park, C.C.; Hilsenbeck, S.G.; Ward, R.; Rimawi, M.F.; Wang, Y.-C.; Shou, J.; Bissell, M.J.; Osborne, C.K.; Schiff, R.  $\beta$ 1 integrin mediates an alternative survival pathway in breast cancer cells resistant to lapatinib. *Breast Cancer Res.* **2011**, *13*, R84. [[CrossRef](#)] [[PubMed](#)]
- Hanker, A.B.; Estrada, M.V.; Bianchini, G.; Moore, P.D.; Zhao, J.; Cheng, F.; Koch, J.P.; Gianni, L.; Tyson, D.R.; Sánchez, V.; et al. Extracellular matrix/integrin signaling promotes resistance to combined inhibition of HER2 and PI3K in HER2+ breast cancer. *Cancer Res* **2017**, *77*, 3280–3292. [[CrossRef](#)]
- Carbonell, W.S.; DeLay, M.; Jahangiri, A.; Park, C.C.; Aghi, M.K.  $\beta$ 1 integrin targeting potentiates antiangiogenic therapy and inhibits the growth of bevacizumab-resistant glioblastoma. *Cancer Res.* **2013**, *73*, 3145–3154. [[CrossRef](#)] [[PubMed](#)]



18. Jahangiri, A.; Nguyen, A.; Chandra, A.; Sidorov, M.K.; Yagnik, G.; Rick, J.; Han, S.W.; Chen, W.; Flanigan, P.M.; Schneidman-Duhovny, D.; et al. Cross-activating c-Met/ $\beta$ 1 integrin complex drives metastasis and invasive resistance in cancer. *Proc. Natl. Acad. Sci. USA* **2017**, *114*, E8685–E8694. [[CrossRef](#)] [[PubMed](#)]
19. Seguin, L.; Kato, S.; Franovic, A.; Camargo, M.F.; Lesperance, J.; Elliott, K.C.; Yebra, M.; Mielgo, A.; Lowy, A.M.; Husain, H.; et al. An integrin  $\beta$ 3-KRAS-RalB complex drives tumour stemness and resistance to EGFR inhibition. *Nat. Cell Biol.* **2014**, *16*, 457–468. [[CrossRef](#)]
20. Yue, J.; Lv, D.; Wang, C.; Li, L.; Zhao, Q.; Chen, H.; Xu, L. Epigenetic silencing of miR-483-3p promotes acquired gefitinib resistance and EMT in EGFR-mutant NSCLC by targeting integrin  $\beta$ 3. *Oncogene* **2018**, *37*, 4300–4312. [[CrossRef](#)]
21. Shin, D.H.; Lee, H.-J.; Min, H.-Y.; Choi, S.P.; Lee, M.-S.; Lee, J.W.; Johnson, F.M.; Mehta, K.; Lippman, S.M.; Glisson, B.S.; et al. Combating resistance to anti-IGFR antibody by targeting the integrin  $\beta$ 3-Src pathway. *J. Natl. Cancer Inst.* **2013**, *105*, 1558–1570. [[CrossRef](#)]
22. Yi, H.; Zeng, D.; Shen, Z.; Liao, J.; Wang, X.; Liu, Y.; Zhang, X.; Kong, P. Integrin  $\alpha$ v $\beta$ 3 enhances  $\beta$ -catenin signaling in acute myeloid leukemia harboring Fms-like tyrosine kinase-3 internal tandem duplication mutations: Implications for microenvironment influence on sorafenib sensitivity. *Oncotarget* **2016**, *7*, 40387–40397. [[CrossRef](#)]
23. Zhang, P.-F.; Li, K.-S.; Shen, Y.; Gao, P.-T.; Dong, Z.-R.; Cai, J.-B.; Zhang, C.; Huang, X.-Y.; Tian, M.-X.; Hu, Z.-Q.; et al. Galectin-1 induces hepatocellular carcinoma EMT and sorafenib resistance by activating FAK/PI3K/AKT signaling. *Cell Death Dis.* **2016**, *7*, e2201. [[CrossRef](#)]
24. Guo, W.; Pylayeva, Y.; Pepe, A.; Yoshioka, T.; Muller, W.J.; Inghirami, G.; Giancotti, F.G.  $\beta$ 4 integrin amplifies ErbB2 signaling to promote mammary tumorigenesis. *Cell* **2006**, *126*, 489–502. [[CrossRef](#)]
25. Yang, X.H.; Flores, L.M.; Li, Q.; Zhou, P.; Xu, F.; Krop, I.E.; Hemler, M.E. Disruption of laminin-integrin-CD151-focal adhesion kinase axis sensitizes breast cancer cells to ErbB2 antagonists. *Cancer Res.* **2010**, *70*, 2256–2263. [[CrossRef](#)]
26. Huafeng, J.; Deqing, Z.; Yong, D.; Yulian, Z.; Ailing, H. A cross-talk between integrin  $\beta$ 4 and epidermal growth factor receptor induces gefitinib chemoresistance to gastric cancer. *Cancer Cell Int.* **2018**, *18*. [[CrossRef](#)]
27. Giannelli, G.; Azzariti, A.; Fransvea, E.; Porcelli, L.; Antonaci, S.; Paradiso, A. Laminin-5 offsets the efficacy of gefitinib ('Iressa') in hepatocellular carcinoma cells. *Br. J. Cancer* **2004**, *91*, 1964–1969. [[CrossRef](#)] [[PubMed](#)]
28. Howe, G.A.; Xiao, B.; Zhao, H.; Al-Zahrani, K.N.; Hasim, M.S.; Villeneuve, J.; Sekhon, H.S.; Goss, G.D.; Sabourin, L.A.; Dimitroulakos, J.; et al. Focal adhesion kinase inhibitors in combination with erlotinib demonstrate enhanced anti-tumor activity in non-small cell lung cancer. *PLoS ONE* **2016**, *11*, e0150567. [[CrossRef](#)]
29. Ichihara, E.; Westover, D.; Meador, C.B.; Yan, Y.; Bauer, J.A.; Lu, P.; Ye, F.; Kulick, A.; de Stanchina, E.; McEwen, R.; et al. SFK/FAK signaling attenuates osimertinib efficacy in both drug-sensitive and drug-resistant models of EGFR-mutant lung cancer. *Cancer Res.* **2017**, *77*, 2990–3000. [[CrossRef](#)]
30. Murakami, Y.; Sonoda, K.; Abe, H.; Watari, K.; Kusakabe, D.; Azuma, K.; Kawahara, A.; Akiba, J.; Oneyama, C.; Pachter, J.A.; et al. The activation of SRC family kinases and focal adhesion kinase with the loss of the amplified, mutated EGFR gene contributes to the resistance to afatinib, erlotinib and osimertinib in human lung cancer cells. *Oncotarget* **2017**, *8*, 70736–70751. [[CrossRef](#)]
31. Solanki, H.S.; Raja, R.; Zhavoronkov, A.; Ozerov, I.V.; Artemov, A.V.; Advani, J.; Radhakrishnan, A.; Babu, N.; Puttamalles, V.N.; Syed, N.; et al. Targeting focal adhesion kinase overcomes erlotinib resistance in smoke induced lung cancer by altering phosphorylation of epidermal growth factor receptor. *Oncoscience* **2018**, *5*, 21–38.
32. Barkan, D.; Chambers, A.F.  $\beta$ 1-Integrin: A potential therapeutic target in the battle against cancer recurrence. *Clin. Cancer Res.* **2011**, *17*, 7219–7223. [[CrossRef](#)]
33. Cordes, D.N.; Park, C.C.  $\beta$ 1 integrin as a molecular therapeutic target. *Int. J. Radiat. Biol.* **2007**, *83*, 753–760. [[CrossRef](#)]
34. Schaffner, F.; Ray, A.M.; Dontenwill, M. Integrin  $\alpha$ 5 $\beta$ 1, the fibronectin receptor, as a pertinent therapeutic target in solid tumors. *Cancers* **2013**, *5*, 27–47. [[CrossRef](#)]
35. Blandin, A.-F.; Renner, G.; Lehmann, M.; Lelong-Rebel, I.; Martin, S.; Dontenwill, M.  $\beta$ 1 integrins as therapeutic targets to disrupt hallmarks of cancer. *Front. Pharmacol.* **2015**, *6*. [[CrossRef](#)]
36. Chen, M.B.; Lamar, J.M.; Li, R.; Hynes, R.O.; Kamm, R.D. Elucidation of the roles of tumor integrin  $\beta$ 1 in the extravasation stage of the metastasis cascade. *Cancer Res.* **2016**, *76*, 2513–2524. [[CrossRef](#)]

37. Lahlou, H.; Muller, W.J.  $\beta$ 1-integrins signaling and mammary tumor progression in transgenic mouse models: Implications for human breast cancer. *Breast Cancer Res.* **2011**, *13*, 229. [[CrossRef](#)]
38. Morello, V.; Cabodi, S.; Sigismund, S.; Camacho-Leal, M.P.; Repetto, D.; Volante, M.; Papotti, M.; Turco, E.; Defilippi, P.  $\beta$ 1 integrin controls EGFR signaling and tumorigenic properties of lung cancer cells. *Oncogene* **2011**, *30*, 4087–4096. [[CrossRef](#)]
39. White, D.E.; Kurpios, N.A.; Zuo, D.; Hassell, J.A.; Blaess, S.; Mueller, U.; Muller, W.J. Targeted disruption of  $\beta$ 1-integrin in a transgenic mouse model of human breast cancer reveals an essential role in mammary tumor induction. *Cancer Cell* **2004**, *6*, 159–170. [[CrossRef](#)]
40. Aoudjit, F.; Vuori, K. Integrin signaling inhibits paclitaxel-induced apoptosis in breast cancer cells. *Oncogene* **2001**, *20*, 4995–5004. [[CrossRef](#)]
41. Hartmann, T.N.; Burger, J.A.; Glodek, A.; Fujii, N.; Burger, M. CXCR4 chemokine receptor and integrin signaling co-operate in mediating adhesion and chemoresistance in small cell lung cancer (SCLC) cells. *Oncogene* **2005**, *24*, 4462–4471. [[CrossRef](#)]
42. Janouskova, H.; Maglott, A.; Leger, D.Y.; Bossert, C.; Noulet, F.; Guerin, E.; Guenot, D.; Pinel, S.; Chastagner, P.; Plenat, F.; et al. Integrin  $\alpha$ 5 $\beta$ 1 plays a critical role in resistance to temozolomide by interfering with the p53 pathway in high-grade glioma. *Cancer Res.* **2012**, *72*, 3463–3470. [[CrossRef](#)]
43. Janouskova, H.; Ray, A.-M.; Noulet, F.; Lelong-Rebel, I.; Choulier, L.; Schaffner, F.; Lehmann, M.; Martin, S.; Teisinger, J.; Dontenwill, M. Activation of p53 pathway by Nutlin-3a inhibits the expression of the therapeutic target  $\alpha$ 5 integrin in colon cancer cells. *Cancer Lett.* **2013**, *336*, 307–318. [[CrossRef](#)]
44. Klobučar, M.; Grbčić, P.; Pavelić, S.K.; Jonjić, N.; Visentin, S.; Sedić, M. Acid ceramidase inhibition sensitizes human colon cancer cells to oxaliplatin through downregulation of transglutaminase 2 and  $\beta$ 1 integrin/FAK-mediated signalling. *Biochem. Biophys. Res. Commun.* **2018**, *503*, 843–848. [[CrossRef](#)] [[PubMed](#)]
45. Maglott, A.; Bartik, P.; Cosgun, S.; Klotz, P.; Rondé, P.; Fuhrmann, G.; Takeda, K.; Martin, S.; Dontenwill, M. The small  $\alpha$ 5 $\beta$ 1 integrin antagonist, SJ749, reduces proliferation and clonogenicity of human astrocytoma cells. *Cancer Res.* **2006**, *66*, 6002–6007. [[CrossRef](#)]
46. Naci, D.; El Azreq, M.-A.; Chetoui, N.; Lauden, L.; Sigaux, F.; Charron, D.; Al-Daccak, R.; Aoudjit, F.  $\alpha$ 2 $\beta$ 1 integrin promotes chemoresistance against doxorubicin in cancer cells through extracellular signal-regulated kinase (ERK). *J. Biol. Chem.* **2012**, *287*, 17065–17076. [[CrossRef](#)] [[PubMed](#)]
47. Naci, D.; Vuori, K.; Aoudjit, F.  $\alpha$ 2 $\beta$ 1 integrin in cancer development and chemoresistance. *Semin. Cancer Biol.* **2015**, *35*, 145–153. [[CrossRef](#)]
48. Pontiggia, O.; Sampayo, R.; Raffo, D.; Motter, A.; Xu, R.; Bissell, M.J.; de Kier Joffé, E.B.; Simian, M. The tumor microenvironment modulates tamoxifen resistance in breast cancer: A role for soluble stromal factors and fibronectin through  $\beta$ 1 integrin. *Breast Cancer Res. Treat.* **2012**, *133*, 459–471. [[CrossRef](#)] [[PubMed](#)]
49. Renner, G.; Janouskova, H.; Noulet, F.; Koenig, V.; Guerin, E.; Bär, S.; Nuesch, J.; Rechenmacher, F.; Neubauer, S.; Kessler, H.; et al. Integrin  $\alpha$ 5 $\beta$ 1 and p53 convergent pathways in the control of anti-apoptotic proteins PEA-15 and survivin in high-grade glioma. *Cell Death Differ.* **2016**, *23*, 640–653. [[CrossRef](#)]
50. Yang, D.; Shi, J.; Fu, H.; Wei, Z.; Xu, J.; Hu, Z.; Zhang, Y.; Yan, R.; Cai, Q. Integrin $\beta$ 1 modulates tumour resistance to gemcitabine and serves as an independent prognostic factor in pancreatic adenocarcinomas. *Tumour Biol.* **2016**, *37*, 12315–12327. [[CrossRef](#)]
51. Dickreuter, E.; Eke, I.; Krause, M.; Borgmann, K.; van Vugt, M.A.; Cordes, N. Targeting of  $\beta$ 1 integrins impairs DNA repair for radiosensitization of head and neck cancer cells. *Oncogene* **2016**, *35*, 1353–1362. [[CrossRef](#)]
52. Eke, I.; Dickreuter, E.; Cordes, N. Enhanced radiosensitivity of head and neck squamous cell carcinoma cells by  $\beta$ 1 integrin inhibition. *Radiother. Oncol.* **2012**, *104*, 235–242. [[CrossRef](#)]
53. Eke, I.; Zscheppang, K.; Dickreuter, E.; Hickmann, L.; Mazzeo, E.; Unger, K.; Krause, M.; Cordes, N. Simultaneous  $\beta$ 1 integrin-EGFR targeting and radiosensitization of human head and neck cancer. *JNCI J. Natl. Cancer Inst.* **2015**, *107*, dju419. [[CrossRef](#)]
54. Koppenhagen, P.; Dickreuter, E.; Cordes, N. Head and neck cancer cell radiosensitization upon dual targeting of c-Abl and  $\beta$ 1-integrin. *Radiother. Oncol.* **2017**, *124*, 370–378. [[CrossRef](#)]
55. Ahmed, K.M.; Zhang, H.; Park, C.C. NF- $\kappa$ B regulates radioresistance mediated by  $\beta$ 1-integrin in three-dimensional culture of breast cancer cells. *Cancer Res.* **2013**, *73*, 3737–3748. [[CrossRef](#)]
56. Nam, J.-M.; Onodera, Y.; Bissell, M.J.; Park, C.C. Breast cancer cells in three-dimensional culture display an enhanced radioresponse after coordinate targeting of integrin  $\alpha$ 5 $\beta$ 1 and fibronectin. *Cancer Res.* **2010**, *70*, 5238–5248. [[CrossRef](#)]

57. Dong, X.; Luo, Z.; Liu, T.; Chai, J.; Ke, Q.; Shen, L. Identification of integrin  $\beta 1$  as a novel PAG1-interacting protein involved in the inherent radioresistance of human laryngeal carcinoma. *J. Cancer* **2018**, *9*, 4128–4138. [[CrossRef](#)]
58. Li, L.; Dong, X.; Peng, F.; Shen, L. Integrin  $\beta 1$  regulates the invasion and radioresistance of laryngeal cancer cells by targeting CD147. *Cancer Cell Int.* **2018**, *18*, 80. [[CrossRef](#)]
59. Petrás, M.; Lajtos, T.; Friedländer, E.; Klekner, A.; Pintye, E.; Feuerstein, B.G.; Szöllosi, J.; Vereb, G. Molecular interactions of ErbB1 (EGFR) and integrin- $\beta 1$  in astrocytoma frozen sections predict clinical outcome and correlate with Akt-mediated in vitro radioresistance. *Neuro Oncol.* **2013**, *15*, 1027–1040. [[CrossRef](#)]
60. Vehlow, A.; Klapproth, E.; Storch, K.; Dickreuter, E.; Seifert, M.; Dietrich, A.; Bütof, R.; Temme, A.; Cordes, N.; Vehlow, A.; et al. Adhesion- and stress-related adaptation of glioma radiochemoresistance is circumvented by  $\beta 1$  integrin/JNK co-targeting. *Oncotarget* **2017**, *8*, 49224–49237. [[CrossRef](#)]
61. Moro, L.; Venturino, M.; Bozzo, C.; Silengo, L.; Altruda, F.; Beguinot, L.; Tarone, G.; Defilippi, P. Integrins induce activation of EGF receptor: Role in MAP kinase induction and adhesion-dependent cell survival. *EMBO J.* **1998**, *17*, 6622–6632. [[CrossRef](#)]
62. Miyamoto, S.; Teramoto, H.; Gutkind, J.S.; Yamada, K.M. Integrins can collaborate with growth factors for phosphorylation of receptor tyrosine kinases and MAP kinase activation: Roles of integrin aggregation and occupancy of receptors. *J. Cell Biol.* **1996**, *135*, 1633–1642. [[CrossRef](#)]
63. Al-Akhrass, H.; Naves, T.; Vincent, F.; Magnaudeix, A.; Durand, K.; Bertin, F.; Melloni, B.; Jauberteau, M.-O.; Lalloué, F. Sortilin limits EGFR signaling by promoting its internalization in lung cancer. *Nat. Commun.* **2017**, *8*, 1182. [[CrossRef](#)]
64. Caswell, P.T.; Chan, M.; Lindsay, A.J.; McCaffrey, M.W.; Boettiger, D.; Norman, J.C. Rab-coupling protein coordinates recycling of  $\alpha 5 \beta 1$  integrin and EGFR1 to promote cell migration in 3D microenvironments. *J. Cell Biol.* **2008**, *183*, 143–155. [[CrossRef](#)]
65. Hang, Q.; Isaji, T.; Hou, S.; Im, S.; Fukuda, T.; Gu, J. Integrin  $\alpha 5$  suppresses the phosphorylation of epidermal growth factor receptor and its cellular signaling of cell proliferation via N-glycosylation. *J. Biol. Chem.* **2015**, *290*, 29345–29360. [[CrossRef](#)] [[PubMed](#)]
66. Mattila, E.; Pellinen, T.; Nevo, J.; Vuoriluoto, K.; Arjonen, A.; Ivaska, J. Negative regulation of EGFR signalling through integrin- $\alpha 1 \beta 1$ -mediated activation of protein tyrosine phosphatase TCPTP. *Nat. Cell Biol.* **2005**, *7*, 78–85. [[CrossRef](#)]
67. Cabodi, S.; Morello, V.; Masi, A.; Cicchi, R.; Broglio, C.; Distefano, P.; Brunelli, E.; Silengo, L.; Pavone, F.; Arcangeli, A.; et al. Convergence of integrins and EGF receptor signaling via PI3K/Akt/FoxO pathway in early gene Egr-1 expression. *J. Cell. Physiol.* **2009**, *218*, 294–303. [[CrossRef](#)] [[PubMed](#)]
68. Mocanu, M.-M.; Fazekas, Z.; Petrás, M.; Nagy, P.; Sebestyén, Z.; Isola, J.; Timár, J.; Park, J.W.; Vereb, G.; Szöllösi, J. Associations of ErbB2,  $\beta 1$ -integrin and lipid rafts on Herceptin (Trastuzumab) resistant and sensitive tumor cell lines. *Cancer Lett.* **2005**, *227*, 201–212. [[CrossRef](#)]
69. Klapproth, E.; Dickreuter, E.; Zakrzewski, F.; Seifert, M.; Petzold, A.; Dahl, A.; Schröck, E.; Klink, B.; Cordes, N. Whole exome sequencing identifies mTOR and KEAP1 as potential targets for radiosensitization of HNSCC cells refractory to EGFR and  $\beta 1$  integrin inhibition. *Oncotarget* **2018**, *9*, 18099–18114. [[CrossRef](#)]
70. Zscheppang, K.; Kurth, I.; Wachtel, N.; Dubrovska, A.; Kunz-Schughart, L.A.; Cordes, N. Efficacy of Beta1 integrin and EGFR targeting in sphere-forming human head and neck cancer cells. *J. Cancer* **2016**, *7*, 736. [[CrossRef](#)] [[PubMed](#)]
71. Poschau, M.; Dickreuter, E.; Singh-Müller, J.; Zscheppang, K.; Eke, I.; Liersch, T.; Cordes, N. EGFR and  $\beta 1$ -integrin targeting differentially affect colorectal carcinoma cell radiosensitivity and invasion. *Radiother. Oncol.* **2015**, *116*, 510–516. [[CrossRef](#)] [[PubMed](#)]
72. Morgillo, F.; Della Corte, C.M.; Fasano, M.; Ciardiello, F. Mechanisms of resistance to EGFR-targeted drugs: Lung cancer. *ESMO Open* **2016**, *1*, e000060. [[CrossRef](#)] [[PubMed](#)]
73. Deng, Q.-F.; SU, B.; ZHAO, Y.-M.; TANG, L.; ZHANG, J.; ZHOU, C.-C. Integrin  $\beta 1$ -mediated acquired gefitinib resistance in non-small cell lung cancer cells occurs via the phosphoinositide 3-kinase-dependent pathway. *Oncol. Lett.* **2016**, *11*, 535–542. [[CrossRef](#)] [[PubMed](#)]
74. Ju, L.; Zhou, C.; Li, W.; Yan, L. Integrin beta1 over-expression associates with resistance to tyrosine kinase inhibitor gefitinib in non-small cell lung cancer. *J. Cell. Biochem.* **2010**, *111*, 1565–1574. [[CrossRef](#)]
75. Ju, L.; Zhou, C. Association of integrin beta1 and c-MET in mediating EGFR TKI gefitinib resistance in non-small cell lung cancer. *Cancer Cell Int.* **2013**, *13*, 15. [[CrossRef](#)]

76. Mousson, A.; Sick, E.; Carl, P.; Dujardin, D.; De Mey, J.; Rondé, P. Targeting focal adhesion kinase using inhibitors of protein-protein interactions. *Cancers* **2018**, *10*, 278. [[CrossRef](#)] [[PubMed](#)]
77. Nixon, N.A.; Hannouf, M.B.; Verma, S. A review of the value of human epidermal growth factor receptor 2 (HER2)-targeted therapies in breast cancer. *Eur. J. Cancer* **2018**, *89*, 72–81. [[CrossRef](#)] [[PubMed](#)]
78. Huck, L.; Pontier, S.M.; Zuo, D.M.; Muller, W.J.  $\beta$ 1-integrin is dispensable for the induction of ErbB2 mammary tumors but plays a critical role in the metastatic phase of tumor progression. *Proc. Natl. Acad. Sci. USA* **2010**, *107*, 15559–15564. [[CrossRef](#)] [[PubMed](#)]
79. Lesniak, D.; Xu, Y.; Deschenes, J.; Lai, R.; Thoms, J.; Murray, D.; Gosh, S.; Mackey, J.R.; Sabri, S.; Abdulkarim, B. Beta1-integrin circumvents the antiproliferative effects of trastuzumab in human epidermal growth factor receptor-2-positive breast cancer. *Cancer Res.* **2009**, *69*, 8620–8628. [[CrossRef](#)] [[PubMed](#)]
80. Campbell, M.R.; Zhang, H.; Ziaee, S.; Ruiz-Saenz, A.; Gulizia, N.; Oeffinger, J.; Amin, D.N.; Ahuja, D.; Moasser, M.M.; Park, C.C. Effective treatment of HER2-amplified breast cancer by targeting HER3 and  $\beta$ 1 integrin. *Breast Cancer Res. Treat.* **2016**, *155*, 431–440. [[CrossRef](#)]
81. Lewis Phillips, G.D.; Li, G.; Dugger, D.L.; Crocker, L.M.; Parsons, K.L.; Mai, E.; Blättler, W.A.; Lambert, J.M.; Chari, R.V.J.; Lutz, R.J.; et al. Targeting HER2-positive breast cancer with trastuzumab-DM1, an antibody-cytotoxic drug conjugate. *Cancer Res.* **2008**, *68*, 9280–9290. [[CrossRef](#)]
82. Endo, Y.; Shen, Y.; Youssef, L.A.; Mohan, N.; Wu, W.J. T-DM1-resistant cells gain high invasive activity via EGFR and integrin cooperated pathways. *mAbs* **2018**, *10*, 1003–1017. [[CrossRef](#)] [[PubMed](#)]
83. Sauveur, J.; Matera, E.-L.; Chettab, K.; Valet, P.; Guitton, J.; Savina, A.; Dumontet, C. Esophageal cancer cells resistant to T-DM1 display alterations in cell adhesion and the prostaglandin pathway. *Oncotarget* **2018**, *9*, 21141–21155. [[PubMed](#)]
84. Mahdi, A.; Darvishi, B.; Majidzadeh-A, K.; Salehi, M.; Farahmand, L. Challenges facing antiangiogenesis therapy: The significant role of hypoxia-inducible factor and MET in development of resistance to anti-vascular endothelial growth factor-targeted therapies. *J. Cell Physiol.* **2019**, *234*, 5655–5663. [[CrossRef](#)]
85. Avraamides, C.J.; Garmy-Susini, B.; Varner, J.A. Integrins in angiogenesis and lymphangiogenesis. *Nat. Rev. Cancer* **2008**, *8*, 604–617. [[CrossRef](#)] [[PubMed](#)]
86. Jahangiri, A.; Aghi, M.K.; Carbonell, W.S.  $\beta$ 1 Integrin: Critical path to antiangiogenic therapy resistance and beyond. *Cancer Res.* **2014**, *74*, 3–7. [[CrossRef](#)]
87. Ferrara, N.; Hillan, K.J.; Gerber, H.-P.; Novotny, W. Discovery and development of bevacizumab, an anti-VEGF antibody for treating cancer. *Nat. Rev. Drug Discov.* **2004**, *3*, 391–400. [[CrossRef](#)] [[PubMed](#)]
88. DeLay, B.M.; Jahangiri, A.; Carbonell, W.S.; Hu, Y.-L.; Tsao, S.; Tom, M.W.; Paquette, J.; Tokuyasu, T.A.; Aghi, M.K. Microarray analysis verifies two distinct phenotypes of glioblastomas resistant to anti-angiogenic therapy. *Clin. Cancer Res.* **2012**, *18*, 2930–2942. [[CrossRef](#)]
89. Shojaei, F.; Lee, J.H.; Simmons, B.H.; Wong, A.; Esparza, C.O.; Plumlee, P.A.; Feng, J.; Stewart, A.E.; Hu-Lowe, D.D.; Christensen, J.G. HGF/c-Met acts as an alternative angiogenic pathway in sunitinib-resistant tumors. *Cancer Res.* **2010**, *70*, 10090–10100. [[CrossRef](#)]
90. Mitra, A.K.; Sawada, K.; Tiwari, P.; Mui, K.; Gwin, K.; Lengyel, E. Ligand-independent activation of c-Met by fibronectin and  $\alpha(5)\beta(1)$ -integrin regulates ovarian cancer invasion and metastasis. *Oncogene* **2011**, *30*, 1566–1576. [[CrossRef](#)]
91. Hongu, T.; Yamauchi, Y.; Funakoshi, Y.; Katagiri, N.; Ohbayashi, N.; Kanaho, Y. Pathological functions of the small GTPase Arf6 in cancer progression: Tumor angiogenesis and metastasis. *Small GTPases* **2016**, *7*, 47–53. [[CrossRef](#)]
92. Mai, A.; Muharram, G.; Barrow-McGee, R.; Baghirov, H.; Rantala, J.; Kermorgant, S.; Ivaska, J. Distinct c-Met activation mechanisms induce cell rounding or invasion through pathways involving integrins, RhoA and HIP1. *J. Cell Sci.* **2014**, *127*, 1938–1952. [[CrossRef](#)]
93. Alanko, J.; Mai, A.; Jacquemet, G.; Schauer, K.; Kaukonen, R.; Saari, M.; Goud, B.; Ivaska, J. Integrin endosomal signalling suppresses anoikis. *Nat. Cell Biol.* **2015**, *17*, 1412–1421. [[CrossRef](#)]
94. Tripolitsioti, D.; Kumar, K.S.; Neve, A.; Migliavacca, J.; Capdeville, C.; Rushing, E.J.; Ma, M.; Kijima, N.; Sharma, A.; Pruschy, M.; et al. MAP4K4 controlled integrin  $\beta$ 1 activation and c-Met endocytosis are associated with invasive behavior of medulloblastoma cells. *Oncotarget* **2018**, *9*, 23220–23236. [[CrossRef](#)]
95. Barrow-McGee, R.; Kishi, N.; Joffre, C.; Ménard, L.; Hervieu, A.; Bakhouché, B.A.; Noval, A.J.; Mai, A.; Guzmán, C.; Robbez-Masson, L.; et al. Beta 1-integrin-c-Met cooperation reveals an inside-in survival signalling on autophagy-related endomembranes. *Nat. Commun.* **2016**, *7*, 11942. [[CrossRef](#)]

96. Weis, S.M.; Cheresch, D.A.  $\alpha$ v integrins in angiogenesis and cancer. *Cold Spring Harb. Perspect. Med.* **2011**, *1*. [[CrossRef](#)]
97. Nieberler, M.; Reuning, U.; Reichart, F.; Notni, J.; Wester, H.-J.; Schwaiger, M.; Weinmüller, M.; Räder, A.; Steiger, K.; Kessler, H. Exploring the role of RGD-recognizing integrins in cancer. *Cancers* **2017**, *9*, 116. [[CrossRef](#)]
98. He, J.; Wang, F.; Qi, H.; Li, Y.; Liang, H. Down-regulation of  $\alpha$ v integrin by retroviral delivery of small interfering RNA reduces multicellular resistance of HT29. *Cancer Lett.* **2009**, *284*, 182–188. [[CrossRef](#)]
99. Maubant, S.; Cruet-Hennequart, S.; Poulain, L.; Carreiras, F.; Sichel, F.; Luis, J.; Staedel, C.; Gauduchon, P. Altered adhesion properties and alpha v integrin expression in a cisplatin-resistant human ovarian carcinoma cell line. *Int. J. Cancer* **2002**, *97*, 186–194. [[CrossRef](#)] [[PubMed](#)]
100. Malric, L.; Monferran, S.; Delmas, C.; Arnauduc, F.; Dahan, P.; Boyrie, S.; Deshors, P.; Lubrano, V.; Da Mota, D.F.; Gilhodes, J.; et al. Inhibiting integrin  $\beta$ 8 to differentiate and radiosensitize glioblastoma-initiating cells. *Mol. Cancer Res.* **2019**, *17*, 384–397. [[CrossRef](#)] [[PubMed](#)]
101. Mikkelsen, T.; Brodie, C.; Finniss, S.; Berens, M.E.; Rennert, J.L.; Nelson, K.; Lemke, N.; Brown, S.L.; Hahn, D.; Neuteboom, B.; et al. Radiation sensitization of glioblastoma by cilengitide has unanticipated schedule-dependency. *Int. J. Cancer* **2009**, *124*, 2719–2727. [[CrossRef](#)] [[PubMed](#)]
102. Monferran, S.; Skuli, N.; Delmas, C.; Favre, G.; Bonnet, J.; Cohen-Jonathan-Moyal, E.; Toulas, C. Alphavbeta3 and alphavbeta5 integrins control glioma cell response to ionising radiation through ILK and RhoB. *Int. J. Cancer* **2008**, *123*, 357–364. [[CrossRef](#)]
103. Ning, S.; Tian, J.; Marshall, D.J.; Knox, S.J. Anti- $\alpha$ v integrin monoclonal antibody intetumumab enhances the efficacy of radiation therapy and reduces metastasis of human cancer xenografts in nude rats. *Cancer Res.* **2010**, *70*, 7591–7599. [[CrossRef](#)] [[PubMed](#)]
104. Ou, J.; Luan, W.; Deng, J.; Sa, R.; Liang, H.  $\alpha$ V integrin induces multicellular radioresistance in human nasopharyngeal carcinoma via activating SAPK/JNK pathway. *PLoS ONE* **2012**, *7*, e38737. [[CrossRef](#)]
105. Cai, W.; Chen, X. Anti-angiogenic cancer therapy based on integrin alphavbeta3 antagonism. *Anticancer Agents Med. Chem.* **2006**, *6*, 407–428. [[CrossRef](#)]
106. Hsu, A.R.; Veeravagu, A.; Cai, W.; Hou, L.C.; Tse, V.; Chen, X. Integrin alpha v beta 3 antagonists for anti-angiogenic cancer treatment. *Recent Pat. Anticancer Drug Discov.* **2007**, *2*, 143–158.
107. Zhang, D.; Pier, T.; McNeel, D.G.; Wilding, G.; Friedl, A. Effects of a monoclonal anti-alphavbeta3 integrin antibody on blood vessels - a pharmacodynamic study. *Invest. New Drugs* **2007**, *25*, 49–55. [[CrossRef](#)]
108. Eskens, F.A.L.M.; Dumez, H.; Hoekstra, R.; Perschl, A.; Brindley, C.; Böttcher, S.; Wynendaele, W.; Drevs, J.; Verweij, J.; van Oosterom, A.T. Phase I and pharmacokinetic study of continuous twice weekly intravenous administration of Cilengitide (EMD 121974), a novel inhibitor of the integrins alphavbeta3 and alphavbeta5 in patients with advanced solid tumours. *Eur. J. Cancer* **2003**, *39*, 917–926. [[CrossRef](#)]
109. Mas-Moruno, C.; Rechenmacher, F.; Kessler, H. Cilengitide: The first anti-angiogenic small molecule drug candidate. design, synthesis and clinical evaluation. *Anticancer Agents Med. Chem.* **2010**, *10*, 753–768. [[CrossRef](#)] [[PubMed](#)]
110. Stupp, R.; Hegi, M.E.; Neyns, B.; Goldbrunner, R.; Schlegel, U.; Clement, P.M.J.; Grabenbauer, G.G.; Ochsenbein, A.F.; Simon, M.; Dietrich, P.-Y.; et al. Phase I/IIa study of cilengitide and temozolomide with concomitant radiotherapy followed by cilengitide and temozolomide maintenance therapy in patients with newly diagnosed glioblastoma. *J. Clin. Oncol.* **2010**, *28*, 2712–2718. [[CrossRef](#)]
111. Khasraw, M.; Lee, A.; McCowatt, S.; Kerestes, Z.; Buyse, M.E.; Back, M.; Kichenadasse, G.; Ackland, S.; Wheeler, H. Cilengitide with metronomic temozolomide, procarbazine, and standard radiotherapy in patients with glioblastoma and unmethylated MGMT gene promoter in ExCentric, an open-label phase II trial. *J. Neurooncol.* **2016**, *128*, 163–171. [[CrossRef](#)]
112. Nabors, L.B.; Fink, K.L.; Mikkelsen, T.; Grujicic, D.; Tarnawski, R.; Nam, D.H.; Mazurkiewicz, M.; Salacz, M.; Ashby, L.; Zagonel, V.; et al. Two cilengitide regimens in combination with standard treatment for patients with newly diagnosed glioblastoma and unmethylated MGMT gene promoter: Results of the open-label, controlled, randomized phase II CORE study. *Neuro Oncol.* **2015**, *17*, 708–717. [[CrossRef](#)]
113. Stupp, R.; Hegi, M.E.; Gorlia, T.; Erridge, S.C.; Perry, J.; Hong, Y.-K.; Aldape, K.D.; Lhermitte, B.; Pietsch, T.; Grujicic, D.; et al. Cilengitide combined with standard treatment for patients with newly diagnosed glioblastoma with methylated MGMT promoter (CENTRIC EORTC 26071-22072 study): A multicentre, randomised, open-label, phase 3 trial. *Lancet Oncol.* **2014**, *15*, 1100–1108. [[CrossRef](#)]

114. Cosset, É.; Ilmjärv, S.; Dutoit, V.; Elliott, K.; von Schalscha, T.; Camargo, M.F.; Reiss, A.; Moroishi, T.; Seguin, L.; Gomez, G.; et al. Glut3 addiction is a druggable vulnerability for a molecularly defined subpopulation of glioblastoma. *Cancer Cell* **2017**, *32*, 856–868.e5. [[CrossRef](#)]
115. Desgrosellier, J.S.; Barnes, L.A.; Shields, D.J.; Huang, M.; Lau, S.K.; Prévost, N.; Tarin, D.; Shattil, S.J.; Cheresch, D.A. Integrin  $\alpha\beta3/c$ -src “Oncogenic Unit” promotes anchorage-independence and tumor progression. *Nat. Med.* **2009**, *15*, 1163–1169. [[CrossRef](#)]
116. Seguin, L.; Camargo, M.F.; Wettersten, H.I.; Kato, S.; Desgrosellier, J.S.; von Schalscha, T.; Elliott, K.C.; Cosset, E.; Lesperance, J.; Weis, S.M.; et al. Galectin-3, a druggable vulnerability for KRAS-addicted cancers. *Cancer Discov.* **2017**, *7*, 1464–1479. [[CrossRef](#)] [[PubMed](#)]
117. Wdowiak, K.; Francuz, T.; Gallego-Colon, E.; Ruiz-Agamez, N.; Kubezcko, M.; Grochoła, I.; Wojnar, J. Galectin targeted therapy in oncology: Current knowledge and perspectives. *Int. J. Mol. Sci.* **2018**, *19*, 210. [[CrossRef](#)]
118. Chen, X.; Zhu, L.; Ma, Z.; Sun, G.; Luo, X.; Li, M.; Zhai, S.; Li, P.; Wang, X. Oncogenic miR-9 is a target of erlotinib in NSCLCs. *Sci. Rep.* **2015**, *5*, 17031. [[CrossRef](#)]
119. Gao, Y.; Fan, X.; Li, W.; Ping, W.; Deng, Y.; Fu, X. miR-138-5p reverses gefitinib resistance in non-small cell lung cancer cells via negatively regulating G protein-coupled receptor 124. *Biochem. Biophys. Res. Commun.* **2014**, *446*, 179–186. [[CrossRef](#)]
120. Li, B.; Ren, S.; Li, X.; Wang, Y.; Garfield, D.; Zhou, S.; Chen, X.; Su, C.; Chen, M.; Kuang, P.; et al. MiR-21 overexpression is associated with acquired resistance of EGFR-TKI in non-small cell lung cancer. *Lung Cancer* **2014**, *83*, 146–153. [[CrossRef](#)]
121. Shen, H.; Zhu, F.; Liu, J.; Xu, T.; Pei, D.; Wang, R.; Qian, Y.; Li, Q.; Wang, L.; Shi, Z.; et al. Alteration in Mir-21/PTEN Expression Modulates Gefitinib Resistance in Non-Small Cell Lung Cancer. *PLoS ONE* **2014**, *9*, e103305. [[CrossRef](#)] [[PubMed](#)]
122. Wang, S.; Su, X.; Bai, H.; Zhao, J.; Duan, J.; An, T.; Zhuo, M.; Wang, Z.; Wu, M.; Li, Z.; et al. Identification of plasma microRNA profiles for primary resistance to EGFR-TKIs in advanced non-small cell lung cancer (NSCLC) patients with EGFR activating mutation. *J. Hematol. Oncol.* **2015**, *8*, 127. [[CrossRef](#)] [[PubMed](#)]
123. Yan, G.; Yao, R.; Tang, D.; Qiu, T.; Shen, Y.; Jiao, W.; Ge, N.; Xuan, Y.; Wang, Y. Prognostic significance of microRNA expression in completely resected lung adenocarcinoma and the associated response to erlotinib. *Med. Oncol.* **2014**, *31*, 203. [[CrossRef](#)] [[PubMed](#)]
124. Zhang, N.; Li, Y.; Zheng, Y.; Zhang, L.; Pan, Y.; Yu, J.; Yang, M. miR-608 and miR-4513 significantly contribute to the prognosis of lung adenocarcinoma treated with EGFR-TKIs. *Lab. Invest.* **2019**, *99*, 568–576. [[CrossRef](#)] [[PubMed](#)]
125. Vansteenkiste, J.; Barlesi, F.; Waller, C.F.; Bennouna, J.; Gridelli, C.; Goekkurt, E.; Verhoeven, D.; Szczesna, A.; Feurer, M.; Milanowski, J.; et al. Cilengitide combined with cetuximab and platinum-based chemotherapy as first-line treatment in advanced non-small-cell lung cancer (NSCLC) patients: Results of an open-label, randomized, controlled phase II study (CERTO). *Ann. Oncol.* **2015**, *26*, 1734–1740. [[CrossRef](#)]
126. Cedra, S.; Wiegand, S.; Kolb, M.; Dietz, A.; Wichmann, G. Reduced cytokine release in ex vivo response to cilengitide and cetuximab is a marker for improved survival of head and neck cancer patients. *Cancers (Basel)* **2017**, *9*.
127. Wichmann, G.; Cedra, S.; Schlegel, D.; Kolb, M.; Wiegand, S.; Boehm, A.; Hofer, M.; Dietz, A. cilengitide and cetuximab reduce cytokine production and colony formation of head and neck squamous cell carcinoma cells ex vivo. *Anticancer Res.* **2017**, *37*, 521–527. [[CrossRef](#)]
128. Élez, E.; Kocáková, I.; Höhler, T.; Martens, U.M.; Bokemeyer, C.; Van Cutsem, E.; Melichar, B.; Smakal, M.; Csósz, T.; Topuzov, E.; et al. Abituzumab combined with cetuximab plus irinotecan versus cetuximab plus irinotecan alone for patients with KRAS wild-type metastatic colorectal cancer: The randomised phase I/II POSEIDON trial. *Ann. Oncol.* **2015**, *26*, 132–140. [[CrossRef](#)]
129. Maki, R.G. Small is beautiful: insulin-like growth factors and their role in growth, development, and cancer. *J. Clin. Oncol.* **2010**, *28*, 4985–4995. [[CrossRef](#)]
130. Chen, H.X.; Sharon, E. IGF-1R as an anti-cancer target—trials and tribulations. *Chin. J. Cancer* **2013**, *32*, 242. [[CrossRef](#)]
131. Saegusa, J.; Yamaji, S.; Ieguchi, K.; Wu, C.-Y.; Lam, K.S.; Liu, F.-T.; Takada, Y.K.; Takada, Y. The direct binding of insulin-like growth factor-1 (igf-1) to integrin  $\alpha\beta3$  is involved in igf-1 signaling. *J. Biol. Chem.* **2009**, *284*, 24106–24114. [[CrossRef](#)]

132. Fujita, M.; Takada, Y.K.; Takada, Y. Insulin-like growth factor (IGF) signaling requires  $\alpha\beta 3$ -IGF1-IGF type 1 receptor (IGF1R) ternary complex formation in anchorage independence, and the complex formation does not require IGF1R and Src activation. *J. Biol. Chem.* **2013**, *288*, 3059–3069. [[CrossRef](#)]
133. Fujita, M.; Ieguchi, K.; Cedano-Prieto, D.M.; Fong, A.; Wilkerson, C.; Chen, J.Q.; Wu, M.; Lo, S.-H.; Cheung, A.T.W.; Wilson, M.D.; et al. An integrin binding-defective mutant of insulin-like growth factor-1 (R36E/R37E IGF1) acts as a dominant-negative antagonist of the IGF1 receptor (IGF1R) and suppresses tumorigenesis but still binds to IGF1R. *J. Biol. Chem.* **2013**, *288*, 19593–19603. [[CrossRef](#)]
134. Takada, Y.; Takada, Y.K.; Fujita, M. Crosstalk between insulin-like growth factor (IGF) receptor and integrins through direct integrin binding to IGF1. *Cytokine Growth Factor Rev.* **2017**, *34*, 67–72. [[CrossRef](#)] [[PubMed](#)]
135. Hasskarl, J. Sorafenib. *Recent Results Cancer Res.* **2010**, *184*, 61–70. [[PubMed](#)]
136. Chong, Y.; Tang, D.; Xiong, Q.; Jiang, X.; Xu, C.; Huang, Y.; Wang, J.; Zhou, H.; Shi, Y.; Wu, X.; et al. Galectin-1 from cancer-associated fibroblasts induces epithelial-mesenchymal transition through  $\beta 1$  integrin-mediated upregulation of Gli1 in gastric cancer. *J. Exp. Clin. Cancer Res.* **2016**, *35*, 175. [[CrossRef](#)]
137. Nam, K.; Son, S.; Oh, S.; Jeon, D.; Kim, H.; Noh, D.-Y.; Kim, S.; Shin, I. Binding of galectin-1 to integrin  $\beta 1$  potentiates drug resistance by promoting survivin expression in breast cancer cells. *Oncotarget* **2017**, *8*, 35804–35823. [[CrossRef](#)]
138. He, X.-J.; Tao, H.-Q.; Hu, Z.-M.; Ma, Y.-Y.; Xu, J.; Wang, H.-J.; Xia, Y.-J.; Li, L.; Fei, B.-Y.; Li, Y.-Q.; et al. Expression of galectin-1 in carcinoma-associated fibroblasts promotes gastric cancer cell invasion through upregulation of integrin  $\beta 1$ . *Cancer Sci.* **2014**, *105*, 1402–1410. [[CrossRef](#)]
139. Liebert, M.; Washington, R.; Wedemeyer, G.; Carey, T.E.; Grossman, H.B. Loss of co-localization of alpha 6 beta 4 integrin and collagen VII in bladder cancer. *Am. J. Pathol.* **1994**, *144*, 787–795. [[PubMed](#)]
140. Rodius, S.; Indra, G.; Thibault, C.; Pfister, V.; Georges-Labouesse, E. Loss of alpha6 integrins in keratinocytes leads to an increase in TGFbeta and AP1 signaling and in expression of differentiation genes. *J. Cell. Physiol.* **2007**, *212*, 439–449. [[CrossRef](#)]
141. Raymond, K.; Kreft, M.; Janssen, H.; Calafat, J.; Sonnenberg, A. Keratinocytes display normal proliferation, survival and differentiation in conditional  $\beta 4$ -integrin knockout mice. *J. Cell. Sci.* **2005**, *118*, 1045–1060. [[CrossRef](#)]
142. Faure, E.; Garrouste, F.; Parat, F.; Monferran, S.; Leloup, L.; Pommier, G.; Kovacic, H.; Lehmann, M. P2Y2 receptor inhibits EGF-induced MAPK pathway to stabilise keratinocyte hemidesmosomes. *J. Cell. Sci.* **2012**, *125*, 4264–4277. [[CrossRef](#)]
143. Frijns, E.; Sachs, N.; Kreft, M.; Wilhelmsen, K.; Sonnenberg, A. EGF-induced MAPK signaling inhibits hemidesmosome formation through phosphorylation of the integrin  $\beta 4$ . *J. Biol. Chem.* **2010**, *285*, 37650–37662. [[CrossRef](#)]
144. Frijns, E.; Kuikman, I.; Litjens, S.; Raspe, M.; Jalink, K.; Ports, M.; Wilhelmsen, K.; Sonnenberg, A. Phosphorylation of threonine 1736 in the C-terminal tail of integrin  $\beta 4$  contributes to hemidesmosome disassembly. *Mol. Biol. Cell* **2012**, *23*, 1475–1485. [[CrossRef](#)]
145. Margadant, C.; Frijns, E.; Wilhelmsen, K.; Sonnenberg, A. Regulation of hemidesmosome disassembly by growth factor receptors. *Curr. Opin. Cell Biol.* **2008**, *20*, 589–596. [[CrossRef](#)] [[PubMed](#)]
146. Mariotti, A.; Kedeshian, P.A.; Dans, M.; Curatola, A.M.; Gagnoux-Palacios, L.; Giancotti, F.G. EGF-R signaling through Fyn kinase disrupts the function of integrin  $\alpha 6\beta 4$  at hemidesmosomes: Role in epithelial cell migration and carcinoma invasion. *J. Cell Biol.* **2001**, *155*, 447–458. [[CrossRef](#)] [[PubMed](#)]
147. Wilhelmsen, K.; Litjens, S.H.M.; Kuikman, I.; Margadant, C.; van Rheenen, J.; Sonnenberg, A. Serine phosphorylation of the integrin  $\beta 4$  subunit is necessary for epidermal growth factor receptor-induced hemidesmosome disruption. *Mol. Biol. Cell* **2007**, *18*, 3512–3522. [[CrossRef](#)]
148. Ramovs, V.; Te Molder, L.; Sonnenberg, A. The opposing roles of laminin-binding integrins in cancer. *Matrix Biol.* **2017**, *57–58*, 213–243. [[CrossRef](#)]
149. Stewart, R.L.; O'Connor, K.L. Clinical significance of the integrin  $\alpha 6\beta 4$  in human malignancies. *Lab. Invest.* **2015**, *95*, 976–986. [[CrossRef](#)]
150. De Arcangelis, A.; Hamade, H.; Alpy, F.; Normand, S.; Bruyère, E.; Lefebvre, O.; Méchine-Neuville, A.; Siebert, S.; Pfister, V.; Lepage, P.; et al. Hemidesmosome integrity protects the colon against colitis and colorectal cancer. *Gut* **2017**, *66*, 1748–1760. [[CrossRef](#)]
151. Laval, S.; Laklai, H.; Fanjul, M.; Pucelle, M.; Laurell, H.; Billon-Galés, A.; Le Guellec, S.; Delisle, M.-B.; Sonnenberg, A.; Susini, C.; et al. Dual roles of hemidesmosomal proteins in the pancreatic epithelium: The phosphoinositide 3-kinase decides. *Oncogene* **2014**, *33*, 1934–1944. [[CrossRef](#)] [[PubMed](#)]

152. Yu, P.T.; Babicky, M.; Jaquish, D.; French, R.; Marayuma, K.; Mose, E.; Niessen, S.; Hoover, H.; Shields, D.; Cheresch, D.; et al. The RON-receptor regulates pancreatic cancer cell migration through phosphorylation-dependent breakdown of the hemidesmosome. *Int. J. Cancer* **2012**, *131*, 1744–1754. [[CrossRef](#)] [[PubMed](#)]
153. Trusolino, L.; Bertotti, A.; Comoglio, P.M. A Signaling Adapter Function for  $\alpha 6 \beta 4$  Integrin in the Control of HGF-Dependent Invasive Growth. *Cell* **2001**, *107*, 643–654. [[CrossRef](#)]
154. Scartozzi, M.; Giampieri, R.; Loretelli, C.; Mandolesi, A.; del Prete, M.; Biagetti, S.; Alfonsi, S.; Faloppi, L.; Bianconi, M.; Bittoni, A.; et al. Role of  $\beta 4$  integrin in HER-3-negative, K-RAS wild-type metastatic colorectal tumors receiving cetuximab. *Future Oncol.* **2013**, *9*, 1207–1214. [[CrossRef](#)] [[PubMed](#)]
155. Martins Cavaco, A.C.; Rezaei, M.; Caliandro, M.F.; Martins Lima, A.; Stehling, M.; Dhayat, S.A.; Haier, J.; Brakebusch, C.; Eble, J.A. The interaction between laminin-332 and  $\alpha 3 \beta 1$  integrin determines differentiation and maintenance of CAFs, and supports invasion of pancreatic duct adenocarcinoma cells. *Cancers (Basel)* **2018**, *11*.
156. Kalluri, R. The biology and function of fibroblasts in cancer. *Nat. Rev. Cancer* **2016**, *16*, 582–598. [[CrossRef](#)]
157. Fiori, M.E.; Di Franco, S.; Villanova, L.; Bianca, P.; Stassi, G.; De Maria, R. Cancer-associated fibroblasts as abettors of tumor progression at the crossroads of EMT and therapy resistance. *Mol. Cancer* **2019**, *18*, 70. [[CrossRef](#)]
158. Daverey, A.; Drain, A.P.; Kidambi, S. Physical intimacy of breast cancer cells with mesenchymal stem cells elicits trastuzumab resistance through Src activation. *Sci. Rep.* **2015**, *5*. [[CrossRef](#)] [[PubMed](#)]
159. Marusyk, A.; Tabassum, D.P.; Janiszewska, M.; Place, A.E.; Trinh, A.; Rozhok, A.I.; Pyne, S.; Guerriero, J.L.; Shu, S.; Ekram, M.; et al. Spatial proximity to fibroblasts impacts molecular features and therapeutic sensitivity of breast cancer cells influencing clinical outcomes. *Cancer Res.* **2016**, *76*, 6495–6506. [[CrossRef](#)]
160. McFarlane, S.; McFarlane, C.; Montgomery, N.; Hill, A.; Waugh, D.J.J. CD44-mediated activation of  $\alpha 5 \beta 1$ -integrin, cortactin and paxillin signaling underpins adhesion of basal-like breast cancer cells to endothelium and Fibronectin-enriched matrices. *Oncotarget* **2015**, *6*, 36762–36773. [[CrossRef](#)]
161. Blandin, A.-F.; Noulet, F.; Renner, G.; Mercier, M.-C.; Choulier, L.; Vauchelles, R.; Ronde, P.; Carreiras, F.; Etienne-Selloum, N.; Vereb, G.; et al. Glioma cell dispersion is driven by  $\alpha 5$  integrin-mediated cell–matrix and cell–cell interactions. *Cancer Lett.* **2016**, *376*, 328–338. [[CrossRef](#)]
162. Gao, Q.; Yang, Z.; Xu, S.; Li, X.; Yang, X.; Jin, P.; Liu, Y.; Zhou, X.; Zhang, T.; Gong, C.; et al. Heterotypic CAF-tumor spheroids promote early peritoneal metastasis of ovarian cancer. *J. Exp. Med.* **2019**, *216*, 688. [[CrossRef](#)]
163. Wang, Y.; Zhang, T.; Guo, L.; Ren, T.; Yang, Y. Stromal extracellular matrix is a microenvironmental cue promoting resistance to EGFR tyrosine kinase inhibitors in lung cancer cells. *Int. J. Biochem. Cell Biol.* **2019**, *106*, 96–106. [[CrossRef](#)]
164. Yamazaki, S.; Higuchi, Y.; Ishibashi, M.; Hashimoto, H.; Yasunaga, M.; Matsumura, Y.; Tsuchihara, K.; Tsuboi, M.; Goto, K.; Ochiai, A.; et al. Collagen type I induces EGFR-TKI resistance in EGFR-mutated cancer cells by mTOR activation through Akt-independent pathway. *Cancer Sci.* **2018**, *109*, 2063–2073. [[CrossRef](#)]
165. Brighton, H.E.; Angus, S.P.; Bo, T.; Roques, J.; Tagliatela, A.C.; Darr, D.B.; Karagoz, K.; Sciaky, N.; Gatza, M.L.; Sharpless, N.E.; et al. New mechanisms of resistance to MEK inhibitors in melanoma revealed by intravital imaging. *Cancer Res.* **2018**, *78*, 542–557. [[CrossRef](#)]
166. Hirata, E.; Girotti, M.R.; Viros, A.; Hooper, S.; Spencer-Dene, B.; Matsuda, M.; Larkin, J.; Marais, R.; Sahai, E. Intravital imaging reveals how BRAF inhibition generates drug-tolerant microenvironments with high integrin  $\beta 1$ /FAK signaling. *Cancer Cell* **2015**, *27*, 574–588. [[CrossRef](#)]
167. Fedorenko, I.V.; Abel, E.V.; Koomen, J.M.; Fang, B.; Wood, E.R.; Chen, Y.A.; Fisher, K.J.; Iyengar, S.; Dahlman, K.B.; Wargo, J.A.; et al. Fibronectin induction abrogates the BRAF inhibitor response of BRAF V600E/PTEN-null melanoma cells. *Oncogene* **2016**, *35*, 1225–1235. [[CrossRef](#)]
168. Margue, C.; Philippidou, D.; Kozar, I.; Cesi, G.; Felten, P.; Kulms, D.; Letellier, E.; Haan, C.; Kreis, S. Kinase inhibitor library screening identifies synergistic drug combinations effective in sensitive and resistant melanoma cells. *J. Exp. Clin. Cancer Res.* **2019**, *38*, 56. [[CrossRef](#)]
169. Dupont, S. Role of YAP/TAZ in cell-matrix adhesion-mediated signalling and mechanotransduction. *Exp. Cell Res.* **2016**, *343*, 42–53. [[CrossRef](#)]
170. Elbediwy, A.; Thompson, B.J. Evolution of mechanotransduction via YAP/TAZ in animal epithelia. *Curr. Opin. Cell Biol.* **2018**, *51*, 117–123. [[CrossRef](#)]



171. Kapoor, A.; Yao, W.; Ying, H.; Hua, S.; Liewen, A.; Wang, Q.; Zhong, Y.; Wu, C.-J.; Sadanandam, A.; Hu, B.; et al. Yap1 activation enables bypass of oncogenic Kras addiction in pancreatic cancer. *Cell* **2014**, *158*, 185–197. [[CrossRef](#)] [[PubMed](#)]
172. Shao, D.D.; Xue, W.; Krall, E.B.; Bhutkar, A.; Piccioni, F.; Wang, X.; Schinzel, A.C.; Sood, S.; Rosenbluh, J.; Kim, J.W.; et al. KRAS and YAP1 converge to regulate EMT and tumor survival. *Cell* **2014**, *158*, 171–184. [[CrossRef](#)] [[PubMed](#)]
173. Kim, M.H.; Kim, J.; Hong, H.; Lee, S.-H.; Lee, J.-K.; Jung, E.; Kim, J. Actin remodeling confers BRAF inhibitor resistance to melanoma cells through YAP/TAZ activation. *EMBO J.* **2016**, *35*, 462–478. [[CrossRef](#)] [[PubMed](#)]
174. Lin, L.; Sabnis, A.J.; Chan, E.; Olivass, V.; Cade, L.; Pazarentzos, E.; Asthana, S.; Neel, D.; Yan, J.J.; Lu, X.; et al. The Hippo effector YAP promotes resistance to RAF- and MEK-targeted cancer therapies. *Nat. Genet.* **2015**, *47*, 250–256. [[CrossRef](#)] [[PubMed](#)]
175. Chang, C.-C.; Hsieh, T.-L.; Tiong, T.-Y.; Hsiao, C.-H.; Ji, A.T.-Q.; Hsu, W.-T.; Lee, O.K.; Ho, J.H. Regulation of metastatic ability and drug resistance in pulmonary adenocarcinoma by matrix rigidity via activating c-Met and EGFR. *Biomaterials* **2015**, *60*, 141–150. [[CrossRef](#)]
176. Lin, C.-H.; Pelissier, F.A.; Zhang, H.; Lakins, J.; Weaver, V.M.; Park, C.; LaBarge, M.A. Microenvironment rigidity modulates responses to the HER2 receptor tyrosine kinase inhibitor lapatinib via YAP and TAZ transcription factors. *Mol. Biol. Cell* **2015**, *26*, 3946–3953. [[CrossRef](#)]
177. Nguyen, T.V.; Sleiman, M.; Moriarty, T.; Herrick, W.G.; Peyton, S.R. Sorafenib resistance and JNK signaling in carcinoma during extracellular matrix stiffening. *Biomaterials* **2014**, *35*, 5749–5759. [[CrossRef](#)] [[PubMed](#)]
178. Attieh, Y.; Clark, A.G.; Grass, C.; Richon, S.; Pocard, M.; Mariani, P.; Elkhatib, N.; Betz, T.; Gurchenkov, B.; Vignjevic, D.M. Cancer-associated fibroblasts lead tumor invasion through integrin- $\beta$ 3-dependent fibronectin assembly. *J. Cell Biol.* **2017**, *216*, 3509–3520. [[CrossRef](#)]
179. Erdogan, B.; Ao, M.; White, L.M.; Means, A.L.; Brewer, B.M.; Yang, L.; Washington, M.K.; Shi, C.; Franco, O.E.; Weaver, A.M.; et al. Cancer-associated fibroblasts promote directional cancer cell migration by aligning fibronectin. *J. Cell Biol.* **2017**, *216*, 3799–3816. [[CrossRef](#)]
180. Gaggioli, C.; Hooper, S.; Hidalgo-Carcedo, C.; Grosse, R.; Marshall, J.F.; Harrington, K.; Sahai, E. Fibroblast-led collective invasion of carcinoma cells with differing roles for RhoGTPases in leading and following cells. *Nat. Cell Biol.* **2007**, *9*, 1392–1400. [[CrossRef](#)] [[PubMed](#)]
181. Goetz, J.G.; Minguet, S.; Navarro-Lérida, I.; Lazcano, J.J.; Samaniego, R.; Calvo, E.; Tello, M.; Osteso-Ibáñez, T.; Pellinen, T.; Echarri, A.; et al. Biomechanical remodeling of the microenvironment by stromal caveolin-1 favors tumor invasion and metastasis. *Cell* **2011**, *146*, 148–163. [[CrossRef](#)]
182. Navab, R.; Strumpf, D.; To, C.; Pasko, E.; Kim, K.S.; Park, C.J.; Hai, J.; Liu, J.; Jonkman, J.; Barczyk, M.; et al. Integrin  $\alpha$ 11 $\beta$ 1 regulates cancer stromal stiffness and promotes tumorigenicity and metastasis in non-small cell lung cancer. *Oncogene* **2016**, *35*, 1899–1908. [[CrossRef](#)]
183. Levental, K.R.; Yu, H.; Kass, L.; Lakins, J.N.; Egeblad, M.; Erler, J.T.; Fong, S.F.T.; Csiszar, K.; Giaccia, A.; Wenginger, W.; et al. Matrix crosslinking forces tumor progression by enhancing integrin signaling. *Cell* **2009**, *139*, 891–906. [[CrossRef](#)]
184. Alkasalias, T.; Moyano-Galceran, L.; Arsenian-Henriksson, M.; Lehti, K. Fibroblasts in the tumor microenvironment: Shield or spear? *Int. J. Mol. Sci.* **2018**, *19*, 1532. [[CrossRef](#)]
185. Cooper, J.; Giancotti, F.G. Integrin signaling in Cancer: Mechanotransduction, stemness, epithelial plasticity, and therapeutic resistance. *Cancer Cell* **2019**, *35*, 347–367. [[CrossRef](#)]
186. Löffek, S.; Franzke, C.-W.; Helfrich, I. Tension in cancer. *Int. J. Mol. Sci.* **2016**, *17*, 1910. [[CrossRef](#)]
187. Mercier, M.-C.; Dontenwill, M.; Choulier, L. Selection of nucleic acid aptamers targeting tumor cell-surface protein biomarkers. *Cancers (Basel)* **2017**, *9*.




188. Camorani, S.; Crescenzi, E.; Gramanzini, M.; Fedele, M.; Zannetti, A.; Cerchia, L. Aptamer-mediated impairment of EGFR-integrin  $\alpha v \beta 3$  complex inhibits vasculogenic mimicry and growth of triple-negative breast cancers. *Sci. Rep.* **2017**, *7*, 46659. [[CrossRef](#)]
189. Laurenzana, A.; Margheri, F.; Biagioni, A.; Chillà, A.; Pimpinelli, N.; Ruzzolini, J.; Peppicelli, S.; Andreucci, E.; Calorini, L.; Serrati, S.; et al. EGFR/uPAR interaction as druggable target to overcome vemurafenib acquired resistance in melanoma cells. *EBioMedicine* **2019**, *39*, 194–206. [[CrossRef](#)]



© 2019 by the authors. Licensee MDPI, Basel, Switzerland. This article is an open access article distributed under the terms and conditions of the Creative Commons Attribution (CC BY) license (<http://creativecommons.org/licenses/by/4.0/>).

## Annexe 3 Publication in collaboration with Dr. Guy Zuber team

# Synthesis and biological evaluation of 2.4 nm thiolate-protected gold nanoparticles conjugated to Cetuximab for targeting glioblastoma cancer cells via the EGFR

Nadja Groysbeck<sup>1</sup> , Audrey Stoessel<sup>1</sup>, Mariel Donzeau<sup>1</sup>,  
Elisabete Cruz da Silva<sup>2</sup>, Maxime Lehmann<sup>2</sup>, Jean-Marc Strub<sup>3</sup> ,  
Sarah Cianferani<sup>3</sup>, Kassioyé Dembélé<sup>4</sup> and Guy Zuber<sup>1</sup> 

<sup>1</sup>Université de Strasbourg—CNRS, UMR 7242, Laboratoire de Biotechnologie et Signalisation Cellulaire, Boulevard Sébastien Brant, F-67400 Illkirch, France

<sup>2</sup>Université de Strasbourg—CNRS, UMR 7021, Laboratoire de Bioimagerie et Pathologies, Faculté de Pharmacie F-67401 Illkirch, France

<sup>3</sup>Université de Strasbourg—CNRS, IPHC UMR 7178, Laboratoire de Spectrométrie de Masse BioOrganique, F-67000 Strasbourg, France

<sup>4</sup>Université de Strasbourg—Institut de Physique et Chimie des Matériaux de Strasbourg (IPCMS) 23 rue du Loess, F-67034 Strasbourg, France

E-mail: [zuber@unistra.fr](mailto:zuber@unistra.fr)

Received 29 October 2018, revised 7 January 2019

Accepted for publication 16 January 2019

Published 21 February 2019



## Abstract

Therapeutic monoclonal antibodies benefit to patients and the conjugation to gold nanoparticles (AuNPs) might bring additional activities to these macromolecules. However, the behavior of the conjugate will largely depend on the bulkiness of the AuNP and small sizes are moreover preferable for diffusion. Water-soluble thiolate-protected AuNPs having diameters of 2–3 nm can be synthesized with narrow polydispersity and can selectively react with incoming organic thiols *via* a S<sub>N</sub>2-like mechanism. We therefore synthesized a mixed thionitrobenzoic acid-, thioaminobenzoic acid-monolayered AuNP of 2.4 nm in diameter and developed a site-selective conjugation strategy to link the AuNP to Cetuximab, an anti-epidermal growth factor receptor (EGFR) antibody used in clinic. The water-soluble 80 kDa AuNP was fully characterized and then reacted to the hinge area of Cetuximab, which was selectively reduced using mild concentration of TCEP. The conjugation proceeded smoothly and could be analyzed by polyacrylamide gel electrophoresis, indicating the formation of a 1:1 AuNP-IgG conjugate as the main product. When added to EGFR expressing glioblastoma cells, the AuNP-Cetuximab conjugate selectively bound to the cell surface receptor, inhibited EGFR autophosphorylation and entered into endosomes like Cetuximab. Altogether, we describe a simple and robust protocol for a site-directed conjugation of a thiolate-protected AuNP to Cetuximab, which could be easily monitored, thereby allowing to assess the quality of the product formation. The conjugated 2.4 nm AuNP did not majorly affect the biological behavior of Cetuximab, but provided it with the electronic properties of the AuNP. This offers the ability to detect the tagged antibody and opens application for targeted cancer radiotherapy.

Supplementary material for this article is available [online](#)

Keywords: gold nanoparticle, site-directed bioconjugation, antibody, targeted cancer therapy, epidermal growth factor receptor

(Some figures may appear in colour only in the online journal)

## 1. Introduction

Nanoparticles (NPs) are particles of sizes ranging between 1 and 100 nm that have important biomedical applications [1]. Some NPs can be functionalized with multiple elements, which permits to provide the nanomaterial with new properties. The coalescence of several functions allows dealing with the complexity of biological systems and might help for diagnosing and treating diseases [2, 3]. Several sophisticated systems demonstrated some efficiencies at preclinical stages for imaging modalities [4], nucleic acid delivery [5], protein delivery [6], tissue-targeted drug delivery [7], hyperthermia and photothermal therapy [8]. Gold nanoparticles (AuNPs) have been extensively investigated for biomedical application, because they have a low toxicity profile and their unique optic and electronic properties can trigger cellular damage upon application of light [9] or radiation [10, 11]. Furthermore, AuNPs can be equipped with organic molecules, including antibodies, which facilitate accumulation of the AuNPs within selected tissues or cancer lesions [12]. AuNPs with diameters above 5 nm display a large surface area that can be used for tight adsorption of antibodies and other proteins [13, 14]. For example, El-Sayed *et al* coated 40 nm AuNPs with monoclonal antibodies targeting the epidermal growth factor receptor (EGFR) by random adsorption in order to target oral squamous carcinoma cells. The antibody-mediated accumulation of these AuNPs into the cancer cells was then used to promote cell death *via* a photothermal treatment [9]. Patra *et al* synthesized 5 nm AuNPs that were also surface-coated with anti-EGFR antibodies, as well as with gemcitabine for targeting the drug to cancer cells [15]. Although of straightforward practicability, the functionalization of AuNPs *via* adsorption to the particle's surface has limitations. Firstly, a control over the orientation and stoichiometry of the adsorbed molecules onto the AuNP is challenging [16]. Secondly, the physicochemical properties of the antibody and its subsequent cellular response are impacted by the AuNP's size [17, 18]. When the properties of an AuNP-IgG conjugate should resemble the ones of an antibody, AuNPs of smaller sizes should be selected. However, since antibodies do not tightly adsorb to the surface of small-sized AuNPs, the functionalization method must be adjusted by the formation of an Au-S coordination bond.

Small-sized and uniform AuNPs with diameters between 0.8 and 2 nm are easily prepared by reduction of chloroauric acid in the presence of organic thiols [19]. Thiobenzoate-protected AuNPs of such small sizes and of rather precise chemical composition can be directly prepared in aqueous solutions leading to water-soluble AuNPs. These AuNPs can be further grafted with biological macromolecules, such as oligonucleotides, peptides and proteins [20, 21], or viruses [22] by exchanging the thiobenzoate ligands with incoming

thiol-containing macromolecules. To diminish unspecific association to cellular constituents and to enhance the ligand exchange reaction, we have previously developed a mixed thionitrobenzoic acid (TNBA), thioaminobenzoic acid (TABA) protected-AuNP of 1.4 nm diameter that showed diffusion abilities inside living cells after grafting with bioactive peptides [23]. This type of AuNP appeared to be particularly suited for the site-directed conjugation to an IgG at the antibody's hinge region. The hinge region of an IgG connects the complement-activating Fc domain to the antigen-binding (Fab) domain and contains disulfide bonds that can be selectively reduced to liberate nucleophilic thiols. These liberated thiols can then react with electrophiles, thereby forming covalent bonds [24, 25]. Moreover, they can also exchange with the ligands of thiolate-protected AuNPs [26]. When the antibody is tagged at the hinge area, the antibody functionality is generally untouched since the Fab and the Fc domain, which both are implicated in the IgG cellular action, remain unmodified [27]. It should be however mentioned that the thiol-specific conjugation of AuNPs [28] and thiolate-protected AuNPs [26] at the hinge area is not always easy to achieve, likely due to steric hindrance.

In the presented study, we first modified a synthetic protocol for making a TNBA-, TABA-protected AuNP of 2.4 nm. Secondly, we evaluated the ability of this AuNP to react with the thiols of reduced IgGs at the hinge region (AuNP synthesis scheme and bioconjugation strategy illustrated in figure 1). As models, we selected the anti-EGFR antibody Cetuximab (Cmab) and the anti-vascular endothelial growth factor (VEGF) antibody Bevacizumab (Bmab). The direct ligand exchange proceeded seamlessly at near stoichiometric ratio and the AuNP-antibody link remained intact, even after addition of the CALNNG peptide in large excess, which served the purpose of exchanging the remaining reactive TNBA/TABA ligands with a passive CALNNG layer [29]. Thirdly, the ability of the AuNP-Cetuximab conjugate to bind to its cellular target was assayed using cell line models. Biological evaluation using living cells with or without cell surface EGFR demonstrated that the AuNP-Cetuximab conjugate behaved very similarly to Cetuximab, despite being tagged with a 2.4 nm AuNP.

## 2. Materials and methods

### 2.1. Chemicals

Water was purified with a Millipore Q-POD apparatus. The paraformaldehyde (PFA 16% solution) and the glutaraldehyde (25% solution) solutions were of Electron Microscopy quality grade and purchased from electron microscopy sciences. The jet PRIME siRNA transfection reagent was

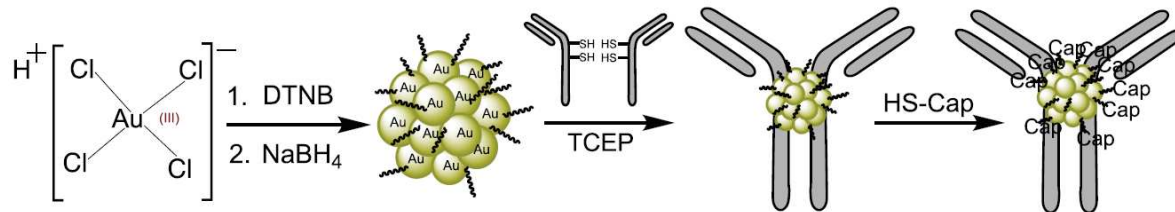


**Figure 1.** Scheme of gold nanoparticle (AuG) synthesis and bioconjugation to antibody. 1st step: synthesis of AuG. Reduction of  $\text{HAuCl}_4 \cdot 3\text{H}_2\text{O}$  to organothiolate gold nanoparticle using  $\text{NaBH}_4$  in the presence of DTNB (dithionitrobenzoic acid) in  $\text{CH}_3\text{CN}/\text{H}_2\text{O}$  (80:20) pH = 13. 2nd step: thiolate-for-thiolate exchange of the selectively reduced antibody's hinge thiols and the AuG-ligands TNBA (thionitrobenzoic acid) and TABA (thioaminobenzoic acid). 3rd step: passivation of the AuNP-IgG conjugate using excess of peptide CALNNG (HS-Cap).

from PolyPlus-transfection. Other chemical reagents and solvents were obtained from commercial sources (Sigma Aldrich, Carl Roth, Honeywell, VWR Chemicals) and used without further purification. The protein ladder for SDS-PAGE analysis was the Precision Plus Protein Standard Dual Xtra (BioRad). Peptides were purchased from GeneCust and the antibodies bevacizumab (Bmab) and cetuximab (Cmab) were provided by Centre de lutte contre le Cancer Paul Strauss (France) and originally purchased from Merck KGaA and Roche laboratory, respectively. The initial buffer solution of the antibodies Cmab and Bmab was changed to PBS using illustra NAP-10 column (GE Healthcare). Antibodies used for the western blot analysis were purchased from Cell Signaling.

## 2.2 Materials

The pH of the solution was measured using a HI 2210 pH meter. Centrifugation of 50 ml tubes was performed with an Eppendorf 5810R centrifuge using an A-4-81 rotor. Centrifugation of smaller volumes (0.2–2 ml) was done using an Eppendorf 5415 R centrifuge. A Heidolph Rotamax 120 rocking platform was used for mixing the gold reaction solution. Peptide coated AuNPs were purified and concentrated using Amicon Ultra 0.5 ml centrifugal filter devices (MWCO 10 kDa) if not stated otherwise. UV-vis spectroscopy was performed on a Varian Cary 100Bio spectrometer.

## 2.3. Synthesis of the AuG gold nanoparticles

Solutions of 0.4 M  $\text{HAuCl}_4 \cdot 3\text{H}_2\text{O}$  (90  $\mu\text{l}$ , 36  $\mu\text{mol}$ ) and 50 mM DTNB (5,5'-dithiobis-(2-nitrobenzoic acid), 1.08 ml, 54  $\mu\text{mol}$ ) in 0.3 M NaOH were added to 80:20  $\text{CH}_3\text{CN}/\text{H}_2\text{O}$  mixture (10.8 ml) under stirring. The mixture was agitated for 6 h at room temperature before addition of a freshly prepared 0.75 M  $\text{NaBH}_4$  solution in water (240  $\mu\text{l}$ , 180  $\mu\text{mol}$ ). The orange colored solution immediately turned to black. After an overnight stirring, the precipitated AuNPs were recovered by centrifugation, washed with acetonitrile and then dried to yield the AuNP (named AuG) as a black powder.

## 2.4. Synthesis of AuNP-antibody conjugate

A 2 mg  $\text{ml}^{-1}$  antibody solution (225  $\mu\text{l}$ , 0.45 mg) was treated with a 7 mM Tris(2-carboxyethyl)phosphine-HCl (TCEP) solution, pH 7.0 (90  $\mu\text{l}$ , 0.63  $\mu\text{mol}$ ) for 1.5 h at 37 °C. The

AuG (73  $\mu\text{l}$  of a 42  $\mu\text{M}$ , 3.06 nmol) was then added to the reduced antibody (297  $\mu\text{l}$ , 0.42 mg) in 0.1 M HEPES buffer, pH 7.5 at 25 °C and the reaction was let to proceed overnight. The next day the AuNP-antibody conjugate was passivated with a 1 mM solution of peptide CALNNG (123  $\mu\text{l}$ , 123 nmol or 40 molar eq. of AuNP-antibody conjugate) for 4 h at 25 °C in 0.1 M HEPES buffer, pH 7.5. The exchanged AuG-ligands (TNBA and TABA) and excess CALNNG peptides were removed by ultrafiltration using Amicon 100 K ultra-centrifugal devices.

## 2.5. Mass spectrometry analysis

Mass spectra were recorded with a MALDI-TOF MS operating in positive ion mode on an Autoflex<sup>TM</sup> system (Bruker Daltonics GmbH, Bremen, Germany). The system was used at an accelerating potential of 20 kDa in linear and reflector mode. The nitrogen laser (337 nm) was used at a frequency of 5 Hz and the acquisition mass range was set to 5000–30 000 m/z with a matrix suppression deflection of 500 m/z. Samples were prepared by the dried droplet method. The matrix solution consisted of a saturated solution of  $\alpha$ -cyano-4-hydroxycinnamic acid in  $\text{H}_2\text{O}/\text{CH}_3\text{CN}$  (50:50), which was threefold diluted in  $\text{H}_2\text{O}/\text{CH}_3\text{CN}/\text{TFA}$  (50:49.9:0.1).

## 2.6. Electron microscopy and EDX analysis

Images of the AuNPs were obtained by performing microscopy experiments using a  $\text{C}_s$ -corrected JEOL JEM-2100F scanning transmission electron microscope (STEM) operating at 200 keV. Energy dispersive x-ray (EDX) analysis was carried out on the same instrument, being equipped with an EDX detector. Samples were prepared by adding 10  $\mu\text{l}$  of a 5  $\mu\text{M}$  AuNP solution onto the Carbon film support of a ultrathin carbon 400 mesh Cu grid (Ted Pella Product No 01822-F, Redding, CA). After 2 min, excess liquid was blotted with a filter paper and the grid was dried for 48 h.

## 2.7. FTIR analysis

Fourier-transform infrared (FTIR) spectrum of AuNPs was recorded using a Nicolet 380 FTIR spectrometer and a diamond ATR by Thermo Fisher Scientific (supporting

information, figure S1 is available online at [stacks.iop.org/NANO/30/184005/mmedia](https://stacks.iop.org/NANO/30/184005/mmedia)).

### 2.8. SDS-PAGE

SDS-PAGE was performed according to a published protocol of Laemmli *et al* on 10% and 15% acrylamide gels [30]. The gels were pre-run for 20 min in a tris-glycine buffer (0.25 M Tris, 1.92 M glycine, 1% SDS, pH 8.5) at 20 mA. For loading 50% (v/v) glycerol solution was added to the AuNP solutions to a 5% final proportion. After electrophoresis, the AuNPs were seen as black-brown bands. Few amounts of AuNPs could be further visualized by silver enhancement. Proteins were revealed by Coomassie blue staining.

### 2.9. Cell culture

Cell lines were maintained in a 37 °C humidified incubator with 5% CO<sub>2</sub>. The human U87 glioblastoma cells (U87 MG, ATCC HTB-14) and the human fibrosarcoma cells (HT-1080, ATCC CCL-121) were maintained in Eagle's minimum essential medium containing 10% fetal bovine serum, 1% sodium pyruvate and 1% nonessential amino acids. Human foreskin fibroblast (HFF) cells (HFF-1, ATCC SCRC-1041) were cultured in Dulbecco's modified eagle medium supplemented with 2 mM L-glutamine, HEPES buffer, 10% heat inactivated fetal calf serum (FCS) and 50 µg ml<sup>-1</sup> gentamycin. The U87 and HFF cells co-culture was done in Opti-MEM cell culture medium containing 10% FCS. The EGFR (+) U87 cell line was a gift from Professor Furnari [31]. The MTT assay was performed according to a published procedure [32].

### 2.10. Downregulation of EGFR expression in U87 cells

Expression of EGFR was down-regulated using the synthetic interfering RNAs (siRNAs) methodology. The U87 cell line was seeded in 6-well plates at 250 000 cells/well the day before the siRNA transfection experiment. For one well, a 50 nM siRNA solution (200 µl jetPrime buffer, 10 pmol siEGFR) was mixed with 4 µl of jetPrime reagent. After 10 min incubation at room temperature, the complexes were added to the cells by dilution into the cell culture medium. To ensure maximum gene silencing the cells were incubated for 48 h before use [33]. The human EGFR siRNA solution (siGENOME Human EGFR(1956) siRNA Smart pool) was purchased from Dharmacon. The solution contained 4 siRNA molecules, which target the following mRNA sequences. Sequence 1: CCGCAAUCCGA-GACGAA, sequence 2: CAAAGUGUGUAACGGAAUA, sequence 3: GUAACAAGCUCACG-CAGUU, sequence 4: GAGGAAUAUGUACUACGA.

### 2.11. EGFR binding assay

Cells were seeded in 24-well plates and let to adhere on fibronectin-coated (20 µg ml<sup>-1</sup>) glass coverslips the day before the assay. The cell culture medium was then replaced with a serum-free cell culture medium and the cells were

incubated at 37 °C for 30 min. This starvation step aimed at optimizing EGFR presentation on the cell surface [34]. Culture medium was then carefully removed and replaced with a serum-free medium containing the AuNP-antibody conjugate. After 30 min of incubation, the cell culture medium was removed. Cells were washed with PBS and then fixed with either 4% PFA in PBS (10 min) or 2.5% glutaraldehyde in Sorenson's Buffer (1 h).

### 2.12. Assay of EGFR-mediated endocytosis

Cells were seeded in 24-well plates and let to adhere on fibronectin-coated (20 µg ml<sup>-1</sup>) glass coverslips the day before the assay. The cell culture medium was then replaced with serum-depleted culture medium and the cells were let in this medium for 30 min at 37 °C. After serum-depletion, cells were incubated in ice-cooled serum-free medium containing 167 nM of the AuNP-antibody conjugate. After 30 min of incubation on ice, the cell culture medium was replaced with pre-warmed serum-containing cell culture medium and the cells were incubated at 37 °C for different time periods. The cell surface-bound antibodies were detached with a 0.2 M sodium acetate solution (pH 2.7). The cells were then washed with PBS and fixed with 4% PFA.

### 2.13. Preparation of the cell specimen for AuNP detection

The AuNPs were detected using a modified Danscher method [23, 35]. Briefly, after the 2.5% glutaraldehyde fixation step, the cells were incubated with a 0.1 M Sorenson's buffer, pH 7.4 containing 50 mM glycine for 20 min. The cell membrane was then permeabilized using a Sorenson's buffer, pH 7.4 containing 0.05% (w/v) saponine. The buffered solution was then replaced by a 0.1 M citrate solution, pH 6.7 containing 2% (w/v) sucrose. Development of the AuNPs was done in a dark room for 8 min using a freshly prepared 6 mM silver acetate solution in 0.16 M sodium citrate, pH 6.7 containing 2 mM propyl gallate and 20% (w/v) gum arabic. Development of the silver-mediated AuNP staining was stopped by washing the cell specimen with 0.16 M sodium citrate solution, pH 6.7.

### 2.14. Western blot

Cells were lysed in Laemmli loading buffer, the lysate was fractionated by SDS-PAGE and transferred onto a polyvinylidene difluoride membrane. The anti-EGFR D38B1, anti-pEGFR Tyr1068 and anti-GAPDH antibodies were used to detect EGFR, phosphorylated EGFR and GAPDH respectively.

## 3. Results

### 3.1. Gold nanoparticle synthesis and characterization

We previously described the synthesis of a TNBA-, TABA-protected AuNP of circa 102 gold atoms that could be grafted with thiolated peptides by exchanging most of the

TNBA-ligands, leaving a surrounding zwitterionic protecting shell consisting of gold-coordinated TABAs [23]. In an initial stage, we explored the possibility of preparing the same type of TNBA-, TABA-protected AuNP, but of larger diameter. The nature and proportion of the solvents were seen to dramatically alter the production of thiolate-protected AuNPs [36]. We therefore assayed the reduction of  $\text{HAuCl}_4$  with  $\text{NaBH}_4$  and DTNB in various co-solvents. It was observed that a  $\text{HAuCl}_4/\text{DTNB}/\text{NaBH}_4$  ratio of 1:1.5:5 in a solvent mixture of  $\text{CH}_3\text{CN}/\text{H}_2\text{O}$  (80:20) yielded to a AuNP population migrating as a discrete band when subjected to a sodium dodecyl sulfate polyacrylamide gel electrophoresis (SDS-PAGE) analysis, suggesting a homogenous population (figure 2(a)). This AuNP population (named AuG) was further characterized by UV-vis spectroscopy (figure 2(b)). Data showed that the absorption gradually increases for decreasing wavelengths. The spectrum contains a hump with a maximum absorption at 520 nm, corresponding to the weak surface plasmon resonance absorption of 2 nm diameter AuNPs [37]. The STEM analysis of the AuNP revealed a homogenous population of spherical particles (figure 2(c)) with a mean diameter of  $2.4 \pm 0.28$  nm ( $n = 61$ ). The observation of a crystalline lattice at high resolution (inset image in figure 2(c)) confirmed that the metallic core of AuG was massive ( $\text{Au}^0$ ). A MALDI-TOF mass spectrometry analysis of the AuNP (figure 2(d)) displayed a narrow distribution of masses at 80 kDa, confirming the SDS-PAGE and EM data. By combining the different data and a volumetric density of  $19.3 \text{ g cm}^{-3}$  for Au, we estimated that the AuNP contains on average about 420 gold atoms and 130 ligands. Further calculations and a test reaction using increasing ratios of a thiol-containing cationic peptide to the AuNP suggested that the ligand to peptide substitution saturates at about 35 exchanges per particle (figure S2, supporting information). EDX analysis was also performed (figures 2(e) and (f)). The spectrum displayed the characteristic peaks of gold ( $\text{Au}_{M\alpha}$  at 2.12 keV;  $\text{Au}_{L\alpha}$  at 9.712 eV) along with peaks corresponding to carbon and copper resulting from the carbon film-coated copper grid, on which the AuNPs were deposited for the analysis.

### 3.2. Conjugation to antibodies

The weakly nucleophilic and thiol-free reducing agent TCEP was used to reduce the antibody disulfide bridges [38]. For optimizing the reduction condition, the Cetuximab antibody (Cmab) was incubated with increasing TCEP concentrations and the reactions were monitored by SDS-PAGE analysis using non-reducing conditions (supporting information, figure S3). Data showed that a final 2 mM TCEP concentration produced a complete reduction of the 150 kDa band to the expected 75 kDa band. Cmab was hence reduced with 2 mM TCEP in PBS for 90 min and the water-soluble 2.4 nm AuNP (AuG) was then directly added to the TCEP-reduced antibody mixture at a 1:1.2 (Cmab:AuNP) stoichiometry. The formation of the AuNP-Cetuximab conjugate (Au-Cmab) was monitored by SDS-PAGE using 10% acrylamide gels (figure 3). To enable dual detection of the protein and the AuNP, the gel was firstly stained using Coomassie blue and then silver ions. The

conjugation reaction based on the substitution of an AuG ligand with a thiol group of the antibody's hinge area proceeded seamlessly, which could be concluded from the observation of a black colored 150 kDa band and no remaining band at 75 kDa in the lane of Au-Cmab (figure 3, lane 5). An apparent 250 kDa band was also observed suggesting dimerization of the IgG, but the proportion was estimated to be lower than 10%. We assumed that the major apparent 150 kDa band corresponds to a 1:1 AuNP-IgG conjugate, whereas the 250 kDa species possibly represents either a  $\text{AuNP}-(\text{IgG})_2$  product or an aggregate of two 1:1 AuNP-IgGs. The observation that the electrophoretic mobility of the main Au-Cmab conjugate was similar to the one of unreacted 150 kDa Cmab is puzzling. However, the AuNP migrated within the migration front and not as classical 80 kDa protein. This high electrophoretic mobility likely results from the high volumetric mass density of gold ( $19.3 \text{ g cm}^{-3}$ ) and the electronegative charge of AuG. A small amount of unreacted AuG was still detectable in the crude Au-Cmab solution (figure 3, lane 5, faint band at the bottom of the gel), which likely resulted from the slight excess of AuG used for the reaction. Finally, the released ligands, as well as excess peptides and AuNPs were removed using a 100 kDa cut-off ultracentrifugation device. At the present stage, we were unable to remove all the AuNPs as judged by SDS-PAGE analysis, but obtained a batch with less than 5% of free AuNPs.

The conjugation of AuG to Bmab and the purification procedure were performed in a similar manner, but using a TCEP concentration of 0.1 mM for reduction of the hinge disulfide bonds (supporting information, figure S4).

### 3.3. Biological evaluation of the Au-Cmab conjugate

The ability of the Au-Cmab to bind to EGFR, present on the surface of various cancer cells, was examined using a U87 glioblastoma cell line overexpressing the EGFR [31], hereafter referred to as EGFR(+) U87 cells. The Au-Bmab conjugate, which does not target the EGFR, but the (VEGF), was used as the control. In a parallel control experiment, the EGFR expression of U87 wild type cells was almost abolished using the siRNA-mediated gene silencing technology to obtain EGFR(−) U87 cells (western blot confirming the successful downregulation of EGFR depicted in figure S5, supporting information). The Cmab, Au-Cmab and Au-Bmab were added to living cells at a concentration of 167 nM by dilution into the cell culture medium. After 30 min of incubation, the cells were fixed and each domain of the conjugate was separately tracked (figure 4). The antibody was detected by immunofluorescence (IF) [39] (figure 4(a)). Green fluorescence (IgG) was only observed when Cmab and Au-Cmab were added to EGFR(+) U87 cells. Next, the AuNP moiety was revealed by gold-induced silver staining (figure 4(b)). Analogous to the IF results, the strongest silver staining pattern was only seen for Au-Cmab-treated EGFR(+) U87 cells. Some silver staining was nonetheless observed within the endosomes of EGFR(−) and EGFR(+) cells for Au-Bmab and for Au-Cmab, suggesting that the AuNP domain



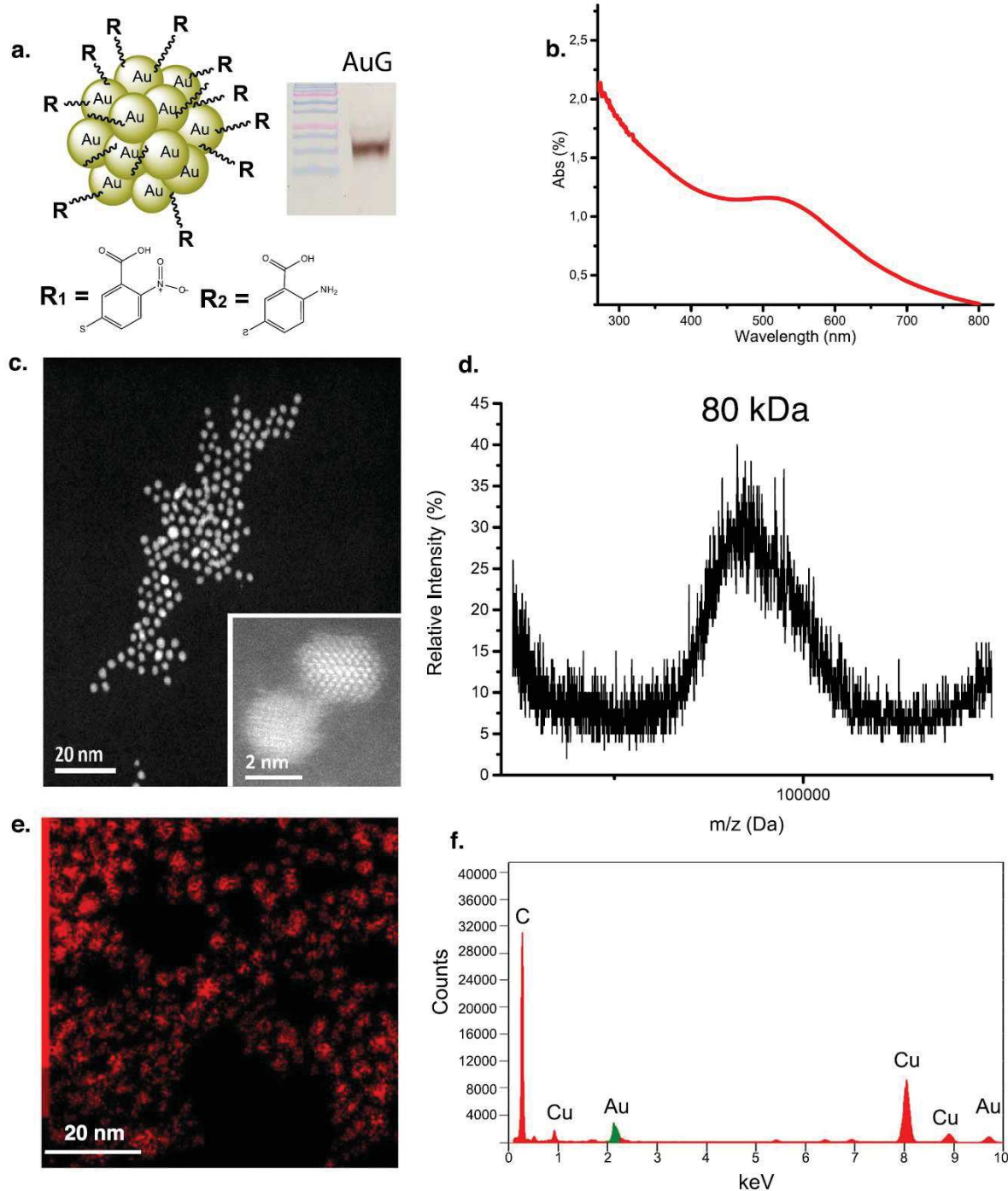


**Figure 2.** Characterization of 2.4 nm AuNP (AuG) (a) structure and SDS-PAGE analysis of AuG (15% acrylamide gel). Structure of organothiolate ligands building the surface coating of AuG are depicted below the nanoparticle: R<sub>1</sub> = TNBA (thionitrobenzoic acid), R<sub>2</sub> = TABA (thioaminobenzoic acid); (b) UV-vis spectrum of AuG (small peak at 520 nm corresponding to weak surface plasmon resonance absorption); (c) scanning transmission electron microscopy image of AuG particles. Inset image in right corner shows magnification (scale bar of main image: 20 nm, scale bar of inset image: 2 nm); (d) MALDI-TOF mass spectrum of AuG ( $MW^{\text{obs}} = 80$  kDa); (e) elemental EDX mapping of AuG (scale bar: 20 nm); (f) EDX spectrum of AuG ( $C_{K\alpha} = 0.277$  keV,  $Cu_{L\alpha} = 0.93$  keV,  $Au_{M\alpha} = 2.12$  keV,  $Cu_{K\alpha} = 8.04$  keV,  $Cu_{K\beta} = 8.9$  keV,  $Au_{L\alpha} = 9.71$  eV).

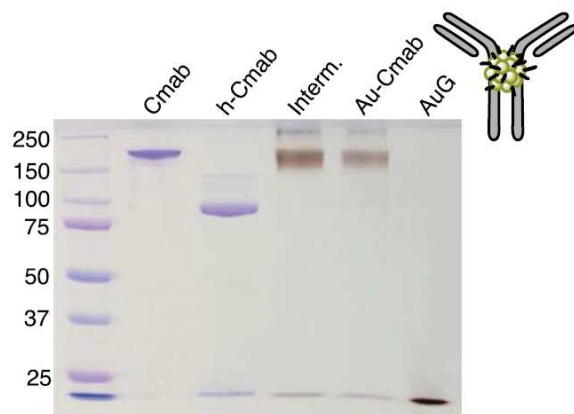


**Figure 3.** SDS-10% PAGE of gold nanoparticle-antibody-conjugate (Au-Cmab) formation under non-reducing conditions. Order on the gel from left to right: Cetuximab (Cmab), selectively reduced Cetuximab (h-Cmab), AuNP-Cetuximab conjugate before passivation (Interm.), AuNP-Cetuximab conjugate after passivation with peptide CALNNG (Au-Cmab), gold nanoparticle AuG.

somehow favors adherence to cell surfaces and subsequent endocytosis. It should be however mentioned that the silver-enhancement procedure is highly sensitive and not a quantitative method.

The ability of Au-Cmab to bind to EGFR-overexpressing cells was confirmed using an other EGFR-expressing cancer cell line (human fibrosarcoma cells, HT-1080; Supporting Information, Figure S6). As previously described for binding experiments using EGFR(+) U87 cells, the Au-Cmab bound to the surface of HT-1080 cells, whereas the control conjugate Au-Bmab did not show this pattern. Here again, we noticed some silver staining of the cells incubated with Au-Bmab, reinforcing the assumption that the AuNP domain slightly promotes adherence to the cell surface and subsequent endocytosis.

These experiments convincingly demonstrated that Cmab and the Au-Cmab conjugate selectively bind to EGFR of living EGFR-presenting cells. We then evaluated the impact of the AuNP on the ability of Cmab to bind to the cell surface receptors. Cmab and Au-Cmab were incubated with the EGFR(+) U87 cells at concentrations ranging from 0.67 pM to 167 nM. The cells were fixed and the cell-attached antibodies were qualitatively detected by IF. An on/off fluorescence detection threshold was used and the on/off detection data were plotted as a function of the initial material concentration (supporting information, figure S7). This rough quantitative analysis showed that the detection of the EGFR onto the cells required 10 times more of the Au-Cmab conjugate, than of Cmab, suggesting that appending the 2.4 nm AuNP at the hinge area may not be fully innocuous.

Next, we assayed the ability of the Au-Cmab to get internalized into cells, as it is described for Cmab [40]. Both compounds (Cmab and Au-Cmab) were incubated with living serum-starved EGFR(+) U87 cells for 30 min on ice to allow for receptor binding, but not for internalization. Afterwards, the sample- and non-serum-containing medium was

exchanged for serum-containing cell culture medium and the cells were incubated at 37 °C for 30 and 60 min, to allow internalization. At the end of the incubation, the nanomaterials bound to the cell surface receptors were washed away using a mild acidic treatment [41]. The cells were then fixed, the plasma membrane permeabilized with detergent, and the components detected by IF (figure 5). The time-course experiment showed that binding of Cmab and Au-Cmab to the cell surface receptors is followed by internalization into intracellular vesicular compartments. Although the intracellular fate of Cmab and Au-Cmab was similar, slight differences were observed at the 30 min incubation time-point. Cmab mainly localized into perinuclear compartments, whereas the Au-Cmab was still seen inside vesicles closer to the plasma membrane.

To further examine whether the biological function of Cmab was affected by the conjugation to AuG, we compared the ability of Cmab and Au-Cmab to inhibit EGFR autophosphorylation after induction with EGF. The serum-starved EGFR(+) U87 cells were incubated with Cmab and Au-Cmab together with EGF for 15 min at 37 °C. Afterwards, the cells were lysed and the cell extracts were fractionated by SDS-PAGE to quantify the intracytosolic levels of EGFR and EGFR-pTyr1068 by western blot analysis (figure 6). Data showed that the Au-Cmab inhibited the phosphorylation of EGFR similarly to Cmab [42].

Even though Cmab and the Au-Cmab inhibited EGFR phosphorylation, their addition to EGFR(+) U87 cells at a concentration of 167 nM did not apparently impact the cellular viability, as judged by a MTT assay (supporting information, figure S8).

Finally, we examined whether the Au-Cmab conjugate is able to distinguish between EGFR-overexpressing cancer cells and non-cancerous cells. The EGFR(+) U87 cells were co-cultured with the non-cancerous HFF cells and the Au-Cmab was then added to the cell culture medium. After 30 min the cells were fixed and the presence of the Au-Cmab conjugate was revealed by IF and silver staining (figure 7). The two cell types were easily distinguishable by their cell morphology. EGFR(+) U87 cells (figure 7(a): black arrows) are much smaller and thinner than HFF cells (figure 7(a): red arrow; figure 7(b): cells encircled in red). Only the EGFR(+) U87 cells were engulfing a large proportion of Cmab and Au-Cmab, confirming that the Au-Cmab conjugate might be useful to selectively target EGFR-overexpressing tumor cells while not affecting non-cancerous cells.

#### 4. Discussion

NPs, including AuNPs, can be prepared at various sizes and be equipped with functional organic components, which makes them useful for a multitude of different applications [43–48]. For biological applications, the AuNP size plays a major role. Particles having sizes above 4–5 nm offer the advantage to be easily detectable by electron microscopy and they can also be easily surface-coated with several antibodies using strong non-covalent binding or be coordinated to

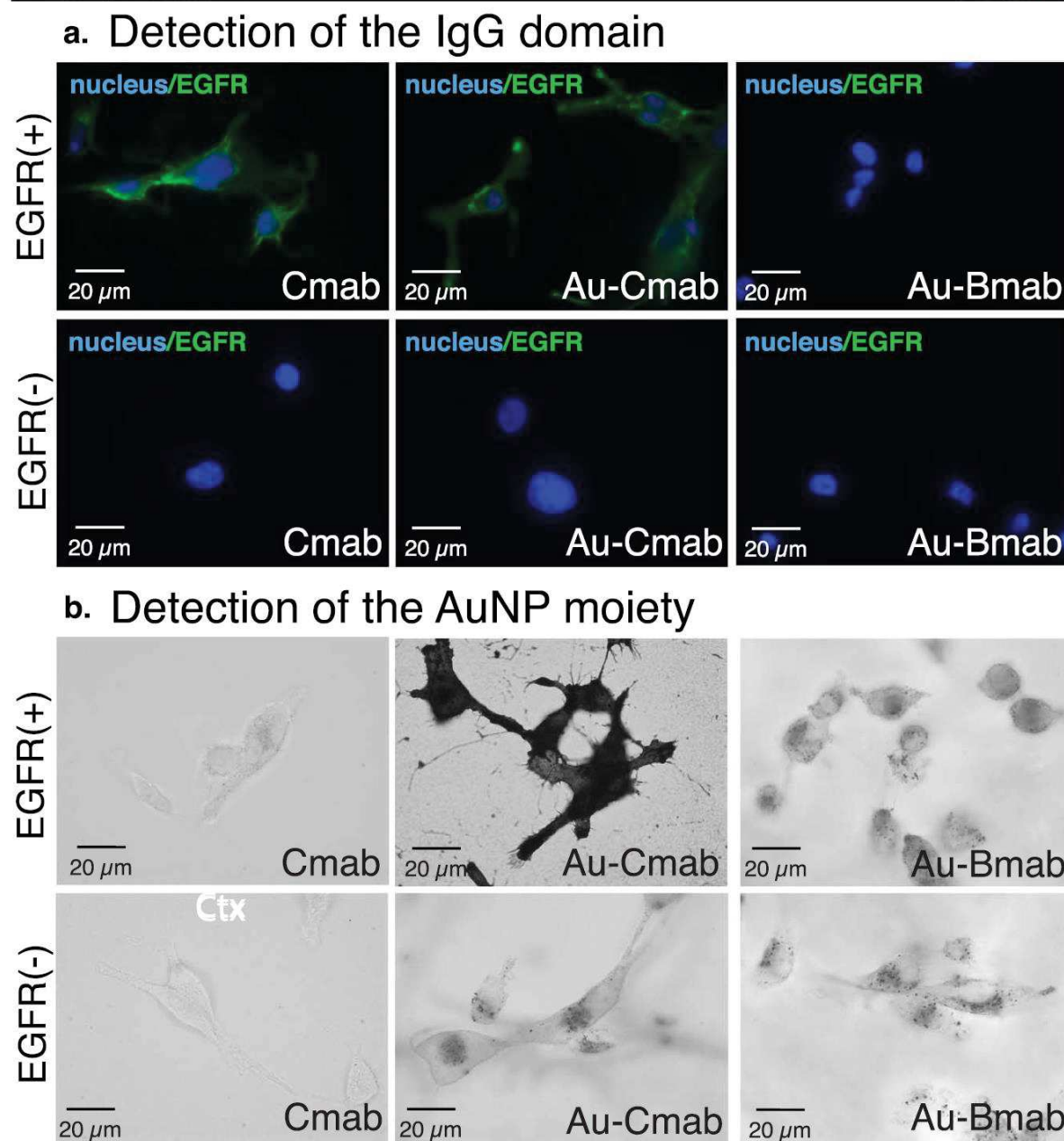


**Figure 4.** Analysis of the EGFR binding ability of the anti-EGFR C-mab, Au-C-mab and Au-B-mab to living EGFR(+) U87 glioblastoma cells and EGFR(-) U87 cells. (a) Detection of the antibody domain of the nanomaterial by immunofluorescence; (b) detection of the AuNP domain by silver staining. Cells were incubated with 167 nM of antibody or AuNP-antibody conjugate for 30 min at 37 °C. Scale bar: 20  $\mu$ m.

organic molecules *via* an Au-S coordination [49, 50]. However, presentation of a large surface to macromolecules present in the solvent is not without consequence. When AuNPs are mixed with serum, a large protein corona is forming around the AuNPs [51] that can impact cellular interactions [52]. Beside these variations in physicochemical properties, the size plays an important role for the ADME (absorption, distribution, metabolism, excretion) profile of the particles

[53–55]. Another parameter that is clearly impacting the ADME profile of NPs, such as elimination from the body, is the particle's coverage [56–58]. For inorganic non-biodegradable AuNPs, renal excretion should be undoubtedly favored, giving priority to the development of small AuNPs. Based on the work of Ackerson [59] we have prepared a novel type of AuNPs containing a mixed TABA, TNBA layer of circa 102 gold atoms that showed extremely promising

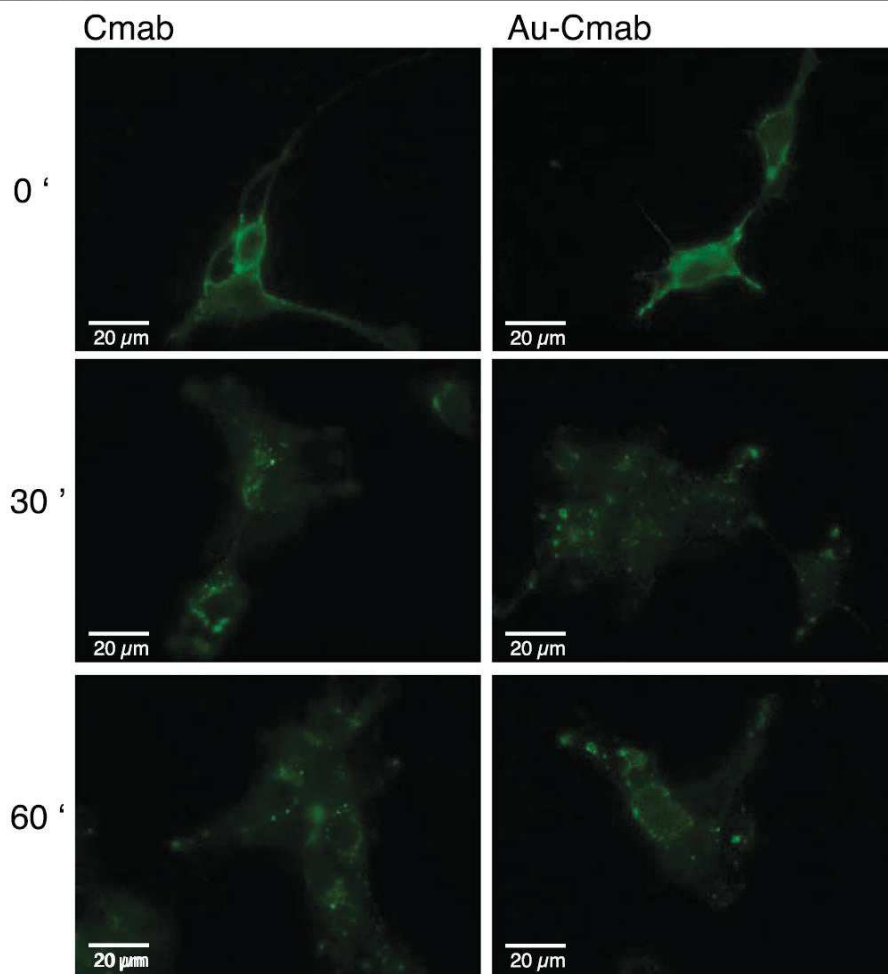


**Figure 5.** Assay of EGFR-mediated endocytosis. Cetuximab (Cmab) and AuNP-Cetuximab conjugate (Au-Cmab) were added to living EGFR(+) U87 cells for 30 min (37 °C) at concentrations of 167 nM. The cell endocytosis was then evaluated immediately (image on top: 0'), as well as after 30 and 60 min of further incubation in complete medium (not containing antibody and conjugate samples). The nanomaterial was detected by immunofluorescence. Scale bar: 20  $\mu\text{m}$

usage for biological application, due to its abilities to be functionalized with peptides and to be stabilized with zwitterionic ligands [23]. Although we could have used this AuNP for conjugation, we wished to prepare slightly larger NPs for increasing the quantity of gold atoms within the system on the one side, but also to increase the conjugation challenge as bulkiness provides steric hindrance and unspecific interactions [60, 61]. While it is well described that increasing the NP size can increase the formation of protein corona [62], the size-threshold for the occurrence of protein corona for thiolate-protected AuNPs and the associated change in the particle's physicochemical properties, is unknown. To start answering to this question, we have hence privileged to work with AuNPs of 2.4 nm, instead of with AuNPs of 1.4 nm.

A previous investigation showed that mercaptobenzoic acid-protected AuNPs can be prepared at various sizes by adjusting the type and composition of the solvent mixture

used for the particle synthesis [36]. In our case, a solvation of the gold-DTNB complex in an acetonitrile/water (80:20) mixture led to 2.4 nm AuNPs showing a high degree of monodispersity that could be characterized by SDS-PAGE analysis, MALDI-TOF mass spectrometry, STEM, EDX and UV-vis spectroscopy.

The site-directed bioconjugation of the antibodies Cmab and Bmab to the AuG *via* simple thiolate-for-thiolate ligand exchange proceeded smoothly and could be monitored by non-reducing SDS-PAGE. Until today there are very few reports about the controlled conjugation of large biomolecules to small-sized AuNPs. Ackerson and coworkers attempted the 'direct' labeling of cysteine-containing proteins with Au<sub>144</sub>NPs, however the reaction seemed to require a large excess of NPs, as a large quantity of unreacted AuNPs could be detected on the SDS gels, indicating that the reaction did not proceed as straightforward as it was the case in the present study [26]. The following reason could be hypothesized. The

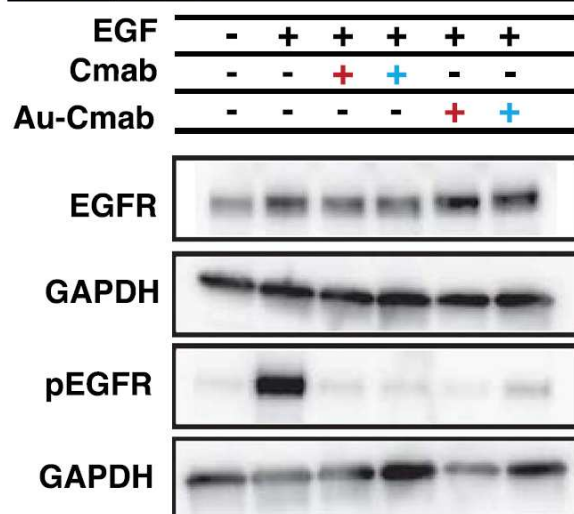


**Figure 6.** Western blot analysis of EGFR and phosphorylated EGFR (pEGFR) levels after addition of Cmab and Au-Cmab to EGF-stimulated EGFR(+) U87 cells. GAPDH was used as a loading control. Cmab and Au-Cmab were used at concentrations of 787 nM (left red +) and 394 nM (right blue +). EGF was used at a concentration of 8 nM.

AuNPs produced by Ackerson *et al* were coated with mercaptobenzoic acid, while the particles of the present study contained zwitterionic thioaminobenzoate ligands. This zwitterionic coating might diminish unspecific associations between the NP and the biomolecule, thereby favoring the accessibility of the AuNP to the antibody's hinge thiols and consequently the  $S_N2$ -like substitution.

The ability of Au-Cmab to selectively bind to EGFR present on living cells was assayed using U87 glioblastoma cells that were engineered to overexpress the EGFR, as well as using the human HT-1080 fibrosarcoma cell line, which also overexpresses the EGFR. The glioblastoma cell model system was chosen, because 40% of all glioblastoma patients overexpress the EGFR, however the response to any EGFR-based therapeutic treatment is extremely low, an issue, which remains unresolved until today [63–65]. As a consequence approaches have been developed to use the anti-EGFR antibody Cmab as a cancer targeting agent to deliver active payloads [63]. These active payloads can hence induce cell damage of the targeted cells, without relying on a 'normal functioning' EGFR signaling pathway. The data obtained from the EGFR binding assays of the present study showed that the Au-Cmab conjugate selectively binds to the EGFR on living cells in an analogous, but not identical manner than Cmab. The following AuNP-mediated differences were observed. First, an AuNP-mediated endocytosis was noted, suggesting that the 2.4 nm AuNPs slightly bind by themselves to cell surfaces. The association of the AuNP to the cell membrane was moreover promoting a small change in the intracellular trafficking of the Au-Cmab, confirming some AuNP-mediated non-selective associations to cell surface membranes. The relevance of this slight, but apparent

difference between Cmab and AuCmab is unclear but deserves careful attention. Finally, the conjugation of the AuNP decreased the apparent binding affinity. However, it should be emphasized that we have not comprehensively optimized the quality of the Au-Cmab conjugate and the magnitude in decrease of binding affinity, which we have observed (10 times difference), might be reduced.

The cell viability of the EGFR(+) U87 cells was not diminished by incubation with Cmab or Au-Cmab. This absence of toxicity has already been reported for cultured glioblastoma cells [66] and we hypothesize that this issue has the same background as the resistance of glioblastoma tumors to EGFR-based therapies.

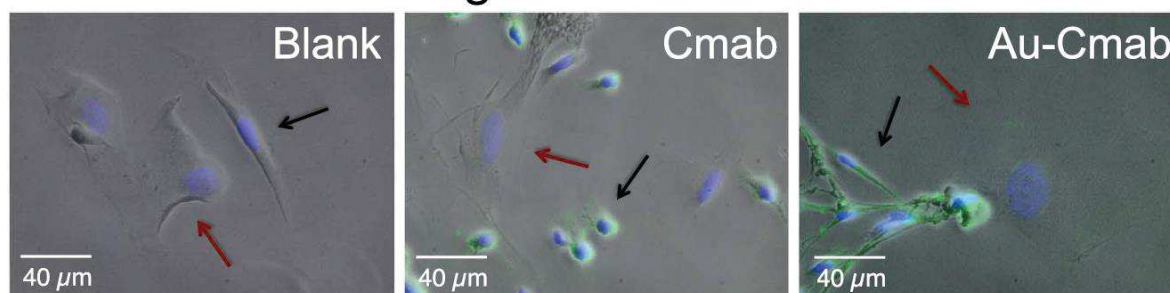
Altogether, we reported a synthesis of highly uniform 2.4 nm AuNPs that can be site-directly conjugated to the antibodies Cmab and Bmab *via* a straightforward thiolate-for-thiolate exchange mechanism. Data from *in vitro* studies showed that the Au-Cmab conjugate was able to specifically bind and internalize into glioblastoma cells after binding to EGFR, demonstrating that a targeted accumulation of AuNPs within cancerous cells is achievable. Since AuNPs allow for radiosensitization [67, 68], can be readily conjugated to drugs [69], or can be prepared from  $\beta$ -emitting radioactive gold-189 [70, 71], the Au-Cmab conjugate holds promise for targeted anticancer therapy of glioblastoma tumors, which are resistant to traditional EGFR-based therapeutic treatments.

At the present stage of investigation and knowledge, antibodies and by extension 'antibody-like' conjugates should circulate in the blood after intravenous injection. Assuming that the pharmacokinetic properties of Au-Cmab are identical to the ones of Cmab, a blood half-life of 18–21 d can be expected with an elimination by intracellular catabolism [72], rather than by renal filtration or hepato-biliary mode [73]. This pharmacokinetic behavior should facilitate targeted accumulation of the conjugate at cancer lesions, but raises issues about the reminiscence of AuNPs inside the body after degradation of the antibody moiety. Although it is generally accepted that particles having a hydrodynamic diameter <6 nm are rapidly cleared from the body by renal filtration [73], the elimination of the 2.4 nm AuNPs needs to be examined by *in vivo* studies. Moreover, *in vivo* experiments should be performed to study the route of administration, the biodistribution and the fate of the Au-Cmab conjugate.

## 5. Conclusion

A highly defined 2.4 nm AuNP, displaying an inner metallic core and an Au-S coordinated organic ligand shell, was synthesized by  $\text{NaBH}_4$  reduction of chloroauric acid in the presence of the Ellman's reagent in a 80:20 acetonitrile/water mixture. This 2.4 nm AuNP could be characterized using several methods including MALDI-TOF mass spectrometry, SDS-PAGE, UV-vis spectroscopy, electron microscopy, FTIR and EDX analysis, thereby facilitating the reproducibility of production. The AuNP was subsequently functionalized with the anti-EGFR antibody Cmab *via* a simple thiolate-for-thiolate exchange of the AuG ligands (TNBA and TABA) and the hinge thiols of the

## a. Detection of the IgG domain



## b. Detection of the AuNP moiety

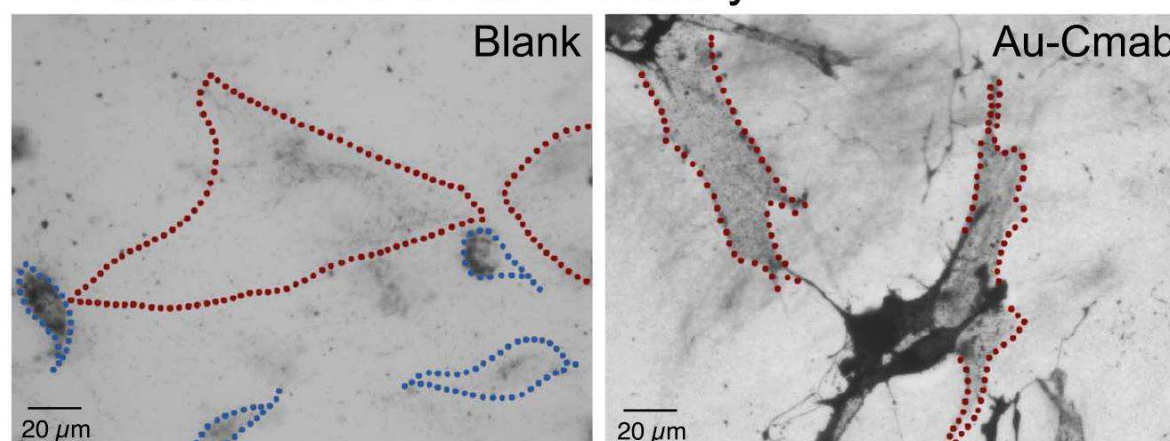


**Figure 7.** Evaluation of cell selectivity towards EGFR using a co-culture of EGFR(+) U87 cancer cells and non-cancerous human foreskin fibroblast (HFF) cells. Cmab or Au-Cmab were added to the co-culture by dilution in the cell culture medium. After 30 min incubation at 37 °C the antibody domain and the AuNP moiety were detected by immunofluorescence (a) and silver staining (b). The nuclei were stained in blue (DAPI). (a) HFF cells indicated by red arrow, EGFR(+) U87 cells indicated by black arrow. (b) HFF cells are encircled in red, EGFR(+) U87 cells are encircled in blue (in blank image only). Cmab and Au-Cmab concentrations used for incubation: 167 nM. Scale bar in (a): 40  $\mu$ m, scale bar in (b) : 20  $\mu$ m

selectively reduced antibody—a site-directed conjugation strategy, which has not been explored before for antibodies and small-sized AuNPs. To minimize the formation of protein corona and to prevent NP aggregation, the Au-Cmab conjugate was passivated with peptide CALNNG in a second step. To demonstrate that the conjugation strategy is generally applicable, the AuNP was also conjugated to the VEGF-targeting antibody Bmab. Besides, the Au-Bmab conjugate served as control in the EGFR binding assays. The conjugation reactions could be readily visualized using non-reductive SDS-PAGE analysis, from which it was assessed that the major conjugation products consist of one IgG and one AuNP. The generated Au-Cmab conjugate was seen to behave similarly to Cmab when added to living cells, suggesting that the site-directed conjugation to the AuNP did not destroy the biological activity of the antibody, thereby demonstrating the value of the designed functionalization strategy. The possibility to produce very defined AuNP-IgG conjugates opens now new ways to assay the Au-Cmab

conjugate for cancer therapy, either for sensitizing tumor cells to external radiation [10], or as a vehicle for the delivery of radioactive gold isotopes to tumor sites [70, 71, 74].

### Acknowledgments

This research was supported by the ANR-10-LABX-0026\_CSC and the French Proteomic Infrastructure (ProFI, ANR-10-INBS-08-03). NG received a PhD fellowship from the IdEX Unistra (Université de Strasbourg and Investissements d'Avenir).

The authors and co-authors have no conflicts of interest.

### ORCID iDs

Nadja Groysbeck <https://orcid.org/0000-0002-8672-555X>  
 Jean-Marc Strub <https://orcid.org/0000-0001-6224-3428>  
 Guy Zuber <https://orcid.org/0000-0001-8032-2410>

## References

- [1] McNamara K and Tofail S A M 2016 Nanoparticles in biomedical applications *Adv. Phys.* **X** 2 54–88
- [2] Ma X, Xiong Y and Lee L T O 2018 Application of nanoparticles for targeting g protein-coupled receptors *Int. J. Mol. Sci.* **19** 2006
- [3] Muhamad N, Plengsuriyakarn T and Na-Bangchang K 2018 Application of active targeting nanoparticle delivery system for chemotherapeutic drugs and traditional/herbal medicines in cancer therapy: a systematic review *Int. J. Nanomed.* **13** 3921–35
- [4] Tong L *et al* 2009 Gold nanorods as contrast agents for biological imaging: optical properties, surface conjugation and photothermal effects *Photochem. Photobiol.* **85** 21–32
- [5] Zuber G, Dontenwill M and Behr J P 2009 Synthetic viruslike particles for targeted gene delivery to  $\alpha_v\beta_3$  integrin-presenting endothelial cells *Mol. Pharm.* **6** 1544–52
- [6] Chiper M, Niederreither K and Zuber G 2018 Transduction methods for cytosolic delivery of proteins and bioconjugates into living cells *Adv. Healthc. Mater.* **7** e1701040
- [7] Farooq M U *et al* 2018 Gold nanoparticles-enabled efficient dual delivery of anticancer therapeutics to hela cells *Sci. Rep.* **8** 2907
- [8] Dykman L and Khlebtsov N 2012 Gold nanoparticles in biomedical applications: recent advances and perspectives *Chem. Soc. Rev.* **41** 2256–82
- [9] El-Sayed I H, Huang X and El-Sayed M A 2006 Selective laser photo-thermal therapy of epithelial carcinoma using anti-EGFR antibody conjugated gold nanoparticles *Cancer Lett.* **239** 129–35
- [10] Hainfeld J F and Furuya F R 1991 Gold nanoparticles for radiation enhancement in vivo *J. Histochem. Cytochem.* **40** 177–84
- [11] Chattopadhyay N *et al* 2013 Molecularly targeted gold nanoparticles enhance the radiation response of breast cancer cells and tumor xenografts to x-radiation *Breast Cancer Res. Treat.* **137** 81–91
- [12] Nie S 2010 Understanding and overcoming major barriers in cancer nanomedicine *Nanomedicine* **5** 523–8
- [13] Dixit V *et al* 2006 Synthesis and grafting of thioctic acid-PEG-folate conjugates onto Au nanoparticles for selective targeting of folate receptor-positive tumor cells *Bioconjug. Chem.* **17** 603–9
- [14] Haller E, Lindner W and Lammerhofer M 2015 Gold nanoparticle-antibody conjugates for specific extraction and subsequent analysis by liquid chromatography-tandem mass spectrometry of malondialdehyde-modified low density lipoprotein as biomarker for cardiovascular risk *Anal. Chim. Acta.* **857** 53–63
- [15] Patra C R *et al* 2008 Targeted delivery of gemcitabine to pancreatic adenocarcinoma using cetuximab as a targeting agent *Cancer Res.* **68** 1970–8
- [16] Montenegro J M *et al* 2013 Controlled antibody/(bio-) conjugation of inorganic nanoparticles for targeted delivery *Adv. Drug. Deliv. Rev.* **65** 677–88
- [17] Jiang W *et al* 2008 Nanoparticle-mediated cellular response is size-dependent *Nat. Nanotechnol.* **3** 145–50
- [18] Bhattacharyya S *et al* 2010 Nanoconjugation modulates the trafficking and mechanism of antibody induced receptor endocytosis *Proc. Natl Acad. Sci. USA* **107** 14541–6
- [19] Brust M *et al* 1994 Synthesis of thiol-derivatised gold nanoparticles in a two-phase liquid-liquid system *J. Chem. Soc., Chem. Commun.* **0** 801–2
- [20] Ackerson C J *et al* 2010 Synthesis and bioconjugation of 2 and 3 nm-diameter gold nanoparticles *Bioconjug. Chem.* **21** 214–8
- [21] Levi-Kalisman Y *et al* 2011 Synthesis and characterization of  $\text{Au}_{102}(\text{p-MBA})_{44}$  nanoparticles *J. Am. Chem. Soc.* **133** 2976–82
- [22] Marjomaki V *et al* 2014 Site-specific targeting of enterovirus capsid by functionalized monodisperse gold nanoclusters *Proc. Natl Acad. Sci. USA* **111** 1277–81
- [23] Desplancq D *et al* 2018 Cytosolic diffusion and peptide-assisted nuclear shuttling of peptide-substituted circa 102 gold atom nanoclusters in living cells *ACS Appl. Nano Mater.* **1** 4236–46
- [24] Yao H *et al* 2016 Methods to design and synthesize antibody-drug conjugates (ADCs) *Int. J. Mol. Sci.* **17** 194
- [25] Billah M M *et al* 2010 Directed immobilization of reduced antibody fragments onto a novel SAM on gold for myoglobin impedance immunosensing *Bioelectrochemistry* **80** 49–54
- [26] Ackerson C J, Powell R D and Hainfeld J F 2010 Site-specific biomolecule labeling with gold clusters *Methods Enzymol.* **481** 195–230
- [27] Diebold C A *et al* 2014 Complement is activated by IgG hexamers assembled at the cell surface *Science* **343** 1260–3
- [28] He W *et al* 2007 A freeze substitution fixation-based gold enlarging technique for EM studies of endocytosed nanogold-labeled molecules *J. Struct. Biol.* **160** 103–13
- [29] Lévy R *et al* 2004 Rational and combinatorial design of peptide capping ligands for gold nanoparticles *J. Am. Chem. Soc.* **126** 10076–84
- [30] Laemmli U K 1970 Cleavage of structural proteins during the assembly of the head of bacteriophage T4 *Nature* **227** 680
- [31] Bonavia R *et al* 2012 EGFRvIII promotes glioma angiogenesis and growth through the NF-kappaB, interleukin-8 pathway *Oncogene* **31** 4054–66
- [32] Chiper M *et al* 2017 Self-aggregating 1.8kDa polyethylenimines with dissolution switch at endosomal acidic pH are delivery carriers for plasmid DNA, mRNA, siRNA and exon-skipping oligonucleotides *J. Control. Release* **246** 60–70
- [33] Pinel S *et al* 2014 Quantitative measurement of delivery and gene silencing activities of siRNA polyplexes containing pyridylthiourea-grafted polyethylenimines *J. Control. Release* **182** 1–12
- [34] Fraser-Pitt D J *et al* 2011 Phosphorylation of the epidermal growth factor receptor (EGFR) is essential for interleukin-8 release from intestinal epithelial cells in response to challenge with escherichia coli O157 : H7 flagellin *Microbiology* **157** 2339–47
- [35] Danscher G and Nørsgaard J O R 1983 Light microscopic visualization of colloidal gold on resin-embedded tissue *J. Histochem. Cytochem.* **31** 1394–8
- [36] Wong O A, Compel W S and Ackerson C J 2015 Combinatorial discovery of cosolvent systems for production of narrow dispersion thiolate-protected gold nanoparticles *ACS Comb. Sci.* **17** 11–8
- [37] Amendola V and Meneghetti M 2009 Size evaluation of gold nanoparticles by UV-vis spectroscopy *J. Phys. Chem. C* **113** 4277–85
- [38] Makaraviciute A *et al* 2016 Considerations in producing preferentially reduced half-antibody fragments *J. Immunol. Methods.* **429** 50–6
- [39] Desplancq D *et al* 2016 Targeting the replisome with transduced monoclonal antibodies triggers lethal DNA replication stress in cancer cells *Exp. Cell Res.* **342** 145–58
- [40] Okada Y *et al* 2017 EGFR downregulation after anti-EGFR therapy predicts the antitumor effect in colorectal cancer *Mol. Cancer Res.* **15** 1445–54
- [41] Sorkin A and Duex J E 2010 Quantitative analysis of endocytosis and turnover of epidermal growth factor (EGF) and EGF receptor *Curr. Protoc Cell Biol.* **46** 15.14.1–20

- [42] Brand T M, Iida M and Wheeler D L 2011 Molecular mechanisms of resistance to the EGFR monoclonal antibody cetuximab *Cancer Biol. Ther.* **11** 777–92
- [43] Bowman M C *et al* 2008 Inhibition of HIV fusion with multivalent gold nanoparticles *J. Am. Chem. Soc.* **130** 6896–7
- [44] Hainfeld J F *et al* 2013 Gold nanoparticle imaging and radiotherapy of brain tumors in mice *Nanomedicine* **8** 1601–9
- [45] Polyakov A *et al* 2018 Gold decoration and photoresistive response to nitrogen dioxide of WS<sub>2</sub> nanotubes *Chemistry* **24** 18952–62
- [46] Choi B J *et al* 2018 A gold nanoparticle system for the enhancement of radiotherapy and simultaneous monitoring of reactive-oxygen-species formation *Nanotechnology* **29** 504001
- [47] Cole L E *et al* 2018 Effects of bisphosphonate ligands and pegylation on targeted delivery of gold nanoparticles for contrast-enhanced radiographic detection of breast microcalcifications *Acta Biomater.* **82** 122–32
- [48] Mahmoodzadeh F *et al* 2018 A novel gold-based stimuli-responsive theranostic nanomedicine for chemo-photothermal therapy of solid tumors *Mater. Sci. Eng. C* **93** 880–9
- [49] Chattopadhyay N *et al* 2010 Design and characterization of HER-2-targeted gold nanoparticles for enhanced X-radiation treatment of locally advanced breast cancer *Mol. Pharm.* **7** 2194–206
- [50] Qian Y *et al* 2014 Enhanced cytotoxic activity of cetuximab in EGFR-positive lung cancer by conjugating with gold nanoparticles *Sci. Rep.* **4** 7490
- [51] Monopoli M P *et al* 2012 Biomolecular coronas provide the biological identity of nanosized materials *Nat. Nanotechnol.* **7** 779–86
- [52] Walkey C D *et al* 2014 Protein corona fingerprinting predicts the cellular interaction of gold and silver nanoparticles *ACS Nano* **8** 2439–55
- [53] Perrault S D *et al* 2009 Mediating tumor targeting efficiency of nanoparticles through design *Nano Lett.* **9** 1909–15
- [54] Wong O A *et al* 2013 Structure-activity relationships for biodistribution, pharmacokinetics, and excretion of atomically precise nanoclusters in a murine model *Nanoscale* **5** 10525–33
- [55] Choi H S *et al* 2007 Renal clearance of quantum dots *Nat. Biotechnol.* **25** 1165–70
- [56] Shah N B *et al* 2012 Blood-nanoparticle interactions and in vivo biodistribution: impact of surface PEG and ligand properties *Mol. Pharm.* **9** 2146–55
- [57] Storm G *et al* 1995 Surface modification of nanoparticles to oppose uptake by the mononuclear phagocyte system *Adv. Drug. Deliv. Rev.* **17** 31–48
- [58] Morais T *et al* 2012 Effect of surface coating on the biodistribution profile of gold nanoparticles in the rat *Eur. J. Pharm. Biopharm.* **80** 185–93
- [59] Jadzinsky P D *et al* 2007 Structure of a thiol monolayer-protected gold nanoparticle at 1.1 Å resolution *Science* **318** 430–3
- [60] Piella J, Bastus N G and Puntès V 2017 Size-dependent protein-nanoparticle interactions in citrate-stabilized gold nanoparticles: the emergence of the protein corona *Bioconjug. Chem.* **28** 88–97
- [61] Saha K *et al* 2016 Regulation of macrophage recognition through the interplay of nanoparticle surface functionality and protein corona *ACS Nano* **10** 4421–30
- [62] Al-Jawad S M H *et al* 2018 Synthesis and characterization of small-sized gold nanoparticles coated by bovine serum albumin (BSA) for cancer photothermal therapy *Photodiagn. Photodyn. Ther.* **21** 201–10
- [63] Westphal M, Maire C L and Lamszus K 2017 EGFR as a target for glioblastoma treatment: an unfulfilled promise *CNS Drugs* **31** 723–35
- [64] Hatanpää K J *et al* 2010 Epidermal growth factor receptor in glioma: signal transduction, neuropathology, imaging, and radioresistance *Neoplasia* **12** 675–84
- [65] Zhu J J and Wong E T 2013 Personalized medicine for glioblastoma: current challenges and future opportunities *Curr. Mol. Med.* **13** 358–67
- [66] Kaluzova M *et al* 2015 Targeted therapy of glioblastoma stem-like cells and tumor non-stem cells using cetuximab-conjugated iron-oxide nanoparticles *Oncotarget* **6** 8788–806
- [67] Hainfeld J F *et al* 2008 Radiotherapy enhancement with gold nanoparticles *J. Pharm. Pharmacol.* **60** 977–85
- [68] Her S, Jaffray D A and Allen C 2017 Gold nanoparticles for applications in cancer radiotherapy: mechanisms and recent advancements *Adv. Drug. Deliv. Rev.* **109** 84–101
- [69] Vigderman L and Zubarev E R 2013 Therapeutic platforms based on gold nanoparticles and their covalent conjugates with drug molecules *Adv. Drug. Deliv. Rev.* **65** 663–76
- [70] Chanda N *et al* 2010 Radioactive gold nanoparticles in cancer therapy: therapeutic efficacy studies of GA-198AuNP nanoconstruct in prostate tumor-bearing mice *Nanomedicine* **6** 201–9
- [71] Shukla R *et al* 2012 Laminin receptor specific therapeutic gold nanoparticles (<sup>198</sup>AuNP-EGCg) show efficacy in treating prostate cancer *Proc. Natl Acad. Sci. USA* **109** 12426–31
- [72] Ryman J T and Meibohm B 2017 Pharmacokinetics of monoclonal antibodies *CPT Pharmacometr. Syst. Pharmacol.* **6** 576–88
- [73] Longmire M, Choyke P L and Kobayashi H 2008 Clearance properties of nano-sized particles and molecules as imaging agents: considerations and caveats *Nanomedicine* **3** 703–17
- [74] Rovais M R A *et al* 2018 Internalization capabilities of gold-198 nanoparticles: comparative evaluation of effects of chitosan agent on cellular uptake into MCF-7 *Appl. Radiat. Isot.* **142** 85–91



## Strategy of non-physiological EGFR endocytosis and aptamer-vectorization

### Résumé

La progression du glioblastome (GBM), tumeur cérébrale la plus fréquente, est associée à la surexpression du récepteur du facteur de croissance épidermique (EGFR) et de l'intégrine  $\alpha_5\beta_1$ . Par des études *in vitro*, nous proposons de nouvelles pistes pour améliorer les thérapies ciblant ces récepteurs et de nouveaux outils diagnostiques. 1) Nous avons montré que des médicaments, inhibiteurs de la tyrosine kinase de l'EGFR, comme le géfitinib, augmentent l'endocytose de l'EGFR et des intégrines et que l'inhibition de l'endocytose confère aux cellules une résistance contre le géfitinib. 2) Nous avons identifié et caractérisé un nouvel aptamère sélectif de l'intégrine  $\alpha_5\beta_1$  et aspirons à valider l'utilisation des aptamères ciblant  $\alpha_5\beta_1$  et l'EGFR comme outils de diagnostic pertinents dans le GBM. 3) Enfin, nous avons observé que le géfitinib augmente l'endocytose d'anticorps et d'aptamères anti-EGFR. Nos travaux positionnent i) le trafic endomembranaire en tant que cible thérapeutique, ii) les aptamères en tant que possibles outils diagnostiques et thérapeutiques, iii) le géfitinib en tant que co-traitement potentiel pour accroître la délivrance d'agents (cyto-toxiques ou siRNA) à l'aide de vecteurs à base d'aptamères ou d'anticorps anti-EGFR.

**Mots- clés :** glioblastoma, trafic endomembranaire, récepteurs membranaires, aptamères

### Abstract

The progression of glioblastoma (GBM), the most common brain tumor, is associated with overexpression of the epidermal growth factor receptor (EGFR) and the  $\alpha_5\beta_1$  integrin. Through *in vitro* studies, we are proposing new approaches to improve therapies targeting these receptors and new diagnostic tools. 1) We have shown that drugs inhibiting EGFR tyrosine kinase, such as gefitinib, increase EGFR and integrin endocytosis and that inhibition of endocytosis confers resistance to gefitinib. 2) We identified and characterized a novel selective  $\alpha_5\beta_1$  integrin aptamer and aim to validate the use of aptamers targeting  $\alpha_5\beta_1$  integrin and EGFR as relevant diagnostic tools in GBM. 3) Finally, we observed that gefitinib increases the endocytosis of anti-EGFR antibodies and aptamers. Our work highlights i) endomembrane trafficking as a therapeutic target, ii) aptamers as potential diagnostic and therapeutic tools, iii) gefitinib as a potential co-treatment to increase the delivery of drugs (toxic agents or siRNA) using vectors based on aptamers or anti-EGFR antibodies.

**Keywords:** glioblastoma, membrane trafficking, cell surface receptors, aptamers